frontiers | Research Topics

Advances in the diagnosis and management of infectious diseases

Edited by
Diana Manolescu and Ariadna Petronela Fildan

Coordinated by
Emil Robert Stoicescu

Published in
Frontiers in Cellular and Infection Microbiology

ISSN 1664-8714
ISBN 978-2-8325-7376-1
DOI 10.3389/978-2-8325-7376-1

Generative AI statement
Any alternative text (Alt text) provided alongside figures in the articles in this ebook has been generated by Frontiers with the support of artificial intelligence and reasonable efforts have been made to ensure accuracy, including review by the authors wherever possible. If you identify any issues, please contact us.

About Frontiers

Frontiers is more than just an open access publisher of scholarly articles: it is a pioneering approach to the world of academia, radically improving the way scholarly research is managed. The grand vision of Frontiers is a world where all people have an equal opportunity to seek, share and generate knowledge. Frontiers provides immediate and permanent online open access to all its publications, but this alone is not enough to realize our grand goals.

Frontiers journal series

The Frontiers journal series is a multi-tier and interdisciplinary set of open-access, online journals, promising a paradigm shift from the current review, selection and dissemination processes in academic publishing. All Frontiers journals are driven by researchers for researchers; therefore, they constitute a service to the scholarly community. At the same time, the *Frontiers journal series* operates on a revolutionary invention, the tiered publishing system, initially addressing specific communities of scholars, and gradually climbing up to broader public understanding, thus serving the interests of the lay society, too.

Dedication to quality

Each Frontiers article is a landmark of the highest quality, thanks to genuinely collaborative interactions between authors and review editors, who include some of the world's best academicians. Research must be certified by peers before entering a stream of knowledge that may eventually reach the public - and shape society; therefore, Frontiers only applies the most rigorous and unbiased reviews. Frontiers revolutionizes research publishing by freely delivering the most outstanding research, evaluated with no bias from both the academic and social point of view. By applying the most advanced information technologies, Frontiers is catapulting scholarly publishing into a new generation.

What are Frontiers Research Topics?

Frontiers Research Topics are very popular trademarks of the *Frontiers journals series*: they are collections of at least ten articles, all centered on a particular subject. With their unique mix of varied contributions from Original Research to Review Articles, Frontiers Research Topics unify the most influential researchers, the latest key findings and historical advances in a hot research area.

Find out more on how to host your own Frontiers Research Topic or contribute to one as an author by contacting the Frontiers editorial office: frontiersin.org/about/contact

Advances in the diagnosis and management of infectious diseases

Topic editors
Diana Manolescu — Victor Babes University of Medicine and Pharmacy, Romania
Ariadna Petronela Fildan — Ovidius University, Romania

Topic coordinator
Emil Robert Stoicescu — Victor Babes University of Medicine and Pharmacy, Romania

Citation
Manolescu, D., Fildan, A. P., Stoicescu, E. R., eds. (2026). *Advances in the diagnosis and management of infectious diseases*. Lausanne: Frontiers Media SA.
doi: 10.3389/978-2-8325-7376-1

Table of contents

frontiers | Frontiers in Cellular and Infection Microbiology

TYPE Editorial
PUBLISHED 06 January 2026
DOI 10.3389/fcimb.2025.1765521

OPEN ACCESS

EDITED AND REVIEWED BY
Rodolfo García-Contreras,
National Autonomous University of Mexico, Mexico

*CORRESPONDENCE
Emil Robert Stoicescu
stoicescu.emil@umft.ro

RECEIVED 11 December 2025
ACCEPTED 16 December 2025
PUBLISHED 06 January 2026

CITATION
Manolescu D, Stoicescu ER and Fildan AP (2026) Editorial: Advances in the diagnosis and management of infectious diseases. *Front. Cell. Infect. Microbiol.* 15:1765521. doi: 10.3389/fcimb.2025.1765521

Editorial: Advances in the diagnosis and management of infectious diseases

Diana Manolescu[1,2], Emil Robert Stoicescu[1,3,4]* and Ariadna Petronela Fildan[5]

[1]Radiology and Medical Imaging University Clinic, 'Victor Babes' University of Medicine and Pharmacy Timisoara, Timisoara, Romania, [2]Center for Research and Innovation in Precision Medicine of Respiratory Diseases (CRIPMRD), 'Victor Babes' University of Medicine and Pharmacy Timisoara, Timisoara, Romania, [3]Research Center for Medical Communication, 'Victor Babes' University of Medicine and Pharmacy Timisoara, Timisoara, Romania, [4]Research Center for Pharmaco-Toxicological Evaluations, 'Victor Babes' University of Medicine and Pharmacy Timisoara, Timisoara, Romania, [5]Faculty of Medicine, "Ovidius" University of Constanta, Constanta, Romania

KEYWORDS

antimicrobial resistance (AMR), biomarker discovery, diagnostic stewardship, infectious diseases, molecular sequencing, point-of-care testing, precision medicine

Editorial on the Research Topic
Advances in the diagnosis and management of infectious diseases

Introduction

Infectious diseases continue to represent one of the most dynamic and rapidly evolving domains of modern medicine. Global interconnectedness, climate change, and microbial adaptation have contributed to the continuous emergence and re-emergence of pathogens, while the parallel rise of antimicrobial resistance (AMR) challenges conventional therapeutic paradigms. Against this complex backdrop, diagnostic innovation has become the cornerstone of effective clinical and public-health response. Advances in molecular detection, sequencing technologies, point-of-care testing, and quantitative biomarker analysis are redefining how clinicians detect, characterize, and monitor infectious processes.

The present Research Topic, *"Advances in the Diagnosis and Management of Infectious Diseases,"* compiles twenty peer-reviewed studies that collectively capture the ongoing transition from laboratory innovation to clinical translation. The selected papers span a broad scientific and geographical spectrum, encompassing next-generation sequencing (NGS), chemiluminescent and immunoassay technologies, imaging biomarkers, antimicrobial stewardship strategies, and outcome-oriented clinical research. Taken together, these studies exemplify a global research effort directed toward improving diagnostic accuracy, therapeutic precision, and patient prognosis through technological convergence and multidisciplinary collaboration.

To synthesize this body of work, the articles were organized into five major research directions:

(1) Innovations in Molecular and Sequencing-Based Diagnostics;
(2) Clinical Impact of Metagenomic Sequencing in Infectious Diseases;
(3) Development of Rapid and Point-of-Care Diagnostic Tools;
(4) Diagnostic Performance and Biomarker Discovery; and
(5) Antimicrobial Resistance, Stewardship, and Clinical Outcomes.

Each direction reflects a distinct yet interconnected facet of the current diagnostic landscape and collectively illustrates how precision technology and clinical integration are reshaping infectious disease management worldwide.

Innovations in molecular and sequencing-based diagnostics

The first cluster of studies underscores the growing maturity of molecular and sequencing-based platforms capable of delivering comprehensive pathogen detection with clinical-grade accuracy. Technologies such as third-generation nanopore sequencing, targeted NGS (tNGS), and metagenomic NGS (mNGS) now offer near-real-time identification of microorganisms and resistance determinants directly from clinical specimens, reducing dependence on culture and expediting targeted therapy.

A large retrospective study evaluating third-generation nanopore sequencing in non-tuberculous mycobacterial pulmonary disease (NTMPD) demonstrated 81.3% sensitivity and 98.8% specificity, outperforming culture and identifying numerous low-burden or mixed infections undetected by conventional methods. Similarly, validation of the MeltPlus TB-NTM/RIF assay confirmed its capacity to simultaneously identify *Mycobacterium tuberculosis* complex, non-tuberculous mycobacteria, and rifampicin resistance with high accuracy within three hours—an achievement of substantial operational relevance for tuberculosis-endemic settings (Zhao et al., Wang et al.).

Complementing these advances, a multiplex molecular point-of-care platform (fastNTM) achieved near-perfect agreement with the Xpert MTB/RIF Ultra assay, reducing total diagnostic time to 90 minutes and demonstrating the feasibility of decentralizing complex molecular testing. Parallel studies comparing tNGS and mNGS in respiratory infections revealed equivalent diagnostic performance but lower cost and faster turnaround for tNGS, emphasizing the importance of targeted panels as cost-effective alternatives to broad metagenomic approaches. In fungal respiratory infections, both modalities far outperformed culture, with *Pneumocystis jirovecii*, *Candida albicans*, and *Aspergillus fumigatus* emerging as the most prevalent organisms (Yi et al., Kuang et al.).

Collectively, these studies illustrate the ongoing convergence between sequencing depth, diagnostic speed, and cost-efficiency. The data support an impending shift from exploratory sequencing toward standardized, clinically integrated molecular workflows, where sequencing informs real-time antimicrobial and infection-control decisions.

Clinical impact of metagenomic sequencing in infectious diseases

The second group of articles focuses on the clinical translation of metagenomic sequencing in complex or atypical infections, particularly those affecting immunocompromised hosts. The ability of mNGS to detect microbial DNA or RNA directly from plasma, cerebrospinal fluid, or bronchoalveolar lavage fluid (BALF) has transformed the diagnostic outlook for disseminated and opportunistic diseases that are frequently missed by culture.

In a study on disseminated tuberculosis, plasma mNGS detected *Mycobacterium tuberculosis* in two-thirds of confirmed cases, achieving 100% specificity and outperforming traditional immune-based assays, especially in HIV-positive patients (Ma et al.).

Another large retrospective analysis from Wuhan evaluated BALF mNGS in nearly 300 patients with suspected pneumonia and demonstrated a diagnostic sensitivity of 87.9%, significantly higher than that of conventional microbial tests. The inclusion of immunocompromised and oncologic populations emphasized the added value of mNGS in guiding tailored therapy for patients with ambiguous or culture-negative infections (Zhou et al.).

The same principle was applied in non-endemic visceral leishmaniasis, where mNGS successfully identified *Leishmania infantum* and *L. donovani* in peripheral blood and bone marrow samples of previously misdiagnosed patients. Early molecular identification allowed rapid initiation of specific antiprotozoal therapy and complete recovery—highlighting mNGS as a powerful tool for identifying imported or unexpected pathogens (Zhao et al.).

Taken together, these studies demonstrate that the clinical utility of mNGS extends beyond discovery; it meaningfully alters diagnostic certainty, accelerates therapeutic decisions, and supports differential diagnosis in both endemic and non-endemic contexts. However, they also underscore the need for standardized interpretation frameworks and cost-effectiveness analyses before universal adoption.

Development of rapid and point-of-care diagnostic tools

Rapid, field-deployable diagnostics are indispensable for outbreak response, rural healthcare, and veterinary surveillance. The third research direction presents a suite of isothermal amplification-based assays, often combined with CRISPR/Cas detection systems or lateral flow devices (LFDs), which achieve high analytical performance without sophisticated infrastructure.

A recombinase polymerase amplification (RPA)/LFD assay for *Dengue virus* type 2 detection achieved a limit of detection of approximately 40 copies per reaction within 20 minutes, maintaining stability across variable temperatures and multiple freeze–thaw cycles. This portability renders it particularly valuable for tropical regions where dengue is endemic but laboratory capacity limited (Prescott et al.).

Similarly, a CRISPR-Cas12a-enhanced RPA assay for *goose parvovirus* achieved single-digit copy detection in under an hour, outperforming qPCR in sensitivity and specificity and allowing naked-eye readout under blue light. These designs collectively demonstrate how CRISPR and RPA technologies are merging into flexible, low-cost diagnostic systems adaptable across species and pathogens (Chen et al.).

A third innovation, the immunoassay–mass spectrometry (MS) method for *Brucella melitensis*, integrated magnetic nanoparticle capture with MALDI-TOF identification, eliminating the need for lengthy culture of hazardous organisms. With a detection limit of 50 CFU/mL and completion within 60 minutes, the method markedly improves biosafety and turnaround time for a major zoonotic pathogen (Sharif et al.).

Collectively, these studies reinforce the promise of next-generation point-of-care (POC) platforms: assays that combine analytical sensitivity approaching laboratory methods with operational simplicity suitable for decentralized or emergency settings. Their broad adoption could bridge existing gaps between molecular capability and field applicability, thereby extending the reach of precision diagnostics to low-resource environments.

Diagnostic performance and biomarker discovery

The fourth group of studies emphasizes quantitative biomarkers and advanced immunoassays that transcend binary diagnostic outcomes by offering dynamic measures of disease burden and therapeutic response. As infectious disease management evolves toward precision medicine, such biomarkers serve as vital adjuncts to guide initiation, monitoring, and discontinuation of therapy.

A multicenter comparison of chemiluminescent immunoassay (CLIA) and lateral flow assay (LFA) for cryptococcal antigen detection revealed near-perfect agreement (99.2%) but highlighted CLIA's superiority for longitudinal monitoring (Tang et al.).

In musculoskeletal infections, synovial fluid fibrin degradation product (sFDP) emerged as a robust biomarker for periprosthetic joint infection (PJI), showing diagnostic accuracy comparable to CRP and ESR but with greater procedural practicality. The study advocates combined biomarker approaches to refine preoperative evaluation, particularly when culture or histopathology is delayed (Huang et al.).

Meanwhile, analysis of plasma *Epstein–Barr virus* (EBV) DNA load in intestinal EBV infection established its dual diagnostic and prognostic value. Defined thresholds accurately distinguished infection types and predicted six-month outcomes, with viral load correlating closely with tissue EBER positivity. The work supports integration of plasma EBV quantification into monitoring algorithms for EBV-associated intestinal disorders and lymphoproliferative disease (Ma et al.).

These contributions collectively signal a transition from static qualitative tests toward dynamic, data-rich biomarker systems capable of stratifying risk, quantifying disease progression, and informing therapeutic decisions in real time.

Antimicrobial resistance, stewardship, and clinical outcomes

The final thematic group addresses the intertwined challenges of antimicrobial resistance (AMR), clinical stewardship, and outcome prediction—domains where diagnostic precision directly influences survival and antibiotic sustainability.

A 2023 cohort of 190 patients with carbapenem-resistant *Klebsiella pneumoniae* (CRKP) identified ICU admission, co-infection with CRAB or CRPA, and elevated neutrophil-to-lymphocyte ratio (NLR) as independent predictors of mortality, whereas timely appropriate therapy was protective. The NLR, a simple hematologic parameter, demonstrated moderate predictive accuracy (AUC 0.696) and offers a practical adjunct for early risk stratification in critically ill patients (Wang et al.).

From a systems perspective, a six-year initiative at the Central Texas Veterans Health Care System examined the impact of discontinuing automatic reflex urine cultures after urinalysis. The policy reduced culture volume by 42%, lowered unnecessary antibiotic use, and shifted prescribing patterns toward narrower agents such as nitrofurantoin—an exemplary case of diagnostic stewardship aligning laboratory practice with evidence-based care (Berger et al.).

Two COVID-19-related studies further elucidate the interplay between diagnostics, host factors, and outcomes. A Romanian cohort comparing lopinavir/ritonavir and darunavir/ritonavir demonstrated a survival advantage only for lopinavir-based therapy, highlighting the importance of comparative effectiveness data during therapeutic repurposing. Another investigation during the Omicron wave in China revealed a high incidence (29%) of COVID-19-associated pulmonary aspergillosis (CAPA), with mortality exceeding 50%. Diabetes, chronic lung disease, corticosteroid exposure, and mechanical ventilation emerged as key risk factors, emphasizing the need for routine fungal screening and judicious use of immunomodulators. (Paroczai et al., Xiao et al.).

Additional studies addressed diagnostic limitations and epidemiologic trends. Evaluation of HTLV-1 antibody testing in endemic Chinese hospitals revealed insufficient sensitivity at current cutoff levels, supporting combined serologic and nucleic-acid testing for high-risk cases (Chen et al.).

A regional surveillance study from Shijiazhuang documented post-pandemic resurgence and compositional shifts in acute respiratory infection (ARI) pathogens, with *Mycoplasma pneumoniae* prevalence rising sharply after withdrawal of non-pharmaceutical interventions (Zheng et al.).

Together, these investigations illustrate how accurate diagnostics underpin not only pathogen detection but also the broader ecosystem of stewardship, surveillance, and patient safety.

They collectively argue for an integrated approach linking laboratory insight to clinical policy and outcome analysis.

Future directions and perspectives

The twenty studies represented in this Research Topic converge on a clear trajectory: the integration of multimodal, data-driven, and personalized strategies into infectious disease diagnostics and management. Several cross-cutting trends emerge.

First, the acceleration of molecular turnaround time—from days to minutes—signals an imminent reconfiguration of diagnostic algorithms. As nanopore and RPA-based assays mature, decentralization of advanced molecular testing will become feasible even in resource-limited settings. However, harmonization of analytic performance metrics and quality assurance frameworks remains an essential prerequisite for equitable global adoption.

Second, data integration and artificial intelligence (AI) are poised to transform diagnostic interpretation. Sequencing output, biomarker kinetics, and radiologic patterns can be synthesized through machine-learning models to enable predictive diagnostics, capable of forecasting resistance emergence or treatment response before clinical deterioration occurs. Embedding these models into electronic health record systems will be critical to realizing their full potential.

Third, the field must address economic and operational scalability. Despite demonstrated accuracy, mNGS and other high-throughput platforms remain cost-intensive and technically demanding. Development of streamlined bioinformatic pipelines, cloud-based analysis, and standardized reporting formats will be key to reducing barriers to clinical implementation.

Finally, interdisciplinary collaboration stands as the defining catalyst for sustained progress. The convergence of microbiology, molecular engineering, informatics, imaging, and clinical medicine exemplified in this Research Topic underscores that infectious disease diagnostics can no longer operate in disciplinary isolation. Future research should continue to pursue multicenter validation, longitudinal follow-up, and implementation science to ensure that innovation translates into measurable public-health benefit.

Conclusion

This Research Topic encapsulates a vibrant and rapidly advancing research landscape in infectious disease diagnostics and management. Collectively, these works demonstrate that the future of infection control and clinical microbiology lies in precision, speed, and integration—precision through genomics and quantitative biomarkers, speed through point-of-care technologies, and integration through stewardship frameworks and digital analytics.

By uniting technological innovation with clinical applicability, the contributions in this Research Topic offer a roadmap toward more personalized, predictive, and preventive infectious disease care. Continued global collaboration, standardization, and equitable dissemination of these advances will be essential to translate diagnostic excellence into improved outcomes for patients worldwide.

Author contributions

DM: Data curation, Writing – original draft, Conceptualization, Project administration, Methodology, Visualization, Investigation, Supervision, Resources, Funding acquisition, Validation, Writing – review & editing, Software, Formal Analysis. ES: Data curation, Writing – original draft, Project administration, Validation, Resources, Methodology, Conceptualization, Supervision, Funding acquisition, Investigation, Visualization, Software, Formal Analysis, Writing – review & editing. AF: Writing – original draft, Methodology, Data curation, Conceptualization, Supervision, Visualization, Investigation, Funding acquisition, Validation, Resources, Project administration, Formal Analysis, Writing – review & editing, Software.

Conflict of interest

The authors declared that this work was conducted in the absence of any commercial or financial relationships that could be construed as a potential conflict of interest.

Generative AI statement

The author(s) declared that generative AI was used in the creation of this manuscript. Generative AI was used in the preparation of this manuscript solely for grammar correction and to improve the professional tone of the text. The authors verify and take full responsibility for the content of the manuscript and for the use of generative AI tools as described.

Any alternative text (alt text) provided alongside figures in this article has been generated by Frontiers with the support of artificial intelligence and reasonable efforts have been made to ensure accuracy, including review by the authors wherever possible. If you identify any issues, please contact us.

Publisher's note

frontiers | Frontiers in Cellular and Infection Microbiology

TYPE Original Research
PUBLISHED 28 November 2024
DOI 10.3389/fcimb.2024.1486953

OPEN ACCESS

EDITED BY
Diana Manolescu,
Victor Babes University of Medicine and Pharmacy, Romania

REVIEWED BY
Shobha Broor,
Shree Guru Gobind Singh Tricentenary University, India
Tatina Todorova Todorova,
Medical University of Varna, Bulgaria

*CORRESPONDENCE
Zan-chao Liu
liuzanchao2007@163.com

†These authors have contributed equally to this work

RECEIVED 27 August 2024
ACCEPTED 29 October 2024
PUBLISHED 28 November 2024

CITATION
Zheng P-p, Zhao Y-n, Wang Z-k, Wang M-z, Li R, Zhang J, Li N, Zhang Z-f, Rong R-j, Sun Y-c and Liu Z-c (2024) Prevalence of respiratory pathogens among hospitalised patients with acute respiratory infection during and after the COVID-19 pandemic in Shijiazhuang, China.
Front. Cell. Infect. Microbiol. 14:1486953.
doi: 10.3389/fcimb.2024.1486953

Prevalence of respiratory pathogens among hospitalised patients with acute respiratory infection during and after the COVID-19 pandemic in Shijiazhuang, China

Pan-pan Zheng[1†], Ya-nan Zhao[2†], Zhi-kai Wang[3], Min-zhen Wang[4], Rong Li[1], Jing Zhang[2], Nan Li[2], Zi-feng Zhang[2], Rui-juan Rong[2], Yi-chan Sun[2] and Zan-chao Liu[1*]

[1]Hebei Key Laboratory of Basic Medicine for Diabetes, Shijiazhuang Second Hospital, Shijiazhuang, Hebei, China, [2]Shijiazhuang Technology Innovation Center of Precision Medicine for Diabetes, Shijiazhuang Second Hospital, Shijiazhuang, Hebei, China, [3]School of Clinical Medicine, Hebei Medical University, Shijiazhuang, Hebei, China, [4]Institute of Epidemiology and Health Statistics, School of Public Health, Lanzhou University, Lanzhou, Gansu, China

Background: The COVID-19 pandemic and the resulting non-pharmaceutical interventions (NPIs) have led to changes in the epidemiology of other respiratory pathogens. This study was conducted to explore the epidemiological characteristics of 13 respiratory pathogens, including 11 respiratory viruses and 2 non-classical microorganisms, in hospitalised patients with acute respiratory tract infections (ARTIs) and to compare the prevalence of respiratory pathogens during and after the COVID-19 pandemic.

Methods: We conducted a single-centre retrospective study involving 8979 patients with ARTIs in Shijiazhuang City from December 2019 to December 2023. The GeXP analysis platform and multiple reverse transcription–PCR (mRT–PCR) technology were used to simultaneously detect 13 respiratory pathogens. The ARIMA model was constructed to predict the pathogen detection rate in each quarter of Shijiazhuang City in the next 2 y.

Results: Among the 8979 patients, 4169 (46.43%) tested positive for respiratory pathogens. The total pathogen detection rate rebounded in the year after the COVID-19 pandemic. After the COVID-19 pandemic, the positive rates in men were slightly higher than those in women and the positive rates in spring and winter were significantly higher than those in summer. The dominant pathogens during the COVID-19 pandemic were Influenza A viru (InfA; 24.08%) and Human Rhinovirus (HRV; 21.77%), and after the COVID-19 pandemic were InfA (27.92%) and H3 (21.17%). During the COVID-19 pandemic, InfA and HRV frequently occurred in all age groups. After the COVID-19 pandemic, InfA and Seasonal Influenza virus H3N2 (H3) frequently occurred in all age groups.

Conclusions: A series of NPIs introduced by the Chinese government during the COVID-19 pandemic had a significant impact on acute upper respiratory pathogenic infections. After the withdrawal of the NPIs, the spectrum of respiratory pathogens changed.

KEYWORDS

COVID-19, respiratory pathogens, non-classical microorganisms, ARTIs/ILI, epidemiology

Nearly 30% of hospitalised cases and 30%–60% of outpatient visits are related to respiratory infections (Albogami et al., 2018). Acute respiratory tract infections (ARTIs) are responsible for the high childhood morbidity and mortality in developing countries and are a major global health burden (World Health Organization, 2019). Viral ARTIs are one of the leading causes of hospital and outpatient visits in children and the elderly (Huang et al., 2018). Respiratory virus infection is one of the main causes of ARTIs, particularly upper respiratory tract infections, where viral infection accounts for 70%–80% of cases (Woodhead et al., 2011). An epidemiological investigation of respiratory pathogens is conducive to recovery from infection and control of pathogen outbreaks to avoid wider spread (Giamberardin et al., 2016; Ojuawo et al., 2020).

Because of the non-specific symptoms and the lack of rapid and sensitive diagnostic methods, including antigen-based testing and viral isolation culture, the use of empirical antibiotics in patients with viral ARTIs not only delays the time for treatment but also increases resistance (Benezit et al., 2020). The recommended method for diagnosing respiratory virus infections is nucleic acid testing, i.e. molecular detection methods, the use of which will reduce the turnaround time of diagnosis and will enable the detection of multiple pathogens simultaneously (Bibby et al., 2022). We used the GeXP genetic analysis platform and multiple reverse transcription–PCR (mRT–PCR) method (Wang et al., 2021) to simultaneously detect 13 major respiratory viruses and non-classical microorganisms.

The epidemiological pattern of respiratory pathogens is easily affected by factors such as the environment, geographical region, climate, human mobility and socioeconomic status (Albogami et al., 2018; Wu et al., 2023). In December 2019, the novel coronavirus (SARS-CoV-2) was first detected in China. Because humans have no natural immunity to the virus, COVID-19 eventually became a pandemic even with strict lockdown measures (Tan et al., 2022). SARS-CoV-2 infection can be transmitted by aerosols and respiratory droplets, sharing the same route of transmission as that of other respiratory pathogens (Zeng et al., 2021; Al et al., 2023). During the COVID-19 pandemic, the Chinese government used effective measures to treat COVID-19 patients and implemented non-pharmaceutical interventions (NPIs), including social distancing, closing schools, wearing masks, restricting travel, strengthening personal hygiene and closing borders, to curb disease transmission (Wu et al., 2023) while reducing the spread of viruses such as influenza A and B (Al et al., 2023). After the withdrawal of the NPIs in 2022–2023, viral ARTI-related hospitalisations increased and the influenza virus is currently co-circulating with SARS-CoV-2 in the UK (Nguyen et al., 2023), however, the situation in the Shijiazhuang area of China is unclear. This study analysed the incidence rate, gender, age of onset, seasonal changes of respiratory pathogens, and changes during and after the COVID-19 outbreak in all age groups.

Methods

Study population

We enrolled 8979 patients with suspected ARTIs who were hospitalised in Shijiazhuang Second Hospital from December 2019 to December 2023. The inclusion criteria were the following: (1) disease duration less than 3 days accompanied by cough or sore throat, nasal congestion, runny nose, sputum and other upper respiratory tract symptoms; (2) complete data. The exclusion criteria were the following: (1) acute respiratory inflammation caused by non-infectious factors; (2) parenchymatous organs or haematopoietic stem cell transplantation, immunodeficiency diseases such as human immunodeficiency virus infection, and cancer chemotherapy; and (3) incomplete data or patients not agreeing to participate in this study. This study was approved by the Ethics Committee of Shijiazhuang Second Hospital, and oral informed consent was obtained from all patients.

Clinical data and sample collection

Demographic data were collected from the laboratory information system, including sex, age, clinical diagnosis, date of hospitalisation and date of pathogen testing. Nasopharyngeal swab samples were collected by professional clinicians and submitted for examination within 2 h. The collection of clinical data was de-identified and anonymous.

GeXP-based multiple reverse transcription–polymerase chain reaction

A nucleic acid extraction BD-Micro kit (ZD Biotech, Zhejiang, China) was used to extract nucleic acid according to the manufacturer's instructions. Multiple detection kits for 13 respiratory pathogens (ZD Biotech, Zhejiang, China) were used for respiratory pathogen detection. The multiple reverse transcription–PCR (mRT–PCR) reaction system and procedure are described in the kit instructions. The mRT–PCR products were separated in the GenomeLab™ GeXP (Beckman Coulter, USA) platform according to fragment size and migration rate and were analysed using the fluorescence signal intensity data. The 13 pathogens included Influenza A viru (InfA), Influenza A virus H1N1 (InfAH1N1), Seasonal Influenza virus H3N2 (H3), Influenza B virus (InfB), Human Adenovirus (HADV), Boca virus (Boca), Human Rhinovirus (HRV), Human Parainfluenza virus (HPIV), Human Coronavirus (HCOV), Human Respiratory Syncytial virus (HRSV), Human Metapneumovirus (HMPV), Mycoplasma Pneumoniae (MP) and Chlamydia (Ch). Quality control was performed during pathogen testing.

Statistical analysis

The SPSS 21.0 statistical software and GraphPad Prism 5 were used to process and analyses the data. Categorical variables were compared using the chi-square test or Fisher's exact test. A bilateral P value of <0.05 was considered statistically significant. The base, tseries, forecast and other software packages of R4.0.3 were used to construct the ARIMA prediction model for time series analysis, and the smaller the MAPE value was, the better was the fitting effect. Positive rate or positive detection rate refers to the frequency of positive detections. Positive proportion refers to the positive detection of a pathogen in the positive detection of all 13 pathogens. Positive cases refers to the number of positive patients.

Results

Characteristics of the respiratory pathogenic infection

A total of 8979 cases were collected from inpatients with ARTIsadmitted to the hospital, of whom 4801 (53.47%) were males and 4178 (46.53%) were females. The patient age range was from 9 months to 105 y. The socio-demographic variables are summarised in Table 1. A total of 4169 cases tested positive for respiratory pathogens, and the total positive detection rate was 46.43% (4169/8979). The positive detection rate of the InfAH1N1 virus and total infection rate in males were significantly higher than those in females (1.7% vs. 1.0%, P = 0.004; 24.15% vs. 22.29%, P = 0.020), and the positive detection rate of the H3 virus in females was significantly higher than that in males (9.3% vs. 7.9%, P = 0.042). The total pathogen detection rate was highest in the age group of 0–4 y (102.1%). With the exception of InfAH1N1, HCOV and Ch, there were significant differences in pathogen detection rates among different age groups (P < 0.001).

Distribution of the pathogen positive detection rate in different years

In December 2019, the first pandemic strain 19A was found in Wuhan, China, and since then, China's epidemic prevention and control has started. China launched an emergency management mechanism for the first time and began to implement strict epidemic prevention and control measures until December 2022, when the State Council's epidemic prevention measures to optimise the 'new 10' (Rongfeng et al., 2024). Therefore, we collected data for 3 y during the COVID-19 outbreak and for 1 y after the COVID-19 pandemic, as shown in Figure 1.

The number of pathogens detected in the first 3 y ranged from 1000 to 2000 and rebounded to more than 4,600. The positive detection rates of InfA, InfAH1N1, H3, HRV, HPIV, HMPV and MP were significantly different among the four time periods, which were all higher from December 2022 to December 2023 than from the other three time periods, except for HRV (P < 0.01) (Figure 1A). From December 2019 to November 2020, the main pathogenic infections were InfA, H3 and HRV; from December 2020 to November 2021, the pathogenic infection was mainly HRV; from December 2021 to November 2022, the main pathogenic infections were InfB and HRV; and from December 2022 to December 2023, the pathogenic infections were mainly InfA, H3 and MP (Figure 1B).

Monthly activity patterns of the respiratory pathogen positive rate

We analysed the monthly distribution of respiratory pathogens by gender and during and after the COVID-19 outbreak in the study period, as shown in Figure 2. In the four time periods, there was no significant difference in the positive rates of males and females. In the first year of the pandemic, the positive rate of males was highest in December (75.31%) and lowest in July (4.44%), and the positive rate of females was highest in January (78.43%) and lowest in June (1.79%) (Figure 2A). In the second year, the positive rate of males was highest in October (30.16%) and lowest in March (4.00%), and the positive rate of females was highest in October (28.00%) and lowest in February (0.00%). The highest positivity rates for males and females were much lower than those in the first year (Figure 2B). In the third year, the positive rate of males was highest in January (25.00%) and lowest in July (10.00%), and the positive rate of females was highest in December (40.98%) and lowest in July (6.67%) (Figure 2C). In the fourth year, the positive rates were higher in spring and winter than in summer and autumn. The positive rate of males was highest in December (58.54%) and lowest in January (0.93%). The positive rate of females was highest in October (60.53%) and lowest in January (0.00%). The total

TABLE 1 Characteristics of respiratory pathogen detection in hospitalized patients of different gender and age groups.

	Gender			Age n (%)							
	Male n (%) n=4801	Female n (%) n=4178	*P*	0-4y n (%) n=756 (M:F=1.2)	5-18y n (%) n=1183 (M:F=)1.2	19-49y n (%) n=1250 (M:F=1.1)	50-64y n (%) n=1760 (M:F=1.0)	65-74y n (%) n=1836 (M:F=1.3)	75-84y n (%) n=1320 (M:F=1.2)	≥85y n (%) n=874 (M:F=1.2)	*P*
InfA	591 (12.3)	545 (13.0)	0.360	143 (18.9)	205 (17.3)	165 (13.2)	207 (11.8)	221 (12.0)	122 (9.2)	73 (8.3)	<0.001
InfAH1N1	84 (1.7)	42 (1.0)	0.004	2 (0.3)	17 (1.4)	19 (1.5)	38 (2.2)	27 (1.5)	15 (1.1)	8 (0.9)	0.802
H3	381 (7.9)	387 (9.3)	0.042	94 (12.4)	144 (12.2)	111 (8.9)	127 (7.2)	149 (8.1)	90 (6.8)	53 (6.1)	<0.001
InfB	62 (1.3)	74 (1.8)	0.069	10 (1.3)	24 (2.0)	56 (4.5)	18 (1.0)	14 (0.8)	5 (0.4)	9 (1.0)	<0.001
HADV	121 (2.5)	98 (2.4)	0.632	43 (5.7)	81 (6.8)	20 (1.6)	22 (1.2)	27 (1.5)	18 (1.4)	8 (0.9)	<0.001
Boca	28 (0.6)	20 (0.5)	0.563	31 (4.1)	2 (0.2)	3 (0.2)	3 (0.2)	5 (0.3)	3 (0.2)	1 (0.1)	<0.001
HRV	290 (6.0)	228 (5.5)	0.277	102 (13.5)	131 (11.1)	63 (5.0)	75 (4.3)	57 (3.1)	53 (4.0)	37 (4.2)	<0.001
HPIV	83 (1.7)	82 (2.0)	0.423	70 (9.3)	32 (2.7)	4 (0.3)	18 (1.0)	20 (1.1)	10 (0.8)	11 (1.3)	<0.001
HCOV	57 (1.2)	51 (1.2)	0.923	14 (1.8)	16 (1.4)	12 (1.0)	11 (0.6)	19 (1.0)	23 (1.7)	13 (1.5)	0.853
HRSV	125 (2.6)	118 (2.8)	0.558	144 (19.0)	40 (3.4)	5 (0.4)	9 (0.5)	15 (0.8)	17 (1.3)	13 (1.5)	<0.001
HMPV	120 (2.5)	132 (3.2)	0.073	84 (11.1)	72 (3.6)	16 (1.3)	31 (1.8)	26 (1.4)	15 (1.1)	8 (0.9)	<0.001
MP	221 (4.6)	220 (5.3)	0.171	33 (4.4)	316 (26.7)	52 (4.2)	24 (1.4)	14 (0.8)	2 (0.1)	0 (0.0)	<0.001
Ch	5 (0.1)	4 (0.1)	1.000	2 (0.3)	1 (0.1)	3 (0.2)	0 (0.0)	3 (0.2)	0 (0.0)	0 (0.0)	0.080
Total	2168 (45.2)	2001 (47.9)	0.119	772 (102.1)	1081 (91.4)	529 (42.3)	583 (33.1)	597 (32.5)	373 (28.3)	234 (26.8)	<0.001

10.3389/fcimb.2024.1486953

A

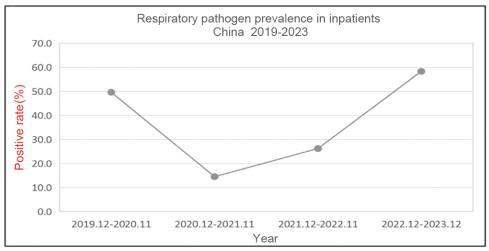

	2019.12-2020.11 n(%) n=1980	2020.12-2021.11 n(%) n=1266	2021.12-2022.11 n(%) n=1108	2022.12-2023.12 n(%) n=4652	*P*
InfA	350(17.7)	5(0.4)	24(2.2)	757(16.3)	0.006
InfAH1N1	6(0.3)	0(0.0)	0(0.0)	120(2.6)	<0.001
H3	171(8.6)	0(0.0)	23(2.1)	574(12.3)	<0.001
InfB	18(0.9)	4(0.3)	87(7.9)	27(0.6)	0.765
HADV	63(3.2)	14(1.1)	31(2.8)	111(2.4)	0.418
Boca	11(0.6)	4(0.3)	3(0.3)	30(0.6)	0.412
HRV	152(7.7)	84(6.6)	45(4.1)	237(5.1)	<0.001
HPIV	9(0.5)	15(1.2)	18(1.6)	123(2.6)	<0.001
HCOV	25(1.3)	16(1.3)	6(0.5)	61(1.3)	0.884
HRSV	80(4.0)	17(1.3)	12(1.1)	134(2.9)	0.161
HMPV	40(2.0)	14(1.1)	13(1.2)	185(4.0)	<0.001
MP	54(2.7)	9(0.7)	25(2.3)	353(7.6)	<0.001
Ch	3(0.2)	1(0.1)	3(0.3)	2(0.0)	0.234
Total	982 (49.6)	183(14.5)	290(26.2)	2714(58.3)	<0.001

B

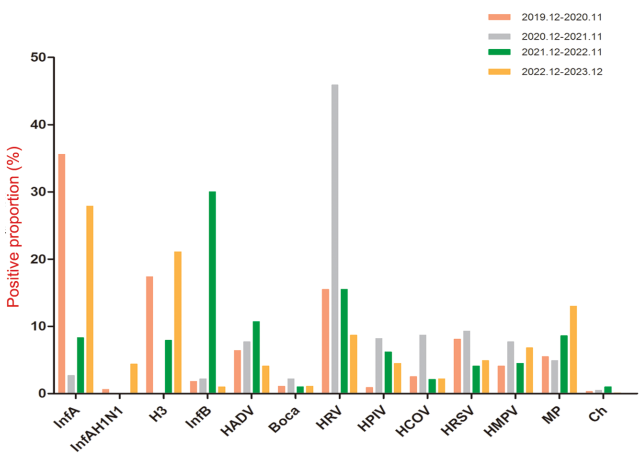

FIGURE 1
Respiratory pathogen detection among hospitalized patients in 2019.12-2023.12. **(A)** Respiratory pathogen detection rate from December 2019 to December 2023. **(B)** Differences of positive rates of each respiratory pathogen in four time periods from December 2019 to December 2023. Positive rate refers to the frequency of positive detections in the current year. Positive proportion refers to the positive detection of a pathogen in the positive detection of all 13 pathogens.

positive rate of males was significantly higher than that of females ($P < 0.001$) (Figure 2D).

We then statistically analysed the changes in pathogen positive rates (only one count of overlapping infections) and positive detection rates (including overlapping infections) during and after the COVID-19 pandemic. From December 2019 to November 2022, the positive rate of pathogens showed a downwards trend without seasonal dependence, and from December 2022 to December 2023, the positive rate of pathogens showed an upwards trend and the positive rates in spring and winter were higher than those in summer and autumn (Figure 2E). The positive detection rate of pathogens showed the same trend (Figure 2F). These results suggest that an increase in pathogen positive rates is accompanied by an increase in overlapping infections.

Monthly distribution of 13 respiratory pathogens

The monthly distribution of each respiratory pathogen during and after the COVID-19 pandemic is shown in Figure 3. During the COVID-19 pandemic, the peak of InfA and H3 virus infection occurred in winter (January and December) and the lowest activity was in spring and summer (from March to July). There was no clear

10.3389/fcimb.2024.1486953

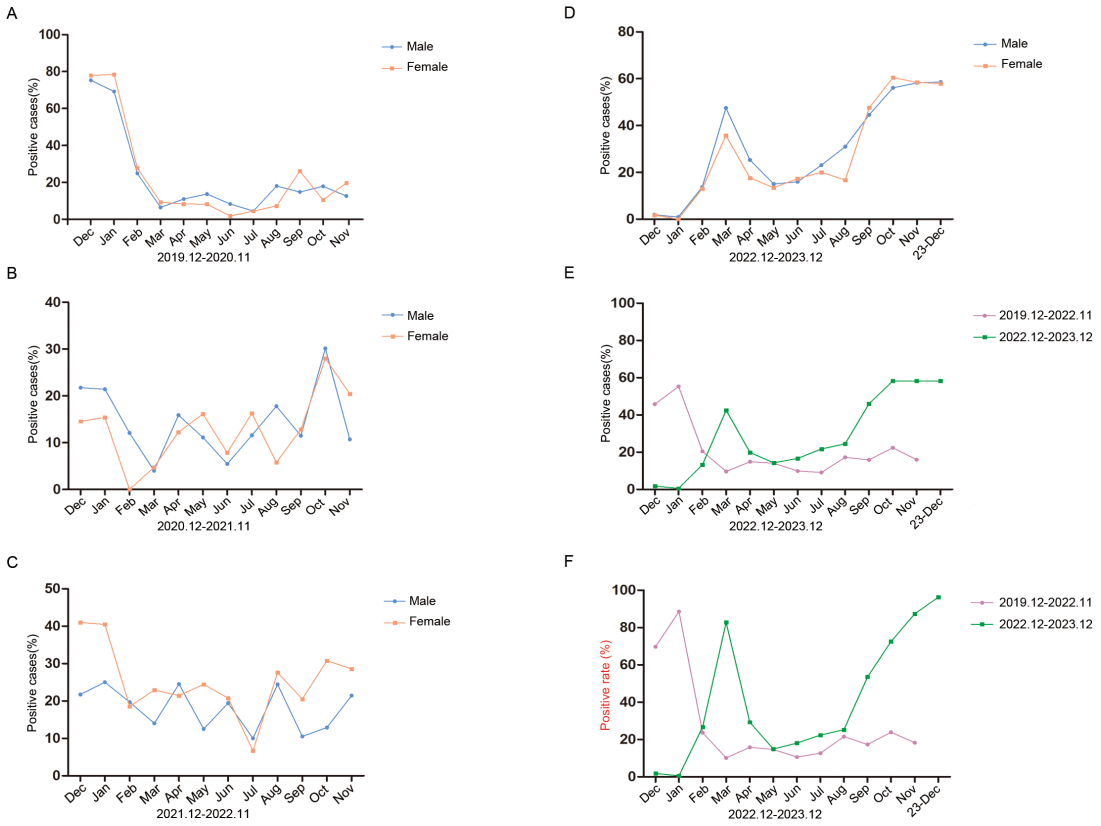

FIGURE 2
Monthly activity patterns of respiratory pathogens positive rate. **(A)** Monthly activity patterns of respiratory pathogens positive rate from December 2019 to November 2020. **(B)** Monthly activity patterns of respiratory pathogens positive rate from December 2020 to November 2021. **(C)** Monthly activity patterns of respiratory pathogens positive rate from December 2021 to November 2022. **(D)** Monthly activity patterns of respiratory pathogens positive rate from December 2022 to December 2023. Different monthly activity patterns of respiratory pathogens positivity rates **(E)** and positive detection rates **(F)** during the two time periods of December 2019 to November 2022 and December 2022 to December 2023. Positive cases (%) refers to the number of positive patients in the total number of patients tested. Positive rate refers to the frequency of postive detections.

seasonal distribution for HRV, and infections were high throughout the year (Figure 3A). However, as shown in Figure 3C, it can be seen that the higher number of infections in December was mainly contributed by December 2019. After the COVID-19 pandemic, InfA and H3 virus infections peaked in spring (March) and winter (October), with the lowest activity in summer and autumn (from May to September). MP dramatically increased in winter (from October to November). HRV infection increased significantly in autumn and winter (from September to November). HRSV had a small increase in April and May. The number of positive samples for the other pathogens was smaller but significantly higher than that during the COVID-19 pandemic, and the peak of infection was also in autumn and winter (Figure 3B). However, as shown in Figure 3D, it can be seen that because of the seasonal advantage of winter, the number of pathogenic infections in December 2023 was still increasing dramatically. Since the first positive case of COVID-19 was found in Shijiazhuang (also Hebei Province) in January 2020, and nucleic acid inspection was lifted from January 2023, and according to the actual monthly change distribution of respiratory viruses, we strictly referred to the 2020.01-2022.12 as 3 y of pandemic, and the 2023.01-2023.12 as 1 y after the pandemic.

During the COVID-19 pandemic, the total number of positive pathogens was 1217 and the dominant pathogens were InfA and HRV, accounting for 24.08% and 21.77% of the total number of positive pathogens, respectively, followed by H3, accounting for 10.35% (Figure 3E). After COVID-19 pandemic, the total number of positive pathogens was 2711 and the dominant pathogens were InfA and H3, accounting for 27.92% and 21.17% of the total number of positive pathogens, respectively, followed by MP, accounting for 13.02% (Figure 3F). Both during and after the COVID-19 pandemic, InfA/H3 had the highest proportion of co-infection among all tested samples, respectively, accounting for 35.13% (124/353) and 58.81% (574/976), which was not shown in the figure because it was much higher than the other co-infections (Figure 3G).

Comparison of pathogenic epidemiological characteristics during and after the COVID-19 pandemic

During the COVID-19 pandemic, male and female positive samples accounted for 49.83% and 50.17%, respectively, and the

10.3389/fcimb.2024.1486953

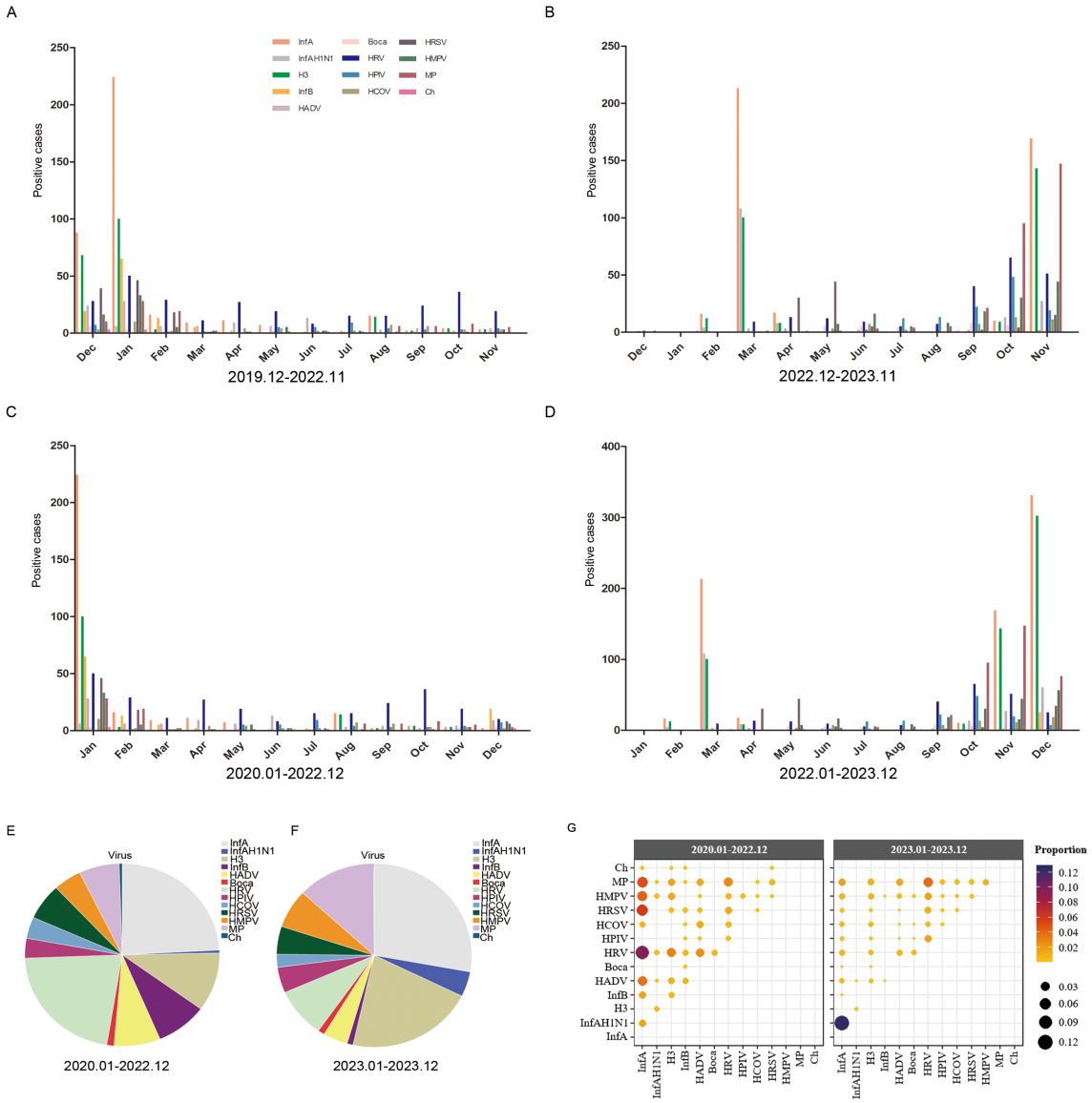

FIGURE 3
The monthly distribution of different respiratory pathogens. **(A)** The monthly distribution of different respiratory pathogens from December 2019 to November 2022. **(B)** The monthly distribution of different respiratory pathogens from December 2022 to November 2023. **(C)** The monthly distribution of different respiratory pathogens from January 2022 to December 2022. **(D)** The monthly distribution of different respiratory pathogens from January 2023 to December 2023. **(E)** The proportions of different pathogens from January 2022 to December 2022. **(F)** The porportions of different pathogens from January 2023 to December 2023. **(G)** The proportion of each co-infection pair among all co-infected samples shown by color and size from January 2022 to December 2022 and January 2023 to December 2023. Positive cases refers to the number of positive patients.

difference was not statistically significant ($P = 0.861$) (Figure 4A). After the COVID-19 outbreak, the proportion of males in positive samples was significantly higher than that of females (53.78% vs. 46.22%, $P = 0.001$) (Figure 4B). During the COVID-19 pandemic, HRV and InfA were the main pathogens in males. InfA and HRV were the main pathogens in females (Figure 4C). After the COVID-19 pandemic, the main pathogens in males and females were InfA, H3 and MP. The proportions of InfA, H3 and MP in males were higher than those in females (Figure 4D). The number of positive samples in all age groups was higher after the COVID-19 outbreak than during the pandemic (Figure 4E). During the COVID-19 pandemic, InfA and HRV frequently occurred in all age groups. HRSV infection also frequently occurred in the age group of 0–4 y, and InfB and MP infections frequently occurred in the age group of 19–49 y and were much higher than those in the other age groups (Figure 4F). After the COVID-19 pandemic, InfA and H3 frequently occurred in all age groups. HRSV infection also frequently occurred in the age group of 0–4 y, and MP infection frequently occurred in the age group of 5–18 y and was much higher than that in the other age groups (Figure 4G). ARIMA time series prediction modelling was performed on the overall respiratory

10.3389/fcimb.2024.1486953

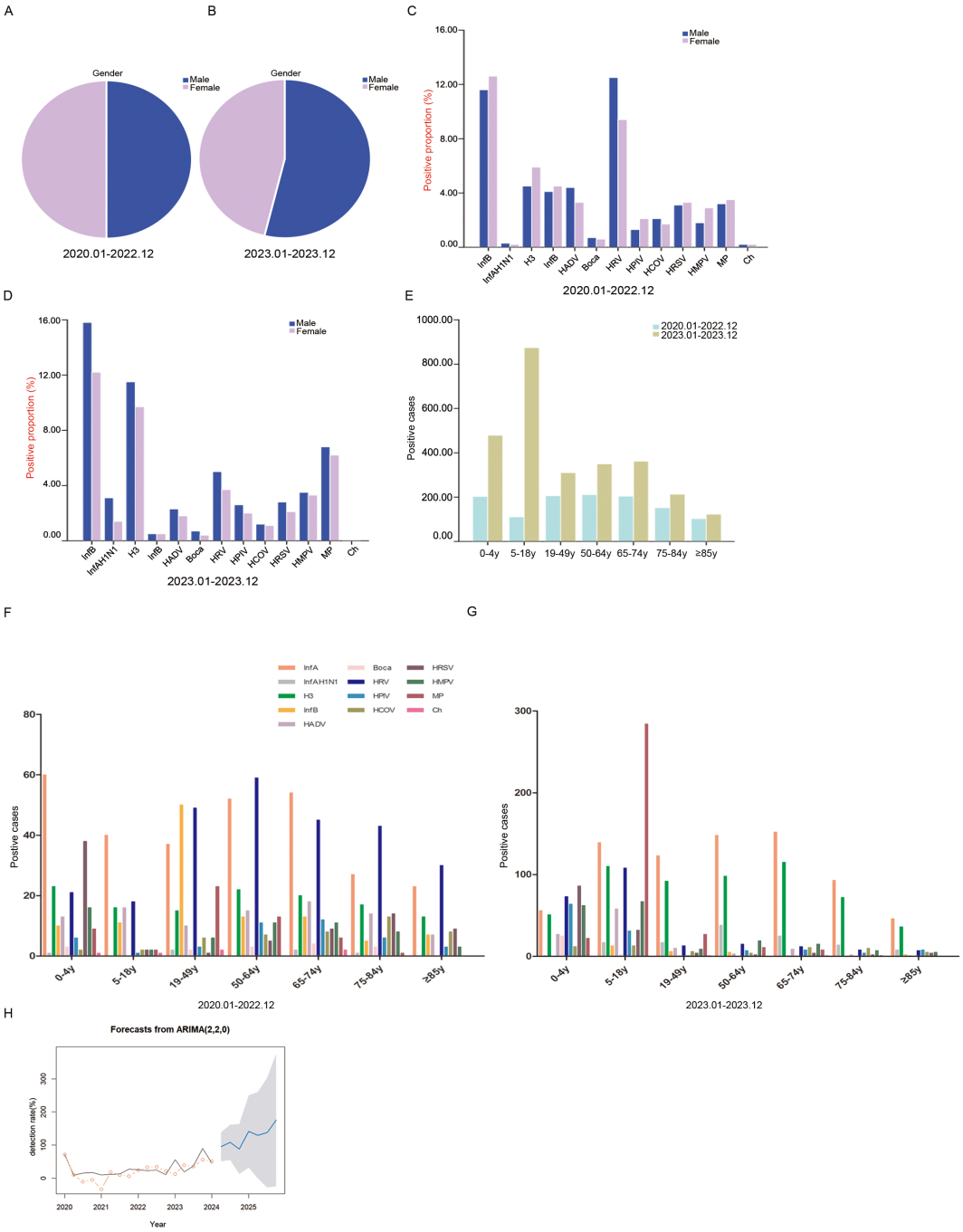

FIGURE 4
The demographic characteristics of respiratory pathogens during and after the COVID-19. **(A)** The proportions of different sexes among positive samples during the COVID-19. **(B)** The proportions of different sexes among positive samples after the COVID-19. **(C)** The proportions of different pathogens in sex-specific positive samples during the COVID-19. **(D)** The proportions of different pathogens in sex-specific positive samples after the COVID-19. **(E)** The proportions of different ages of positive samples. **(F)** The distribution of pathogens in positive samples among different ages during the COVID-19. **(G)** The distribution of pathogens in positive samples among different ages after the COVID-19. **(H)** The AMIRA time series model predicted the respiratory pathogen detection rates from April 2024 to December 2025. The black line is the actual value, the red circle is the fitting value, the blue is the predicted value, and the gray area is the 95% confidence interval. Positive proportion refers to the positive detection of a pathogen in the positive detection of all 13 pathogens. Positive cases refers to the number of positive patients.

pathogenic infections, and the total predicted pathogen detection rates for seven quarters from April 2024 to December 2025 in Shijiazhuang City were obtained. The optimal model of acute upper respiratory tract infection in Shijiazhuang was ARIMA (2,2,0), and MAPE was 75.92 (Figure 4H).

Discussion

Respiratory pathogens are common in the general population, placing a heavy economic burden on the public health system. As a double-edged sword, the national action plan during the COVID-19

period while controlling the spread of the pandemic can easily lead to the continuous recurrence of respiratory pathogens due to the lack of long-term immunity, and it is urgent to adjust the immunisation strategy in time. This study focused on the epidemiological characteristics of respiratory pathogens causing ARTIs in North China during and after the COVID-19 pandemic period from December 2019 to December 2023 and compared the changes in the pathogen epidemic spectra before and after the COVID-19 pandemic to help actively cope with the 'immunity debt' after the COVID-19 pandemic.

Most pre-COVID-19 studies showed that men were more susceptible than women, possibly because of more social and hormonal influences (Richter et al., 2016; Wang et al., 2016; Albogami et al., 2018). We found that the positive detection rate of InfAH1N1 and total infection rate in males were significantly higher than those in females and the positive detection rate of the H3 virus in females was significantly higher than that in males, which was also different from the results reported during the COVID-19 period that boys may be more susceptible to respiratory pathogenic infection than girls (Yassine et al., 2020), which may be related to the impact of the NPIs on the trajectory of human flow. We found that the total pathogen detection rates were highest in the age group of 0–4 y, which was consistent with the facts that despite general population susceptibility, children are the main source of respiratory infections and that younger children are more susceptible to viral infections than older children (Williams et al., 2002; Wan et al., 2023). The detection rates of most pathogens were different between age groups, so the infection appeared to be closely related to age. We found that compared with the downwards trend during the COVID-19 pandemic, the total pathogen detection rate rebounded after the COVID-19 outbreak, similar to what was reported in a study in Guangzhou, China (Zeng et al., 2021). Our results are consistent with recent literature reporting that HRVs are very prevalent viruses during the COVID-19 pandemic and the rebound of influenza viruses after COVID-19 pandemic (Lai et al., 2022; Regina et al., 2024). ARTIs are the leading cause of medical visits in winter and spring for all age groups before COVID-19 (Li et al., 2019). Our results showed that there was no significant seasonal distribution of positive rates of patients regardless of gender during the COVID-19 pandemic, with a dramatic decrease beginning in January 2020. However, after the COVID-19 pandemic, the infection rate of men were slightly higher than that of women, and the infection rate of spring and winter were significantly higher than that of summer. The first peak of respiratory infections after the COVID-19 outbreak was in March. These results were consistent with many studies showing large reductions in outpatient and inpatient visits in many countries in 2020 (the COVID-19 began) (Friedrich et al., 2021; Pines et al., 2021). This suggests that respiratory pathogens begin to resume their original transmission characteristics after the NPIs were withdrawn.

It has been reported that the NPIs during the COVID-19 pandemic typically slow down and alleviate the spread of respiratory pathogens in populations (Kaleta et al., 2022). A series of comprehensive new public health preventive measures in response to the COVID-19 pandemic have resulted in significant reductions in the prevalence of non-SARS-CoV-2 infections (Olsen et al., 2021; Ren et al., 2023). Rare studies of pathogenic infection characteristics after the COVID-19 pandemic have been reported. Our study showed that the dominant pathogens during the COVID-19 pandemic were InfA (24.08%) and HRV (21.77%) and the dominant pathogens after COVID-19 were InfA (27.92%) and H3 (21.17%), followed by MP (13.02%). InfA/H3 had the highest proportion of co-infections among all tested samples during (35.13%) and after (58.81%) the COVID-19 pandemic. These results demonstrated that NPIs can indeed be very effective against influenza (Wan et al., 2023; Gao et al., 2024), influenza virus infection resumed after the withdrawal of the NPIs and the transmission of MP in the population is significantly enhanced. During the COVID-19 pandemic, there was no significant difference in the proportion of positive samples between males and females and the infection rate of men were slightly higher than that of women after the COVID-19, indicating that NPIs changed the distribution of sexual respiratory pathogens and the distribution of sexual respiratory pathogens recovered after the withdrawal of the NPIs. Our results showed that during the COVID-19 pandemic, InfA and HRV frequently occurred in all age groups. HRSV infection also frequently occurred in the age group of 0–4 y, and InfB and MP infections frequently occurred in the age group of 19–49 y and were much higher than those in the other age groups. After the COVID-19 pandemic, InfA and H3 frequently occurred in all age groups. HRSV infection also frequently occurred in the age group of 0–4 y, and MP infection frequently occurred in the age group of 5–18 y and was much higher than that in the other groups. Previous epidemiological survey data show that HRSV is the most common respiratory virus in children in Vietnam (Lu et al., 2020), and another study in Beijing found that influenza A is the most important virus, followed by HRSV (Li et al., 2020). However, our data showed that during the COVID-19 period, InfA was the most common virus in children in Shijiazhuang, followed by HRSV. After the COVID-19 pandemic, HRSV was the most important respiratory virus in children. In any case, HRSV was the primary pathogen in children aged 0–4 y during or after the COVID-19 pandemic, which is consistent with reports from China and other countries (Duan et al., 2021; Li et al., 2021; Wan et al., 2023). These results suggest that SARS-CoV-2 infection did not change the primary population of HRSV infection and that pathogenic infection varies by geographical characteristics or living environment as children's playgrounds change from home or community to school after the outbreak. Another study in Sichuan, China, confirmed that SARS-CoV-2 had no effect on the positive rate of seven respiratory viruses, including HRSV, in children (Duan et al., 2021). Our results also revealed that young and middle-aged people should be alert to the prevalence of MP.

This study compared the prevalence of 13 pathogens during and after the COVID-19 pandemic and found that the removal of the

NPIs after the pandemic resulted in the rebound of respiratory pathogens, which may cause 'immunity debt'. At the same time, the time series model established using the data from December 2091 to January 2024 suggests that the positive detection rate of pathogens is still at a relatively high level in the short term, suggesting that clinical workers should strengthen the monitoring and management of non-SARS-CoV-2 infections. There are still some shortcomings, although our study applied the gold standard method of real-time PCR. First, there might be some viruses that were not taken into account. Second, our study was limited to the Shijiazhuang region and may not be applicable to other regions. Third, fewer outpatient visits during the COVID-19 pandemic might have resulted in lower test samples. Fourth, some factors that influence positive rates, including the influenza vaccine coverage, were not taken into account.

Conclusion

This report is the first to identify the prevalence of respiratory pathogens in hospitalised patients of all ages during and after the COVID-19 pandemic in Shijiazhuang, which is generally consistent with other reports before, during and after the COVID-19 pandemic, demonstrating that non-drug interventions have a significant negative impact on the transmission of other respiratory pathogens. In the past 3 y of the COVID-19 outbreak, surveillance efforts mainly focused on SARS-CoV-2. Future studies need to combine SARS-CoV-2 with ARTIs to achieve comprehensive, active and sustained epidemiological surveillance and alert to 'immunity debt'.

Data availability statement

The raw data supporting the conclusions of this article will be made available by the authors, without undue reservation.

Ethics statement

The studies involving humans were approved by Shijiazhuang Second Hospital medical Ethics Committee. The studies were conducted in accordance with the local legislation and institutional requirements. The participants provided their written informed consent to participate in this study.

Author contributions

PZ: Conceptualization, Investigation, Methodology, Project administration, Writing – original draft, Writing – review & editing. YZ: Data curation, Investigation, Project administration, Resources, Software, Writing – review & editing. ZW: Formal Analysis, Methodology, Validation, Writing – original draft. MW: Data curation, Formal Analysis, Project administration, Supervision, Writing – review & editing. RL: Methodology, Software, Validation, Writing – original draft. JZ: Resources, Writing – original draft. NL: Software, Visualization, Writing – original draft. ZZ: Data curation, Project administration, Writing – review & editing. RR: Investigation, Visualization, Writing – original draft. YS: Formal Analysis, Methodology, Resources, Writing – original draft. ZL: Formal Analysis, Funding acquisition, Project administration, Resources, Writing – original draft, Writing – review & editing, Conceptualization, Investigation.

Funding

The author(s) declare that financial support was received for the research, authorship, and/or publication of this article. This work was supported by the Funding for Construction of Hebei Provincial Key Laboratory of Basic Medicine for Diabetes (Grants No.226790187H), the Funding for Post-performance subsidy of Shijiazhuang Technology Innovation Center of Precision Medicine for Diabetes (Grants No.227790657A), and the Medical Science Research Project of Hebei Provincial Health Commission (Grant No.20221655; 20240133).

Conflict of interest

The authors declare that the research was conducted in the absence of any commercial or financial relationships that could be construed as a potential conflict of interest.

Publisher's note

Supplementary material

The Supplementary Material for this article can be found online at: https://www.frontiersin.org/articles/10.3389/fcimb.2024.1486953/full#supplementary-material

References

Al, K. H., Meredith, L. W., Al-Jardani, A., Sajina, F., Al, S. I., Al, H. R., et al. (2023). Time trend of respiratory viruses before and during the COVID-19 pandemic in severe acute respiratory virus infection in the Sultanate of Oman between 2017 and 2022. *Influenza Other Respir. Viruses* 17, e13233. doi: 10.1111/irv.13233

Albogami, S. S., Alotaibi, M. R., Alsahli, S. A., Masuadi, E., and Alshaalan, M. (2018). Seasonal variations of respiratory viruses detected from children with respiratory tract infections in Riyadh, Saudi Arabia. *J. Infect. Public Health* 11, 183–186. doi: 10.1016/j.jiph.2017.06.001

Benezit, F., Loubet, P., Galtier, F., Pronier, C., Lenzi, N., Lesieur, Z., et al. (2020). Non-influenza respiratory viruses in adult patients admitted with influenza-like illness: a 3-year prospective multicenter study. *Infection* 48, 489–495. doi: 10.1007/s15010-019-01388-1

Bibby, H. L., de Koning, L., Seiden-Long, I., Zelyas, N., and Church, D. L. (2022). A pragmatic randomized controlled trial of rapid on-site influenza and respiratory syncytial virus PCR testing in paediatric and adult populations. *BMC Infect. Dis.* 22, 854. doi: 10.1186/s12879-022-07796-3

Duan, Y., He, J., Cui, Y., Li, W., and Jiang, Y. (2021). Characteristics and forecasting of respiratory viral epidemics among children in west China. *Med. (Baltimore)* 100, e25498. doi: 10.1097/MD.0000000000025498

Friedrich, F., Ongaratto, R., Scotta, M. C., Veras, T. N., Stein, R. T., Lumertz, M. S., et al. (2021). Early impact of social distancing in response to coronavirus disease 2019 on hospitalizations for acute bronchiolitis in infants in Brazil. *Clin. Infect. Dis.* 72, 2071–2075. doi: 10.1093/cid/ciaa1458

Gao, Z., Wang, Y., Yan, L., Liu, T., and Peng, L. (2024). Epidemiological characteristics of respiratory viruses in children during the COVID-19 epidemic in Chengdu, China. *Microbiol. Spectr.* 12, e261423. doi: 10.1128/spectrum.02614-23

Giamberardin, H. I., Homsani, S., Bricks, L. F., Pacheco, A. P., Guedes, M., Debur, M. C., et al. (2016). Clinical and epidemiological features of respiratory virus infections in preschool children over two consecutive influenza seasons in southern Brazil. *J. Med. Virol.* 88, 1325–1333. doi: 10.1002/jmv.24477

Huang, H. S., Tsai, C. L., Chang, J., Hsu, T. C., Lin, S., and Lee, C. C. (2018). Multiplex PCR system for the rapid diagnosis of respiratory virus infection: systematic review and meta-analysis. *Clin. Microbiol. Infect.* 24, 1055–1063. doi: 10.1016/j.cmi.2017.11.018

Kaleta, M., Kesik-Brodacka, M., Nowak, K., Olszewski, R., Sliwinski, T., and Zoltowska, I. (2022). Long-term spatial and population-structured planning of non-pharmaceutical interventions to epidemic outbreaks. *Comput. Oper Res.* 146, 105919. doi: 10.1016/j.cor.2022.105919

Lai, S. Y., Liu, Y. L., Jiang, Y. M., and Liu, T. (2022). Precautions against COVID-19 reduce respiratory virus infections among children in Southwest China. *Med. (Baltimore)* 101, e30604. doi: 10.1097/MD.0000000000030604

Li, Y., Johnson, E. K., Shi, T., Campbell, H., Chaves, S. S., Commaille-Chapus, C., et al. (2021). National burden estimates of hospitalisations for acute lower respiratory infections due to respiratory syncytial virus in young children in 2019 among 58 countries: a modelling study. *Lancet Respir. Med.* 9, 175–185. doi: 10.1016/S2213-2600(20)30322-2

Li, Y., Reeves, R. M., Wang, X., Bassat, Q., Brooks, W. A., Cohen, C., et al. (2019). Global patterns in monthly activity of influenza virus, respiratory syncytial virus, parainfluenza virus, and metapneumovirus: a systematic analysis. *Lancet Glob Health* 7, e1031–e1045. doi: 10.1016/S2214-109X(19)30264-5

Li, Y., Wang, J., Wang, C., Yang, Q., Xu, Y., Xu, J., et al. (2020). Characteristics of respiratory virus infection during the outbreak of 2019 novel coronavirus in Beijing. *Int. J. Infect. Dis.* 96, 266–269. doi: 10.1016/j.ijid.2020.05.008

Lu, L., Robertson, G., Ashworth, J., Pham, H. A., Shi, T., Ivens, A., et al. (2020). Epidemiology and phylogenetic analysis of viral respiratory infections in Vietnam. *Front. Microbiol.* 11, 833. doi: 10.3389/fmicb.2020.00833

Nguyen, V. H., Ashraf, M., and Mould-Quevedo, J. F. (2023). Estimating the impact of influenza vaccination of low-risk 50-64-year-olds on acute and ICU hospital bed usage in an influenza season under endemic COVID-19 in the UK. *Hum. Vaccin Immunother.* 19, 2187592. doi: 10.1080/21645515.2023.2187592

Ojuawo, O. B., Desalu, O. O., Fawibe, A. E., Ojuawo, A. B., Aladesanmi, A. O., Opeyemi, C. M, et al. (2020). Clinical and microbiological profile of adult inpatients with community acquired pneumonia in Ilorin, North Central, Nigeria. *Afr Health Sci.* 20, 1655–1668. doi: 10.4314/ahs.v20i4.18

Olsen, S. J., Winn, A. K., Budd, A. P., Prill, M. M., Steel, J., Midgley, C. M., et al. (2021). Changes in influenza and other respiratory virus activity during the COVID-19 pandemic-United States, 2020-2021. *Am. J. Transplant.* 21, 3481–3486. doi: 10.1111/ajt.16049

Pines, J. M., Zocchi, M. S., Black, B. S., Carlson, J. N., Celedon, P., Moghtaderi, A., et al. (2021). Characterizing pediatric emergency department visits during the COVID-19 pandemic. *Am. J. Emerg. Med.* 41, 201–204. doi: 10.1016/j.ajem.2020.11.037

Regina, M. I. C., Santos, M. O., de Oliveira, C. M., de Araujo, K. M., de Souza, G., Rezio, G. S., et al. (2024). Rhinovirus infection and co-infection in children with severe acute respiratory infection during the COVID-19 pandemic period. *Virulence* 15, 2310873. doi: 10.1080/21505594.2024.2310873

Ren, L., Lin, L., Zhang, H., Wang, Q., Cheng, Y., Liu, Q., et al. (2023). Epidemiological and clinical characteristics of respiratory syncytial virus and influenza infections in hospitalized children before and during the COVID-19 pandemic in Central China. *Influenza Other Respir. Viruses* 17, e13103. doi: 10.1111/irv.13103

Richter, J., Panayiotou, C., Tryfonos, C., Koptides, D., Koliou, M., Kalogirou, N., et al. (2016). Aetiology of acute respiratory tract infections in hospitalised children in Cyprus. *PLoS One* 11, e147041. doi: 10.1371/journal.pone.0147041

Rongfeng, Z., Kai, S., Fang, X., Hongzhou, L., et al. (2024). Changes in China's Prevention and control policies of the Novel Coronavirus Pneumonia Epidemic. *Fudan J. (Medical Edition)* 51, 109–114. Available online at: https://link.cnki.net/urlid/31.1885.r.20240108.1025.012

Tan, M. P., Leong, C. L., Pang, Y. K., Razali, R. M., Ismail, A. I., Sam, I. C., et al. (2022). Dearth of influenza among older adults admitted with respiratory symptoms in Malaysia during the coronavirus disease 2019 pandemic in 2021. *Front. Med. (Lausanne)* 9, 977614. doi: 10.3389/fmed.2022.977614

Wan, L., Li, L., Zhang, H., Liu, C., Li, R., Wu, X., et al. (2023). The changing pattern of common respiratory viruses among children from 2018 to 2021 in Wuhan, China. *Arch. Virol.* 168, 291. doi: 10.1007/s00705-023-05891-7

Wang, H., Gu, J., Li, X., van der Gaast-de, J. C., Wang, W., He, X., et al. (2021). Broad range detection of viral and bacterial pathogens in bronchoalveolar lavage fluid of children to identify the cause of lower respiratory tract infections. *BMC Infect. Dis.* 21, 152. doi: 10.1186/s12879-021-05834-0

Wang, H., Zheng, Y., Deng, J., Wang, W., Liu, P., Yang, F., et al. (2016). Prevalence of respiratory viruses among children hospitalized from respiratory infections in Shenzhen, China. *Virol. J.* 13, 39. doi: 10.1186/s12985-016-0493-7

Williams, B. G., Gouws, E., Boschi-Pinto, C., Bryce, J., and Dye, C. (2002). Estimates of world-wide distribution of child deaths from acute respiratory infections. *Lancet Infect. Dis.* 2, 25–32. doi: 10.1016/S1473-3099(01)00170-0

Woodhead, M., Blasi, F., Ewig, S., Garau, J., Huchon, G., Ieven, M., et al. (2011). Guidelines for the management of adult lower respiratory tract infections–full version. *Clin. Microbiol. Infect.* 17 Suppl 6, E1–E59. doi: 10.1111/j.1469-0691.2011.03672.x

World Health Organization (2019).International statistical classification of diseases and related health problems 10th revision. Available online at: https://icd.who.int/browse10/2019/en/.

Wu, R., Zhang, J., and Mo, L. (2023). Analysis of respiratory virus detection in hospitalised children with acute respiratory infection during the COVID-19 pandemic. *Virol. J.* 20, 253. doi: 10.1186/s12985-023-02218-5

Yassine, H. M., Sohail, M. U., Younes, N., and Nasrallah, G. K. (2020). Systematic review of the respiratory syncytial virus (RSV) prevalence, genotype distribution, and seasonality in children from the middle east and north Africa (MENA) region. *Microorganisms* 8 (5), 713. doi: 10.3390/microorganisms8050713

Zeng, Z., Guan, W., Liu, Y., Lin, Z., Liang, W., Liang, J., et al. (2021). Different circulation pattern of multiple respiratory viruses in southern China during the COVID-19 pandemic. *Front. Microbiol.* 12, 801946. doi: 10.3389/fmicb.2021.801946

frontiers | Frontiers in Cellular and Infection Microbiology

TYPE Original Research
PUBLISHED 28 November 2024
DOI 10.3389/fcimb.2024.1461325

OPEN ACCESS

EDITED BY
Ariadna Petronela Fildan,
Ovidius University, Romania

REVIEWED BY
Nazan Tuna,
Namik Kemal University, Türkiye
Verena Zerbato,
Azienda Sanitaria Università Integrata di Trieste, Italy

*CORRESPONDENCE
Keli Qian
qiankeli86@163.com

RECEIVED 08 July 2024
ACCEPTED 04 November 2024
PUBLISHED 28 November 2024

CITATION
Wang Z, Li R, Yuan Z, Zhang Z and Qian K (2024) The prognostic value of neutrophil-to-lymphocyte ratio in adult carbapenem-resistant *Klebsiella pneumoniae* infection: a retrospective cohort study. *Front. Cell. Infect. Microbiol.* 14:1461325. doi: 10.3389/fcimb.2024.1461325

The prognostic value of neutrophil-to-lymphocyte ratio in adult carbapenem-resistant *Klebsiella pneumoniae* infection: a retrospective cohort study

Zhongjie Wang[1], Renhua Li[1], Zhe Yuan[1], Zuli Zhang[2] and Keli Qian[1]*

[1]Department of Infection Control, The First Affiliated Hospital of Chongqing Medical University, Chongqing, China, [2]Department of Respiratory and Critical Care Medicine, The First Affiliated Hospital of Chongqing Medical University, Chongqing, China

Background: Systemic inflammatory indicators such as neutrophil-to-lymphocyte ratio (NLR) can effectively predict the prognosis of various inflammatory diseases. However, its prognostic effect on patients with carbapenem-resistant *Klebsiella pneumoniae* (CRKP) infection is little known. The objective of this study was to investigate the risk factors for mortality associated with CRKP infection and the clinical value of NLR in predicting prognosis in these patients.

Methods: A total of 190 inpatients with CRKP infection from 1 January 2023 to 31 December 2023 were enrolled in this study, namely, 73 fatal cases and 117 survival cases in hospital. The medical data and examination results of these patients were collected. A logistic regression analysis was performed to assess the association between the NLR on the day of CRKP infection onset and all-cause mortality in hospital.

Results: The overall mortality rate of patients with CRKP infection was 38.42% (73/190). Of the 190 patients, 91 were co-infected with carbapenem-resistant *Acinetobacter baumannii*/carbapenem-resistant *Pseudomonas aeruginosa* (CRAB/CRPA). Multifactor regression analysis confirmed that carbapenem exposure in the past 14 days, central line insertion, and chronic Foley catheter requirement were independent risk factors for carbapenem-resistant bacteria co-infection. The multivariate analysis shows that admission to an ICU, co-infection with CRAB/CRPA, and higher NLR were independent risk factors for the mortality in hospital, while appropriate treatment within 3 days was an independent protective factor. The area under the curve (AUC) of the NLR was 0.696, and the cutoff value of the NLR was 10.73.

Conclusions: The NLR on the day of CRKP infection onset, admission to an ICU, and co-infection with CRAB/CRPA were identified as independent risk factors for

all-cause mortality of patients with CRKP infection, while appropriate treatment within 3 days was recognized as an independent protective factor. The NLR serves as a conveniently accessible and independent prognostic biomarker for patients with CRKP infection.

KEYWORDS

carbapenem-resistant *Klebsiella pneumoniae*, risk factors, neutrophil-to-lymphocyte ratio, co-infection, prognosis

Introduction

Carbapenem-resistant Gram-negative bacilli such as carbapenem-resistant *Klebsiella pneumoniae* (CRKP), carbapenem-resistant *Pseudomonas aeruginosa* (CRPA), and carbapenem-resistant *Acinetobacter baumanii* (CRAB) are major pathogens of hospital-acquired infections, and are all contained in the bacterial pathogen priority list issued by the WHO in 2024 (World Health Organization (WHO), 2024). As one of the bacteria of the critical group, CRKP has widely spread around the world in the past 20 years and has also shown a rapid rising trend in Chinese medical institutions. According to the China Antimicrobial Surveillance Network, carbapenem resistance of *K. pneumoniae* has increased significantly from 3% to 26% between 2005 and 2023 (http://www.chinets.com/Data/GermYear).

The mortality rate of patients with CRKP infection was higher than that of patients with carbapenem-sensitive *Klebsiella pneumoniae* (CSKP) infection (Falagas et al., 2014; Budhram et al., 2020). Several studies have suggested that patients infected with CRKP have a mortality rate of up to 70% (Iredell et al., 2016; Han et al., 2022; Giacobbe et al., 2023). At present, the antimicrobial options for CRKP infection is still very limioted (Karampatakis et al., 2023). Meanwhile, in daily monitoring, we found that there were often cases in which multiple carbapenem-resistant bacteria were detected in one patient during the same hospitalization; in particular, CRKP and CRAB or CRPA were detected simultaneously. This phenomenon has also been reported in other studies. A study in the United States suggested that approximately 9% of patients had two or more different carbapenem-resistant negative bacteria co-colonized (Adediran et al., 2020). Another study found that over 30% of CRKP-positive patients were co-colonized with CRAB or CRPA (Sophonsri et al., 2023).

The treatment of carbapenem-resistant bacterial co-infections may be more complex, while the prognosis may be worse. Therefore, it is necessary to explore the risk factors for mortality associated with CRKP infection, especially co-infection of multiple carbapenem-resistant bacteria, to help clinicians to choose more appropriate empirical treatment and consequently improve the prognosis. However, studies on risk factors for mortality of patients with CRKP infection have been inconsistent; in addition, fewer studies have been conducted on co-infection with multiple carbapenem-resistant bacteria (Chen et al., 2022; Lv et al., 2022; Wu et al., 2022).

Leukocytes, neutrophils, or procalcitonins (PCTs) are usually used to reflect the level of inflammation in patients. However, these indicators can be influenced by many aspects; the accuracy of using one indicator alone to assess infection status is limited (Li et al., 2021). A growing number of research is combining these parameters to more effectively reflect inflammation levels. Neutrophil-to-lymphocyte ratio (NLR) was one of the important indicators used as an additional infection marker in clinical intensive care unit practice. Li et al. found that NLR was a risk factor for postoperative complication sepsis in patients with ureteral stones (Li et al., 2024). Zhang et al. observed that NLR first increased and then decreased during intracerebral hemorrhage, which had a high predictive value for pneumonia 30 days after surgery (Zhang et al., 2024).

Therefore, the primary objective of this study was to implore the risk factors of mortality associated with CRKP infection, especially the co-infection and mortality of multiple carbapenem-resistant bacteria, and secondly to evaluate NLR as a predictor of the prognosis of CRKP infection.

Materials and methods

Study design and data collection

This was a retrospective descriptive analysis conducted from 1 January 2023 to 31 December 2023 at a large tertiary hospital with 3,200 beds in Chongqing, China. The study was approved by the ethical research committee of The First Affiliated Hospital of Chongqing Medical University and was performed in accordance with the Declaration of Helsinki and its amendments. All data in this study were from medical records and stripped of identifying information. The predefined route of this study is shown in Figure 1.

We included patients with CRKP mono-infection and CRKP co-infection with CRAB or CRPA from the database with their medical records. Only the initial positive culture of target strains were included. The exclusion criteria were as follows: (i) patients aged 0–14 years, (ii) positive culture only without any evidence of infection; and (iii) medical records were unavailable for analysis.

All data for the same patient were collected by the same person, and another person checked the data entry to ensure accuracy. Gather information from medical records: age, gender, length of

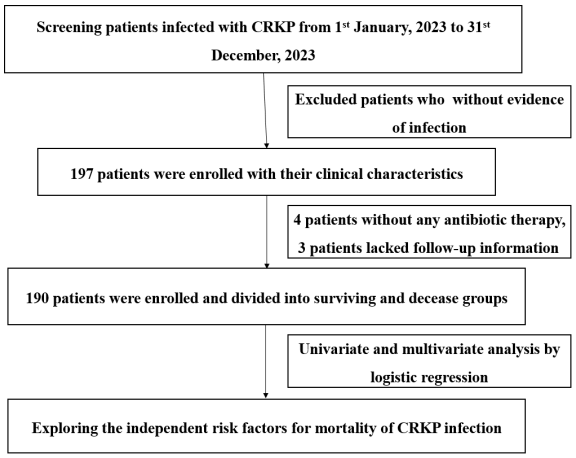

FIGURE 1
Flowchart of the study design.

hospitalization, course of treatment [intensive care unit (ICU) stay, invasive procedures, and equipment], site of infection, antibiotics exposure, baseline diseases, and outcome. All blood laboratory results were obtained on the day of bacterial culture specimen collected.

Study definitions

The onset of CRKP infection was defined as the collection date of a positive culture. Co-infection is defined based on the detection of ≥2 carbapenem-resistant bacteria in the same sample during hospitalization. A diagnosis of infection rather than colonization is confirmed by the clinician based on clinical signs and symptoms, imaging reports, and assessable clinical indicators. Carbapenem exposure meant that carbapenem antibiotics were administered for more than 48 h within the past 14 days. Appropriate treatments within 3 days were defined as administration of one or more antimicrobial agents proven effective by *in vitro* susceptibility testing within 72 h of definitive diagnosis of CRKP infection. All-cause mortality was defined as death from any cause during hospitalization.

Statistical analysis

Statistical analysis was performed using IBM SPSS version 18.0 (IBM Corp., Armonk, NY, USA). Continuous variables are presented as mean ± standard deviation or median (interquartile range), Student's *t*-test was used to compare normally distributed variables, and Mann–Whitney *U*-test was used to compare non-normally distributed variables. Categorical variables are presented as percentages, evaluated by chi-square or Fisher's exact tests. Risk factors for mortality and co-infection were analyzed using logistic regression. Variables with $p < 0.05$ in the univariate analysis were included in a multivariate backward logistic regression analysis. $p < 0.05$ was considered to be statistically significant in multivariate logistic regression. The prediction accuracy was evaluated using the area under the receiver operating characteristic (ROC) curves.

Results

Characteristics of patients

From 1 January 2023 to 31 December 2023, a total of 197 patients met study inclusion criteria, but 4 patients did not undergo antibiotic therapy and 3 patients lacked follow-up information; thus, 190 patients were ultimately enrolled, of whom 73 died in hospital and 117 survived. The overall mortality rate was 38.42% (73/190). The clinical and demographic characteristics of cohort patients with CRKP infection are shown in Table 1 according to the in-hospital survival status.

Characteristics of patients with co-infection and mono-infection

Of 146 patients, 99 had CRKP mono-infection and 91 had co-infection with CRKP and CRPA or CRAB. Of those with co-2infections, 62.64% (57/91) had CRKP and CRAB, 12.09% (11/91) had CRKP and CRPA, while 25.27% (23/91) had all three pathogens (CRKP, CRPA, and CRAB). There was no difference in the proportion of patients admitted to ICU and who underwent surgery between the two groups. However, patients in the co-infected group had higher rates of use of medical devices, including mechanical ventilation ($p = 0.003$), central line insertion ($p = 0.002$), and chronic Foley catheter requirement ($p < 0.001$). The sites of infection differed between the two groups (Table 2). The predominant source of infection in both groups was the respiratory tract, but the proportion was higher in the co-infection group ($p = 0.004$), while the urinary tract infection was more common in patients with mono-infection ($p = 0.035$). Antimicrobial exposure before the onset of CRKP infection was compared between the two groups. Notably, a higher proportion of co-infected patients were exposed to carbapenems, and a lower proportion were exposed to beta-lactam/beta-lactamase inhibitor than the mono-infection group. Meanwhile, meropenem was found to be the dominant carbapenem antibiotic, and more than 80% of patients in both groups were on combination therapy.

Risk factors associated with CRKP co-infection with CRAB/CRPA

By multivariable logistic regression analysis, the following clinical variables were identified for our cohort as independent risk factors that were significantly associated with co-infection: carbapenem exposure in past 14 days, central line insertion, and chronic Foley catheter requirement (Table 3).

Risk factors associated with mortality of CRKP infection

To identify the potential risk factors for mortality of CRKP infection, we conducted univariate analyses between the surviving

10.3389/fcimb.2024.1461325

TABLE 1 Clinical and demographic characteristics of 190 patients with CRKP infection and risk factors for mortality in hospital.

	Total *N* = 190	Death in hospital *N* = 73	Surviving in hospital *N* = 117	*p*
Demographic				
Age	62.75 ± 17.22	67.03 ± 16.80	60.09± 17.01	0.007
Male, *n* (%)	136 (71.58)	51 (69.86)	85 (72.65)	0.679
Admission to an ICU, *n* (%)	84 (44.21)	63 (86.30)	21 (17.95)	<0.001
Duration of hospitalization in the ICU ≤ 3 days, *n* (%)	53 (27.89%)	5 (6.85%)	48 (41.03%)	<0.001
Total hospital stay, days (median, IQR)	50.00 (28.00, 80.00)	34.00 (20.00, 58.00)	57.00 (33.00, 87.00)	<0.001
Surgery, *n* (%)	76 (40.00)	23 (31.51)	53 (45.30)	0.059
Baseline disease				
Diabetes	30 (15.79)	13 (17.81)	17 (14.53)	0.547
Hypertension	39 (20.51)	14(19.18)	25(21.37)	0.854
Heart disease	15 (7.89)	12 (16.44)	3 (2.56)	0.001
Neurologic disease	55 (28.95)	15(20.55)	40(34.19)	0.049
Chronic nephritis	9 (4.74)	5(6.85)	4(3.42)	0.309
Immunosuppression	10 (5.26)	5(6.85)	5(4.27)	0.511
Pulmonary disease	29 (15.26)	16(21.92)	13(11.11)	0.061
Malignancy	33 (17.37)	12(16.44)	21(17.95)	0.846
Antimicrobial therapy				
Carbapenems exposure in past 2 weeks	97 (51.05)	39 (53.42)	58 (49.57)	0.605
Appropriate treatments within 3 days	131 (68.95)	32 (43.84)	99 (84.62)	<0.001
Infection situation				
Co-infection, *n* (%)	100 (52.63)	48 (65.75)	52 (44.44)	0.004
Pneumonia	126 (66.32)	52 (71.23)	74 (63.25)	0.274
Sepsis	29 (15.26)	14 (19.17)	15 (12.82)	0.300
Urinary tract infection	12 (6.32)	1 (1.37)	12 (6.32)	0.018
Abdominal infection	18 (9.47)	18 (9.47)	18 (9.47)	0.355
Intracranial infection	2(1.05)	0(0)	2(1.71)	0.524
Skin and soft tissue infection	3(1.58)	0(0)	3(2.56)	0.286
Use of medical device				
Mechanical ventilation, *n* (%)	113 (59.47)	59 (80.82)	54 (46.15)	<0.001
Central line insertion, *n* (%)	146 (76.84)	68 (93.15)	78 (66.67)	<0.001
Chronic Foley catheter requirement, *n* (%)	174 (91.58)	69 (94.52)	105 (89.74)	0.249
Laboratory variables from blood				
WBC (10^9/L)	12.15 ± 6.48	15.26 ± 6.93	10.23 ± 5.38	<0.001
NEUT (10^9/L)	10.01 ± 6.15	13.11 ± 6.75	8.10 ± 4.87	<0.001
LY (10^9/L)	1.15 ± 1.29	1.18 ± 1.94	1.13 ± 0.65	0.82
PLT (10^9/L)	232.99± 135.59	224.89± 154.68	238.02± 122.71	0.52
PT (s)	14.25 ± 3.65	15.11 ± 5.30	13.72 ± 1.90	0.036

(Continued)

TABLE 1 Continued

	Total N = 190	Death in hospital N = 73	Surviving in hospital N = 117	p
Laboratory variables from blood				
A (g/L)	32.21 ± 4.79	31.29 ± 4.40	32.78 ± 4.95	0.038
TP (g/L)	61.95 ± 8.41	62.14 ± 8.20	61.84 ± 8.57	0.812
Cr (μmol/L)	80.59 ± 122.78	99.77 ± 129.95	68.79 ± 117.16	0.092
CRP (mg/L)	82.33 ± 83.77	107.28 ± 99.88	65.33 ± 66.10	0.005
PCT (ng/mL)	12.99 ± 36.18	16.43 ± 45.32	10.75 ± 28.74	0.312
Blood glucose (mmol/L)	7.38 ± 3.63	9.64 ± 5.26	6.36 ± 1.91	0.008
TC (mmol/L)	3.71 ± 1.19	3.41 ± 1.28	3.88 ± 1.12	0.045
TG (mmol/L)	1.63 ± 1.06	1.73 ± 1.30	1.57 ± 0.91	0.463
NLR	15.88 ± 22.23	26.74 ± 32.27	9.25 ± 7.01	<0.001

ICU, intensive care unit; WBC, white blood cell; NEUT, neutrophil; LY, lymphocyte count; PLT, platelet; PT, prothrombin time; A, albumin; TP, total protein; Cr, creatinine; CRP, C-reactive protein; PCT, procalcitonin; TC, total cholesterol; TG, triglyceride; NLR, neutrophil-to-lymphocyte count ratio; CRKP, carbapenem-resistant *Klebsiella pneumoniae*.

and deceased groups. The results (Table 2) revealed that admission to an ICU ($p < 0.001$), co-infection with CRAB/CRPA ($p = 0.005$), use of mechanical ventilation ($p < 0.001$), central line insertion ($p < 0.001$), higher white blood cell ($p = 0.009$), higher neutrophil ($p = 0.002$), higher prothrombin time ($p = 0.004$), lower albumin ($p = 0.005$), higher C-reactive protein ($p = 0.004$), higher blood glucose ($p = 0.007$), and higher NLR ($p < 0.001$) were more likely to be associated with mortality in hospital. In addition, the multivariate analysis (Table 4) shows that admission to an ICU ($p < 0.001$), co-infection with CRAB/CRPA ($p = 0.005$), and higher NLR ($p < 0.001$) were independent risk factors for mortality in hospital, while appropriate treatment within 3 days ($p < 0.001$) was an independent protective factor. The ROC curves of the NLR and in-hospital mortality are shown in Figure 2, and the area under the curve (AUC) was 0.696 (95% CI 0.615–0.777, $p < 0.001$); the NLR value with the highest Youden index was also the cutoff value of the NLR, which was 10.73.

Co-infection with CRAB/CRPA; a higher NLR may increase 28-day mortality

According to survival at 28 days after the onset of CRKP infection, we divided the patients who died into those who died within 28 days and those who died after 28 days. After univariate and multifactorial regression analysis, it was found that co-infection with CRAB/CRPA and high NLR at the onset of CRKP infection were risk factors for death within 28 days (Table 5).

Discussion

CRKP infection is an urgent public health problem. Because of the limited treatment availability coupled with the rapid spread of CRKP infection, the treatment of patients after infection is difficult, the case fatality rate is high, and the length of hospital stay and the cost are significantly increased, which increases the burden of patients and consumes more medical resources (Kohler et al., 2017). Owing to the abuse of antibiotics, environmental transmission, quorum sensing, and host adaptive response, CRKP co-infection with other carbapenem-resistant bacteria further increased the difficulty of clinical treatment (Marchaim et al., 2011; Sophonsri et al., 2023).

In the surveillance data for 2023, we found that the incidence of CRKP and CRAB/CRPA co-infection was significantly higher. A recent study has suggested that *P. aeruginosa* and *K. pneumoniae* are common co-isolates of *Acinetobacter baumannii*, which is consistent with our findings (Karakonstantis et al., 2022). In this study, 48.35% of co-infected patients were admitted to the ICU. A previous study has shown that 31.3% of the high-frequency contact surface cultures in the ICU bed units had one or more CRKP positive (Yan et al., 2019). At the same time, there was also a correlation between co-infection and ICU stay time. We found that the rate of co-infection was relatively lower in an ICU stay of less than 3 days (co-infection 16.48% vs. mono-infection 38.39%, $p \leq 0.001$).

An investigation into the outbreak of multidrug-resistant bacterial hospital infections in the ICU found that environmental contamination played an important role in some instances. Drug-resistant bacteria that are airborne or transmitted through contact may lead to healthcare-acquired infections or colonization, and even co-infections with multidrug-resistant carbapenemase-producing bacteria (Marchaim et al., 2012). Compared with CRKP mono-infection patients, co-infected patients were more likely to undergo invasive procedures, and we found that up to 98.90% of the co-infected patients in this study required urinary catheters and that 70.33% and 79.8% required the use of ventilators and central line insertion, respectively. Consistent with the results of another study, it was suggested that patients with co-infection were severely debilitated and lacked a functional state of activities of daily living, especially incontinence (Sophonsri et al., 2023). Simultaneously, these invasive

10.3389/fcimb.2024.1461325

TABLE 2 Comparison of co-infection and mono-infection. ICU, intensive care unit. * Carbapenem was used in monotherapy.

	Co-infection, *N* = 91	Mono-infection, *N* = 99	*p*-value
Therapeutic processes before infection			
Admission to an ICU, *n* (%)	44 (48.35)	40 (40.40)	0.307
Duration of hospitalization in the ICU ≤ 3 days, *n* (%)	15 (16.48%)	38 (38.39%)	0.001
Surgery, *n* (%)	36 (39.56)	40 (40.40)	0.534
Mechanical ventilation, *n* (%)	64 (70.33)	49 (49.50)	0.003
Central line insertion, *n* (%)	79 (79.80)	67 (67.68)	0.002
Chronic Foley catheter requirement, *n* (%)	90 (98.90)	84 (84.85)	<0.001
Infection situation			
Pneumonia, *n* (%)	70 (76.92)	56 (56.57)	0.004
Sepsis, *n* (%)	9 (9.89)	20 (20.20)	0.068
Urinary tract infection, *n* (%)	2 (2.20)	10 (10.10)	0.035
Abdominal infection, *n* (%)	7 (7.69)	11 (11.11)	0.466
Intracranial infection, *n* (%)	0 (0)	2 (2.02)	0.498
Skin and soft tissue infection, *n* (%)	3 (3.30)	0 (0)	0.108
Antimicrobial exposure in the past 14 days			
Carbapenems, *n* (%)	71 (78.02)	42 (42.42)	<0.001
Meropenem	58	32	0.483
Imipenem	13	10	
Monotherapy*	9	4	0.612
Beta-lactam/beta-lactamase inhibitor, *n* (%)	57 (62.64)	88 (88.89)	<0.001
Tigecycline, *n* (%)	5 (5.49)	6 (6.06)	0.558
Fluoroquinolones, *n* (%)	10 (10.99)	10 (10.10)	0.514
Sulfamethoxazole, *n* (%)	6 (6.59)	7 (7.07)	0.564
Aminoglycosides, *n* (%)	8 (8.79)	9 (9.09)	0.583

procedures also increased the risk of patients contracting or colonizing multidrug-resistant bacteria. The respiratory tract was the main infection site, and the proportion of patients in the co-infected group were higher, which may be related to the higher utilization rate of ventilators in the co-infected group.

A higher proportion of patients with co-infections had been exposed to carbapenem antibiotics within 14 days prior to the onset of CRKP infection. Carbapenem overexposure may select carbapenem-resistant organisms through different mechanisms, such as porin deletion or mutation, efflux pump overexpression, and upregulation of carbapenem resistance genes such as blaKPC (Tsao et al., 2018; Zou et al., 2018). Meanwhile, all patients were exposed to antibiotics within 14 days, including beta-lactam/beta-lactamase inhibitor and fluoroquinolones in addition to carbapenems. The complex underlying medical conditions of our patients likely required the use of broad-spectrum agents to provide adequate coverage but also predisposing them to infections caused by multidrug-resistant organisms. By multivariate analysis, clinical features identified to be significantly associated with co-infection in our study cohort were use of central line insertion, chronic Foley catheter requirement, and carbapenem exposure in the past 14 days.

TABLE 3 Multivariate analysis of risk factors for CRKP co-infection with CRAB/CRPA.

	Exp (B)	95% CI Exp (B)	*p*-value
Central line insertion	2.688	1.24–5.825	0.012
Chronic Foley catheter requirement	15.793	1.975–126.314	0.009
Carbapenems exposure in the past 14 days	0.472	0.243–0.917	0.027

CRKP, carbapenem-resistant *Klebsiella pneumoniae*; CRAB, carbapenem-resistant *Acinetobacter baumanii*; CRPA. carbapenem-resistant *Pseudomonas aeruginosa*.

10.3389/fcimb.2024.1461325

TABLE 4 Multivariate logistic regression analysis of risk factors for mortality in hospital of patients with CRKP infection.

	Univariate analysis			Multivariate analysis		
	Exp (B)	95% CI Exp (B)	*p*-value	Exp (B)	95% CI Exp (B)	*p*-value
Admission to an ICU	0.035	0.015–0.079	<0.001	0.034	0.012–0.091	<0.001
Duration of hospitalization in the ICU ≤ 3 days, *n* (%)	0.106	0.040–0.282	<0.001			
Co-infection with CRAB/CRPA	0.417	0.227–0.763	0.005	0.141	0.024–0.841	0.032
Appropriate treatments within 3 days	7.047	3.561–13.946	<0.001	7.928	2.627–20.271	<0.001
Mechanical ventilation	0.203	0.102–0.404	<0.001			
Central line insertion	0.147	0.055–0.394	<0.001			
WBC	0.939	0.895–0.984	0.009			
NEUT	0.923	0.877–0.972	0.002			
PT	0.806	0.696–0.932	0.004			
A	1.101	1.03–1.176	0.005			
CRP	0.994	0.989–0.998	0.004			
Blood glucose	0.801	0.682–0.942	0.007			
NLR	0.933	0.902–0.964	<0.001	0.968	0.935–1.001	0.036

CRKP, carbapenem-resistant *Klebsiella pneumoniae*; ICU, intensive care unit; CRAB, carbapenem-resistant *Acinetobacter baumanii*; CRPA. carbapenem-resistant *Pseudomonas aeruginosa*; WBC, white blood cell; NEUT, neutrophil; PT, prothrombin time; A, albumin; CRP, C-reactive protein; NLR, neutrophil-to-lymphocyte count ratio.

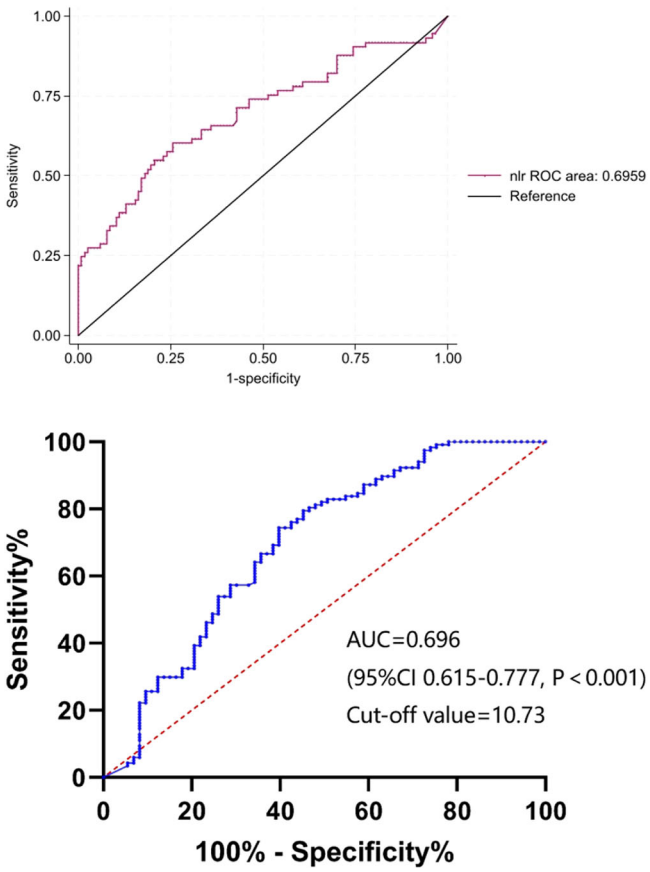

FIGURE 2
The ROC curves of NLR. ROC, receiver operating characteristic; NLR, neutrophil-to-lymphocyte count ratio; AUC, area under the curve.

TABLE 5 Multivariate logistic regression analysis of risk factors for 28-day mortality of patients with CRKP infection.

	Exp (B)	95% CI Exp (B)	*p*-value
Co-infection with CRAB/CRPA	6.415	1.526–26.978	0.011
NLR	1.204	1.071–1.353	0.002

CRKP, carbapenem-resistant *Klebsiella pneumoniae*; CRAB, carbapenem-resistant *Acinetobacter baumanii*; CRPA, carbapenem-resistant *Pseudomonas aeruginosa*; NLR, neutrophil-to-lymphocyte count ratio.

This study observed an all-cause mortality of 38.42% in patients with CRKP infection, similar to the mortality reported in previous studies (Chen et al., 2021; Barbosa et al., 2022). The mean age of patients in the hospital death group was higher than that in the hospital survival group, while the total hospital stay was shorter. In the hospital death group, admission to an ICU, neurologic disease, the use of medical device (mechanical ventilation, central line insertion, and chronic Foley catheter requirement), and co-infection with CRAB/CRPA were significantly more common than in the hospital survival group. It was found that patients in the death group whose duration of hospitalization in the ICU was ≤3 days were significantly less than those in the surviving group, suggesting that the patients in the death group may have more complex and severe diseases and were more likely to have co-infection during their stay in the ICU, which aggravated their disease. We also found that WBC, neutrophils, CRP, and NLR were higher; albumin was lower; and blood glucose and total cholesterol levels were higher in the hospital death group.

In the multivariate logistic regression analysis, admission to an ICU and co-infection with CRAB/CRPA were independent risk factors for all-cause mortality of CRKP infection patients. Previous studies suggest that age is a restrictive factor for ICU admission and determines treatment intensity (Tian et al., 2016). Among patients admitted to the ICU, there is an increased risk of antibiotic-resistant microbial infections and increased mortality due to comorbidities, critical conditions, frequent use of antimicrobials, and invasive procedures. Because of the age-related decline in immune function, age-related changes in organ structure and function, malnutrition, and comorbidities, elderly patients are susceptible to infections (Çölkesen et al., 2023), increasing the likelihood of admission to the ICU (Zhou et al., 2023). Age was not found to be an independent risk factor for morbidity, and this may be due to the fact that the study enrolled patients who were primarily elderly, with an average age of over 60 years.

Gender was not associated with mortality, but it is interesting to note that 71.58% of patients with CRKP infection were male. This is consistent with the findings of other literatures, which show that the proportion of male patients with CRKP infection is relatively high (Wang et al., 2022). One possible reason is that the common infection site of CRKP in China is the respiratory tract, and it is well known that men are more likely to develop respiratory tract infection due to smoking.

Because of the failure to implement early and rapid diagnosis, many patients were initially treated with inappropriate antibiotics, which may cause several serious comorbidities such as infectious shock, further increasing mortality. In this study, multivariate regression analysis results suggested that appropriate treatment within 3 days was a protective factor for mortality from CRKP infection. As mentioned earlier, carbapenem exposure increased the risk of co-infection. These data showed that inappropriate antibiotic exposure not only increased the risk of carbapenem-resistant bacteria infection but also increased mortality. Thus, a rational use of antibiotics can contribute to the decrease in morbidity and mortality associated with CRKP infection.

Studies have confirmed that early and appropriate anti-infective therapy can effectively reduce the mortality of CRKP infection (Kohler et al., 2017). Hence, exploring the prognostic value of potential biomarkers early on is important. A suitable biomarker must provide additional information to what is presently available; it should be able to predict outcomes or evaluate the efficacy of treatment, and it should be immediately available and cost-effective. In clinical practice, leukocytes, neutrophils, or PCTs are usually used to reflect the level of inflammation in patients. However, these indicators' infection status is limited. As a reaction product in the acute phase, CRP increases when inflammation, infection, or tissue damage occurs in the body (Sproston and Ashworth, 2018; Tan et al., 2019), while PCT is also not a perfect marker of inflammation, as it can be elevated in any cellular injury, whether direct tissue injury or non-infectious ischemia–reperfusion injury, such as myocardial infarction or cancer, which can lead to misdiagnosis by clinicians (Paudel et al., 2020). Univariate analysis revealed that CRP was a prognostic factor in patients with CRKP infection in this study, but after multivariate analysis, we found that CRP did not effectively predict the prognosis of patients with CRKP infection.

Neutrophils is the first line of defense against bacterial infections, and they rapidly recruit and phagocytose to kill pathogenic microorganisms after bacterial infections. At the same time, lymphocyte apoptosis is accelerated, leading to immune system suppression and multiorgan dysfunction (Kobayashi et al., 2018). In some studies, NLR has been observed to be more effective than conventional inflammatory biomarkers in adult diseases such as community-acquired pneumonia (De Jager et al., 2012) and sepsis (Huang et al., 2020). This study indicated the NLR was an independent risk factor for all-cause mortality of CRKP infection patients. We conducted this study to evaluate NLR as a predictor of the prognosis of patients infected with CRKP, along with other biomarkers and therapy strategies. We found that NLR on the day of CRKP infection onset could be an independent risk factor for all-cause mortality and 28-day mortality. To the best of our knowledge, this is the first study to explore the value of the NLR in predicting

all-cause mortality of patients with CRKP infection. It suggests that NLR can be used as a useful and economical marker with the function of indicating the severity of CRKP infection in patients and whether anti-infection treatment is appropriate for patients.

There are several limitations to this study. First, this was a single-center retrospective study, which may have introduced bias in data interpretation. Second, owing to the limitation of the retrospective study, we did not perform a dynamic analysis of NLR in patients with CRKP infection. Third, the ability to capture data pertinent to outside hospitalizations such as antimicrobial administration as well as readmissions to outside institutions also poses limitations to the completeness of data collection.

Conclusion

Together, we observed that co-infection with CRKP and another carbapenem-resistant pathogen significantly increased morbidity and healthcare burden. Our study revealed that NLR on the day of CRKP infection onset, admission to an ICU, and co-infection with CRAB/CRPA were independent risk factors for all-cause mortality of patients with CRKP infection, while appropriate treatment within 3 days was an independent protective factor.

Data availability statement

The original contributions presented in the study are included in the article/supplementary material. Further inquiries can be directed to the corresponding author.

Author contributions

ZW: Data curation, Investigation, Writing – review & editing. ZY: Conceptualization, Writing – review & editing. RL: Investigation, Writing – review & editing. KQ: Data curation, Formal analysis, Investigation, Writing – original draft, Writing – review & editing. ZZ: Data curation, Writing – review & editing.

Funding

The author(s) declare that no financial support was received for the research, authorship, and/or publication of this article.

Conflict of interest

The authors declare that the research was conducted in the absence of any commercial or financial relationships that could be construed as a potential conflict of interest.

Publisher's note

All claims expressed in this article are solely those of the authors and do not necessarily represent those of their affiliated organizations, or those of the publisher, the editors and the reviewers. Any product that may be evaluated in this article, or claim that may be made by its manufacturer, is not guaranteed or endorsed by the publisher.

References

Adediran, T., Harris, A. D., Johnson, J. K., Calfee, D. P., Miller, L. G., Nguyen, M. H., et al. (2020). Epidemiologic and microbiologic characteristics of hospitalized patients co-colonized with multiple species of carbapenem-resistant enterobacteriaceae in the United States. *Open Forum Infect. Dis.* 7, Ofaa386. doi: 10.1093/ofid/ofaa386

Barbosa, L. C. G., Silva, J. A.S. E., Bordoni, G. P., Barbosa, G. D., and Carneiro, L. C. (2022). Elevated mortality risk from crkp associated with comorbidities: systematic review and meta-analysis. *Antibiotics (Basel Switzerland)* 11, 1. doi: 10.3390/antibiotics11070874

Budhram, D. R., Mac, S., Bielecki, J. M., Patel, S. N., and Sander, B.. (2020). Health outcomes attributable to carbapenemase-producing enterobacteriaceae infections: A systematic review and meta-analysis. *Infection Control And Hosp. Epidemiol.* 41, 37–43. doi: 10.1017/ice.2019.282

Chen, I. R., Huang, P. H., Wu, P. F., Wang, F. D., and Lin, Y. T. (2021). Clinical characteristics and outcomes of 56 patients with pneumonia caused by carbapenem-resistant klebsiella pneumoniae. *J. Global Antimicrobial Resistance* 25, 1. doi: 10.1016/j.jgar.2021.03.028

Chen, Y., Ying, S., Jiang, L., Dong, S. H., Dai, J. Y., and Jin, X. H. (2022). A novel nomogram for predicting risk factors and outcomes in bloodstream infections caused by klebsiella pneumoniae. *Infection And Drug Resistance* 15, 1. doi: 10.2147/IDR.S349236

Çölkesen, F., Tarakçı, A., Eroğlu, E., Kacar, F., Armagan, S. Ö., and Can, S. (2023). Carbapenem-resistant klebsiella pneumoniae infection and its risk factors in older adult patients. *Clin. Interventions In Aging* 18, 1. doi: 10.2147/CIA.S406214

De Jager, C. P., Wever, P. C., Gemen, E. F., Kusters, R., van Gageldonk-Lafeber, A. B., van der Poll, T., et al. (2012). The neutrophil-lymphocyte count ratio in patients with community-acquired pneumonia. *PloS One* 7, e46561. doi: 10.1371/journal.pone.0046561

Falagas, M. E., Tansarli, G. S., Karageorgopoulos, D. E., and Vardakas, K. Z. (2014). Deaths attributable to carbapenem-resistant enterobacteriaceae infections. *Emerging Infect. Dis.* 20, 1170–1175. doi: 10.3201/eid2007.121004

Giacobbe, D. R., Marelli, C., Cattardico, G., Fanelli, C., Signori, A., Di Meco, G., et al. (2023). Mortality in kpc-producing klebsiella pneumoniae bloodstream infections: A changing landscape. *J. Antimicrobial Chemotherapy* 78, 2505–2514. doi: 10.1093/jac/dkad262

Han, Y. L., Wen, X. H., Zhao, W., Cao, X. S., Wen, J. X., and Wang, J. R. (2022). Epidemiological characteristics and molecular evolution mechanisms of carbapenem-resistant hypervirulent klebsiella pneumoniae. *Front. Microbiol.* 13. doi: 10.3389/fmicb.2022.1003783

Huang, Z. W., Fu, Z. Y., Huang, W. J., and Huang, K. G. (2020). Prognostic value of neutrophil-to-lymphocyte ratio in sepsis: A meta-analysis. *Am. J. Emergency Med.* 38, 641–647. doi: 10.1016/j.ajem.2019.10.023

Iredell, J., Brown, J., and Tagg, K. (2016). Antibiotic resistance in enterobacteriaceae: mechanisms and clinical implications. *BMJ (Clinical Res. Ed)* 352, 1. doi: 10.1136/bmj.h6420

Karakonstantis, S., Ioannou, P., and Kritsotakis, E. I. (2022). Co-isolates of acinetobacter baumannii complex in polymicrobial infections: A meta-analysis. *Access Microbiol.* 4, Acmi000348. doi: 10.1099/acmi.0.000348

Karampatakis, T., Tsergouli, K., and Behzadi, P. (2023). Carbapenem-resistant klebsiella pneumoniae: virulence factors, molecular epidemiology and latest updates in treatment options. *Antibiotics (Basel Switzerland)* 12, 1. doi: 10.3390/antibiotics12020234

Kobayashi, S. D., Malachowa, N., and Deleo, F. R. (2018). Neutrophils and bacterial immune evasion. *J. Innate Immun.* 10, 432–441. doi: 10.1159/000487756

Kohler, P. P., Volling, C., Green, K., Uleryk, E. M., Shah, P. S., McGeer, A., et al. (2017). Carbapenem Resistance, Initial antibiotic therapy, and mortality in klebsiella pneumoniae bacteremia: A systematic review and meta-analysis. *Infection Control And Hosp. Epidemiol.* 38, 1319–1328. doi: 10.1017/ice.2017.197

Li, B., Li, X., Zhao, J., Wang, X. Y., and Ma, L. (2024). Analysis and modelling of the predictive value of pct, plr and nlr for ureteric sepsis after ureteral stone surgery: A

retrospective cohort study. *Archivos Espanoles Urologia* 77, 498–504. doi: 10.56434/j.arch.esp.urol.20247705.69

Li, Y., Min, L., and Zhang, X. (2021). Usefulness of procalcitonin (Pct), C-reactive protein (Crp), and white blood cell (Wbc) levels in the differential diagnosis of acute bacterial, viral, and mycoplasmal respiratory tract infections in children. *BMC Pulmonary Med.* 21, 386. doi: 10.1186/s12890-021-01756-4

Lv, D. M., Zuo, Y., Wang, Y. R., Wang, Z. X., and Xu, Y. H. (2022). Predictors of occurrence and 30-day mortality for co-infection of carbapenem-resistant klebsiella pneumoniae and carbapenem-resistant acinetobacter baumannii. *Front. Cell Infect. Microbiol.* 12, 1. doi: 10.3389/fcimb.2022.919414

Marchaim, D., Chopra, T., Perez, F., Hayakawa, K., Lephart, P. R., and Bheemreddy, S. (2011). Outcomes and genetic relatedness of carbapenem-resistant enterobacteriaceae at detroit medical center. *Infection Control And Hosp. Epidemiol.* 32, 861–871. doi: 10.1086/661597

Marchaim, D., Perez, F., Lee, J., Bheemreddy, S., Hujer, A. M., Rudin, S., et al. (2012). Swimming in resistance": co-colonization with carbapenem-resistant enterobacteriaceae and acinetobacter baumannii or pseudomonas aeruginosa. *Am. J. Infection Control* 40, 830–835. doi: 10.1016/j.ajic.2011.10.013

Paudel, R., Dogra, P., Montgomery-Yates, A. A., and Yataco, A. C. (2020). Procalcitonin: A promising tool or just another overhyped test? *Int. J. Med. Sci.* 17, 332–337. doi: 10.7150/ijms.39367

Sophonsri, A., Kelsom, C., Lou, M., Nieberg, P., and Wong-Beringer, A. (2023). Risk factors and outcome associated with coinfection with carbapenem-resistant klebsiella pneumoniae and carbapenem-resistant pseudomonas aeruginosa or acinetobacter baumanii: A descriptive analysis. *Front. Cell Infect. Microbiol.* 13. doi: 10.3389/fcimb.2023.1231740

Sproston, N. R., and Ashworth, J. J. (2018). Role of C-reactive protein at sites of inflammation and infection. *Front. Immunol.* 9. doi: 10.3389/fimmu.2018.00754

Tan, M., Lu, Y., Jiang, H., and Zhang, L. D. (2019). The diagnostic accuracy of procalcitonin and C-reactive protein for sepsis: A systematic review and meta-analysis. *J. Cell. Biochem.* 120, 5852–5859. doi: 10.1002/jcb.v120.4

Tian, L., Tan, R., Chen, Y., Sun, J. Y., Liu, J. L., Qu, H. P., et al. (2016). Epidemiology of klebsiella pneumoniae bloodstream infections in A teaching hospital: factors related to the carbapenem resistance and patient mortality. *Antimicrobial Resistance And Infection Control* 5, 10. doi: 10.1186/s13756-016-0145-0

Tsao, L. H., Hsin, C. Y., Liu, H. Y., Chuang, H. C., Chen, L. Y., Lee, Y. J., et al. (2018). Risk factors for healthcare-associated infection caused by carbapenem-resistant pseudomonas aeruginosa. *J. Microbiol. Immunol. Infect.* 51, 359–366. doi: 10.1016/j.jmii.2017.08.015

Wang, M. G., Earley, M., Chen, L., Hanson, B. M., Yu, Y. S., and Liu, Z. Y. (2022). Clinical outcomes and bacterial characteristics of carbapenem-resistant klebsiella pneumoniae complex among patients from different global regions (Crackle-2): A prospective, multicentre, cohort study. *Lancet Infect. Dis.* 22, 401–412. doi: 10.1016/S1473-3099(21)00399-6

World Health Organization (WHO). (2024). *WHO bacterial priority pathogens list, 2024: Bacterial pathogens of public health importance to guide research, development and strategies to prevent and control antimicrobial resistance*. Available online at: https://www.who.int/publications/i/item/9789240093461 (accessed November 20, 2024).

Wu, C., Zheng, L., and Yao, J. (2022). Analysis of risk factors and mortality of patients with carbapenem-resistant klebsiella pneumoniae infection. *Infect. Drug Resist.* 15, 1. doi: 10.2147/IDR.S362723

Yan, Z. Q., Zhou, Y., Du, M. M., Bai, Y. L., Liu, B. W., Gong, M. L., et al. (2019). Prospective Investigation Carbapenem-Resistant Klebsiella Pneumonia Transmission Among The Staff, Environment and patients in five major intensive care units, beijing. *J. Hosp. Infection* 101, 150–157. doi: 10.1016/j.jhin.2018.11.019

Zhang, J., Liu, C., Xiao, X., Xie, H., Zhang, Y., Hong, Y., et al (2024). Neutrophil-to-lymphocyte ratio, platelet-to-lymphocyte ratio, and systemic immunoinflammatory index in patients with intracerebral hemorrhage and clinical value in predicting pneumonia 30 days after surgery. *World Neurosurg.* 188, 1. doi: 10.1016/j.wneu.2024.05.048

Zhou, C. E., Sun, L. Y., Li, H. X., Huang, L., and Liu, X. M. (2023). Risk factors and mortality of elderly patients with hospital-acquired pneumonia of carbapenem-resistant klebsiella pneumoniae infection. *Infection And Drug Resistance* 16, 1. doi: 10.2147/IDR.S431085

Zou, Y. M., Lian, J. P., Di, Y., You, H. S., Yao, H. P., and Liu, J. H. (2018). The quick loss of carbapenem susceptibility in pseudomonas aeruginosa at intensive care units. *Int. J. Clin. Pharm.* 40, 175–182. doi: 10.1007/s11096-017-0524-5

frontiers | Frontiers in Cellular and Infection Microbiology

TYPE Original Research
PUBLISHED 28 November 2024
DOI 10.3389/fcimb.2024.1451539

OPEN ACCESS

EDITED BY
Diana Manolescu,
Victor Babes University of Medicine and Pharmacy, Romania

REVIEWED BY
Lorena V. N. Oliveira,
University of Massachusetts Medical School, United States
Michał Jacek Sobkowiak,
Karolinska Institutet (KI), Sweden
Catalin Marian,
Victor Babes University of Medicine and Pharmacy, Romania

*CORRESPONDENCE
Dong-Dong Li
jiangxili1219@163.com

†These authors have contributed equally to this work

RECEIVED 19 June 2024
ACCEPTED 28 October 2024
PUBLISHED 28 November 2024

CITATION
Tang Z-Y, Xu P, Wang Z-H, Wang T-T, Zhou D, Ao K-P, Song H-F, Yin X-Y and Li D-D (2024) Evaluation of cryptococcal antigen testing using a novel chemiluminescence assay in two medical centers of China.
Front. Cell. Infect. Microbiol. 14:1451539.
doi: 10.3389/fcimb.2024.1451539

Evaluation of cryptococcal antigen testing using a novel chemiluminescence assay in two medical centers of China

Zhuo-Yun Tang[1†], Ping Xu[2†], Zhong-Hao Wang[1], Ting-Ting Wang[1], Dan Zhou[1], Ke-Ping Ao[1], Hua-Feng Song[2], Xiao-Yun Yin[2] and Dong-Dong Li[1*]

[1]Department of Laboratory Medicine, West China Hospital of Sichuan University, Chengdu, Sichuan, China, [2]Department of Clinical Laboratory, The Fifth People's Hospital of Suzhou, Infectious Disease Hospital Affiliated to Soochow University, Suzhou, Jiangsu, China

Objective: This study aimed to assess the efficacy of innovative Chemiluminescence Immunoassay (CLIA) in testing Cryptococcal Antigen (CrAg) across two medical centers, employing the FDA-approved CrAg Lateral Flow Assay (LFA) by IMMY as a reference standard.

Methods: The study encompassed patients diagnosed with cryptococcosis at West China Hospital of Sichuan University (HX) between July 2022 and May 2023, and Suzhou Fifth People's Hospital (SZ) from September 2020 to September 2023. All specimens underwent simultaneous detection using the LFA (IMMY, Norman, USA) and CLIA (Chuanglan, Suzhou, China).

Results: A total of 628 patients were enrolled, revealing a remarkable 99.20% concordance between LFA and CLIA (623/628, 99.20%). The LFA exhibited a sensitivity of 96.83% (244/252) and specificity of 98.35% (179/182). Among the 42 patients with unaltered CrAg titers, the changes of Signal-to-Cut-Off ratio (ΔS/CO) results exhibited a noteworthy discrepancy, with 71.43% (30/42) demonstrating a decreasing trend in ΔS/CO of at least 10%.

Conclusions: The CLIA method demonstrated commendable specificity and sensitivity, exhibiting a high level of agreement with the FDA-approved LFA method. Additionally, CLIA demonstrated superior utility for treatment monitoring compared to LFA, offering continuous insight into the fluctuation of CrAg concentrations.

KEYWORDS

cryptococcal antigen, cryptococcosis, chemiluminescence assay (CLIA), lateral flow assay (LFA), diagnostic performance, treatment monitoring

1 Background

Cryptococcosis constitutes a severe invasive fungal ailment associated with significant morbidity and mortality on a global scale (Benedict et al., 2022; Rajasingham et al., 2022). Cryptococcal antigenemia and meningitis predominantly afflict individuals experiencing immunosuppression due to conditions such as HIV, malignancies, organ transplantation, and similar states (Marr et al., 2020; Liang et al., 2023). While cryptococcal antigenemia and meningitis are prevalent among those with HIV globally (Rajasingham et al., 2017; Bive et al., 2022), an increasing number of non-HIV individuals in China are falling victim to cryptococcosis due to variations in population susceptibility (Chen et al., 2020; Zhao et al., 2021). The recognition of cryptococcosis in seemingly immunocompetent patients is also on the rise (George et al., 2018; Hevey et al., 2019; Li et al., 2021; Pinheiro et al., 2021). Given that early identification and intervention can mitigate morbidity and mortality, comprehending testing trends for cryptococcosis is imperative in estimating its public health impact (Baddley et al., 2021; Benedict et al., 2022; Liang et al., 2023).

Laboratory methodologies employed for cryptococcosis diagnosis typically involve culture, microscopic examination of cerebrospinal fluid (CSF), and the detection of cryptococcal antigen (CrAg) in bodily fluids (Osaigbovo and Bongomin, 2021; Benedict et al., 2022). Among these, CrAg detection stands out as the most expeditious and widely employed diagnostic approach, owing to its elevated sensitivity and specificity (Dubbels et al., 2017; Tugume et al., 2023). Latex agglutination, enzyme immunoassay and lateral flow assay (LFA), represent common techniques for CrAg detection (Kamble et al., 2021; Macrae et al., 2023). CrAg titers serve as prognostic indicators for mortality and can supplement therapeutic assessments (Wang et al., 2020; Tadeo et al., 2021). While LFA are straightforward, rapid, and economical diagnostic methods, determining titers using LFA necessitates an ample supply of strips and reagents, coupled with technical proficiency. The chemiluminescence assay (CLIA) has the advantages of simple operation, low cost, high sensitivity and stable reagents (Li and Guo, 2024). Consequently, CLIA emerges as an appealing alternative, potentially enabling precise management decisions based on titers at a reduced cost (Dubbels et al., 2017; Wang et al., 2020; Macrae et al., 2023; McHale et al., 2023).

The objective of this study was to assess the efficacy of a novel chemiluminescence assay for testing CrAg and CrAg titers in two medical centers, utilizing the FDA-approved CrAg LFA (IMMY) as a benchmark.

2 Materials and methods

2.1 Cohort population

All patients diagnosed with cryptococcosis at West China Hospital of Sichuan University (HX) between July 2022 and May 2023 and Suzhou Fifth People's Hospital (SZ) from September 2020 to September 2023 were enrolled in this study. Patient samples with the following conditions were excluded: 1) serum samples with severe hemolysis and lipidemia; 2) CSF samples with fatty turbidity; 3) samples with insufficient amount. Cryptococcal infection was defined as the presence of a positive serum or CSF CrAg test, isolation of Cryptococcus neoformans in culture, or pertinent clinical information. The date of the diagnostic specimen was utilized as the time of diagnosis. Patient demographics, laboratory testing, treatment data, and outcomes were extracted from the medical charts and subsequently analyzed. The negative group comprised individuals with a negative serum or CSF CrAg result determined by LFA (IMMY, Norman, USA). The interference group included cases with conditions such as bacterial encephalitis, viral encephalitis, autoimmune encephalitis, tuberculous encephalitis, rheumatoid factor and systemic lupus erythematosus. All samples used in this study were acquired from remaining samples after clinical testing.

2.2 Testing methods

All specimens underwent concurrent assessment using LFA (IMMY, Norman, USA) and CLIA (Chuanglan, Suzhou, China). Qualitative outcomes were categorized as negative or positive, while semiquantitative results were expressed as tiers (IMMY), and quantitative results were presented as numerical values (Chuanglan).

The operation steps were carried out in accordance with the reagent instructions. For LFA, it was a "sandwich" immunochromatographic test strip for the detection of CrAg. A positive test resulted in two lines (the control line and the test line), and a negative test resulted only one line (the control line), and if the band did not appear, the test was invalid. The LFA assay gave semiquantitative results as 1:5, 1:10, 1:20 and so on.

The novel CLIA method used magnetic particle directly to detect the concentration of CrAg in human serum and cerebrospinal fluid based on a two-step immune response sandwiched with bispecific antibodies: 1) The first step was to bind the CrAg to the magnetic particle-coated anti-capsular polysaccharide monoclonal antibody through an immune response. 2) The second step was to add acridine ester-labeled anti-GXM monoclonal antibody to form a complex. 3) After washing, added pre-excitation and excitation solution and its luminescence intensity was positively correlated with the concentration of capsular polysaccharides in serum or cerebrospinal fluid. The range of the kit was 2-160 ng/mL. If the concentration of CrAg < 2ng/mL, it was considered negative; if the sample was above the upper limit of detection, it was reported as greater than that value (>160 ng/mL).

2.3 Statistical methods

Categorical variables were scrutinized utilizing Fisher's exact test and the chi-square test, as deemed appropriate. Continuous variables were analyzed through the t-test and the Mann-Whitney

U test if the assumption of normality was violated. P values of <0.05 were considered statistically significant. The analyses were executed using SPSS [V25] (IBM, Armonk, NY, USA) and Origin [V2022] (OriginLab, Northampton, Massachusetts, USA).

3 Results

3.1 Comparison of the consistency of LFA and CLIA in qualitative results

We conducted a comprehensive review of 901 samples meeting the enrolment criteria for the positive group, negative group, and interference group from September 2020 to September 2023. A total of 273 samples, identified as replicates, were excluded from the analysis. The resultant cohort comprised 628 patients, revealing a noteworthy 99.20% consistency between LFA and CLIA (623/628, 99.20%) (Table 1). Among these, 377 samples originated from West China Hospital (HX), while 251 samples were obtained from The Fifth People's Hospital of Suzhou (SZ). The positive group consisted of 278 samples, the negative group included 330 samples, and 20 samples were designated as interference group. Each group exhibited substantial consistency between the two methods (271/278, 97.48%; 330/330, 100.00%; 20/20, 100.00%). Notably, 5 samples exhibited inconsistent results, and 80.00% (4/5) of the inconsistent samples were serum samples, with merely one originating from CSF (Table 2).

3.2 Specificity and sensitivity of LFA and CLIA

Demographic data were available for 456 patients across the two centers, excluding 22 patients who either missed the clinical diagnosis or could not be diagnosed with cryptococcosis. The cohort from the two centers comprised 155 women and 279 men, with a mean age of 50.35 years (Table 3). The LFA demonstrated a sensitivity of 96.83% (244/252) and a specificity of 98.35% (179/182). Similarly, the CLIA exhibited a sensitivity of 97.22% (245/252) and a specificity of 96.70% (176/182). In HX center, a more detailed analysis of 377 samples was carried out with the sensitivity and specificity was 96.96% (126/132) and 98.24% (112/114) for serum samples; the sensitivity and specificity were 100.00% (67/67) and 97.67% (42/43) for CSF samples.

TABLE 1 The results of LFA and CLIA in 628 patients.

Test	Results	LFA		Total
		Positive	Negative	
CLIA	Positive	271 (99.63%)	4 (1.12%)	275
	Negative	1 (0.37%)	352 (98.88%)	353
Total		272	356	628

3.3 Performance evaluation for the same patient surveillance

A total of 195 samples from 69 patients were available for therapy surveillance, wherein certain patients contributed more than one sample across different time points. All samples underwent both LFA and CLIA testing, revealing 42 patients (60.86%,42/69) maintained the same CrAg titer by LFA but exhibited markedly different CLIA results (ΔS/CO ≥ 10%, $\Delta S/CO = \left|\frac{S/COsecond - S/COfirst}{S/COfirst}\right|$) (Figure 1; Supplementary Table 1). The median of ΔS/CO was 0.36 (Interquartile range [IQR], 0.21 to 0.80). Of these patients, 23.81% (10/42) witnessed an increase in ΔS/CO, 71.43% (30/42) experienced a decrease, and 4.76% (2/42) displayed fluctuating changes in CrAg (Figure 2).

3.4 LFA and CLIA assist in clinical judgment of the timing of drug discontinuation

A compilation of 153 samples with negative fungal cultures of Cryptococcus in CSF was analyzed for LFA, CLIA results, and clinical information on drug discontinuation. Among these samples, only three patients opted for discontinuation of antifungal therapy (Table 4). These three patients, all of advanced age, had been orally administered voriconazole for an extended duration of antifungal therapy post-diagnosis. Despite the persistence of CrAg, clinicians chose to discontinue antifungal therapy upon obtaining negative cultures.

4 Discussion

Cryptococcus capsular polysaccharide antigen stands out as an optimal biomarker for screening cryptococcal infections (Wang et al., 2022; Liang et al., 2023). The LFA currently enjoys global recognition and widespread use for CrAg detection, demonstrating high specificity and sensitivity (Borges et al., 2019; Ware et al., 2023). In contrast to conventional culture, ink staining, and Next-Generation Sequencing (NGS) methods, LFA offers the distinct advantages of speed, accuracy, and cost-effectiveness. However, when utilized for CrAg titer detection, LFA can only provide results in a semi-quantitative format (Skipper et al., 2020; Tenforde et al., 2020). With the increasing adoption of chemiluminescence methodology, the use of the CLIA for CrAg detection addresses the limitations of semi-quantitation, providing results that are more rapid, accurate, and quantitative.

The primary objective of this study was to assess the diagnostic performance of a novel CLIA CrAg assay, using the FDA-approved CrAg LFA test (IMMY) as the reference method. The new CLIA CrAg assay demonstrated perfect consistency with IMMY, showing a 99.20% agreement between LFA and CLIA across the positive group, negative group, and interference group. Both the negative and interference groups exhibited 100.00% consistency, with only 5 out of 278 positive samples displaying inconsistencies. Among these incongruities, 80.00% originated from serum samples, while 20.00%

10.3389/fcimb.2024.1451539

TABLE 2 The baseline results of five inconsistent samples.

Sample	Age	Gender	Clinical diagnosis	Sample type	LFA result	CLIA result (S/CO)
1	48	Male	Cryptococcosis	Serum	Positive(+)	0.076(-)
2	22	Male	Cryptococcal meningitis	CSF	Negative(-)	3.424(+)
3	57	Female	NP*	Serum	Positive(+)	0.598(-)
4	40	Male	Cryptococcosis	Serum	Positive(+)	1.236(-)
5	25	Female	Cryptococcosis	Serum	Positive(+)	0.021(-)

*NP, not provided.

TABLE 3 Baseline characteristics of LFA and CLIA performed by HX and SZ.

	Total	LFA		CLIA	
		Positive	Negative	Positive	Negative
Mean age (year)	50.35	49.21	51.81	49.04	52.09
Gender					
Male	279 (64.29%)	168 (68.85%)	111 (58.42%)	171 (69.80%)	108 (57.14%)
Female	155 (35.71%)	76 (31.15%)	79 (4158%)	74 (30.20%)	81 (42.86%)
Clinical diagnosis					
Cryptococcosis	211 (48.62%)	204 (83.61%)	7 (3.68%)	200 (81.63%)	13 (6.88%)
Cryptococcal meningitis	41 (0.92%)	40 (16.39%)	4 (2.11%)	45 (18.37%)	0 (0)
Non-cryptococcal infections	182 (43.94%)	0 (0)	179 (94.21%)	0 (0)	176 (93.12%)
Total	434	244	190	245	189

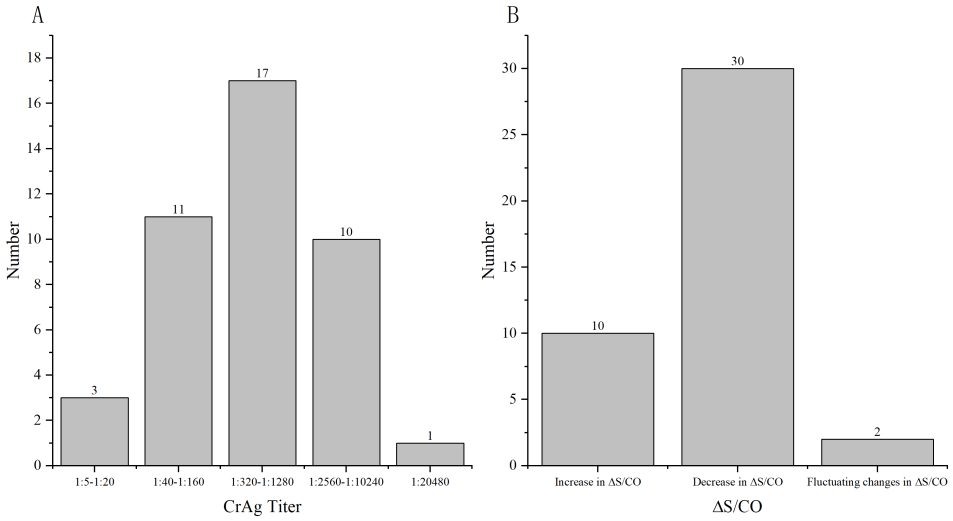

FIGURE 1
ΔS/CO and LFA results of 42 patients who were available for surveillance. **(A)** The distribution of different CrAg titer of 42 patients by LFA; **(B)** The distribution of different changes in CrAg by CLIA.

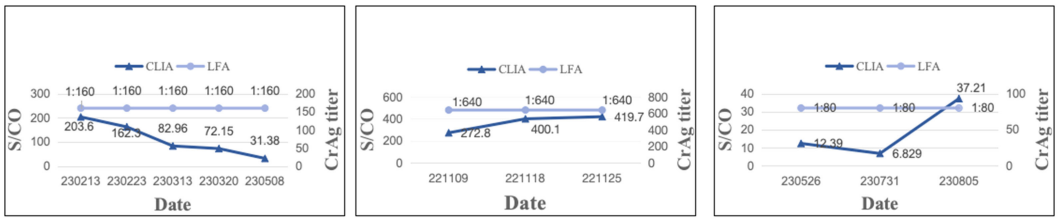

FIGURE 2
Depiction of three typical patients maintaining the same CrAg titer but exhibiting significantly different S/CO results. Patient 4 had a CrAg titer of 1:160, yet S/CO results decreased. Patient 7 maintained a CrAg titer of 1:640, with increased S/CO results. Patient 16 had a CrAg titer of 1:80, but S/CO displayed fluctuating changes.

were from CSF. Of the five discordant cases, four were diagnosed with cryptococcal infection, three of which were accurately identified as positive by LFA but incorrectly deemed false-negative by CLIA. One case was falsely negative by LFA but correctly identified as positive by CLIA.

The study evaluated the diagnostic performance of the new CLIA CrAg assay (Chuanglan) in comparison to the LFA CrAg assay (IMMY). Both CLIA and LFA demonstrated excellent test performance, boasting 97.22% sensitivity and 96.70% specificity (CLIA) versus 96.83% sensitivity and 98.35% specificity (LFA). CLIA was more sensitive but less specific. However, the sensitivity and specificity of the IMMY test in this study were marginally lower than in previous studies (Jarvis et al., 2020; Skipper et al., 2020; Kwizera et al., 2021; Noguera et al., 2021; Langner and Yang, 2022), potentially attributed to variations in the testing population (Zhang et al., 2023). Notably, the predominant characteristic of the testing population in China was the prevalence of immunocompetent individuals among cryptococcus-infected patients, in contrast to populations largely comprising immunocompromised individuals such as people living with HIV (PLWH) or organ transplant recipients (Rajasingham et al., 2017; Zhang et al., 2023). Literature reports on non-HIV populations revealed LFA detection performance with 96.00% sensitivity and 96.00% specificity, consistent with our findings (Macrae et al., 2023). This observation is significant as cryptococcal disease, while predominantly affecting PLWH, is increasingly affecting HIV-negative individuals, particularly in regions with advanced healthcare systems.

In this study, 69 patients maintaining the same CrAg titer (IMMY) over an extended period were examined innovatively, revealing that 42 of them experienced a change of more than 10% in S/CO value by CLIA. The median value of ΔS/CO was 36.00%, with 71.43% of patients exhibiting a decreasing trend in CrAg concentration, indicative of the efficacy of antifungal therapy [35]. Conversely, 23.81% and 4.76% of patients showed an increasing and fluctuating trend in CrAg concentration, respectively, suggesting a suboptimal response to antifungal therapy. CrAg concentration serves as an indicator of the rate of cryptococcal clearance, making it a valuable tool for treatment monitoring. The prolonged nature of antifungal therapy renders the LFA method capable of only providing semi-quantitative results, leading to scenarios where the CrAg titer may persist unchanged despite gradual elimination of the pathogen. In such cases, CLIA's quantitative results offer a superior method for therapeutic monitoring, providing continuous presentation of results and enabling the monitoring of CrAg concentration changes at multiple time points to reflect the efficacy of antifungal therapy.

In this study, we examined 153 patients with negative CSF fungal cultures, subjecting both their serum and CSF to testing with both LFA and CLIA, while reviewing their treatment outcomes. Merely three patients opted to discontinue antifungal therapy upon obtaining negative cultures. The LFA results were 1:2, 1:10, and 1:80, with corresponding CLIA results of 0.144, 3.365, and 8.766, respectively, showing low levels of CrAg. The best time to discontinue the antifungal therapy should be further discussed, and therefore, we proposed a hypothesis and plan to expand the dataset to establish a "gray zone" based on LFA and CLIA results. CrAg values below this "gray zone" might signal antifungal discontinuation, potentially reducing drug side effects and fungal resistance. This prompts the consideration of methodological limitations contributing to the continued detection of CrAg even in the absence of fungal growth.

There were also some shortcomings in this study. Firstly, there were two medical centers, covering only the southwest and eastern parts of China, which was not a good representation of the overall situation in China. Second, there were few data for drug and treatment monitoring, and this part can be further focused on in follow-up studies. In addition, the CLIA assay were not commercially available and it will take time to be used in the clinic.

TABLE 4 Baseline characteristics of three patients discontinuation of antifungal therapy.

Sample	Age	Gender	Clinical diagnosis	Sample type	CrAg titer (LFA)	S/CO (CLIA)
1	57	Female	Cryptococcal meningitis	Serum	1:10 (+)	3.365 (+)
2	48	Male	Cryptococcosis	Serum	1:2 (+)	0.144 (-)
3	47	Male	Cryptococcal meningitis	Serum	1:80 (+)	8.766 (+)

In conclusion, this study assessed a novel CLIA method for CrAg detection, demonstrating high consistency with the FDA-approved LFA method and exhibiting commendable specificity and sensitivity (both > 96.00%). Owing to methodological disparities, CLIA showcased superior application value compared to LFA for treatment monitoring, offering continuous reflection of CrAg concentration changes. Additionally, we anticipate that in subsequent studies, the establishment of a CrAg "gray zone" for patients with negative cultures could provide supplementary guidance for drug discontinuation decisions.

Data availability statement

The raw data supporting the conclusions of this article will be made available by the authors, without undue reservation.

Ethics statement

The studies involving humans were approved by Ethies Committce on Clinical Trial. West China Hospital of Sichunn University (No.202318). The studies were conducted in accordance with the local legislation and institutional requirements. The human samples used in this study were acquired from Samples were acquired from remaining samples after clinical testing. Written informed consent for participation was not required from the participants or the participants' legal guardians/next of kin in accordance with the national legislation and institutional requirements.

Author contributions

ZT: Conceptualization, Data curation, Formal analysis, Methodology, Software, Validation, Writing – original draft, Writing – review & editing. PX: Conceptualization, Data curation, Formal analysis, Writing – review & editing. ZW: Data curation, Investigation, Methodology, Writing – review & editing. TW: Formal analysis, Methodology, Resources, Software, Visualization, Writing – review & editing. DZ: Formal analysis, Resources, Visualization, Writing – review & editing. KA: Data curation, Methodology, Supervision, Writing – review & editing. HS: Formal analysis, Investigation, Methodology, Writing – review & editing. XY: Methodology, Project administration, Resources, Visualization, Writing – review & editing. DL: Project administration, Resources, Visualization, Writing – review & editing.

Funding

The author(s) declare that no financial support was received for the research, authorship, and/or publication of this article.

Conflict of interest

The authors declare that the research was conducted in the absence of any commercial or financial relationships that could be construed as a potential conflict of interest.

Publisher's note

Supplementary material

The Supplementary Material for this article can be found online at: https://www.frontiersin.org/articles/10.3389/fcimb.2024.1451539/full#supplementary-material

References

Baddley, J. W., Chen, S. C., Huisingh, C., Benedict, K., DeBess, E. E., Galanis, E., et al. (2021). MSG07: An International Cohort Study Comparing Epidemiology and Outcomes of Patients With Cryptococcus neoformans or Cryptococcus gattii Infections. *Clin. Infect. Dis.* 73, 1133–1141. doi: 10.1093/cid/ciab268

Benedict, K., Gold, J. A. W., Dietz, S., Anjum, S., Williamson, P. R., and Jackson, B. R.. (2022). Testing for cryptococcosis at a major commercial laboratory-United States, 2019-2021. *Open Forum Infect. Dis.* 9, ofac253. doi: 10.1093/ofid/ofac253

Bive, B. Z., Sacheli, R., Situakibanza Nani-Tuma, H., Kabututu Zakayi, P., Ka, A., Mbula Mambimbi, M., et al. (2022). Clinical epidemiology and high genetic diversity amongst Cryptococcus spp. isolates infecting people living with HIV in Kinshasa, Democratic Republic of Congo. *PLoS One* 17, e0267842. doi: 10.1371/journal.pone.0267842

Borges, M. A. S. B., Araújo Filho, J. A., Soares, R. B. A., Vidal, J. E., and Turchi, M. D. (2019). False-negative result of serum cryptococcal antigen lateral flow assay in an HIV-infected patient with culture-proven cryptococcaemia. *Med. Mycol Case Rep.* 26, 64–66. doi: 10.1016/j.mmcr.2019.10.009

Chen, M., Xu, N., and Xu, J. (2020). Cryptococcus Neoformans Meningitis Cases Among China's HIV-Infected Population may have been Severely Under-Reported. *Mycopathologia* 185, 971–974. doi: 10.1007/s11046-020-00491-4

Dubbels, M., Granger, D., and Theel, E. S. (2017). Low cryptococcus antigen titers as determined by lateral flow assay should be interpreted cautiously in patients without prior diagnosis of Cryptococcal infection. *J. Clin. Microbiol.* 55, 2472–2479. doi: 10.1128/JCM.00751-17

George, I. A., Spec, A., Powderly, W. G., and Santos, C. A. Q. (2018). Comparative epidemiology and outcomes of human immunodeficiency virus (HIV), non-HIV non-transplant, and solid organ transplant associated cryptococcosis: A population-based study. *Clin. Infect. Dis.* 66, 608–611. doi: 10.1093/cid/cix867

Hevey, M. A., George, I. A., Raval, K., Powderly, W.G., and Spec, A. (2019). Presentation and mortality of cryptococcal infection varies by predisposing illness: A retrospective cohort study. *Am. J. Med.* 132, 977–983.e1. doi: 10.1016/j.amjmed.2019.04.026

Jarvis, J. N., Tenforde, M. W., Lechiile, K., Milton, T., Boose, A., Leeme, T. B., et al. (2020). Evaluation of a novel semiquantitative cryptococcal antigen lateral flow assay in patients with advanced HIV disease. *J. Clin. Microbiol.* 58, e00441–e00420. doi: 10.1128/JCM.00441-20

Kamble, U., Dheeresh, K. H., Bhosale, K., Indu, M. B., Sharma, B., and Chowdhary, A. (2021). Evaluation of point of care serum cryptococcal antigen by lateral flow

immunoassay for diagnosis of cryptococcosis and cryptococcal meningitis in HIV-positive patients. *Indian J. Sex Transm Dis. AIDS.* 42, 14–18. doi: 10.4103/ijstd.IJSTD_94_19

Kwizera, R., Omali, D., Tadeo, K., Kasibante, J., Rutakingirwa, M. K., Kagimu, E., et al. (2021). Evaluation of the dynamiker cryptococcal antigen lateral flow assay for the diagnosis of HIV-associated cryptococcosis. *J. Clin. Microbiol.* 59, e02421–e02420. doi: 10.1128/JCM.02421-20

Langner, K. F. A., and Yang, W. J. (2022). Clinical performance of the IMMY cryptococcal antigen lateral flow assay in dogs and cats. *J. Vet. Intern. Med.* 36, 1966–1973. doi: 10.1111/jvim.16555

Li, H., Li, X., Zhang, L., Fang, W., Zhang, K., Arastehfar, A., et al. (2021). The clinical profiles and outcomes of HIV-negative cryptococcal meningitis patients in type II diabetes mellitus. *BMC Infect. Dis.* 21, 224. doi: 10.1186/s12879-021-05867-5

Li, J., and Guo, Y. (2024). A sandwich chemiluminescent magnetic microparticle immunoassay for cryptococcal antigen detection. *Expert Rev. Mol. Diagn.* 24, 533–540. doi: 10.1080/14737159.2024.2369243

Liang, B., Lin, Z., Li, J., Jiang, R., Zhan, W., and Jian, X. (2023). Diagnostic accuracy of cryptococcal antigen test in pulmonary cryptococcosis: a protocol for a systematic review and meta-analysis. *BMJ Open* 13, e070994. doi: 10.1136/bmjopen-2022-070994

Macrae, C., Ellis, J., Keddie, S. H., Falconer, J., Bradley, J., Keogh, R., et al. (2023). Diagnostic performance of the IMMY cryptococcal antigen lateral flow assay on serum and cerebrospinal fluid for diagnosis of cryptococcosis in HIV-negative patients: a systematic review. *BMC Infect. Dis.* 23, 209. doi: 10.1186/s12879-023-08135-w

Marr, K. A., Sun, Y., Spec, A., Lu, N., Panackal, A., Bennett, J., et al. (2020). Cryptococcus infection network cohort study working group. A multicenter, longitudinal cohort study of cryptococcosis in human immunodeficiency virus-negative people in the United States. *Clin. Infect. Dis.* 70, 252–261. doi: 10.1093/cid/ciz193

McHale, T. C., Boulware, D. R., Kasibante, J., Ssebambulidde, K., Skipper, C. P., and Abassi, M. (2023). Diagnosis and management of cryptococcal meningitis in HIV-infected adults. *Clin. Microbiol. Rev.* 28, e0015622. doi: 10.1128/cmr.00156-22

Noguera, M. C., Escandón, P., Rodríguez, J., Parody, A., and Camargo, L. (2021). Comparison of two commercial tests (Immy vs. Dynamiker) for cryptococcal capsular antigen. *Rev. Soc. Bras. Med. Trop.* 54, e03072021. doi: 10.1590/0037-8682-0307-2021

Osaigbovo, I. I., and Bongomin, F. (2021). Point of care tests for invasive fungal infections: a blueprint for increasing availability in Africa. *Ther. Adv. Infect. Dis.* 8, 20499361211034266. doi: 10.1177/20499361211034266

Pinheiro, S. B., Sousa, E. S., Cortez, A. C. A., da Silva Rocha, D. F., Menescal, L. S. F., Chagas, V. S., et al. (2021). Cryptococcal meningitis in non-HIV patients in the State of Amazonas, Northern Brazil. *Braz. J. Microbiol.* 52, 279–288. doi: 10.1007/s42770-020-00383-1

Rajasingham, R., Govender, N. P., Jordan, A., Loyse, A., Shroufi, A., Denning, D. W., et al. (2022). The global burden of HIV-associated cryptococcal infection in adults in 2020: a modelling analysis. *Lancet Infect. Dis.* 22, 1748–1755. doi: 10.1016/S1473-3099(22)00499-6

Rajasingham, R., Smith, R. M., Park, B. J., Jarvis, J. N., Govender, N. P., Chiller, T. M., et al. (2017). Global burden of disease of HIV-associated cryptococcal meningitis: an updated analysis. *Lancet Infect. Dis.* 17, 873–881. doi: 10.1016/S1473-3099(17)30243-8

Skipper, C., Tadeo, K., Martyn, E., Nalintya, E., Rajasingham, R., Meya, D. B., et al. (2020). Evaluation of serum cryptococcal antigen testing using two novel semiquantitative lateral flow assays in persons with cryptococcal antigenemia. *J. Clin. Microbiol.* 58, e02046–e02019. doi: 10.1128/JCM.02046-19

Tadeo, K. K., Nimwesiga, A., Kwizera, R., Apeduno, L., Martyn, E., Okirwoth, M., et al. (2021). Evaluation of the diagnostic performance of a semiquantitative cryptococcal antigen point-of-care assay among HIV-infected persons with cryptococcal meningitis. *J. Clin. Microbiol.* 59, e0086021. doi: 10.1128/JCM.00860-21

Tenforde, M. W., Boyer-Chammard, T., Muthoga, C., Tawe, L., Milton, T., Rulaganyang, I., et al. (2020). Diagnostic accuracy of the biosynex cryptoPS cryptococcal antigen semiquantitative lateral flow assay in patients with advanced HIV disease. *J. Clin. Microbiol.* 59, e02307–e02320. doi: 10.1128/JCM.02307-20

Tugume, L., Ssebambulidde, K., Kasibante, J., Ellis, J., Wake, R. M., Gakuru, J., et al. (2023). Cryptococcal meningitis. *Nat. Rev. Dis. Primers.* 9, 62. doi: 10.1038/s41572-023-00472-z

Wang, C., Li, R., Ma, C., Du, J., and Gu, L. (2022). Early diagnosis of disseminated cryptococcosis by cryptococcal antigen lateral-flow assay. *J. Microbiol. Immunol. Infect.* 55, 177–179. doi: 10.1016/j.jmii.2021.08.006

Wang, X., Cheng, J. H., Zhou, L. H., Zhu, J. H., Wang, R. Y., Zhao, H. Z., et al. (2020). Evaluation of low cryptococcal antigen titer as determined by the lateral flow assay in serum and cerebrospinal fluid among HIV-negative patients: a retrospective diagnostic accuracy study. *IMA Fungus.* 11, 6. doi: 10.1186/s43008-020-00028-w

Ware, C., Meledathu, S., Tariq, Z., Yee, R., Lichtenberger, J. P. 3rd, and Siegel, M. O. (2023). Cryptococcal pneumonia and meningitis in a renal transplant recipient with a false negative serum cryptococcal antigen due to postzone phenomenon. *IDCases* 34, e01898. doi: 10.1016/j.idcr.2023.e01898

Zhang, L., Wang, S., Hong, N., Li, M., Liu, Y., Zhou, T., et al (2023). Genotypic diversity and antifungal susceptibility of Cryptococcus neoformans species complex from China, including the diploid VNIII isolates from HIV-infected patients in Chongqing region. *Med. Mycol.* 61, myad119. doi: 10.1093/mmy/myad119

Zhao, H., Zhou, M., Zheng, Q., Zhu, M., Yang, Z., Hu, C., et al. (2021). Clinical features and Outcomes of Cryptococcemia patients with and without HIV infection. *Mycoses* 64, 656–667. doi: 10.1111/myc.13261

frontiers | Frontiers in Cellular and Infection Microbiology

TYPE Original Research
PUBLISHED 09 December 2024
DOI 10.3389/fcimb.2024.1456119

OPEN ACCESS

EDITED BY
Ariadna Petronela Fildan,
Ovidius University, Romania

REVIEWED BY
Ajoy Kumar Verma,
National Institute of Tuberculosis and Respiratory Diseases, India
Emil Robert Stoicescu,
Victor Babes University of Medicine and Pharmacy, Romania

*CORRESPONDENCE
Huaying Zhou
zhouhuaying200@csu.edu.cn

RECEIVED 28 June 2024
ACCEPTED 12 November 2024
PUBLISHED 09 December 2024

CITATION
Ma J, Jiang Y, He Y and Zhou H (2024) The value of metagenomic next-generation sequencing with blood samples for the diagnosis of disseminated tuberculosis. *Front. Cell. Infect. Microbiol.* 14:1456119. doi: 10.3389/fcimb.2024.1456119

The value of metagenomic next-generation sequencing with blood samples for the diagnosis of disseminated tuberculosis

Jing Ma[1], Yongfang Jiang[1,2,3], Yan He[1] and Huaying Zhou[1]*

[1]Department of Infectious Diseases, the Second Xiangya Hospital, Central South University, Changsha, Hunan, China, [2]FuRong Laboratory, Changsha, Hunan, China, [3]Clinical Medical Research Center for Viral Hepatitis in Hunan Province, Changsha, Hunan, China

Objective: The aim of this study was to assess the clinical value of metagenomic next-generation sequencing (mNGS) of blood samples for the identification of disseminated tuberculosis (DTB).

Methods: A total of 48 individuals suspected of DTB were enrolled. All patients underwent mNGS of peripheral blood and conventional microbiological tests. Patient characteristics were collected from their medical records.

Results: A total of 28 patients were diagnosed with DTB, whereas 20 patients were confirmed as non-DTB cases. In the DTB groups, 19 (67.9%) contained TB sequences, with specific reads of TB ranging from 1 to 219. The TB sequence was more detectable by mNGS in male patients, those with elevated PCT levels, those who are HIV positive, and those with a decreased CD4 T-cell count. The HIV-positive group shows higher TB mNGS reads (p = 0.012) and TB mNGS sensitivity (p = 0.05). The sensitivity of TB mNGS in blood samples was 80% for HIV-infected patients and 44.4% for non-HIV-infected individuals (p = 0.05). The non-HIV group had a higher prevalence of miliary tuberculosis (p = 0.018), and extrapulmonary tuberculosis was more prevalent in the HIV-positive group.

Conclusion: Our research has shown that the mNGS of blood samples has excellent sensitivity for the diagnosis of DTB. The TB sequence was more detectable by mNGS in patients with elevated PCT levels, those who are HIV positive, and those with a decreased CD4 T-cell count.

KEYWORDS

metagenomic next-generation sequencing, peripheral blood, disseminated tuberculosis, clinical diagnosis, diagnosis performance

Introduction

Tuberculosis (TB) is the leading cause of morbidity and mortality in the HIV and non-HIV immunocompromised populations. TB primarily targets the respiratory system but can disseminate to other organs in the body. Disseminated TB (DTB), also known as miliary TB (MTB), is characterized by the systemic spread of the disease through tiny millet-sized lesions (1–4 mm) that can rapidly develop in various organs. DTB has become increasingly diagnosed in adults due to the growing prevalence of immunocompromising conditions such as diabetes, malignancy, and HIV/AIDS infections, as well as the increased use of immunosuppressive medications (Abuabat et al., 2023; Shafer et al., 1991; Sharma et al., 2012, 2016; Hassanein and Elbadry, 2016).

Diagnosing DTB is challenging due to nonspecific symptoms, atypical presentations, difficulties getting patient samples, and false-negative findings, leading to a delay in the diagnosis and increased mortality (Sharma et al., 2012; Hassanein and Elbadry, 2016). DTB has received less research attention than other forms of TB, at least in part because mycobacterial blood cultures are unavailable in most high-burden settings and have limited diagnostic value because median time to positivity is longer than median time from admission to death in fatal cases of DTB.

Metagenomic next-generation sequencing (mNGS) has been used to identify specific infectious pathogens in a timely, unbiased, and hypothesis-free manner (Zhang et al., 2014; Pang et al., 2024; Wu et al., 2024; Li et al., 2023; Liu et al., 2023; Gao et al., 2024; Shi et al., 2021; Zhou et al., 2019). It also has the ability to recognize co-infecting microbes. Furthermore, research indicates that mNGS can detect hematologic dissemination using blood tests, which may obviate the need for invasive procedures (Pang et al., 2024; Wu et al., 2024; Zhou et al., 2019). In recent years, accumulating data showed that mNGS is effective for diagnosing TB in direct clinical samples with excellent accuracy and specificity (Li et al., 2023; Liu et al., 2023; Gao et al., 2024; Shi et al., 2021; Zhou et al., 2019). Nevertheless, no research assessed the diagnostic accuracy of mNGS in patients with DTB. In this study, we explored the diagnostic efficacy of mNGS in DTB patients using blood samples.

Patients and methods

This retrospective analysis consecutively enrolled 48 suspected DTB patients admitted to the Second Xiangya Hospital, Central South University (Changsha, China) from 1 May 2021 to 31 May 2024. Patients were eligible for enrollment if they met all the following criteria: (1) consent to undergo the plasma mNGS examination and (2) suspected DTB. Patients were excluded if they met any of the following criteria: (1) incomplete medical record and (2) patients already receiving antituberculosis therapy. Suspected DTB patients were included if they met at least one of the following criteria: (1) miliary pattern on chest imaging and (2) suspected bloodstream infections and TB exposure history. The final clinical diagnostic criteria for DTB include the following: (1) identifying either a miliary pattern on chest imaging and a positive MTB in sputum (culture, acid-fast staining smears, Xpert, or NGS) or lung biopsy showing granulomas, (2) active TB clinical manifestations and positive plasma mNGS results for MTB, or (3) detecting caseating granulomas in a biopsy from any other organ, along with the presence of a miliary pattern on chest imaging or a positive sputum culture for MTB. In the absence of microbiological evidence, the attending physician may diagnose DTB infection clinically by relating the patient's clinical manifestations and imaging results to exclude other diseases, together with the patient's confirmed responsiveness to anti-TB treatment after 1 month of follow-up. This study was approved by the Research Ethics Committee of the Second Xiangya Hospital, and the need for written informed consent was waived owing to its retrospective design.

Clinical data collection

Data were collected from the patients' medical records. The following details at diagnosis were gathered: demographics, presenting symptoms, imaging, and histopathological data, as well as risk factors and mortality rates. Mycobacterial blood culture and TB polymerase chain reaction (PCR)-based assays of blood samples cannot be collected due to the limitations of routine methods. In cases of incomplete data, historical manual files were retrieved and examined.

Detection method (mNGS)

Specimens were obtained from patients according to standard procedures. Briefly, 3 mL of blood was collected in sterile DNase-free tubes. Plasma was separated by centrifuging the blood at 1,600 × *g* at 4°C for 10 min within 8 h of collection. Using high-throughput sequencing technology, the DNA sequence of the microorganisms in the sample was obtained and compared with that of the microbial gene bank to identify pathogenic microorganisms. The detection process includes nucleic acid extraction, library construction, computer sequencing, bioinformatic analysis, and report interpretation (Liu et al., 2023). The detection process was based on the Illumina NextSeq550Dx (Illumina) sequencing system, and reference databases for classification were downloaded from NCBI. RefSeq contains 11,958 bacterial genomes or scaffolds, 1,714 fungi related to human infection, 7,373 whole-genome sequences of viral taxa, and 343 parasites associated with human diseases. The number of TB reads was defined as the number of unique reads for the standardized species. MTB was considered positive when the mapping read number (genus or species level) was in the top 20 in the bacteria list (Miao et al., 2018).

Statistical analysis

Continuous data are deemed as nonparametric. Continuous variables were expressed as median and interquartile range (IQR),

and the Shapiro–Wilk test ($p < 0.05$) was used for continuous variables that exhibited non-normal distribution. The categorized data were represented by case number (n) and percentage (%). The chi-square test (McNemar test) was employed for comparison. $p < 0.05$ was statistically significant without adjustment for multiple tests. All analyses were conducted with the IBM SPSS statistical software, version 26.0.

Results

Patient profiles

Among 48 individuals with suspected DTB infection, 20 were identified as non-DTB cases (Figure 1). A total of 28 cases were confirmed DTB. Table 1 summarizes the demographic characteristics of the 28 enrolled individuals diagnosed with DTB. The median age was 55 years, nearly 50% were over 60 years old, and 17 individuals (60.7%) were male. The predominant risk factor was HIV infection, present in 10 (35.7%) patients. Diabetes or pneumoconiosis was observed in four patients (14.3%); chronic liver disease was detected in 7.14% of patients; chronic kidney disease, anorexia, or pregnancy was observed in 3.6% of patients; and four (14.3%) patients had immunocompromising conditions, including malignancy or use of immunosuppressive agents. The most common presenting symptoms observed were fever, fatigue, and weight loss, occurring in 24 (85.7%), 20 (71.4%), and 23 (82.1%) patients, respectively. Cough was reported in 10 (35.7%) patients, night sweats in 14 (50%) patients, and hepatosplenomegaly in 16 (57.1%) patients. Regarding the anatomical site of TB infection at the time of diagnosis, the majority of patients had pulmonary MTB, which accounted for over half of the cases (16 patients; 57.1%). TB lymphadenitis and gastrointestinal involvement were the second most common sites, observed in six patients (21.4%), followed by pleural or peritoneal involvement in four patients(14.3%); and urogenital TB in one patient (3.6%).

Table 2 outlines the most frequently observed laboratory findings in the study population. The most common laboratory abnormality was elevated ESR, present in 26 (92.9%) patients. Anemia was the second most prevalent laboratory finding, observed in 25 (89.3%) patients. Elevated liver enzymes were also frequently observed, with aspartate aminotransferase elevated in 12 (42.9%) patients, and alanine transaminase elevated in 11 (39.3%) patients. Leukopenia was present in 2 (7.14%) patients, thrombocytopenia in 4 (14.3%) patients, thrombocytosis or leukocytosis in 7 (25%) patients, and elevated creatinine in 7 (25%) patients. Positive T-SPOT.TB results were reported in 23 (82.1%) patients. CD4 T-cell subsets in the peripheral blood were analyzed in 22 individuals, of whom 16 (72.7%) showed a reduction. mNGS of blood samples was conducted on all patients; 19 (67.9%) contained TB sequences, with specific reads of TB ranging from 1 to 219. TB sequences were identified in 15 patients (53.6%) with over two reads and in 12 patients (42.9%) with over three reads. A total of 18 acid-fast bacilli (AFB) smears from sputum, pleural, or ascitic fluid were performed, of which 8 showed positive results. Bronchoalveolar lavage was performed five times, with two positive results. X-pert MTB/RIF was taken 14 times, with 6 positive outcomes. Positive biopsy results were observed in four patients with caseating granuloma.

Comparison of clinical features of DTB in patients with HIV infection and non-HIV infection

Table 3 assesses the clinical characteristics of 18 DTB persons with non-HIV infections and 10 DTB patients with HIV infections. The HIV-positive group exhibits elevated TB mNGS readings ($p = 0.012$) and TB mNGS sensitivity ($p = 0.05$) compared to the non-HIV group. The sensitivity of TB mNGS in blood samples was 80% for HIV-infected patients and 44.4% for non-HIV-infected individuals ($p = 0.05$). The non-HIV cohort had a higher

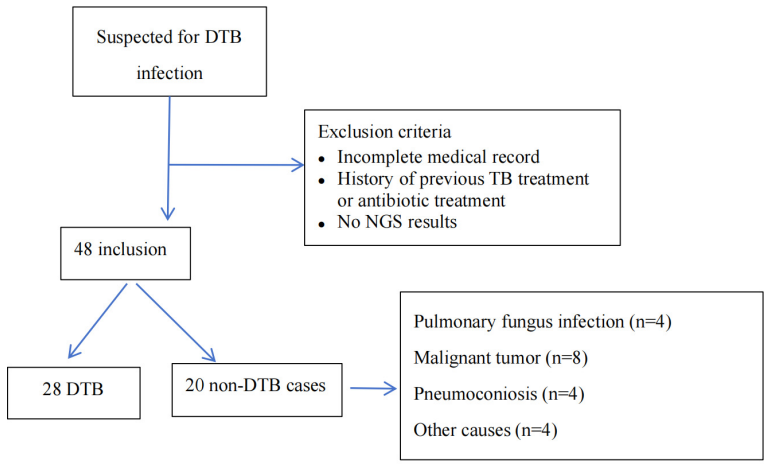

FIGURE 1
Flowchart of enrollment, exclusion criteria, and study procedures, by mNGS blood assay result. DTB, disseminated TB; NGS, next-generation sequencing.

10.3389/fcimb.2024.1456119

TABLE 1 Demographic characteristics.

Characteristics [median (IQR) or *n* (%)]	*n* (%)
Age (years)	55 (38.75–64.75)
Elders (age ≥ 60 years)	13 (46.4%)
Male, *n* (%)	17 (60.7%)
Comorbidities	
HIV positive	10 (35.7%)
Chronic liver disease	2 (7.14%)
Diabetes	4 (14.3%)
Immunosuppression	4 (14.3%)
CKD	1 (3.6%)
Pneumoconiosis	4 (14.3%)
pregnancy	1 (3.6%)
Anorexia	1 (3.6%)
Symptoms	
Fever	24 (85.7%)
Cough	10 (35.7%)
Weight loss	23 (82.1%)
Night sweats	14 (50%)
Fatigue	20 (71.4%)
Hepatosplenomegaly	16 (57.1%)
TB type	
Miliary	16 (57.1%)
Lymphadenitis	6 (21.4%)
CNS	2 (7.14%)
Skeletal	2 (7.14%)
Gastrointestinal	6 (21.4%)
Pleural or Peritoneal	4 (14.3%)
Urogenital	1 (3.6%)
Hepatosplenic	2 (7.14%)

IQR, interquartile range; HIV, human immunodeficiency; CKD, chronic kidney disease; CNS, central nervous system.

TABLE 2 Laboratory findings.

	N = 28 (%)
Elevated ESR	26 (92.9%)
Anemia	25 (89.3%)
Leukopenia	2 (7.14%)
Thrombocytopenia	4 (14.3%)
Thrombocytosis	7 (25%)
Leukocytosis	7 (25%)
Elevated ALT	11 (39.3%)
Elevated AST	12 (42.9%)
Elevated creatinine	7 (25%)
Positive T-SPOT.TB results	23 (82.1%)
Decreased CD4 cells	16/22
TB reads by plasma mNGS > 2	15 (53.6%)
TB reads by plasma mNGS > 3	12 (42.9%)
Positive TB by plasma mNGS	19 (67.9%)
AFB smears taken	18
Positive AFB smears	8
BAL done	5
Positive BAL results	2
Xpert® MTB/RIF taken	14
Positive Xpert® MTB/RIF	6
Positive biopsy result	4

ESR, erythrocyte sedimentation rate; ALT, alanine aminotransferase; AST, aspartate aminotransferase; TB, tuberculosis; mNGS, metagenomic next-generation sequencing; AFB, acid-fast bacilli; BAL, bronchoalveolar lavage.

prevalence of MTB ($p = 0.018$), but extrapulmonary TB was more prevalent in the HIV-positive group. An older age was observed, although it lacked statistical significance in the non-HIV groups. No significant differences were seen between the two groups in regard to AST, ALT, WBC, HB, PLT, CRP, PCT, and Cr levels.

Comparison of clinical features of DTB in mNGS-positive and -negative patients with TB

Table 4 illustrates that mNGS of blood samples was performed in all patients; the diagnostic sensitivity of mNGS was calculated using the clinical composite diagnosis as reference standard. TB was identified by mNGS in 19 (67.9%) cases. The sensitivity of mNGS was 67.9%. In a comparison of TB mNGS-positive and -negative groups, TB sequences were more detectable by mNGS in male patients, those with elevated PCT levels, those who are HIV positive, and those with a decreased CD4 T-cell count. There were no significant differences between the two groups in terms of age, AST, ALT, WBC, HB, PLT, CRP, and Cr levels.

Diagnostic performance of blood mNGS and T-SPOT.TB assay in confirmed DTB

We assessed the diagnostic performance for blood mNGS and T-SPOT.TB methods compared with the clinical final diagnosis of DTB (Figure 2). Of the 28 patients with confirmed DTB, 23 cases were detected by T-SPOT.TB, with a positive rate of 82.1%, while mNGS found 19 cases, with a positive rate of 67.8%. Among the 19 patients with positive mNGS, 4 patients had negative T-SOPT.TB assays, whereas the remaining 15 patients had both positive mNGS and T-SPOT.TB assay. In these 28 patients, the positive rates of mNGS and TSPOT were not ($p > 0.05$) statistically different. With

10.3389/fcimb.2024.1456119

TABLE 3 Comparison of clinical features of DTB in patients with HIV infection and non-HIV infection.

Characteristics [median (IQR) or n (%)]	HIV Positve (10)	HIV Negative (18)	p
Age (years)	48.50 (28.50-61.50)	59.00 (40.25-72.25)	0.861
Elders (age>=60 years)	3 (30%)	10 (55.6%)	0.206
Male, n (%)	7 (70%)	10 (55.6%)	0.206
WBC	6.88 (5.80-9.85)	6.46 (5.37-13.90)	0.205
HB	93.00 (74.25-110.50)	85.00 (74.00-108.75)	0.886
PLT	257.00 (162.75-308.50)	203.00(124.25-326.25)	0.714
CRP	48.41(34.15-80.69)	75.43 (42.47-121.73)	0.968
ESR	68.50 (57.00-101.00)	53.00 (27.50-96.50)	0.896
PCT	0.51 (0.12-0.80)	0.75 (0.43-2.88)	**0.003**
ALT	31.60 (19.60-57.10)	24.10 (13.88-64.25)	0.769
AST	30.35 (26.58-52.60)	41.50 (26.05-61.98)	0.967
CD4	23.5(9.75-64.00)	218(121.00-408.00)	**0.012**
Military	2 (20%)	14 (82.3%)	**0.018**
TB mNGS sensitivity	8 (80.0%)	11 (44.4%)	**0.050**
Postive T-SPOT.TB results	9 (90.0%)	14 (82.3%)	0.080
TB reads by mNGS	3.00 (0.75-9.75)	1.00 (0-9.25)	**0.012**

DTB; disseminated tuberculosis; HIV, human immunodeficiency; IQR, interquartile range; WBC, white blood cell; HB, hemoglobin; PLT, platelets; CRP, C-reactive protein; ESR, erythrocyte sedimentation rate; PCT, procalcitonin; ALT, alanine aminotransferase; AST, aspartate aminotransferase; mNGS, metagenomic next-generation sequencing; TB, tuberculosis.
The bold values mean statistically significant values.

TABLE 4 Comparison of clinical features of DTB in mNGS-positive and mNGS-negative patients with TB.

Characteristics [median (IQR) or n (%)]	mNGS positive (19)	mNGS negative (9)	p
Age (years)	55.00(46.00-60.00)	59.00(34.50-71.50)	0.908
Elders (age>=60 years)	8 (42.1%)	5 (55.5%)	0.739
Male, n (%)	14(73.7%)	3(33.3%)	**0.039**
WBC	6.75(4.36-12.41)	6.61(6.15-14.06)	0.555
HB	91.00(70.00-104.00)	86.00(75.50-110.50)	0.751
PLT	201.00(150.00-279.00)	303(154.50-463.50)	0.957
CRP	56.88(44.22-56.88)	44.09(18.8-131.91)	0.686
ESR	60.00(35.25-84.75)	88.00(37.5-100.00)	0.872
PCT	0.67(0.44-2.27)	0.63(0.12-2.05)	**0.021**
ALT	27.60(20.60-64.00)	22.60(9.70-51.00)	0.832
AST	33.30(26.80-64.00)	32.10(21.70-57.30)	0.422
Cr	69.50(53.00-91.50)	66.00(47.00-93.40)	0.973
Hepatosplenomegaly	11 (57.9%)	5 (55.6%)	0.491
Positive T-SPOT.TB results	15(78.9%)	8(88.9%)	0.220
CD4	71.00(17.75-160.25)	147.00(37-354.00)	**0.010**
Military	10 (52.6%)	6(66.6%)	0.491
HIV positive	8(42.1%)	2 (22.2%)	**0.009**

DTB, disseminated tuberculosis; TB, tuberculosis; mNGS, metagenomic next-generation sequencing; IQR, interquartile range; WBC, white blood cell; HB, hemoglobin; PLT, platelets; CRP, C-reactive protein; ESR, erythrocyte sedimentation rate; PCT, procalcitonin; ALT, alanine aminotransferase; AST, aspartate aminotransferase; Cr, creatinine; HIV, human immunodeficiency.
The bold values mean statistically significant values.

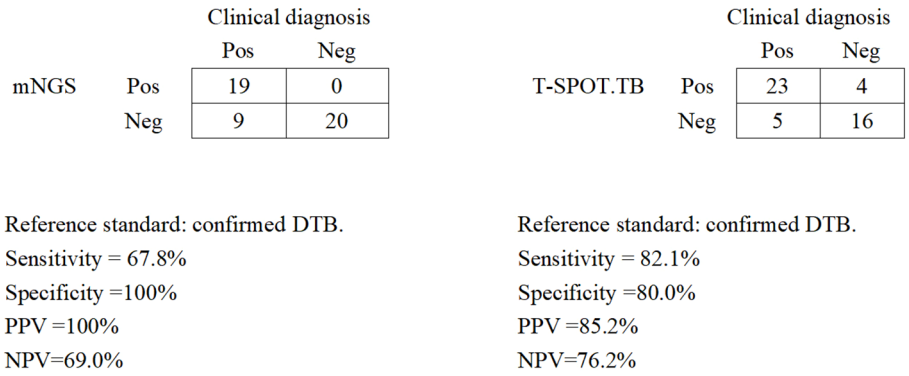

FIGURE 2
Diagnostic performance of mNGS and the T-SPOT.TB assay for DTB using blood samples. Pos, positive; Neg, negative; mNGS, metagenomic next-generation sequencing; DTB, disseminated tuberculosis; PPV, positive predictive value; NPV, negative predictive value.

clinically confirmed DTB as the reference standard, mNGS demonstrated a clinical sensitivity of 67.8%, a clinical specificity of 100%, a positive predictive value of 100%, and a negative predictive of 69.0%. With clinically verified DTB as the reference standard, the T-SPOT.TB assay had a clinical sensitivity of 82.1%, a clinical specificity of 80%, a positive predictive value of 85.2%, and a negative predictive value of 76.2%.

Discussion

In light of the continuing HIV/AIDS epidemic and increasing use of immunosuppressive and cytotoxic drugs, the burden of DTB will continue to rise (Meira et al., 2019). DTB is a notoriously difficult disease to diagnose, with nonspecific symptoms and clinical abnormalities that are shared by many other infectious and noninfectious diseases. Mortality from this disease has remained high despite effective therapy being available. The early, timely, and correct diagnosis of DTB is a key factor for reducing mortality. This study applied mNGS of blood samples to evaluate its diagnostic efficacy for DTB and chose the use of clinical diagnosis rather than mycobacterial blood culture as a comparison because of the limitation of routine methods. Despite the lack of culture for clinical diagnosis, pathological findings and follow-up greatly reduced the possibility of misdiagnosis.

This study revealed HIV infection as the most prevalent risk factor for DTB, accounting for 35.7%; other risk factors were pharmacological immunosuppression, diabetics, chronic liver disease, and chronic kidney disease. Consistent with those reported in the literature (Ye et al., 2021; Crump et al., 2012; Kerkhoff et al., 2017), the importance of cell-mediated immunity was further illustrated by the inverse correlation found between the CD4+ T-cell count in HIV patients and the frequency of cases of DTB. Previous studies have highlighted the prognostic value of T-cell count in this context (Ye et al., 2021; Crump et al., 2012).

Several investigations from Africa with blood culture have shown that TB is a common cause of bloodstream infections (Crump et al., 2012; Kerkhoff et al., 2017). Blood is an attractive sample type for diagnosing DTB, especially for HIV-infected individuals, due to their higher probability of sputum culture-negative, disseminated, or extrapulmonary TB. Various studies on *Mycobacterium tuberculosis* bacteremia have established the potential of blood for TB detection by both culture and nucleic acid amplification test (NAAT) (Lima et al., 2009; Taci et al., 2003).

Mycobacterial blood culture is not available in most settings. Even where available, an average 3-week delay between culture and identification, combined with high early mortality, means that TB blood culture has limited diagnostic value. NAAT-based *M. tuberculosis* bacteremia studies have had different results, with sensitivities of TB detection in peripheral blood of 2% to 55% (Lima et al., 2009; Taci et al., 2003; Rebollo et al., 2006). Patients with DTB are at high risk for early death, and this sequential approach to empirical therapy introduces a potentially fatal delay in the commencement of anti-TB chemotherapy (ATC). Rapid testing of blood for TB with the mNGS may facilitate the rapid diagnosis of DTB and consequently the early initiation of ATC. Our findings revealed that 19 blood samples contained TB sequences from 28 diagnoses as DTB, indicating that plasma mNGS had a high sensitivity (67.9%) and that circulating cfDNA sequencing contributed to an improvement in the diagnosis of DTB. Our results demonstrated that TB sequence was more detectable by plasma mNGS in patients with HIV infection, elevated PCT levels, and decreased CD4 T-cell count. Patients who were HIV positive had higher TB mNGS reads and TB mNGS sensitivity. The sensitivity of TB mNGS in blood samples was 80% for HIV-infected patients and 44.4% for non-HIV-infected individuals. The data also revealed that immunocompromised patients were more likely to yield positive mNGS results, and detection of *M. tuberculosis* bacteremia by mNGS was rapid and had high specificity (100%) and high sensitivity (67.9%) compared to blood culture and NAAT.

In the diagnostic specificity of DTB, mNGS is better than T-SPOT.TB, although the T-SPOT.TB assay is slightly more sensitive than mNGS for DTB; a cost/time trade-off would be beneficial. In China, the mNGS test costs between $300 and $450 per sample, whereas the cost of the TSOPT.TB assay ranges from approximately $84 to $100. The detection period for mNGS is 1 day, while the detection time for TSPOT.TB assay takes approximately 48 h, and

research indicates that mNGS can identify drug-resistant genes or mixed pathogens, altering the therapeutic management of TB patients and reducing the cost-effectiveness (Brown et al.,2015; Doyle et al.,2018; Votintseva et al., 2017).

mNGS is not recommended for routine use in mild/moderate infections due to its high cost (Chiu and Miller, 2019; Miller et al., 2018). Nonetheless, it is necessary to carry out adequate development in complex patients. MTB is an intracellular bacterium, and its DNA extraction is challenging, which may result in reduced susceptibility to mNGS. Moreover, the false positives of mNGS should be carefully monitored and assessed. MTB is not a common background bacteria in laboratory settings; the possibility for contamination of MTB in blood samples is lower than that in other sample types. Therefore, even when one specific read of a taxon is mapped to either the species or genus level, MTB infection should be considered. MTB was considered positive if it meets the following criteria: (1) its genus or species level is among the top 20 with the highest standardized specific reading number (SDSMRN); (2) it ranks first within its genus; and (3) its SDSMRN exceeds 1. To reduce the risk of contamination introduced before mNGS procedures, we made a strict sterile procedure during sample collection and a relative nucleic acid-free guideline during specimen preparation. In addition, two independent experienced clinics analyzed the mNGS results to see whether they were in accordance with the patient's clinical manifestation and diagnosis.

There are some limitations to this study. First, the sample size included was relatively small, comprising only 28 cases. Thus, the sensitivity of diagnosis DTB for mNGS may not be accurately evaluated, *M. tuberculosis* bloodstream infection is underdiagnosed, false negatives will increase, and the negative predictive value could be overestimated. Prospective studies with a bigger sample size are needed to further evaluate the diagnostic value of mNGS in DTB. Second, the patients included did not undergo traditional culture; comparative analysis with conventional methods was limited by lack of information; therefore, prospective studies are needed to compare mNGS with traditional detection methods. Third, biases resulting from the selection and referral processes are potentially important, since these investigations were conducted in single centers. Despite some limitations, this investigation provides useful insights into the clinical value of plasma mNGS for identifying DTB. A comprehensive, multicenter study is needed to verify our findings.

In conclusion, our study showed that mNGS of blood samples exhibits exceptional sensitivity for diagnosing DTB. The TB sequence was more detectable by peripheral blood mNGS in patients who were HIV positive or with other immunosuppressive diseases. Blood mNGS should be conducted when diagnosing DTB is challenging, particularly in areas with a high prevalence of HIV presenting with severe sepsis in order to prevent the high early death rate. However, further refinement and larger-scale validation studies are necessary, especially in HIV-positive or other immunosuppressive populations.

Data availability statement

The raw data supporting the conclusions of this article will be made available by the authors, without undue reservation.

Ethics statement

The studies involving humans were approved by Ethics Committee of the Second Xiangya Hospital of the Central South University. The studies were conducted in accordance with the local legislation and institutional requirements. Written informed consent for participation was not required from the participants or the participants' legal guardians/next of kin in accordance with the national legislation and institutional requirements.

Author contributions

JM: Writing – original draft. YJ: Formal analysis, Funding acquisition, Writing – review & editing. YH: Formal analysis, Data curation, Supervision, Writing – review & editing. HZ: Conceptualization, Project administration, Writing – review & editing.

Funding

The author(s) declare financial support was received for the research, authorship, and/or publication of this article. This study was supported by grants from the Scientific Research Program of FuRong Laboratory (No. 2023SK2108), the Clinical Medical Research Center for Viral Hepatitis in Hunan Province (No. 2023SK4009), and the Hunan Provincial Health Commission Research Program (No. 202303088786).

Conflict of interest

The authors declare that the research was conducted in the absence of any commercial or financial relationships that could be construed as a potential conflict of interest.

Publisher's note

References

Abuabat, F., Badri, M., and Abuabat, S. (2023). Sultan Alsultan, Salim Baharoon, Abdullah Alharbi,et al; Disseminated tuberculosis: Clinical presentation, diagnosis, and outcomes in a tertiary-care hospital in Saudi Arabia. *Int. J. Mycobacteriol* 12, 407–411. doi: 10.4103/ijmy.ijmy_141_23

Brown, A. C., Bryant, J. M., and Einer-Jensen, K. (2015). Rapid whole-genome sequencing of Mycobacterium tuberculosis isolates directly from clinical samples, et al; Rapid whole-genome sequencing of Mycobacterium tuberculosis isolates directly from clinical samples. *J. Clin. Microbiol.* 53, 2230–2237. doi: 10.1128/JCM.00486-15

Chiu, C. Y., and Miller, S. A. (2019). Clinical metagenomics. *Nat. Rev. Genet.* 20, 341–355. doi: 10.1038/s41576-019-0113-7

Crump, J. A., Ramadhani, H. O., Morrissey, A. B., Morrissey, A. B., Saganda, W., Mwako, M. S., et al. (2012). Bacteremic disseminated tuberculosis in sub-saharan Africa: a prospective cohort study. *Clin. Infect. Dis.* 55, 242—250. doi: 10.1093/cid/cis409

Doyle, R. M., Burgess, C., Williams, R., Gorton, R., Booth, H., Brown, J., et al. (2018). Direct whole-genome sequencing of sputum accurately identifies drugresistant Mycobacterium tuberculosis faster than MGIT culture sequencing. *J. Clin. Microbiol.* 56, e00666–e00618. doi: 10.1128/JCM.00666-18

Gao, J., Zhao, L., Chen, G., Huang, C., Kong, W., Feng, Y., et al. (2024). The value of metagenomic next-generation sequencing for the diagnosis of pulmonary tuberculosis using bronchoalveolar lavage fluid. *Lab. Med.* 55, 96–102. doi: 10.1093/labmed/lmad041

Hassanein, H. A., and Elbadry, M. I. (2016). Selective immunoglobulin M deficiency in an adult with miliary tuberculosis: A clinically interesting coexistence. A case report and review of the literature. *Int. J. Mycobacteriol.* 5, 106–110. doi: 10.1016/j.ijmyco.2015.11.002

Kerkhoff, A. D., Barr, D. A., Schutz, C., Burton, R., Nicol, M. P., Lawn, S. D., et al. (2017). Disseminated tuberculosis among hospitalised HIV patients in South Africa: a common condition that can be rapidly diagnosed using urine-based assays. *Sci. Rep.* 7, 10931. doi: 10.1038/s41598-017-09895-7

Li, Y., Bian, W., Wu, S., Zhang, J., and Li, D. (2023). Metagenomic next-generation sequencing for Mycobacterium tuberculosis complex detection: a meta-analysis. *Front. Public. Health* 11. doi: 10.3389/fpubh.2023.1224993

Lima, J., Montenegro, L., de Albuquerque, M., Cabral, M., Lima, A., Abath, F., et al. (2009). Performance of nested PCR in the specific detection of Mycobacterium tuberculosis complex in blood samples of pediatric patients. *J. Bras. Pneumol.* 35, 690–6697. doi: 10.1590/S1806-37132009000700011

Liu, Y., Wang, H., Li, Y., and Yu, Z. (2023). Clinical application of metagenomic next-generation sequencing in tuberculosis diagnosis. *Front. Cell. Infect. Microbiol.* 12. doi: 10.3389/fcimb.2022.984753

Meira, L., Chaves, C., Araújo, D., Almeida, L., Boaventura, R., Ramos, A., et al. (2019). Predictors and outcomes of disseminated tuberculosis in an intermediate burden setting. *Pulmonology* 25, 320–327. doi: 10.1016/j.pulmoe.2018.11.001

Miao, Q., Ma, Y., Wang, Q., Pan, J., Zhang, Y., Jin, W., et al. (2018). Microbiological diagnostic performance of metagenomic next-generation sequencing when applied to clinical practice. *Clin. Infect. Dis.* 67, S231–S240. doi: 10.1093/cid/ciy693

Miller, J. M., Binnicker, M. J., Campbell, S., Campbell, S., Carroll, K. C., Chapin, K. C., et al. (2018). A guide to utilization of the microbiology laboratory for diagnosis of infectious diseases: 2018 update by the infectious diseases society of America and the American society for microbiology. *Clin. Infect. Dis.* 67, e1–e94. doi: 10.1093/cid/ciy381

Pang, F., Xu, W., Zhao, H., Chen, S., Tian, Y., Fu, J., et al. (2014). Comprehensive evaluation of plasma microbial cell-free DNA sequencing for predicting bloodstream and local infections in clinical practice: a multicenter retrospective study.Front. *Cell. Infect. Microbiol.* 13. doi: 10.3389/fcimb.2023.1256099

Rebollo, M. J., San Juan Garrido, R., Folgueira, D., Palenque, E., DiazPedroche, C., Lumbreras, C., et al. (20062006). Blood and urine samples as useful sources for the direct detection of tuberculosis by polymerase chain reaction. *Diagn. Microbiol. Infect. Dis.* 56, 141–146. doi: 10.1016/j.diagmicrobio.2006.03.018

Shafer, R. W., Kim, D. S., Weiss, J. P., and Quale, J. M. (1991). Extrapulmonary tuberculosis in patients with human immunodeficiency virus infection. *Med. (Baltimore)* 70, 384–397. doi: 10.1097/00005792-199111000-00004

Sharma, S. K., Mohan, A., and Sharma, A. (2012). Challenges in the diagnosis & treatment of miliary tuberculosis. *Indian. J. Med. Res.* 135, 703–730.

Sharma, S. K., Mohan, A., and Sharma, A. (2016). Miliary tuberculosis: A new look at an old foe. *J. Clin. Tuberc. Other. Mycobact. Dis.* 3, 13–27. doi: 10.1016/j.jctube.2016.03.003

Shi, Y. F., Shi, X. H., Zhang, Y., Chen, J. X., Lai, W. X., Luo, J. M., et al. (2021). Disseminated tuberculosis associated hemophagocytic lymphohistiocytosis in a pregnant woman with Evans syndrome: A case report and literature review. *Front. Immunol.* 12. doi: 10.3389/fimmu.2021.676132

Taci, N., Yurdakul, A. S., Ceyhan, I., Berktas, M. B., and Ogretensoy, M. (2003). Detection of Mycobacterium tuberculosis DNA from peripheral blood in patients with HIV-seronegative and new cases of smear-positive pulmonary tuberculosis by polymerase chain reaction. *Respir. Med.* 97, 676–6681. doi: 10.1053/rmed.2003.1500

Votintseva, A. A., Bradley, P., Pankhurst, L., Elias, C. D. O., Loose, M., Nilgiriwala, K., et al. (2017). Same-day diagnostic and surveillance data for tuberculosis via whole-genome sequencing of direct respiratory samples. *J. Clin. Microbiol.* 55, 1285–1298. doi: 10.1128/JCM.02483-16

Wu, J., Song, W., Yan, H., Luo, C., Hu, W., Xie, L., et al. (2024). Metagenomic next-generation sequencing in detecting pathogens in pediatric oncology patients with suspected bloodstream infections. *Pediatr. Res.* 95, 843–851. doi: 10.1038/s41390-023-02776-y

Ye, Y., Yang, N., Zhou, J., Qian, G., and Chu, J. (2021). Case report: metagenomic next-generation sequencing in diagnosis of disseminated tuberculosis of an immunocompetent patient. *Front. Med. (Lausanne)* 8. doi: 10.3389/fmed.2021.687984

Zhang, H., Zhou, F., Liu, X., and Huang, J. (2014). Clinical application of metagenomic next-generation sequencing in patients with different organ system infection: A retrospective observational study. *Med. (Baltimore).* 103, e36745. doi: 10.1097/MD.0000000000036745

Zhou, X., Wu, H., Ruan, Q., Luo, C., Hu, W., Xie, l., et al. (2019). Clinical Evaluation of Diagnosis Efficacy of Active Mycobacterium tuberculosis Complex Infection via Metagenomic Next-Generation Sequencing of Direct Clinical Samples. *Front. Cell. Infect. Microbiol.* 9. doi: 10.3389/fcimb.2019.00351

frontiers | Frontiers in Cellular and Infection Microbiology

TYPE Original Research
PUBLISHED 12 December 2024
DOI 10.3389/fcimb.2024.1498512

OPEN ACCESS

EDITED BY
Diana Manolescu,
Victor Babes University of Medicine and Pharmacy, Romania

REVIEWED BY
Taj Azarian,
University of Central Florida, United States
Derrick Chen,
University of Wisconsin Hospital and Clinics, United States

*CORRESPONDENCE
Ke-Jing Tang
tangkj@mail.sysu.edu.cn
Zunfu Ke
kezunfu@mail.sysu.edu.cn

†These authors have contributed equally to this work and share first authorship

RECEIVED 19 September 2024
ACCEPTED 13 November 2024
PUBLISHED 12 December 2024

CITATION
Kuang Y, Tan W, Hu C, Dai Z, Bai L, Wang J, Liao H, Chen H, He R, Zhu P, Liu J, Xie C, Ke Z and Tang K-J (2024) Diagnosis value of targeted and metagenomic sequencing in respiratory tract infection.
Front. Cell. Infect. Microbiol. 14:1498512.
doi: 10.3389/fcimb.2024.1498512

Diagnosis value of targeted and metagenomic sequencing in respiratory tract infection

Yukun Kuang[1,2†], Weiping Tan[1,2†], Chaohui Hu[3†], Zehan Dai[3†], Lihong Bai[1,2†], Jiyu Wang[1,2], Huai Liao[1,2], Haihong Chen[1,2], Rongling He[1,2], Pengyuan Zhu[3], Jun Liu[3], Canmao Xie[1,2], Zunfu Ke[4,5,6*] and Ke-Jing Tang[1,2,7*]

[1]Department of Pulmonary and Critical Care Medicine, The First Affiliated Hospital, Sun Yat-sen University, Guangzhou, China, [2]Institute of Respiratory Diseases of Sun Yat-sen University, Guangzhou, China, [3]Guangzhou Kingcreate Biotechnology Co., Ltd., Guangzhou, China, [4]Molecular Diagnosis and Gene Testing Center, The First Affiliated Hospital, Sun Yat-sen University, Guangzhou, China, [5]Department of Pathology, The First Affiliated Hospital, Sun Yat-sen University, Guangzhou, China, [6]Institute of Precision Medicine, The First Affiliated Hospital, Sun Yat-sen University, Guangzhou, China, [7]Department of Pharmacy, The First Affiliated Hospital, Sun Yat-sen University, Guangzhou, China

Background: Targeted next-generation sequencing (tNGS) has become a trending tool in the field of infection diagnosis, but concerns are also raising about its performance compared with metagenomic next-generation sequencing (mNGS). This study aims to explore the clinical feasibility of a tNGS panel for respiratory tract infection diagnosis and compare it with mNGS in the same cohort of inpatients.

Methods: 180 bronchoalveolar lavage fluid samples were collected and sent to two centers for mNGS and tNGS blinded tests, respectively. The concordance between pathogen reports of both methods and the clinical significance among samples with/without known etiology was further evaluated.

Results: Overall, both methods displayed high agreement on pathogen reports, as the average percent agreement reached 95.29%. But tNGS presented a slightly higher detection rate per species than mNGS ($P_{Wilcoxon}$=1.212e-05; standard mean difference = 0.2887091), as detection rates for 32 out of 48 species were higher than those of mNGS. Due to limitations of panel coverage, tNGS identified 28 fewer species than mNGS, among which only 3 were considered clinically relevant. In reference to composite reference standard, accuracy, sensitivity, and specificity combining both tNGS and mNGS reached 95.61%, 96.71%, and 95.68%, respectively, while positive prediction value (PPV) was low at 48.13%, which was caused by low agreement regarding opportunistic pathogens. tNGS and mNGS improved the etiology identification in 30.6% (55/180) and 33.9% (61/180) cases, respectively.

Conclusion: Collectively, tNGS presented a similar overall performance in pathogen identification compared to mNGS, but outperformed in some pathogens. This study also demonstrated that deployment of tNGS significantly improves etiology identification in routine practice and provides hints for clinical

decisions. The low agreement between clinical diagnosis and NGS reports towards opportunistic pathogens implies that adjudication is essential for report interpretation. Finally, We proposed tNGS as a diagnosis option in clinical practice due to its cost-efficiency.

KEYWORDS

broad-spectrum pathogen identification, targeted next-generation sequencing (tNGS), metagenomic next-generation sequencing (mNGS), diagnosis value, respiratory tract infection

1 Introduction

Respiratory tract infections (RTIs) pose a severe threat to global health, causing great morbidity and mortality on a global scale (Lozano et al., 2012). Severe RTIs may lead to life-threatening pneumonia and acute respiratory distress syndrome. Accurate pathogen identification is essential in clinical practice, as delayed or incorrect diagnosis may result in adverse outcomes, such as misuse of antibiotics, and may worsen the prognosis for patients (Ewig et al., 2002; Bleeker-Rovers et al., 2007; Weng et al., 2017).

Determining the etiology of RTI is usually a formidable task in clinical practice. As an opening to the environment, the respiratory tract is exposed to an extensive list of pathogenic factors, either infectious or non-infectious (Dickson et al., 2016; Man et al., 2017), which sometimes lead to the development of various symptoms, including expectoration, cough, fever, hemoptysis etc. Such symptomatology drives pulmonologists to employ comprehensive settings to identify the etiology in routine practice, during which multiple tests are usually employed, including, but not limited to, microscopic examination, imaging, immunology, and molecular testing. A common limitation of these methods is their narrow spectrum, thus the choice of these methods is made accordingly based on presumed pathogens. But still, employing a selection of tests may fail to confirm the causal factor, and pulmonologists may have to resort to empirical treatment for critically ill patients before etiology is determined.

Next-generation sequencing (NGS) has been proposed as a promising tool for resolving difficulties of identifying etiology (Zhong et al., 2021). NGS could be introduced in parallel with routine laboratory tests (RLT), providing comprehensive reports with candidate pathogens and serving as additional evidence for clinical diagnosis. The values of metagenomic next-generation sequencing (mNGS) in RTI diagnosis have been demonstrated (Dong et al., 2022; Li et al., 2022; Xie et al., 2021; Miao et al., 2018; Li et al., 2018; Yang et al., 2019; Shi et al., 2020; Duan et al., 2021). In recent years, targeted next-generation sequencing (tNGS) based on highly-multiplex-PCR is emerging in China, and presents as a competitor for mNGS in pathogen detection. The most distinctive feature of the tNGS panel is its focus on target organisms with clinical relevance, which also benefits from increased sensitivity to low-abundant pathogens. Target amplification could also eliminate interference from a high host genetic background (Mamanova et al., 2010; Dennis et al., 2022), and this further increases data usage efficiency and reduces costs. A primary concern regarding tNGS is its diagnostic performance, particularly in comparison to mNGS, a similar approach that has garnered substantial recognition. The second question is to what extent these methods can aid in precise etiology determination, especially considering that tNGS has a target spectrum. Unfortunately, the real-world differences between both methods in clinical practice haven't yet been explored. The answers to these questions should enhance our understanding of these methods and similar technologies, and may potentially improve diagnosis and therapeutic processes.

In this study, a two-center, retrospective, blinded comparison was conducted to evaluate the pathogen detection performance of tNGS and mNGS in clinical samples. A total of 199 bronchoalveolar lavage fluid (BALF) samples from 190 inpatients with respiratory infections were collected, and eligible samples were sent to two commercial companies for tNGS and mNGS testing, respectively. After the generated pathogen reports underwent case-by-case scrutiny, the method-wise consistency, the accuracy of identifying etiology and the clinical significance were evaluated. Technical comparison, potential pitfalls, and clinical applications of both methods were also discussed.

2 Methods and materials

2.1 Study design

The workflow of this study is depicted in Figure 1. A total of 199 BALF samples were collected from 190 patients admitted to the Department of Pulmonary and Critical Care Medicine, First Affiliated Hospital of Sun Yat-sen University (FAH-SYU). The test results of routine laboratory tests, combined with all information collected during all medical procedures, served as a clinical reference standard for pulmonologists to make a conclusive

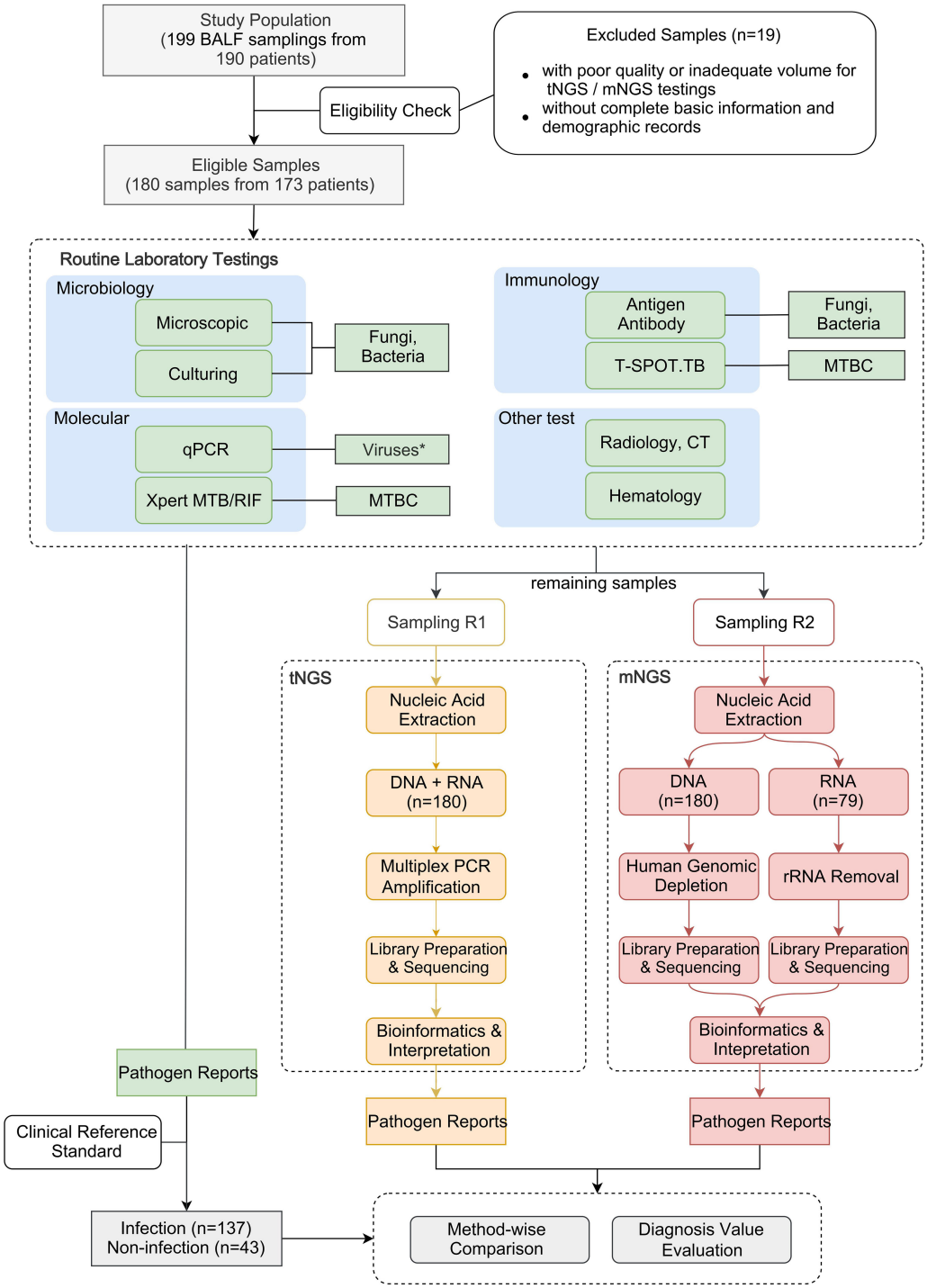

FIGURE 1
Schematic presentation of the workflow in this study. *qPCR was employed solely for routine virus detection in this study, although it can be used to detect all types of microorganisms.

diagnosis. The remaining samples were stored at -80°C until May 2023, divided into two parts, namely R1 and R2, and sent individually to Kingmed Diagnostics Group Co., Ltd., Guangzhou and VisionMedical Co., Ltd., Guangzhou for tNGS and mNGS. Eligibility criteria: 1) all patients presented typical symptoms of RTI; 2) remaining samples were qualified and sufficient for sequencing; 3) with complete basic information and demographic records. Due to the limitations of mNGS, DNA and RNA samples were extracted and sent for library construction, respectively. Both companies produced pathogen reports independently without

knowledge of each other's and results of any routine laboratory tests until the completion of all data collection. Qualified tNGS and mNGS pathogen reports underwent downstream comparative analysis and evaluation of diagnosis value.

2.2 Routine laboratory testing and clinical diagnosis

Different tests were conducted as part of standard routine practice. These tests were selectively conducted based on pathogen suspicion or for exclusion purposes. Results serve as evidence to assist in making a diagnosis. Regular laboratory tests were conducted as part of standard clinical practice. This included conventional microbiological tests (CMTs), such as microbial culture and bacterial and fungal stains, as well as immunological and molecular tests (e.g., qPCR) for pathogen identification and disease diagnosis. These tests were performed by the Department of Laboratory Medicine at FAH-SYU. In addition, acid-fast bacilli staining and culture, Xpert MTB/RIF, and T-cell-based tests for tuberculosis infection (T-SPOT.TB) were also performed for cases with clinical suspicion of *Mycobacterium tuberculosis* (MTB). Each of these methods was developed for the identification of specific types of pathogens and was utilized based on the individual cases. For practical considerations, these tests were selectively conducted based on clinical suspicion and were not used indiscriminately on all samples. Thus, data of specific methods in some samples may not be available, but results of at least two microbial tests were employed for all samples. Intermediate results of individual methods would not be considered positive unless consistency was observed from at least two methods. Results of all tests were combined and taken into consideration to conclude a diagnosis. The positive calling criteria for each method are summarized in Supplementary Table 1.

A composite reference standard for etiology identification was established to serve as a criterion for physicians to make initial clinical diagnoses. In brief, two experienced physicians independently reviewed the medical records, including the chart interview process, routine laboratory test results, treatment responses and other information from all medical procedures, to determine whether the patients had infections or non-infections and to identify potential causal pathogens. Disagreements between physicians were resolved through in-depth discussions, during which senior physicians participated until a consensus was reached.

2.3 Targeted NGS pathogen detection

Samples were sent to Kingmed Diagnostics Group Co., Ltd., Guangzhou, China for tNGS sequencing. In brief, the development of the tNGS panel first started with a rigorous and exhaustive survey of different types of reference materials, including academic papers, books, and expert consensus, to determine the target spectrum. A corresponding reference database consisting of representative sequences of these microbes described above was curated from NCBI NT database. For tNGS, the panel was designed to cover a spectrum of 153 microorganisms, including 68 viruses, 65 bacteria, 14 fungi, 3 chlamydiae, and 3 mycoplasmas. A full list of all target species was detailed in Supplementary Table 2. Primer design was guided by several critical parameters, including GC content, primer length, amplicon size, melting temperature, and potential secondary structures, followed by a specificity check. For more details of it, please refer to Yin's study (Yin et al., 2024). The BALF samples with high viscosity were diluted 1:1 with 0.1 M dithiothreitol prior to nucleic acid extraction. Automated nucleic acid extraction was performed using MagPure Pathogen DNA/RNA Kit B (Magen Biotechnology, Guangzhou, Guangdong, China) on KingFisher™ Flex Purification System (Thermo Fisher Scientific, Waltham, MA, USA). Nuclease-free water (Invitrogen, Waltham, MA, USA) was used as a non-template control to detect contamination.

Multiplex PCR pre-amplification of target loci and library preparation were performed using a respiratory pathogen test kit, RP100 (KingCreate, Guangzhou, Guangdong, China). Generated libraries were quantified using Equalbit DNA HS Assay Kit (Vazyme Biotech, Nanjing, Jiangsu, China) with an Invitrogen™ Qubit™ 3.0/4.0 (Thermo Fisher Scientific, Waltham, MA, USA) Fluorometer to ensure that all samples had library densities ≥ 0.5 ng/μL, otherwise, they were subjected to library reconstruction. DNA fragment analysis was performed using the Qsep100 Capillary Electrophoresis System™ (BiOptic Inc., Jiangsu, China) and its compatible Standard Cartridge Kit. After library qualification, sequencing was performed using KM MiniSeqDx-CN Sequencing Kit on the sequencing platform KM MiniSeq Dx-CN (KingCreate, Guangzhou, Guangdong, China).

Generated sequencing data was analyzed using a customized bioinformatic workflow. Generated sequencing raw read data underwent quality control procedures. The fastp v0.20.1 (Chen et al., 2018) was employed for adapter trimming and low-quality filtering using default parameters followed by reference-based assembly using Bowtie2 v2.4.1 (Langmead and Salzberg, 2012) in 'very-sensitive' mode. For a specific pathogen species or group, the normalized matched read count must reach matched reads per 100,000 reads (RPhK) ≥ 10 to be considered positive. Interpreters conducted the interpretation of the generated pathogen reports, often cooperating with bioinformaticians, before releasing the report.

2.4 Metagenomic NGS pathogen detection

Criterion was set up for selecting representative reference sequences of microorganisms from the NCBI NT and NCBI Genome databases. The pathogen list was determined in reference to Johns Hopkins ABX Guide, Manual of Clinical Microbiology, clinical case reports, and peer-reviewed articles, which was detailed in Liu's study (Liu et al., 2022). Using the QIAamp® UCP Pathogen DNA Kit (Qiagen, Nordrhein-Westfalen, Germany) and following the manufacturer's instructions, DNA extraction was performed on all samples. Human DNA was eliminated from the samples by using Benzonase (Qiagen, Nordrhein-Westfalen, Germany) and Tween 20

(Sigma, Indiana, U.S.). Total RNA was extracted from the specimens by using the QIAamp® Viral RNA Kit (Qiagen, Nordrhein-Westfalen, Germany) and ribosomal RNA was removed by utilizing the Ribo-Zero rRNA Removal Kit (Illumina, California, USA). The generated cDNA was obtained through reverse transcription (Thermo Fisher Scientific, Waltham, MA, USA).

The Nextera XT DNA Library Prep Kit (Illumina, San Diego, CA, USA) was utilized to create libraries for both the DNA and cDNA samples. The Qubit dsDNA HS Assay Kit (Thermo Fisher Scientific, Waltham, MA, USA) was used to evaluate the quality of the libraries, followed by the High Sensitivity DNA Kit (Agilent, California, USA) on the Agilent 2100 Bioanalyzer (Agilent, California, USA). Each library was subjected to 75 cycles of single-end sequencing on an Illumina NextSeq 550Dx Sequencer (Illumina, San Diego, CA, USA) to generate approximately 20 million reads. Deionized water was included in the extraction process as a negative control to function as a non-template control alongside the specimens.

Trimmomatic (Bolger et al., 2014) was used for low-quality read filtering and adapter trimming. The Burrows-Wheeler Aligner software (Li and Durbin, 2009) was used to exclude reads of human genomes in reference to the human reference genome hg38. For microbial species identification, a curated reference database consisting of > 20000 genomes spanning bacteria, viruses, fungi, protozoa, to other multicellular eukaryotic organisms was employed, as depicted in a previous study (Liu et al., 2022). Microbial reads were aligned to the database using SNAP v1.0 beta.1810 (Zaharia et al., 2011). Positive detection of a given species or genus was reported if the reads per million (RPM) ratio (Miller et al., 2019), or RPM-r, was ≥ 5. The RPM-r was defined as the RPM of the sample divided by the RPM of the negative control. To minimize cross-species misalignments among closely related microorganisms, a penalty mechanism was introduced (Gu et al., 2021). Bioinformaticians conducted the interpretation of the pathogen identification results, generated the pathogen report and approved it before release.

TABLE 1 Criteria for determining the diagnosis value of NGS methods.

Value	Type	Etiology	Clinical Presumption	NGS Report	NGS-DTP Match*	Criteria Description
Agree	infectious	determined	species level	+	yes	NGS concluded the potential pathogens identified through DTP.
	non-infectious	unknown	–	–	yes	For non-infectious cases determined through DTP, NGS reported no potential pathogens.
Support/Extend	infectious	suspected	genus level or higher	+	yes	Support: diagnosis has a general presumption of potential pathogen (genus level or higher), potential pathogens reported by NGS were consistent with DTP, and thus considered to be clinically revelant.
		unknown	–			Extend: no pathogen presumption was made in clinical diagnosis, potential pathogens reported by NGS were considered to be consistent with DTP.
Noncontributory	non-infectious	unknown	–	+†	no	Microbes reported by NGS were clinically insignificant.
Unlikely	infectious	determined	species level or higher	+	no	None of the microbes reported by NGS matched the suspected pathogen identified in the clinical diagnosis or DTP.
	non-infectious	unknown	–	+‡	no	The clinical diagnosis was non-infectious. However, the "potential pathogens" reported by NGS were either considered highly pathogenic based on clinical experience or documented as acute pathogens (e.g. *Mycobacterium tuberculosis*), and these pathogens did not match DTP.
Disagree	infectious	determined	species level	–	no	For infectious cases in which potential pathogens were identified through DTP, NGS failed to detect any microorganisms.

*DTP, Diagnostic and therapeutic process. NGS-DTP Match indicates whether the reported organisms matched DTP.
"+" indicates either clinical diagnosis has determined potential pathogen or at least one pathogen was reported by NGS.
"†" and "‡" indicate that the reported pathogen candidates in cases labeled as "Noncontributory" and "Unlikely" are opportunistic pathogens and acute pathogens, respectively.
"-" indicates no pathogens.

2.5 Pathogen report review and refinement

The initial pathogen reports generated from both NGS approaches underwent a pairwise blind review by two experienced physicians. The physicians scrutinized each sample and pathogen report carefully to identify any ambiguous results. After completing this step, the chief researchers unblinded the tNGS and mNGS reports to analyze the results in preparation for the next step. In cases of controversial conclusions concerning any pathogen or patient, a review of the entire workflow was conducted with input from pulmonologists, bioinformaticians, and lab technicians to reach a final conclusion, which was based on the data generated by all methods and sampling.

2.6 Clinical value evaluation

To assess the diagnosis value of NGS methods in clinical decision-making and ensure an intuitive understanding, all reports were evaluated by pulmonologists and assigned labels to represent NGS's contribution to pathogen identification in various scenarios. The five labels used are Agree, Support/Extend, Disagree, Unlikely, and Noncontributory. In general, these labels express agreement on the reports grouped by disease status and qualify whether NGS aided in identifying etiology. Agree and Support/Extend present positive attitudes on cases of infectious samples, while Disagree and Unlikely present disagreement, and Noncontributory presents an intermediate attitudes towards clinically insignificant microbes. The criteria for each label are described in detail in Table 1.

2.7 Statistical analysis

Wilcoxon test and Kruskal Wallis test were used to test the pairwise variance for all quantitative measurements (Andrews, 1954). The normal distribution of data was determined by the Shapiro-Wilk test prior to t-test (Shapiro and Wilk, 1965). Linearity between two variables was checked using the *Spearman* rank correlation test (Fieller et al., 1957). These analyses were all conducted using the corresponding functions implemented in base R 4.1.1. The standard mean difference (SMD) was used to measure the degree of variance given two groups of variables with the assistance of the R package *smd* (https://rdrr.io/cran/smd/). A SMD value of "$0.20 \leq$ estimate ≤ 0.50" is considered to indicate a small effect size (Faraone, 2008).

Positive percent agreement (PPA, percent of the concordant positives), negative percent agreement (NPA, percent of the concordant negatives), sensitivity, specificity, accuracy, positive predictive value (PPV), negative predictive value (NPV), and 95% confidence interval (CI) were all manually calculated following the formulas described in previous studies (Altman and Bland, 1994a, Altman and Bland, 1994b; Bland and Altman, 1996; van Stralen et al., 2009). Percent agreement, PPA and NPA were used for evaluating the agreement of measurement between two NGS approaches. To estimate the clinical agreement of these qualitative tests, the conclusion of clinical diagnosis was used as the reference to determine true positives, true negatives, false positives, false negatives. Based on these, specificity, sensitivity, and accuracy were further calculated.

2.8 Sample size estimation

Sample size was estimated as below:

$$N = \frac{(Z_{\alpha}^{C} + Z_{\beta}^{C})^2}{d^2}$$

In this formula, N represents the total sample size, C denotes confidence level, Z_{α} is the critical value of the standard normal distribution corresponding to the significance level α, β represents the power level, and Z_{β} is the critical value of the standard normal distribution corresponding to the power level. The effect size d, computed as minimum mean difference divided by standard deviation.

Assuming a confidence level of 0.99, the value of Z_{α} is 2.576. Assuming a power level of 0.95, the value of Z_{β} is 1.645. Based on preliminary experimental data (not published), the estimated effect size is 32%. The minimum required sample size is calculated as:

$$N = \frac{(2.576 + 1.645)^2}{0.31^2} \approx 173$$

The estimated sample size is 173. Considering the possible insufficiency of remaining samples and possibility of unqualified sequencing test, additional 10% was added to this estimate. The final expected sample size is 190.

3 Results

3.1 Baseline demographics and clinical characteristics

A total of 199 samples were collected from 190 patients with suspected pneumonia, among which 180 eligible samples passed the enrollment criteria and were included in the following analysis. All samples were randomly selected and collected between July 2021 and October 2022. Although different types of samples were collected for routine clinical practice, only BALF samples were selected for this study. Basic information of the study population is summarized in Table 2. All the patients included were over 18 years old, with ages ranging from 19 to 89 (Supplementary Figure 1). The majority of study subjects (over 75%) were aged between 40 and 80. 68% of the selected patients were male and 32% were female. All patients had typical pneumonia symptoms. The proportions of patients with cough, expectoration, fever, and hemoptysis account for 72.22%, 52.78%, 39.44%, and 10.00%, respectively (Table 2). Some patients had chronic diseases, such as diabetes, cardiovascular disease, hypertension, and issues in other organs. Patients with cardiovascular disease and hypertension represent the highest proportions (29.44% and 31.67%). BALF samples were first taken

10.3389/fcimb.2024.1498512

TABLE 2 Characteristics and history of patients in the study (n=173).

Examinations	Reference Range	Measurements
Clinical manifestation (count; percentage)		
Cough	–	130 (72.22%)
Expectoration	–	95 (52.78%)
Fever	–	71 (39.44%)
Hemoptysis	–	18 (10.00%)
Dyspnea	–	1 (0.56%)
Chest tightness	–	1 (0.56%)
Hematology parameters (median; lower/upper quartile)		
White cell count (× 10^9/L)	3.50-9.50	8.26 (5.46-11.23)
Platelet count (× 10^9/L)	100-300	251 (176-335)
Neutrophil (%)	45.0-75.0	75.5 (64.8-83.8)
Lymphocyte (%)	20.0-50.0	14.4 (7.9-23.6)
Eosinophil (%)	0.5~5	9 (2-19)
Hemoglobin (g/L)	115-150	118 (99-138)
Plateletcrit (mg/ml)	<0.1	0.09 (0.05-0.26)
C-reactive protein (mg/L)	<5.0	26.93 (7.68-107.09)
Underlying Disease (count; percentage)		
Hypertension	–	57 (31.67%)
Cardiovascular disease	–	53 (29.44%)
Cerebrovascular disease	–	37 (20.56%)
Diabetes	–	28 (15.56%)
Chronic liver disease	–	27 (15.00%)
Chronic kidney disease	–	14 (7.78%)
Chronic obstructive pulmonary disease	–	10 (5.56%)

from these patients for selected laboratory tests to serve as part of routine practice for helping pulmonologists with decision making. After hospitalization/administration of all inpatients, the remaining samples were sent for nucleic acid extraction to facilitate downstream NGS analysis

3.2 Method-wise concordance between tNGS and mNGS

The general performance comparison between tNGS and mNGS is summarized in Figure 2. A significant positive correlation in detection frequencies per species was observed between tNGS and mNGS (*Spearman* test, P=1.39e-14, Figure 2A). However, tNGS reported more positives than mNGS, as evidenced by the deviated fitted line and a correlation coefficient less than 1 ($\rho_{spearman}$=0.85, Figure 2A). It is interesting that although tNGS has a much narrower spectrum (153 species, detailed in Supplementary Table 2) than mNGS (~20,000), tNGS reported significantly more potential pathogens per sample than mNGS. Such a difference was more pronounced when considering only the targets covered by both the tNGS panel and mNGS (P=1.374e-13, Figure 2B). Such variance could be further demonstrated at organism level. An overall difference could be observed between tNGS and mNGS regarding detection frequencies (P-value=1.212e-05, Paired Wilcoxon test). In detail, tNGS exhibited higher detection frequencies for 32 organisms, equal detection frequencies for 12 organisms, and lower detection frequencies for 4 organisms when compared to mNGS. Ten species were identified exclusively by either tNGS or mNGS, each appearing in only one sample (Figure 2C). Additionally, mNGS exclusively reported 28 species that are not covered in the tNGS panel (Supplementary Table 3). However, 25 of them were considered clinically insignificant by composite reference standard. Although the

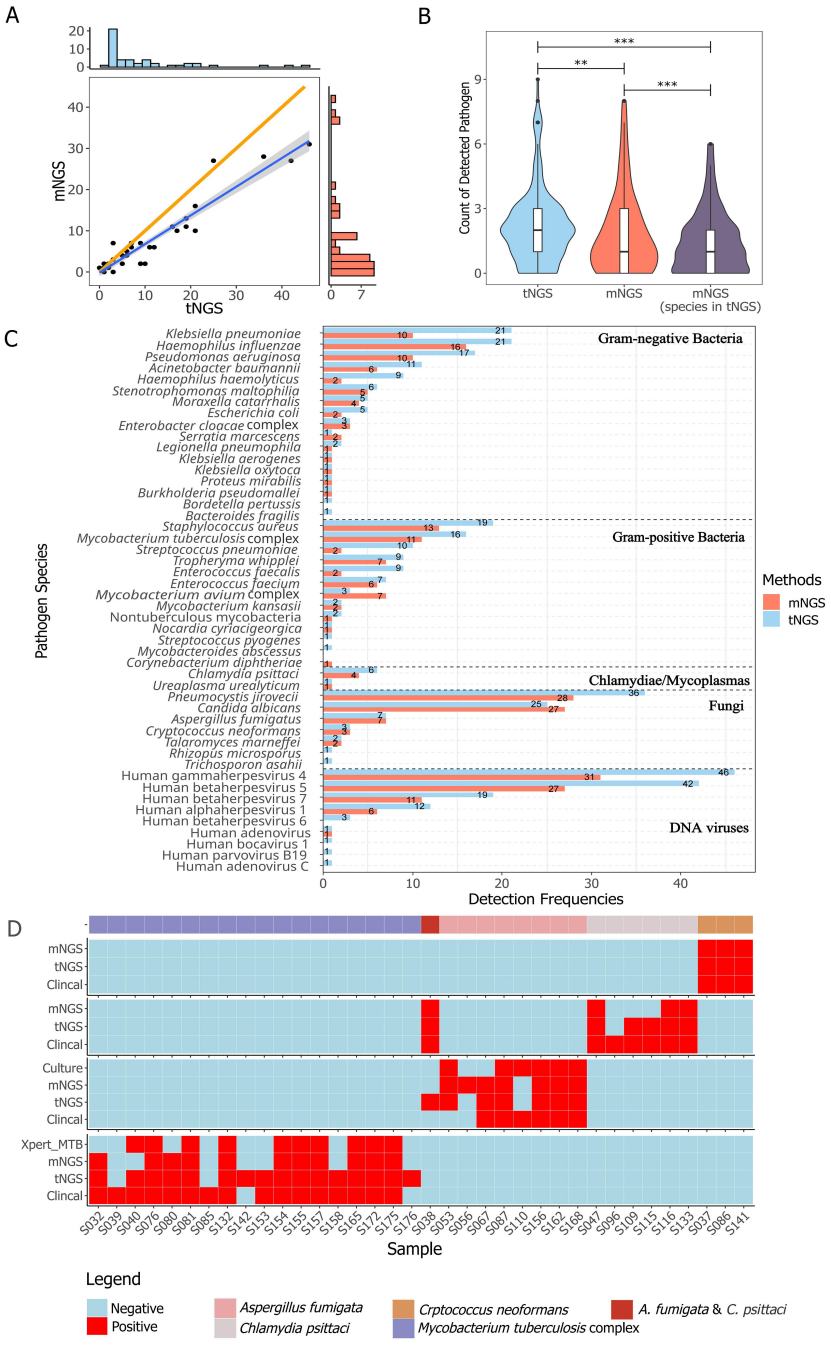

FIGURE 2
Method-wise comparison of pathogen detection. **(A)** The correlation of identified pathogens between tNGS and mNGS is illustrated with a highlighted blue regression line to emphasize the linearity of positive calls, while an orange line represents the reference line of equality. The correlation was determined using Spearman rank test ($P < 0.01$). **(B)** Counts of detected pathogen species per sample with group-wise statistical differences confirmed by paired Wilcoxon test ($P < 0.01$). "**" and "***" indicates a P value of ≤0.05 and ≤0,01, respectively. **(C)** The detection frequency of each pathogen with a method-wise statistical difference confirmed by paired Wilcoxon test ($P < 0.01$). All the pathogens described or taken into analysis are microbes with DNA genome. Only species covered in the tNGS panel and mNGS were included. **(D)** Comparison of different methods for detection of *Aspergillus fumigata*, *Chlamydia psittaci*, *Crptococcus neoformans*, and *Mycobacterium tuberculosis* complex.

overall percent agreements of all shared targets showed high concordance between both methods (82.78% ~ 100%) (Supplementary Table 4), the PPAs of some species were low (e.g. *Mycobacterium avium* complex at 42.86%). These results highlight the differences in detection prevalence between mNGS and tNGS.

3.3 Agreement of tNGS and mNGS with clinical diagnosis

In reference to diagnoses, the overall accuracy, sensitivity, specificity, and negative percent value (NPV) of tNGS/mNGS all

TABLE 3 Detection performance of NGS methods on specific pathogens in reference to clinical diagnosis.

Pathogen	Method	Accuracy% ($CI_{95\%}$)	Sensitivity% ($CI_{95\%}$)	Specificity% ($CI_{95\%}$)	PPV% ($CI_{95\%}$)	NPV% ($CI_{95\%}$)
Cryptococcus neoformans	tNGS	99.44%	100%	99.44%	66.67%	100%
		(96.9%-99.9%)	(15.8%-100%)	(96.9%-99.9%)	(9.4%-99.16%)	(97.9%-100%)
	mNGS	99.44%	100%	99.44%	66.67%	100%
		(96.9%-99.9%)	(15.8%-100%)	(96.9%-99.9%)	(9.4%-99.2%)	(97.9%-100%)
Aspergillus fumigata	tNGS	99.44%	100%	99.43%	85.71%	100%
		(96.9%-100%)	(54.1%-100%)	(96.8%-100%)	(42.1%-99.6%)	(97.9%-100%)
	mNGS	99.44%	100%	99.43%	85.71%	100%
		(96.9%-100%)	(54.1%-100%)	(96.8%-100%)	(42.1%-99.6%)	(97.9%-100%)
Mycobacterium tuberculosis complex	tNGS	98.89%	93.75%	99.39%	93.75%	99.39%
		(96.0%-99.9%)	(69.8%-99.8%)	(96.7%-100%)	(69.8%-99.8%)	(96.7%-99.9%)
	mNGS	97.22%	68.75%	100%	100%	97.04%
		(93.6%-99.1%)	(41.3%-89.0%)	(97.8%-100%)	(71.5%-100%)	(93.2%-99.0%)
Chlamydia psittaci	tNGS	100%	100%	100%	100%	100%
		(98.0%-100%)	(54.1%-100%)	(98.0%-100%)	(54.1%-100%)	(97.9%-100%)
	mNGS	98.89%	66.67%	100%	100%	98.86%
		(96.0%-99.9%)	(22.3%-95.7%)	(98.0%-100%)	(39.8%-100%)	(96.0%-99.9%)
all pathogens	tNGS	94.56%	98.86%	94.52%	42.09%	99.95%
		(91.5%~97.1%)	(97.0%~100%)	(91.4%~97.7%)	(27.6%~56.6%)	(99.9%~100.0%)
	mNGS	96.54%	94.82%	96.70%	53.47%	99.78%
		(94.6%~98.5%)	(90.3%~99.4%)	(94.7%~98.7%)	(38.7%~68.2%)	(99.5%~100.0%)
all pathogens	total	95.61%	96.72%	95.68%	48.13%	99.86%
		(93.9%~97.4%)	(94.2%~99.3%)	(93.9%~97.5%)	(38.0%~58.3%)	(99.7%~100.0%)

PPV, Positive predictive value; NPV, Negative predictive value.

exceeded 95%, while the overall PPVs were relatively low at 42.09% ($CI_{95\%}$: 27.6%~56.6%) and 53.47% ($CI_{95\%}$: 38.7%~68.2%) (Table 3). Further inspection revealed that this may be due to the predominance of opportunistic pathogens, as PPVs of opportunistic pathogens by tNGS and mNGS were 15.71% and 21.88%, respectively. An extreme case is Human gammaherpesvirus 4, as only 1 positive was considered clinically relevant out of all 46 positives (for all pathogens, see Supplementary Table 5). On the other hand, four selected pathogens - *Cryptococcus neoformans*, *Aspergillus fumigata*, *Mycobacterium tuberculosis* complex, and *Chlamydia psittaci* - considered empirically to be highly pathogenic, had high PPVs (66.7% to 100%) (Table 3). Agreement of positive results between clinical diagnosis and other methods regarding these species is summarized in Figure 2D. tNGS and mNGS confirmed most of the positive results identified by clinical diagnosis and outperformed other methods. Taking *Mycobacterium tuberculosis* complex as an example, tNGS, mNGS and Xpert reported 14, 11, and 10 positives out of 16 clinically positive samples, respectively. This was also observed in *Aspergillus fumigatus*, *Cryptococcus neoformans*, and *Chlamydia psittaci* (Figure 2D).

3.4 Accessing the diagnosis value of NGS

To access the diagnosis value of NGS reports, we scrutinized all reports, adjudicated the reported organisms and categorized the reports based on agreement labeling (namely Agree, Support/Extend, Noncontributory, Unlikely, Disagree, see Table 1 for criteria), assessing whether NGS aided in etiology determination. Tags of Agree and Support/Extend indicate that NGS assisted in identifying potential pathogens, and the total number of reports marked by these two tags reached 124 (68.9%) and 118 (65.6%) for tNGS and mNGS, respectively. In contrast, the total counts of Disagree, Unlikely, and Noncontributory are relatively low, at 31.1% and 34.4%, where most reported pathogens were considered to be clinically insignificant (Figure 3A). A preference could be observed between tNGS and mNGS, as the etiology of

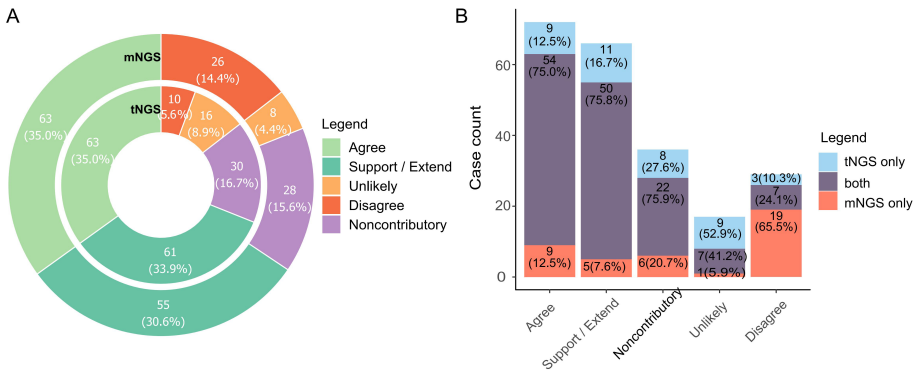

FIGURE 3
Diagnosis value of NGS methods towards pathogen determination. **(A)** Barplot summarizing cases with different tags of diagnosis value. Pathogen reports were adjudicated by pulmonologists and assigned labels according to the extent they assisted in identifying possible causal pathogens. Label explanation: Agree, NGS reported potential pathogens that was/were consistent with clinical diagnosis (either infectious or non-infectious). Support/Extend, NGS reported unexpected potential pathogens in cases with unknown etiology, and they matched diagnosis (by routine laboratory test) and treatment response. Noncontributory, all microbes reported in non-infectious cases were clinically insignificant. Unlikely, reported microbes did not match diagnosis and treatment response. Disagree, NGS failed to identify any microorganism in infection cases in which important casual pathogens were identified. Full criteria for each label are listed in Table 1. **(B)**. Comparison of preference based on value tags between tNGS and mNGS.

some cases was identified only by either tNGS or mNGS. tNGS tended to report more cases of Unlikely while mNGS reported more cases of Disagree (Figure 3B). We assume that this may be due to sensitivity differences between NGS methods, which will be discussed later.

Figure 3A depicts the comprehensive efficacy of NGS in ascertaining etiological factors. Subsequent analyses were conducted on cases where NGS-based determinations of etiology were provided at a report level. We primarily focused on the cases that highlighted the enhanced capability of NGS to identify potential pathogens. At least one NGS method, either tNGS or mNGS, identified the primary pathogen *Mycobacterium tuberculosis*, supported by RLT, in 15 cases. However, no single RLT was capable of detecting *Mycobacterium tuberculosis* in all these instances (Table 4). The RLT with the highest number of positives was the Xpert MTB/RIF assay, confirming the pathogen in 10 out of 15 cases, which was less effective than tNGS (14/15), and mNGS(11/15) (Table 4). Furthermore, tNGS provided assistance in identifying potential *Mycobacterium tuberculosis* infections in cases where RLT results were negative. Additionally, in four cases, both tNGS and mNGS were instrumental in identifying non-tuberculous mycobacteria to the species level (S075, S085, S120, S149). Regarding the detection of *Aspergillus fumigatus*, it relies on serological tests, culture, and microscopic observation. Serological tests, such as ELISA, depend on an infection window to achieve optimal sensitivity, which may explain the positive results in only three out of the total seven cases. Moreover, the culture method - a time-intensive and comparatively less sensitive approach - yielded positive results in five cases. In contrast, both NGS methods achieved a 100% detection rate (7/7). In six cases, *Chlamydia psittaci* was detected exclusively by NGS methods, with no RLTs providing corroborative evidence. Diagnosis of these cases was definitively attributed to a composite reference standard, reinforced by the clinical context of primary pathogenicity and the patients' history of frequent poultry exposure.

4 Discussion

NGS was initially proposed as a promising tool for pathogen identification in the early 2010s (Yongfeng et al., 2011; Miller et al., 2013), but has not gained popularity till recent years, particularly with the advent of mNGS, whose robustness in detecting respiratory pathogens has been demonstrated (Chen et al., 2020; Fang et al., 2020; Li et al., 2020; Shi et al., 2020; Jiang et al., 2021; Peng et al., 2021; Gaston et al., 2022; Miller et al., 2019). The emerging highly-multiplex-PCR-based tNGS has gained significant acceptance in China since the introduction of commercial products in 2021. In some prestigious hospitals, there have been arguments advocating for the implementation of tNGS and mNGS as routine testing procedures. While tNGS shows feasibility in diagnosing RTIs, its true value and efficacy still require solid evidence to be substantiated. In this study, we evaluated the pathogen detection performance of tNGS and mNGS based on the same clinical cohort of 180 enrolled BALF samples. Tests of tNGS and mNGS were conducted and reports were interpreted by two units. Pulmonologists evaluated the diagnosis value of pathogen reports case by case. Strict rules were set up during this stage, and all details were collected and taken into consideration to implement an objective, bias-free validation for both NGS approaches. Overall, the results demonstrated that tNGS had similar detection performance to mNGS although some variance was observed when identifying specific species. Both methods assist in etiology identification but tend to identify opportunistic pathogens with low clinical relevance.

In general, tNGS exhibited a high overall consistency with mNGS in detecting pathogens, as supported by the linearity (Figure 2A) and performance metrics (Supplementary Table 4). Small variance effect (standard median deviation = 0.288) and significance by Wilcoxon rank test implied that tNGS had a slightly higher chance of identifying organisms than mNGS, which was supported by higher detection rates per species

10.3389/fcimb.2024.1498512

TABLE 4 Comparison of etiology determined in selected cases by NGS and RLTs.

Sample	Potential Pathogen	Routine Laboratory Test	tNGS	mNGS
RLT-supported etiology				
S032	*Mycobacterium tuberculosis* complex	T-SOPT.TB (+)	tNGS (+)	mNGS (+)
S039	*Mycobacterium tuberculosis* complex	Acid Fast Bacteria Stain (+)	–	–
S040	*Mycobacterium tuberculosis* complex	Xpert MTB (+)	tNGS (+)	–
S076	*Mycobacterium tuberculosis* complex	Xpert MTB (+)	tNGS (+)	mNGS (+)
S080	*Mycobacterium tuberculosis* complex	Acid Fast Bacteria Stain (+)	tNGS (+)	mNGS (+)
S081	*Mycobacterium tuberculosis* complex	Xpert MTB (+)	tNGS (+)	mNGS (+)
S132	*Aspergillus* fungi	*Aspergillus* Elisa (+), fungal fluorescent staining (+), suspected *Aspergillus* hyphae and spores	–	mNGS (+)
	Penicillium marneffei	Sputum culture (+), BALF culture (+)	tNGS (+)	mNGS (+)
	Mycobacterium tuberculosis complex	Xpert MTB (+)	tNGS (+)	mNGS (+)
S153	*Pseudomonas aeruginosa*	Sputum culture (+), BALF culture (+)	tNGS (+)	mNGS (+)
	Mycobacterium tuberculosis complex	Acid Fast Bacteria Stain (+)	tNGS (+)	–
S154	*Mycobacterium tuberculosis* complex	Xpert MTB (+)	tNGS (+)	mNGS (+)
S155	*Mycobacterium tuberculosis* complex	Xpert MTB (+)	tNGS (+)	mNGS (+)
S157	*Mycobacterium tuberculosis* complex	Xpert MTB (+)	tNGS (+)	mNGS (+)
S165	*Mycobacterium tuberculosis* complex	Xpert MTB (+)	tNGS (+)	mNGS (+)
S172	*Mycobacterium tuberculosis* complex	Xpert MTB (+), Acid Fast Bacteria Stain (+)	tNGS (+)	mNGS (+)
S175	*Mycobacterium tuberculosis* complex	Xpert MTB (+), Acid Fast Bacteria Stain (+)	tNGS (+)	mNGS (+)
S176	*Mycobacterium tuberculosis* complex	Acid Fast Bacteria Stain (+)	tNGS (+)	–
S053	*Aspergillus fumigatus*	Sputum culture (+), BALF culture (+)	tNGS (+)	mNGS (+)
	Staphylococcus aureus	BALF culture (+)	tNGS (+)	mNGS (+)
S067	*Aspergillus fumigatus*	*Aspergillus* Elisa (+)	tNGS (+)	mNGS (+)
S087	*Aspergillus fumigatus*	*Aspergillus* Elisa (+), fungal fluorescent staining (+)	tNGS (+)	mNGS (+)
S156	*Aspergillus fumigatus*	Sputum culture (+), BALF culture (+), *Aspergillus* Elisa (+)	tNGS (+)	mNGS (+)
S162	*Aspergillus fumigatus*	Sputum culture (+), BALF culture (+)	tNGS (+)	mNGS (+)
S168	*Aspergillus fumigatus*	Sputum culture (+), BALF culture (+)	tNGS (+)	mNGS (+)
S087	*Aspergillus fumigatus*	*Aspergillus* Elisa(+), suspected *Aspergillus* hyphae and spores	tNGS (+)	mNGS (+)
S099	*Streptococcus pneumoniae*	BALF culture (+)	tNGS (+)	–
	Candida albicans	BALF culture (+)	tNGS (+)	mNGS (+)
S151	*Candida albicans*	Sputum culture (+), BALF culture (+)	–	mNGS (+)
S145	*Candida albicans*	BALF culture (+)	tNGS (+)	mNGS (+)
S146	*Candida albicans*	BALF culture (+)	tNGS (+)	mNGS (+)
S110	*Enterococcus faecium*	Pleural and peritoneal effusions (+)	tNGS (+)	mNGS (+)
S002	CMV	PCR(+), antibody(+)	tNGS (+)	mNGS (+)
	EB	PCR(+)	–	–
RLT-negative				
S158	*Mycobacterium tuberculosis*	–	tNGS (+)	–
S075	*Mycobacterium avium* complex	–	tNGS (+)	mNGS (+)

(Continued)

10.3389/fcimb.2024.1498512

TABLE 4 Continued

Sample	Potential Pathogen	Routine Laboratory Test	tNGS	mNGS
RLT-negative				
S085	*Mycobacterium avium* complex	–	tNGS (+)	mNGS (+)
S120	*Mycobacterium avium* complex	–	tNGS (+)	mNGS (+)
S149	*Mycobacterium kensasii*	–	tNGS (+)	mNGS (+)
S038	*Chlamydia psittaci*	–	tNGS (+)	mNGS (+)
	Aspergillus fumigatus	–	tNGS (+)	
S047	*Chlamydia psittaci*	–	tNGS (+)	mNGS (+)
S109	*Chlamydia psittaci*	–	tNGS (+)	–
S115	*Chlamydia psittaci*	–	tNGS (+)	–
S116	*Chlamydia psittaci*	–	tNGS (+)	mNGS (+)
S133	*Chlamydia psittaci*	–	tNGS (+)	mNGS (+)
S098	*Pneumocystis jirovecii*	–	tNGS (+)	mNGS (+)
	Rhinovirus	–	tNGS (+)	–
S074	*Pneumocystis jirovecii*	–	tNGS (+)	mNGS (+)
S064	*Pneumocystis jirovecii*	–	tNGS (+)	mNGS (+)
S012	*Pneumocystis jirovecii*	–	tNGS (+)	mNGS (+)
	HCMV	–	tNGS (+)	mNGS (+)
S019	*Pneumocystis jirovecii*	–	tNGS (+)	mNGS (+)
S026	*Pneumocystis jirovecii*	–	tNGS (+)	mNGS (+)
S104	*Pneumocystis jirovecii*	–	tNGS (+)	mNGS (+)
S107	*Pneumocystis jirovecii*	–	tNGS (+)	mNGS (+)
S128	*Pneumocystis jirovecii*	–	tNGS (+)	–
S177	*Pneumocystis jirovecii*	–	tNGS (+)	mNGS (+)
S101	Rhinovirus	–	tNGS (+)	–
S111	Human metapneumovirus	–	tNGS (+)	–
S114	Rhinovirus	–	tNGS (+)	–
S137	Influenza A virus	–	tNGS (+)	mNGS (+)

(Figure 2C). This may be thanks to the pre-amplification procedure, which could overcome interference by high level of human genomic fragments and increase sensitivity to low abundant targets.

Unlike tNGS, additional workflow is required for mNGS to detect RNA targets, which doubles the cost and resource consumption. Due to the expense of mNGS and our initial focus not including RNA viruses, a total of 102 samples did not undergo mNGS-RNA test, among which tNGS identified RNA viruses in 13 samples. Regarding samples with both mNGS-RNA and tNGS reports, both methods detected 12 RNA species, indicating their similar abilities to identify RNA viruses, as most detection frequencies for each species were equal (Supplementary Figure 2).

The agreement between NGS outputs and clinical diagnosis is the key concern in this study. As a broad-spectrum molecular detection method, NGS tends to output a comprehensive list of microbes once the targets are detected. Such a list usually includes opportunistic pathogens which only cause diseases on hosts with immunocompromised conditions. The less likelihood for a pathogen causing observable symptoms, the less likelihood clinicians link it to casual factors. This may explain the low PPVs for all opportunistic pathogens (Supplementary Table 5). One extreme case is Human gammaherpesvirus 4, with PPVs of 2.17% and 3.23% for tNGS and mNGS, respectively. Meanwhile, four selected microbes, *Aspergillus fumigata*, *Chlamydia psittaci*, *Crptococcus neoformans*, and *Mycobacterium tuberculosis* had higher PPVs (66.7%~100%, Table 3), demonstrating high agreement on these organisms as "pathogen" in clinical prospect.

A classification system was established to assess the diagnosis value of NGS methods to clinical decision under different scenarios (Figure 3; Table 1). All reports were adjudicated and labeled as Agree, Extend/Support, Noncontributory, Unlikely, or Disagree to ensure an intuitive summary. An ideal method should output a

higher percentage of "good" results, that is those reports with Agree or Support/Extend tags. Both tNGS and mNGS had a combined ratio of 65.6% (119/180) and 68.9% (124/180), indicating that NGS methods could assist in identifying potential pathogens. The cases labeled as 'Support' or 'Extend' had their etiology undetermined until the introduction of NGS, which enabled identification at the species level, reflecting NGS's ability to improve etiology determination. Such cases accounted for 33.9% and 30.6% for tNGS and mNGS, respectively. These findings suggest that tNGS may enhance medical service similarly to mNGS, as illustrated in Figure 3A.

Cases categorized as Noncontributory, Unlikely, or Disagree for tNGS and mNGS, respectively revealed NGS's limitations in some clinical cases. A preference of tNGS in Unlikely cases and mNGS in Disagree cases was observed (Figure 3B). We hypothesize that it might be due to the differences in sensitivity. The pathogen detection ability of mNGS was interfered by a high host genetic background (Miller et al., 2019) while the targeted amplification strategy makes tNGS avoid such interference and increase sensitivity. This could also apply to the Noncontributory cases, as a majority of the cases reported opportunistic pathogens, accounting for 13.9%/13.9% of all samples for tNGS/mNGS. This further supports our hypothesis that pathogenicity significantly influences the agreement between NGS results and clinical diagnosis. However, it is hard to conclude that NGS is Noncontributory. Firstly, pathogen reports at the early stage of infection could serve as an indicator of potential threat for immunocompromised patients with poor prognosis. Secondly, it is hard to exclude the role of opportunistic pathogens in exacerbating illness in cases of co-infection. In our opinion, both NGS methods are better suited as tools for profiling potential organism threats while it is the medical personnel's responsibility to conclude the relevance of the threats. This holds true for any detection tool, not just NGS. Therefore, interpretation is critical when employing NGS in pathogen detection.

Table 5 highlights several technical and practical considerations of mNGS and tNGS for pathogen identification. The tNGS panel focuses on specific pathogen species with high clinical relevance while mNGS detects all microbes without bias. Additionally, tNGS utilizes a panel design and pre-amplification strategy, resulting in high data usage and minimized data throughput requirement (100K for tNGS, 20M for mNGS). The cost of mNGS in this study ranged from 289.2 to 462.7 USD per assay (batch run), while tNGS was roughly a quarter of that cost. Moreover, regular mNGS requires additional nucleic acid extraction, library construction, and sequencing steps to detect RNA viruses, making the whole procedure of mNGS more complicated than tNGS. Overall, these advantages make tNGS a cost-efficient fit for clinical microbiology. The overall TAT of tNGS and mNGS were 12h and 17h, respectively, representing the internal time from sample preprocessing to report output. When combined with the delivery time, the total TAT may reach 1~2d, depending on the distance from sampling location to the third-party sequencing laboratory, which may delay the NGS report/service in meeting clinical needs. Delivery is one of the issues that NGS service providers need to improve through speeding up transportation by constructing an intensive network, or achieving sequencing laboratory localization. The laboratory–developed test (LDT) should be one of the trending solutions for NGS in the upcoming decade, allowing hospitals to develop LDT in place, which should significantly shorten the TAT in the future.

TABLE 5 Technical comparison of NGS in RTI diagnosis.

Features	mNGS	tNGS
Spectrum	Broad (target species > 20,000)	Broad (target species = 153)
Target Limit	Theoretically unlimited in sequencing level but pathogen calling limited to the reference database	Limited to the panel; may miss causal pathogens
Interference		
- high host genetic background	Major impact	Minor impact
- low-titer target species	Major impact	Minor impact
Simultaneous DNA + RNA Pathogen Identification	No, separate nucleic acid extraction, library and sequencing procedures are required for DNA and RNA pathogens, individually	Yes
Prior-knowledge Requirement	Yes, required downstream of sequencing (bioinformatics analysis step)	Yes, required prior to sequencing (enrichment step) bioinformatics analysis step
Prepossessing	Host depletion	Target amplification by multiplex PCR
Processing and Library Construction	Relatively more complicated processing procedures, more reagent cost (human depletion; additional extraction for RNA library)	Simple procedure
Average Output Size for Qualified Report	20 million reads	100 kilo reads
Effective Data %	Low, require host depletion	High
Interpretation	Required to determine potential pathogens from a comprehensive list, markedly more pathogens require interpretation	Fewer pathogens reported, but still requires interpretation
Turn Around Time	~17 h	~12 h
Cost per Assay/Patient	mNGS(DNA): ~600 USD	~120 USD
	mNGS(DNA+RNA): ~1000 USD	(pending on panel)

It's hard to conclude that tNGS is a substitute for mNGS in pathogen identification. The specificity and target spectrum of a multiplex-PCR-based tNGS largely depend on the primer set design. In this study, a total of 28 species were missed by the

tNGS panel, as summarized in Supplementary Table 3. However, only 3 of them were clinically significant. The inability of tNGS to identify unknown pathogens could be problematic when an acute infection is caused by new/unknown pathogens, e.g. SARS-COV-2 pandemic in 2019. Although the spectrum limit of tNGS could be resolved by increasing target species, the difficulty of primer set design significantly increases, and pre-amplification may enhance contamination signals, posing another challenge to tNGS application. Thus, the decision to use either mNGS or tNGS should be guided by several factors, including the clinical scenario, technical distinctions, emergence, and cost. For cases requiring rapid identification of an etiology, tNGS is recommended due to its shorter turnaround time (TAT). In contrast, for severe infections where a comprehensive report on pathogens and drug resistance is crucial, mNGS may be prioritized over tNGS, given its broader target spectrum. In some situations, employing both mNGS and tNGS concurrently might be beneficial. Moreover, for cases where there is a suspicion of new or unknown pathogens, or where routine clinical laboratory tests have returned negatives or have an inadequate spectrum, mNGS is recommended. While this study only included bronchoalveolar lavage fluid (BALF) samples, it is important to note that other sample types, including more complex samples like formalin-fixed, paraffin-embedded (FFPE) tissues or blood samples with low host genetic material, could also be effectively analyzed. This approach ensures that the choice between mNGS and tNGS is aligned with the specific needs of the clinical context, leveraging each method's strengths to optimize pathogen identification and patient outcomes.

A recent study compared the performance of tNGS and mNGS in RTI diagnosis on the same cohort (Sun et al., 2024), which employed a similar design as ours. Both Sun's study and this study remonstrated that the overall performance of tNGS and mNGS in pathogen detection was relatively similar while significant differences were noted in the detection of specific pathogens. For Human gammaherpesvirus 4, Human betaherpesvirus 7, and Human betaherpesvirus 5, which were focal points of Sun's study, our findings indicate significant differences between tNGS and mNGS ($P<0.05$) and tNGS presented higher detection frequencies for all these viruses, aligning with the Sun's study. Conversely, in the case of Human betaherpesvirus 6, our analysis identified only three positives by tNGS whereas mNGS yielded non, thus it could not be directly compared to Sun's result (12 verse 4). Nonetheless, it's also difficult to conduct direct parallel comparison regarding other pathogens. First, Sun's study employed a relatively small sample size of 80, which is hard to confirm such sample size is robust enough for reliable conclusions, especially for the pathogens with low detection rates (25 species had only 1 positive in Sun's study), let alone Sun's study didn't involve mNGS-RNA procedures. In contrast, our study was informed by prior exploratory research and adopted a sample size exceeding 190 to ensure robustness (demonstrated in Methods and materials 2.8). Secondly, the sensitivity and specificity of pathogen detection are heavily contingent upon the primer sets utilized. Without transparency of primer settings in these commercial tNGS panels in these two studies, it is difficult to critically evaluate these differences. Thirdly, our study opted for simultaneous application of both mNGS and tNGS, whereas the other study subjected residual mNGS samples to freeze-thaw cycles before conducting tNGS, which could have inadvertently compromised the sensitivity of tNGS for certain samples. Also, Our study design did not include an orthogonal validation, like the retrospective PCR in Sun's study, since we have already employed a composite reference standard, which takes results from single to multiple prior microbial testings for robust etiology.

In conclusion, this study demonstrates the robustness of a highly-multiplex PCR based tNGS method in respiratory pathogen detection, as an economical alternative to mNGS. Although mNGS offers theoretically unlimited sequencing depth, it requires a higher cost per assay than tNGS. Conversely, tNGS is more cost-effective and less susceptible to inference impact, but restricted to specific panel targets. The sequencing methods, therefore, should be selected based on specific goals, available resources, and trade-offs between sensitivity, specificity, and cost. Our recommendation is to prioritize tNGS as a primary option for RTI diagnosis due to its lower cost, while keeping mNGS available as an alternative if tNGS proves inadequate in clinical practice. Although tNGS and mNGS are complementary in pathogen detection, reliable results must be obtained in combination with sophisticated interpretation and adjudication. Validating the clinical relevance of NGS reports requires taking into account the pathogenicity of the reported organisms and low-abundance candidates. Overall, these findings offer valuable insights for decision-making in microbial identification and can assist researchers in optimizing the use of sequencing technologies for medical purposes.

Data availability statement

All sequencing data generated for this study, including tNGS and mNGS, have been deposited in the Genome Sequence Archive (Chen et al., 2021) database of National Genomics Data Center under the accession number PRJCA018285.

Ethics statement

The study protocol was reviewed and approved by the Independent Ethics Committee for Clinical Research and Animal Trials of the First Affiliated Hospital of Sun Yat-sen University (protocol code [2023]357) and conformed to the ethical standards for medical research involving human subjects, as laid out in the newest versions of ICH-GCP, China GCP, and Declaration of Helsinki. This study involved retrospective information and material collection and has been approved by the ethics committee as exempt from informed consent.

Author contributions

YK: Data curation, Methodology, Validation, Writing – original draft. WT: Conceptualization, Validation, Writing – original draft. CH: Conceptualization, Methodology, Writing – review & editing.

ZD: Software, Validation, Visualization, Writing – review & editing, Formal analysis. LB: Data curation, Investigation, Validation, Writing – original draft, Writing – review & editing, Software. JW: Data curation, Formal analysis, Investigation, Methodology, Writing – review & editing. HL: Data curation, Formal analysis, Investigation, Methodology, Writing – review & editing. HC: Data curation, Formal analysis, Investigation, Methodology, Writing – review & editing. RH: Data curation, Formal analysis, Investigation, Methodology, Writing – review & editing. PZ: Methodology, Resources, Writing – review & editing. JL: Methodology, Resources, Writing – review & editing. CX: Writing – review & editing, Methodology. ZK: Conceptualization, Funding acquisition, Methodology, Project administration, Resources, Supervision, Validation, Writing – original draft, Writing – review & editing. K-JT: Conceptualization, Methodology, Project administration, Resources, Supervision, Validation, Writing – original draft, Writing – review & editing.

Funding

The author(s) declare financial support was received for the research, authorship, and/or publication of this article. This work was funded by National Natural Science Foundation of China (81773299), which is granted to ZK.

Acknowledgments

The authors would like to express their gratitude to Dr. Pei Li from Guangzhou KingMed Diagnostics Group Co., Ltd., Professor Guobao Tian from School of Medicine, Sun Yat-sen University, and Professor Jingxian Chen from National Clinical Research Center for Respiratory Disease for their valuable comments on this project. Additionally, the authors would like to thank Guangzhou KingMed Diagnostics Group Co., Ltd. and Vision Medicals Technology Co., Ltd. for their service and support in tNGS and mNGS, respectively.

Conflict of interest

CH, ZD, PZ, and JL are employees or executives of Guangzhou Kingcreate Biotechnology Co., Ltd.

The remaining authors declare that the research was conducted in the absence of any commercial or financial relationships that could be construed as a potential conflict of interest.

Publisher's note

Author disclaimer

Commercial products mentioned in this study are only for describing materials to make this study possible.

Supplementary material

The Supplementary Material for this article can be found online at: https://www.frontiersin.org/articles/10.3389/fcimb.2024.1498512/full#supplementary-material

References

Altman, D. G., and Bland, J. M. (1994a). Diagnostic tests 1: sensitivity and specificity. *BMJ.* 308, 1552. doi: 10.1136/bmj.308.6943.1552

Altman, D. G., and Bland, J. M. (1994b). Diagnostic tests 2: Predictive values. *BMJ.* 309, 102. doi: 10.1136/bmj.309.6947.102

Andrews, F. C. (1954). Asymptotic behavior of some rank tests for analysis of variance. *Ann. Inst. Stat. Math.* 25, 724–736. doi: 10.1214/aoms/1177728658

Bland, J. M., and Altman, D. G. (1996). Transformations, means and confidence intervals. *BMJ.* 312, 1079. doi: 10.1136/bmj.312.7038.1079

Bleeker-Rovers, C. P., Vos, F. J., de Kleijn, E. M. H. A., Mudde, A. H., Dofferhoff, T. S. M., Richter, C., et al. (2007). A prospective multicenter study on fever of unknown origin: the yield of a structured diagnostic protocol. *Medicine* 86, 26–38. doi: 10.1097/MD.0b013e31802fe858

Bolger, A. M., Lohse, M., and Usadel, B. (2014). Trimmomatic: A flexible trimmer for Illumina sequence data. *Bioinformatics* 30, 2114–2120. doi: 10.1093/bioinformatics/btu170

Chen, T. T., Chen, X., Zhang, S., Zhu, J., Tang, B., Wang, A., et al. (2021). The Genome Sequence Archive Family: toward explosive data growth and diverse data types. *Genomics Proteomics Bioinf.* 19, 578–583. doi: 10.1016/j.gpb.2021.08.001

Chen, X., Ding, S., Lei, C., Qin, J., Guo, T., Yang, D., et al. (2020). Blood and bronchoalveolar lavage fluid metagenomic next-generation sequencing in pneumonia. *Can. J. Infect. Dis. Med. Microbiol.* 2020, 6839103. doi: 10.1155/2020/6839103

Chen, S., Zhou, Y., Chen, Y., and Gu, J. (2018). fastp: an ultra-fast all-in-one FASTQ preprocessor. *Bioinformatics* 34, i884–i890. doi: 10.1093/bioinformatics/bty560

Dennis, T. P. W., Mable, B. K., Brunelle, B., Devault, A., Carter, R. W., Ling, C. L., et al. (2022). Target-enrichment sequencing yields valuable genomic data for challenging-to-culture bacteria of public health importance. *Microb. Genom.* 8, mgen000836. doi: 10.1099/mgen.0.000836

Dickson, R. P., Erb-Downward, J. R., Martinez, F. J., and Huffnagle, G. B. (2016). The microbiome and the respiratory Tract. *Annu. Rev. Physiol.* 78, 481–504. doi: 10.1146/annurev-physiol-021115-105238

Dong, Y. L., Chen, Q. Q., Tian, B., Li, J., and Hu, Z. (2022). Advancing microbe detection for lower respiratory tract infection diagnosis and management with metagenomic next-generation sequencing. *Infect. Drug Resist.* 16, 677–694. doi: 10.2147/IDR.S387134

Duan, H. X., Li, X., Mei, A. H., Li, P., Liu, Y., Li, X. F., et al. (2021). The diagnostic dalue of metagenomic next-generation sequencing in infectious diseases. *BMC. Infect. Dis.* 21, 62. doi: 10.1186/s12879-020-05746-5

Ewig, S., Torres, A., Angeles Marcos, M., Angrill, J., Rañó, A., de Roux, A., et al. (2002). Factors associated with unknown aetiology in patients with community-acquired pneumonia. *Eur. Respir. J.* 20, 1254–1262. doi: 10.1183/09031936.02.01942001

Fang, X., Mei, Q., Fan, X., Zhu, C., Yang, T., Zhang, L., et al. (2020). Diagnostic value of metagenomic next-generation sequencing for the detection of pathogens in bronchoalveolar lavage fluid in ventilator-associated pneumonia patients. *Front. Microbiol.* 11. doi: 10.3389/fmicb.2020.599756

Faraone, S. V. (2008). Interpreting estimates of treatment effects: implications for managed care. *P. T.* 33, 700–711.

Fieller, C., Hartley, H. O., and Pearson, E. S. (1957). Tests for rank correlation coefficients. I. *Biometrika.* 44, 470–481. doi: 10.1093/biomet/44.3-4.470

Gaston, D. C., Miller, H. B., Fissel, J. A., Jacobs, E., Gough, E., Wu, J., et al. (2022). Evaluation of metagenomic and targeted next-generation sequencing workflows for detection of respiratory pathogens from bronchoalveolar lavage fluid specimens. *J. Clin. Microbiol.* 60, e0052622. doi: 10.1128/jcm.00526-22

Gu, W., Deng, X., Lee, M., Yasemin, D. S., Arevalo, S., Stryke, D., et al. (2021). Rapid pathogen detection by metagenomic next-generation sequencing of infected body fluids. *Nat. Med.* 27, 115–124. doi: 10.1038/s41591-020-1105-z

Jiang, J., Bai, L., Yang, W., Peng, W., An, J., Wu, Y., et al. (2021). Metagenomic next-generation sequencing for the diagnosis of *Pneumocystis jirovecii* pneumonia in non-HIV-infected patients: a retrospective study. *Infect. Dis. Ther.* 10, 1733–1745. doi: 10.1007/s40121-021-00482-y

Langmead, B., and Salzberg, S. L. (2012). Fast gapped-read alignment with Bowtie 2. *Nat. Methods* 9, 357–359. doi: 10.1038/nmeth.1923

Li, H., and Durbin, R. (2009). Fast and accurate short read alignment with Burrows-Wheeler transform. *Bioinformatics* 25, 1754–1760. doi: 10.1093/bioinformatics/btp324

Li, H. N., Gao, H., Meng, H., Wang, Q., Li, S., Chen, H., et al. (2018). Detection of pulmonary infectious pathogens from lung biopsy tissues by metagenomic next-generation sequencing. *Front. Cell. Infect. Microbiol.* 8. doi: 10.3389/fcimb.2018.00205

Li, Y., Sun, B., Tang, X., Liu, Y. L., He, H. Y., Li, X. Y., et al. (2020). Application of metagenomic next-generation sequencing for bronchoalveolar lavage diagnostics in critically ill patients. *Eur. J. Clin. Microbiol. Infect. Dis.* 39, 369–374. doi: 10.1007/s10096-019-03734-5

Li, S., Tong, J., Liu, Y., Shen, W., and Hu, P. (2022). Targeted next generation sequencing is comparable with metagenomic next generation sequencing in adults with pneumonia for pathogenic microorganism detection. *J. Infect.* 85, e127–e129. doi: 10.1016/j.jinf.2022.08.022

Liu, H., Zhang, Y., Chen, G., Sun, S., Wang, J., Chen, F., et al. (2022). Diagnostic significance of metagenomic next-generation sequencing for community-acquired pneumonia in southern China. *Front. Med.* 9, 807174. doi: 10.3389/fmed.2022.807174

Lozano, R., Naghavi, M., Foreman, K. K., Lim, S., Shibuya, K., Aboyans, V., et al. (2012). Global and regional mortality from 235 causes of death for 20 age groups in 1990 and 2010: a systematic analysis for the global burden of disease study 2010. *Lancet* 2012, 2095–2128. doi: 10.1016/S0140-6736(12)61728-0

Mamanova, L., Coffey, A. J., Scott, C. E., Kozarewa, I., Turner, E. H., Kumar, A., et al. (2010). Target-enrichment strategies for next-generation sequencing. *Nat. Meth.* 7, 111–118. doi: 10.1038/nmeth.1419

Man, W. H., de Steenhuijsen Piters, W. A., and Bogaert, D. (2017). The microbiota of the respiratory tract: gatekeeper to respiratory health. *Nat. Rev. Microbiol.* 15, 259–270. doi: 10.1038/nrmicro.2017.14

Miao, Q., Ma, Y. Y., Wang, Q. Q., Pan, J., Zhang, Y., Jin, W., et al. (2018). Microbiological diagnostic performance of metagenomic next-generation sequencing when applied to clinical practice. *Clin. Infect. Dis.* 67, S231–S240. doi: 10.1093/cid/ciy693

Miller, R. R., Montoya, V., Gardy, J. L., Patrick, D. M., and Tang, P. (2013). Metagenomics for pathogen detection in public health. *Genome Med.* 5, 81. doi: 10.1186/gm485

Miller, S., Naccache, S. N., Samayoa, E., Messacar, K., Arevalo, S., Federman, S., et al. (2019). Laboratory validation of a clinical metagenomic sequencing assay for pathogen detection in cerebrospinal fluid. *Genome Res.* 29, 831–842. doi: 10.1101/gr.238170.118

Peng, J. M., Du, B., Qin, H. Y., Wang, Q., and Shi, Y. (2021). Metagenomic next-generation sequencing for the diagnosis of suspected pneumonia in immunocompromised patients. *J. Infect.* 82, 22–27. doi: 10.1016/j.jinf.2021.01.029

Shapiro, S. S., and Wilk, M. B. (1965). An analysis of variance test for normality (complete samples). *Biometrika.* 52, 591–611. doi: 10.1093/biomet/52.3-4.591

Shi, C. L., Han, P., Tang, P. J., Chen, M. M., Ye, Z. J., Wu, M. Y., et al. (2020). Clinical metagenomic sequencing for diagnosis of pulmonary tuberculosis. *J. Infect.* 81, 567–574. doi: 10.1016/j.jinf.2020.08.004

Sun, W., Zheng, L., Kang, L., Chen, C., Wang, L., Lu, L., et al. (2024). Comparative analysis of metagenomic and targeted next-generation sequencing for pathogens diagnosis in bronchoalveolar lavage fluid specimens. *Front. Cell Infect. Mi.* 14. doi: 10.3389/fcimb.2024.1451440

van Stralen, K. J., Stel, V. S., Reitsma, J. B., Dekker, F. W., Zoccali, C., Jager, K. J., et al. (2009). Diagnostic methods I: sensitivity, specificity, and other measures of accuracy. *Kidney Int.* 75, 1257–1263. doi: 10.1038/ki.2009.92

Weng, Q. Y., Raff, A. B., Cohen, J. M., Gunasekera, N., Okhovat, J. P., Vedak, P., et al. (2017). Costs and consequences associated with misdiagnosed lower extremity cellulitis. *JAMA. Dermatol.* 153, 141–146. doi: 10.1001/jamadermatol.2016.3816

Xie, F., Duan, Z. M., Zeng, W. Q., Xie, S., Xie, M., Fu, H., et al. (2021). Clinical Metagenomics Assessments improve diagnosis and outcomes in community-acquired pneumonia. *BMC. Infect. Dis.* 21, 352. doi: 10.1186/s12879-021-06039-1

Yang, L. B., Haidar, G., Zia, H., Nettles, R., Qin, S., Wang, X., et al. (2019). Metagenomic identification of severe pneumonia pathogens in mechanically-ventilated patients: a feasibility and clinical validity study. *Respir. Res.* 20, 265. doi: 10.1186/s12931-019-1218-4

Yin, Y., Zhu, P., Guo, Y., Li, Y., Chen, H., Liu, C., et al. (2024). Enhancing lower respiratory tract infection diagnosis: implementation and clinical assessment of multiplex PCR-based and hybrid capture-based targeted next-generation sequencing. *EBioMedicine.* 15, 9:807174. doi: 10.1016/j.ebiom.2024.105307

Yongfeng, H., Fan, Y., Jie, D., Jian, Y., Ting, Z., Lilian, S., et al. (2011). Direct pathogen detection from swab samples using a new high-throughput sequencing technology. *Clin. Microbiol. Infect.* 17, 241–244. doi: 10.1111/j.1469-0691.2010.03246.x

Zaharia, M., Bolosky, W. J., Curtis, K., Fox, A., Patterson, D., Shenker, S., et al. (2011). Faster and more accurate sequence alignment with SNAP. *arXiv1111.5572v1.* doi: 10.48550/arXiv.1111.5572

Zhong, Y., Xu, F., Wu, J., Schubert, J., and Li, M. M. (2021). Application of next generation sequencing in laboratory medicine. *Ann. Lab. Med.* 41, 25–43. doi: 10.3343/alm.2021.41.1.25

frontiers | Frontiers in Cellular and Infection Microbiology

TYPE Original Research
PUBLISHED 07 January 2025
DOI 10.3389/fcimb.2024.1526633

OPEN ACCESS

EDITED BY
Ariadna Petronela Fildan,
Ovidius University, Romania

REVIEWED BY
Tatina Todorova,
Medical University of Varna, Bulgaria
Shigao Huang,
Air Force Medical University, China

*CORRESPONDENCE
Hu Zhang
zhanghu@scu.edu.cn

†These authors have contributed equally to this work and share first authorship

RECEIVED 12 November 2024
ACCEPTED 16 December 2024
PUBLISHED 07 January 2025

CITATION
Ma C, Jiang M, Li J, Zeng Z, Wu Y, Cheng R, Lin H, Pang J, Yin F, Jia Y, Li L and Zhang H (2025) Plasma Epstein-Barr Virus DNA load for diagnostic and prognostic assessment in intestinal Epstein-Barr Virus infection. *Front. Cell. Infect. Microbiol.* 14:1526633. doi: 10.3389/fcimb.2024.1526633

Plasma Epstein-Barr Virus DNA load for diagnostic and prognostic assessment in intestinal Epstein-Barr Virus infection

Chunxiang Ma[1,2,3†], Mingshan Jiang[1,2,3†], Jiaxin Li[1,2,3†], Zhen Zeng[1,2,3], Yushan Wu[1,2,3], Rui Cheng[1,2,3], Hao Lin[1,2,3], Jiangmei Pang[1,2,3], Fang Yin[1,2,3], Yongbin Jia[1,2,3], Lili Li[1,2,3] and Hu Zhang[1,2,3*]

[1]Department of Gastroenterology, West China Hospital, Sichuan University, Chengdu, China, [2]Centre for Inflammatory Bowel Disease, West China Hospital, Sichuan University, Chengdu, China, [3]Lab of Inflammatory Bowel Disease, Frontiers Science Center for Disease-Related Molecular Network, West China Hospital, Sichuan University, Chengdu, China

Background: The prospective application of plasma Epstein-Barr virus (EBV) DNA load as a noninvasive measure of intestinal EBV infection remains unexplored. This study aims to identify ideal threshold levels for plasma EBV DNA loads in the diagnosis and outcome prediction of intestinal EBV infection, particularly in cases of primary intestinal lymphoproliferative diseases and inflammatory bowel disease (IBD).

Methods: Receiver operating characteristic (ROC) curves were examined to determine suitable thresholds for plasma EBV DNA load in diagnosing intestinal EBV infection and predicting its prognosis.

Results: 108 patients were retrospectively assigned to the test group, while 56 patients were included in the validation group. Plasma EBV DNA loads were significantly higher in the intestinal EBV infection group compared to the non-intestinal EBV infection group (Median: 2.02×10^2 copies/mL, interquartile range [IQR]: 5.49×10^1-6.34×10^3 copies/mL versus 4.2×10^1 copies/mL, IQR: 1.07×10^1-6.08×10^1 copies/mL; $P < 0.0001$). Plasma EBV DNA levels at 9.21×10^1 and 6.77×10^1 copies/mL proved beneficial for the identification and prognostication in intestinal EBV infection, respectively. Values of 0.82 and 0.71 were yielded by the area under the ROC curve (AUC) in the test cohort, corresponding to sensitivities of 84.38% (95% confidence interval [95%CI]: 68.25%-93.14%) and 87.5% (95%CI: 69%-95.66%), specificities of 83.33% (95% CI: 64.15%-93.32%) and 68.09% (95%CI: 53.83%-79.6%), positive predictive values (PPV) of 87.1% (95%CI: 71.15%-94.87%) and 58.33% (95%CI: 42.2%-72.86%), and positive likelihood ratios (LR^+) of 5.06 and 2.74 in the validation cohort, respectively. Furthermore, a plasma EBV DNA load of 5.4×10^2 copies/mL helped differentiate IBD with intestinal EBV infection from primary intestinal EBV-positive lymphoproliferative disorders (PIEBV+LPDs), achieving an AUC of 0.85 within the test cohort, as well as 85% sensitivity (95%CI: 63.96%-94.76%), 91.67%

specificity (95%CI: 64.61%-99.57%), 94.44% PPV (95%CI: 74.24%-99.72%), and an LR^+ of 10.2 in the validation cohort.

Conclusions: Plasma EBV DNA load demonstrates notable potential in distinguishing between different patient cohorts with intestinal EBV infection, although its sensitivity requires further optimization for clinical application.

KEYWORDS

Epstein-Barr virus DNA load, diagnosis, prognosis, inflammatory bowel diseases, primary intestinal lymphoproliferative diseases, intestinal Epstein-Barr Virus infection

1 Introduction

Epstein-Barr virus (EBV), a pervasive herpesvirus, is particularly recognized for its oncogenic potential in various malignancies and its association with autoimmune diseases (Young et al., 2016). The pathogenic role of EBV has been well established in multiple diseases, such as infectious mononucleosis (Lennon et al., 2015), Burkitt lymphoma (BL) (López et al., 2022), and nasopharyngeal cancer (NPC) (Wong et al., 2021). However, research into the impact of EBV on intestinal diseases, particularly inflammatory bowel disease (IBD), together with primary intestinal lymphoproliferative diseases (PILPDs), is just beginning (Rizzo et al., 2017; Dang et al., 2023; Chen L. et al., 2024). IBD is a multifaceted disease characterized by persistent inflammation within the gastrointestinal tract, which is often exacerbated by opportunistic infections (Cao et al., 2022; Zeng et al., 2023; Li et al., 2024; Pu et al., 2024). Evidence highlights that the incidence of positive EBV DNA detection from intestinal resection specimens in patients with IBD is 55%-76%, which is markedly higher than the 19% observed in a non-IBD group (Xu et al., 2020). Furthermore, EBV infection is intricately linked to clinical manifestations (Dimitroulia et al., 2013), therapeutic responses (Pezhouh et al., 2018; Chen Y. et al., 2024), surgical interventions (Hosomi et al., 2018), and lymphoma incidence (Nissen et al., 2015; de Francisco et al., 2018) in IBD patients. Moreover, the diagnosis of intestinal diseases is significantly influenced by EBV infection. PILPDs encompass a spectrum of diseases characterized by abnormal lymphocyte proliferation in the intestine, with manifestations ranging from benign to malignant; notably, aggressive PILPDs are linked to an extremely high risk of mortality (Cohen et al., 2009; Montes-Mojarro et al., 2020). Our previous study revealed that 67% of 12 patients with primary intestinal EBV-positive lymphoproliferative disorders (PIEBV+LPDs) were initially diagnosed with IBD, and half of the 12 patients ultimately succumbed to PIEBV+LPDs (Wang Z. et al., 2018). This underscores the fact that overlooking intestinal EBV infection can lead to fatal outcomes. It is equally important to acknowledge that the gold standard for diagnosing EBV infection is histological analysis using EBV-encoded small RNAs *in situ* hybridization (EBER-ISH) (Weiss and Chen, 2013). However, given the anatomical location of the intestine, the intestinal EBER-ISH test requires invasive procedures, such as endoscopy or surgery. Therefore, the clinical significance of other noninvasive, dependable, and accessible methods for diagnosing intestinal EBV infection needs to be explored.

Measuring peripheral EBV DNA levels shows superiority in simplicity and non-invasiveness for diagnosing and surveilling EBV infection when compared with the histological EBER-ISH test. However, the value of the test is significantly influenced by the choice of peripheral blood components analyzed, such as whole blood, plasma, and peripheral blood mononuclear cells (PBMCs), which may affect sensitivity and specificity. Owing to the latent characteristics of EBV, research proved that measuring EBV DNA levels in plasma has advantages over measuring them in whole blood and PBMCs as indicators of active replication of the virus, thereby improving the diagnostic and prognostic power of diseases associated with EBV (Tsai et al., 2015; Kanakry et al., 2016; Ludvigsen et al., 2023). For instance, the diagnostic sensitivity of a detectable plasma EBV DNA load can reach up to 90% in BL (Hohaus et al., 2011) and as high as 93.2% in NPC (Lou et al., 2023). Furthermore, plasma EBV DNA levels showed considerable predictive power for the outcomes of these diseases (Hui et al., 2020; Qiu et al., 2020). However, in EBV-associated intestinal diseases, although a study reported that IBD patients infected with intestinal EBV exhibited heightened concentrations of EBV DNA within their peripheral whole blood (Xu et al., 2020), no study has employed plasma EBV DNA load, an indicative marker of active infection, to establish definitive thresholds for aiding diagnostic and prognostic assessment of intestinal EBV infection.

Therefore, we conducted a retrospective investigation to define the diagnostic and prognostic cut-off values for intestinal EBV infection based on plasma EBV DNA loads. This approach will facilitate the differential diagnosis of intestinal EBV infections in the clinical setting.

2 Materials and methods

2.1 Study population and design

This retrospective investigation was performed at the Gastroenterology Department of West China Hospital between January 2013 and January 2024. Initially, patients with positive plasma EBV DNA loads and intestinal diseases were screened through electronic medical record system, followed by verification through the pathology system to confirm whether they had also undergone intestinal EBER-ISH test. Patients with intestinal diseases who tested positive for peripheral blood EBV DNA and completed the intestinal EBER-ISH test were included in the study, while those who did not complete both tests, had incomplete clinical data, or had unclear diagnoses were excluded. Immunomodulator usage was defined as treatment with steroids, immunosuppressants, or biological agents within three months prior to the intestinal EBER-ISH test, and intestinal EBV infection was defined as positive EBER-ISH test in the intestine. The diagnosis of IBD followed recognized criteria, including typical clinical presentations, endoscopic findings, radiological assessments, and histological results (Gomollón et al., 2017; Magro et al., 2017). The diagnostic criteria for PILPDs require the presence of gastrointestinal symptoms and confirmation of abnormal proliferation of lymphocytes within the intestinal tissues through pathology, while excluding primary lymphoproliferative diseases at other sites (Wang Z. et al., 2018). On this basis, a positive result for intestinal EBER-ISH test was defined as PIEBV+LPDs, while a negative result was defined as primary intestinal non-EBV-associated lymphoproliferative diseases (PINEBV+LPDs). Data from the electronic medical record system were also collected to analyze clinical data, such as sex, age, plasma EBV DNA load, and other factors. Furthermore, a follow-up on the prognosis of all patients was conducted, where events such as intestinal resection or death within six months after undergoing intestinal EBER-ISH test were defined as fatal events, while all other outcomes were considered benign events. Ethics approval for the present investigation was obtained from the ethics board of West China Hospital. (Number: 2023-22).

2.2 EBV test

As directed by the manufacturer, quantitative measurement of EBV DNA in the plasma was performed using an EBV detection kit with polymerase chain reaction (PCR) fluorescence (Shen Xiang Gene Co.). The EBER gene was amplified using a Bio-Rad CFX96 PCR instrument. A Ct value ≤39 was interpreted as positive, and a standard curve was used to calculate the quantity of EBV DNA copies. EBER-ISH was used to investigate intestinal EBV infection, and the EBV-encoded small RNAs (EBER) peptide nucleic acid probe was sourced from ZSGB-BIO (China). Specifically, tissues from intestinal biopsies of patients were deparaffinized, rehydrated, and permeabilized with proteinase K, followed by overnight hybridization at 37°C with digoxigenin-labeled EBER probes. After incubation with horseradish peroxidase-conjugated anti-digoxigenin antibody, EBER-positive cells were identified by diaminobenzidine staining and exhibited brown-stained nuclei. These cells were quantitatively scored by two experienced pathologists in high-power field (HPF).

2.3 Statistical analysis

Statistical evaluation was performed using SPSS and GraphPad Prism (version 26.0 and 9.5, respectively). This investigation of the demographic and basic features of the patients utilized both frequency distributions and descriptive statistical methods. To compare patient characteristics among different cohorts, either the chi-squared hypothesis evaluation or the exact significance test using Fisher's exact test was employed, contingent on the distributional features inherent in these data. To evaluate the role of plasma EBV DNA load in the diagnostic and prognostic assessment of intestinal EBV infection, a stepwise analysis was conducted using both the train and validation cohorts. In the first stage, receiver operating characteristic (ROC) curves were utilized to analyze plasma EBV DNA concentrations for diagnosing intestinal EBV infection and predicting its prognosis. These optimal cutoff values were determined based on the maximum Youden's index, which maximizes the sum of sensitivity and specificity (Youden's index = sensitivity + specificity-1). This approach ensures the identification of the threshold that achieves the best trade-off between true-positive and true-negative rates for each cohort. In the next stage, the performance of these cutoff values was assessed in the validation cohort by calculating sensitivity, specificity, positive predictive value (PPV), negative predictive value (NPV), positive likelihood ratio (LR^+), and negative likelihood ratio (LR^-). These metrics were used to confirm the robustness of the cutoff values derived from the train cohort. Statistical significance was represented by a p-value of < 0.05.

3 Results

3.1 Clinical characteristics among train cohort

Our investigation began with the identification of 213 patients diagnosed with intestinal diseases and tested positive for plasma EBV DNA. After excluding patients with unclear diagnoses and incomplete clinical data, the remaining patients were randomly assigned in a 2:1 ratio, resulting in a cohort of 108 patients in the train group and 56 patients in the validation group (Supplementary Figure 1; Supplementary Table 1). The train cohort consisted of 60 patients (55.56%) who tested negative for intestinal EBER-ISH and 48 patients (44.44%) who tested positive for intestinal EBER-ISH. The median age of the EBER-negative group was 42 years, which was comparable to that of the EBER-positive group (median age, 44 years). Moreover, neither sex distribution nor disease course demonstrated notable differences between the two groups.

Additionally, the EBER-positive group did not exhibit a significantly higher frequency of immunomodulator use within three months preceding the intestinal EBER-ISH test than the EBER-negative group. However, a disparity in disease type was observed between the two groups. The EBER-positive group predominantly consisted of patients with PILPDs (50%), followed by IBD (47.9%) and other diseases (2.1%), whereas IBD was the most prevalent disease in the EBER-negative group (76.7%). The symptoms in both groups also differed significantly in clinical terms, with the EBER-positive group showing a higher incidence of fever and hematochezia than the EBER-negative group (Table 1).

3.2 Distribution of plasma EBV DNA loads in intestinal EBV infection

In this study, we conducted comparative analyses of the distribution of plasma EBV DNA load across various intestinal diseases. The findings revealed that the majority of patients (88.3%) in the EBER-negative group had EBV DNA loads $<10^1$ copies/ml, with only 11.7% having loads of 10^2-10^3 copies/ml, whereas the EBER-positive group exhibited a wider distribution of higher plasma EBV DNA loads, with 33.3% having loads $>10^3$ copies/ml and 25% having loads between 10^2 and 10^3 copies/ml ($P < 0.001$; Figure 1A). Additionally, when focusing on patients with IBD, we observed that EBER-positive IBD patients exhibited a notably elevated proportion of plasma EBV DNA loads (10^2-10^3 copies/ml) compared to their EBER-negative counterparts (30.4% vs. 6.5%, $P = 0.013$; Figure 1B). Among patients with PILPDs, 66.6% of PIEBV+LPD patients had EBV DNA loads $>10^3$ copies/ml, whereas no patients in the PINEBV +LPD group exhibited similarly high viral loads ($P = 0.001$; Figure 1C). Despite the overall high occurrence of elevated plasma EBV DNA loads in the EBER-positive IBD and PIEBV+LPD groups, a notable difference was observed in the distribution of viral loads between these two groups. In the PIEBV+LPD group, 66.6% of the patients had EBV DNA loads $>10^3$ copies/ml, whereas none of the EBER-positive IBD patients were present within this viral load range ($P < 0.001$; Figure 1D).

Further analysis was conducted to compare plasma EBV DNA levels across EBER-negative and EBER-positive populations. Among the 48 patients in the intestinal EBER-positive group, the plasma EBV DNA level had a median value of 2.02×10^2 copies/mL (Interquartile Range [IQR]: 5.49×10^1-6.34×10^3 copies/mL), which represented a significantly elevated level compared to the median of 4.2×10^1 copies/mL (IQR: 1.07×10^1-6.08×10^1 copies/mL) observed in 60 patients in the intestinal EBER-negative group (Figure 1E). These median plasma EBV DNA loads were notably elevated in comparison to the respective EBER-negative control groups, including the IBD and PILPD groups, as detailed in Figures 1F, G. Notably, within the intestinal EBER-positive cohort, patients diagnosed with PIEBV+LPDs demonstrated the highest median plasma EBV DNA level at 6.18×10^3 copies/mL (IQR 1.8×10^2-5.91×10^4 copies/mL), significantly surpassing the levels in EBER-positive IBD patients (5.96×10^1 copies/mL [IQR 2.23×10^1-2.45×10^2 copies/mL]), with a P-value of <0.0001 (Figure 1H).

TABLE 1 Clinical data of patients in the training and validation cohort.

Characteristics	Test cohort			Validation cohort		
	Intestinal EBER-negative group (N=60)	Intestinal EBER-positive group (N=48)	*P* value	Intestinal EBER-negative group (N=24)	Intestinal EBER-positive group (N=32)	*P* value
Age (year), median ± SD	42 ± 17	44 ± 15	0.431	47 ± 16	41 ± 16	0.815
Male, n (%)	40 (66.7%)	28 (58.3%)	0.373	14 (58.3%)	22 (68.8%)	0.421
Disease duration (months), median ± SD	40 ± 48	44 ± 86	0.7696	32 ± 43	33 ± 60	0.938
IMM use within three months prior to intestinal EBER-ISH test, n (%)	14 (23.3%)	14 (29.2%)	0.492	5 (20.8%)	8 (25%)	0.715
IBD	46 (76.7%)	23 (47.9%)	0.079	18 (75%)	12 (37.5%)	0.125
PILPDs	7 (11.7%)	24 (50%)		3 (12.5%)	20 (62.5%)	
Other diseases	7 (11.7%)	1 (2.1%)		3 (12.5%)	0 (0%)	
Fever	10 (16.7%)	26 (54.2%)	<0.0001	7 (29.2%)	20 (62.5%)	0.013
Abdominal pain	41 (68.3%)	38 (79.2%)	0.207	17 (70.8%)	21 (65.6%)	0.68
Diarrhea	32 (53.3%)	31 (64.6%)	0.239	13 (54.2%)	20 (62.5%)	0.53
Haematochezia	31 (51.7%)	35 (72.9%)	0.024	15 (62.5%)	24 (75%)	0.314
Weight loss	34 (56.7%)	32 (66.7%)	0.289	11 (45.8%)	19 (59.4%)	0.315

SD, standard deviation; IMM, immunomodulators.

10.3389/fcimb.2024.1526633

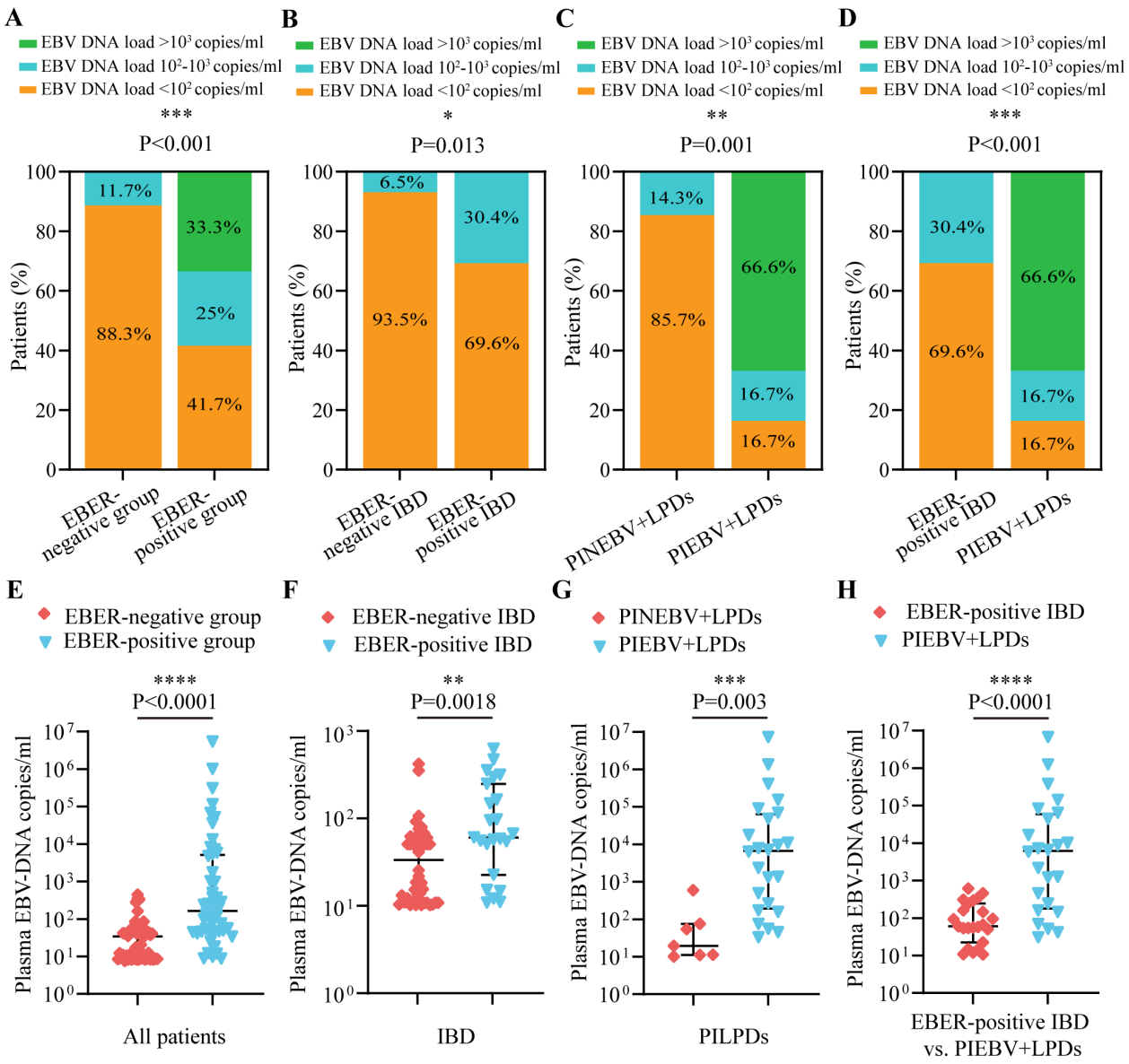

FIGURE 1
Comparisons of the distribution and quantification of plasma EBV DNA load between EBER-negative and EBER-positive groups. The comparisons include intestinal EBER-positive group vs. intestinal EBER-negative group **(A, E)**, EBER-negative IBD vs. EBER-positive IBD **(B, F)**, PINEBV+LPDs vs. PIEBV+LPDs **(C, G)**, and EBER-positive IBD vs. PIEBV+LPDs **(D, H)**. *$p \leq 0.05$, **$p \leq 0.01$, ***$p \leq 0.001$, and ****$p \leq 0.0001$.

3.3 Correlation analysis of EBER-positive cell counts with plasma EBV DNA levels in intestinal EBV infection

According to the consensus established on tissue identification and diagnostic pathology of intestinal EBV infection from the Chinese Medical Association (Ye et al., 2019), we divided these patients into three categories based on the number of cells positive for EBER-ISH per HPF: <10 cells per HPF, 10-50 cells per HPF, and >50 cells per HPF. We analyzed the interrelationship between plasma EBV DNA load and the frequency of intestinal EBER-positive cells per HPF in the intestinal EBER-positive cohort and found that the largest segment comprised patients with <10 cells positive for EBER-ISH per HPF (50%), followed by those with 10-50 cells positive for EBER-ISH per HPF (31.3%), and then patients with >50 cells positive for EBER-ISH per HPF (18.7%; Figure 2A). Notably, there was a notable disparity between PIEBV+LPDs and EBER-positive IBD, with 79.2% of PIEBV+LPD patients exhibiting more than 10 cells positive for EBER-ISH per HPF, compared to only 17.4% in the EBER-positive IBD group ($P < 0.001$; Figure 2A).

For a profound evaluation of EBV DNA load in plasma within intestinal EBV infection, we assessed the median plasma EBV DNA concentrations across different count ranges of EBER-positive cells per HPF, and we discovered that the median plasma DNA concentrations of EBV in the group with >50 EBER-positive cells per HPF (6.41×10^4copies/mL) and in the group with 10-50 EBER-positive cells per HPF (4.62×10^2 copies/mL) were both markedly elevated compared to the level within the group with <10 EBER-positive cells

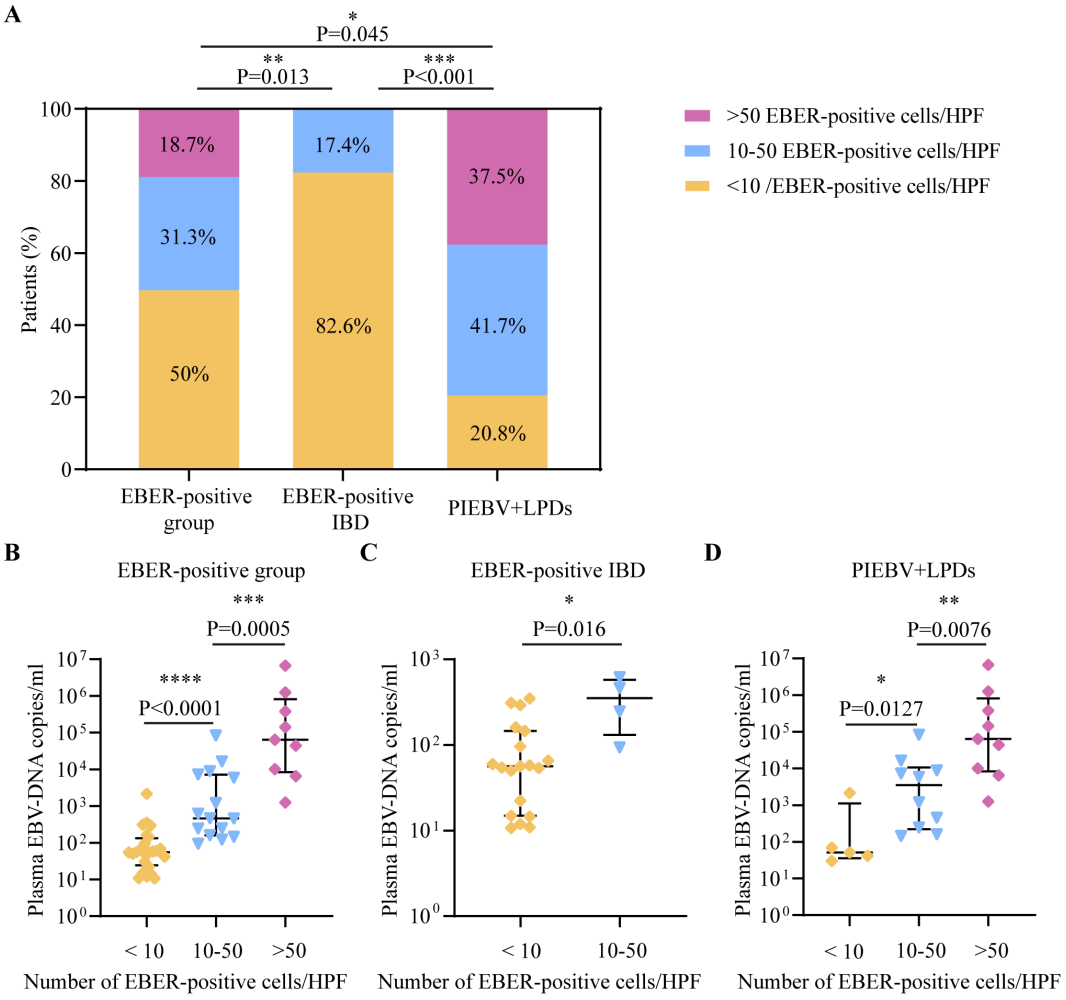

FIGURE 2
Comparative analysis of EBV DNA concentrations in plasma in accordance with total count of cells positive for EBER per HPF in intestinal tissue. **(A)** Distribution of total cells positive for EBER-ISH per HPF in intestinal tissue across different intestinal diseases with EBV infection. **(B)** Plasma EBV DNA quantity within EBER-positive patients. **(C)** Plasma EBV DNA quantity in EBER-positive IBD. **(D)** Plasma EBV-DNA quantity in PIEBV +LPDs. *$p \leq 0.05$, **$p \leq 0.01$, ***$p \leq 0.001$, and ****$p \leq 0.0001$.

per HPF (5.53×10^1 copies/mL), as shown in Figure 2B. Similarly, within the EBER-positive IBD subgroup, patients with 10-50 EBER-positive cells per HPF demonstrated significantly elevated plasma EBV DNA levels compared to those with <10 EBER-positive cells per HPF (3.54×10^2 copies/mL vs. 5.62×10^1 copies/mL; Figure 2C). Furthermore, in PIEBV+LPD group, patients with >50 EBER-positive cells per HPF exhibited markedly higher plasma EBV DNA levels (median 6.41×10^4 copies/mL), which were much superior in comparison with those with 10-50 EBER-positive cells per HPF (median 3.52×10^3 copies/mL, $P = 0.0076$) and those with <10 EBER-positive cells per HPF (median 5.09×10^1 copies/mL, $P = 0.0127$), as delineated in Figure 2D.

3.4 Diagnostic implication of plasma EBV DNA quantification in intestinal EBV infection

Considering that the density of intestinal cells positive for EBER-ISH per HPF exhibited a positive correlation with plasma EBV DNA levels, receiver operating characteristic (ROC) curve examination was initiated to ascertain the potency of plasma EBV DNA load for screening intestinal EBV infection in the test cohort. The analysis indicated that the area under the ROC curve (AUC) for distinguishing intestinal EBER positivity from EBER negativity was 0.82 at a concentration of 9.21×10^1 copies/mL of EBV DNA in plasma (Figure 3A), with a sensitivity of 64.58% and a specificity of 88.33%, indicating its potential utility in initial screening for EBV status. Furthermore, subgroup analyses stratified by intestinal EBER-ISH status identified 5.28×10^1 copies/mL as the cutoff value for differentiating EBV infection from non-EBV infection in IBD, yielding an AUC of 0.73 (Figure 3B), with a sensitivity of 69.57% and a specificity of 71.74%. This result suggests that plasma EBV DNA load has moderate discriminatory power in distinguishing EBV-positive IBD from EBV-negative IBD. Additionally, the analysis was extended to differentiate between EBER-positive IBD and PIEBV+LPDs. The ROC curve analysis for these two diseases produced an AUC of 0.85, with a discriminative threshold established at 5.4×10^2 copies/mL with high specificity

10.3389/fcimb.2024.1526633

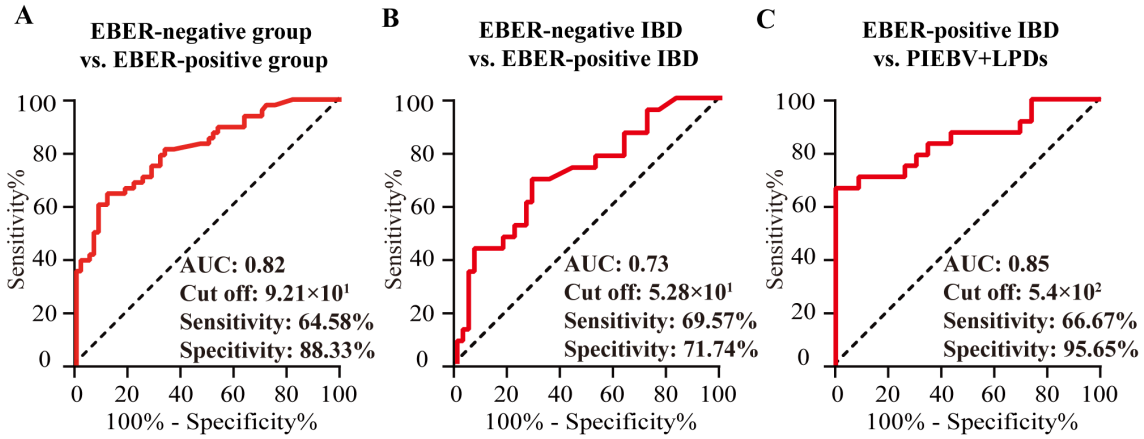

FIGURE 3
Analysis in the test cohort to assess the diagnostic utility of plasma EBV DNA quantification. **(A)** EBER-negative vs. EBER-positive group; **(B)** EBER-negative vs. EBER-positive IBD. **(C)** EBER-positive IBD vs. PIEBV+LPDs.

(95.65%) to ensure diagnostic accuracy for this rare but severe condition (Figure 3C).

The detection capacity achieved by plasma EBV DNA cutoff values indicating intestinal EBV infection was evaluated in the validation cohort. Analysis of clinical characteristics revealed no significant differences in demographic features and clinical presentations within the test and validation cohorts (Supplementary Table S1). In the validation cohort, a threshold of 9.21×10^1 copies/mL for EBV DNA load in plasma demonstrated an LR^+ calculated at 5.06, attaining values of 83.33%, 84.38%, 80%, and 87.1% in terms of specificity, sensitivity, NPV, and PPV, respectively, for identifying intestinal EBER-positive and EBER-negative diseases (Table 2). For IBD, the sensitivity, specificity, PPV, NPV, and LR^+ of a threshold of 5.28×10^1 copies/mL to differentiate intestinal EBV infection from non-EBV infection were 66.67%, 55.56%, 50%, 71.43%, and 1.5, respectively (Table 2). Furthermore, at a cutoff value of 5.4×10^2 copies/mL, the sensitivity for distinguishing PIEBV+LPDs from EBER-positive IBD reached 85%, with an LR^+ of 10.2 (Table 2).

3.5 Prognostic implication of plasma EBV DNA quantification in intestinal EBV infection

The analysis further explored and compared the six-month prognosis following intestinal EBER-ISH test among patients with intestinal diseases who were positive for EBV DNA load in plasma. The results confirmed that individuals in the intestinal EBER-positive group displayed significantly poorer prognoses than those in the EBER-negative group of the test cohort (50% vs. 15%, $P < 0.001$). Moreover, EBER-positive IBD and PIEBV+LPD patients demonstrated worse outcomes than their EBER-negative counterparts (26.1% vs. 15.2%, P =0.334 and 75% vs. 28.6%, P = 0.067, respectively). Details comparing the prognostic outcomes of various intestinal diseases are presented in Supplementary Table 2.

Comparative analyses of plasma EBV DNA concentrations between the fatal and benign groups with various intestinal diseases were also conducted. As depicted in Figure 4A, patients with a fatal prognosis had greater median plasma EBV DNA loads

TABLE 2 Detection capacity of plasma EBV DNA cutoff values for intestinal EBV infection within the validation subset.

Cut off values of plasma EBV DNA load (copies/ml)	Sensitivity (%) (95%CI)	Specificity (%) (95%CI)	PPV (%) (95%CI)	NPV (%) (95%CI)	LR^+	LR^-
9.21×10^1	84.38 (68.25, 93.14)	83.33 (64.15, 93.32)	87.1 (71.15, 94.87)	80 (60.87, 91.14)	5.06	0.19
5.28×10^1	66.67 (39.06, 86.19)	55.56 (33.72, 75.44)	50 (28, 72)	71.43 (45.35, 88,28)	1.5	0.6
5.4×10^2	85 (63.96, 94.76)	91.67 (64.61, 99.57)	94.44 (74.24, 99.72)	78.57 (52.41, 92.43)	10.2	0.16

LR^-, negative likelihood ratio; NPV, negative predictive value; LR^+, positive likelihood ratio; PPV, positive predictive value; 95%CI: 95% confidence interval.

10.3389/fcimb.2024.1526633

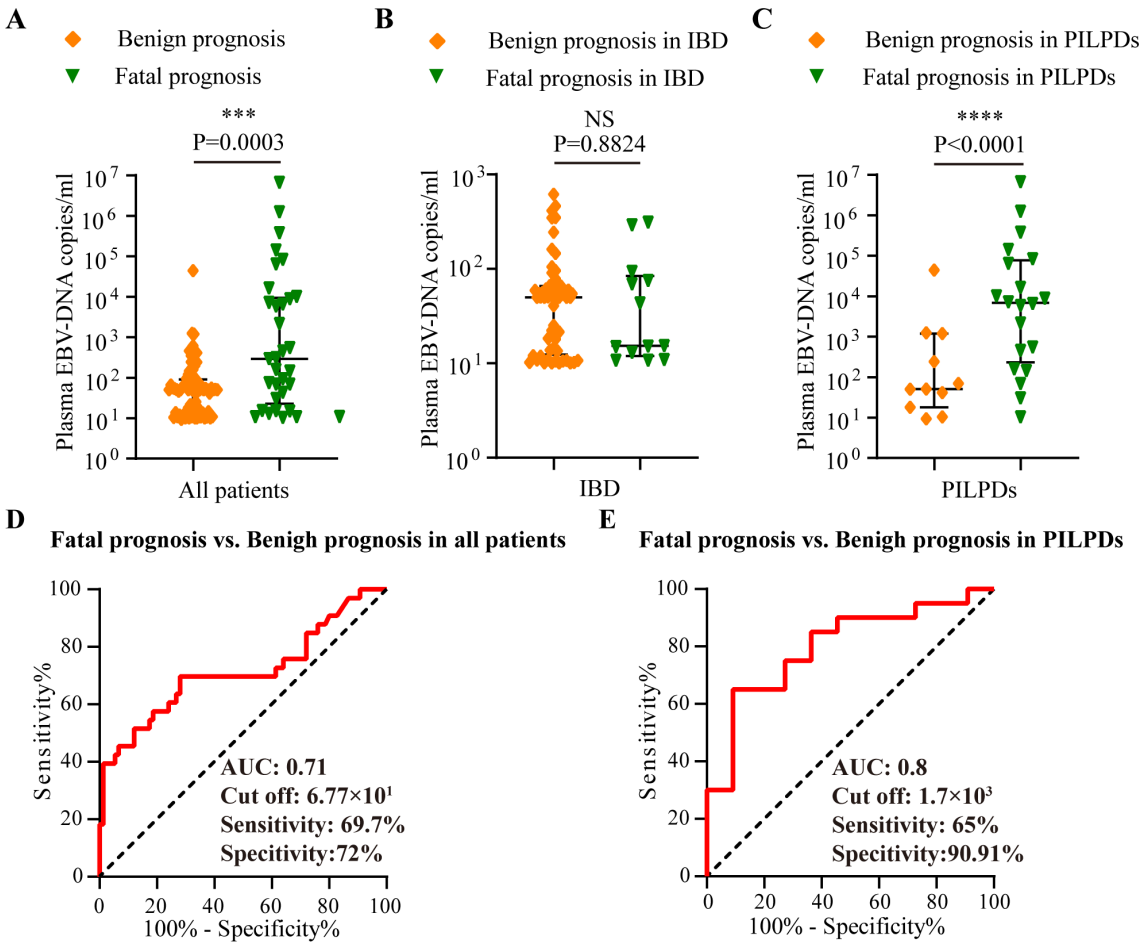

FIGURE 4
Analysis in the test cohort to assess the prognostic utility of plasma EBV DNA quantification. Comparative analysis of plasma EBV-DNA concentrations among various prognosis within the test cohort, including **(A)** Overall cohort, **(B)** IBD cohort, and **(C)** PILPD cohort. **(D)** ROC curve comparing fatal versus benign prognoses in all patients. **(E)** ROC curve comparing the fatal and benign prognoses in patients with PILPDs. ***p < 0.001, ****p < 0.0001. NS, not significant.

than those with a benign outcome (2.9×10^2 copies/mL vs. 5.02×10^1 copies/mL, P = 0.0003). Furthermore, patients with PIEBV+LPDs and those with PINEBV+LPDs had significantly different median plasma EBV DNA levels (6.86×10^2 copies/mL vs. 5.09×10^1 copies/mL, P < 0.0001, Figure 4C). However, patients with fatal prognosis did not show a statistically significant difference in plasma EBV DNA load compared to those with benign prognosis in IBD (P=0.8824) (Figure 4B).

ROC curve analysis revealed that there was an excellent connection between plasma EBV DNA concentrates and prognosis for intestinal EBV infection, demonstrating an AUC of 0.71 in the test cohort (Figure 4D), with a sensitivity of 69.7% and a specificity of 72%, demonstrating moderate ability to differentiate between fatal and benign prognoses. By establishing a threshold of 6.77×10^1 copies/mL for plasma EBV DNA load, we established the sensitivity, specificity, PPV, NPV, LR^+, and LR^- for differentiating between fatal and benign prognoses in the validation cohort. The resulting values were 87.5%, 68.09%, 58.33%, 91.43%, 2.74, and 0.18, respectively (Table 3). Furthermore, plasma EBV DNA concentration at 1.7×10^3 copies/mL was shown to be the most

TABLE 3 The ability to evaluate prognostic outcomes based on plasma EBV DNA cutoff values for intestinal EBV infection within the validation subset.

Cut off values of plasma EBV DNA load (copies/ml)	Sensitivity (%) (95%CI)	Specificity (%) (95%CI)	PPV (%) (95%CI)	NPV (%) (95%CI)	LR^+	LR^-
6.77×10^1	87.5 (69, 95.66)	68.09 (53.83, 79.6)	58.33 (42.2, 72.86)	91.43 (77.62, 97.04)	2.74	0.18
1.7×10^3	64.71 (41.3, 82.69)	83.33 (43.65, 99.15)	91.67 (64.61, 99.57)	45.45 (21.27, 71.99)	3.88	0.42

LR^-, negative likelihood ratio; NPV, negative predictive value; LR^+, positive likelihood ratio; PPV, positive predictive value; 95%CI: 95% confidence interval.

effective threshold for predicting PILPD prognosis, with an AUC of 0.8 (Figure 4E), with a high specificity of 90.91% and relatively low sensitivity of 65%, ensuring the accurate identification of patients at risk of severe outcomes of PILPDs. Within the validation subset, the established cutoff offered a sensitivity of 64.71%, specificity of 83.33%, PPV of 91.67%, NPV of 45.45%, LR^+ of 3.88, and LR^- of 0.42, effectively distinguishing between benign and fatal outcomes in PILPDs (Table 3).

4 Discussion

This investigation found a positive alignment between plasma EBV DNA quantification and the number of cells positive for EBER-ISH per HPF in intestinal diseases. Further studies were performed to determine the significance of EBV DNA concentrations in plasma with respect to identifying intestinal EBV infection and predicting its outcome, and specific threshold values were established. These results indicate that the EBV DNA quantity in plasma functions as a credible marker for the diagnostic and prognostic assessment of intestinal EBV infection.

Emphasizing clinical characteristics plays a crucial role in identifying EBV infection. Our study found no difference in immunosuppressant use between infected and non-infected patients, whereas previous studies have identified immunosuppressant administration as a pivotal element in triggering intestinal EBV activation (Ford and Peyrin-Biroulet, 2013; Magro et al., 2013; Lapsia et al., 2016). This may be due to the fact that all participants in both cohorts of this study were patients with detectable plasma EBV DNA, indicating that both groups were already in a state of EBV activation, which could mask the potential impact of immunosuppressant use. Research has shown that the main clinical manifestations of primary EBV infection include fever, pharyngitis, lymphadenopathy, and hepatosplenomegaly (Song et al., 2023; Ye et al., 2023). Consistent with this, our research demonstrated that compared to those who did not have EBV infection in their intestines, those with intestinal EBV infection exhibited fever symptoms more frequently. Moreover, our investigation is the first cohort study to affirm that patients with intestinal EBV infection strongly exhibit a higher predisposition to gastrointestinal manifestations with hematochezia than those without infection, which aligns with sporadic reports of primary intestinal EBV infection (Karlitz et al., 2011; Chen et al., 2016; Wang Y. et al., 2018). Therefore, our study suggests that it is essential to raise clinical vigilance in screening for intestinal EBV infection in patients with gastrointestinal complaints and fever symptoms.

In general, EBV maintains latency within a robust immune system. However, immunodeficiencies triggered by many factors can result in the reactivation of EBV (Chan et al., 2021). In such scenarios, a detectable level of EBV DNA signifies that the virus is actively undergoing infection and replication, whereas the histological EBER-ISH test is used to ascertain the presence of EBV in tissue samples (Kanakry et al., 2013; Liang et al., 2015; Zhou et al., 2020a). In this study, a substantial increase in the detection of plasma EBV DNA was observed among patients suffering from intestinal EBV infection, in contrast to those who were unaffected. The median plasma EBV DNA loads were reported as 2.02×10^2 copies/ml in infected patients versus 4.2×10^1 copies/ml in non-infected individuals, corroborating the findings of prior studies on EBV-associated diseases (Yu et al., 2021; Shen et al., 2022). This discrepancy indicates that patients with intestinal EBV infection typically experience persistent viral replication, leading to elevated plasma viral loads. Furthermore, consistent with earlier studies (Zhou et al., 2020b; Wang et al., 2022), our study found that IBD patients with intestinal EBV infection showed higher plasma EBV DNA levels than those not infected. Even though the value of EBV DNA load varies across studies owing to the different samples and methods used for EBV DNA testing, the trends observed in these studies are consistent.

The results of our study indicate that plasma EBV DNA load is positively correlated with the number of intestinal EBER-positive cells per HPF. This is consistent with the findings reported by Zhou et al. (Zhou et al., 2020b) in IBD patients with intestinal EBV infection, and aligns with the results from other studies related to EBV-associated diseases (Kanakry et al., 2016; Yu et al., 2021; Shen et al., 2022). Moreover, an indicator of intestinal EBER positivity based on plasma EBV DNA levels was examined using ROC analysis, revealing an AUC of 0.82. The optimal cut-off was established at 9.21×10^1 copies/ml, which is sensitive to 64.58% and specific to 88.33% in distinguishing intestinal EBV infection from non-infection. This is consistent with a previous study that used detectable EBV DNA to segregate EBV-associated diseases from those unrelated to EBV, exhibiting a sensitivity of 83.9% and specificity of 93.5% (Yu et al., 2021). It is evident that our investigation proposed an EBV DNA cut-off value with greater precision for diagnosing intestinal EBV infection. Moreover, our study revealed that patients with IBD with intestinal EBV infection can be distinguished from those with PIEBV+LPDs when their plasma EBV DNA concentration is below 5.4×10^2 copies/ml, which contributes to the differential diagnosis of the two diseases. Hence, our study demonstrates that it is possible to use plasma DNA load as a screening and monitoring tool for intestinal EBV infection. Nevertheless, it is vital to recognize that histological EBER-ISH test might yield underestimations of EBV infection because of the minimal thickness of tissue sections, whereas the high sensitivity of PCR technology in detecting EBV DNA might lead to overestimation of EBV infection. Furthermore, in clinical practice, IBD with intestinal EBV infection is generally regarded as an opportunistic infection, whereas PIEBV+LPDs represent conditions in which EBV acts as a direct pathogenic factor (Ye et al., 2019). This fundamental difference explains the distinct cutoff values derived for each cohort in this study, reflecting their unique disease contexts. Therefore, selecting an appropriate test method and cutoff value of plasma EBV DNA load, based on real-world clinical needs, is essential to achieve optimal diagnostic performance and prognostic assessment for intestinal EBV infection, such as improving the detection accuracy of EBV infection in IBD patients or ensuring precise differentiation in PIEBV+LPDs.

The heterogeneity of outcomes associated with EBV infection spans a continuum from benign to malignant manifestations,

leading to prognostic variability in EBV-associated diseases. Prior studies have demonstrated plasma EBV DNA load for predicting the outcome and therapeutic response of EBV-associated diseases (Kanakry et al., 2013; Ito et al., 2016). In cases of intestinal EBV infection, EBV infection has been linked to refractory responses and the necessity for surgical treatment in patients with IBD (Hosomi et al., 2018; Pezhouh et al., 2018). Analysis of a cohort of 12 patients with PIEBV+LPDs revealed a 50% mortality rate within a follow-up interval of 1-21 months (Wang Z. et al., 2018). Our investigation contributes to this body of evidence by demonstrating a significant correlation between elevated plasma EBV DNA levels and fatal prognoses in patients with intestinal EBV infection within six months after the intestinal EBER-ISH test, marked by an AUC of 0.71. Additionally, for patients with PILPDs, when the plasma EBV DNA load exceeds 1.7×10^3 copies/ml, there is a significant increase in the occurrence of severe adverse outcomes, with an AUC of 0.8. These results further confirm the utility of monitoring plasma EBV DNA load as an indicator of poor outcomes in patients with intestinal EBV-infected infection.

This is an initial investigation to assess the EBV DNA load in plasma as a diagnostic and prognostic tool for intestinal EBV infection. This noninvasive approach promises to diminish the reliance on invasive diagnostic interventions for patients with intestinal EBV infection during the initial diagnosis and subsequent follow-up and holds particular significance for diagnosing and differentiating intestinal diseases associated with EBV. Nonetheless, our study has several limitations. First, our research did not explore the diagnostic and prognostic utility of other types of blood samples, such as whole blood or PBMCs, for intestinal EBV infection. This omission leaves a gap in our understanding of the optimal blood sample type for the accurate diagnosis and prognosis of intestinal EBV infection. Future studies should address this gap by comparing the effectiveness of EBV DNA quantification in different types of blood samples. Second, the retrospective, single-center nature of our study, coupled with a limited sample size, introduces potential biases and limits the generalizability of our findings. To mitigate these limitations and validate the proposed cut-off values for plasma EBV DNA levels, extensive multicenter studies with larger cohorts are essential. Third, the sensitivity of our study was relatively low. To address this limitation, future studies should incorporate additional biomarkers, such as EBV antibody levels and inflammatory markers, as well as other factors, including clinical characteristics and histopathological features, which could collectively enhance the overall diagnostic and prognostic accuracy of plasma EBV DNA load in intestinal EBV infection. Lastly, IBD and PILPD patients constituted the majority of the subjects in this study. Thus, our data do not rule out intestinal EBV infection in patients with other EBV-associated diseases who did not undergo colonoscopy for intestinal EBER-ISH. Studies on a greater variety of study populations with other EBV-associated diseases are needed to evaluate intestinal EBV infection.

The conclusions drawn from this investigation reinforce the importance of plasma EBV DNA quantification in the detection and outcome prediction of intestinal EBV infection. Specifically, the cutoff values of EBV DNA in the plasma at 9.21×10^1 and 6.77×10^1 copies/mL facilitate the diagnosis and prognosis of this disease, respectively. This noninvasive method provides robust evidence for the management of intestinal EBV infection. Detection of EBV DNA using various blood samples and larger-scale multicenter studies will be pivotal in advancing the clinical use of EBV DNA quantification in peripheral blood for managing intestinal EBV infection.

Data availability statement

The raw data supporting the conclusions of this article will be made available by the authors, without undue reservation.

Ethics statement

The studies involving humans were approved by the ethics board of West China Hospital. The studies were conducted in accordance with the local legislation and institutional requirements. The ethics committee/institutional review board waived the requirement of written informed consent for participation from the participants or the participants' legal guardians/next of kin because This study is a retrospective analysis.

Author contributions

CM: Formal analysis, Investigation, Methodology, Validation, Visualization, Writing – original draft. MJ: Formal analysis, Investigation, Visualization, Writing – original draft. JL: Data curation, Investigation, Writing – original draft. ZZ: Investigation, Writing – review & editing. YW: Methodology, Validation, Writing – review & editing. RC: Investigation, Validation, Writing – review & editing. HL: Investigation, Writing – review & editing. JP: Investigation, Writing – review & editing. FY: Investigation, Writing – review & editing. YJ: Investigation, Writing – review & editing. LL: Investigation, Writing – review & editing. HZ: Conceptualization, Funding acquisition, Project administration, Resources, Supervision, Writing – original draft, Writing – review & editing.

Funding

The author(s) declare financial support was received for the research, authorship, and/or publication of this article. This research was funded by the Science and Technology Foundation of Sichuan Province of China (2023YFS0279 and 2024YFFK0347).

Conflict of interest

The authors declare that the research was conducted in the absence of any commercial or financial relationships that could be construed as a potential conflict of interest.

Generative AI statement

The author(s) declare that no Generative AI was used in the creation of this manuscript.

Publisher's note

All claims expressed in this article are solely those of the authors and do not necessarily represent those of their affiliated organizations, or those of the publisher, the editors and the reviewers. Any product that may be evaluated in this article, or claim that may be made by its manufacturer, is not guaranteed or endorsed by the publisher.

Supplementary material

The Supplementary Material for this article can be found online at: https://www.frontiersin.org/articles/10.3389/fcimb.2024.1526633/full#supplementary-material

References

Cao, X., Dong, A., Kang, G., Wang, X., Duan, L., Hou, H., et al. (2022). Modeling spatial interaction networks of the gut microbiota. *Gut. Microbes* 14, 2106103. doi: 10.1080/19490976.2022.2106103

Chan, J. Y., Lim, J. Q., and Ong, C. K. (2021). Checkpoint immunotherapy for NK/T cell lymphoma-Time for a showdown? *Precis. Clin. Med.* 4, 70–72. doi: 10.1093/pcmedi/pbab004

Chen, H., Zhang, Y., Jiang, Z., Zhou, W., and Cao, Q. (2016). A case report of NK-cell lymphoproliferative disease with a wide involvement of digestive tract develop into Epstein-Barr virus associated NK/T cell lymphoma in an immunocompetent patient. *Med. (Baltimore).* 95, e3176. doi: 10.1097/md.0000000000003176

Chen, L., Wang, Y., Zhou, H., Liang, Y., Zhu, F., and Zhou, G. (2024). The new insights of hyperbaric oxygen therapy: focus on inflammatory bowel disease. *Precis. Clin. Med.* 7, pbae001. doi: 10.1093/pcmedi/pbae001

Chen, Y., Xiao, L., Zhou, M., and Zhang, H. (2024). The microbiota: a crucial mediator in gut homeostasis and colonization resistance. *Front. Microbiol.* 15. doi: 10.3389/fmicb.2024.1417864

Cohen, J. I., Kimura, H., Nakamura, S., Ko, Y. H., and Jaffe, E. S. (2009). Epstein-Barr virus-associated lymphoproliferative disease in non-immunocompromised hosts: a status report and summary of an international meeting, 8-9 September 2008. *Ann. Oncol.* 20, 1472–1482. doi: 10.1093/annonc/mdp064

Dang, Y., Ma, C., Chen, K., Chen, Y., Jiang, M., Hu, K., et al. (2023). The effects of a high-fat diet on inflammatory bowel disease. *Biomolecules* 13, 905. doi: 10.3390/biom13060905

de Francisco, R., Castaño-García, A., Martínez-González, S., Pérez-Martínez, I., González-Huerta, A. J., Morais, L. R., et al. (2018). Impact of Epstein-Barr virus serological status on clinical outcomes in adult patients with inflammatory bowel disease. *Aliment. Pharmacol. Ther.* 48, 723–730. doi: 10.1111/apt.14933

Dimitroulia, E., Pitiriga, V. C., Piperaki, E. T., Spanakis, N. E., and Tsakris, A. (2013). Inflammatory bowel disease exacerbation associated with Epstein-Barr virus infection. *Dis. Colon. Rectum.* 56, 322–327. doi: 10.1097/DCR.0b013e31827cd02c

Ford, A. C., and Peyrin-Biroulet, L. (2013). Opportunistic infections with anti-tumor necrosis factor-α therapy in inflammatory bowel disease: meta-analysis of randomized controlled trials. *Am. J. Gastroenterol.* 108, 1268–1276. doi: 10.1038/ajg.2013.138

Gomollón, F., Dignass, A., Annese, V., Tilg, H., Van Assche, G., Lindsay, J. O., et al. (2017). 3rd European evidence-based consensus on the diagnosis and management of Crohn's disease 2016: part 1: diagnosis and medical management. *J. Crohns. Colitis.* 11, 3–25. doi: 10.1093/ecco-jcc/jjw168

Hohaus, S., Santangelo, R., Giachelia, M., Vannata, B., Massini, G., Cuccaro, A., et al. (2011). The viral load of Epstein-Barr virus (EBV) DNA in peripheral blood predicts for biological and clinical characteristics in Hodgkin lymphoma. *Clin. Cancer. Res.* 17, 2885–2892. doi: 10.1158/1078-0432.Ccr-10-3327

Hosomi, S., Watanabe, K., Nishida, Y., Yamagami, H., Yukawa, T., Otani, K., et al. (2018). Combined infection of human herpes viruses: A risk factor for subsequent colectomy in ulcerative colitis. *Inflamm. Bowel. Dis.* 24, 1307–1315. doi: 10.1093/ibd/izy005

Hui, E. P., Li, W. F., Ma, B. B., Lam, W. K. J., Chan, K. C. A., Mo, F., et al. (2020). Integrating postradiotherapy plasma Epstein-Barr virus DNA and TNM stage for risk stratification of nasopharyngeal carcinoma to adjuvant therapy. *Ann. Oncol.* 31, 769–779. doi: 10.1016/j.annonc.2020.03.289

Ito, Y., Suzuki, M., Kawada, J., and Kimura, H. (2016). Diagnostic values for the viral load in peripheral blood mononuclear cells of patients with chronic active Epstein-Barr virus disease. *J. Infect. Chemother.* 22, 268–271. doi: 10.1016/j.jiac.2015.11.002

Kanakry, J. A., Hegde, A. M., Durand, C. M., Massie, A. B., Greer, A. E., Ambinder, R. F., et al. (2016). The clinical significance of EBV DNA in the plasma and peripheral blood mononuclear cells of patients with or without EBV diseases. *Blood* 127, 2007–2017. doi: 10.1182/blood-2015-09-672030

Kanakry, J. A., Li, H., Gellert, L. L., Lemas, M. V., Hsieh, W. S., Hong, F., et al. (2013). Plasma Epstein-Barr virus DNA predicts outcome in advanced Hodgkin lymphoma: correlative analysis from a large North American cooperative group trial. *Blood* 121, 3547–3553. doi: 10.1182/blood-2012-09-454694

Karlitz, J. J., Li, S. T., Holman, R. P., and Rice, M. C. (2011). EBV-associated colitis mimicking IBD in an immunocompetent individual. *Nat. Rev. Gastroenterol. Hepatol.* 8, 50–54. doi: 10.1038/nrgastro.2010.192

Lapsia, S., Koganti, S., Spadaro, S., Rajapakse, R., Chawla, A., and Bhaduri-McIntosh, S. (2016). Anti-TNFα therapy for inflammatory bowel diseases is associated with Epstein-Barr virus lytic activation. *J. Med. Virol.* 88, 312–318. doi: 10.1002/jmv.24331

Lennon, P., Crotty, M., and Fenton, J. E. (2015). Infectious mononucleosis. *BMJ* 350, h1825. doi: 10.1136/bmj.h1825

Li, L., Cheng, R., Wu, Y., Lin, H., Gan, H., and Zhang, H. (2024). Diagnosis and management of inflammatory bowel disease. *J. Evid. Based. Med.* 17, 409–433. doi: 10.1111/jebm.12626

Liang, J. H., Lu, T. X., Tian, T., Wang, L., Fan, L., Xu, J., et al. (2015). Epstein-Barr virus (EBV) DNA in whole blood as a superior prognostic and monitoring factor than EBV-encoded small RNA in *situ* hybridization in diffuse large B-cell lymphoma. *Clin. Microbiol. Infect.* 21, 596–602. doi: 10.1016/j.cmi.2015.02.017

López, C., Burkhardt, B., Chan, J. K. C., Leoncini, L., Mbulaiteye, S. M., Ogwang, M. D., et al. (2022). Burkitt lymphoma. *Nat. Rev. Dis. Primers.* 8, 78. doi: 10.1038/s41572-022-00404-3

Lou, P. J., Jacky Lam, W. K., Hsu, W. L., Pfeiffer, R. M., Yu, K. J., Chan, C. M. L., et al. (2023). Performance and operational feasibility of Epstein-Barr virus-based screening for detection of nasopharyngeal carcinoma: direct comparison of two alternative approaches. *J. Clin. Oncol.* 41, 4257–4266. doi: 10.1200/jco.22.01979

Ludvigsen, L. U. P., Andersen, A. S., Hamilton-Dutoit, S., Jensen-Fangel, S., Bøttger, P., Handberg, K. J., et al. (2023). A prospective evaluation of the diagnostic potential of EBV-DNA in plasma and whole blood. *J. Clin. Virol.* 167, 105579. doi: 10.1016/j.jcv.2023.105579

Magro, F., Gionchetti, P., Eliakim, R., Ardizzone, S., Armuzzi, A., Barreiro-de Acosta, M., et al. (2017). Third European evidence-based consensus on diagnosis and management of ulcerative colitis. Part 1: definitions, diagnosis, extra-intestinal manifestations, pregnancy, cancer surveillance, surgery, and Ileo-anal Pouch disorders. *J. Crohns. Colitis.* 11, 649–670. doi: 10.1093/ecco-jcc/jjx008

Magro, F., Santos-Antunes, J., Albuquerque, A., Vilas-Boas, F., Macedo, G. N., Nazareth, N., et al. (2013). Epstein-Barr virus in inflammatory bowel disease-correlation with different therapeutic regimens. *Inflamm. Bowel. Dis.* 19, 1710–1716. doi: 10.1097/MIB.0b013e318281f31c

Montes-Mojarro, I. A., Kim, W. Y., Fend, F., and Quintanilla-Martinez, L. (2020). Epstein - Barr virus positive T and NK-cell lymphoproliferations: Morphological features and differential diagnosis. *Semin. Diagn. Pathol.* 37, 32–46. doi: 10.1053/j.semdp.2019.12.004

Nissen, L. H., Nagtegaal, I. D., de Jong, D. J., Kievit, W., Derikx, L. A., Groenen, P. J., et al. (2015). Epstein-Barr virus in inflammatory bowel disease: the spectrum of intestinal lymphoproliferative disorders. *J. Crohns. Colitis.* 9, 398–403. doi: 10.1093/ecco-jcc/jjv040

Pezhouh, M. K., Miller, J. A., Sharma, R., Borzik, D., Eze, O., Waters, K., et al. (2018). Refractory inflammatory bowel disease: is there a role for Epstein-Barr virus? A case-controlled study using highly sensitive Epstein-Barr virus-encoded small RNA1 in *situ* hybridization. *Hum. Pathol.* 82, 187–192. doi: 10.1016/j.humpath.2018.08.001

Pu, D., Yao, Y., Zhou, C., Liu, R., Wang, Z., Liu, Y., et al. (2024). FMT rescues mice from DSS-induced colitis in a STING-dependent manner. *Gut. Microbes* 16, 2397879. doi: 10.1080/19490976.2024.2397879

Qiu, M. Z., He, C. Y., Lu, S. X., Guan, W. L., Wang, F., Wang, X. J., et al. (2020). Prospective observation: Clinical utility of plasma Epstein-Barr virus DNA load in

EBV-associated gastric carcinoma patients. *Int. J. Cancer.* 146, 272–280. doi: 10.1002/ijc.32490

Rizzo, A. G., Orlando, A., Gallo, E., Bisanti, A., Sferrazza, S., Montalbano, L. M., et al. (2017). Is Epstein-Barr virus infection associated with the pathogenesis of microscopic colitis? *J. Clin. Virol.* 97, 1–3. doi: 10.1016/j.jcv.2017.10.009

Shen, Z., Hu, L., Yao, M., He, C., Liu, Q., Wang, F., et al. (2022). Disparity analysis and prognostic value of pretreatment whole blood Epstein-Barr virus DNA load and Epstein-Barr encoding region status in lymphomas: A retrospective multicenter study in Huaihai Lymphoma Working Group. *Int. J. Cancer.* 150, 327–334. doi: 10.1002/ijc.33802

Song, J., Zhu, K., Wang, X., Yang, Q., Yu, S., Zhang, Y., et al. (2023). Utility of clinical metagenomics in diagnosing Malignancies in a cohort of patients with Epstein-Barr virus positivity. *Front. Cell. Infect. Microbiol.* 13. doi: 10.3389/fcimb.2023.1211732

Tsai, D. E., Luskin, M. R., Kremer, B. E., Chung, A. K., Arnoldi, S., Paralkar, V. R., et al. (2015). A pilot trial of quantitative Epstein-Barr virus polymerase chain reaction in patients undergoing treatment for their Malignancy: potential use of Epstein-Barr virus polymerase chain reaction in multiple cancer types. *Leuk. Lymphoma.* 56, 1530–1532. doi: 10.3109/10428194.2014.963577

Wang, W., Chen, X., Pan, J., Zhang, X., and Zhang, L. (2022). Epstein-Barr virus and human cytomegalovirus infection in intestinal mucosa of Chinese patients with inflammatory bowel disease. *Front. Microbiol.* 13. doi: 10.3389/fmicb.2022.915453

Wang, Y., Li, Y., Meng, X., Duan, X., Wang, M., Chen, W., et al. (2018). Epstein-Barr virus-associated T-cell lymphoproliferative disorder presenting as chronic diarrhea and intestinal bleeding: A case report. *Front. Immunol.* 9. doi: 10.3389/fimmu.2018.02583

Wang, Z., Zhang, W., Luo, C., Zhu, M., Zhen, Y., Mu, J., et al. (2018). Primary intestinal Epstein-Barr virus-associated natural killer/T-cell lymphoproliferative disorder: A disease mimicking inflammatory bowel disease. *J. Crohns. Colitis.* 12, 896–904. doi: 10.1093/ecco-jcc/jjy043

Weiss, L. M., and Chen, Y. Y. (2013). EBER in *situ* hybridization for Epstein-Barr virus. *Methods Mol. Biol.* 999, 223–230. doi: 10.1007/978-1-62703-357-2_16

Wong, K. C. W., Hui, E. P., Lo, K. W., Lam, W. K. J., Johnson, D., Li, L., et al. (2021). Nasopharyngeal carcinoma: an evolving paradigm. *Nat. Rev. Clin. Oncol.* 18, 679–695. doi: 10.1038/s41571-021-00524-x

Xu, S., Chen, H., Zu, X., Hao, X., Feng, R., Zhang, S., et al. (2020). Epstein-Barr virus infection in ulcerative colitis: a clinicopathologic study from a Chinese area. *Therap. Adv. Gastroenterol.* 13, 1756284820930124. doi: 10.1177/1756284820930124

Ye, Y., Xiao, S., Zhao, J., Shi, X., Zheng, R., Wang, X., et al. (2019). Consensus on tissue detection and pathological diagnosis of intestinal EB virus infection. *Chi. J. Dig.* 39, 433–437. doi: 10.3760/cma.j.issn.0254-1432.2019.07.001

Ye, Z., Chen, L., Zhong, H., Cao, L., Fu, P., and Xu, J. (2023). Epidemiology and clinical characteristics of Epstein-Barr virus infection among children in Shanghai, China 2017-2022. *Front. Cell. Infect. Microbiol.* 13. doi: 10.3389/fcimb.2023.1139068

Young, L. S., Yap, L. F., and Murray, P. G. (2016). Epstein-Barr virus: more than 50 years old and still providing surprises. *Nat. Rev. Cancer.* 16, 789–802. doi: 10.1038/nrc.2016.92

Yu, S., Yang, Q., Wu, J., Zhu, M., Ai, J., Zhang, H., et al. (2021). Clinical application of Epstein-Barr virus DNA loads in Epstein-Barr virus-associated diseases: A cohort study. *J. Infect.* 82, 105–111. doi: 10.1016/j.jinf.2020.11.027

Zeng, Z., Jiang, M., Li, X., Yuan, J., and Zhang, H. (2023). Precision medicine in inflammatory bowel disease. *Precis. Clin. Med.* 6, pbad033. doi: 10.1093/pcmedi/pbad033

Zhou, J. Q., Zeng, L., Zhang, Q., Wu, X. Y., Zhang, M. L., Jing, X. T., et al. (2020a). Clinical features of Epstein-Barr virus in the intestinal mucosa and blood of patients with inflammatory bowel disease. *Saudi. J. Gastroenterol.* 26, 312–320. doi: 10.4103/sjg.SJG_30_20

Zhou, X. H., Liang, J. H., Wang, L., Zhu, H. Y., Wu, J. Z., Xia, Y., et al. (2020b). High viral loads of circulating Epstein-Barr virus DNA copy number in peripheral blood is associated with inferior prognosis in patients with mantle cell lymphoma. *J. Cancer.* 11, 4980–4988. doi: 10.7150/jca.37484

frontiers | Frontiers in Cellular and Infection Microbiology

TYPE Original Research
PUBLISHED 16 January 2025
DOI 10.3389/fcimb.2024.1496176

OPEN ACCESS

EDITED BY
Ariadna Petronela Fildan,
Ovidius University, Romania

REVIEWED BY
German Gornalusse,
University of Washington, United States
Michael Z. Zulu,
University of Cape Town, South Africa

*CORRESPONDENCE
Ana Lascu
lascu.ana@umft.ro

RECEIVED 13 September 2024
ACCEPTED 26 December 2024
PUBLISHED 16 January 2025

CITATION
Paróczai D, Bikov A, Blidaru A, Bobu E, Lascu A, Mot CI, Mihaicuta S and Frent S (2025) Comparative efficacy of repurposed drugs lopinavir-ritonavir and darunavir-ritonavir in hospitalised COVID-19 patients: insights from a tertiary centre cohort. *Front. Cell. Infect. Microbiol.* 14:1496176. doi: 10.3389/fcimb.2024.1496176

Comparative efficacy of repurposed drugs lopinavir-ritonavir and darunavir-ritonavir in hospitalised COVID-19 patients: insights from a tertiary centre cohort

Dóra Paróczai[1,2], András Bikov[3,4], Andreea Blidaru[5], Emanuel Bobu[6], Ana Lascu[7,8]*, Cristian Ion Mot[9,10], Stefan Mihaicuta[5,11] and Stefan Frent[5,11]

[1]Department of Medical Microbiology, University of Szeged, Szeged, Hungary, [2]Albert Szent-Györgyi Health Center, Pulmonology Clinic, University of Szeged, Deszk, Hungary, [3]North West Lung Centre, Wythenshawe Hospital, Manchester University NHS Foundation Trust, Manchester, United Kingdom, [4]Division of Immunology, Immunity to Infection and Respiratory Medicine, University of Manchester, Manchester, United Kingdom, [5]Department of Infectious Diseases, Infectious Diseases and Pulmonology Clinical Hospital, Timisoara, Romania, [6]Department of Pulmonology, University of Medicine and Pharmacy Timisoara, Timisoara, Romania, [7]Department of Functional Sciences, Discipline of Pathophysiology, Centre for Translational Research and Systems Medicine, University of Medicine and Pharmacy Timisoara, Timisoara, Romania, [8]Institute for Cardiovascular Diseases of Timisoara, Clinic for Cardiovascular Surgery, Timisoara, Romania, [9]ENT Department, Municipal Emergency Hospital Timisoara, Timisoara, Romania, [10]Department of Surgery, University of Medicine and Pharmacy Timisoara, Timisoara, Romania, [11]Centre for Research and Innovation in Precision Medicine of Respiratory Diseases, Department of Pulmonology, University of Medicine and Pharmacy Timisoara, Timisoara, Romania

Background: Drug repurposing has become a widely adopted strategy to minimise research time, costs, and associated risks. Combinations of protease inhibitors such as lopinavir and darunavir with ritonavir have been repurposed as treatments for COVID-19. Although lopinavir-ritonavir (LPV/r) and darunavir-ritonavir (DRV/r) have shown *in vitro* efficacy against COVID-19, the results in human studies have been inconsistent. Therefore, our objective was to compare the efficacy of LPV/r and DRV/r in COVID-19 patients admitted to a tertiary centre in Romania.

Research design and methods: A clinical dataset from 417 hospitalised patients was analysed. Patients were assigned to the LPV/r, DRV/r, or control (standard-of-care) group based on clinical decisions made by the attending infectious disease specialists, aligned with national treatment protocols. Kaplan-Meier and Cox proportional hazards regression analyses were conducted to compare in-hospital mortality and to identify factors associated with clinical improvement or fatal outcomes.

Results: By day 10, more patients showed improvement with LPV/r and DRV/r (p=0.03 and 0.01, respectively), but only LPV/r was associated with improved survival compared to the control group (p=0.05). Factors associated with mortality included male gender (HR: 3.63, p=0.02), diabetes (HR: 2.49, p=0.03), oxygen saturation below 90% at admission (HR: 5.23, p<0.01), high

blood glucose levels (HR: 3.68, p=0.01), age (HR: 1.04, p=0.02), and more than 25% lesion extension on chest CT scan (HR: 2.28, p=0.03).

Conclusions: LPV/r, but not DRV/r, showed a survival benefit in patients hospitalised with COVID-19, but these findings deserve further investigation in a randomised clinical trial.

KEYWORDS

COVID-19, darunavir, lopinavir, propensity score matching, ritonavir

Introduction

The COVID-19 pandemic, caused by severe acute respiratory syndrome coronavirus 2 (SARS-CoV-2), emerged in late 2019 (Kumar et al., 2021) and evolved into a global health crisis within the first few months of 2020 (Mallah et al., 2021). Despite extensive research, the effectiveness of some proposed treatments for COVID-19 remains uncertain. The pandemic affected over 650 million individuals worldwide, resulting in more than 6 million deaths. The burden on healthcare systems, as well as the lack of efficient medications, prompted drug regulators, including agencies such as The Food and Drug Administration (FDA), to authorise the use of repurposed drugs and off-label medications (Singh et al., 2020). Humans across the globe are regularly infected with endemic coronaviruses, which typically result in respiratory illnesses with mild symptoms (Li et al., 2005). These viruses have not been deemed a significant public health threat, and thus the development of specific antiviral treatments or preventive vaccines was not prioritised. Consequently, when SARS-CoV-2 appeared, no specific antiviral treatments for coronavirus diseases, including COVID-19, were available. Traditional methods for discovering new antiviral compounds and developing new therapeutic options are lengthy and complex, often taking several years. In this scenario, drug repurposing has emerged as a promising and potentially valuable strategy for identifying already approved drugs for the treatment of other diseases, including COVID-19.

Drug repurposing offers a cost-effective and time-efficient alternative to developing new drugs. As a result, medications like remdesivir, favipiravir, umifenovir, lopinavir, ritonavir, and darunavir were utilised in clinical practice to treat COVID-19. Some of these drugs such as lopinavir, remdesivir and darunavir derivates demonstrated inhibitory effects on SARS-CoV-2 replication *in vitro* on cell cultures (Choy et al., 2020; Wang et al., 2020; Ma et al., 2022). Protease inhibitors, originally developed to target aspartate protease in HIV treatment, have been among the most extensively studied repurposed drugs and were found to inhibit the 3C-like protease of SARS-CoV-2 (Nutho et al., 2020).

Both LPV/r and DRV/r target the viral protease necessary for SARS-CoV-2 replication. However, LPV/r primarily inhibits the 3CL-like protease, while DRV/r demonstrates activity at higher concentrations and was initially designed to target only the HIV-1 protease. An *in vitro* study clarified that darunavir derivates can also inhibit 3CL-like protease like LPV/r (Ma et al., 2022). However, they have distinct pharmacodynamic properties: their inhibitory action differs in affinity and efficacy for SARS-CoV-2 protease target, with LPV/r showing greater efficacy at clinically achievable concentrations (Choy et al., 2020; Kang et al., 2020).

Moreover, protease inhibitors showed *in vitro* efficacy against coronaviruses causing severe acute respiratory syndrome (SARS) and Middle-East respiratory syndrome (MERS) (Chu et al., 2004). Studies conducted to evaluate the protease inhibitors combination of lopinavir-ritonavir with ribavirin reduced the mortality and viral load of SARS patients (Chu et al., 2004). Similarly, in MERS, lopinavir-ritonavir was effective both *in vitro* and in animal models, decreasing the viral load and improving clinical and radiological outcomes (de Wilde et al., 2014; Chan et al., 2015). Although the clinical impact of lopinavir-ritonavir in SARS or MERS was scarce, *in vitro* and animal studies revealed the potential inhibitory effect on SARS-CoV-2. Based on the structural similarities of the coronaviruses, lopinavir and ritonavir showed favourable inhibitory action on the replication of SARS-CoV-2 *in vitro* (Choy et al., 2020; Kang et al., 2020). Another protease inhibitor, darunavir-cobicistat was also found to have *in vitro* inhibitory effect on SARS-CoV-2, but only at higher concentrations (Yamamoto et al., 2020). The initiation of lopinavir-ritonavir and darunavir-cobicistat into COVID-19 treatments was based on the previous experience in SARS and MERS, however, in the last two years several clinical trials were conducted in SARS-CoV-2 infection and most showed no significant improvement in mortality, viral load, hospital stay or the need for ventilation support. Of note, the design of some of these clinical trials raised several bias concerns in terms of patient enrolment and sample size, the start of anti-viral therapy after

Abbreviations: COVID-19, coronavirus disease 2019; CRP, C-reactive protein; CT, computed tomography; DRV/r, darunavir-ritonavir; LMWH, low molecular weight heparin; LPV/r, lopinavir-ritonavir; MERS, Middle-East respiratory syndrome; RT-PCR, real-time polymerase chain reaction; SaO2, oxygen saturation; SARS, severe acute respiratory syndrome; SARS-CoV-2, severe acute respiratory syndrome coronavirus 2.

disease onset, underpowered statistics and the lack of control group (Cao et al., 2020b; Patel et al., 2021). Lopinavir-ritonavir was abandoned as a therapeutic option based on these studies with few concerns, including the trial conducted by Cao et al., which failed to demonstrate a significant benefit of lopinavir-ritonavir in decreasing mortality rates (Cao et al., 2020a; Owa and Owa, 2020). However, patients receiving lopinavir-ritonavir showed lower 28-day mortality rates and had a shorter intensive care unit (ICU) stay with a median of 6 days, compared to 11 days in the standard of care group. Data of this trial were reanalysed and a 73% a posteriori probability of clinical improvement in case of the protease inhibitors was found (Carmona-Bayonas et al., 2020). Along with this observation, a report by Lim et al. confirmed the beneficial clinical effects of lopinavir-ritonavir (Lim et al., 2020).

To our knowledge, data is lacking on the efficacy of lopinavir-ritonavir compared to the standard of care and to an additional protease inhibitor alternative, darunavir-ritonavir combination. Thus, we conducted a retrospective study to assess the differences between various protease inhibitors on comparable patient groups, from a Romanian cohort of patients hospitalised for COVID-19.

Patients and methods

Study design

We conducted a retrospective, single-site, tertiary care center-based, observational study to compare several clinical outcomes in patients taking lopinavir-ritonavir (Kaletra, 200 mg/50 mg, 1 tablet orally twice daily) or darunavir/ritonavir (800 mg darunavir/100 mg ritonavir 1 tablet once daily). We included consecutive patients hospitalised for COVID-19 in the Pulmonology and Infectious Diseases departments of our hospital, between July and October 2020. Concomitantly hospitalised COVID-19 patients, who received standard of care only including antibiotics, anticoagulants, dexamethasone and oxygen therapy via nasal cannula or oxygen mask, served as our controls. Patients were assigned to receive lopinavir/ritonavir, darunavir/ritonavir or standard of care only based on the infectious diseases' specialist advice concordant with a national treatment protocol, and the treatment duration with the protease inhibitors was 7 - 14 days. Of note, the antiviral treatment in eligible patients was started on or the next day of hospital admission. The research project was approved by the hospital's Ethics Committee on 16th of November 2020, on the condition of respect for the confidentiality of personal data and compliance with all applicable data protection laws and regulations. Given the retrospective design of data collection, there was no request from the Ethics Committee to obtain informed consent from the subjects included in the study. The research was conducted in accordance with the principles of the Declaration of Helsinki and its later amendments.

Study population and data collection

We collected data from a cohort compromising 824 hospitalised COVID-19 patients, with confirmed SARS-CoV-2 infection. Male and non-pregnant female patients older than 18 years were eligible if they needed hospitalisation, had a positive quantitative real-time polymerase chain reaction (RT-PCR) for SARS-CoV-2 infection, suggestive symptomatology and chest imaging. Exclusion criteria included pregnancy, prior use of protease inhibitors, necessity of invasive ventilation before considering antivirals, history of known cardiac arrhythmias, known drug allergy, a history of severe liver conditions such as cirrhosis and/or elevated alanine aminotransferase or aspartate aminotransferase level, and inability to swallow the medications.

The diagnosis of COVID-19 was confirmed by the detection of SARS-CoV-2 nucleocapsid genes with Exicycler^{TM} 96 – Bioneer (Korea) RT-PCR system. We collected medical data, including demographics, laboratory tests results, chest CT scan reports, symptomatology, current medication use and comorbidities. Data were obtained from the hospital available documents (i.e., patients' files, discharge letters, electronic database) as recorded by the treating physicians and were assessed for accuracy by the investigators. As a standard of care, all COVID-19 hospitalised patients underwent a chest CT scan upon admission, which was interpreted by experienced radiologists. The extension of lung lesions was graded as mild (<25%), moderate (25-50%) or severe (>50%).

Statistical analysis

Propensity score matching based on age, gender, oxygen use, steroid therapy and chest computed tomography (CT) imaging was used to divide the source population consisting of 824 patients. As 139 patients received LPV/r combination, all three groups (LPV/r, DRV/r, and control) comprised in the end the same number of patients.

Baseline characteristics were expressed as average ± standard deviation (SD) or proportions. The time to death or clinical improvement were assessed by Kaplan-Meier plot using log-rank test. In order to assess the relationship between mortality and drug administration, we used the Cox proportional hazard model and hazard ratios were shown with 95% CIs. All $p<0.05$ values were considered significant, adjusted p values were calculated with the Bonferroni method. We performed sensitivity analyses in pre-defined subgroups [male gender, age>50 years, >25% lesions on chest CT, presence of obesity, arterial hypertension or diabetes, high blood glucose level, low SaO2, high C- reactive protein (CRP) level, and the use of oxygen, dexamethasone and low molecular weight heparin (LMWH)]. Statistics were performed with R version 4.2.2 (R Project for Statistical Computing) and the Graphpad Prism 8.0.1 software.

Results

Patient characteristics

The flowchart for patient selection is summarised on Figure 1.

With respect to age, gender, and comorbidities, the three groups were generally balanced. Table 1 summarised the pre-treatment demographic and clinical characteristics. Patients in the LPV/r showed less 25-50% lesion extension on chest CT, compared to DRV/r group ($p<0.05$) and fewer patients had obesity or diabetes, compared to the control and DRV/r group. In both treatment arms gastrointestinal symptoms, headache and myalgia were the most common symptoms and occurred more frequently than in the control group (Table 1).

Table 2 shows the main clinical characteristics at admission and discharge including vital parameters, laboratory tests results and adjuvant therapies. Heart rate, blood pressure, body temperature and SaO2 did not show significant differences between the groups both at admission and at discharge. Although more patients had known diabetes in the DRV/r group, the LPV/r and control group had comparable glycaemia at admission. In both antiviral groups, dexamethasone and LMWH were more frequently administered, and patients receiving DRV/r more commonly needed oxygen supplementation (Table 2).

Outcomes

Although the mean duration of hospitalisation and the time to clinical improvement were significantly higher in both treated groups compared to controls ($p<0.01$), in-hospital mortality rate was decreased by lopinavir/ritonavir compared to the control and darunavir/ritonavir groups. As compared to the control group, univariable hazard ratios for death were 0.39 (95% CI 0.19-0.99) and 1.49 (95% CI 0.71-3.12) for LPV/r and for DRV/r, respectively (Table 3).

Several confounding factors may have contributed due to the retrospective nature of the study, thus the Cox proportional hazards model was adjusted for significant and clinically relevant baseline variables. These factors include comorbidities, oxygen saturation, high glucose levels and radiological abnormalities. In this multivariate analysis, the association with decreased mortality rates in LPV/r group remained significant (HR=0.25, 95% CI 0.09-0.66), while the administration of DRV/r was associated with higher risk for mortality (HR=2.60, 95% CI 1.37-4.92) (Table 4).

Kaplan-Meier analysis on antiviral treatment which was used to compare survival curves using the log-rank test, revealed that unlike DRV/r, LPV/r was associated with higher probability of survival (Figure 2A). Interestingly, clinically improved alive patients showed significant improvement at day 10 with both LPV/r and DRV/r, but not with standard care ($p< 0.05$, Figure 2B). Clinically improved patients were defined as those who were alive and demonstrated stabilised vital signs, improved oxygen saturation, better laboratory markers, and readiness for discharge.

In a subgroup analysis, LPV/r demonstrated improved survival in the group of patients with >25% lesion extension on the chest CT scan, however, the presence of comorbidities such as arterial hypertension, diabetes and the need for oxygen therapy significantly decreased the benefits of LPV/r. (Table 5).

Discussion

In this single centre, retrospective study we compared the efficacy of LPV/r and DRV/r combinations for the treatment of patients with COVID-19 during the second wave of pandemic. We found that the treatment with LPV/r was associated with better survival in hospitalised patients, but not with DRV/r. Comorbidities such as diabetes increased the risk of mortality in case of DRV/r but not with LPV/r. Lopinavir-ritonavir was particularly beneficial in patients with moderate-to-severe lesions on chest CT scan; however, arterial hypertension and the need for oxygen supplementation reduced its effectiveness.

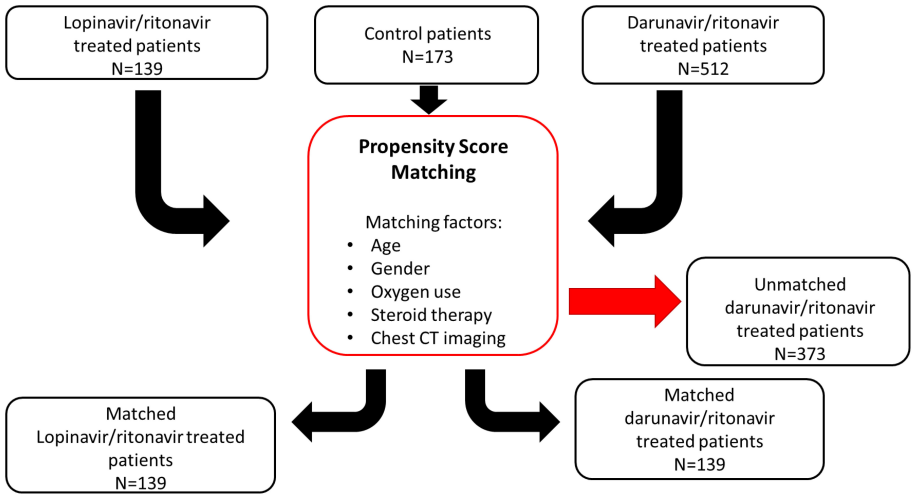

FIGURE 1
Flowchart for the patient selection pathway with propensity score matching method. A population of 824 patients was assigned using propensity score matching based on age, sex, oxygen use, steroid therapy, and chest CT imaging. 139 out of 824 patients received LPV/r combination, so the three groups (LPV/r, DRV/r, and control) comprised in the end the same number of patients.

10.3389/fcimb.2024.1496176

TABLE 1 General characteristics of COVID-19 patients, assigned to lopinavir/ritonavir (LPV/r), darunavir/ritonavir (DRV/r) use or standard care.

	Control N=139	LPV/r N=139	Unadjusted P value	Adjusted P value	DRV/r N=139	Unadjusted P value	Adjusted P value
Age (mean, SD)	50.5 ± 16.9	50.2 ± 15.3	0.98	ns	52.5 ± 5.8	0.45	ns
Male sex No (%)	75 (54%)	62 (45%)	0.06	ns	72 (52%)	0.36	ns
Smoking history	14 (10.1%)	21 (15.8%)	0.1	ns	31 (22.3%)	0.44	ns
Disease severity on chest CT No (%)							
Grade <25%	101 (73%)	95 (68%)	0.18	ns	69 (49%)	<0.01	
Grade 25-50%	29 (21%)	37 (26%)	0.16		62 (45%)	<0.01	
Grade >50%	9 (6%)	7 (5%)	0.35		8 (5.7%)	0.45	
Hospital-onset COVID-19	4 (2.9%)	8 (5.8%)	0.11	ns	2 (1.5%)	0.2	ns
Coexisting conditions No (%)							
Diabetes	30 (21.6%)	15 (10.8%)	0.007	ns	31 (22.3%)	0.44	ns
Arterial hypertension	50 (35.6%)	52 (37.4%)	0.4	ns	62 (44.6%)	0.07	ns
Chronic kidney disease	5 (3.6%)	1 (0.7%)	0.05	ns	6 (4.3%)	0.38	ns
Obesity	35 (25.2%)	18 (13%)	0.004	0.116	67 (48.2%)	<0.001	0.01
Asthma	4 (2.8%)	8 (5.7%)	0.12	0.99	13 (9.5%)	0.01	0.39
Other cardiovascular comorbidities	20 (14.4%)	16 (11.5%)	0.23	ns	21 (15.1%)	0.43	ns
Other pulmonary conditions	6 (4.3%)	8 (5.7%)	0.29	Ns	11 (7.9%)	0.1	ns
Neurological disorders	3 (2.1%)	8 (5.7%)	0.06	Ns	10 (7.2%)	0.02	0.78
Symptoms							
Asymptomatic	18 (13%)	4 (2.8%)	0.001	0.029	6 (4.31%)	0.005	0.19
Asthenia	47 (33.8%)	53 (38.1%)	0.22	Ns	54 (38.8%)	0.19	ns
Fever	55 (39.5%)	67 (48.2%)	0.07	Ns	84 (60.4%)	<0.001	0.01
Sweats	10 (7.2%)	24 (17.3%)	0.005	0.145	15 (10.8%)	0.14	ns
Fatigue	69 (49.6%)	73 (52.5%)	0.31	Ns	63 (45.3%)	0.23	ns
Dyspnea	35 (25.1%)	27 (19.4%)	0.12	Ns	55 (39.5%)	0.005	0.19
Dry cough	66 (47.5%)	77 (55.4%)	0.09	Ns	86 (61.8%)	0.008	0.31
Productive cough	9 (6.5%)	16 (11.5%)	0.07	Ns	17 (12.2%)	0.05	ns
Chills	17 (12.2%)	31 (22.3%)	0.01	0.3	43 (30.9%)	<0.001	0.003
Headache	33 (23.7%)	57 (41%)	0.001	0.03	50 (35.9%)	0.01	0.39
Diarrhoea	10 (7.2%)	16 (11.5%)	0.1	Ns	24 (17.3%)	0.005	ns
Nausea	7 (5%)	19 (13.7%)	0.007	0.2	22 (15.8%)	0.001	0.04
Vomiting	7 (5%)	12 (8.6%)	0.11	Ns	18 (12.9%)	0.01	0.4
Altered general condition	73 (52.5%)	73 (52.5%)	0.5	Ns	108 (77.7%)	<0.001	0.003
Loss of appetite	15 (10.8%)	29 (20.1%)	0.01	0.29	9 (6.5%)	0.1	ns
Ageusia	15 (10.8%)	13 (9.3%)	0.34	Ns	24 (17.3%)	0.06	ns
Dysphagia	19 (13.7%)	27 (19.4%)	0.09	Ns	26 (18.7%)	0.12	ns
Myalgia	23 (16.5%)	35 (25.2%)	0.03	0.87	56 (40.3%)	<0.001	0.004

Data are expressed as number (percentage).

10.3389/fcimb.2024.1496176

TABLE 2 Patient status and treatments administered at the time of enrolment and discharge.

	Control	LPV/r	p (vs. control)	DRV/r	p (vs. control)
SaO2 (admission)	95.2 ± 4.4	95 ± 5.7	0.86	94.6 ± 3.4	0.99
Low SaO2 at admission (<90%)	12 (8.6%)	13 (9.4%)	0.4	20 (14%)	0.07
SaO2 (discharge)	95.4 ± 6.2	95.7 ± 5.7	0.92	94.8 ± 6.3	0.81
Blood pressure admission (systole, mmHg)	129.31 ± 18.79	128.48 ± 17.52	0.92	130.82 ± 19.54	0.77
Blood pressure admission (diastole, mmHg)	80.34 ± 12.35	80.52 ± 10.23	0.99	82.76 ± 12.47	0.2
Heart rate admission	84.86 ± 14.13	85.06 ± 14.55	0.99	87.46 ± 15.54	0.31
Body temperature admission (°C)	36.21 ± 2.85	36.57 ± 0.71	0.21	36.51 ± 0.65	0.33
Blood pressure discharge (systole, mmHg)	124.63 ± 15.63	125.43 ± 16.13	0.91	126.39 ± 18.79	0.66
Blood pressure discharge(diastole, mmHg)	78.58 ± 11.0	78.51 ± 10.56	0.99	80.01 ± 12.22	0.54
Heart rate discharge	79.52 ± 12.32	81.32 ± 13.78	0.51	80.67 ± 14.60	0.76
Body temperature discharge (°C)	36.32 ± 0.46	36.27 ± 0.46	0.97	36.31 ± 0.36	0.99
Na (mmol/l)	135.88 ± 3.95	136.98 ± 3.07	0.047	136.68 ± 4.16	0.14
K (mmol/l)	4.26 ± 0.63	4.12 ± 0.51	0.12	4.34 ± 0.65	0.71
CRP (mg/ml)	39.3 ± 59.2	37.5 ± 58.5	0.8	63.7 ± 88.6	<0.01
Glycaemia (admission)	136.9 ± 79.8	136.7 ± 73.6	0.99	145.9 ± 73	0.55
Impaired glucose >110 mg/dl	54 (39%)	67 (48%)	0.065	87 (62.6%)	<0.01
High glucose >125 mg/dl	41 (29.5%)	48 (34.5%)	0.18	87 (62.6%)	<0.01
Fibrinogen	4.43 ± 1.48	4.52 ± 1.78	0.96	5.07 ± 4.2	0.14
GOT (U/ml)	27.98 ± 19.89	40.50 ± 71.31	0.76	59.61 ± 238.26	0.52
GPT (U/ml)	35.88 ± 36.65	68.84 ± 192.92	0.07	54.74 ± 66.17	0.41
Oxygen therapy	33 (23.7%)	30 (21.6%)	0.33	74 (53.2%)	<0.01
Ceftriaxone	34 (24.5)	24 (17.3%)	0.06	55 (39.6%)	<0.01
Azithromycin	56 (40.3%)	58 (41.7%)	0.4	68 (48.9%)	0.07
Dexamethasone	58 (41.7%)	59 (42.4%)	0.45	116 (83.4%)	<0.01
LMWH	84 (60.4%)	110 (79.1%)	<0.01	136 (97.8%)	<0.01

Data are expressed as number (percentage) or mean± standard deviation (SD). CRP, C-reactive protein; GOT, glutamate oxaloacetate transaminase; GPT, glutamate pyruvate transaminase; LMWH, Low molecular weight heparin; SaO2, arterial oxygen saturation.

Similarly to the HIV aspartic protease, the cysteine protease of SARS-CoV-2 was hypothesised to be a reasonable target of repurposed antiretroviral protease inhibitors (Magro et al., 2021). *In vitro* studies demonstrated the efficacy of lopinavir-ritonavir against SARS-CoV-2 and its ability to bind to SARS-CoV 3C-like protease, thus inhibiting viral replication (Zumla et al., 2016; Choy et al., 2020). Apart from lopinavir- ritonavir, another protease inhibitor combination darunavir-cobicistat was tested in silico and found to have theoretical affinity to 3C-like protease and potential inhibitory effect on viral replication (Sang et al., 2020). Later, an *in vitro* research demonstrated the lack of antiviral effects of darunavir on SARS-CoV-2 (De Meyer et al., 2020). In the early desperate times of the pandemic, protease inhibitors came into focus again after successful treatment of a patient with mild COVID-19 (Lim et al., 2020). Although lopinavir-ritonavir and hydroxychloroquine reduced organ support-free days and worsened the clinical outcomes among critically ill patients at an intensive care unit (Arabi et al., 2021), protease inhibitors remained still a potential option for hospitalised mild to severe COVID-19 patients. In a randomised, controlled, open-label trial by Cao et al., the authors suggested that lopinavir-ritonavir has no benefit in hospitalised patients compared to standard care (Cao et al., 2020a). Although the clinicians started to abandon lopinavir-ritonavir based on the results of this trial, several arguments should be taken into consideration: the trial was underpowered due to small sample size (N=199) and arguably, the treatment started at a median time of 13 days after symptom onset. Of note, the same trial reported several interesting findings with regard to the secondary outcomes suggesting lopinavir-ritonavir may be associated with reduced all-cause mortality (19% of patients in the lopinavir-ritonavir group vs. 25% of control group), decreased risk of severe adverse events (20% in lopinavir-ritonavir vs 32% of control group) and lower risk of severe respiratory failure (13% vs. 27%, respectively) (Dalerba et al., 2020). Another group reanalysed

TABLE 3 Mortality data of study population by treatment allocation.

	Control N=139	LPV/r N=139	Difference	Adj.p (vs. control)	DRV/r N=139	Difference	Adj.p (vs. control)	LPV/r vs. DRV/r difference	Adj.p LPV/r vs. DRV/r
Days spent in hospital	8.09 ± 6.0	10.63 ± 5.5	-2.54 (-4.24 to -0.83)	<0.001	12.83 ± 6.4	-4.73(-6.42 to -3.044)	<0.001	-2.193 (-3.89 to -0.48)	0.007
Time to clinical improvement (average days ± SD)	7.9 ± 5.9	10.6 ± 5.4	-2.69 (-4.41 to -0.97)	<0.001	11 ± 6.3	-3.13 (-4.87 to -1.37)	<0.001	-0.43 (-2.16 to 1.30)	0.82
In-hospital mortality	10 (7.2%)	5 (3.6%)		0.09	14 (10%)		0.19		0.016
Time to death	10.1 ± 6.7	13.8 ± 8.4	-3.7 (-13.68 to 6.27	0.63	13.4 ± 7.1	-3.32 (-10.87 to 4.21)	0.52	0.37 (-9.11 to 9.8)	0.99
Univariate analysis (HR, 95% CI)	–	0.39 (0.19-0.99)	–	0.04	1.49 (0.71-3.12)	–	0.28		

Data is expressed as mean ± SD. CI, confidence interval; HR, hazard ratio.

these data and found that lopinavir-ritonavir can contribute to clinical improvement (Carmona-Bayonas et al., 2020). In this aspect, our results were consistent with their observation that lopinavir-ritonavir reduced mortality. A further publication advised to consider starting lopinavir-ritonavir earlier and speculated about the favourable effects of LPV/r, supporting the need for further clinical studies in this field (Owa and Owa, 2020).

In the RECOVERY trial LPV/r was not associated with reduced 28-day mortality, duration of hospital stay or the risk of progression to invasive mechanical ventilation. However, we have to evaluate these results cautiously as an overall 74% of patients required respiratory support in form of oxygen therapy at baseline and both the usual care and LPV/r were started at an average 8 days after symptom onset (RECOVERY Collaborative Group, 2020). In line with this, oxygen therapy was associated with worse outcomes in the LPV/r group in our study. Additionally, the WHO SOLIDARITY trial included primarily patients already being ventilated or using respiratory support at the time of their recruitment.

Patients assigned to antiviral treatment had severe COVID-19, most of them lived in Asia and Africa where limited treatment resources were available, and some patients would have needed respiratory support (WHO Solidarity Trial Consortium, 2022). Although the final results concentrated on the effects of remdesivir therapy, the interim research results suggested that LPV/r can have benefits in a defined group of patients (< 50 years) (WHO Solidarity Trial Consortium et al., 2021). Further studies compared LPV/r to other drug combinations, and one of them found that a triple combination with LPV/r, interferon beta -1b and ribavirin significantly improved National Early Warning Score (NEWS2), Sequential Organ Failure Assessment (SOFA) scores, hospital stay and decreased the time to negative viral load in nasopharyngeal specimens only if the patient allocation was done prior to 7 days after symptom onset (Hung et al., 2020). These data also pointed out that similar to MERS and SARS, the early antiviral treatment may be crucial against SARS-CoV-2, and one should consider the wide randomisation windows in the evaluation of clinical trial results (de Wit et al., 2016). Additional studies aimed to compare LPV/r alone to other drugs such as umifenovir, novaferon or hydroxychloroquine, and to their combinations. However, these studies had no standard care group, had small sample size, poor statistical power and different control groups with various study population heterogeneity, therefore they have to be interpreted cautiously (Li et al., 2020; Nojomi et al., 2020; Zheng et al., 2020). The TOGETHER trial enrolled COVID-19 patients with at least one clinical criterion for high risk and compared the effects of LPV/r or hydroxychloroquine to placebo. Although the participants received the treatment less than 8 days from symptom onset, the trial confirmed that neither LPV/r, nor hydroxychloroquine showed associations with COVID-19 mortality or hospitalisation (Reis et al., 2021). Another study confirmed that all paediatric patients with

TABLE 4 Hazard ratios for the risk factor of death in the study population.

	HR	CI 95%	p value
Age	1.04	1.00-1.07	0.02
Male sex	3.63	1.23-10.68	0.02
LPV/r	0.25	0.09-0.66	<0.01
DRV/r	2.60	1.37-4.92	<0.01
Obesity	1.49	0.65-3.43	0.34
Diabetes	2.49	1.05-5.58	0.03
Low SaO2 (<90%)	5.23	2.45-11.17	<0.001
High glucose >125 mg/dl	3.68	1.23-10.91	0.01
Grade1 lesion (<25%)	0.12	0.02-0.53	0.005
Grade3 lesion (>50%)	2.67	1.12-6.39	0.03
Dexamethasone	1.69	0.55-5.18	0.36
Oxygen therapy	1.37	0.57-3.31	0.47

Cox proportional hazard model was used to determine the relationship of clinical factors and in-hospital mortality in the treated and control groups (n=417). Hazard ratios are shown with 95% CIs. All COVID-19 hospitalised patients underwent a chest CT scan and the extension of lung lesions was graded as mild (<25%, Grade 1), moderate (25-50%, Grade 2) or severe (>50%, Grade 3).

10.3389/fcimb.2024.1496176

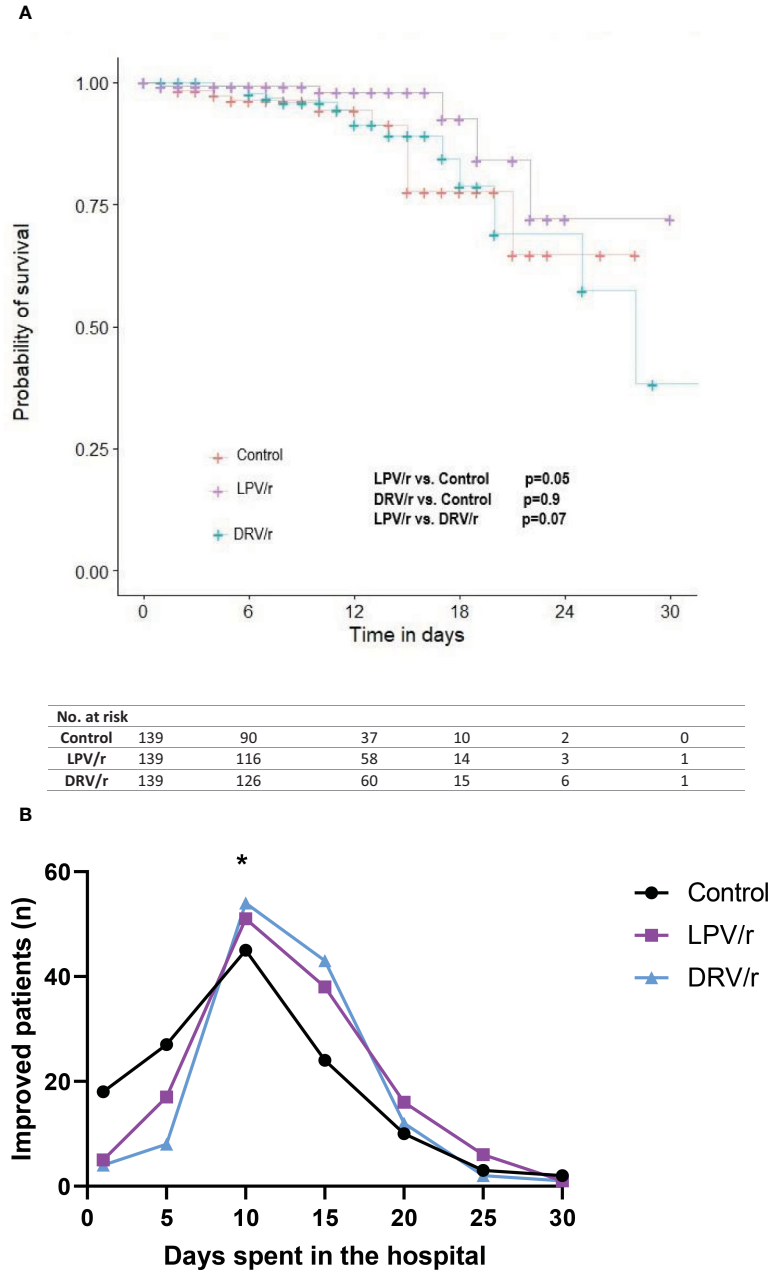

FIGURE 2
(A) Survival curves according to LPV/r or DRV/r use. A Kaplan-Meier analysis was performed to evaluate in-hospital mortality. Significance was calculated by using log-rank test. **(B)** Patient improvement on LPV/r or DRV/r therapy. Patient improvement was expressed according to the days patients spent in hospital. At day 10 both the LPV/r and DRV/r treated patients showed significant improvement compared to control participants. n= number of patients, *$p<0.05$.

mild or moderate COVID-19 receiving LPV/r were cured and had reduced hospital stay (Qiu et al., 2020). Taken together, these data suggest that LPV/r may have clinical benefits in a predefined subgroup of hospitalised patients without baseline respiratory support. Indeed, our data is consistent with this theory, as patients without severe comorbidities or oxygen supplementation receiving LPV/r showed association with lower risk of COVID-19 associated death.

Darunavir, another protease inhibitor, was identified as a promising hit by computational methods which indicated it to be more effective against COVID-19 than LPV/r (Khan et al., 2021). Darunavir was mostly used in combination with cobicistat (DRV/c), but this drug combination did not meet the initial expectations. DRV/c was effective at high concentrations against SARS-CoV-2 *in vitro* and proved to be more tolerable and safer than LPV/r (Orkin et al., 2013; Yamamoto et al., 2020). However, a study by Milic et al. confirmed that patients on DRV/c had higher mortality rate and risk for mechanical ventilation, compared to patients received standard care (Milic et al., 2021). A further study compared DRV/c with LPV/r and revealed that DRV/c was associated with 89% increased risk of death if the patients were women, older, had

10.3389/fcimb.2024.1496176

TABLE 5 Hazard ratios for mortality according to LPV/r and DRV/r use in different subgroups.

	HR (95% CI)	
Subgroups	LPV/r vs. control	DRV/r vs. control
Demographics		
Men (N=209)	0.45 (0.15-1.35)	0.71 (0.50-1.01)
Age >50 years (N=223)	0.54 (0.14-1.66)	0.78 (0.28-2.09)
Comorbidities		
Obesity		
Yes (N=120)	0.55 (0.06-5.13)	0.89 (0.28-2.74)
No (N=297)	0.35 (0.09-1.35)	0.93 (0.28-3.07)
Diabetes		
Yes (N=76)	0.93 (0.16-5.16)	2.10 (0.61-7.21)
No (N=341)	0.23 (0.06-0.96) p=0.044	0.61 (0.20-1.84)
Arterial hypertension		
Yes (N=164)	1.02 (0.26-3.89)	1.30 (0.42-4.05)
No (N=253)	0.07 (0.0086-0.67) P= 0.021	0.56 (0.17-1.88)
Patient status		
Degree of COVID-19 severity on chest CT scan		
Grade<25% (N=265)	NA (1)	NA (2)
Grade>25% (N=152)	0.35 (0.12-1.03) p=0.05	0.63 (0.27-1.48)
Impaired glucose metabolism (>110 mg/dl)		
Yes (N=208)	0.42 (0.12-1.51)	1.28 (0.48-3.39)
No (N=263)	0.18 (0.02-1.6)	NA (1)
Low SaO2 (<90%)		
Yes (N=45)	0.47 (0.11-1.97)	0.58 (0.16-2.02)
No (N=372)	0.29 (0.05-1.54)	1.49 (0.45-4.91)
High CRP (10 mg/dl)		
Yes (N=243)	0.29 (0.07-1.14) P=0.07	1.15 (0.44-2.80)
No (N=174)	NA	NA
Therapies		
Use of oxygen		
Yes (N=137)	0.65 (0.16-2.59)	1.14 (0.40-3.03)
No (N=280)	0.18 (0.03-1.12) p=0.05	0.62 (0.13-2.85)
Use of dexamethasone		
Yes (N=228)	0.73 (0.22-2.39)	1.16 (0.44-3.04)
No (N=189)	NA	NA
Use of LMWH		
Yes (N=330)	0.61 (0.18-2.00)	1.41 (0.54-3.69)
No (N=87)	NA	NA

A subgroup analysis was conducted to reveal the main risk factors in mortality according to protease inhibitor use. Hazard ratios are shown with 95% CIs. Values showed NA (not applicable) meaning the inability to calculate values due to low number of patients. CRP, C-reactive protein; LMWH, Low molecular weight heparin; SaO2, arterial oxygen saturation.

severe infection and received hydroxychloroquine. Additionally, a subgroup analysis of data from this study showed a lower risk of death in patients with mild disease treated with LPV/r (Di Castelnuovo et al., 2021). Another observational study comparing the efficacy of early administered DRV/c versus LPV/r unravelled that LPV/r was associated with faster time to recovery and virological clearance, but not DRV/c (Elmekaty et al., 2022). These findings can be also attributed to the unfavourable toxic side-effects of DRV/c (Hunt et al., 2011). The majority of darunavir is bound to plasma proteins and metabolised by CYP3A4. As ritonavir is a known CYP3A4 inhibitor, their combination can be theoretically a more efficacious drug against COVID-19 as DRV/c, however, there is an increasing risk of drug interactions and severe side-effects (Hsu et al., 1998; Rittweger and Arastéh, 2007). In fact, our study is the first that evaluated the clinical outcomes of DRV/r on COVID-19 patients, compared to LPV/r or standard care group. Based on our results, DRV/r was associated with increased mortality rates compared to LPV/r treated patients, showed higher rates of impaired glucose metabolism and oxygen support, but we did not observe higher frequency of cardiovascular alterations.

To our knowledge, our study is the first to compare the clinical effects of LPV/r and DRV/r protease inhibitors in hospitalised patients with mild-to-severe COVID-19, however, our results have some limitations. Firstly, we checked the effects in a retrospective observational nature. The treatment options were highly dependent on the accessibility of LPV/r and DRV/r in our centre. A placebo-controlled project would have been also not accepted during the early desperate time of the pandemic, so we tried to exclude the potential confounding factors with propensity-score matching method. Additionally, our study was launched relatively early during the pandemic and it would have been complicated to set up a randomised prospective study and get an ethical approval for these combinations.

Conclusions

The main benefits of drug repurposing include the existing knowledge of a drug's pharmacokinetics, pharmacodynamics, and toxicity. Employing similar strategies to find anti-SARS-CoV-2 compounds could significantly reduce the time required to identify an effective treatment for COVID-19, thereby lessening the disease's impact, including hospital admissions, deaths, and long-term consequences. The global health crisis caused by the

COVID-19 pandemic has necessitated the urgent acceleration of drug discovery and the swift identification of effective treatments and therapeutic options. While repurposed drugs must still undergo clinical trials, it is evident that this approach can quickly uncover effective treatments, even among those drugs that did not succeed for their initial intended use. Despite the widespread administration of COVID-19 vaccinations, COVID-19 continues to pose significant financial and public health challenges globally. Furthermore, vaccinations are not equally accessible to all populations; hence, repurposed drugs for the treatment of COVID-19 remain a viable option.

This retrospective study demonstrated that early treatment with lopinavir-ritonavir was associated with significantly improved survival and mortality rates compared to darunavir-ritonavir. Lopinavir-ritonavir exhibited a higher probability of survival compared to both the darunavir-ritonavir and standard care groups. Therefore, in the event of a future medication shortage during the COVID-19 pandemic, it would remain a favourable option for a carefully selected subgroup of patients. Despite some studies, the long-term effects of lopinavir-ritonavir in these patients await confirmation in a prospective, randomised, controlled trial. Our findings suggest that lopinavir-ritonavir should not be entirely disregarded for the treatment of COVID-19 and confirm that the combination of darunavir-ritonavir offers no additional clinical benefit for these patients.

Data availability statement

The raw data supporting the conclusions of this article will be made available by the authors, without undue reservation.

Ethics statement

The studies involving humans were approved by Infectious Diseases and Pulmonology Clinical Hospital Timisoara - Ethics Committee. The studies were conducted in accordance with the local legislation and institutional requirements. The ethics committee/institutional review board waived the requirement of written informed consent for participation from the participants or the participants' legal guardians/next of kin because the study design was retrospective.

Author contributions

DP: Conceptualization, Formal analysis, Methodology, Validation, Visualization, Writing – original draft, Writing – review & editing. ABi: Conceptualization, Formal analysis, Methodology, Supervision, Validation, Visualization, Writing – original draft, Writing – review & editing. ABl: Data curation, Investigation, Project administration, Software, Validation, Writing – review & editing. EB: Data curation, Project administration, Software, Validation, Writing – review & editing. AL: Data curation, Formal analysis, Project administration, Software, Validation, Writing – review & editing. CM: Data curation, Formal analysis, Project administration, Software, Validation, Writing – review & editing. SM: Data curation, Formal analysis, Project administration, Software, Validation, Visualization, Writing – review & editing. SF: Conceptualization, Data curation, Formal analysis, Methodology, Project administration, Resources, Software, Supervision, Validation, Visualization, Writing – review & editing.

Funding

The author(s) declare that financial support was received for the research, authorship, and/or publication of this article. We would like to acknowledge VICTOR BABES UNIVERSITY OF MEDICINE AND PHARMACY TIMISOARA for their support in covering the costs of publication of this research paper. DP was supported by the University Research Fellowship Program (EKÖP) of the Ministry for Culture and Innovation from the source of the National Research, Development and Innovation Fund (EKÖP-24-4 - SZTE-376).

Conflict of interest

The authors declare that the research was conducted in the absence of any commercial or financial relationships that could be construed as a potential conflict of interest.

Publisher's note

References

Arabi, Y. M., Gordon, A. C., Derde, L. P. G., Nichol, A. D., Murthy, S., Beidh, F. A., et al. (2021). Lopinavir-ritonavir and hydroxychloroquine for critically ill patients with COVID-19: REMAP-CAP randomized controlled trial. *Intensive Care Med.* 47, 867–886. doi: 10.1007/s00134-021-06448-5

Cao, B., Wang, Y., Wen, D., Liu, W., Wang, J., Fan, G., et al. (2020a). A trial of lopinavir-ritonavir in adults hospitalized with severe covid-19. *N. Engl. J. Med.* 382, 1787–1799. doi: 10.1056/NEJMoa2001282

Cao, B., Zhang, D., and Wang, C. A. (2020b). Trial of lopinavir-ritonavir in covid-19. Reply. *N. Engl. J. Med.* 382, e68. doi: 10.1056/NEJMc2008043

Carmona-Bayonas, A., Jimenez-Fonseca, P., and Castañón, E. A. (2020). Trial of lopinavir-ritonavir in covid-19. *N. Engl. J. Med.* 382, e68. doi: 10.1056/NEJMc2008043

Chan, J. F.-W., Yao, Y., Yeung, M.-L., Deng, W., Bao, L., Jia, L., et al. (2015). Treatment with lopinavir/ritonavir or interferon-B1b improves outcome of MERS-

CoV infection in a nonhuman primate model of common marmoset. *J. Infect. Dis.* 212, 1904–1913. doi: 10.1093/infdis/jiv392

Choy, K.-T., Wong, A. Y.-L., Kaewpreedee, P., Sia, S. F., Chen, D., Hui, K. P. Y., et al. (2020). Remdesivir, lopinavir, emetine, and homoharringtonine inhibit SARS-coV-2 replication *in vitro*. *Antiviral Res.* 178, 104786. doi: 10.1016/j.antiviral.2020.104786

Chu, C. M., Cheng, V. C. C., Hung, I. F. N., Wong, M. M. L., Chan, K. H., Chan, K. S., et al. (2004). Role of lopinavir/ritonavir in the treatment of SARS: initial virological and clinical findings. *Thorax* 59, 252–256. doi: 10.1136/thorax.2003.012658

Dalerba, P., Levin, B., and Thompson, J. L. A. (2020). Trial of lopinavir-ritonavir in covid-19. *N. Engl. J. Med.* 382, e68. doi: 10.1056/NEJMc2008043

De Meyer, S., Bojkova, D., Cinatl, J., Van Damme, E., Buyck, C., Van Loock, M., et al. (2020). Lack of antiviral activity of darunavir against SARS-CoV-2. *Int. J. Infect. Dis. IJID Off. Publ. Int. Soc Infect. Dis.* 97, 7–10. doi: 10.1016/j.ijid.2020.05.085

de Wilde, A. H., Jochmans, D., Posthuma, C. C., Zevenhoven-Dobbe, J. C., van Nieuwkoop, S., Bestebroer, T. M., et al. (2014). Screening of an FDA-approved compound library identifies four small-molecule inhibitors of middle east respiratory syndrome coronavirus replication in cell culture. *Antimicrob. Agents Chemother.* 58, 4875–4884. doi: 10.1128/AAC.03011-14

de Wit, E., van Doremalen, N., Falzarano, D., and Munster, V. J. (2016). SARS and MERS: recent insights into emerging coronaviruses. *Nat. Rev. Microbiol.* 14, 523–534. doi: 10.1038/nrmicro.2016.81

Di Castelnuovo, A., Costanzo, S., Antinori, A., Berselli, N., Blandi, L., Bonaccio, M., et al. (2021). Lopinavir/ritonavir and darunavir/cobicistat in hospitalized COVID-19 patients: findings from the multicenter italian CORIST study. *Front. Med.* 8. doi: 10.3389/fmed.2021.639970

Elmekaty, E. Z. I., Alibrahim, R., Hassanin, R., Eltaib, S., Elsayed, A., Rustom, F., et al. (2022). Darunavir-cobicistat versus lopinavir-ritonavir in the treatment of COVID-19 infection (DOLCI): A multicenter observational study. *PloS One* 17, e0267884. doi: 10.1371/journal.pone.0267884

Hsu, A., Granneman, G. R., and Bertz, R. J. (1998). Ritonavir. Clinical pharmacokinetics and interactions with other anti-HIV agents. *Clin. Pharmacokinet.* 35, 275–291. doi: 10.2165/00003088-199835040-00002

Hung, I. F.-N., Lung, K.-C., Tso, E. Y.-K., Liu, R., Chung, T. W.-H., Chu, M.-Y., et al. (2020). Triple combination of interferon beta-1b, lopinavir-ritonavir, and ribavirin in the treatment of patients admitted to hospital with COVID-19: an open-label, randomised, phase 2 trial. *Lancet Lond. Engl.* 395, 1695–1704. doi: 10.1016/S0140-6736(20)31042-4

Hunt, K., Hughes, C. A., and Hills-Nieminen, C. (2011). Protease inhibitor-associated QT interval prolongation. *Ann. Pharmacother.* 45, 1544–1550. doi: 10.1345/aph.1Q422

Kang, C. K., Seong, M.-W., Choi, S.-J., Kim, T. S., Choe, P. G., Song, S. H., et al. (2020). *In Vitro* Activity of Lopinavir/Ritonavir and Hydroxychloroquine against Severe Acute Respiratory Syndrome Coronavirus 2 at Concentrations Achievable by Usual Doses. *Korean J. Intern. Med.* 35, 782–787. doi: 10.3904/kjim.2020.157

Khan, S. A., Zia, K., Ashraf, S., Uddin, R., and Ul-Haq, Z. (2021). Identification of chymotrypsin-like protease inhibitors of SARS-CoV-2 via integrated computational approach. *J. Biomol. Struct. Dyn.* 39, 2607–2616. doi: 10.1080/07391102.2020.1751298

Kumar, A., Singh, R., Kaur, J., Pandey, S., Sharma, V., Thakur, L., et al. (2021). Wuhan to world: the COVID-19 pandemic. *Front. Cell. Infect. Microbiol.* 11. doi: 10.3389/fcimb.2021.596201

Li, Y., Xie, Z., Lin, W., Cai, W., Wen, C., Guan, Y., et al. (2020). Efficacy and safety of lopinavir/ritonavir or arbidol in adult patients with mild/moderate COVID-19: an exploratory randomized controlled trial. *Med. N. Y. N* 1, 105–113.e4. doi: 10.1016/j.medj.2020.04.001

Li, W., Zhang, C., Sui, J., Kuhn, J. H., Moore, M. J., Luo, S., et al. (2005). Receptor and viral determinants of SARS-coronavirus adaptation to human ACE2. *EMBO J.* 24, 1634–1643. doi: 10.1038/sj.emboj.7600640

Lim, J., Jeon, S., Shin, H. Y., Kim, M. J., Seong, Y. M., Lee, W. J., et al. (2020). Case of the index patient who caused tertiary transmission of COVID-19 infection in Korea: the application of lopinavir/ritonavir for the treatment of COVID-19 infected pneumonia monitored by quantitative RT-PCR. *J. Korean Med. Sci.* 35, e79. doi: 10.3346/jkms.2020.35.e79

Ma, L., Xie, Y., Zhu, M., Yi, D., Zhao, J., Guo, S., et al. (2022). Identification of darunavir derivatives for inhibition of SARS-coV-2 3CLpro. *Int. J. Mol. Sci.* 23, 16011. doi: 10.3390/ijms232416011

Magro, P., Zanella, I., Pescarolo, M., Castelli, F., and Quiros-Roldan, E. (2021). Lopinavir/ritonavir: repurposing an old drug for HIV infection in COVID-19 treatment. *Biomed. J.* 44, 43–53. doi: 10.1016/j.bj.2020.11.005

Mallah, S. I., Ghorab, O. K., Al-Salmi, S., Abdellatif, O. S., Tharmaratnam, T., Iskandar, M. A., et al. (2021). COVID-19: breaking down a global health crisis. *Ann. Clin. Microbiol. Antimicrob.* 20, 35. doi: 10.1186/s12941-021-00438-7

Milic, J., Novella, A., Meschiari, M., Menozzi, M., Santoro, A., Bedini, A., et al. (2021). Darunavir/cobicistat is associated with negative outcomes in HIV-negative patients with severe COVID-19 pneumonia. *AIDS Res. Hum. Retroviruses* 37, 283–291. doi: 10.1089/AID.2020.0305

Nojomi, M., Yassin, Z., Keyvani, H., Makiani, M. J., Roham, M., Laali, A., et al. (2020). Effect of arbidol (Umifenovir) on COVID-19: A randomized controlled trial. *BMC Infect. Dis.* 20, 954. doi: 10.1186/s12879-020-05698-w

Nutho, B., Mahalapbutr, P., Hengphasatporn, K., Pattaranggoon, N. C., Simanon, N., Shigeta, Y., et al. (2020). Why Are Lopinavir and Ritonavir Effective against the Newly Emerged Coronavirus 2019? Atomistic Insights into the Inhibitory Mechanisms. *Biochemistry* 59, 1769–1779. doi: 10.1021/acs.biochem.0c00160

Orkin, C., DeJesus, E., Khanlou, H., Stoehr, A., Supparatpinyo, K., Lathouwers, E., et al. (2013). Final 192-week efficacy and safety of once-daily darunavir/ritonavir compared with lopinavir/ritonavir in HIV-1-infected treatment-naïve patients in the ARTEMIS trial. *HIV Med.* 14, 49–59. doi: 10.1111/j.1468-1293.2012.01060.x

Owa, A. B., and Owa, O. T. (2020). Lopinavir/ritonavir use in Covid-19 infection: is it completely non-beneficial? *J. Microbiol. Immunol. Infect. Wei Mian Yu Gan Ran Za Zhi* 53, 674–675. doi: 10.1016/j.jmii.2020.05.014

Patel, T. K., Patel, P. B., Barvaliya, M., Saurabh, M. K., Bhalla, H. L., and Khosla, P. P. (2021). Efficacy and safety of lopinavir-ritonavir in COVID-19: A systematic review of randomized controlled trials. *J. Infect. Public Health* 14, 740–748. doi: 10.1016/j.jiph.2021.03.015

Qiu, H., Wu, J., Hong, L., Luo, Y., Song, Q., and Chen, D. (2020). Clinical and epidemiological features of 36 children with coronavirus disease 2019 (COVID-19) in Zhejiang, China: an observational cohort study. *Lancet Infect. Dis.* 20, 689–696. doi: 10.1016/S1473-3099(20)30198-5

RECOVERY Collaborative Group (2020). Lopinavir-ritonavir in patients admitted to hospital with COVID-19 (RECOVERY): A randomised, controlled, open-label, platform trial. *Lancet Lond. Engl.* 396, 1345–1352. doi: 10.1016/S0140-6736(20)32013-4

Reis, G., Moreira Silva, E. A. D. S., Medeiros Silva, D. C., Thabane, L., Singh, G., Park, J. J. H., et al. (2021). Effect of early treatment with hydroxychloroquine or lopinavir and ritonavir on risk of hospitalization among patients with COVID-19: the TOGETHER randomized clinical trial. *JAMA Netw. Open* 4, e216468. doi: 10.1001/jamanetworkopen.2021.6468

Rittweger, M., and Arastéh, K. (2007). Clinical pharmacokinetics of darunavir. *Clin. Pharmacokinet.* 46, 739–756. doi: 10.2165/00003088-200746090-00002

Sang, P., Tian, S.-H., Meng, Z.-H., and Yang, L.-Q. (2020). Anti-HIV drug repurposing against SARS-CoV-2. *RSC Adv.* 10, 15775–15783. doi: 10.1039/d0ra01899f

Singh, T. U., Parida, S., Lingaraju, M. C., Kesavan, M., Kumar, D., and Singh, R. K. (2020). Drug repurposing approach to fight COVID-19. *Pharmacol. Rep. PR* 72, 1479–1508. doi: 10.1007/s43440-020-00155-6

Wang, M., Cao, R., Zhang, L., Yang, X., Liu, J., Xu, M., et al. (2020). Remdesivir and chloroquine effectively inhibit the recently emerged novel coronavirus (2019-nCoV) *in vitro*. *Cell Res.* 30, 269–271. doi: 10.1038/s41422-020-0282-0

WHO Solidarity Trial Consortium (2022). Remdesivir and three other drugs for hospitalised patients with COVID-19: final results of the WHO solidarity randomised trial and updated meta-analyses. *Lancet Lond. Engl.* 399, 1941–1953. doi: 10.1016/S0140-6736(22)00519-0

WHO Solidarity Trial Consortium, Pan, H., Peto, R., Henao-Restrepo, A.-M., Preziosi, M.-P., Sathiyamoorthy, V., et al. (2021). Repurposed antiviral drugs for covid-19 - interim WHO solidarity trial results. *N. Engl. J. Med.* 384, 497–511. doi: 10.1056/NEJMoa2023184

Yamamoto, N., Matsuyama, S., Hoshino, T., and Yamamoto, N. (2020). Nelfinavir inhibits replication of severe acute respiratory syndrome coronavirus 2 *in vitro*. doi: 10.1101/2020.04.06.026476

Zheng, F., Zhou, Y., Zhou, Z., Ye, F., Huang, B., Huang, Y., et al. (2020). SARS-CoV-2 clearance in COVID-19 patients with novaferon treatment: A randomized, open-label, parallel-group trial. *Int. J. Infect. Dis. IJID Off. Publ. Int. Soc Infect. Dis.* 99, 84–91. doi: 10.1016/j.ijid.2020.07.053

Zumla, A., Chan, J. F. W., Azhar, E. I., Hui, D. S. C., and Yuen, K.-Y. (2016). Coronaviruses - drug discovery and therapeutic options. *Nat. Rev. Drug Discovery* 15, 327–347. doi: 10.1038/nrd.2015.37

frontiers | Frontiers in Cellular and Infection Microbiology

TYPE Original Research
PUBLISHED 04 February 2025
DOI 10.3389/fcimb.2025.1531018

OPEN ACCESS

EDITED BY
Diana Manolescu,
Victor Babes University of Medicine and Pharmacy, Romania

REVIEWED BY
Mirella Luciani,
Experimental Zooprophylactic Institute of Abruzzo and Molise G. Caporale, Italy
Neelja Singhal,
University of Delhi, India

*CORRESPONDENCE
Alireza Ghassempour
a_ghassempour@yahoo.com

RECEIVED 19 November 2024
ACCEPTED 09 January 2025
PUBLISHED 04 February 2025

CITATION
Sharif A, Nejad RB and Ghassempour A (2025) Immunoassay–mass spectrometry to identify *Brucella melitensis*. *Front. Cell. Infect. Microbiol.* 15:1531018. doi: 10.3389/fcimb.2025.1531018

Immunoassay–mass spectrometry to identify *Brucella melitensis*

Amirreza Sharif[1], Ramin Bagheri Nejad[2] and Alireza Ghassempour[1]*

[1]Medicinal Plants and Drugs Research Institute, Shahid Beheshti University, Tehran, Iran, [2]Razi Vaccine & Serum Research Institute, Agricultural Research, Education and Extension Organization, Karaj, Iran

Two factors frequently impede accurate bacterial identification using matrix-assisted laser desorption ionization time-of-flight mass spectrometry (MALDI-TOF MS): inadequate bacterial abundance in real samples and bacterial combinations. For MALDI-TOF MS analysis and libraries for bacterial identification, time-consuming culture procedures are necessary to achieve sufficient concentration and isolation of a single bacterium. When dealing with hazardous bacteria like *Brucella*, which are more difficult to handle and cure, this problem becomes even more crucial. To overcome these obstacles, Fe_3O_4 magnetic nanoparticles (MNPs) linked with *Brucella*-specific antibodies and MALDI-TOF MS analysis have been used to create a quick and accurate technique for direct bacterial separation and identification in complex samples. This method allows MNPs to immune-selectively collect *Brucella* cells, which are then deactivated and ready for MALDI-TOF MS analysis by a formic acid/acetonitrile wash. Rabbits were used to manufacture brucella antibodies, which have effectively adsorbed onto the MNPs–protein A. Any particular *Brucella* bacteria found in the media might be absorbed by this MNPs–protein A–antibody immunoprobe. The concentration of *Brucella* bacterial cells increases the protein spectrum's visibility by a factor of 10^3, making it possible to quickly identify *Brucella* spp. without first growing them in cultural conditions. This method has been successfully used to achieve a limit of detection (LOD) of 50 CFU/mL in an aqueous medium and genuine sample—milk. The diagnostic time for this harmful bacterium is greatly decreased because the entire procedure from bacterial isolation to species identification is finished in less than 60 min. High sensitivity and specificity are demonstrated by the immunoassay–MS approach, as the spectral pattern it produces matches well-known databases like SPECLUST and Ribopeaks.

KEYWORDS

immunoassay-mass spectrometry, *Brucella* spp., magnetic nanoparticles, milk, MALDI-TOF MS

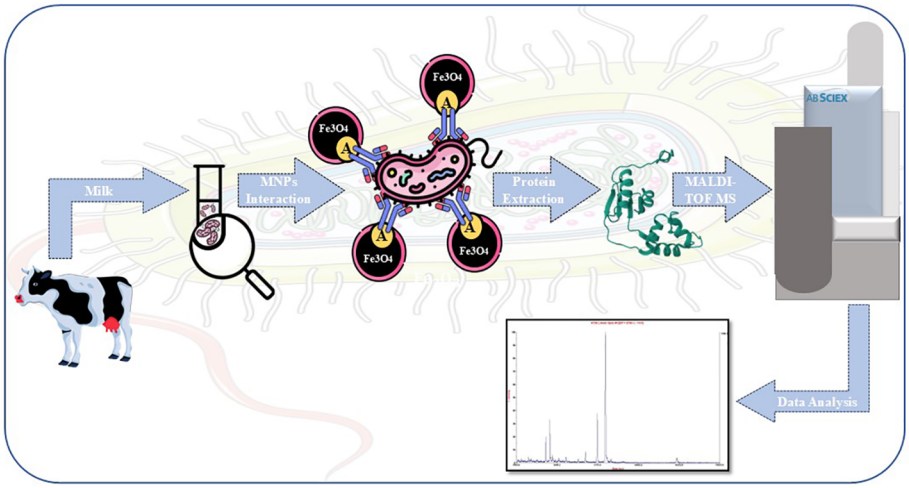

GRAPHICAL ABSTRACT

1 Introduction

The world's health is being threatened by infectious germs, which have the capacity to start pandemics in the future (Nieto and Salvetti, 2014; Cloeckaert, 2024). Bacteria have historically caused a wide range of infectious diseases that impact people, animals, and plants (Dharmarajan et al., 2022; Tiedje et al., 2022; Glajzner et al., 2024). An estimated 420,000 deaths are attributed to foodborne pathogens alone each year, with the largest burden occurring in areas of poverty (Olivares et al., 2013; Schaumburg et al., 2019; de Oliveira et al., 2024). Therefore, bacterial illnesses must be properly diagnosed and treated in order to protect the public's health (Zia and Alkheraije, 2023). Brucellosis is also known as "Mediterranean fever", "undulant fever," and "Malta fever". Because of its low infectious dosage and ability to spread through inhaling contaminated aerosols, it is considered an infectious bacterial zoonosis (Qin et al., 2023; Zhang et al., 2024). Rapid and accurate identification of pathogenic microorganisms is necessary to comprehend these diseases (Wang et al., 2022; Kang et al., 2024). Matrix-assisted laser desorption ionization time-of-flight mass spectrometry (MALDI-TOF MS) utilizes a mass spectrum library derived from sufficient microbial proteins, allowing the matching of the obtained mass spectrum of one bacteria with known profiles for species identification (Cheng et al., 2016; Kurli et al., 2018; Rahi and Vaishampayan, 2020; Han et al., 2021; Lorente-Leal et al., 2022; Peng et al., 2022; Tsuchida and Nakayama, 2022; Becker and Lupetti, 2023; Foster and Khaiboullina, 2023).

Notable commercial kits include the developed fast BACpro® II kit (Nittobo Medical Co., Tokyo, Japan) (Wang et al., 2016; Oviaño et al., 2021), the Vitek MS blood culture kit (bioMérieux, Inc.) (Nomura et al., 2020), and the Sepsityper® kit (Bruker Daltonics) (Perše et al., 2022). For bacterial analysis in microbiology labs, including cultivation, inactivation, isolation, and data interpretation, the Food and Drug Administration (FDA) has authorized MALDI-TOF MS (Bauermeister et al., 2022; Li et al., 2022; Haider et al., 2023; Pastrone et al., 2023).

A potential method for quick and precise microbiological identification is the combination of MNPs and MALDI-TOF MS (Kumari et al., 2023). Detection limits as low as 10^2 CFU/mL are made possible by MNPs (Xiao et al., 2022; Abafogi et al., 2024). This technique improves operating speed and accuracy by streamlining processes by doing away with the requirement to culture samples, particularly for highly virulent pathogens such as *Brucella* (Ha and Kim, 2022). Furthermore, MNPs' capacity to functionalize and attach selectively to bacterial cells enhances detection specificity in complicated biological samples, contributing to their high selectivity (Houser et al., 2024). Because of protein A's high affinity for the Fc region of immunoglobulins (IgGs), antibodies on MNPs can be effectively immobilized, greatly enhancing their ability to ensnare target microorganisms (Xu et al., 2019).

Serological tests are usually preferred because determining the source of brucellosis is crucial due to its current threats and takes a lot of time, often requiring highly qualified specialists (Padilla et al., 2010). Serological techniques, however, frequently encounter obstacles like a lack of standardization, validation issues, and restrictions on precisely identifying the species and strain of *Brucella* implicated (Yagupsky et al., 2019).

In our last study, we used bioinformatics in conjunction with MALDI-TOF MS proteomics analysis to find biomarkers for brucellosis (Hamidi et al., 2022). Additionally, we used MALDI-TOF MS in conjunction with single-chain variable fragment (scFv) antibody-conjugated MNPs as highly sensitive and selective probes to quickly and precisely detect and identify the fig mosaic virus (Soleimani Mashhadi et al., 2020).

Using Fe_3O_4 MNPs modified with protein A and particular antibodies produced in rabbits, an immunoaffinity probe was created in this study to selectively isolate *Brucella* bacteria from contaminated samples at low concentration levels. This was

followed by identification using the MALDI-TOF MS technique. This proposed technique increased the limit of detection (LOD) of *Brucella* bacteria by a factor of 1,000 in aqueous medium and milk samples.

2 Materials and methods

2.1 Material

2.1.1 Chemicals and solutions

In this investigation, the following substances were used: CHEM LAB Co. (Zedelgem, Belgium) provided the sodium carbonate and sodium dodecyl sulfate (SDS). Sigma-Aldrich Co. (Altenburg, USA) provided the magnetic iron oxide nanoparticles (Fe_3O_4 MNPs), acrylamide, N,N'-methylene bisacrylamide, sinapinic acid, and α-cyano-4-hydroxycinnamic acid (CHCA).

The following additional reagents were obtained from Merck Co. (Darmstadt, Germany): tetramethylethylenediamine (TEMED), Tris (hydroxymethyl) aminomethane, silver nitrate, tetraethyl orthosilicate (TEOS), N,N-dimethylformamide (DMF), succinic anhydride, disodium phosphate, potassium dihydrogen phosphate, glycine, ammonia solution (28%), acetonitrile (HPLC grade), absolute ethanol, formic acid, and trifluoroacetic acid (TFA).

The supplier of formaldehyde was Ghatranshimi Co. in Tehran, Iran. The supplier of ammonium persulfate (APS) was GE Healthcare Co. (Chicago, USA). We purchased 3-aminopropyltriethoxysilane (APTES), 1-ethyl-3-(3-dimethylaminopropyl) carbodiimide (EDC), and N-hydroxysuccinimide (NHS) from Exir GmbH Co. (Vienna, Austria). Lastly, BIOCHEM Chemopharma Co. (Burgundy, France) was the supplier of potassium chloride and sodium chloride.

2.2 Preparation of antibody immobilized on magnetic iron oxide nanoparticles

Initially, 100 mg of MNPs was subjected to a 10-min sonication. After adding ethanol (EtOH), water, ammonia, and TEOS, the mixture was sonicated for 3 h at room temperature. After that, ethanol was used to wash the MNPs. After adding APTES, water, ammonia, and EtOH, the mixture was sonicated for an hour at room temperature and then washed with ethanol to aminate the MNPs.

After the MNPs were cleaned, succinic anhydride was added, and the reaction was left to continue stirring all night. EDAC and NHS were added to the succinylated MNPs after they had been dissolved in 50 mM phosphate-buffered saline (PBS, pH 6.6) to activate the carboxyl groups (Mahmoud et al., 2005).

Following washing, the suspension was vortexed for 3 h and 2 mL of 500 ppm protein A solution was added (Ramandi et al., 2022). Two milliliters of 50 mM PBS (pH 6.6) was used to wash the MNPs three times for 10 min each time. For the SDS-PAGE analysis, 30 µL of each sample was kept. A Tris-HCl buffer (pH 8) was used to quench the MNPs' unreacted sites.

The buffer was switched out for 50 mM PBS (pH 7.4) in order to encapsulate the antibody. After adding 2 mL of a 500 ppm *Brucella* antibody solution to the MNPs–protein A complex, the mixture was vortexed for 3 h. Two milliliters of 50 mM PBS (pH 7.4) was used to wash the MNPs three times for 10 min each time. Once more, 30 µL of every sample was saved for SDS-PAGE examination. For bacterial enrichment, the resultant MNPs–protein A–antibody complex was utilized (Figure 1).

2.3 SDS-PAGE analysis

Using the Bio-Rad system (Hercules, CA, USA), one-dimensional SDS-PAGE was performed. A 15% polyacrylamide gel made with Tris-glycine buffer was loaded with protein samples. For the best protein band separation, electrophoresis was carried out at a steady voltage.

To see the separated proteins, a silver nitrate staining procedure was used on the gel following electrophoresis. In short, the gel was sensitized in a sodium thiosulfate solution after being fixed in a methanol, acetic acid, and water solution to maintain the protein bands. After staining the gel with silver nitrate, it was developed with a developer solution based on formaldehyde until protein bands were visible. The gel was submerged in a stop solution to stop the reaction. High-sensitivity protein band detection was made possible by this procedure, guaranteeing that the separated proteins could be seen for further examination.

2.4 *Brucella* culture

The reference strain *Brucella melitensis* 16M was obtained from the Razi Vaccine and Serum Research Institute (Karaj, Iran). The bacteria were cultured on *Brucella* agar plates (BBL Microbiological Systems, Cockeysville, MD, USA), a selective medium specifically designed to support the growth of *Brucella* species. The plates were incubated under aerobic conditions at 37°C for 6 days to allow for sufficient bacterial growth.

To ensure optimal bacterial proliferation, the agar plates were prepared fresh and maintained in sterile conditions. Colony morphology was observed daily to confirm the growth characteristics of *B. melitensis* 16M, and any contamination was ruled out through visual inspection. After the incubation period, bacterial colonies were harvested under aseptic conditions and prepared for downstream applications, such as protein extraction, immunoassay development, or mass spectrometric analysis.

2.5 Produce antibody in rabbit

A fresh overnight culture was diluted in PBS to create a bacterial solution with a concentration of 10^8 CFU/mL to generate antibodies against *B. melitensis*. Two doses of this suspension were administered to New Zealand White rabbits, with a 3-week gap between the first and booster shots. Two weeks following the booster injection, jugular

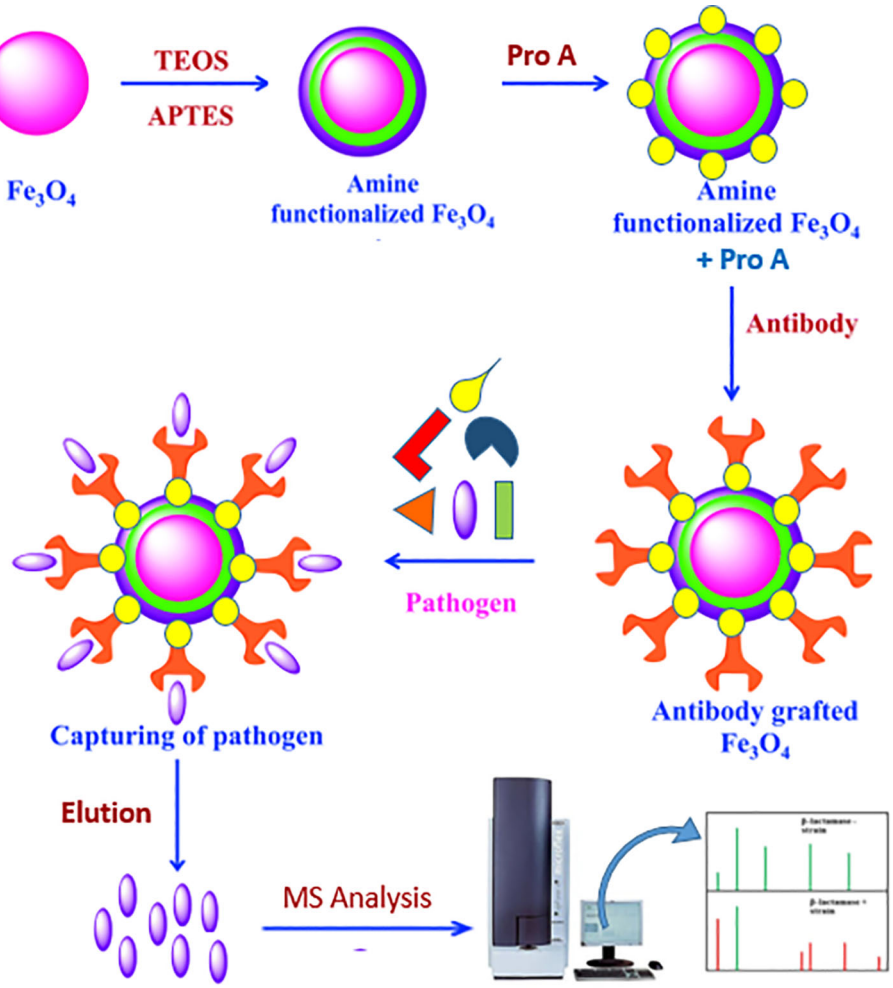

FIGURE 1
Activation of MNPs and immobilization of protein A and adsorption of antibody on it: TEOS (tetraethyl orthosilicate) and APTES (3-aminopropyltriethoxysilan).

vein blood samples were taken to extract antibody production. MNPs were employed to extract *B. melitensis* antibodies from the serum, which were then utilized for the following procedures.

2.6 Extraction of bacteria from samples with MNPs–protein A–antibody

The initial sample was diluted to reach a concentration of 50 billion bacteria after bacterial growth, then subsequent dilutions (50 to 5×10^8 CFU/mL) were made. Different concentrations of MNPs–protein A–antibody were applied to 5×10^6 CFU/mL of bacterial suspension to maximize bacterial separation. Bacteria attached to the MNPs–protein A–antibody conjugates were collected after 30 min of incubation at 37°C with constant shaking. They were then rinsed for 10 min with 1,000 µL of PBS (pH 7.4) and then again for 10 min with 1,000 µL of deionized water. After resuspending the particles in 15 µL of 70% formic acid and MS-grade acetonitrile, they were shaken to break down the bacterial cell walls and extract the proteins. The supernatant was spotted on a MALDI plate using the CHCA matrix for analysis.

2.7 MALDI-TOF MS analysis

An Applied Biosystems 4800 MALDI-TOF MS equipped with a Nd laser (200 Hz, AB Sciex, Canada) was used to obtain the mass spectra of bacterial proteins. CHCA (10.0 mg/mL in 2.5% TFA and 50% acetonitrile). The sample solution was added to the MALDI plate after 1 µL of the matrix solution. With a mass range of 2–20 kDa, the analysis was carried out in positive ion linear mode. Each sample received between 600 and 1,000 laser pulses, and the Data Explorer software (version 4.0) was used to create the average mass spectrum.

For bacterial inactivation and extraction, we employed a formic acid–ethanol extraction strategy. A bacterial suspension containing 6 to 10 colonies in 600 µL of water was vortexed for 10 s, followed by the addition of 1,000 µL of absolute ethanol. The mixture was carefully mixed and incubated at 20–25°C for 30 min and then centrifuged at 10,000 rpm for 10 min. The supernatant was removed, and the pellet was resuspended in 10 µL of 70% formic acid. Ten microliters of acetonitrile was added to ensure thorough mixing.

After centrifuging the mixture for 2 min at 11,000 rpm and 20–25°C, the supernatant was gathered and placed in a separate tube. The supernatant was put onto *Brucella* agar and cultured for 6 days at 37°C in order to evaluate the vitality of the bacteria. The effectiveness of the chemical procedures in deactivating *Brucella* spp. was validated by the lack of bacterial colonies.

3 Results

The SDS-PAGE analysis revealed successful immobilization of protein A on MNPs. The presence of protein A was confirmed in the supernatant, wash 1, and wash 2, indicating that protein A was effectively fixed on the MNPs and was ready for antibody binding to capture specific antigens (S1). Additionally, *Brucella* antibodies are produced in rabbits and purified via MNPs–protein A. The SDS-PAGE gel demonstrating the MNPs–protein A–antibody compared to pure antibodies is illustrated (S2). The non-covalent bond formed between protein A and the *Brucella* antibody allows for the potential purification of the *Brucella* antibody through elution from the MNPs–protein A–antibody surface.

A dilution of 5×10^3 CFU/mL of *Brucella* bacteria was incubated with the antibody-coated substrate, and the results were compared to a substrate devoid of antibodies to verify the development of the antibody–antigen bond. The proteins of the *Brucella* bacteria that were isolated from the antibody-coated substrate produced the anticipated protein spectrum, while no such spectrum was seen from the substrate without antibodies. Additionally, MNPs–protein A–antibody was given to 5×10^3 CFU/mL of *Escherichia coli* to verify its specificity, and no peaks were observed. Considering the necessity to optimize the amount of MNPs–protein A–antibody for isolation, we tested different substrate concentrations (0.5, 1, 2, and 5 mg/mL) using 5×10^3 CFU/mL of *Brucella* bacteria (Table 1). Significant variations in protein spectrum intensity across the different substrate amounts led to the conclusion that 2 mg/mL was the ideal substrate concentration.

The antibody-coated substrate was also kept in PBS buffer at 4°C for 3 months to evaluate its shelf life. Effective contact with bacteria was validated by post-storage analysis, which also showed that the produced MNPs–protein A–antibody remained functional for a minimum of 3 months.

To assess the pre-concentration effectiveness of the MNPs–protein A–antibody, both with the optimal quantity of MNPs–protein A–antibody after extraction using MALDI-TOF MS and without trapping the bacteria on the substrate, bacterial proteins were examined at various dilutions. The colony count in the initial suspension was 5×10^8 CFU/mL. To extract the *Brucella* bacteria, several aqueous bacterial suspensions were made at dilutions ranging from 5×10^8 to 50 CFU/mL. A LOD of 5×10^4 and 50 CFU/mL in the aqueous environment without and with pre-concentration, respectively, was found in the mass spectra derived from these investigations.

To verify the analysis of *B. melitensis* 16M, the obtained mass spectra were compared to reference spectra, which showed a sizable number of similar peaks. They were generated in an aqueous medium to continue a series of dilutions that interacted with 2 mg/mL of the substrate, ranging from 5×10^8 to 50 CFU/mL of the original bacterial suspension. After the proteins from the *Brucella* bacteria were extracted, the data were examined and are shown in Table 2. The average standard deviation (SD) was 12.3, and the linear discriminating range (LDR) was 10^7, signifying a noteworthy 10^3-fold increase in the concentration coefficient.

We referred to the average total viable count in urban samples, which is reported to be between 10^8 and 10^5 CFU/mL (Berhe et al., 2020; Mukhopadhyay et al., 2024), in order to further modify this method for biological applications. Therefore, we made bacterial dilutions ranging from 5×10^4 to 50 CFU/mL and added them to low-fat pasteurized milk as an actual sample analysis. Following the established procedure, we extracted the protein after permitting contact with the substrate. Figure 2 displays the outcome of the 50 CFU/mL dilution analysis.

The mass spectrum displayed significant interference from milk proteins (Šebela, 2022; Cuccato et al., 2022), prompting the exploration of several strategies to enhance the detection of bacterial protein peaks. The approaches employed included centrifugation of contaminated milk, followed by dilution of the sediment in water prior to interaction with the substrate (Punyapornwithaya et al., 2009; Tiedje et al., 2022), washing with a Tween-20-containing buffer, and adding additional

TABLE 1 Comparison amount of the ability of MNPs–protein A–antibody to achieve bacteria.

MNPs (mg/mL)	Intensity
0.5	64.3
1	264.0
2	987.5
5	1,085.8

TABLE 2 Evaluate the pre-concentration efficacy of the MNPs–protein A–antibody, without trapping the bacteria on the substrate and with the optimized amount of MNPs–protein A–antibody following extraction via MALDI-TOF MS.

Bacterial dilution (CFU/mL)	Intensity Non-interaction ± *SD*	Intensity Interaction ± *SD*
5×10^8	2923.4 ± 12.2	3536.1 ± 12.8
5×10^7	1978.7 ± 11.4	2488.5 ± 13.7
5×10^6	1696.0 ± 13.1	2430.4 ± 11.8
5×10^5	1589.2 ± 12.6	1886.6 ± 12.3
5×10^4	1071.1 ± 11.9	1785.7 ± 12.6
5×10^3	–	1553.0 ± 11.2
5×10^2	–	1433.9 ± 10.9
50	–	537.0 ± 13.4

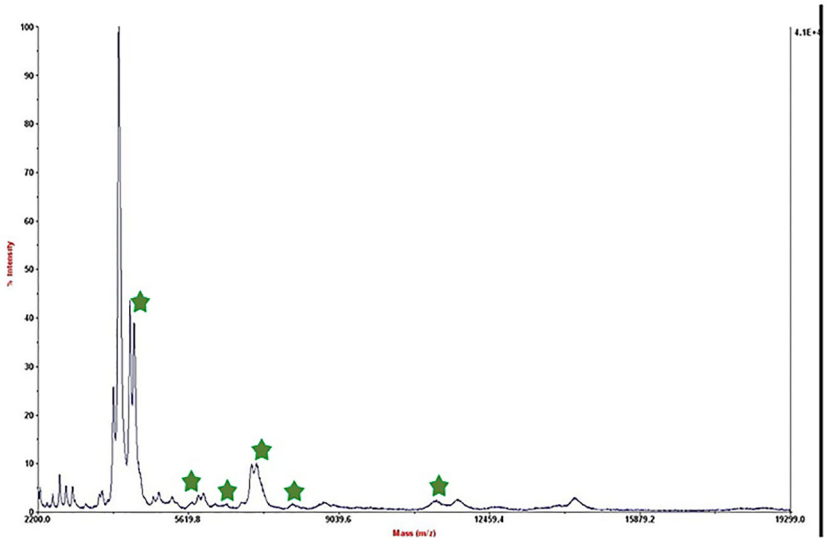

FIGURE 2
Mass spectrum of *B. melitensis* in 50 CFU/mL dilution in milk after interaction with MNPs–protein A–antibody.

washing steps (Barreiro et al., 2012). These methods were applied to bacterial dilutions of 5×10^4 to 50 CFU/mL, resulting in notable improvements, as shown in Figure 3. Ongoing efforts are focused on optimizing the analysis of smaller bacterial quantities. It means that the LOD of this technique is 50 CFU/mL and we can detect bacteria in milk samples. The significance of this method lies in its potential for rapid and accurate pathogen identification, thereby aiding medical professionals and contributing to public health. This report details our progress to date, with continued work aimed at validating the method for practical applications in clinical settings.

4 Discussion

We found that 2 mg/mL of MNPs–protein A–antibody is the ideal concentration for efficiently isolating pathogens in complex matrices like milk, where proteins and lipids can make isolation difficult. Our findings concur with those of Xiao et al (Xiao et al., 2022), who emphasized the significance of optimal MNP concentrations for raising the sensitivity of detection. Using MNPs in conjunction with immunoassay methods, we were able to detect *B. melitensis* in milk and water samples with an LOD of 50 CFU/mL. The application of polydopamine-coated MNPs for

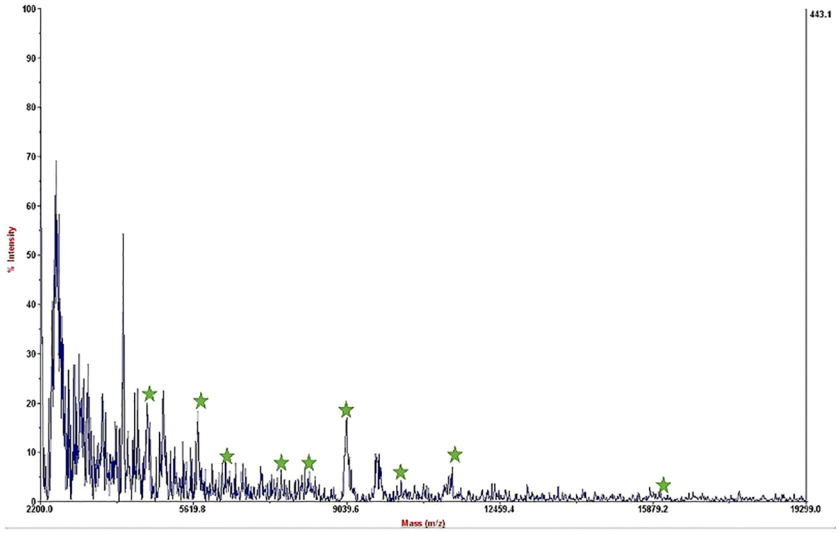

FIGURE 3
Mass spectrum of *B. melitensis* in 50 CFU/mL dilution in milk after interaction with MNPs–protein A–antibody and improvement.

automated sepsis detection was recently demonstrated by Zhang et al., who achieved remarkable sensitivity with detection limits as low as 10^2 CFU/mL across a variety of bacterial species in blood samples (Houser et al., 2024).

Similar to our strategy of using MNPs for bacterial collection from milk, this degree of sensitivity highlights how well MNPs work to capture and concentrate germs from complicated matrices. Furthermore, Chen et al. reported that MNPs grafted with antibodies can greatly increase detection sensitivity (Chen et al., 2022). Our findings that antibody-functionalized MNPs improve the overall sensitivity of bacterial protein spectra by a factor of 10^3 detection and expedite the isolation procedure are corroborated by this evidence. When compared to traditional culture methods, our method of using MALDI-TOF MS in conjunction with MNPs provides rapid identification capabilities in less than 60 min, which is a significant reduction in the time needed for bacterial identification. For prompt clinical decision-making and efficient patient care, this quick turnaround is essential.

Additionally, the significant problem of low bacterial abundance in samples is resolved by integrating MNPs with MALDI-TOF MS. Furthermore, new research highlights the adaptability and efficiency of iron oxide-based MNPs in the identification and management of bacteria (Svadlakova et al (Svadlakova et al., 2020)). Improvements in magnetic nanoparticle-based microfluidic systems that allow for the quick and accurate identification of harmful bacteria in a variety of sample types, including food and water, were covered by Han et al (Han et al., 2021). Furthermore, Ha et al. described methods that increase sensitivity and specificity even in complex food matrices (Ha and Kim, 2022) and demonstrated how magnetic nanoparticles improve immunoassays for pathogen detection.

By offering prompt and precise bacterial identification that is essential for efficient patient care and treatment, this quick turnaround has the potential to completely transform clinical microbiology. Although this approach may have a significant impact on clinical microbiology, its wider application will require additional verification of its precision and consistency across a range of bacterial strains and clinical settings.

Adapting this technique to a range of diseases requires high-affinity antibodies that target specific pathogen indicators, such as lipopolysaccharides or cell wall proteins for bacteria and capsid or envelope proteins for viruses. These antibodies ensure the sensitivity and specificity of the immunoaffinity enrichment. The high-throughput, rapid, and cost-effective technique of MALDI-TOF mass spectrometry enhances bacterial identification. However, in settings with limited resources, its high initial costs, maintenance needs, and reliance on skilled personnel may make it less accessible. Continuous sample preparation and efficient processes are necessary for scalability. Despite these challenges, MALDI-TOF offers scalable, cost-effective diagnostics with exceptional mass accuracy and precision.

Although MNPs have several drawbacks when used in therapeutic settings, they provide intriguing applications for bacterial enrichment. It is difficult to achieve specificity across a variety of bacterial populations; thus, current research attempts to improve the identification of mixed pathogens by developing particular substrates based on patient clinical circumstances and protein biomarkers (Sandrin and Demirev, 2018; Yang et al., 2018; Han et al., 2021). The efficiency of magnetic separation is affected by factors such as flux and magnetic field strength, which can be improved by synthesizing smaller MNPs and their quantity optimization for bacterial extraction (Socas-Rodríguez et al., 2020). Furthermore, complex biological matrices often interfere with binding and enrichment processes, requiring preconcentration methods such as centrifugation to clean up samples (Xu et al., 2019). Moreover, implementing MNP-based methods in clinical settings requires compliance with regulatory standards, which presents challenges in standardizing protocols across laboratories (Takallu et al., 2024). It will be essential to highlight these challenges to advance the use of MNPs in routine microbiological diagnostics.

Using this method within the context of an automated diagnostic platform or a field-deployable kit, MS is thus a viable strategy for advancing microbial diagnostics. Future research should involve the development of automated magnetic separation techniques that will improve the method's efficiency as shown by various studies that have used vancomycin- and allantoin-conjugated MNPs for the rapid concentration of bacteria from the complex samples (Han et al., 2021; Abafogi et al., 2024). In addition, the development of portable diagnostic kits that contain MNPs will help in the identification of pathogens in the affected regions (Wen et al., 2017). The specificity, sensitivity, and selectivity of MNPs can be increased further to capture a wider range of bacterial strains through the use of new conjugation techniques (Gao et al., 2016). In general, these developments can be viewed as having the capacity to enhance microbial diagnostic capabilities in the clinical setting with speed and efficiency.

Data availability statement

The datasets presented in this study can be found in online repositories. The names of the repository/repositories and accession number(s) can be found in the article/Supplementary Material.

Ethics statement

The experiments were conducted in accordance with the ethical standards of the National Institute of Genetic Engineering and Biotechnology (NIGEB) (IR.NIGEB.EC.1394.8.10).

Author contributions

AS: Conceptualization, Data curation, Formal analysis, Investigation, Methodology, Resources, Software, Writing – original draft. RN: Writing – review & editing, Data curation, Methodology, Resources. AG: Writing – review & editing, Supervision, Validation, Visualization.

Funding

The author(s) declare that no financial support was received for the research, authorship, and/or publication of this article.

Acknowledgments

The authors would like to thank Dr. Autosa AliAhmadi, Dr. MohammadAli As'habi, Dr. Hamideh Hamidi, Ms. Negar Saeedi, Dr. Marjan Talebi, Mr. Mohammad-Amin Ensandoost, and Mr. Saeed Nowrozi for their valuable and helpful comments to improve this manuscript.

Conflict of interest

The authors declare that the research was conducted in the absence of any commercial or financial relationships that could be construed as a potential conflict of interest.

Generative AI statement

The author(s) declare that no Generative AI was used in the creation of this manuscript.

Publisher's note

Supplementary material

The Supplementary Material for this article can be found online at: https://www.frontiersin.org/articles/10.3389/fcimb.2025.1531018/full#supplementary-material

References

Abafogi, A. T., et al. (2024). Automated sepsis detection with vancomycin-and allantoin-polydopamine magnetic nanoparticles. *Sci. Rep.* 14, 3693. doi: 10.1038/s41598-024-54236-0

Barreiro, J. R., et al. (2012). Nonculture-based identification of bacteria in milk by protein fingerprinting. *Proteomics* 12, 2739–2745. doi: 10.1002/pmic.201200053

Bauermeister, A., Mannochio-Russo, H., Costa-Lotufo, L. V., Jarmusch, A. K., and Dorrestein, P. C. (2022). Mass spectrometry-based metabolomics in microbiome investigations. *Nat. Rev. Microbiol.* 20, 143–160. doi: 10.1038/s41579-021-00621-9

Becker, K., and Lupetti, A. (2023). MALDI-TOF MS in microbiological diagnostics: future applications beyond identification. *Front. Microbiol.* 14, 1204452. doi: 10.3389/fmicb.2023.1204452

Berhe, G., Wasihun, A. G., Kassaye, E., and Gebreselasie, K. (2020). Milk-borne bacterial health hazards in milk produced for commercial purpose in Tigray, northern Ethiopia. *BMC Public Health* 20, 1–8. doi: 10.1186/s12889-020-09016-6

Chen, Y.-J., et al. (2022). Microneedle patches integrated with lateral flow cassettes for blood-free chronic kidney disease point-of-care testing during a pandemic. *Biosens. Bioelectron.* 208, 114234. doi: 10.1016/j.bios.2022.114234

Cheng, K., Chui, H., Domish, L., Hernandez, D., and Wang, G. (2016). Recent development of mass spectrometry and proteomics applications in identification and typing of bacteria. *PROTEOMICS–Clinical Appl.* 10, 346–357. doi: 10.1002/prca.201500086

Cloeckaert, A. (2024). Insights in infectious agents and disease: 2022. *Front. Microbiol.* 15, 1443636. doi: 10.3389/fmicb.2024.1443636

Cuccato, M., Divari, S., Sacchi, P., Girolami, F., and Cannizzo, F. T. (2022). MALDI-TOF mass spectrometry profiling of bovine skim milk for subclinical mastitis detection. *Front. Vet. Sci.* 9, 1009928. doi: 10.3389/fvets.2022.1009928

de Oliveira, L. M. A., Ribeiro, R. L., and Ganda, E. (2024). Foodborne bacterial pathogens under the One Health perspective-antimicrobial resistance, epidemiology, virulence, and zoonotic impact. *Front. Cell. Infection Microbiol.* 14, 1379188. doi: 10.3389/fcimb.2024.1379188

Dharmarajan, G., et al. (2022). The animal origin of major human infectious diseases: what can past epidemics teach us about preventing the next pandemic? *Zoonoses* 2, 989. doi: 10.15212/ZOONOSES-2021-0028

Foster, T., and Khaiboullina, S. (2023). Community series-innovative approaches in diagnosis of emerging/re-emerging infectious diseases, volume II. *Front. Microbiol.* 14, 1193841. doi: 10.3389/fmicb.2023.1193841

Gao, X.-L., et al. (2016). Non-selective separation of bacterial cells with magnetic nanoparticles facilitated by varying surface charge. *Front. Microbiol.* 7, 1891. doi: 10.3389/fmicb.2016.01891

Glajzner, P., Bernat, A., and Jasińska-Stroschein, M. (2024). Improving the treatment of bacterial infections caused by multidrug-resistant bacteria through drug repositioning. *Front. Pharmacol.* 15, 1397602. doi: 10.3389/fphar.2024.1397602

Ha, Y., and Kim, I. (2022). Recent developments in innovative magnetic nanoparticles-based immunoassays: from improvement of conventional immunoassays to diagnosis of COVID-19. *BioChip J.* 16, 351–365. doi: 10.1007/s13206-022-00064-1

Haider, A., Ringer, M., Kotroczó, Z., Mohácsi-Farkas, C., and Kocsis, T. (2023). The current level of MALDI-TOF MS applications in the detection of microorganisms: a short review of benefits and limitations. *Microbiol. Res. (Pavia).* 14, 80–90. doi: 10.3390/microbiolres14010008

Hamidi, H., Bagheri Nejad, R., Es-Haghi, A., and Ghassempour, A. (2022). A combination of MALDI-TOF MS proteomics and species-unique biomarkers' discovery for rapid screening of brucellosis. *J. Am. Soc Mass Spectrom.* 33, 1530–1540. doi: 10.1021/jasms.2c00110

Han, H., Sohn, B., Choi, J., and Jeon, S. (2021). Recent advances in magnetic nanoparticle-based microfluidic devices for the pretreatment of pathogenic bacteria. *Biomed. Eng. Lett.* 11, 297–307. doi: 10.1007/s13534-021-00202-y

Houser, B. J., et al. (2024). Bacterial binding to polydopamine-coated magnetic nanoparticles. *ACS Appl. Mater. Interfaces.* doi: 10.1021/acsami.4c11169

Kang, H., et al. (2024). Rapid identification of bloodstream infection pathogens and drug resistance using Raman spectroscopy enhanced by convolutional neural networks. *Front. Microbiol.* 15, 1428304. doi: 10.3389/fmicb.2024.1428304

Kumari, M., Klodzinska, S. N., and Chifiriuc, M. C. (2023). Microbe-nanoparticle interactions: a mechanistic approach. *Front. Microbiol.* 14, 1273364. doi: 10.3389/fmicb.2023.1273364

Kurli, R., et al. (2018). Cultivable microbial diversity associated with cellular phones. *Front. Microbiol.* 9, 1229. doi: 10.3389/fmicb.2018.01229

Li, B., et al. (2022). Performance evaluation and clinical validation of optimized nucleotide MALDI-TOF-MS for mycobacterial identification. *Front. Cell. Infect. Microbiol.* 12, 1079184. doi: 10.3389/fcimb.2022.1079184

Lorente-Leal, V., et al. (2022). MALDI-TOF mass spectrometry as a rapid screening alternative for non-tuberculous mycobacterial species identification in the veterinary laboratory. *Front. Vet. Sci.* 9, 827702. doi: 10.3389/fvets.2022.827702

Mahmoud, K. A., Long, Y., Schatte, G., and Kraatz, H. (2005). Rearrangement of the active ester intermediate during HOBt/EDC amide coupling. *Eur. J. Inorg. Chem.* 2005, 173–180. doi: 10.1002/ejic.200400504

Mukhopadhyay, M., Malviya, J., Barik, A., and Asthana, N. (2024). Assessing the microbial contamination levels in milk samples from rural and urban areas: A focus on raisen and bhopal districts. *Macromol. Symp.* 413, 2300093. doi: 10.1002/masy.202300093

Nieto, K., and Salvetti, A. (2014). AAV vectors vaccines against infectious diseases. *Front. Immunol.* 5, 5. doi: 10.3389/fimmu.2014.00005

Nomura, F., Tsuchida, S., Murata, S., Satoh, M., and Matsushita, K. (2020). Mass spectrometry-based microbiological testing for blood stream infection. *Clin. Proteomics* 17, 1–11. doi: 10.1186/s12014-020-09278-7

Olivares, J., et al. (2013). The intrinsic resistome of bacterial pathogens. *Front. Microbiol.* 4, 103. doi: 10.3389/fmicb.2013.00103

Oviaño, M., et al. (2021). Multicenter evaluation of rapid BACpro® II for the accurate identification of microorganisms directly from blood cultures using MALDI-TOF MS. *Diagnostics* 11, 2251.

Padilla, P. F., Nielsen, K., Ernesto, S. L., and Ling, Y. W. (2010). Diagnosis of brucellosis. *Open Vet. Sci. J.* 4, 46–60. doi: 10.2174/1874318801004010046

Pastrone, L., et al. (2023). Evaluation of two different Preparation protocols for MALDI-TOF MS nontuberculous mycobacteria identification from Liquid and Solid Media. *Microorganisms* 11, 120. doi: 10.3390/microorganisms11010120

Peng, J., Tang, Y.-W., and Xiao, D. (2022). Progress in pathogen identification based on mass spectrometry. *Front. Cell. Infection Microbiol.* 11, 813133. doi: 10.3389/fcimb.2021.813133

Perše, G., et al. (2022). Sepsityper® kit versus in-house method in rapid identification of bacteria from positive blood cultures by MALDI-TOF mass spectrometry. *Life* 12, 1744.

Punyapornwithaya, V., Fox, L. K., Gay, G. M., Hancock, D. D., and Alldredge, J. R. (2009). The effect of centrifugation and resuspension on the recovery of Mycoplasma species from milk. *J. Dairy Sci.* 92, 4444–4447. doi: 10.3168/jds.2009-2182

Qin, S., et al. (2023). Case report: A case of brucellosis misdiagnosed as coronavirus disease 2019/influenza in China. *Front. Public Heal.* 11, 1186800. doi: 10.3389/fpubh.2023.1186800

Rahi, P., and Vaishampayan, P. (2020). MALDI-TOF MS application in microbial ecology studies. *Front. Microbiol.* 10, 2954. doi: 10.3389/fmicb.2019.02954

Ramandi, N. F., et al. (2022). Study of Glutathione S-transferase-P1 in cancer blood plasma after extraction by affinity magnetic nanoparticles and monitoring by MALDI-TOF, IM-Q-TOF and LC-ESI-Q-TOF MS. *J. Chromatogr. B* 1190, 123091.

Sandrin, T. R., and Demirev, P. A. (2018). Characterization of microbial mixtures by mass spectrometry. *Mass Spectrom. Rev.* 37, 321–349. doi: 10.1002/mas.21534

Schaumburg, F., Carrell, C. S., and Henry, C. S. (2019). Rapid bacteria detection at low concentrations using sequential immunomagnetic separation and paper-based isotachophoresis. *Anal. Chem.* 91, 9623–9630. doi: 10.1021/acs.analchem.9b01002

Šebela, M. (2022). Biomolecular profiling by MALDI-TOF mass spectrometry in food and beverage analyses. *Int. J. Mol. Sci.* 23, 13631. doi: 10.3390/ijms232113631

Socas-Rodríguez, B., Herrera-Herrera, A. V., Asensio-Ramos, M., and Rodríguez-Delgado, M.Á. (2020). Recent applications of magnetic nanoparticles in food analysis. *Processes* 8, 1140. doi: 10.3390/pr8091140

Soleimani Mashhadi, I., Safarnejad, M. R., Shahmirzaie, M., Aliahmadi, A., and Ghassempour, A. (2020). Conjugation of single-chain variable fragment antibody to magnetic nanoparticles and screening of fig mosaic virus by MALDI TOF mass spectrometry. *Anal. Chem.* 92, 10460–10469. doi: 10.1021/acs.analchem.0c01119

Svadlakova, T., et al. (2020). Proinflammatory effect of carbon-based nanomaterials: *In vitro* study on stimulation of inflammasome NLRP3 via destabilisation of lysosomes. *Nanomaterials* 10, 418. doi: 10.3390/nano10030418

Takallu, S., et al. (2024). Nanotechnology improves the detection of bacteria: Recent advances and future perspectives. *Heliyon*. doi: 10.1016/j.heliyon.2024.e32020

Tiedje, J. M., et al. (2022). Microbes and climate change: a research prospectus for the future. *MBio* 13, e00800–e00822. doi: 10.1128/mbio.00800-22

Tsuchida, S., and Nakayama, T. (2022). MALDI-based mass spectrometry in clinical testing: Focus on bacterial identification. *Appl. Sci.* 12, 2814. doi: 10.3390/app12062814

Wang, H., et al. (2016). Evaluation of the Bruker Biotyper matrix-assisted laser desorption/ionization time-of-flight mass spectrometry system for identification of clinical and environmental isolates of Burkholderia pseudomallei. *Front. Microbiol.* 7, 415. doi: 10.3389/fmicb.2016.00415

Wang, Y.-C., Lee, Y.-T., Matsuura, K., Liu, X., and Cheng, C.-M. (2022). Detection nanodevices for infectious diseases. *Front. Bioeng. Biotechnol.* 10, 962746. doi: 10.3389/fbioe.2022.962746

Wen, C.-Y., et al. (2017). Efficient enrichment and analyses of bacteria at ultralow concentration with quick-response magnetic nanospheres. *ACS Appl. Mater. Interfaces* 9, 9416–9425. doi: 10.1021/acsami.6b16831

Xiao, F., et al. (2022). Rapid enrichment and detection of Staphylococcus aureus in milk using polyethyleneimine functionalized magnetic nanoparticles. *Microchem. J.* 178, 107388. doi: 10.1016/j.microc.2022.107388

Xu, C., Akakuru, O. U., Zheng, J., and Wu, A. (2019). Applications of iron oxide-based magnetic nanoparticles in the diagnosis and treatment of bacterial infections. *Front. Bioeng. Biotechnol.* 7, 141. doi: 10.3389/fbioe.2019.00141

Yagupsky, P., Morata, P., and Colmenero, J. D. (2019). Laboratory diagnosis of human brucellosis. *Clin. Microbiol. Rev.* 33, 10–1128. doi: 10.1128/CMR.00073-19

Yang, Y., Lin, Y., and Qiao, L. (2018). Direct MALDI-TOF MS identification of bacterial mixtures. *Anal. Chem.* 90, 10400–10408. doi: 10.1021/acs.analchem.8b02258

Zhang, X., Zhang, D., Zhang, X., and Zhang, X. (2024). Artificial intelligence applications in the diagnosis and treatment of bacterial infections. *Front. Microbiol.* 15, 1449844. doi: 10.3389/fmicb.2024.1449844

Zia, S., and Alkheraije, K. A. (2023). Recent trends in the use of bacteriophages as replacement of antimicrobials against food-animal pathogens. *Front. Vet. Sci.* 10, 1162465. doi: 10.3389/fvets.2023.1162465

frontiers | Frontiers in Cellular and Infection Microbiology

TYPE Original Research
PUBLISHED 06 February 2025
DOI 10.3389/fcimb.2025.1517046

OPEN ACCESS

EDITED BY
Ariadna Petronela Fildan,
Ovidius University, Romania

REVIEWED BY
Harry P. De Koning,
University of Glasgow, United Kingdom
Sreenivas Gannavaram,
United States Food and Drug Administration, United States

*CORRESPONDENCE
Xudong Wei
xudongwei@zzu.edu.cn

RECEIVED 25 October 2024
ACCEPTED 13 January 2025
PUBLISHED 06 February 2025

CITATION
Zhao R, He G, Xiang L, Ji M, He R and Wei X (2025) Metagenomic next-generation sequencing assists in the diagnosis of visceral leishmaniasis in non-endemic areas of China. *Front. Cell. Infect. Microbiol.* 15:1517046. doi: 10.3389/fcimb.2025.1517046

Metagenomic next-generation sequencing assists in the diagnosis of visceral leishmaniasis in non-endemic areas of China

Rui Zhao[1], Guilun He[2], Lin Xiang[2], Melinda Ji[3], Rongheng He[1] and Xudong Wei[1]*

[1]Department of Hematopathy, Henan Institute of Hematology, Cancer Hospital Affiliated to Zhengzhou University, Zhengzhou, Henan, China, [2]Science and Technology Service Center, Nanjing Practice Medicine Diagnostics CO., Ltd., Nanjing, Jiangsu, China, [3]Department of Translational Research and Cellular Therapeutics, City of Hope, Duarte, CA, United States

Introduction: Leishmaniasis, a protozoan disease caused by infection by *Leishmania*, is a critical issue in Asia, South America, East Africa, and North Africa. With 12 million cases globally, leishmaniasis is one of the most serious neglected tropical diseases worldwide. Direct identification of infected tissues is currently the primary method of diagnosis; however, the low sensitivity and inconvenience of microscopic examination in detecting amastigotes, parasitic manifestations of *Leishmania*, leads to the possibility of misdiagnosis, delayed diagnosis, and underdiagnosis.

Methods: With the development of metagenomic nextgeneration sequencing (mNGS) technology for pathogen identification, it is possible to detect specific nucleic acid sequences characteristic of *Leishmania* parasites, which opens new avenues for the more accurate diagnosis of leishmaniasis. In this study, we report two cases of leishmaniasis from Henan Province, China, in which *Leishmania* parasites were identified using mNGS technology, massively expediting diagnosis and treatment.

Results: Our report demonstrates that the mNGS method is applicable to peripheral blood samples (PB), which are far more readily available in clinical settings, in addition to bone marrow aspirate samples (BM), which are traditionally used for diagnosis of visceral leishmaniasis.

Conclusion: Our report validates the efficacy of mNGS technology as a rapid and accurate method of diagnosis for leishmaniasis.

KEYWORDS

metagenomic next-generation sequencing assists, therapy, leishmaniasis, endemic area, clinical diagnosis

Highlights

- In non-endemic areas, Leishmania can be easily misdiagnosed, resulting in delayed treatment of patients, which can even be life-threatening.
- mNGS has great advantages over traditional methods in the early diagnosis of Leishmania.

1 Introduction

Leishmaniasis is a serious protozoan disease that poses a major threat to public health and safety (Hirve et al., 2017).It is characterized by numerous clinical manifestations, which vary based on the host immune reaction and infecting species (Maxfield and Crane, 2024). Zoonotic leishmaniasis most commonly involves phlebotomine sandfly vectors and can be spread from dogs, rodents, hyraxes, and bats to humans (Grevelink and Lerner, 1996; Gebremichael, 2018).

Around 50,000 to 90,000 new cases of visceral leishmaniasis, also known as kala-azar, arise each year, with 90% occurring in rural, impoverished areas throughout Africa and South Asia. However, the global incidence of VL is likely significantly higher, as only an estimated 25% to 45% of total cases are reported (Hirve et al., 2017). If left untreated, over 95% of visceral leishmaniasis (VL) cases are ultimately fatal (Grevelink and Lerner, 1996). Additionally, VL is frequently concurrent with HIV and overlaps significantly in geographical range (Lindoso et al., 2016).

As untimely diagnosis and treatment may result in patient mortality (Alves et al., 2018), ensuring a timely diagnosis and appropriate treatment is crucial for patient health, especially in non-endemic areas (Zhou et al., 2020). In clinical practice, microscopic examination based on the detection of amastigotes, serological tests utilizing enzyme-linked immunosorbent assays (ELISA) to detect anti-*Leishmania* IgG antibodies, and molecular analyses using polymerase chain reaction (PCR) to amplify minute concentrations of *Leishmania*-derived nucleic acids are commonly used methods to diagnose leishmaniasis (Welearegay et al., 2018). However, traditional pathogen detection methods exhibit limited sensitivity and specificity. Serological tests, which are generally more sensitive to visceral leishmaniasis than cutaneous or mucosal leishmaniasis, demonstrate very low sensitivity in diagnosing leishmaniasis-HIV coinfections (Lindoso et al., 2016; De Avelar et al., 2023). Furthermore, while PCR-based nucleic acid amplification is a highly sensitive diagnostic tool for the detection of *Leishmania* (Coulborn et al., 2018). Moreover, detection of multiple species distinctly and concurrently requires multiplex PCR assays, and designing a single PCR cycling protocol to suit each primer pair can present assay constraints (De Brito et al., 2020; De Avelar et al., 2023).

In recent years, metagenomic next-generation sequencing (mNGS) technology has undergone rapid development. In comparison to PCR, mNGS is hypothesis-free and untargeted while exhibiting comparably high sensitivity and a rapid turn-around time (Pallen, 2014). Additionally, mNGS demonstrates significantly higher sensitivity during the early stages of infection than serological assays, circumvents the low accuracy of serological tests when immunodeficiencies are present, and is a considerably more consistent, reliable approach than direct microscopic examination (Chen et al., 2020; Han et al., 2022). Therefore, mNGS offers major advantages over conventional methods in the diagnosis of infectious diseases (Chen et al., 2022; Diao et al., 2022).

In this report, we illustrate the significant role of mNGS in enabling the rapid diagnosis of leishmaniasis through two case reports of misdiagnoses and mistreatment in non-endemic areas. Furthermore, we validate the use of PB, which are considerably easier and far safer to obtain than splenic or BM, for diagnosing leishmaniasis with the mNGS method.

2 Materials and methods

Clinical samples for mNGS were obtained from the blood and bronchoalveolar lavage fluid (BALF) of patient 1. BALF was isolated by instilling saline into a pulmonary subsegment, then suctioning and collecting the lavage fluid using a bronchoscope. To isolate the plasma, patient 1's PB were centrifuged at 2100 g for a duration of 5 minutes. For patient 2, blood and BM were drawn, from which mononucleate cells were isolated and stored prior to DNA extraction.

After collecting and processing the clinical samples, the mNGS process was performed as described subsequently. Sterile deionized water was used in addition to clinical samples as a negative control. After vortexing the samples for 5 minutes with 0.5-mm glass beads (1 g) to lyse cells, complete genomic DNA was extracted from these samples using the TIANamp Micro DNA Kit (DP316, TIANGEN Biotech, Beijing, China) according to the manufacturer's protocol. Extracted DNA was then sonicated to yield smaller 250-300 bp fragments, as the method followed uses a short-read, shotgun sequencing approach. The concentration and purity of the extracted genomic DNA were assessed using the Qubit and Nanodrop techniques, while the degradation level of genomic DNA was evaluated through 0.8% agarose gel electrophoresis and Agilent 4200 Bioanalyzer (Agilent Technologies Inc.). Qualified single-end DNA libraries were then prepared using the One Shot DNA Library Prep Kit (PDM602, Nanjing Practice Medicine Diagnostics. Co., Ltd., Nanjing, China) and subjected to quality control assessment via an Agilent 2100 biological fragment analyzer. DNA nanoballs (DNBs) were then prepared from amplified single-stranded circular DNA and loaded onto a sequencing chip for high-throughput sequencing using the MGISEQ-200 gene sequencer.

Following sequencing, raw reads were first filtered by removing low-quality reads (PHRED < 20), reads with read-through adapters, reads with multiple uncalled bases (N's > 2), and short reads (length < 35 bp) using the fastp algorithm (Chen et al., 2018). After adapter trimming and read filtration, low entropy and low-complexity reads consisting mostly of repeats were removed with PRINSEQ software (Schmieder and Edwards, 2011). To account for host-contamination, reads passing quality filters were aligned to the human reference genome (hg38) using Burrows-Wheeler alignment with default parameters inputted into algorithm BWA-MEM

(Li and Durbin, 2010). Any single-end reads not mapped to the human genome were then extracted as non-host reads and were used for taxonomic classification. The microbial genome repository used in pathogen identification was synthesized from several public databases: FDA-ARGOS, BV-BRC (version 3.28.9), EuPathDB (Release 52) and NCBI Genbank (Release 242). When constructing the pathogen reference database, only typical representative genomes were retained from the repositories to mitigate redundancy, yielding a final total of 28,516 bacterial, 8,046 viral, 2,076 fungal, and 429 parasitic taxa. Subsequently, the previously extracted non-host reads were aligned to the pathogen reference database, with parameter '-Y -h 1000' inputted into the BWA-MEM algorithm. A mapping quality threshold of 10 was used, to account for the issue of false positives when using BWA [https://www.ncbi.nlm.nih.gov/pmc/articles/PMC2705234/]. The species-specific read number (SSRN) of each species was calculated based on uniquely mapped reads, while multi-mapping reads were assigned to the genus-specific taxon using the lowest common ancestor annotation (LCA) strategy (Huson et al., 2007). The accuracy of classification was further validated using the NCBI BLAST method based on the NR/NT library, in which confirmation was achieved when the BLAST hit with the lowest E-value corresponded to the previously identified target taxon (Johnson et al., 2008).

3 Results

Two Chinese patients were admitted to the Cancer hospital of Affiliated to Zhengzhou University, assessed via mNGS analysis, were ultimately diagnosed with visceral leishmaniasis (Table 1). mNGS was performed on PB and bronchoalveolar lavage fluid from patient 1, and PB and BM from patient 2. The patients' medical records are summarized below.

3.1 Case 1

A 60-year-old Chinese male patient with intermittent fevers lasting for more than four months was admitted to the Cancer hospital of Affiliated to Zhengzhou University on December 1st, 2022. Throughout the four-month period, the patient experienced unexplained fevers with a peak temperature of 38.1°C, headaches, lower back pain, acid reflux, and heartburn. No other forms of discomfort, including abdominal pain, diarrhea, black stools, and hematemesis, were reported. On August 21, 2022, the patient went to a local hospital where laboratory test results yielded abnormal values: white blood cell (WBC) count, 1.96×10^9/L (normal range, $[4.0\text{-}10]\times10^9$/L); red blood cell (RBC) count of 3.31×10^{12}/L (normal range, $[4.0\text{-}5.0]\times10^{12}$/L); hemoglobin (HB) level of 90g/L (normal range, [120-160] g/L); platelet (PLT) count of 37×10^9/L (normal range, $[100\text{-}300]\times10^9$/L) and ferritin level of 1166 ng/ml (normal range, [40-300] ng/ml). Microscopic examination of the BM showed active hyperplastic bone marrow morphology. The bone marrow biopsy, which revealed a large number of megakaryocytes, suggested hypoplastic anemia. Pleural effusion visible in the chest computed tomography (CT) scan indicated a pulmonary infection (Figure 1), which was supported by mNGS analysis revealing *Leishmania* sequences in BALF samples. The patient was diagnosed with hemophagocytic lymphohistiocytosis (HLH), occasional sinus pauses with atrial fibrillation, and a pulmonary infection.

On December 4th, 2022, HLH-04 protocol was used to treat the patient, but symptoms did not improve. Pathogen metagenomics test results on the patient's blood and bronchoalveolar lavage fluid (BALF) indicated infections with *Klebsiella pneumoniae*, *Aspergillus fumigatus*, cytomegalovirus (CMV), and *Leishmania* parasites (Table 2, Figures 2A, B). However, due to the rarity of the disease in the area and relatively low sequence detection, the patient was not diagnosed with leishmaniasis despite mNGS yielding *Leishmania*-positive results. During hospitalization, the patient was given intravenous imipenem-cilastatin, intravenous capreomycin, intravenous tigecycline, and intravenous ganciclovir to ameliorate infection, but the patient's condition continued to worsen and platelet counts remained low. In order to quickly identify the cause of the disease, an mNGS test was conducted again two weeks later. Results on the patient's blood and sputum indicated an infection with *Leishmania* parasites once again, and the number of *Leishmania*-derived sequences detected in the blood had increased from 277 in the initial reading to 1045 (Table 2, Figures 2C, D). As a result, clinical treatment included therapy specifically targeting *Leishmania* parasites in addition to the original plan. After a four-week period in which the patient underwent daily treatment with sodium stibogluconate, administered via intravenous injection at a standard dose of 20 mg/kg, the patient's symptoms improved. Treatment efficacy was determined based on elimination of fever, pulmonary infection, and return of blood counts to their normal ranges.

TABLE 1 Summary of patient clinical characteristics.

Patient No./Sex/ Age/Ethnicity	Final Diagnosis	Family History	Clinical Symptoms	Travel/Residence in Endemic Area
No. 1/Male/60/Chinese	Visceral leishmaniasis	Normal	Recurrent fevers, pancytopenia, high ferritin, pulmonary infection, atrial fibrillation	None
No.2/Female/10/Chinese	Visceral leishmaniasis	Normal	Recurrent fever, coarse lung texture, splenomegaly	Previous residence in mountainous area with sporadic VL occurrences

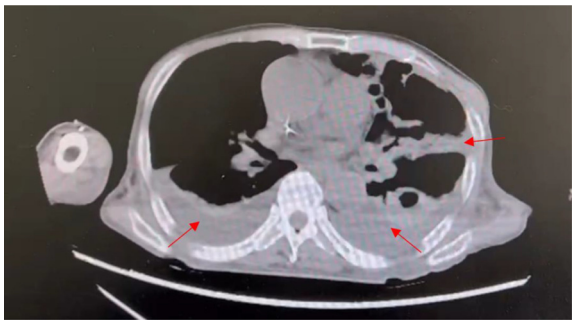

FIGURE 1
Transverse section from chest CT scan of patient 1 showing pleural effusion, hyperdense regions surrounding the lungs, as indicated by the arrows. Pleural effusion is characteristic of pulmonary infection.

3.2 Case 2

A 10-year-old Chinese female patient with intermittent fevers lasting for more than 2 months was admitted to the Cancer hospital of Affiliated to Zhengzhou University on December 31, 2022. During the two-month period, the patient had experienced frequent high fevers with a maximum temperature of 39.5°C, and a routine blood examination on October 30, 2022 yielded a WBC count of 1.52×10^9/L (normal range, $[4.0\text{-}10.0]\times10^9$/L), HB level of 75 g/L (normal range, [120-160] g/L), PLT count of 41×10^9/L (normal range, $[100\text{-}300]\times10^9$/L), and ferritin level of 4180 ng/ml (normal range, [40-300] ng/ml). The concentration of triglycerides in the patient's bloodstream was determined to be 3.10 mmol/L (normal range, [0.45~1.69 mmol/L]), and an NKA assay measured natural killer cell activity to be 17.54% of lymphocytes (normal

TABLE 2 Summary of mNGS results of patient 1.

Sample Type	Date of Testing	Pathogen Detected	Pathogen Category	Relative Abundance	Total Reads	RPM
PB	2022/12/29	*Klebsiella pneumoniae*	B:G-	5.38%	87	2.00
		Aspergillus flavus	F	2.17%	1	0.02
		Human betaherpesvirus 5	V:DNA	42.86%	3	0.07
		Leishmania infantum	Parasites	**16.88%**	**277**	**6.37**
		Leishmania donovani	Parasites	**1.58%**	**26**	**0.60**
BALF	2022/12/29	*Klebsiella pneumoniae*	B:G-	6.19%	81	1.83
		Aspergillus fumigatus	F	22.37%	17	0.38
		Aspergillus flavus	F	14.47%	11	0.25
		Human betaherpesvirus 5	V:DNA	100.00%	5	0.11
		Leishmania infantum	Parasites	**16.53%**	**143**	**3.23**
		Leishmania donovani	Parasites	**0.58%**	**5**	**0.11**
PB	2023/1/11	*Aspergillus fumigatus*	F	16.31%	38	1.26
		Aspergillus flavus	F	3.00%	7	0.23
		Aspergillus niger	F	1.72%	4	0.13
		Human betaherpesvirus 5	V:DNA	94.15%	483	16.04
		Torque teno virus	V:DNA	2.85%	15	0.50
		Leishmania infantum	Parasites	**16.93%**	**1045**	**34.70**
		Leishmania donovani	Parasites	**2.85%**	**176**	**5.84**
Sputum	2023/1/11	*Enterococcus faecium*	B:G+	0.08%	346	11.49
		Candida lusitaniae	F	85.69%	497	16.50
		Aspergillus fumigatus	F	2.59%	15	0.50
		Epstein-Barr virus	V:DNA	48.11%	102	3.39
		Human betaherpesvirus 7	V:DNA	32.55%	69	2.29
		Human betaherpesvirus 5	V:DNA	16.51%	35	1.16
		Leishmania infantum	Parasites	**16.19%**	**102**	**3.39**
		Leishmania donovani	Parasites	**0.95%**	**6**	**0.20**

PB: peripheral blood sample, BALF: bronchoalveolar lavage fluid, B:G+: gram-positive bacteria, B:G-: gram-negative bacteria, F: fungal DNA, V:DNA: viral DNA, RPM: reads per million mapped reads.
Two changes in the number of sequences of leishmania infection were highlighted in bold.

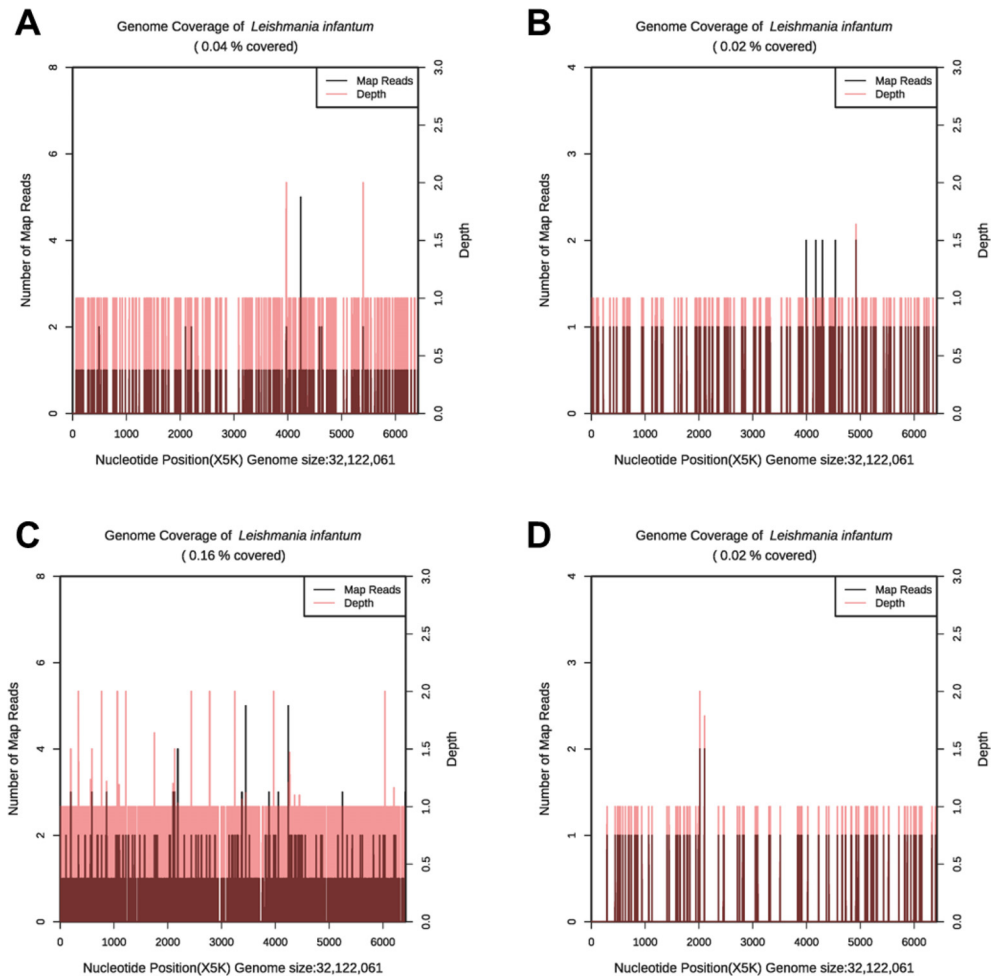

FIGURE 2
The genome coverage map of *Leishmania infantum* as detected by mNGS in case 1. In the first mNGS test, genome coverage of *Leishmania infantum* in the PB sample was 0.04% **(A)** and 0.02% in BALF **(B)**. In the second mNGS test, the genome coverage of *Leishmania infantum* in the PB sample was 0.16% **(C)** and 0.02% in sputum **(D)**.

range, [4.1-17.3%]). The anti-nuclear antibody spectrum (IHF) test result was positive (+), indicating a potential autoimmune response. Analysis of bone marrow puncture aspirate yielded normal results. Color doppler ultrasound indicated splenomegaly. The patient was ultimately diagnosed with hemophagocytic syndrome (HPS). On November 5, 2022, following the HLH-2018 protocol of Chinese Children's Histiocytic Group (CCHG-HLH-2018), the patient began treatment with methylprednisolone (10 mg/kg) and ruxolitinib (10 mg q12h po.). Two days later, her body temperature returned to normal. However, on December 24, 2022, the patient's fever returned at a temperature of 40.0°C. A follow-up routine blood examination supplemented with a C-reactive protein (CRP) test showed a WBC count of 3.27×10^9/L, HB level of 105 g/L, PLT count of 85×10^9/L, and CRP level of 133.74 mg/L. A chest CT indicated a coarse lung texture and splenomegaly. The previously prescribed treatment method failed to improve the patient's fever, suggesting that the patient may have had an infection of another origin.

On January 2, 2023, bone marrow and peripheral blood samples were collected and subjected to mNGS. Additionally, a bone marrow sample originating from the same sample used for mNGS was collected and placed under microscopic examination. Result revealed reticular cells, hemophagocytosis and *Leishmania* amastigotes (Figures 3A–D), indicating a potential *Leishmania* infection. Consistent with these results, the mNGS results of BM sample showed that *Leishmania*-positive sequences were detected at a high relative abundance of 99.52% (Table 3, Figure 4). The patient had no abnormal medical or family history, but had previously resided in a mountainous region where sporadic leishmaniasis had previously occurred. The patient was consequently diagnosed with leishmaniasis, and the clinical treatment strategy was adjusted promptly to include daily intravenous injections of sodium stibogluconate (20 mg/kg), leading symptoms to ultimately improve. Two weeks following treatment, microscopic examination of BM revealed no signs of infection. Treatment efficacy was further confirmed based on elimination of fever and return of blood counts to their normal ranges.

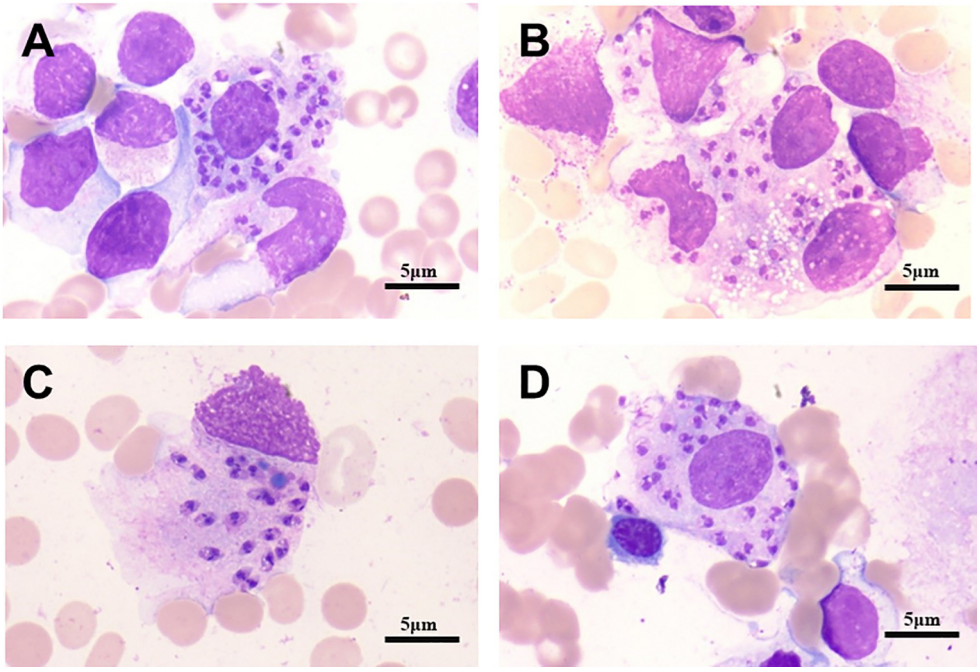

FIGURE 3
Bone marrow micrographs from patient 2. Active bone marrow hyperplasia, reticular cells, hemophagocytosis and Leishmania amastigotes, as indicated by the arrows, can be seen. **(A)** Macrophages contain numerous Leishman-Donovan bodies. **(B)** Leishman-Donovan body infect more circulating or fixed macrophages. **(C)** The macrophage dies, Leishman-Donovan body are released. **(D)** Macrophages engulf a large number of lydosomes. Cells visualized with H&E stain, 100X magnification. Scale bar represents 5 μm.

4 Discussion

Visceral leishmaniasis (VL) was once prevalent in the eastern and central regions of China, with the first reported case of leishmaniasis occurring in 1904. The Henan province, in particular, was once highly endemic for both human and canine visceral leishmaniasis (Yang et al., 2023). However, with the onset of active large-scale prevention and control efforts, the incidence of leishmaniasis in China has decreased annually. According to data published in 2011, the incidence rate of leishmaniasis has decreased to 0.03/100,000 (Guan and Wu, 2014; Lun et al., 2015). Extensive eradication efforts throughout the late 1900s accordingly reduced the incidence of leishmaniasis in Henan. However, beginning in 2016, there has been an upsurge in sporadic cases of local visceral leishmaniasis infections in Henan, with around four cases reported throughout the province each year (Cheng, 2023; Yang et al., 2023).

Based on the species and epidemiological characteristics, visceral leishmaniasis in China is mainly classified into three types: anthroponotic VL (AVL), mountain-type zoonotic VL (MT-ZVL), and desert-type ZVL (DT-ZVL). Research has shown that the average incubation period of visceral leishmaniasis is 3-8 months (Gramiccia et al., 2013; Adamczick et al., 2018). In addition, the clinical symptoms of visceral leishmaniasis such as fever, splenomegaly, and pancytopenia are extensive and overlap with other severe microbial infections, blood diseases, and autoimmune diseases, increasing the difficulty of clinical diagnosis. Furthermore, because of the rarity of the disease in non-endemic areas, underdiagnosis is even more frequent in geographic regions with low incidence (Song et al., 2021).

In this report, both patients developed the disease in the winter without a recent history of travel to endemic areas. Patient 1 had been admitted to another hospital for nearly 3 months, where he had been treated with multiple antibiotics without success. After being transferred to the Cancer hospital of Affiliated to Zhengzhou University, although *Leishmania*-specific sequences were reported in both the peripheral blood and bronchoalveolar lavage fluid in the first mNGS examination, it did not receive significant clinical

TABLE 3 Summary of mNGS results of patient 2.

Sample Type	Date of Testing	Pathogen Detected	Pathogen Category	Relative Abundance	Total Reads	RPM
PB	2023/1/2	*Leishmania infantum*	Parasites	99.49%	15757	650.26
		Leishmania donovani	Parasites	0.51%	80	3.30
BM	2023/1/2	*Leishmania infantum*	Parasites	99.52%	20464	844.51
		Leishmania donovani	Parasites	0.48%	98	4.04

PB: peripheral blood sample, BM: bone marrow aspirate, RPM: reads per million mapped reads.

attention because *Leishmania*-positive reads appeared to be relatively low and *Klebsiella pneumoniae*, *Aspergillus fumigatus*, and cytomegalovirus were concurrently present. It was not until the second mNGS examination of peripheral blood and sputum samples, which revealed an increase in the number of *Leishmania*-positive sequences, that the infection began to be taken seriously. Patient 2 was transferred to the Cancer hospital of Affiliated to Zhengzhou University after ineffective treatment for 2 months at another hospital, where *Leishmania* amastigotes seen in the bone marrow smear suggested leishmaniasis. Both bone marrow and PB from mNGS indicated *Leishmania* infection, and anti-*Leishmania* treatment with sodium stibogluconate was effective.

From the time of initial consultation to the final diagnosis of leishmaniasis, case 1 lasted a total of four and a half months, while case 2 lasted two and a half months. Both cases were initially misdiagnosed as hemophagocytic syndrome and accordingly given chemotherapy to alleviate fever and pancytopenia, causing unnecessary physical, mental, and financial losses to the patients. The considerable delay in diagnosis indicates that traditional diagnostic methods are urgently lacking in reliability, sensitivity, and speed when applied to rare, relapsing infections such as leishmaniasis. Delays are present even in leishmaniasis-endemic areas (Vasconcelos et al., 2024). On average, patients had to visit seven medical services before obtaining an accurate diagnosis (Luz et al., 2019). In non-endemic areas such as the UK, the median time before diagnosis is as long as 6 months (Fletcher et al., 2015). Currently, the clinical diagnosis of visceral leishmaniasis is relatively difficult, with statistical data showing a misdiagnosis rate of around 84.2% (Mondal et al., 2010; Copeland and Aronson, 2015). In case 1 of this report, *Leishmania*-positive reads were initially disregarded despite significantly exceeding the threshold established by Miller et al. for pathogen positivity (10 reads per million) (Miller et al., 2019). Furthermore, for parasites specifically, a stringent-mapped read number (SMRN) of greater than 100 (initial case 1 SMRN of 277) is clinically significant. Because of the rarity of leishmaniasis, especially in a non-endemic area, the possibility of VL was not taken seriously, which contributed to delays in diagnosis and treatment (Diro et al., 2018). Therefore, to ensure an early and accurate diagnosis, mNGS testing should be performed on patients with long-term, re-occurring fevers, abnormal blood counts, and poor responses to previous antimicrobial treatments. If mNGS yields *Leishmania*-positive results, the possibility of leishmaniasis should be considered, and further PCR investigations for different subtypes should be completed.

In recent years, there has been an increase in the use of mNGS to detect *Leishmania* infection (Vogt et al., 2018; Guo et al., 2020; Lin et al., 2021; Gao et al., 2022; Zhang et al., 2022; Chang et al., 2023; Liang et al., 2023).

This report further substantiates the use of mNGS in clinical practice, as it can not only detect *Leishmania* parasites in BM (Chen et al., 2020) but can also be used to test PB, which are significantly more readily obtained. Both patient cases provide incremental evidence of the value of mNGS in detecting specific *Leishmania*-positive sequences from PB, as mentioned previously by Han et al (Han et al., 2022). This further validates the use of PB in identifying leishmaniasis with mNGS, considerably expediting both the sampling and diagnosis process. Interestingly, in the detection results of case 2, we found that the genome coverage map of *Leishmania infantum* (Figure 4) may indicate that Chromosome 31 of *Leishmania infantum* in uncultured clinical samples is tetraploid (4 copies), while other chromosomes tend to be diploid (Extended Data Supplementary Figure S1). These results demonstrate that the mNGS method can identify the copy number of some chromosomes of pathogens, providing a reference for related research (Domagalska et al., 2019; Reis-Cunha et al., 2024).

Research shows that when screening for pathogens in patients with concurrent immunodeficiency syndromes, bloodstream infections, respiratory infections, or general infections, mNGS has a wide detection range and is suitable for discovering unknown pathogens or co-infections with multiple pathogens (Jiang et al).In particular, HIV-*Leishmania* co-infections are frequent and associated with higher fatality rates, but are often difficult to diagnose. As a result of immunosuppression caused concurrently by HIV and *Leishmania* (Da-Cruz et al., 2006), serology assays relying on host-produced immune factors for diagnosis, such as ELISA assays detecting anti-

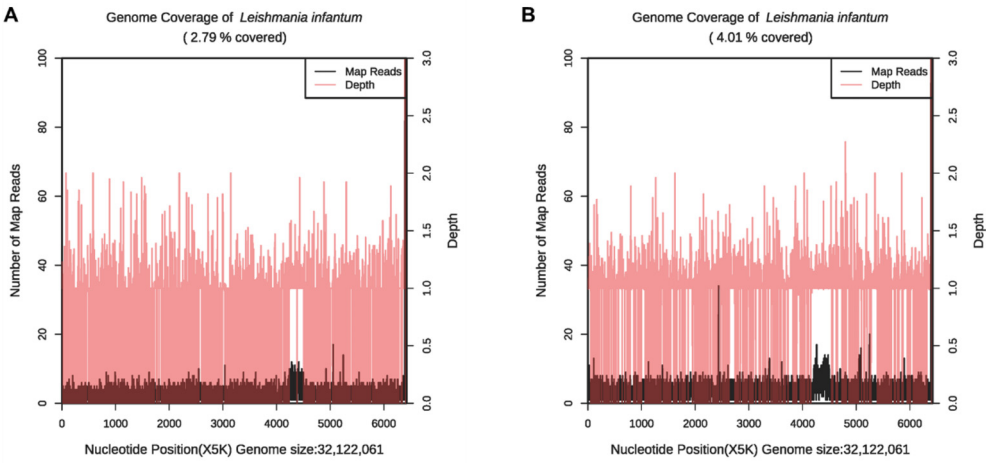

FIGURE 4
The genome coverage map of *Leishmania infantum* as detected by mNGS in case 2. The genome coverage of *Leishmania infantum* in the PB sample was 2.79% **(A)** and 4.01% in BM **(B)**.

Leishmania IgG, are virtually ineffective. Rapid immunoassays detecting rK39 antigens are also rendered ineffective (Lindoso et al., 2018). mNGS does not rely on the host's immune status or antibody production. In contrast, delayed-type hypersensitivity (DTH) requires the host to have a certain immune competence, and DTH may produce false-negative results in immunosuppressed or immunodeficient individuals (Gow et al., 2022). A comparison of mNGS and DTH responses after antigen vaccination in the diagnosis of *Leishmania* is shown in Supplementary Materials Table 1. mNGS, however, has been previously demonstrated by Tang et al. to be a reliable means of detection, even when leishmaniasis is concurrent with HIV (Tang et al., 2022). In addition, mNGS is not dependent on specific targets, as opposed to targeted molecular methods such as PCR. Most notably, unbiased sampling allows for the unbiased detection of a far broader range of rare, low-level infections and co-infections, rather than quantifying only pre-specified pathogenic sequences. Furthermore, mNGS can theoretically not only identify known pathogens, but also recognize unknown pathogens and potentially even reveal novel pathogens (Han et al., 2019; Zhang et al., 2020). Of course, the sensitivity of PCR in detecting Leishmania in acute VL has been repeatedly demonstrated, so mNGS should be promptly selected as an auxiliary test when multiple previous treatments have failed and the pathogen has not been identified (Chen et al., 2022). Additionally, in a previous case study conducted by Chen et al., peripheral plasma samples yielded zero *Leishmania*-positive reads while BM yielded a 99.6% relative abundance of *Leishmania* (Chen et al., 2020), indicating that blood samples may not always be a reliable predictor of visceral leishmaniasis. The use of blood samples alone in mNGS thus requires further investigation.

Considering the limited number of cases discussed in this report, this study has certain limitations. In the case of patient 1, other diseases were present in addition to leishmaniasis, which could pose potential confounding variables. Because only two cases have been presented, the findings described in this study may not be generalizable to all visceral leishmaniasis cases, as the prognosis of VL may vary depending on factors including comorbidities, geographic region, mode of transmission, primary infecting species, and patient characteristics. Moreover, the follow-up time for patients was not long enough to provide significant post-treatment clinical insights, for instance, regarding the efficacy of treatment strategies in preventing relapse. Regarding case 2, microscopic examination of BM taken two weeks after treatment revealed no signs of infection. Both patients reported no longer experiencing symptoms after a 4-week period and 2-week period for cases 1 and 2, respectively. Patients have been verbally followed up leading up to the present and have reported no recurrence of previous symptoms; however, conclusions cannot be made about the possibility of relapse, as only around 14 months have passed since administration of treatment. Additionally, because the same anti-leishmaniasis treatment (intravenously injected sodium stibogluconate) was administered to both patients, additional research evaluating alternative treatment methods could be beneficial. Further case studies could be valuable in determining the long-term efficacy, potential complications, and patient-specific side effects of alternative therapeutic avenues. Because the relapse rate of leishmaniasis is high, the ability of treatments to ameliorate *Leishmania* infections long-term is an important consideration. Furthermore, personalization of treatment based on genetic markers in the host or the host immune response, both of which can be elucidated by mNGS, can also be explored.

Data availability statement

The original contributions presented in the study are publicly available. This data can be found here: https://www.ncbi.nlm.nih.gov/bioproject/?term=1140367.

Ethics statement

The studies involving humans were approved by Life Science Ethics Committee of Zhengzhou University (No. 2021-KY-0214-001). The studies were conducted in accordance with the local legislation and institutional requirements. Written informed consent for participation in this study was provided by the participants' legal guardians/next of kin. Written informed consent was obtained from the individual(s), and minor(s)' legal guardian/next of kin, for the publication of any potentially identifiable images or data included in this article.

Author contributions

RZ: Conceptualization, Methodology, Writing – original draft. GH: Writing – original draft, Investigation, Validation. LX: Writing – review & editing. MJ: Writing – review & editing, Formal Analysis. RH: Formal Analysis, Writing – review & editing. XW: Funding acquisition, Supervision, Writing – review & editing.

Funding

The author(s) declare financial support was received for the research, authorship, and/or publication of this article. This paper supported by grants from National Natural Science Foundation of China, Grant/Award Number: 82170151; Henan medical science and technology project (232102310201), Henan medical science and technology project (LHGJ20220186).

Acknowledgments

The authors thank the patient and her family.

Conflict of interest

Author GH and LX were employed by the company Nanjing Practice Medicine Diagnostics CO., Ltd.

The remaining authors declare that the research was conducted in the absence of any commercial or financial relationships that could be construed as a potential conflict of interest.

Generative AI statement

The author(s) declare that no Generative AI was used in the creation of this manuscript.

Publisher's note

All claims expressed in this article are solely those of the authors and do not necessarily represent those of their affiliated organizations, or those of the publisher, the editors and the reviewers. Any product that may be evaluated in this article, or claim that may be made by its manufacturer, is not guaranteed or endorsed by the publisher.

Supplementary material

The Supplementary Material for this article can be found online at: https://www.frontiersin.org/articles/10.3389/fcimb.2025.1517046/full#supplementary-material

References

Adamczick, C., Dierig, A., Welzel, T., Schifferli, A., Blum, J., and Ritz, N. (2018). Double trouble: visceral leishmaniasis in twins after traveling to Tuscany–a case report. *BMC Infect. Dis.* 18, 1–5. doi: 10.1186/s12879-018-3394-0

Alves, F., Bilbe, G., Blesson, S., Goyal, V., Monnerat, S., Mowbray, C., et al. (2018). Recent development of visceral leishmaniasis treatments: successes, pitfalls, and perspectives. *Clin. Microbiol. Rev.* 31, e00048–e00018. doi: 10.1128/CMR.00048-18

Chang, L., Che, G., Yang, Q., Lai, S., Teng, J., Duan, J., et al. (2023). Leishmania donovani visceral leishmaniasis diagnosed by metagenomics next-generation sequencing in an infant with acute lymphoblastic leukemia: a case report. *Front. Public Health* 11. doi: 10.3389/fpubh.2023.1197149

Chen, Y., Fan, L. C., Chai, Y. H., and Xu, J. F. (2022). Advantages and challenges of metagenomic sequencing for the diagnosis of pulmonary infectious diseases. *Clin. Respir. J.* 16, 646–656. doi: 10.1111/crj.13538

Chen, H., Fan, C., Gao, H., Yin, Y., Wang, X., Zhang, Y., et al. (2020). Leishmaniasis diagnosis via metagenomic next-generation sequencing. *Front. Cell Infect. Microbiol.* 10. doi: 10.3389/fcimb.2020.528884

Chen, S., Zhou, Y., Chen, Y., and Gu, J. (2018). fastp: an ultra-fast all-in-one FASTQ preprocessor. *Bioinformatics* 34, i884–i890. doi: 10.1093/bioinformatics/bty560

Cheng, Y. (2023). Epidemiological investigation on a visceral leishmaniasis case in Zhengzhou city of Henan province. *Zhongguo Xue Xi Chong Bing Fang Zhi Za Zhi.* 34, 635. doi: 10.16250/j.32.1374.2022048

Copeland, N. K., and Aronson, N. E. (2015). Leishmaniasis: treatment updates and clinical practice guidelines review. *Curr. Opin. Infect. Dis.* 28, 426–437. doi: 10.1097/QCO.0000000000000194

Coulborn, R. M., Gebrehiwot, T. G., Schneider, M., Gerstl, S., Adera, C., Herrero, M., et al. (2018). Barriers to access to visceral leishmaniasis diagnosis and care among seasonal mobile workers in Western Tigray, Northern Ethiopia: A qualitative study. *PLoS Negl. Trop. Dis.* 12, e0006778. doi: 10.1371/journal.pntd.0006778

Da-Cruz, A., Rodrigues, A., Mattos, M., Oliveira-Neto, M. P., Sabbaga-Amato, V., Posada, M. P., et al. (2006). Immunopathological changes in HIV-Leishmania co-infection *Rev Soc Bras Med Trop* 39, 75–79.

De Avelar, D. M., Santos, C. C., and Fusaro Faioli, A. (2023). Developments in Leishmaniasis diagnosis: A patent landscape from 2010 to 2022. *PLoS Glob Public Health* 3, e0002557. doi: 10.1371/journal.pgph.0002557

De Brito, R. C. F., Aguiar-Soares, R. D. D. O., Cardoso, J. M. D. O., Coura-Vital, W., Roatt, B. M., Reis, A. B., et al. (2020). Recent advances and new strategies in Leishmaniasis diagnosis. *Appl. Microbiol. Biotechnol.* 104, 8105–8116. doi: 10.1007/s00253-020-10846-y

Diao, Z., Han, D., Zhang, R., and Li, J. (2022). Metagenomics next-generation sequencing tests take the stage in the diagnosis of lower respiratory tract infections. *J. Adv. Res.* 38, 201–212. doi: 10.1016/j.jare.2021.09.012

Diro, E., Ritmeijer, K., Boelaert, M., Alves, F., Mohammed, R., Abongomera, C., et al. (2018). Long-term clinical outcomes in visceral leishmaniasis/human immunodeficiency virus–coinfected patients during and after pentamidine secondary prophylaxis in Ethiopia: a single-arm clinical trial. *Clin. Infect. Dis.* 66, 444–451. doi: 10.1093/cid/cix807

Domagalska, M. A., Imamura, H., Sanders, M., Van den Broeck, F., Bhattarai, N. R., Vanaerschot, M., et al. (2019). Genomes of Leishmania parasites directly sequenced from patients with visceral leishmaniasis in the Indian subcontinent. *PLoS Negl. Trop. Dis.* 13, e0007900. doi: 10.1371/journal.pntd.0007900

Fletcher, K., Issa, R., and Lockwood, D. (2015). Visceral leishmaniasis and immunocompromise as a risk factor for the development of visceral leishmaniasis: a changing pattern at the hospital for tropical diseases, London. *PLoS One* 10, e0121418. doi: 10.1371/journal.pone.0121418

Gao, H., Wang, J., Zhang, S., and Li, T. (2022). A case report of two kala-azar cases in China diagnosed by metagenomic next-generation sequencing. *Front. Microbiol.* 13. doi: 10.3389/fmicb.2022.922894

Gebremichael, D. (2018). Zoonotic impact and epidemiological changes of leishmaniasis in Ethiopia. *Open Vet. J.* 8, 432–440. doi: 10.4314/ovj.v8i4.13

Gow, I., Smith, N. C., Stark, D., and Ellis, J. (2022). Laboratory diagnostics for human Leishmania infections: a polymerase chain reaction-focussed review of detection and identification methods. *Parasites Vectors* 15, 412. doi: 10.1186/s13071-022-05524-z

Gramiccia, M., Scalone, A., Di Muccio, T., Orsini, S., Fiorentino, E., and Gradoni, L. (2013). The burden of visceral leishmaniasis in Italy from 1982 to 2012: a retrospective analysis of the multi-annual epidemic that occurred from 1989 to 2009. *Euro Surveill.* 18, 20535. doi: 10.2807/1560-7917.ES2013.18.29.20535

Grevelink, S., and Lerner, E. (1996). Leishmaniasis. *J. Am. Acad. Dermatol.* 34, 257–272. doi: 10.1016/s0190-9622(96)80121-6

Guan, L.-R., and Wu, Z.-X. (2014). Historical experience in the elimination of visceral leishmaniasis in the plain region of Eastern and Central China. *Infect. Dis. Poverty* 3, 1–12. doi: 10.1186/2049-9957-3-10

Guo, F., Kang, L., and Xu, M. (2020). A case of pediatric visceral leishmaniasis-related hemophagocytic lymphohistiocytosis diagnosed by mNGS. *Int. J. Infect. Dis.* 97, 27–29. doi: 10.1016/j.ijid.2020.05.056

Han, D., Li, Z., Li, R., Zhang, R., and Li, J. (2019). mNGS in clinical microbiology laboratories: on the road to maturity. *Crit. Rev. Microbiol.* 45, 668–685. doi: 10.1080/1040841X.2019.1681933

Han, N., Yu, J., Wang, M., Ma, Y., Yan, L., and Tang, H. (2022). The value of metagenomic next-generation sequencing in leishmaniasis diagnosis: a case series and literature review. *Open Forum Infect. Dis.* 9, ofac511. doi: 10.1093/ofid/ofac511

Hirve, S., Kroeger, A., Matlashewski, G., Mondal, D., Banjara, M. R., Das, P., et al. (2017). Towards elimination of visceral leishmaniasis in the Indian subcontinent—Translating research to practice to public health. *PLoS Negl Trop Dis*11. doi: 10.1371/journal.pntd.0005889

Huson, D. H., Auch, A. F., Qi, J., and Schuster, S. C. (2007). MEGAN analysis of metagenomic data. *Genome Res.* 17, 377–386. doi: 10.1101/gr.5969107

Jiang, X. W., Liang, Z. K., Zeng, L., et al. Zhonghua yu fang yi xue za zhi [Chinese journal of preventive medicine] 57, 1124–1130. doi: 10.3760/cma.j.cn112150-20220824-00836.

Johnson, M., Zaretskaya, I., Raytselis, Y., Merezhuk, Y., McGinnis, S., and Madden, T. L. (2008). NCBI BLAST: a better web interface. *Nucleic Acids Res.* 36, W5–W9. doi: 10.1093/nar/gkn201

Li, H., and Durbin, R. (2010). Fast and accurate long-read alignment with Burrows–Wheeler transform. *Bioinformatics* 26, 589–595. doi: 10.1093/bioinformatics/btp698

Liang, Q., Liang, X., Hong, D., Fang, Y., Tang, L., Mu, J., et al. (2023). Case report: Application of metagenomic next-generation sequencing in the diagnosis of visceral leishmaniasis and its treatment evaluation. *Front. Med. (Lausanne)* 9. doi: 10.3389/fmed.2022.1044043

Lin, Z.-N., Sun, Y.-C., Wang, J.-P., Lai, Y. L., and Sheng, L. X. (2021). Next-generation sequencing technology for diagnosis and efficacy evaluation of a patient with visceral leishmaniasis: a case report. *World J Clin Cases* 9, 9903. doi: 10.12998/wjcc.v9.i32.9903

Lindoso, J., Cunha, M., Queiroz, I., and Moreira, C. H. (2016). Leishmaniasis-HIV coinfection: current challenges. *HIV AIDS (Auckl)* 8, 147–156. doi: 10.2147/HIV.S93789

Lindoso, J., Moreira, C. H. V., Cunha, M. A., and Queiroz, I. T. (2018). Visceral leishmaniasis and HIV coinfection: current perspectives. *HIV AIDS (Auckl)* 10, 193–201. doi: 10.2147/HIV.S143929

Lun, Z.-R., Wu, M.-S., Chen, Y.-F., Wang, J. Y., Zhou, X. N., Liao, L. F., et al. (2015). Visceral leishmaniasis in China: an endemic disease under control. *Clin. Microbiol. Rev.* 28, 987–1004. doi: 10.1128/CMR.00080-14

Luz, J. G. G., Carvalho, A. G. D., Naves, D. B., Dias, J. V. L., and Fontes, C. J. F. (2019). Where, when, and how the diagnosis of human visceral leishmaniasis is defined:

answers from the Brazilian control program. *Mem Inst Oswaldo Cruz* 114, e190253. doi: 10.1590/0074-02760190253

Maxfield, L., and Crane, J. S. (2024). "Leishmaniasis," in *StatPearls* (StatPearls Publishing Copyright © 2024, StatPearls Publishing LLC, Treasure Island (FL).

Miller, S., Naccache, S. N., Samayoa, E., Messacar, K., Arevalo, S., Federman, S., et al. (2019). Laboratory validation of a clinical metagenomic sequencing assay for pathogen detection in cerebrospinal fluid. *Genome Res.* 29, 831–842. doi: 10.1101/gr.238170.118

Mondal, S., Bhattacharya, P., and Ali, N. (2010). Current diagnosis and treatment of visceral leishmaniasis. *QJM* 8, 919–944. doi: 10.1093/qjmed/hct116

Pallen, M. J. (2014). Diagnostic metagenomics: potential applications to bacterial, viral and parasitic infections. *Parasitology* 141, 1856–1862. doi: 10.1017/S0031182014000134

Reis-Cunha, J. L., Pimenta-Carvalho, S. A., Almeida, L. V., Coqueiro-Dos-Santos, A., Marques, C. A., Black, J. A., et al. (2024). Ancestral aneuploidy and stable chromosomal duplication resulting in differential genome structure and gene expression control in trypanosomatid parasites. *Genome Res.* 34, 441–453. doi: 10.1101/gr.278550.123

Schmieder, R., and Edwards, R. (2011). Quality control and preprocessing of metagenomic datasets. *Bioinformatics* 27, 863–864. doi: 10.1093/bioinformatics/btr026

Song, P., Chen, S., Tan, X., Gao, Y., Fu, J., You, Z., et al. (2021). Metagenomic analysis identifying a rare Leishmania infection in an adult with AIDS. *Front. Cell Infect. Microbiol.* 11. doi: 10.3389/fcimb.2021.764142

Tang, C., He, S., Wang, N., and Chen, L. (2022). A case report and literature review: diagnosis and treatment of human immunodeficiency virus coinfected with visceral leishmania by metagenomic next-generation sequencing in China. *Ann. Transl. Med.* 10 (8), 497. doi: 10.21037/atm-22-1351

Vasconcelos, A. D. O., Bedoya-Pacheco, S. J., Cunha E Silva, R. R., Magalhães, M. A. F. M., de Sá, T. P. S. O., Dias, C. M. G., et al. (2024). Spatial-temporal distribution of visceral leishmaniasis in Rio de Janeiro, Brazil, 2001–2020: expansion and challenges. *Trans. R Soc. Trop. Med. Hyg* 118 (7), 448–457. doi: 10.1093/trstmh/trae009

Vogt, F., Mengesha, B., Asmamaw, H., Mekonnen, T., Fikre, H., Takele, Y., et al. (2018). Antigen detection in urine for noninvasive diagnosis and treatment monitoring of visceral leishmaniasis in human immunodeficiency virus coinfected patients: an exploratory analysis from Ethiopia. *Am. J. Trop. Med. Hyg.* 99, 957–966. doi: 10.4269/ajtmh.18-0042

Welearegay, T. G., Diouani, M. F., ÖSterlund, L., Ionescu, F., Belgacem, K., Smadhi, H., et al. (2018). Ligand-capped ultrapure metal nanoparticle sensors for the detection of cutaneous leishmaniasis disease in exhaled breath. *ACS sens* 3, 2532–2540. doi: 10.1021/acssensors.8b00759

Yang, C., Li, S., Lu, D., He, Z., Wang, D., Qian, D., et al. (2023). Reemergence of visceral leishmaniasis in Henan province. *China Trop. Med. Infect. Dis.* 8, 318. doi: 10.3390/tropicalmed8060318

Zhang, X., Liu, Y., Zhang, M., Wang, Z., Feng, X., Yang, L., et al. (2022). Case report: Diagnosis of visceral leishmaniasis using metagenomic next-generation sequencing and bone marrow smear. *Front. Cell Infect. Microbiol.* 12. doi: 10.3389/fcimb.2022.1095072

Zhang, H. C., Zhang, Q. R., Ai, J. W., Cui, P., Wu, H. L., Zhang, W. H., et al. (2020). The role of bone marrow metagenomics next-generation sequencing to differential diagnosis among visceral leishmaniasis, histoplasmosis, and talaromycosis marneffei. *Int. J. Lab. Hematol.* 42 (2), e52–e54. doi: 10.1111/ijlh.13103

Zhou, Z., Lyu, S., Zhang, Y., Li, Y., Li, S., Zhou, X. N., et al. (2020). Visceral leishmaniasis—China, 2015– 2019. *China CDC Wkly* 2, 625–628. doi: 10.46234/ccdcw2020.173

frontiers | Frontiers in Cellular and Infection Microbiology

TYPE Original Research
PUBLISHED 10 February 2025
DOI 10.3389/fcimb.2025.1534268

OPEN ACCESS

EDITED BY
Ariadna Petronela Fildan,
Ovidius University, Romania

REVIEWED BY
Nathan Mugenyi,
Mbarara University of Science and Technology, Uganda
Nagwan El Menofy,
Al-Azhar University, Egypt
Niyam Dave,
Indian Institute of Science (IISc), India
Dan Zhang,
Zhejiang University, China

*CORRESPONDENCE
Yaping Jiang
18092735535@163.com

RECEIVED 25 November 2024
ACCEPTED 20 January 2025
PUBLISHED 10 February 2025

CITATION
Wang Z, Zou Y, Wei Z, Bai G, Wang X, Qu S, Shi J, Jiang Y and Gu C (2025) Analytical and clinical validation of a novel MeltPlus TB-NTM/RIF platform for simultaneous detection of *Mycobacterium tuberculosis complex*, *Non-Tuberculous Mycobacteria* and rifampicin resistance.
Front. Cell. Infect. Microbiol. 15:1534268.
doi: 10.3389/fcimb.2025.1534268

Analytical and clinical validation of a novel MeltPlus TB-NTM/RIF platform for simultaneous detection of *Mycobacterium tuberculosis complex*, *Non-Tuberculous Mycobacteria* and rifampicin resistance

Zhuo Wang[1], Yuanwu Zou[1], Zihan Wei[2], Guanghong Bai[1], Xiaolin Wang[1], Shaoyi Qu[1], Jie Shi[1], Yaping Jiang[3]* and Cuijiao Gu[1]

[1]Department of Clinical Laboratory, Shaanxi Provincial Hospital of Tuberculosis Prevention and Treatment Hospital, Xian, China, [2]Department of Clinical Laboratory, Shaanxi Provincial People's Hospital, Xian, China, [3]Department of Clinical Laboratory, Xi'an No.3 Hospital, The Affiliated Hospital of Northwest University, Xian, China

Background: Rapid and accurate diagnosis of tuberculosis, particularly rifampin (RIF)-resistant tuberculosis (RR-TB) and *Non-Tuberculous Mycobacteria* (NTM), is essential for implementing appropriate proper therapy to benefit patients and improve TB/NTM patient management.

Methods: In this study, we developed a novel MeltPlus MTB-NTM/RIF platform, designed to simultaneously detect *Mycobacterium tuberculosis complex* (MTBC), NTM and RIF resistance. The platform was evaluated for its limit of detection (LOD) and specificity before clinical validation, followed by a prospective single-center study in patients with presumptive TB cases.

Results: The calculated LOD for MTBC, NTM and RIF susceptibility was found to be 10.31 CFU/mL, 57.55 CFU/mL and 48.584 CFU/mL, respectively. The assay showed a sensitivity of 98.76% (95% CI: 96.41-99.74%) and a specificity of 94.42% (95% CI: 90.82-96.92%) for MTBC detection compared to the bacteriological TB standard. For NTM detection, the assay demonstrated a sensitivity of 91.98% (95% CI: 76.32-98.14%) and a specificity of 99.59% (95% CI: 98.54-99.95%). RIF resistance detection showed a sensitivity of 90.24% (95% CI:76.87-97.28%) and specificity of 95.98% (95% CI: 91.89-98.37%), with a high level of diagnostic agreement (*Kappa*: 0.8338) compared to GeneXpert. Sanger sequencing revealed that novel assay correctly classifies 98.6% of study cases as RIF resistant or susceptible, slightly higher that of GeneXpert.

Discussion: These findings indicate that the novel MeltPlus MTB-NTM/RIF platform provides a rapid and accurate method for the simultaneously detecting MTBC, NTM, and RIF resistance, making it a promising tool for clinical TB/NTM diagnosis and management, further multi-center and field studies are recommended to validate its broader applicability.

KEYWORDS

tuberculosis, *Non-Tuberculous Mycobacteria*, rifampicin resistance, molecular diagnosis, MeltPlus TB-NTM/RIF

1 Introduction

Tuberculosis (TB) remains one of the leading infectious diseases worldwide, with an estimated 10.8 million new cases and 1.25 million deaths reported in 2023 by World Health Organization (W.H.O., 2024). Early and accurate diagnosis is crucial for effective TB control and management, particularly in regions with high disease burden. The *Mycobacterium tuberculosis complex* (MTBC) is the causative agent of TB, but the diagnosis is complicated by the presence of *Non-Tuberculous Mycobacteria* (NTM). NTMs cause similar clinical symptoms but require distinct treatment approaches, presenting a significant challenge in differentiating between the two in clinical settings. Conventional diagnostic methods, such as acid-fast bacillus smears and cultures, cannot reliably distinguish MTBC from NTM, often leading to diagnostic delays or errors. Furthermore, NTMs are increasingly recognized as clinically relevant pathogens, complicating the diagnostic landscape further. Specifically, other studies have revealed that the failure to detect NTM infections frequently results in the misdiagnosis of lung diseases with vague symptoms, leading to inappropriate and potentially harmful treatments and can potentially foster TB drug resistance (Griffith et al., 2007). Moreover, the emergence of multidrug-resistant TB (MDR-TB), with approximately 45,000 new cases reported globally in 2024, particularly resistance to rifampicin, affecting around 104,000 individuals, has further complicated TB control efforts (Lange et al., 2020). Rapid and accurate detection of both MTBC and NTM, as well as rifampicin resistance, is therefore essential for the timely initiation of appropriate treatment regimens and for controlling TB spread.

Traditional diagnostic methods, such as acid-fast bacillus smears (AFB) and cultures, remain widely used but are limited in their effectiveness. Specifically, AFB smears suffer from low sensitivity and cultures are constrained by prolonged turnaround times (Parsons et al., 2011). To overcome these challenges, fluorescence microscopy has emerged as a promising alternative. By enhancing the visibility of bacilli, it offers approximately 10% greater sensitivity compared to traditional AFB smears (Albert et al., 2010; Mugenyi et al., 2024). Moreover, advancements in culture techniques have introduced liquid culture methods, which significantly shorten detection times to 10~14 days, compared to the 2~4 weeks typically required for traditional solid media. These improvements represent significant steps forward, but limitations such as reliance on specialized equipment and longer processing times compared to newer technologies remain. In contrast, molecular diagnostic tools have revolutionized TB diagnostics by not only rapid and accurate detection but also the ability to identify drug resistance patterns within several hours (Sekyere et al., 2019). GeneXpert MTB/RIF assay, endorsed by the WHO, is widely used to detect MTBC and rifampicin resistance directly from clinical specimens within two hours. However, despite its high sensitivity and specificity, GeneXpert MTB/RIF has some limitations, including potential false-positive results for rifampicin resistance and the inability to distinguish between MTBC and NTM (McNerney and Zumla, 2015). False positive results might derive from technical issues such as probe binding delays or the use of specific probes (e.g., probe B) in the GeneXpert assay (Berhanu et al., 2019). Probe binding delays can cause the assay to misinterpret the presence of resistance, particularly when the cycle threshold values are low. On the other hand, the presence of heterogeneous mutations can lead to challenges in accurately identifying the target sequences, thereby reducing the specificity of the assay (Van Rie et al., 2020). In response to these limitations, various other commercial PCR kits have been developed to enhance the detection capabilities for TB diagnostics. These kits aim to offer comprehensive diagnostic information, including the differentiation between MTBC and NTM and detection of rifampicin resistance (Lee et al., 2018; Shin et al., 2020; Fan et al., 2023). Unfortunately, these commercial kits need to be used in combination for these purposes, in other words, there are fewer reports of achieving detection of these targets in the same tube. Given these limitations, there is a clear need for a more efficient, centralized assay that can detect MTBC, NTM and rifampicin resistance in a single tube to streamline the diagnostic process, reduce turnaround time, and lower the costs associated with TB diagnostics.

In the current, we aimed to develop and validate a novel centralized assay, based on asymmetric PCR combined with melting curve analysis, for simultaneous diagnosis of MTBC, NTM and rifampicin resistance in presumptive TB patients at a single center. Specifically, we compare the diagnostic accuracy, sensitivity, and specificity of MeltPlus MTB-NTM/RIF against the GeneXpert MTB/RIF and a commercial PCR kit. By providing a detailed comparative analysis, this study seeks to contribute to the

optimization of TB diagnostic strategies, ultimately enhancing patient outcomes and supporting global TB control efforts, particularly in high-burden settings where rapid and accurate diagnostics are critical for effective disease control.

2 Methods

2.1 Asymmetric PCR-combined MCA assay development

2.1.1 Primer and probe design

Two highly conserved regions, including Insertion Sequence (*IS*) 6110 and gyrB, were selected to design primers and probes for detection of MTBC (Chaudhari et al., 2016; Chen et al., 2021). Detection of NTM was achieved by targeting the *16S* rRNA gene that present in all mycobacterial species, while the target region of *IS* 6110 and gyrB are not present in the NTM species (Uwamino et al., 2023). For rifampicin resistance, 81bp region of the *rpoB* gene, which is crucial for determining rifampicin resistance, is utilized for designing specific primers and probes. Additionally, primers targeting the human tRNA-processing ribonuclease P (RNase P) gene were also included in this study, added as the extraction and amplification control.

2.1.2 PCR amplification and muti-color melting curve analysis

The PCR amplification was performed on the SLAN-96S real-time PCR system (Hongshi Tech Co., ltd, China). Amplification was carried out in 25 μL reaction volumes, including 1×Taq HS Buffer (Mg^{2+} plus) (Nanjing Vazyme, China), 0.1 U/μL Taq HS DNA polymerase (Nanjing Vazyme, China), limiting and excess primers, Taqman probes and 5 μL template. The detailed concentration of primers and probes are presented in Supplementary Table S1. PCR amplification was performed under the following conditions: 95°C for 10 min for initial denaturation, followed by 13 touch down cycles of denaturation at 95°C for 25 s, annealing and extension at 72°C for 30 s (-1°C/cycle). And then 38 cycles of 95°C for 25 s, annealing at 58°C for 30 s, followed by extension at 72°C for 30 s. Melting curve analysis was initiated with a denaturation step of 1 min at 95°C, followed by hybridization for 1 min at 45°C. The temperature was gradually increased from 45°C to 90°C at a rate of 0.04°C/s, with fluorescence signals acquired in the FAM, VIC, ROX and Cy5 channel, allowing for the identification of specific melting peaks corresponding to each target. Double distilled water was added to the tube to serve as the negative control.

2.1.3 Sample processing and DNA extraction

DNA was extracted from the sputum or bronchoalveolar lavage fluid (BALF) sediments using EX-TB DNA extraction kit and GeneFlex 16 Fully automated nucleic acid extraction instrument (Tianlong Tech Co., Ltd.) according to manufacturer's instructions. Briefly, the 1.0 mL of raw sputum or BALF was pipetted to 2mL N-acetylL-cysteine-2% NaOH, vortexed thoroughly and then incubated for 15 min. Subsequently, 1 mL of the liquefied sample was added the sample loading well. DNA extraction carried out using a magnetic bead-based automatic extraction protocol, and the extracted DNA was used as a template for PCR amplification. For the GeneXpert MTB/RIF assay, 1.0 mL of raw sediments was added to 2.0 mL of the liquefying agent according to the manufacturer's instructions. After incubation for 15 min, 2.0 mL of this mixture was pipetted to cartridge and it was loaded subsequently in GeneXpert instrument.

2.2 Analytic evaluation of the assay

The clinical non-infected sputum samples, confirmed to be negative for MTBC and NTM by Mycobacteria Growth Indicator Tube (MGIT) liquid medium inoculation, were selected as model to further evaluation the performance of the established platform. The samples artificially spiked with a known concentration of the reference strain MTB H37Rv at series concentrations, 1 CFU/mL to 500 CFU/mL for MTBC, 10 CFU/mL to 2000 CFU/mL for NTM and rifampicin susceptibility. Each dilution was prepared and tested in twenty replicates to ensure statistic reliability. Negative controls (non-infected sputum samples without bacterial spiking) and positive controls (samples spiked with concentrations well above the detection threshold) were included in each assay run to validate performance. The lower limit of detection (LOD) was determined using probit analysis, defined as the concentration of CFU/mL at the lowest dilution which yield the detection of the targets ≥95% probability. Additionally, the analytical specificity of the novel platform was tested using other respiratory bacterial cultures, of which concentration $\geq 10^6$ CFU/mL, and some commonly NTM isolates are also used to verify the inclusiveness of developed assay (Supplementary Table S2).

2.3 Ethical approval statement

Informed consent was obtained from all subjects, and the study was approved by the Institutional Review Board of Shaanxi Provincial Hospital of Tuberculosis Prevention and Treatment Hospital (Ethics approval number: 2024No.26). This approval was in line with the Helsinki declaration as revised in 2013 and its later amendments.

2.4 Study participants and procedure

In this prospective single-center study, sputum and BALF specimens were collected from 534 presumptive TB cases (between March 2024 and July 2024) following testing with smear microscopy, mycobacterial culture and GeneXpert MTB/RIF (Cepheid Inc., USA) at the clinical laboratory of Shaanxi Provincial Hospital of Tuberculosis Prevention and Treatment Hospital, Xian, China. Sputum and BALF sediments, whether TB positive or negative, regardless of culture status and GeneXpert RIF resistance results, were included in the study. Each specimen was assigned a unique study number, and patient personal information were removed.

2.5 Acid-fast bacillus smears and mycobacterial culture

Samples were smeared onto glass slides, air-dried, and heat-fixed. The smears were then stained using the modified Ziehl-Neelsen staining method. Slides were immersed in carbol fuchsin, decolorized with acid alcohol, and counterstained with methylene blue. After thorough washing, the slides were examined under a light microscope using oil immersion (1000× magnification).

Sputum and BALF were decontaminated using the N-acetyl-L-cysteine (NALC)-NaOH method. The treated samples were then concentrated by centrifugation and inoculated onto both solid (Löwenstein-Jensen medium) or liquid media (MGIT liquid culture system). Solid media were incubated at 37°C and inspected weekly for colony formation for up to 6~8 weeks. Liquid cultures were monitored using an automated detection system, with positive results typically observed within 2~6 weeks. Colony morphology and growth characteristics on the media provided initial identification of the mycobacterial species (Den Hertog et al., 2010; Watanabe Pinhata et al., 2018), which was further confirmed by molecular or biochemical tests (Jung et al., 2016; Kuentzel et al., 2018; Lyamin et al., 2023).

2.6 Statistical analysis

Data were analyzed statistically using IVD Statistics and GraphPad Prism 8.0.2. Sensitivity, specificity, accuracy and their confidence intervals of the assay were calculated by comparing the MeltPlus TB-NTM/RIF with those obtained with the reference methods, including culture, GeneXpert MTB/RIF and a commercial PCR kit (*Mycobacterium* Real Time PCR Detection Test, CapitalBio Tech Co., Ltd. China).

3 Results

3.1 Workflow of the established assay

The present study has developed a novel platform that enables the simultaneous diagnosis of MTBC/NTM and rifampicin resistance in a single tube, offering both rapidity and cost-efficiency. As shown in Figure 1, the platform is comprised of two distinct components: sample processing and PCR amplification with subsequent melting curve analysis, in which the former includes sputum/BALF liquefaction and fully automated nucleic acid extraction. After melting curve analysis, the actual Tm values of the probes ranged from 61°C to 84°C, and each target can be differentiated based on their distinct Tm value and fluorophore (Figure 1). A test was considered positive for MTBC if it was positive for *IS 6110/gyrB* and *RNase P* genes, which Tm values were found to be 63 ± 1°C and 72 ± 1°C in Cy5 channel, respectively. A test was considered positive for NTM if it was positive for *16s RNA* and *RNase P* genes, while negative for *IS 6110/gyrB*, which Tm values were found to be 77 ± 1°C and 72 ± 1°C in Cy5 channel, respectively. Three different Tm peaks, in respect to 83 ± 1°C in FAM channel, 63 ± 1°C in HEX channel and 75 ± 1°C in Texas red channel, would be obtained and it presented that there was no mutation in the 81bp-core region of *rpoB* gene. If ΔTm of any of the three fluorescence channels were greater than 1.5°C, it is considered that there is a mutation in the drug resistance determination area of *rpoB* and the bacteria is resistant to rifampicin.

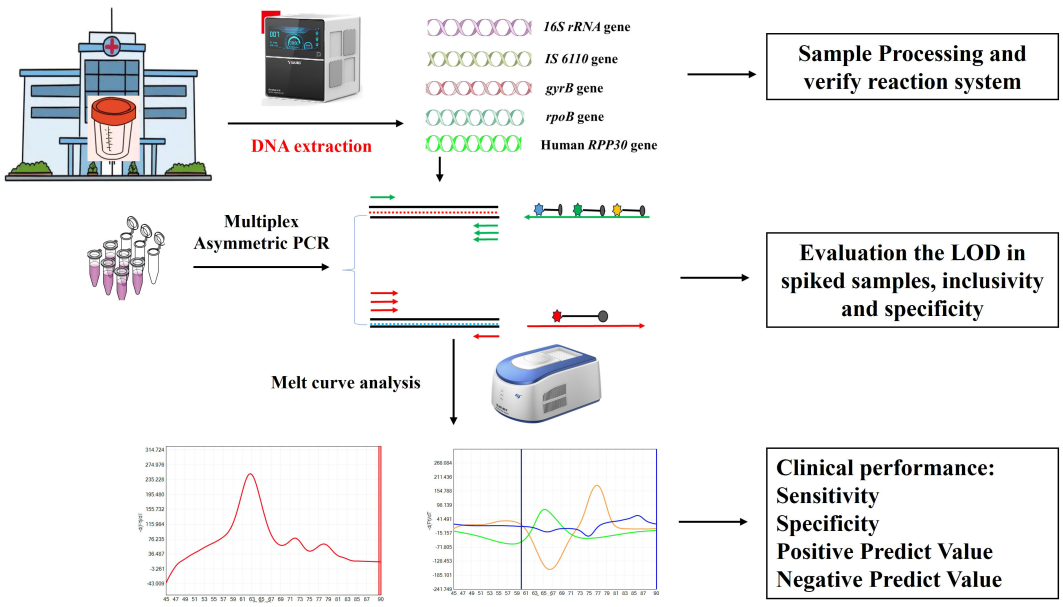

FIGURE 1
Schematic illustration of MeltPlus TB-NTM/RIF platform.

3.2 LOD and specific evaluation

Artificially contaminated sputum samples were prepared by adding varying concentrations of MTB H37Rv to the matrix (from 1 CFU/mL to 2000 CFU/mL), and the assay was then tested on 20 replicates of each concentration to determine the LOD. The results showed that 95% (19/20) of tested 20 samples were successfully detected by MeltPlus TB-NTM/RIF down to dilutions to 10 CFU/mL for MTBC spiked samples. The mycobacterial strains were correctly 100% detected by the specific melting peak of 16S rRNA at 100 CFU/mL (20/20), while only 80% (16/20) at 50 CFU/mL and 35% (7/20) at 10 CFU/mL, respectively. All tested 20 samples successfully detected (100%) of RIF susceptibility up to 100 CFU/mL, while 75% (15/20) for 50 CFU/mL and 48.5% (9/20) for 10 CFU/mL, respectively (Table 1). Therefore, the calculated LOD of MeltPlus TB-NTM/RIF by probit analysis for detection of MTBC, NTM and RIF susceptibility in spiked samples was found to be 10.31 CFU/mL (CI: 8.18-15.23), 57.55 CFU/mL (CI: 44.18-117.03) and 48.584 CFU/mL (CI: 35.48-88.61), respectively (Figure 2).

Five clinical MTBC strains, 10 NTM species and 6 non-TB bacteria were used to verify the inclusivity and specificity of the novel developed assay. The new assay correctly detected all MTBC and 10 NTM species, whereas no cross-reactivity against 6 other respiratory pathogens and distilled water, indicating that the established assay presented high specificity and could be used for clinical evaluation (Supplementary Table S2).

TABLE 1 Limit of detection of the novel platform based on asymmetric PCR-combined MCA assay.

CFU/mL	IS 6110+gyrb for MTBC	16S rRNA for all Mycobacteria	rpob for rifampicin
2000	ND	20/20(100%)	20/20(100%)
1000	ND	20/20(100%)	20/20(100%)
500	20/20(100%)	20/20(100%)	20/20(100%)
200	20/20(100%)	20/20(100%)	20/20(100%)
100	20/20(100%)	20/20(100%)	20/20(100%)
50	20/20(100%)	16/20(80%)	18/20(90%)
25	20/20(100%)	13/20(65%)	14/20(70%)
10	19/20(95%)	7/20(35%)	9/20(48.5%)
5	11/20(55%)	0/20(0)	2/20(10%)
1	4/20(20%)	0/20(0)	0/20(0)

ND, Not detected

3.3 Assay performance with clinical samples

3.3.1 Patient characteristics

To conduct a clinical feasibility evaluation of MeltPlus TB-NTM/RIF, a total of 534 individuals were initially included in this study. Eight individuals were excluded due to following reasons: 3 cases of insufficient sputum or BALF, 3 cases of culture contamination, and 2 cases of unclear diagnosis. Consequently, a total of 526 patients were finally included in the study (as shown in Figure 3). Among them, 383 (72.8%) were diagnosed with PTB or NTM pulmonary disease, including 275 confirmed as *Mycobacteria* infection through culture or GeneXpert (241 TB infections and 34 NTM infections), and 108 clinically diagnosed TB. The remaining 251 (47.7%) were negative for both culture and GeneXpert tests. The other characteristics of these patients were summarized in Table 2.

3.3.2 Accuracy of MTBC diagnostic

Results of the comparison between MeltPlus TB-NTM/RIF and bacteriologically TB standard are shown in Table 3, sensitivity and specificity of the platform was found to be 98.76% (238/241; 95% CI: 96.41%-99.74%) and 94.42% (237/251; 95% CI: 90.82%-96.92%), respectively. The specificity calculation did not include the NTM cases detected. Of the participants, a total of 17 specimen showed discordant results between bacteriologically TB standard and MeltPlus TB-NTM/RIF. Among the 241 TB confirmed patients, 215 were found to be positive for GeneXpert sore use, yielding a sensitivity of 89.2% (95% CI: 85.28%-93.11%). Compared with bacteriologically TB standard, the sensitivity of GeneXpert is significantly lower than that of MeltPlus TB-NTM/RIF ($P<0.001$), and this might result from LOD difference and the nonhomogeneous nature of sputum or BALF (Kennedy et al., 1994). On the other hand, 14 cases without laboratory evidence presented MTBC-positive results, of which 10 cases fulfilled the criteria for clinically diagnosed TB. Therefore, the sensitivity and specificity of novel assay was 71.06% (248/349; 95% CI: 65.99%-75.76%) and 97.18% (138/142; 95% CI: 92.94%-97.18%) when compared with clinically diagnosed results.

3.3.3 Diagnostic performance for NTM

Out of 526 clinical respiratory samples, 34 samples were positive for NTM using the *Mycobacterium* Real Time PCR Detection Test Kit (CapitalBio Tech Co., Ltd. China). After retrospectively reviewed the patients' case information, we confirmed that all 34 cases fulfilled the definition of pulmonary NTM disease, with NTM detected in at least two respiratory

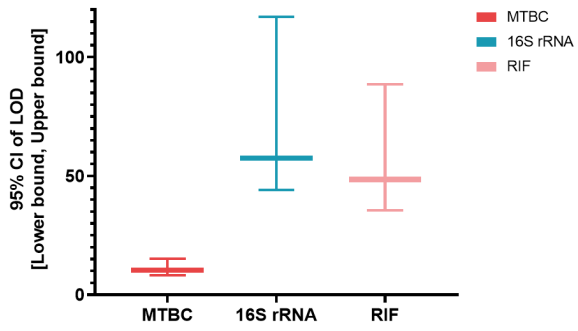

FIGURE 2
The LOD [95% CI: (Lower bound, upper bound)] of the assay for the targeted genes.

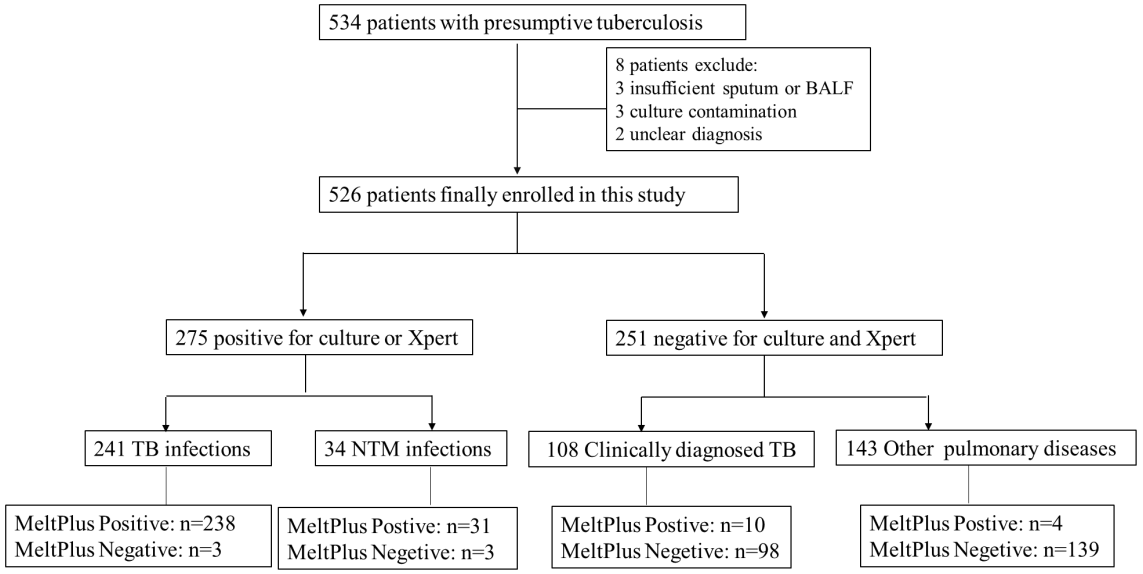

FIGURE 3
Study participants' and exclusions from analysis eligibility.

samples collected at different times, along with the presence of respiratory symptoms similar with TB/NTM infection. Of these 34 cases, 31 were accurately identified by MeltPlus TB-NTM/RIF, while the remaining 3 samples were identified as MTBC (Table 3). This specimen exhibited a weakly positive result for NTM in the commercial PCR kit (with Ct value of *Mycobacterium* gene: 38.11, 36.88, 37.42 and Ct value less than 40 regarded as positive), whereas our assay result was positive for MTBC (Supplementary Table S3). This discrepancy may be attributed to the inconsistency of the LOD values, as LOD of the commercial PCR kit reported to be 5×10^3 CFU/mL. Among the samples that were negative by both culture and GeneXpert, 2 samples were identified as NTM by MeltPlus TB-NTM/RIF, whereas the commercial PCR kit returned negative results. Therefore,

TABLE 2 Demographic and clinical characteristics of the 526 enrolled suspected TB patients.

Characteristics N=526	No. positive for TB N=241(%)	No. (%) positive for NTM N=34(%)	Others N=251(%)
Gender			
Male	170 (70.54%)	26 (76.47%)	136 (53.78%)
Female	71 (29.47%)	8 (23.53%)	115 (45.82%)
Age group			
≤35	49 (20.33%)	6 (17.65%)	61 (24.30%)
35-70	145 (60.17%)	23 (67.65%)	159 (63.35%)
≥70	47 (19.50%)	5 (14.71%)	31 (12.35%)
Sample types			
Sputum	198 (82.16%)	29 (85.29%)	143 (56.98%)
BALF	43 (17.84%)	5 (14.71%)	108 (3.02%)
AFB			
Positive	135 (56.02%)	19 (55.88%)	0
Negative	106 (43.98%)	15 (44.12%)	251 (100%)
Mycobacterial culture			
Positive	212 (87.97%)	34 (100%)	0
Negative	29 (12.03%)	0	251 (100%)

TABLE 3 Diagnostic performance of MeltPlus TB-NTM/RIF for the detection of MTBC and NTM from 526 sputum and BALF specimens.

Analyte	The novel assay	Reference		Sensitivity % (95% CI)	Specificity % (95% CI)	OPA[e] % (95% CI)	Cohen's κ
		P[c]	N[d]				
MTBC[a]	P[c]	238	14	98.76 (96.41-99.74)	94.42 (90.82-96.92)	96.54 (94.53-97.97)	0.9309
	N[d]	3	237				
NTM[b]	P[c]	31	2	91.98 (76.32-98.14)	99.59 (98.54-99.95)	99.05 (97.80-99.69)	0.9203
	N[d]	3	490				

[a]For MTBC detection, the Reference method was microbiological reference standard, including GeneXpert and culture.
[b]For NTM detection, the results was compared with a commercial PCR kit.
[c]P, positive.
[d]N, negative.
[e]OPA, overall percent agreement.

MeltPlus TB-NTM/RIF showed sensitivity and specificity of 91.98% (95% CI: 76.32%-98.14%) and 99.59% (95% CI: 98.54%-99.95%) for directly detection of NTM in clinical sputum and BALF specimens.

3.3.4 Performance for RIF resistance detection

Among 41 patients diagnosed with RIF-resistant by GeneXpert, 37 patients were correctly diagnosed by MeltPlus TB-NTM/RIF with a sensitivity of 90.24% (95% CI: 76.87%-97.28%). In addition, 167 of 174 patients diagnosed as RIF sensitive by GeneXpert were confirmed by MeltPlus TB-NTM/RIF, demonstrating a specificity of 95.98% (95% CI: 91.89%-98.37%). Kappa analysis was conducted to evaluate the consistency between MeltPlus TB-NTM/RIF and GeneXpert in detecting rifampicin susceptibility, yielding a *Kappa* value of 0.8338, which suggests a high level of diagnostic agreement (Table 4). Out of the 215 samples subjected to resistance analysis, 11 samples presented inconsistent results between the novel platform and GeneXpert, of which 4 cases of GeneXpert were diagnosed as RIF resistance and 7 cases were diagnosed as RIF sensitive. We further sequenced the PCR amplified products from the 11 clinical samples to identify presence or absence of the mutations. Results of sanger sequencing revealed that 3 samples of the former cases were diagnosed as RIF sensitive, consistent with MeltPlus TB-NTM/RIF, and 1 sample was diagnosed as RIF resistance. Two patients' samples of the 7 cases were found to be RIF sensitive while 5 cases were found to be RIF resistance by sanger sequencing, respectively. Therefore, MeltPlus TB-NTM/RIF and GeneXpert correctly classifies 98.6% and 96.3% of study cases as RIF resistant or susceptible, respectively. And we speculate that sensitivity and specificity of the novel assay for detection of RIF susceptibility are slightly higher than those of GeneXpert.

4 Discussion

MeltPlus TB-NTM/RIF, integrating the detection of MTBC, NTM and rifampicin resistance into one test, can significantly improve the management of TB or NTM infections, particularly in high-burden settings where rapid and accurate diagnostics are critical for effective disease control. The platform delivers results within 3 hours (from sample to answer) and costs approximately $8 per sample (including nucleic acid extraction), making it a highly cost-effective alternative. In comparison, the commercial Xpert MTB/RIF test costs approximately $65 per sample, as the negotiated lower price is not applicable in China. By integrating the detection of multiple targets into a single assay, the MeltPlus platform also reduces the need for separate tests, further minimizing costs and improving operational efficiency in laboratories with limited resources. These features collectively position the platform as a scalable and practical solution for TB and NTM management in regions with high disease burden and constrained healthcare infrastructure.

The novel centralized platform was further validated and demonstrated to be highly accurate, sensitive and reliable. LODs for MTBC was found to be 10.31CFU/mL, with the sensitivity surpasses the GeneXpert's assay (131CFU/mL) and are comparable to the results for Xpert Ultra (15.6 CFU/mL), iFIND TBR (13.34 CFU/mL) and InnowaveDX MTB/RIF(9.6 CFU/mL) (Helb et al., 2010; Chakravorty et al., 2017; Deng et al., 2023; Ou et al., 2024). The assay also detected MTBC at 100 CFU/mL with 100% accuracy, outperforming some traditional culture methods that typically require higher bacterial loads for reliable detection. The analytical performance for NTM and RIF susceptibility is lower at a detection

TABLE 4 Diagnostic accuracy of MeltPlus TB-NTM/RIF for RIF susceptibility compared with GeneXpert.

The novel assay	GeneXpert		Sensitivity % (95% CI)	Specificity % (95% CI)	OPA[c] % (95% CI)	Cohen's κ
	R[a]	S[b]				
R[a]	37	7	90.24 (76.87-97.28)	95.98 (91.89-98.37)	94.88 (91.03-97.42)	0.8338
S[b]	4	167				

[a]R, rifampin resistant.
[b]S, rifampin susceptible.
[c]OPA, overall percent agreement.

limit of 50 CFU/mL, but it remains comparable to the performance reported for the commercial PCR kit and GeneXpert assay. The increased sensitivity of MeltPlus TB-NTM/RIF undoubtedly assisted diagnosis and guide treatment decision for pulmonary TB.

Clinical validation of MeltPlus TB-NTM/RIF platform involved a comprehensive study with 526 patients, where the assay exhibited remarkable sensitivity (98.76%) and specificity (94.42%) for detecting MTBC. This high performance is comparable to, and in some cases exceeds, that of traditional diagnostic methods. For example, the sensitivity of platform exceeds that of the GeneXpert assay, which demonstrated a sensitivity of 89.2% in our study. This finding is consistent with other reports, wherein the sensitivity of the GeneXpert for tuberculosis diagnosis has been reported to 83% to 90% (Boehme et al., 2010). Increased sensitivity to benefit those at risk for false negatives may reduce the specificity, leading to a higher chance of false positives (Deng et al., 2023). As we evaluated the clinical performance of the new method for the detection of MTBC and NTM, 10 of the 16 samples without TB and NTM etiology met the criteria for clinical diagnosis of TB, but the remaining 6 would be considered as false positives, and these false positives may occur attributable to the sample cross contamination. Pre-PCR sample processing can produce many aerosols, particularly in labs with numerous *Mycobacterial* samples, potentially leading to false positives of MeltPlus MTBC-NTM/RIF in the present study (Mifflin, 2007). On the other hand, increased false-positive results from ultrasensitive molecular assays have also been reported in other studies, highlighting a common challenge with such highly sensitive diagnostic tools. For example, as demonstrated by a study conducted by Zhang et al., the use of Xpert Ultra for tuberculosis diagnosis led to a higher rate of false positives, which the authors attributed to the assay's ability to detect minute amounts of DNA that may not necessarily indicate active infection (Zhang et al., 2020). Similarly, Johnson et al. found that, in patients who had previously undergone treatment for TB, an ultrasensitive assay for detecting MTBC produced false-positive results, likely due to residual DNA from dead bacteria (Boyles et al., 2014). Therefore, clinicians should interpret the results from the MeltPlus TB-NTM platform within the broader clinical context, especially for the patients with a history of TB or NTM infection as the presence of residual DNA from non-viable bacteria might lead to false-positive results.

NTM infections contribute to substantial morbidity and mortality globally, it is not routinely diagnosed despite the availability of treatment in many developing countries (Lange et al., 2020). However, physicians, in these resource-limited regions, often initiate presumptive treatment, which can be toxic and time-consuming (Sarro et al., 2021). Identifying these patients and ensuring appropriate treatment is critical to combat TB drug resistance and effectively treat those with NTM infection or TB. The novel platform presented good sensitivity (91.98%) and specificity (99.59%) for NTM detection in sputum and BALF specimens. We found that the sensitivity of our platform was slightly lower than that of commercial PCR kit in this study, however, the commercial kit's sensitivity for detecting MTBC is relatively low, making it difficult to accurately confirm the validity of our detection results. Unfortunately, we were unable to conduct sanger sequencing to verify the results due to the low bacterial loads. Despite the limitations, we successfully achieved simultaneous detection of MTBC, NTM and RIF resistance in a single tube.

The centralized platform also demonstrated superior sensitivity and specificity compared to the GeneXpert MTB/RIF assay for detection of rifampicin resistance. In our study, discrepancies between two methods were observed in 11 cases. Subsequent analysis using Sanger sequencing revealed that our platform exhibited a higher concordance with sequencing results (72.7% *vs* 27.3%), with 2 cases were defined as false positive and 1 case was defined as false negative. This suggests that our assay may offer improved accuracy in detecting RIF resistance, particularly in cases where the GeneXpert assay may produce false-positive or false-negative results. These findings are especially significant in clinical settings, where precise detection of rifampicin resistance is crucial for the appropriate management of TB. Accurate identification of drug-resistant strains directly influences treatment decisions and patient outcomes. Misidentification of rifampicin resistance could lead to the use of ineffective treatment regimens, potentially contributing to the development of multidrug-resistant TB (MDR-TB) (Makhado et al., 2018).

The evaluation of diagnostic kits for detecting MTBC, NTM, and rifampicin resistance is crucial for improving the management and control of TB and NTM infections. Various nucleic acid amplification tests (NAATs) have been developed to enable rapid and accurate detection of these targets. Among these, the COBAS Amplicor MTB, COBAS TaqMan MTB, and AdvanSure TB/NTM real-time PCR kits are widely used in clinical settings. The COBAS Amplicor MTB assay, while effective, has limitations in specificity, particularly in samples with low optical density, leading to false-positive outcomes (Kim et al., 2011). To address these issues, the COBAS TaqMan MTB assay, which replaced the Amplicor version, demonstrated improved performance with a sensitivity of 88.4% and a specificity of 98.8% for respiratory specimens (Bloemberg et al., 2013). Similarly, the AdvanSure TB/NTM real-time PCR kit was evaluated for its ability to differentiate between MTBC and NTM, showing a sensitivity of 76.7% and a specificity of 99.7% for MTBC detection. In comparison, the MeltPlus MTB-NTM/RIF platform exhibited a significantly higher sensitivity (98.76%) for detecting MTBC. While its specificity was slightly lower than the COBAS TaqMan MTB and AdvanSure TB/NTM assays, it remained within a comparable range, highlighting its reliability in MTBC diagnosis. For NTM detection, the AdvanSure TB/NTM kit achieved a sensitivity of 73.9% and a specificity of 100%, reflecting its high accuracy (Kim et al., 2020). The MeltPlus platform demonstrated slightly lower but comparable sensitivity and specificity, making it a competitive option for NTM diagnosis.

Beyond MTBC and NTM detection, the MeltPlus platform also shows promise in rifampicin resistance diagnosis. It achieved a combined sensitivity of 97.62% (in conjunction with Sanger sequencing: 41/42, 95% CI: 87.43–99.94%), which is slightly lower than BD's Max MDR-TB (99.1%) and iFIND TBR (98.15%), comparable to Bruker/Hain's FluoroType MTBDR (97%), and superior to Roche's cobas MTB-RIF/INH (91%), Abbott's RealTime MTB RIF/INH (94%), and InnowaveDX MTB/RIF (86.4%) (Deng et al., 2023; Xie et al., 2024). Although the clinical

performance of the MeltPlus platform is influenced by factors such as operator variability, population differences, and reagent performance, the current findings suggest that it offers a competitive edge over its counterparts. With its high sensitivity for MTBC detection, reliable performance in NTM detection, and competitive rifampicin resistance diagnosis capabilities, MeltPlus MTB-NTM/RIF platform demonstrates significant potential for enhancing TB and NTM management in clinical practice.

Despite the promising results, some limitations should be noted. The assay's performance in detecting low bacterial loads, particularly for NTM, warrants further investigation. Furthermore, the assay's validation has so far been limited to a relatively narrow range of clinical samples and settings. To confirm its generalizability and robustness, it is essential to expand validation efforts to include a broader array of clinical specimens from diverse patient populations and various geographical regions. This comprehensive validation would help ensure that the assay performs consistently and reliably across different clinical contexts, thus supporting its potential application in routine practice. Additionally, the novel platform cannot accurately detect samples co-infected with MTBC and NTM, the platform tends to misdiagnose the samples as solely MTBC infections. A previous multicenter clinical study in China revealed that the co-infection rate of MTBC and NTM to be approximately 1.2% (Wang et al., 2023). Although this prevalence is relatively low, these co-infection cases pose specific challenges for clinicians in developing effective treatment plans.

5 Conclusion

The diagnostic accuracy of MeltPlus TB-NTM/RIF platform for the detection of MTBC, NTM and rifampicin resistance was highly concordant with that of reference method (Overall percent agreement >95%, *Kappa* value >0.75). It's enhanced sensitivity, specificity and diagnostic accuracy, coupled with the convenience of simultaneous testing, make it a valuable addition to the current diagnostic toolkit for TB/NTM infections. Future studies should focus on validating these findings in larger and more diverse patient populations to further establish the platform's clinical utility. Furthermore, with the development of the isoniazid (INH) detection system, the novel platform is also expected to effectively detection INH resistance, further expanding its clinical applications and enhancing its utility in guiding MDR-TB treatment strategies.

Data availability statement

The original contributions presented in the study are included in the article/Supplementary Material. Further inquiries can be directed to the corresponding author.

Ethics statement

The studies involving humans were approved by Tuberculosis Hospital of Shaanxi Province. The studies were conducted in accordance with the local legislation and institutional requirements. The participants provided their written informed consent to participate in this study.

Author contributions

ZW: Conceptualization, Investigation, Methodology, Writing – original draft. YZ: Conceptualization, Methodology, Writing – original draft. ZHW: Data curation, Formal analysis, Writing – original draft. GB: Data curation, Formal analysis, Writing – original draft. XW: Validation, Visualization, Writing – original draft. SQ: Validation, Visualization, Writing – original draft. JS: Validation, Visualization, Writing – original draft. YJ: Resources, Supervision, Visualization, Writing – review & editing. CG: Data curation, Formal analysis, Writing – review & editing.

Funding

The author(s) declare that no financial support was received for the research, authorship, and/or publication of this article.

Acknowledgments

We are grateful to all the participants who participated in this study, and we also thank the laboratory staff for their valuable technical assistance.

Conflict of interest

The authors declare that the research was conducted in the absence of any commercial or financial relationships that could be construed as a potential conflict of interest.

Generative AI statement

The author(s) declare that no Generative AI was used in the creation of this manuscript.

Publisher's note

All claims expressed in this article are solely those of the authors and do not necessarily represent those of their affiliated organizations, or those of the publisher, the editors and the reviewers. Any product that may be evaluated in this article, or claim that may be made by its manufacturer, is not guaranteed or endorsed by the publisher.

Supplementary material

The Supplementary Material for this article can be found online at: https://www.frontiersin.org/articles/10.3389/fcimb.2025.1534268/full#supplementary-material

References

Albert, H., Manabe, Y., Lukyamuzi, G., Ademun, P., Mukkada, S., Nyesiga, B., et al. (2010). Performance of three LED-based fluorescence microscopy systems for detection of tuberculosis in Uganda. *PloS One* 5, e15206. doi: 10.1371/journal.pone.0015206

Berhanu, R. H., Schnippel, K., Kularatne, R., Firnhaber, C., Jacobson, K. R., Horsburgh, C. R., et al. (2019). Discordant rifampicin susceptibility results are associated with Xpert® MTB/RIF probe B and probe binding delay. *Int. J. Tuberculosis Lung Dis.* 23, 358–362. doi: 10.5588/ijtld.17.0837

Bloemberg, G. V., Voit, A., Ritter, C., Deggim, V., and Böttger, E. C. (2013). Evaluation of cobas taqMan MTB for direct detection of the mycobacterium tuberculosis complex in comparison with cobas amplicor MTB. *J. Clin. Microbiol.* 51, 2112–2117. doi: 10.1128/JCM.00142-13

Boehme, C. C., Nabeta, P., Hillemann, D., Nicol, M. P., Shenai, S., Krapp, F., et al. (2010). Rapid molecular detection of tuberculosis and rifampin resistance. *New Engl. J. Med.* 363, 1005–1015. doi: 10.1056/NEJMoa0907847

Boyles, T. H., Hughes, J., Cox, V., Burton, R., Meintjes, G., and Mendelson, M. (2014). False-positive Xpert® MTB/RIF assays in previously treated patients: need for caution in interpreting results. *Int. J. Tuberculosis Lung Dis.* 18, 876–878. doi: 10.5588/ijtld.13.0853

Chakravorty, S., Simmons, A. M., Rowneki, M., Parmar, H., Cao, Y., Ryan, J., et al. (2017). The new xpert MTB/RIF ultra: improving detection of mycobacterium tuberculosis and resistance to rifampin in an assay suitable for point-of-care testing. *mBio* 8, e00812-17. doi: 10.1128/mbio.00812-00817

Chaudhari, K., Surana, S., Jain, P., and Patel, H. M. (2016). Mycobacterium Tuberculosis (MTB) GyrB inhibitors: An attractive approach for developing novel drugs against TB. *Eur. J. Medicinal Chem.* 124, 160–185. doi: 10.1016/j.ejmech.2016.08.034

Chen, X., Huang, J. F., Xiao, Z. Y., Yang, X. G., Chen, Y. J., Zheng, W. L., et al. (2021). Highly specific and sensitive detection of the Mycobacterium tuberculosis complex using multiplex loop-mediated isothermal amplification combined with a nanoparticle-based lateral flow biosensor. *Braz. J. Microbiol.* 52, 1315–1325. doi: 10.1007/s42770-021-00520-4

Deng, Y., Ma, Z., Su, B., Bai, G., Pan, J., Wang, Q., et al. (2023). Accuracy of the InnowaveDX MTB/RIF test for detection of. *Emerging Microbes Infections* 12, 2151382. doi: 10.1080/22221751.2022.2151382

Den Hertog, A. L., Visser, D. W., Ingham, C. J., Fey, F. H. A. G., Klatser, P. R., and Anthony, R. M. (2010). Simplified automated image analysis for detection and phenotyping of mycobacterium tuberculosis on porous supports by monitoring growing microcolonies. *PloS One* 5, e11008. doi: 10.1371/journal.pone.0011008

Fan, D. P., Yue, Y. N., Li, H., Shang, X. C., Li, H. Y., Xiao, R., et al. (2023). Evaluation of the performances of InnowaveDx MTB-RIF assay in the diagnosis of pulmonary tuberculosis using bronchoalveolar lavage fluid. *Tuberculosis* 140, 1002349. doi: 10.1016/j.tube.2023.102349

Griffith, D. E., Aksamit, T., Brown-Elliott, B. A., Catanzaro, A., Daley, C., Gordin, F., et al. (2007). An official ATS/IDSA statement: Diagnosis, treatment, and prevention of nontuberculous mycobacterial diseases. *Am. J. Respir. Crit. Care Med.* 175, 367–416. doi: 10.1164/rccm.200604-571ST

Helb, D., Jones, M., Story, E., Boehme, C., Wallace, E., Ho, K., et al. (2010). Rapid detection of mycobacterium tuberculosis and rifampin resistance by use of on-demand, near-patient technology. *J. Clin. Microbiol.* 48, 229–237. doi: 10.1128/JCM.01463-09

Jung, Y. J., Kim, J. Y., Song, D. J., Koh, W. J., Huh, H. J., Ki, C. S., et al. (2016). Evaluation of three real-time PCR assays for differential identification of Mycobacterium tuberculosis complex and nontuberculous mycobacteria species in liquid culture media. *Diagn. Microbiol. Infect. Dis.* 85, 186–191. doi: 10.1016/j.diagmicrobio.2016.03.014

Kennedy, N., Gillespie, S. H., Saruni, A. O. S., Kisyombe, G., McNerney, R., Ngowi, F. I., et al. (1994). Polymerase chain-reaction for assessing treatment response in patients with pulmonary tuberculosis. *J. Infect. Dis.* 170, 713–716. doi: 10.1093/infdis/170.3.713

Kim, J., Choi, Q., Kim, J. W., Kim, S. Y., Kim, H. J., Park, Y., et al. (2020). Comparison of the Genedia MTB/NTM Detection Kit and Anyplex plus MTB/NTM Detection Kit for detection of Mycobacterium tuberculosis complex and nontuberculous mycobacteria in clinical specimens. *J. Clin. Lab. Anal.* 34, e23021. doi: 10.1002/jcla.23021

Kim, J. H., Kim, Y. J., Ki, C. S., Kim, J. Y., and Lee, N. Y. (2011). Evaluation of cobas taqMan MTB PCR for detection of mycobacterium tuberculosis. *J. Clin. Microbiol.* 49, 173–176. doi: 10.1128/JCM.00694-10

Kuentzel, A., Oertel, P., Fischer, S., Bergmann, A., Trefz, P., Schubert, J., et al. (2018). Comparative analysis of volatile organic compounds for the classification and identification of mycobacterial species. *PloS One* 13, e0194348. doi: 10.1371/journal.pone.0194348

Lange, C., Aarnoutse, R., Chesov, D., van Crevel, R., Gillespie, S. H., Grobbel, H. P., et al. (2020). Perspective for precision medicine for tuberculosis. *Front. Immunol.* 11, 566608. doi: 10.3389/fimmu.2020.566608

Lee, S., Hwang, K.-A., Ahn, J.-H., and Nam, J.-H. (2018). Evaluation of EZplex MTBC/NTM Real-Time PCR kit: diagnostic accuracy and efficacy in vaccination. *Clin. Exp. Vaccine Res.* 7, 111–118. doi: 10.7774/cevr.2018.7.2.111

Lyamin, A. V., Ereshchenko, A. A., Gusyakova, O. A., Antipov, V. A., Kozlov, A. V., and Ismatullin, D. D. (2023). Application of chromogenic media for preliminary identification of acid-resistant bacteria. *Int. J. Mycobacteriol.* 12, 49–54. doi: 10.4103/ijmy.ijmy_6_23

Makhado, N. A., Matabane, E., Faccin, M., Pinçon, C., Jouet, A., Boutachkourt, F., et al. (2018). Outbreak of multidrug-resistant tuberculosis in South Africa undetected by WHO-endorsed commercial tests: an observational study. *Lancet Infect. Dis.* 18, 1350–1359. doi: 10.1016/S1473-3099(18)30496-1

McNerney, R., and Zumla, A. (2015). Impact of the Xpert MTB/RIF diagnostic test for tuberculosis in countries with a high burden of disease. *Curr. Opin. Pulmonary Med.* 21, 304–308. doi: 10.1097/MCP.0000000000000161

Mifflin, T. E. (2007). Setting up a PCR laboratory. *CSH Protoc.* 2007, pdb top14. doi: 10.1101/pdb.top14

Mugenyi, N., Ssewante, N., Baruch Baluku, J., Bongomin, F., MuKenya Irene, M., Andama, A., et al. (2024). Innovative laboratory methods for improved tuberculosis diagnosis and drug-susceptibility testing. *Front. Tuberculosis* 1. doi: 10.3389/ftubr.2023.1295979

Ou, X. C., Song, Z. X., Xing, R. D., Zhao, B., Pei, S. J., Teng, C., et al. (2024). Development and preliminary assessment of the iFIND TBR: all-in- one molecular diagnostic assay for rapid detection of Mycobacterium tuberculosis and rifampicin resistance. *Front. Cell. Infect. Microbiol.* 14, 1439099. doi: 10.3389/fcimb.2024.1439099

Parsons, L. M., Somoskövi, A., Gutierrez, C., Lee, E., Paramasivan, C. N., Abimiku, A., et al. (2011). Laboratory diagnosis of tuberculosis in resource-poor countries: challenges and opportunities. *Clin. Microbiol. Rev.* 24, 314–350. doi: 10.1128/CMR.00059-10

Sarro, Y. D. S., Butzler, M. A., Sanogo, F., Kodio, O., Tolofoudie, M., Goumane, M. S., et al. (2021). Development and clinical evaluation of a new multiplex PCR assay for a simultaneous diagnosis of tuberculous and nontuberculous mycobacteria. *Ebiomedicine* 70, 103527. doi: 10.1016/j.ebiom.2021.103527

Sekyere, J. O., Maphalala, N., Malinga, L. A., Mbelle, N. M., and Maningi, N.E. (2019). A comparative evaluation of the new genexpert MTB/RIF ultra and other rapid diagnostic assays for detecting tuberculosis in pulmonary and extra pulmonary specimens. *Sci. Rep.* 9, 16587. doi: 10.1038/s41598-019-53086-5

Shin, S., Yoo, I. Y., Shim, H. J., Kang, O. K., Jhun, B. W., Koh, W. J., et al. (2020). Diagnostic performance of the GENEDIA MTB/NTM detection kit for detecting mycobacterium tuberculosis and nontuberculous mycobacteria with sputum specimens. *Ann. Lab. Med.* 40, 173–177. doi: 10.3343/alm.2020.40.2.169

Uwamino, Y., Aono, A., Tomita, Y., Morimoto, K., Kawashima, M., Kamata, H., et al. (2023). Diagnostic utility of a mycobacterium multiplex PCR detection panel for tuberculosis and nontuberculous mycobacterial infections. *Microbiol. Spectr.* 11, 516222. doi: 10.1128/spectrum.05162-22

Van Rie, A., Whitfield, M. G., De Vos, E., Scott, L., Da Silva, P., Hayes, C., et al. (2020). Discordances between molecular assays for rifampicin resistance in Mycobacterium tuberculosis: frequency, mechanisms and clinical impact. *J. Antimicrob. Chemoth.* 75, 1123–1129. doi: 10.1093/jac/dkz564

Wang, D. M., Liu, H., Zheng, Y. L., Xu, Y. H., and Liao, Y. (2023). Epidemiology of nontuberculous mycobacteria in tuberculosis suspects, southwest of China 2017-2022. *Front. Cell. Infect. Microbiol.* 13, 1282902. doi: 10.3389/fcimb.2023.1282902

Watanabe Pinhata, J. M., Felippe, I. M., Gallo, J. F., Chimara, E., Ferrazoli, L., and de Oliveira, R. S. (2018). Growth characteristics of liquid cultures increase the reliability of presumptive identification of Mycobacterium tuberculosis complex. *J. Med. Microbiol.* 67, 828–833. doi: 10.1099/jmm.0.000734

WHO (2024). *Global tuberculosis report 2024* (Geneva: World Health Organization).

Xie, L., Zhu, X. Y., Xu, L., Xu, X. X., Ruan, Z. F., Huang, M. X., et al. (2024). Accurate and affordable detection of rifampicin and isoniazid resistance in Tuberculosis sputum specimens by multiplex PCR-multiple probes melting analysis. *Infection* 52, 2371–2398. doi: 10.1007/s15010-024-02295-w

Zhang, M., Xue, M., and He, J. Q. (2020). Diagnostic accuracy of the new Xpert MTB/RIF Ultra for tuberculosis disease: A preliminary systematic review and meta-analysis. *Int. J. Infect. Dis.* 90, 35–45. doi: 10.1016/j.ijid.2019.09.016

frontiers | Frontiers in Cellular and Infection Microbiology

TYPE Original Research
PUBLISHED 01 April 2025
DOI 10.3389/fcimb.2025.1557079

OPEN ACCESS

EDITED BY
Diana Manolescu,
Victor Babes University of Medicine and Pharmacy, Romania

REVIEWED BY
Meng Fu,
University of Science and Technology of China (USTC), China
Yilian Xie,
Ningbo First Hospital, China

*CORRESPONDENCE
Qing-Dong Zhu
zhuqingdong2003@163.com
Zhou-Hua Xie
1491348066@qq.com

†These authors have contributed equally to this work and share first authorship

RECEIVED 08 January 2025
ACCEPTED 17 March 2025
PUBLISHED 01 April 2025

CITATION
Zhao C-Y, Song C, Lin Y-R, Nong Y-X, Huang A-C, Xi S-Y, Wei X-Y, Zeng C-M, Xie Z-H and Zhu Q-D (2025) The diagnostic value of third-generation nanopore sequencing in non-tuberculous mycobacterial infections.
Front. Cell. Infect. Microbiol. 15:1557079.
doi: 10.3389/fcimb.2025.1557079

The diagnostic value of third-generation nanopore sequencing in non-tuberculous mycobacterial infections

Chun-Yan Zhao[1,2†], Chang Song[1,2†], Yan-Rong Lin[1†], Ying-Xing Nong[3], Ai-Chun Huang[1], Shao-Yong Xi[4], Xiao-Ying Wei[1], Chun-Mei Zeng[1], Zhou-Hua Xie[1*] and Qing-Dong Zhu[1*]

[1]Department of Tuberculosis, The Fourth People's Hospital of Nanning, Nanning, Guangxi, China, [2]Clinical Medical School, Guangxi Medical University, Nanning, Guangxi, China, [3]Department of Medical, The Fourth People's Hospital of Nanning, Nanning, Guangxi, China, [4]Department of Clinical Laboratory, The Fourth People's Hospital of Nanning, Nanning, Guangxi, China

Background: This study aimed to investigate the diagnostic value of nanopore sequencing technology in non-tuberculous mycobacterial pulmonary disease (NTMPD) and compare it with traditional culture methods.

Methods: A retrospective analysis was conducted on 225 suspected NTMPD patients admitted to the Fourth People's Hospital of Nanning City from January 2022 to July 2024. The sensitivity, specificity, positive predictive value (PPV), negative predictive value (NPV), kappa coefficient, and area under the receiver operating characteristic curve (AUC) of nanopore sequencing, culture, and combined diagnostic methods were compared to evaluate their diagnostic performance. In addition, patients were divided into different groups to investigate the detection of NTMPD by nanopore sequencing technology under different pathogen concentrations, in cases of concurrent Mycobacterium tuberculosis (MTB) infection, and among the elderly (aged > 60 years).

Results: Among 139 NTMPD samples, nanopore sequencing detected positives in 113 cases, with a sensitivity of 81.3%, PPV of 99.1%, NPV of 76.6%, kappa coefficient of 0.759, and AUC of 0.901, demonstrating high specificity (98.8%) comparable to culture. The combined diagnostic approach significantly improved the sensitivity (90.6%), NPV (98.4%), kappa coefficient (0.862), and AUC (0.942) of NTMPD diagnosis. Nanopore sequencing showed superior diagnostic value in samples with various bacterial concentrations and in cases of concurrent MTB infection.

Conclusion: Third-generation nanopore sequencing technology serves as a rapid and effective diagnostic tool, which may profoundly impact the current diagnosis of NTMPD.

KEYWORDS

nanopore sequencing, NTMPD, diagnostic value, bacterial concentration, MTB infection

1 Introduction

Non-tuberculous mycobacteria (NTM) constitute a group of mycobacteria other than Mycobacterium tuberculosis and Mycobacterium leprae (Jamal and Hammer, 2022). NTM is free-living and ubiquitous in the natural environment, inhabiting water systems, soil, and vegetation (Falkinham, 2013). While NTM was previously considered a secondary pathogen like Mycobacterium tuberculosis (MTB), NTMPD has garnered increasing attention over the past 30 years (Griffith and Aksamit, 2016). Several studies have shown that in 16% of geographical regions globally, there is a trend opposite to that of tuberculosis, particularly in developed countries where the incidence of NTMPD exceeds that of tuberculosis, including Japan, the United States, and Australia (Chin et al., 2020). The global incidence and prevalence of NTMPD are rising due to continuously improving monitoring and diagnostic techniques, broader population surveys, and the influence of human activities and environmental changes, necessitating urgent treatment and prevention efforts (Stout et al., 2016; Wassilew et al., 2016; Kumar and Loebinger, 2022). Recent reports indicate the possibility of person-to-person transmission (Bryant et al., 2016). Therefore, the control and management of NTMPD can become one of the significant global health challenges.

The early and accurate diagnosis of NTMPD is critical for disease treatment and epidemic control. Whereas NTMPD diseases are unresponsive to anti-tuberculosis drugs with treatment strategies varying with bacterial species, often requiring at least 18 months of therapy and 12 months of negative sputum smears (Gopalaswamy et al., 2020). Because of the morphological similarities between NTM and MTB, their differentiation through commonly used traditional acid-fast staining microscopy methods is challenging. Due to the NTM's slow growth, traditional culture methods require a long time to yield reliable results. NTM is usually present at low concentrations in samples, resulting in a low culture positivity rate and complicating the diagnosis further. Additionally, many clinical symptoms of NTMPD diseases are like tuberculosis, exacerbating the diagnostic process. The challenge of diagnosing NTMPD is further complicated by the fact that individuals may carry these bacteria due to environmental exposure, requiring physicians to distinguish between NTM isolates as commensals or pathogens. This process is significantly more complex than tuberculosis (Gopalaswamy et al., 2020). Due to these characteristics, NTMPD is prevalent globally, leading to a series of misdiagnoses, confirmation difficulties, and treatment challenges, making therapeutic approaches for this disease difficult and complex (Ratnatunga et al., 2020).

Therefore, to improve the diagnostic accuracy and efficiency of NTMPD infections, it is critical to develop rapid and sensitive detection methods. The emergence of third-generation nanopore sequencing technology may revolutionize NTMPD diagnostics. Through real-time analysis of single molecules, nanopore sequencing technology is poised to achieve breakthroughs in speed and sensitivity levels that traditional culture methods cannot attain (Sun et al., 2020; Wang et al., 2021; Pugh, 2023). This technology not only accelerates the analysis and reduces the diagnostic duration but also improves NTMPD 's specific molecular marker identification through high-throughput data generation. Its unique sequencing approach can make it a powerful tool for the rapid diagnosis of NTMPD infections, improving the pathogen detection process, providing molecular diagnostic evidence for personalized treatment of patients, and ultimately achieving better treatment outcomes and quality of life.

Although several studies have explored the diagnostic value of nanopore sequencing in Mycobacterium tuberculosis, to our knowledge, there have been no reports on the diagnostic potential of third-generation nanopore sequencing technology for NTMPD. Therefore, by integrating the clinical characteristics of patients, different bacterial concentrations, co - infection with Mycobacterium tuberculosis (MTB), and the results from the elderly patient population, we aim to evaluate the effectiveness and accuracy of nanopore sequencing as a diagnostic tool for NTMPD.

2 Material and methods

2.1 Subject recruitment

A retrospective cohort analysis was conducted on 225 suspected cases of NTMPD admitted to the Fourth People's Hospital of Nanning City from January 2022 to July 2024. The inclusion criteria were as follows: (1) Patients with typical lung lesions indicative of NTM infection detected using radiological examination, including bronchiectasis, nodules or nodular lesions, fibro cavitary lesions, inflammatory infiltrates and nodules, miliary lesions, or calcified foci; (2) patients with persistent symptoms like chronic cough, sputum production, dyspnea, chest pain, weight loss, fatigue, and fever, with ineffective anti-tuberculosis and conventional antibacterial treatment; (3) patients with initial acid-fast staining positive results but ineffective anti-tuberculosis treatment. The exclusion criteria were as follows: (1) Patients who did not undergo third-generation nanopore sequencing and culture; (2) patients with incomplete clinical data; (3) patients who only underwent either third-generation nanopore sequencing or culture; (4) patients or their legal guardians who did not sign informed consent; (5) patients with unclear final clinical diagnosis.

The final diagnosis of NTMPD is determined in accordance with the 2020 American Thoracic Society (ATS) "Guidelines for the Treatment of NTM Disease" (Daley et al., 2020), the 2017 British Thoracic Society (BTS) "Guidelines for the Management of NTMPD " (Haworth et al., 2017) and the Chinese Medical Association's Diagnosis and Treatment Guidelines for Non-tuberculous Mycobacterial Diseases (2020 version) (Chinese Society for Tuberculosis, 2020). Patients with respiratory symptoms and/or systemic symptoms, who have cavitary shadows, multifocal bronchiectasis, and multiple small nodular lesions detected by chest imaging, and in whom other pulmonary diseases have been excluded, can be diagnosed with NTMPD if any of the following criteria are met under the premise that the specimen is free from exogenous contamination: (1) Two separate

sputum specimens are positive for NTM culture and identified as the same pathogen, and/or NTM molecular biological tests are positive for the same pathogen. (2) NTM culture and/or molecular biological tests of bronchoalveolar lavage fluid (BALF) or bronchial washing fluid are positive. (3) Histopathological features of mycobacterial disease (granulomatous inflammation or acid-fast staining positivity) are found in lung tissue biopsy obtained via bronchoscopy or other means, and NTM culture and/or molecular biological tests are positive. (4) Histopathological features of mycobacterial disease (granulomatous inflammation or acid-fast staining positivity) are found in lung tissue biopsy obtained via bronchoscopy or other means, and NTM culture and/or molecular biological tests are positive in one or more sputum specimens, BALF, or bronchial washing fluid. In this study, a positive result was defined as a final diagnosis of NTMPD, whereas a negative result was defined as the absence of a diagnosis of NTMPD.

The final clinical diagnosis of each pulmonary tuberculosis patient was determined according to the "WS 288-2017 Pulmonary Tuberculosis Diagnostic Criteria" issued by the Chinese Center for Disease Control and Prevention. This study was approved by the Human Research Ethics Committee of the Fourth People's Hospital of Nanning City (Ethics Approval No. [2023]24). All participants or their legal guardians provided informed consent. Moreover, all researchers ensured that the planning, implementation, and reporting of this study complied with the revised Helsinki Declaration of 2013.

2.2 Sample collection

Morning sputum samples were collected. Based on the location of respiratory tract lesions, BALF samples containing cells and secretions from the alveoli, which could be potential hosts for mycobacteria, were obtained using endobronchial ultrasound technology. We strictly adhere to standardized procedures for sample collection and testing, ensuring that every step is carried out with precision and accuracy. This approach effectively minimizes deviations caused by differences in sample handling, thereby guaranteeing the reliability and accuracy of the test results.

2.3 Acid-fast Bacillus culture

An equal volume of 4% NaOH solution was added to approximately 5 mL of the sample, vortexed for 20 s, and allowed to rest at room temperature for 15 min. A phosphate buffer solution with a pH of 7.2 was added, and the mixture was centrifuged and precipitated. The total processing time should not exceed 20 min. Many samples should be processed in batches. Modified Loewenstein culture medium (Beisen Technology Co., Ltd., Zhuhai, China; specification: 50 tubes/box) was used. The culture medium was aseptically inoculated with 0.1 mL of the pretreated sample, and the inoculated slant was shaken to evenly spread the liquid. The bottle cap was secured and incubated flat at 35 °C for 24 h, and then the slant was positioned upright and incubated at 35 °C. The samples were observed three and seven days after inoculation, followed by weekly observations. Positive smear results were reported at any time. A positive result reported within seven days indicates rapid-growing bacteria, while one reported after seven days indicates slow-growing bacteria. Negative results were reported after eight weeks, with possible extension if necessary. Clinical samples should be handled in a biosafety level 2 cabinet as a principle, and contamination should be rigorously avoided. When observing the growth of mycobacteria, if other pathogens are detected, it is reported as contaminated and retested. The contamination rate should be controlled below 2%; if it exceeds 2%, it indicates contamination of the culture medium or improper sample handling.

2.4 Nanopore sequencing

2.4.1 Sequencing protocol expansion

Added explicit library preparation steps (DNA repair, adapter ligation, purification) with commercial kit references (ONT SQK-LSK114, NEB enzymes) to ensure reproducibility. Specified flow cell type (R10.4.1) and voltage parameters, as these critically impact read accuracy and throughput.

2.4.2 Software versioning and parameters

Detailed basecalling tools (Guppy v6.4.6) and quality filters (Q-score ≥7) to align with ONT's latest recommendations. Included post-processing tools (Porechop, NanoFilt, Kraken2) and their parameters to clarify how raw data were refined before analysis.

2.4.3 Database and thresholds for pathogen detection

Defined the microbial reference database (NCBI RefSeq) and statistical criteria for species identification (50% identity, 10× coverage) to address potential false-positive concerns.

In our research, we took the following quality control steps: First, to minimize errors, we used the high - precision model of the latest Guppy base - calling algorithm provided by Oxford Nanopore Technologies to improve the accuracy of base calling. Meanwhile, we performed read filtering by removing low - quality reads with a length of less than 200 nucleotides or more than 1000 nucleotides and a quality score (Q value) of less than 7. In addition, we used the minimap2 tool to align the reads with the reference genome. This tool is optimized for long reads and can effectively identify and filter out reads with alignment errors or structural variations that may lead to errors in variant detection. Second, we combined the read length and quality score thresholds to further filter low - quality reads. We excluded reads shorter than 200 nucleotides or longer than 2000 nucleotides and those with an average Phred quality score (Q value) below 7 to ensure that only high - quality reads were used for downstream analysis. Finally, we calculated the coverage depth of the samples using the Samtools depth function. The average coverage depth was between 90 - fold and 1000 - fold, with a median of 325 - fold. We also visually inspected the distribution of the whole - genome coverage to ensure the uniformity of coverage.

2.5 Data processing and analysis

Statistical analysis was performed using SPSS 23.0 software. The indicators for evaluating diagnostic performance included sensitivity, specificity, PPV, NPV, kappa coefficient, and AUC. To compare the diagnostic performance of nanopore sequencing and solid culture of mycobacteria, McNemar's chi-square test was used to analyze paired data. $P < 0.05$ was considered statistically significant.

3 Results

3.1 Clinical characteristics of participants

This study included 225 individuals, among whom 139 were diagnosed with NTMPD. The diagnosed patients included 48 males (34.53%) and 91 females (65.47%). This finding is consistent with previous studies, indicating that elderly females were more susceptible to the disease (Ku et al., 2020). Among the 225 included samples, 176 were from BALF and 49 were from sputum. Among the 139 NTMPD-positive samples, 50 were co-infected with Mycobacterium tuberculosis, and 81 had bronchiectasis. Specific information on other complications is presented in Table 1. In the NTMPD group, the most common species was Mycobacterium intracellular (48.25%), followed by Mycobacterium abscesses (37.72%), and there were also 6 cases of mixed nontuberculous mycobacterial infections (5.26%) (Figure 1).

TABLE 1 Clinical characteristics of the included patients.

	NTMPD (n=139)	Non-NTMPD (n=86)
Gender		
Male	48	55
Female	91	31
Age (years) (mean ± SD)	56.95 ± 14.81	59.82 ± 13.23
Complications		
Tuberculosis	50	66
Bronchiectasis	81	67
Chronic obstructive pulmonary disease	9	18
Pleural disorders	11	19
Pneumonia or upper respiratory tract inflammation	25	33
Respiratory failure	11	13
Pleural effusion	9	3
Pulmonary arterial diseases (hypertension/fistula)	3	3
Lung cancer	1	2
Sample type		
BALF	106	70
Sputum	33	16

3.2 Efficacy of nanopore sequencing, culture, and combined diagnosis

Among the 139 NTMPD samples, 113 were detected as positive by nanopore sequencing, whereas 93 were detected as positive by culture (Table 2). Nanopore sequencing demonstrated superior sensitivity (81.3%), PPV (99.1%), NPV (76.6%), and Kappa coefficient (0.759) while maintaining a similarly high specificity (98.8%) as culture. Furthermore, combining nanopore sequencing with culture significantly improved the indicators.

The ROC curves for the various diagnostic methods are presented in Figure 2. The AUC for Nanopore sequencing assay and culture was 0.942 (95% CI: 0.908–0.976), which was higher than that of culture alone (0.829 [95% CI: 0.775–0.882]) and standalone nanopore sequencing (0.901 [95% CI: 0.859–0.943]). All P-values were less than 0.05, indicating statistical significance.

3.3 Venn diagram of nanopore sequencing and culture-obtained NTM positive result

All 139 specimens from NTMPD individuals were subjected to nanopore sequencing and culture, yielding 113 positive results (81.29%) and 93 positive results (66.91%), respectively (Figure 3). It is noteworthy that nanopore sequencing successfully identified 33 positive cases missed by culture. However, 13 positive cases detected by culture were overlooked by nanopore sequencing.

3.4 Detection of NTM based on the number of pathogenic bacterial sequences

We classified the pathogenic bacterial sequences into four groups using third-generation nanopore sequencing technology: >1000, 101–1000, 11–100, and 1–10. The positive detection rates of nanopore sequencing assays and culture were compared in different groups. The results revealed that in the groups with >1000 and 100–1000 pathogenic bacterial sequences, culture failed to detect 9 and 7 positive results, respectively. In the group with 10–100 sequences, nanopore sequencing detected 22 positive results (including one false positive), while in the group with 1–10 sequences, culture showed lower positive detection rates, detecting only 5 positive cases (Figure 4).

3.5 Impact of Mycobacterium tuberculosis on NTM detection

To investigate the interference effect of Mycobacterium tuberculosis (MTB) sequences on NTM detection, samples were divided into two groups based on MTB infection status: MTB-

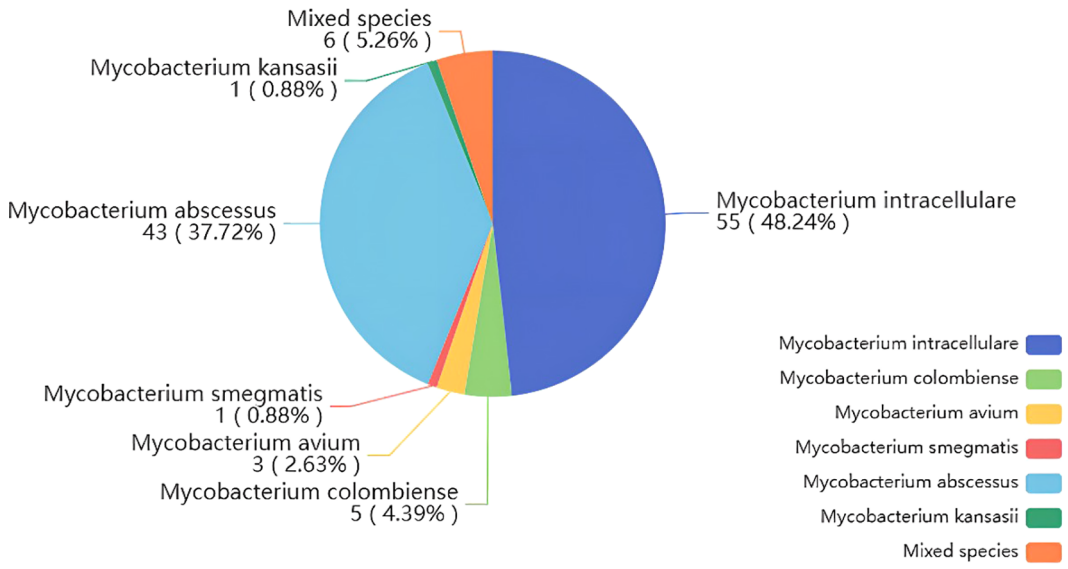

FIGURE 1
Pie chart of the composition ratio of NTM species in the cases diagnosed by nanopore sequencing diagnosis.

positive (n=116) and negative (n=109). NTM detection rates between the two groups were then compared under different conditions. The results indicate that when considering the influence of MTB infection, nanopore sequencing technology exhibited a higher detection rate in the MTB-positive group (74%) than in the detection rate of culture (60%), demonstrating its superiority (Figure 5). In the case of simple NTM infection, the detection rate of NTM by nanopore sequencing is 87.5%, while that by culture is 71.59%.

3.6 Detection efficiency of nanopore sequencing for NTM in different samples and the elderly

Among the 225 patients included in the study, 49 cases were sputum samples, and 176 cases were BALF samples. In the comparison of the detection efficacy of these two sample types, nanopore sequencing showed higher sensitivity (83%), NPV (NPV, 79.3%), and Kappa coefficient (0.784) in BALF samples than in sputum samples (sensitivity 75.8%, NPV 66.7%, Kappa coefficient 0.671). However, in terms of specificity and positive predictive value (PPV), sputum samples performed better, with both specificity and PPV reaching 100%, while the specificity of BALF samples was 98.6% and the PPV was 98.9%. This difference was mainly due to a false - positive result in the BALF samples (Supplementary Tables 1, 2). When further analyzing the elderly patient group, nanopore sequencing was superior to the overall level in all indicators of NTMPD detection. Specifically, the sensitivity was 84.5%, the specificity was 100%, the PPV was 100%, the NPV was 78.4%, and the Kappa coefficient was 0.797 (Supplementary Table 3). This indicates that nanopore sequencing has higher diagnostic efficacy in elderly patients.

TABLE 2 Diagnostic efficacy of nanopore sequencing, culture and combined diagnosis.

	Non-NTMPD	NTMPD	Sensitivity	Specificity	PPV	NPV	Kappa	P value
Nanopore sequencing assay								
Negative	85	26	81.30%	98.80%	99.10%	76.60%	0.759	<0.01
Positive	1	113						
Culture								
Negative	85	46	66.90%	98.80%	98.90%	64.90%	0.598	<0.01
Positive	1	93						
Nanopore sequencing assay & Culture								
Negative	84	13	90.60%	97.70%	98.40%	86.60%	0.862	<0.01
Positive	2	126						

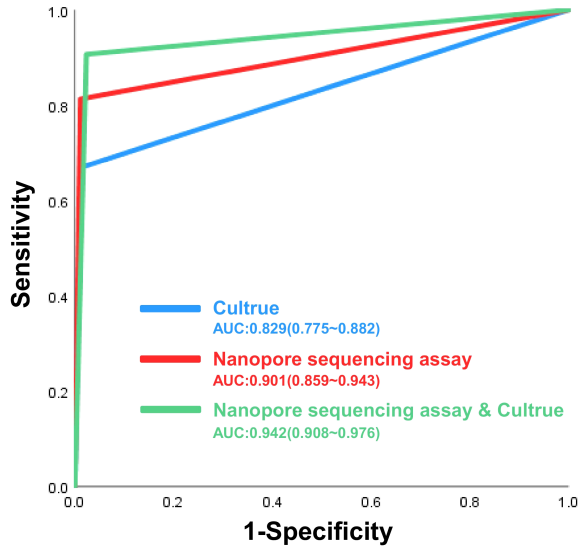

FIGURE 2
The receiver operating characteristic (ROC) curves of nanopore sequencing, culture and Nanopore sequencing in the diagnosis of NTMPD.

4 Discussion

Recently, the incidence and prevalence of pulmonary NTM-related cases have increased globally (Matsuyama et al., 2023). Therefore, it is imperative to improve the understanding, prevention, diagnosis, and treatment of pulmonary NTM disease, especially in tropical and economically underdeveloped countries where NTM is more prevalent (Ratnatunga et al., 2020). Due to its ease of use and versatility, nanopore sequencing is increasingly used in epidemiological research (Lewandowski et al., 2019; Schmidt et al., 2020; Sheka et al., 2021; Tourancheau et al., 2021). Several studies have evaluated the significance of third-generation nanopore sequencing in tuberculosis diagnosis (Yu et al., 2022; Liu et al., 2023; Yang et al., 2023); however, its potential in the diagnosis of NTMPD has not yet been proven.

In this study, among 139 cases of NTMPD, the most common co - existing pulmonary disease was bronchiectasis, followed by Mycobacterium tuberculosis infection, pneumonia, and upper respiratory tract inflammation. There is a close bidirectional relationship between NTM infection and bronchiectasis. The incidence of NTM infection is on the rise globally, especially in Western countries. The common types of NTMPD include the classic cavitary form and the atypical bronchiectasis form, with the latter more likely to occur in elderly women without a history of pulmonary disease (Jamal and Hammer, 2022). Patients with bronchiectasis are more susceptible to NTM infection due to damaged airway structures and impaired mucus clearance, and NTM infection, in turn, can further exacerbate the condition of bronchiectasis (Youssefnia et al., 2022), creating a vicious cycle. Moreover, even after NTM infection is cured, bronchiectasis still requires long-term management (McShane, 2023). Therefore, identifying the presence of NTM infection is crucial for differentiating between simple bronchiectasis and NTM infection-associated bronchiectasis. Detecting the species and drug resistance of NTM helps to formulate targeted treatment plans, avoid unnecessary use of broad-spectrum antibiotics, and thereby reduce the risk of drug resistance and improve treatment efficacy.

In this study, nanopore sequencing and culture were used to identify 139 NTMPD samples. The results revealed that nanopore sequencing detected 114 positive cases, with only 1 false positive, while culture detected 94 positive cases, with 1 false positive. Nanopore sequencing demonstrated higher sensitivity (81.30%), PPV (99.10%), NPV (76.60%), and Kappa coefficient (0.759) compared to culture while maintaining similarly high specificity (98.80%). The combined diagnosis achieved a sensitivity of 90.60%, with a NPV of 86.6%, and a kappa coefficient of 0.862. Furthermore, different diagnostic methods were compared by plotting the ROC curves. The combined application of nanopore sequencing and culture method was 0.942 (95% CI: 0.908 - 0.976), which was significantly higher than that of the culture method used alone (AUC = 0.829, 95% CI 0.775 - 0.882) and the nanopore sequencing method used alone (AUC = 0.901, 95% CI: 0.859 - 0.943). The combination of nanopore sequencing and traditional culture methods offers significant advantages in clinical diagnostics, especially in detecting low-abundance pathogens. Nanopore sequencing, with its rapidity, high sensitivity, and long-read capabilities, can quickly identify potential pathogens, compensating for the time-consuming nature of traditional culture. Meanwhile, culture methods provide precise quantification and validation through live bacterial isolation, ensuring the reliability of diagnostic results. This integration not only enhances diagnostic accuracy and efficiency but also provides robust support for detecting complex and polymicrobial infections. It demonstrates unique value in rapid diagnosis, dynamic monitoring, and evaluating treatment efficacy, offering an important direction for the future development of pathogen detection technologies.

Both culture methods and nanopore sequencing have encountered false positives and false negatives. The possible reasons for these results include false positives mainly stem from non-specific amplification or contamination, limitations of bioinformatics analysis, and misidentification due to the high genetic homology between NTM and Mycobacterium tuberculosis; false negatives may be caused by insufficient detection capability for low-abundance samples, inadequate sequencing depth, and nucleic acid degradation due to improper sample handling.

In 2019, Wei Gu et al. proposed that in clinical metagenomic next-generation sequencing (NGS), counting sequencing reads can provide quantitative or semi-quantitative data on the concentration of organisms in samples, especially for polymicrobial samples or disease processes involving multiple pathogens (Gu et al., 2019). As early as 2014, a case report also mentioned that NGS can comprehensively describe the bacteria causing patient infections. Moreover, its results are consistent with traditional 16S rRNA gene sequencing and can accurately determine the sources of most deep sequencing reads (Salipante et al., 2014). In this study, different pathogen sequences were classified using third-generation nanopore sequencing technology. The results revealed that in the high-concentration

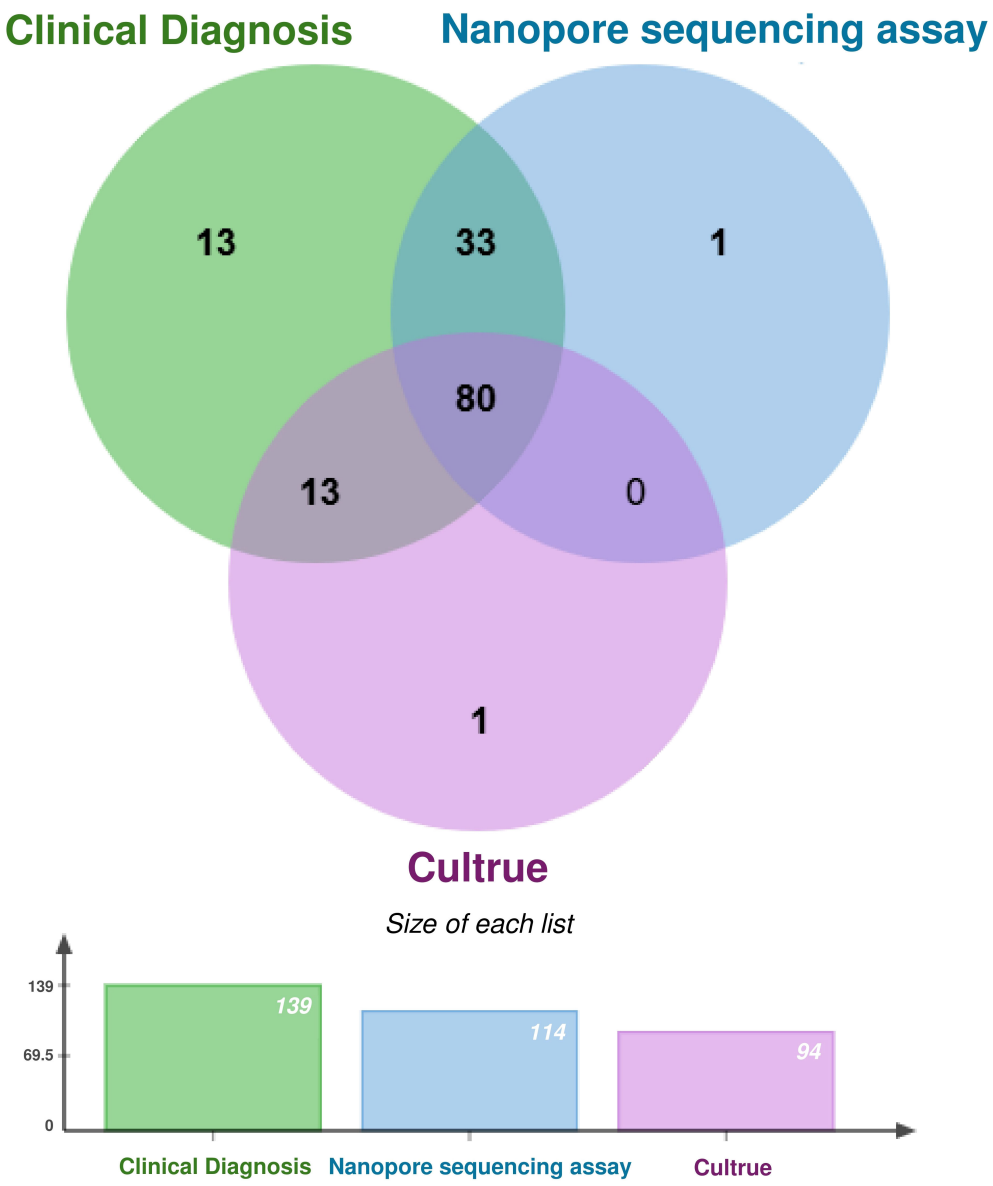

FIGURE 3
Venn diagram of NTM positive results obtained by nanopore sequencing and culture.

pathogen sequence group, culture failed to detect certain pathogens, while nanopore sequencing technology exhibited greater accuracy. Nanopore sequencing demonstrated a higher positive detection rate in the low-concentration sequence group. This study suggests that third-generation nanopore sequencing technology may be a more sensitive tool for identifying and classifying pathogens, especially in cases where traditional diagnostic methods fail to detect low-concentration pathogens.

Conventional diagnostic methods may not accurately distinguish infections caused by different pathogens, where the symptoms and signs of different pathogens may overlap, complicating the diagnosis (Pan et al., 2019). Recurrence is usually assumed when sputum smear/culture results are positive in patients with a history of tuberculosis; however, studies have revealed that a considerable proportion of infections are caused by non-tuberculous mycobacteria (Li et al., 2022). Patients might miss the optimal treatment window while awaiting further testing after culture. Therefore, to investigate the sequence noise interference effect of Mycobacterium tuberculosis sequences in the detection of non-tuberculous mycobacteria, the samples were divided into MTB-positive (n=116) and negative groups (n=109) according to MTB infection and compared the NTM detection rates under different conditions. In this study, only 30 positive cases were detected through culture among NTMPD patients with concurrent Mycobacterium tuberculosis infection, significantly lower than the NTM detection rate of nanopore sequencing technology (87.5%).

The nanopore sequencing had a detection rate 1.22 times higher than traditional culture methods in single-infection groups and 1.23 times higher in mixed-infection groups, with p-values less than 0.05, indicating a more significant advantage in mixed

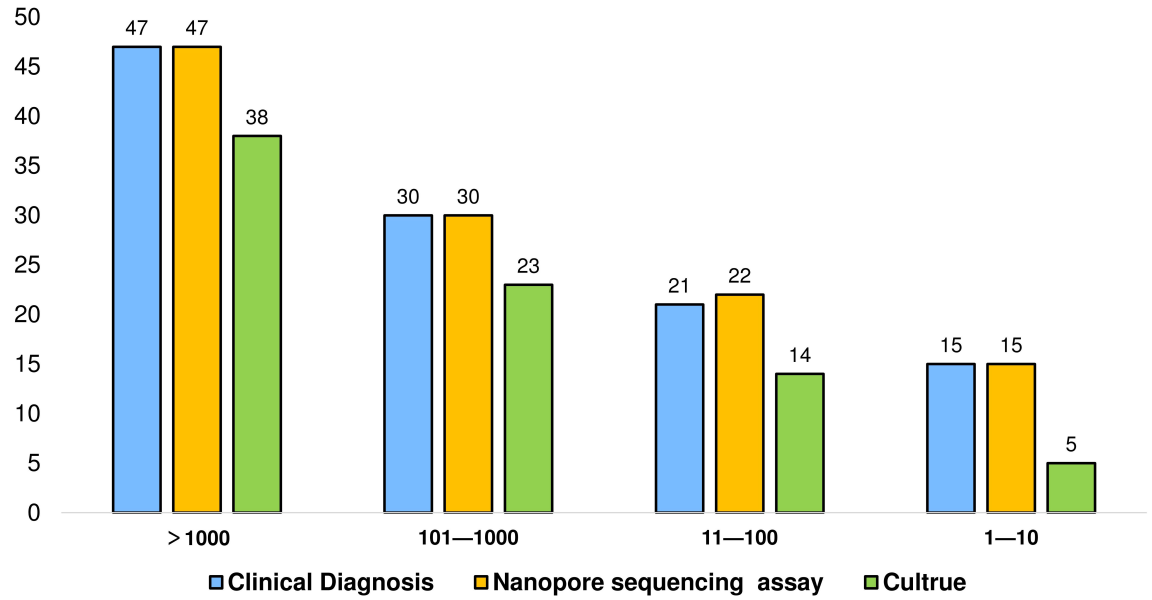

FIGURE 4
Positive detection of different pathogen sequence numbers by nanopore sequencing, culture and γ interferon test (Samples with untyped, mixed infection and unknown final sequence number were not included).

infections. This advantage stems from the limitations of traditional methods. For example, acid-fast staining cannot distinguish between MTB and NTM, while culture methods are time-consuming and have low positive rates. In cases of co-infection with TB and NTM, the rapid growth of MTB may inhibit the growth of NTM, leading to an underestimation of NTM culture positivity (Zaber et al., 2024). Therefore, nanopore sequencing has a greater advantage in detecting NTM, especially in the presence of MTB infection. The development of mycobacteriology relies on the combination of traditional methods and modern molecular techniques, with a focus on shortening diagnostic time and providing more accurate species identification and drug susceptibility results (O'Connor et al., 2015). As an emerging technology, nanopore sequencing has brought breakthroughs to the diagnosis of mycobacteria and is expected to play an important role in the future.

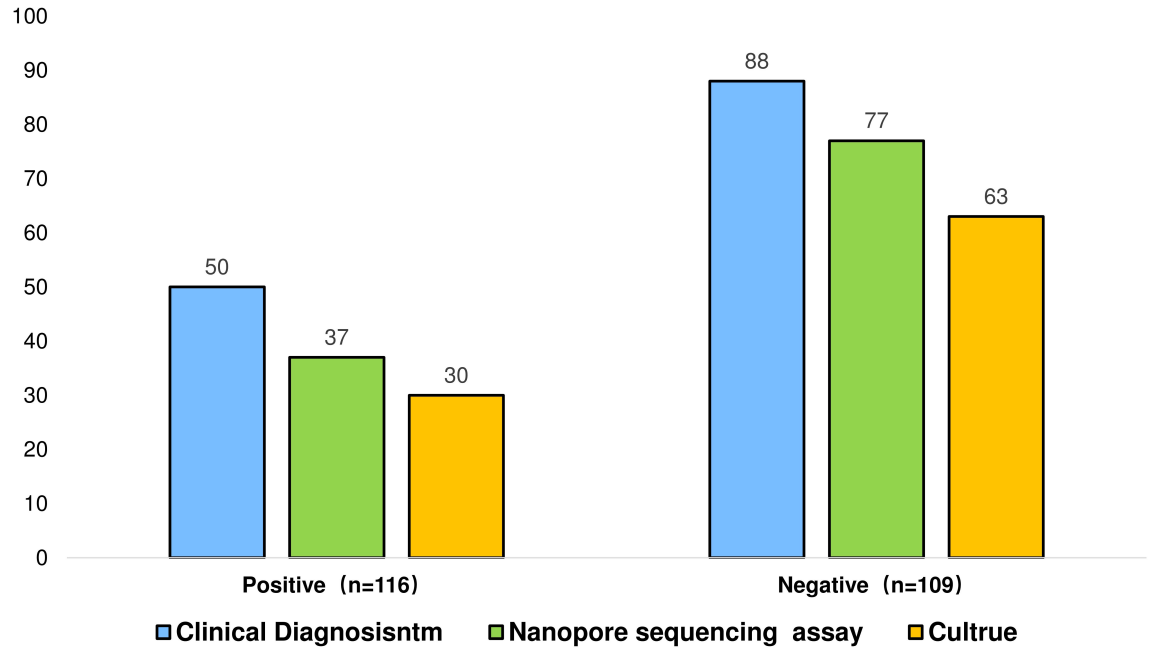

FIGURE 5
Positive detection of MTB infection by nanopore sequencing, culture method and gamma interferon assay.

Nanopore sequencing holds great potential in clinical diagnostics but still faces challenges such as high error rates, low throughput, high costs, and complex bioinformatics analysis, especially in resource-limited settings. To address these issues, the following approaches can be considered: First, improve sequencing accuracy by optimizing nanopore design and signal processing algorithms. Second, reduce costs and simplify operational procedures by developing more affordable reagents and equipment. Third, enhance bioinformatics analysis capabilities through multidisciplinary collaboration. Fourth, prioritize the application of nanopore sequencing in high-demand scenarios, such as rapid pathogen detection and antimicrobial resistance analysis, where its advantages of long-read lengths and quick results can be fully utilized.

This study still had certain limitations. First, study has a relatively small sample size, which may have introduced statistical bias. Second, some NTMPD-positive results in the study were not accurately identified, which could be related to patients' atypical clinical symptoms. Further research is required to determine whether nanopore sequencing can improve the prognosis of NTMPD patients.

5 Conclusion

Third-generation nanopore sequencing excels in diagnosing NTMPD with high accuracy and sensitivity. Combining it with culture improves its accuracy, especially in detecting low pathogen concentrations. It also detects NTM more accurately in patients co-infected with MTB, indicating a more precise identification and treatment. Overall, it is a promising diagnostic tool for NTMPD with the potential to improve medical diagnostics and patient outcomes.

Data availability statement

The original contributions presented in the study are included in the article/Supplementary material. Further inquiries can be directed at the corresponding authors. The data presented in the study are deposited in the SRA repository, accession number PRJNA1228325.

Ethics statement

The studies involving humans were approved by Human Research Ethics Committee of the Fourth People's Hospital of Nanning City. The studies were conducted in accordance with the local legislation and institutional requirements. Written informed consent for participation was not required from the participants or the participants' legal guardians/next of kin in accordance with the national legislation and institutional requirements.

Author contributions

CZ: Conceptualization, Data curation, Formal Analysis, Writing – original draft. CS: Conceptualization, Data curation, Investigation, Writing – original draft. YL: Conceptualization, Data curation, Visualization, Writing – original draft. YN: Conceptualization, Investigation, Software, Writing – original draft. AH: Formal Analysis, Investigation, Software, Writing – original draft. SX: Formal Analysis, Investigation, Software, Writing – review & editing. XW: Data curation, Methodology, Software, Writing – review & editing. CZ: Validation, Visualization, Writing – review & editing. ZX: Methodology, Project administration, Resources, Writing – review & editing. QZ: Funding acquisition, Methodology, Project administration, Resources, Supervision, Writing – review & editing.

Funding

The author(s) declare that financial support was received for the research and/or publication of this article. This research was funded by the Guangxi Zhuang Autonomous Region Health Commission Self-financed Scientific Research Project (Z-A20231211).

Acknowledgments

We acknowledge all the clients who gave consent to be screened and included in this data collection, as well as the Fourth People's Hospital of Nanning City in Guangxi Zhuang Autonomous Region for their support in data collection.

Conflict of interest

The authors declare that the research was conducted in the absence of any commercial or financial relationships that could be construed as a potential conflict of interest.

Generative AI statement

The author(s) declare that no Generative AI was used in the creation of this manuscript.

Publisher's note

Supplementary material

The Supplementary Material for this article can be found online at: https://www.frontiersin.org/articles/10.3389/fcimb.2025.1557079/full#supplementary-material

References

Bryant, J. M., Grogono, D. M., Rodriguez-Rincon, D., Everall, I., Brown, K. P., Moreno, P., et al. (2016). Emergence and spread of a human-transmissible multidrug-resistant nontuberculous mycobacterium. *Science* 354, 751–757. doi: 10.1126/science.aaf8156

Chin, K. L., Sarmiento, M. E., Alvarez-Cabrera, N., Norazmi, M. N., and Acosta, A. (2020). Pulmonary non-tuberculous mycobacterial infections: current state and future management. *Eur. J. Clin. Microbiol. Infect. Dis.* 39, 799–826. doi: 10.1007/s10096-019-03771-0

Chinese Society for Tuberculosis, C.M.A (2020). Chinese medical association's diagnosis and treatment guidelines for non-tuberculous mycobacterial diseases (2020). *Chin. J. Tuberculosis Respir. Dis.* 43, 918–946. doi: 10.3760/cma.j.cn112147-20200508-00570

Daley, C. L., Iaccarino, J. M., Lange, C., Cambau, E., Wallace, R. J. Jr., Andrejak, C., et al. (2020). Treatment of nontuberculous mycobacterial pulmonary disease: an official ATS/ERS/ESCMID/IDSA clinical practice guideline. *Eur. Respir. J.* 56 (1), 2000535. doi: 10.1183/13993003.00535-2020

Falkinham, J. O. (2013). Ecology of nontuberculous mycobacteria–where do human infections come from? *Semin. Respir. Crit. Care Med.* 34, 95–102. doi: 10.1055/s-0033-1333568

Gopalaswamy, R., Shanmugam, S., Mondal, R., and Subbian, S. (2020). Of tuberculosis and non-tuberculous mycobacterial infections - a comparative analysis of epidemiology, diagnosis and treatment. *J. BioMed. Sci.* 27, 74. doi: 10.1186/s12929-020-00667-6

Griffith, D. E., and Aksamit, T. R. (2016). Understanding nontuberculous mycobacterial lung disease: it's been a long time coming. *F1000Res* 5, 2797. doi: 10.12688/f1000research.9272.1

Gu, W., Miller, S., and Chiu, C. Y. (2019). Clinical metagenomic next-generation sequencing for pathogen detection. *Annu. Rev. Pathol.* 14, 319–338. doi: 10.1146/annurev-pathmechdis-012418-012751

Haworth, C. S., Banks, J., Capstick, T., Fisher, A. J., Gorsuch, T., Laurenson, I. F., et al. (2017). British Thoracic Society guidelines for the management of non-tuberculous mycobacterial pulmonary disease (NTM-PD). *Thorax* 72, ii1–ii64. doi: 10.1136/thoraxjnl-2017-210927

Jamal, F., and Hammer, M. M. (2022). Nontuberculous mycobacterial infections. *Radiol. Clin. North Am.* 60, 399–408. doi: 10.1016/j.rcl.2022.01.012

Ku, J. H., Ranches, G., Siegel, S. A. R., and Winthrop, K. L. (2020). [amp]]lsquo;Lady Windermere's counterpart? Pulmonary nontuberculous mycobacteria in men with bronchiectasis. *Diagn. Microbiol. Infect. Dis.* 96, 114916. doi: 10.1016/j.diagmicrobio.2019.114916

Kumar, K., and Loebinger, M. R. (2022). Nontuberculous mycobacterial pulmonary disease: clinical epidemiologic features, risk factors, and diagnosis: the nontuberculous mycobacterial series. *Chest* 161, 637–646. doi: 10.1016/j.chest.2021.10.003

Lewandowski, K., Xu, Y., Pullan, S. T., Lumley, S. F., Foster, D., Sanderson, N., et al. (2019). Metagenomic nanopore sequencing of influenza virus direct from clinical respiratory samples. *J. Clin. Microbiol.* 58 (1), e00963-19. doi: 10.1128/jcm.00963-19

Li, Q., Li, H., An, J., Zhang, X., Wang, W., Wang, Y., et al. (2022). Transition between Mycobacterium tuberculosis and nontuberculous mycobacteria in recurrent "tuberculosis" patients. *Eur. J. Clin. Microbiol. Infect. Dis.* 41, 1127–1132. doi: 10.1007/s10096-022-04477-6

Liu, Z., Yang, Y., Wang, Q., Wang, L., Nie, W., and Chu, N. (2023). Diagnostic value of a nanopore sequencing assay of bronchoalveolar lavage fluid in pulmonary tuberculosis. *BMC Pulm Med.* 23, 77. doi: 10.1186/s12890-023-02337-3

Matsuyama, M., Matsumura, S., Nonaka, M., Nakajima, M., Sakai, C., Arai, N., et al. (2023). Pathophysiology of pulmonary nontuberculous mycobacterial (NTM) disease. *Respir. Investig.* 61, 135–148. doi: 10.1016/j.resinv.2022.12.002

McShane, P. J. (2023). Investigation and management of bronchiectasis in nontuberculous mycobacterial pulmonary disease. *Clin. Chest Med.* 44, 731–742. doi: 10.1016/j.ccm.2023.07.005

O'Connor, J. A., O'Reilly, B., Corcoran, G. D., O'Mahony, J., and Lucey, B. (2015). Mycobacterium diagnostics: from the primitive to the promising. *Br. J. BioMed. Sci.* 72, 32–41. doi: 10.1080/09674845.2015.11666793

Pan, T., Tan, R., Qu, H., Weng, X., Liu, Z., Li, M., et al. (2019). Next-generation sequencing of the BALF in the diagnosis of community-acquired pneumonia in immunocompromised patients. *J. Infect.* 79, 61–74. doi: 10.1016/j.jinf.2018.11.005

Pugh, J. (2023). The current state of nanopore sequencing. *Methods Mol. Biol.* 2632, 3–14. doi: 10.1007/978-1-0716-2996-3_1

Ratnatunga, C. N., Lutzky, V. P., Kupz, A., Doolan, D. L., Reid, D. W., Field, M., et al. (2020). The rise of non-tuberculosis mycobacterial lung disease. *Front. Immunol.* 11. doi: 10.3389/fimmu.2020.00303

Salipante, S. J., Hoogestraat, D. R., Abbott, A. N., SenGupta, D. J., Cummings, L. A., Butler-Wu, S. M., et al. (2014). Coinfection of Fusobacterium nucleatum and Actinomyces Israelii in mastoiditis diagnosed by next-generation DNA sequencing. *J. Clin. Microbiol.* 52, 1789–1792. doi: 10.1128/jcm.03133-13

Schmidt, J., Blessing, F., Fimpler, L., and Wenzel, F. (2020). Nanopore sequencing in a clinical routine laboratory: challenges and opportunities. *Clin. Lab.* 44 (4), 731–742. doi: 10.7754/Clin.Lab.2019.191114

Sheka, D., Alabi, N., and Gordon, P. M. K. (2021). Oxford nanopore sequencing in clinical microbiology and infection diagnostics. *Brief Bioinform.* 22 (5), bbaa403. doi: 10.1093/bib/bbaa403

Stout, J. E., Koh, W. J., and Yew, W. W. (2016). Update on pulmonary disease due to non-tuberculous mycobacteria. *Int. J. Infect. Dis.* 45, 123–134. doi: 10.1016/j.ijid.2016.03.006

Sun, X., Song, L., Yang, W., Zhang, L., Liu, M., Li, X., et al. (2020). Nanopore sequencing and its clinical applications. *Methods Mol. Biol.* 2204, 13–32. doi: 10.1007/978-1-0716-0904-0_2

Tourancheau, A., Mead, E. A., Zhang, X. S., and Fang, G. (2021). Discovering multiple types of DNA methylation from bacteria and microbiome using nanopore sequencing. *Nat. Methods* 18, 491–498. doi: 10.1038/s41592-021-01109-3

Wang, Y., Zhao, Y., Bollas, A., Wang, Y., and Au, K. F. (2021). Nanopore sequencing technology, bioinformatics and applications. *Nat. Biotechnol.* 39, 1348–1365. doi: 10.1038/s41587-021-01108-x

Wassilew, N., Hoffmann, H., Andrejak, C., and Lange, C. (2016). Pulmonary disease caused by non-tuberculous mycobacteria. *Respiration* 91, 386–402. doi: 10.1159/000445906

Yang, J., Ye, W., Zhang, C., Lin, W., Mei, L., Liu, S., et al. (2023). Accuracy of nanopore sequencing as a diagnostic assay for pulmonary tuberculosis versus smear, culture and Xpert MTB/RIF: A head-to-head comparison. *Trop. Med. Infect. Dis.* 8. doi: 10.3390/tropicalmed8090441

Youssefnia, A., Pierre, A., Hoder, J. M., MacDonald, M., Shaffer, M. J. B., Friedman, J., et al. (2022). Ancillary treatment of patients with lung disease due to non-tuberculous mycobacteria: a narrative review. *J. Thorac. Dis.* 14, 3575–3597. doi: 10.21037/jtd-22-410

Yu, G., Shen, Y., Zhong, F., Zhou, L., Chen, G., Fang, L., et al. (2022). Diagnostic accuracy of nanopore sequencing using respiratory specimens in the diagnosis of pulmonary tuberculosis. *Int. J. Infect. Dis.* 122, 237–243. doi: 10.1016/j.ijid.2022.06.001

Zaber, M., Hoque, F., Paean, I. M., and Tarafder, S. (2024). Evaluation of Multiplex loop-mediated isothermal amplification assay for the detection of Mycobacterium tuberculosis complex from clinically suspected cases of pulmonary tuberculosis. *Heliyon* 10, e39847. doi: 10.1016/j.heliyon.2024.e39847

frontiers | Frontiers in Cellular and Infection Microbiology

TYPE Original Research
PUBLISHED 03 April 2025
DOI 10.3389/fcimb.2025.1474526

OPEN ACCESS

EDITED BY
Ariadna Petronela Fildan,
Ovidius University, Romania

REVIEWED BY
Marta Guimarães Cavalcanti,
Federal University of Rio de Janeiro, Brazil
Marina Lobato Martins,
Hemominas Foundation, Brazil

*CORRESPONDENCE
Zhengjun Wu
wuzhengjun1986@163.com
Jianda Hu
drjiandahu@163.com

†These authors have contributed equally to this work and share first authorship

RECEIVED 01 August 2024
ACCEPTED 17 March 2025
PUBLISHED 03 April 2025

CITATION
Chen Y, Chen Y, Zheng J, Yang J, Wu Y, Hu J and Wu Z (2025) Limitations of human t-lymphotropic virus type 1 antibody testing in hospitals of endemic regions in China. *Front. Cell. Infect. Microbiol.* 15:1474526. doi: 10.3389/fcimb.2025.1474526

Limitations of human t-lymphotropic virus type 1 antibody testing in hospitals of endemic regions in China

Yi Chen[1†], Yanxin Chen[1†], Jing Zheng[1†], Jiajie Yang[1,2,3†], Yong Wu[1], Jianda Hu[1,2,3*] and Zhengjun Wu[1*]

[1]Fujian Provincial Key Laboratory on Hematology, Fujian Medical University Union Hospital, Fujian Institute of Hematology, Fuzhou, Fujian, China, [2]Department of Hematology, The Second Affiliated Hospital of Fujian Medical University, Quanzhou, Fujian, China, [3]Institute of Precision Medicine, Fujian Medical University, Fuzhou, Fujian, China

Purpose: This study aims to evaluate the sensitivity and specificity of human T-lymphotropic virus type 1 (HTLV-1) antibody testing within hospitals located in HTLV-1 endemic areas of China.

Method: We performed a retrospective analysis of the clinical records and laboratory results for 1,147 patients who underwent HTLV-1 antibody testing using the Wantai HTLV-1 antibody detection kit and Polymerase Chain Reaction (PCR) testing for HTLV-1 nucleic acids, at Fujian Medical University Union Hospital between 2017 and 2023.

Result: The study population comprised 674 males (58.8%) and 473 females (41.2%), with an age distribution ranging from 7 to 86 years, and a median age of 50 years. Of the patients, 81 (7.1%) tested positive for HTLV-1 antibodies, including 39 males and 42 females. Predominantly, these positive cases were identified within the hematology department (93.8%). The cases originated from several high-prevalence coastal regions in Fujian province, such as Pingtan Island, Fuqing, Changle, Lianjiang, Fuan, Shouning, Xiapu, Zhouning, Fuding, Jiaocheng, Xiuyu, and Licheng. According to current standards for interpreting positive results, only 79.6% of patients with adult T-cell leukemia/lymphoma (ATLL) confirmed by HTLV-1 nucleic acid testing presented positive antibody results. Comparison of HTLV-1 antibody and nucleic acid test results revealed that the antibody test possessed a sensitivity of 63.0% and a specificity of 94.8%. A receiver operating characteristic (ROC) curve analysis determined that a threshold of 0.335 signal-to-cutoff (S/CO) was optimal for classifying positive antibody test results, yielding a sensitivity of 86.3% and a specificity of 94.4%.

Conclusion: The Wantai HTLV-1 antibody test kit, when utilized in hospitals within endemic regions, exhibits a high level of specificity. However, its sensitivity is found to be lacking when evaluated against the current standards for the interpretation of positive results. For patients with a high clinical suspicion of HTLV-1 infection-related diseases, it is crucial to conduct testing of HTLV-1 antibodies and nucleic acids.

KEYWORDS

human T-lymphotropic virus type 1, antibodies, nucleic acid testing, hematology, epidemiology

Introduction

Human T-cell lymphotropic virus (HTLV) is a cell-associated retrovirus, and four types have been identified to date. HTLV type 1 (HTLV-1) infection is a significant pathogenic factor in the development of adult T-cell lymphoma/leukemia (ATLL) and is also a etiologic agent for various infectious disorders, including HTLV-associated myelopathy/tropical spastic paraparesis (HAM/TSP), HTLV-associated uveitis, and infective dermatitis (Proietti et al., 2005; Gessain and Cassar, 2012; Chan et al., 2017; Nozuma and Jacobson, 2019). According to the related literature, HTLV-1 exhibits several endemic zones across the globe. In Japan, the infection prevalence rate of HTLV-1 is approximately 0.07% to 4.6%. In the Caribbean islands, it is around 0.2%. In South America, the rate is about 0.1%, and it is estimated to be between 0.1% and 2.1% in certain regions of the Middle East (Hindawi et al., 2018; Iwanaga, 2020; Gessain et al., 2023; Valcarcel et al., 2023). In China, the prevalence of HTLV-1 infection is generally considered to be low, with reported cases being isolated, particularly in coastal areas of Fujian Province, where the prevalence rate is estimated to be 0.036% (Du et al., 2014; Chen et al., 2019; Zhao et al., 2020; Chang et al., 2021).

The current methods for detecting HTLV-1 involve serological assays such as enzyme-linked immunosorbent assay (ELISA) or chemiluminescence assay (CMIA) for initial screening, followed by confirmatory tests like Western blot or polymerase chain reaction (PCR) assays for the detection of viral nucleic acid (Itabashi et al., 2020; Wolf et al., 2022; Ji et al., 2023). The results of HTLV-1 antibody testing primarily arise from the screening of healthy blood donors or pregnant women and are known to be highly sensitive and specific (San Martín et al., 2016; Hindawi et al., 2018; Itabashi et al., 2020). Typically, for cases with negative initial antibody testing, Western blot or PCR is not performed as a confirmatory test. The Wantai HTLV-1 antibody test kit is extensively employed within the blood donor population in China, having become the predominant screening tool in hospitals for the exclusion of HTLV-1 associated diseases. However, the efficacy of this HTLV-1 antibody testing in hospital populations needs to be further clarified, and there has been a lack of comprehensive data analyzing the sensitivity and specificity of this HTLV-1 antibody testing in high-prevalence regions of China.

Therefore, the primary aim of this study is to assess the efficacy of the current antibody testing methods for HTLV-1 in hospitals situated within endemic areas of China.

Methods

Patients

Fujian Province is located in the southeastern coast of China, with a total area of about 121,400 square kilometers and a permanent resident population of 41.88 million. This study was conducted at Fujian Medical University Union Hospital, which had the largest hematology center in Fujian Province. The study included patients who were suspected of having HTLV-1 infection and had undergone testing for HTLV-1/2 antibodies, as well as individuals who had received clinical and laboratory follow-up and were identified as HTLV-1 carriers, from January 2016 to June 2023. Their medical records were reviewed retrospectively for clinical data and laboratory test outcomes. The study was approved by the Ethics Committee of Fujian Medical University Union Hospital (2024KY128) and was conducted in accordance with the ethical guidelines outlined in the 1964 Declaration of Helsinki.

Assays for HTLV-1/2 antibody screening

All HTLV1/2 antibody detection tests were performed in our laboratory department by using an enzyme-linked immunosorbent assay (ELISA: Beijing Wantai Biological Pharmacy Enterprise Co., Beijing, China). Briefly, 212 amino acids from the envelope region (aa 185–396) of HTLV type 1 fused to 26 amino acids from the envelope region (aa 185–210) of HTLV type 2 were expressed in E. coli. The purified recombinant polypeptide was labeled with horse radish peroxidase (HRP) and coated onto microtiter plate. The assays were performed according to the manufacturers' instruction, which indicated that serum samples that yielded an OD/cut-off ≥1.0

S/CO were considered positive for HTLV-1/2 antibodies. The sensitivity and specificity of the test as described by the manufacturer were 100% and 99.97%, respectively, when applied to the blood donation population.

Confirmatory test

The confirmatory test for HTLV-1 infection was carried out in the hematology laboratory using PCR method. A human T lymphoblastic leukemia cell line, Jurkat, which was uninfected with HTLV-1, served as the negative control, while a patient with ATLL, confirmed by Sanger sequencing, acted as the positive control. Peripheral blood mononuclear cells (PBMCs) were isolated from patients' whole blood using Ficoll-Paque density gradient centrifugation. Genomic DNA was extracted from the PBMCs and Jurkat cell line using a column extraction kit (Tiangen, Beijing, China) or the phenol-chloroform DNA isolation method. The concentration of the purified DNA was determined using a NanoDrop 1000 spectrophotometer (Thermo Scientific, Massachusetts, USA). A dilution of 400 ng of DNA from each sample was subjected to an "in-house" PCR for HTLV-1, with the amplification regions as previously described (Wu et al., 2016). In cases where there is a discrepancy between the detection of HTLV-1 antibodies and the nucleic acid analysis by agarose gel electrophoresis, we will proceed with further confirmation of the diagnosis using TaqMan real-time fluorescent quantitative PCR assay. The detection thresholds for nucleic acid analysis by agarose gel electrophoresis and real-time fluorescent quantitative PCR were 5 × 10^-2 ng/μL and 5 × 10^-4 ng/μL, respectively. All aspects of primer design, PCR experimental procedures, and criteria for result interpretation were detailed in Supplementary File 1. Patients with positive results from HTLV-1 detection by the PCR method were classified as true positive cases, whereas those with negative results were deemed true negative cases.

Statistical analysis

Differences between patient subgroups were assessed using the chi-square test. HTLV-1 antibody and nucleic acid test results were visualized and analyzed using GraphPad Prism 9.5 software (GraphPad Software, San Diego, CA, USA). A Receiver Operating Characteristic (ROC) curve was constructed using R software (version 4.32; R Project for Statistical Computing, Vienna, Austria). In the ROC curve, the HTLV-1 nucleic acid testing results were used as the gold standard. Statistical significance between two groups was determined at $P < 0.05$.

Results

Patient characteristics

This retrospective study encompassed 1,147 patients, with 674 males (58.8%) and 473 females (41.3%). The patients' ages ranged from 7 to 86 years, with a median age of 50 years. The majority population consisted of individuals aged 40 and above, accounting for 70.2% of the total cases. The inpatient department accounted for 84.0% of the total patients, and 16.0% were from the outpatient department. The hematology department was the primary source of cases, accounting for 92.2% of all cases. A small percentage of cases originated from the neurology (4.7%), infectious diseases (0.7%), emergency medicine (0.4%), and dermatology departments (0.1%). Details of patients' characteristics were summarized Table 1.

TABLE 1 Patients characteristics and test results of HTLV-1 antibody.

Parameters	Number, (%)	Positive, n (%)	P-value
Total	1147	81 (7.1)	/
Sex			
Male	673 (58.7)	39 (5.8)	0.0475
Female	474 (41.3)	42 (8.9)	
Age, year	50 (7 - 89)		
<14	13 (1.1)	0 (0)	0.0454
≥14, <30	179 (15.6)	6 (3.4)	
≥30, <40	150 (13.1)	14 (9.3)	
≥40, <60	466 (40.6)	42 (9.0)	
≥60	339 (29.6)	19 (5.6)	
Patient sources			
Inpatient	963 (84.0)	40 (4.2)	<0.0001
Outpatient	184 (16.0)	41 (22.3)	
Department			
Hematology	1058 (92.2)	76 (7.2)	0.1361
Neurology	54 (4.7)	0 (0)	
Emergency medicine	8 (0.7)	2 (25.0)	
Infectious diseases	5 (0.4)	1 (20.0)	
Oncology	1 (0.1)	0 (0)	
Dermatology	1 (0.1)	0 (0)	
Others	20 (1.7)	2 (10.0)	

HTLV-1, human T-lymphotropic virus type 1.

Antibody testing results

According to current standards for interpreting positive results as described by the manufacturer. A total of 81 patients (7.1%) tested positive for HTLV-1 antibodies, consisting of 39 males and 42 females. The majority of these positive cases (93.8%) were from the hematology department, and the details were summarized Table 2. The highest positive detection rate was observed in

TABLE 2 Characteristics of positive samples in hematology department.

Parameters	Number, (%)	Positive rate (%)	P-value
Total	1058 (100.0)	76 (7.2)	/
Age, year			
<40	309 (29.2)	18 (5.8)	0.0744
≥40, <60	413 (39.0)	39 (9.4)	
≥60	336 (31.8)	19 (5.7)	
Sex			
Male	622 (58.8)	36 (5.8)	0.0398
Female	436 (41.2)	40 (9.2)	
Symptoms and laboratory examinations, n (%)			
Skin rash	53 (5.0)	14 (26.4)	<0.0001
Enlarged lymph nodes	513 (48.5)	40 (7.8)	
Fever	233 (22.0)	8 (3.4)	
Elevated serum calcium	255 (24.1)	45 (17.6)	
Increased lymphocyte count	129 (12.2)	25 (19.4)	
Diagnosis			
ATLL	58 (5.5)	45 (77.6)	<0.0001
Immediate family members of ATLL	114 (10.8)	29 (25.4)	
Others	890 (84.1)	4 (0.4)	

ATLL, adult T cell leukemia/lymphoma.

patients aged 40 to 60 years, at 9.4%. Females exhibited a higher positive detection rate (9.2%) compared to males (5.8%) (P = 0.0398). The primary reasons for conducting antibody testing included rash, fever, and lymphadenopathy, as well as elevated serum calcium and lymphocyte counts. Patients with accompanying rash had the highest positive rate at 26.4%. Notably, only 79.6% of patients with ATLL confirmed by HTLV-1 PCR testing presented positive antibody results. Additionally, 25.4% of the immediate family members of ATLL patients displayed positive antibody results, including patients' parents, siblings and children. Two cases with HAM/TSP confirmed by HTLV-1 PCR testing presented negative antibody results.

Geographical distribution of patients

The majority of patients with positive antibody results hailed from several high-prevalence coastal regions in Fujian province (Du et al., 2014; Chen et al., 2019; Zhao et al., 2020; Chang et al., 2021), as they were summarized at Figure 1 and Table 3. In Fuzhou City, Pingtan Island had the highest positive rate at 16.4%, followed by Fuqing, Changle, Lianjiang, and Minhou, with rates of 9.3%, 4.9%, 4.3%, and 3.2%, respectively. In Ningde city, the respective positive rates were as follows: Fuan (29.6%), Shouning (25.0%), Xiapu (21.7%), Zhouning (20.0%), Fuding (17.6%), and Jiaocheng (17.4%). Xiuyu and Licheng in Putian City were also high-prevalence areas, with rates of 27.5% and 13.6%, respectively. No positive cases were detected in the coastal city of Xiamen, and the positive rates in other inland regions were relatively low in this study.

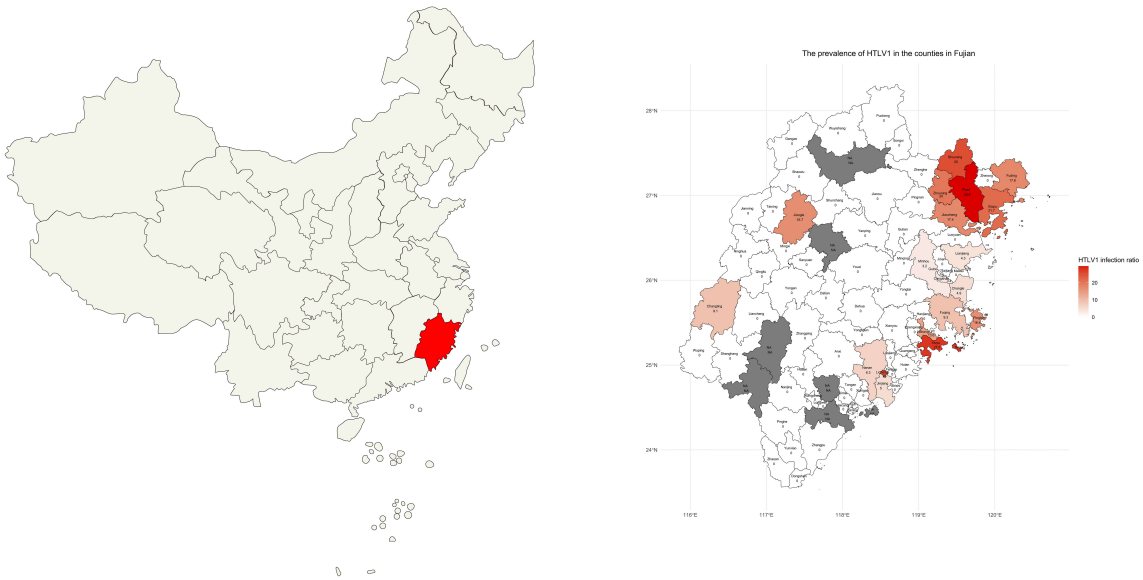

FIGURE 1
Distribution of Patients' Living Areas. A map depicting the geographical distribution of the patients' living areas in Fujian province, highlighting the coastal regions of Pingtan Island, Fuqing, Changle, Lianjiang, Fuan, Shouning, Xiapu, Zhouning, Fuding, Jiaocheng, Xiuyu, and Licheng with a higher prevalence of HTLV-1. NA: no data was available because no patient from this region was tested for HTLV-1.

10.3389/fcimb.2025.1474526

TABLE 3 Distribution of patients' living areas.

Regions	Population (Million)	Number	Positive, n (%)
Fujian Province	41.88	1111	77 (6.9)
Fuzhou	8.29	426	23 (5.4)
Pingtan	0.4	67	11 (16.4)
Fuqing	1.39	75	7 (9.3)
Changle	0.79	41	2 (4.9)
Lianjiang	0.64	23	1 (4.3)
Minhou	0.99	31	1 (3.2)
Cangshan	1.14	29	1 (3.4)
Ningde	3.15	151	28 (18.5)
Fuan	0.61	27	8 (29.6)
Shouning	0.18	8	2 (25.0)
Xiapu	0.48	46	10 (21.7)
Zhouning	0.15	5	1 (20.0)
Fuding	0.55	17	3 (17.6)
Jiaocheng	0.62	23	4 (17.4)
Others	0.70	16	0 (0.0)
Putian	3.21	147	22 (15.0)
Xiuyu	0.32	69	19 (27.5)
Licheng	0.49	22	3 (13.6)
Others	2.40	56	0 (0.0)
Quanzhou	8.78	122	3 (2.5)
Sanming	2.49	58	1 (1.7)
Nanping	2.68	91	0 (0.0)
Longyan	2.72	57	0 (0.0)
Zhangzhou	5.05	43	0 (0.0)
Xiamen	5.16	16	0 (0.0)
Other provinces*	NA	36	4 (11.1)

*In this study, a total of 36 patients from outside Fujian Province underwent HLTV-1 antibody testing. These patients hailed from 14 other provinces and regions. Due to the small number of tests conducted in each area, the total population of these regions was not displayed. NA, not available.

Comparison of antibody and nucleic acid testing for HTLV-1

A total of 216 patients underwent both HTLV-1 antibody and nucleic acid testing, and the results were showed at Table 4. Of these, 81 patients with positive HTLV-1 nucleic acid results (true positive cases) were identified. It was observed that only 51 of these cases (63.0%) were positive in the antibody tests, while 30 cases (37.0%) were negative. The remaining 135 patients with negative HTLV-1 nucleic acid results were considered true negative cases. Among these, 7 cases (5.2%) were positive and 128 cases (94.8%) were negative in antibody testing. In summary, the true positive and false positive rates were 87.9% and 12.1%, respectively, with a sensitivity of 63.0% and a specificity of 94.8%.

TABLE 4 Results of HTLV-1 antibody and nucleic acid testing in 216 cases.

Methods	Results	
	Nucleic acid testing	
Antibody testing	Positive	Negative
Positive	51	7
Negative	30	128

HTLV-1, human T-lymphotropic virus type 1. The true positive rate was 87.9%, and the false positive rate was 12.1%. The sensitivity was 63.0%, and the specificity was 94.8%.

Adjustment of positive criteria for antibody detection

Observing the high specificity (94.8%) but lower sensitivity (63.0%) of antibody testing, it was deemed necessary to reevaluate the positive threshold. A Receiver Operating Characteristic (ROC) curve analysis was performed to determine the optimal cut-off value for positive antibody detection (Figure 2). The analysis revealed that setting the cut-off value at 0.335 S/CO maximized detection efficiency, yielding a sensitivity of 86.3% and a specificity of 94.4%. However, for results below this threshold, there remained a 13.7% chance of a false negative result. HTLV-1 antibody testing results for the overall patient cohort and subgroups, including those with T-cell Lymphoma/Leukemia and those suspected with HAM/TSP based on current and revised positive criteria were summarized at Figures 3, 4.

Dynamic monitoring of HTLV-1 antibody and nucleic acid levels

In the present study, a subset of patients underwent multiple HTLV-1 antibody and nucleic acid tests throughout their disease course. We observed that the antibody levels could fluctuate in certain cases, and the interpretation of these results varied significantly based on the current positive criteria. By adjusting the cut-off value for positive criteria to 0.335 S/CO, we noted that HTLV-1 carriers and patients with ATLL consistently presented positive results for both antibody and nucleic acid tests, even in the absence of allogeneic hematopoietic stem cell transplantation (allo-HSCT), as illustrated in Figures 5A-D. In contrast, for patients with ATLL who underwent allo-HSCT, HTLV-1 nucleic acid levels were undetectable within a specific timeframe post-transplant, yet antibody testing remained persistently positive, as depicted in Figures 5E, F.

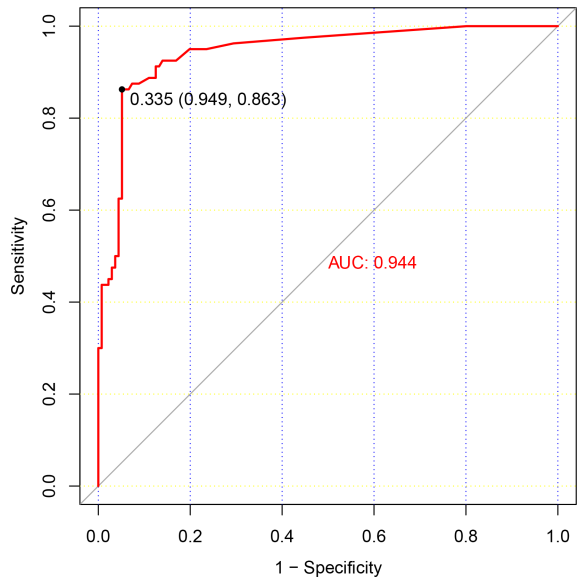

FIGURE 2
ROC Curve Analysis of HTLV-1 Antibody Testing. This figure presents a ROC curve analysis for HTLV-1 antibody testing, depicting the relationship between the sensitivity and specificity of various threshold values. The results of HTLV-1 nucleic acid testing served as the reference standard, with patients testing positive for HTLV-1 nucleic acid being classified as true positive cases. The optimal cut-off value, which maximizes the area under the ROC curve, is indicated by a dashed line at a S/CO ratio of 0.335.

Discussion

HTLV-1 is rare in most regions of China, but it is locally prevalent in coastal areas of Fujian province (Chang et al., 2021). Our team was among the first to report ATLL cases as early as 1992 (Chen et al., 1992), and established a genetic diagnostic system for HTLV-1 and ATLL in 1996 (Hu et al., 1996). To our knowledge, we are currently the only hospital in Fujian province that conducts HTLV-1 viral nucleic acid testing. We have published the largest sample size of ATLL case reports in China (Luo et al., 2024), and HAM/TSP is also reported in our center recently. Currently, antibody testing for HTLV-1 plays a crucial role in identifying individuals who may be afflicted with related diseases. The Wantai HTLV-1 antibody test kit has emerged as the leading screening method utilized in clinical practice for this purpose. However, limited data are available regarding the efficacy of this antibody testing in hospitals situated within HTLV-1 endemic areas of China, and our study contributes to the existing literature by reporting on a substantial number of cases within this setting.

In developed and some developing countries where HTLV-1 is endemic, laboratory screening for HTLV-1/2 infection has become standard practice for blood donors. Antibody testing of HTLV-1/2 is the most commonly employed method (Canavaggio et al., 1990; Fujino et al., 1991; Laperche et al., 2017). Wantai HTLV ELISA kit was one of the main kits in several large-scale epidemiological studies of HTLV-1 infection in China (Du et al., 2014; Chan et al., 2017; Zhao et al., 2020; Chang et al., 2021), and its sensitivity and specificity are 100% and 99.97% in blood donation population. Currently, this HTLV ELISA Kit has been widely adopted for detecting HTLV-1 infection in China. However, we must know that the blood donation population consists of young and healthy individuals, whereas the hospital population includes elderly patients, and patients with immune suppression or immune deficiency due to the disease itself or medical treatment.

Our study observed that the majority of cases originated from the hematology department, primarily among patients suspected or confirmed to have ATLL, or among immediate family members of ATLL patients. Among these high-risk groups for HTLV-1 infection, we identified 81 positive cases through antibody testing. Notably, only 45 out of 58 patients confirmed with ATLL and none out of 2 patients confirmed with HAM/TSP exhibited positive antibody test results for HTLV-1. This suggests that low detection sensitivity by the current ELISA test for HTLV-1 in hospital populations. Therefore, in clinical settings where there is strong suspicion of HTLV-1-related diseases based on symptoms and other laboratory results, it is crucial to conduct confirmatory nucleic acid testing for HTLV-1 through PCR. Moreover, approximately one-fourth of the immediate family members of ATLL patients in our data exhibited positive results for HTLV-1 antibody testing, warranting long-term follow-up for this group.

Comparing antibody testing to PCR testing of HTLV-1, we observed that antibody testing exhibited high specificity but low sensitivity. This implies that individuals with negative antibody testing results are at low risk of HTLV-1 infection, but a considerable proportion of HTLV-1-infected individuals may have negative antibody test results. As we mentioned above, there were significant differences in biological characteristics between the blood donation population and the hospitalized population, so the positive criteria currently based on blood donation population might not be appropriate for the hospital population. Thus, to determine the better optimal positive cut-off value for antibody detection, we conducted a ROC curve analysis. The analysis revealed that adjusting the positive cut-off value to 0.335 S/CO maximized detection efficacy. Additionally, techniques such as CMIA, WB, and Line Immunoassay (LIA) provide valuable confirmatory evidence for HTLV-1 infection, and their use should be considered when appropriate.

Previous studies have indicated that HTLV-1 cause a life-long infection and cannot be cleared (Vallinoto et al., 2019; Zuo et al., 2023). Our findings suggested that among HTLV-1 carriers and patients with ATLL, both antibody and nucleic acid testing remained persistently positive. Interestingly, in some patients with ATLL who underwent allogeneic hematopoietic stem cell transplantation (allo-HSCT), HTLV-1 nucleic acid became undetectable shortly after transplantation, while the antibody levels showed a decreasing trend but persistent positive. This could be attributed to the transplantation process potentially eliminating a majority of the virus, resulting in extremely low viral loads (Okamura et al., 2007). Thus, the interplay between different diagnostic strategies is an important consideration in the comprehensive management of HTLV-1 infection.

Certain limitations should be considered when interpreting the study results. Firstly, this investigation was a single-center retrospective analysis primarily focused on patients within the

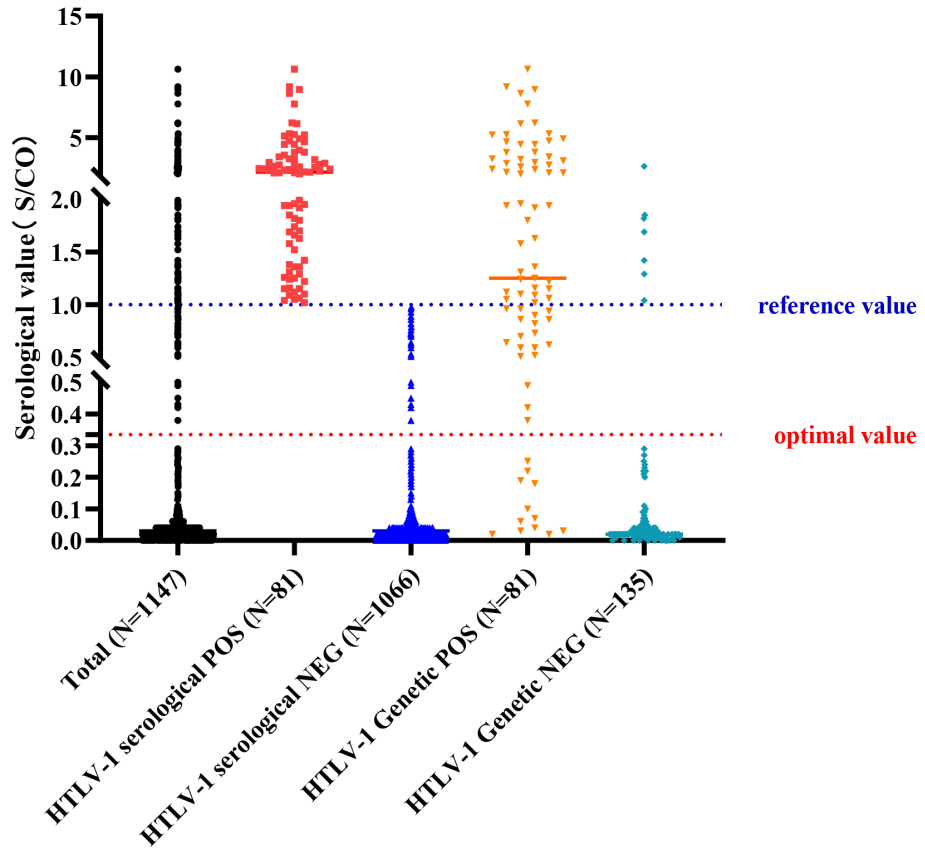

FIGURE 3
Results of Antibody and Nucleic Acid Testing of HTLV-1. A scatter plot summarizing the results of HTLV-1 antibody and nucleic acid testing in the study population, showing the positive and negative rates for each testing method. Reference value: positive judgment criteria described by HLTV-1 test kit; optimal value: positive judgment criteria adjusted with ROC curve.

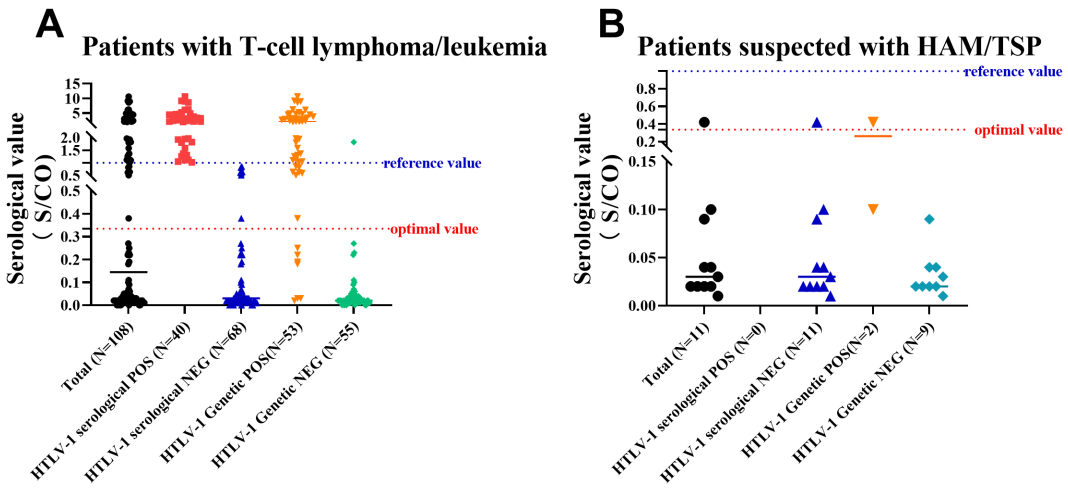

FIGURE 4
Results of Antibody and Nucleic Acid Testing of HTLV-1 in Patients with T-Cell Lymphoma/Leukemia or Suspected with HAM/TSP. **(A)** A scatter plot of results for patients with T-cell lymphoma/leukemia, showing the distribution of positive and negative antibody and nucleic acid test results. **(B)** A scatter plot of results for patients suspected with HAM/TSP, illustrating the distribution of positive and negative antibody and nucleic acid test results. Reference value: positive judgment criteria described by HLTV-1 test kit; optimal value: positive judgment criteria adjusted with ROC curve.

10.3389/fcimb.2025.1474526

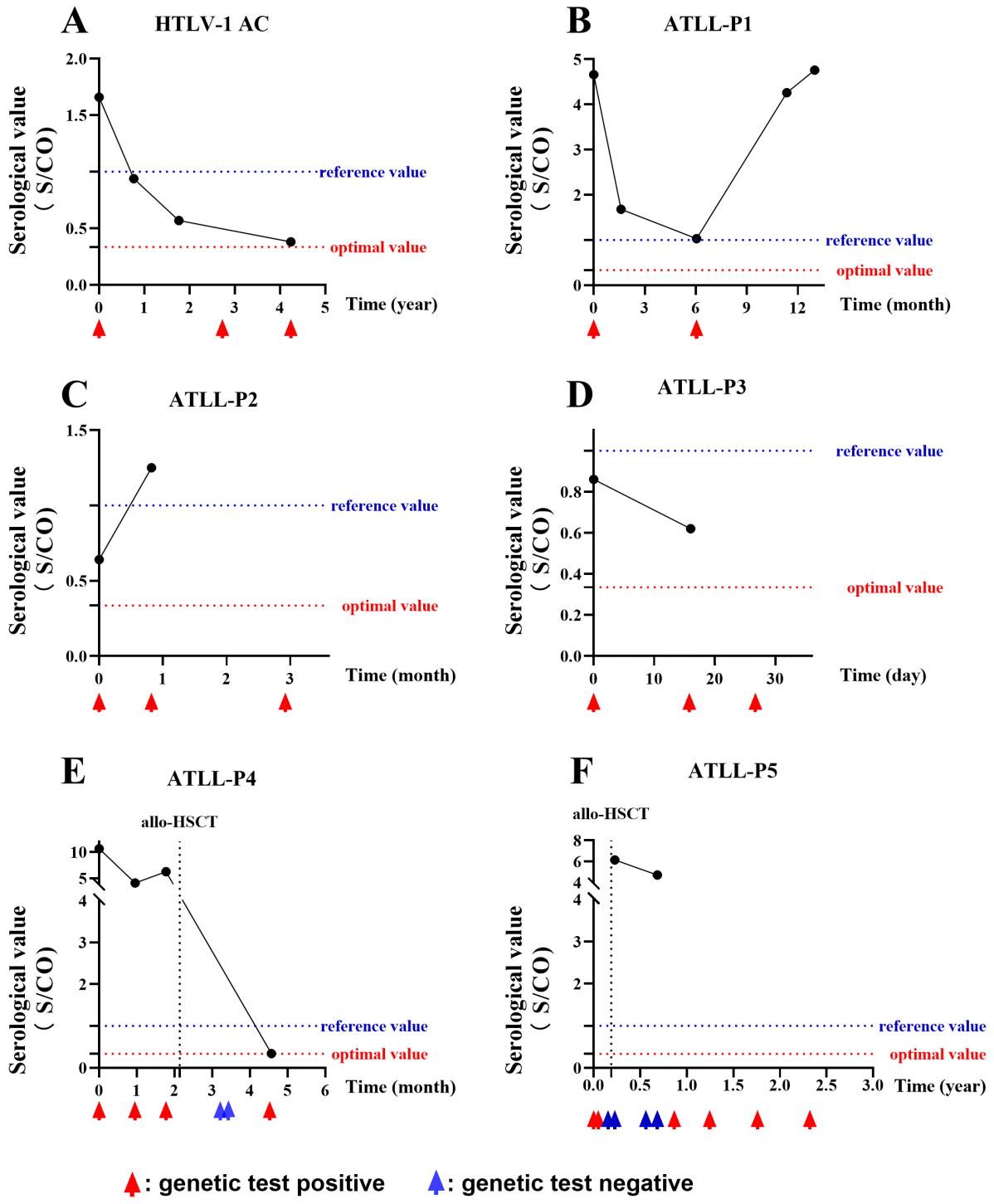

FIGURE 5
Follow-up of HTLV-1 Antibody and Nucleic Acid. A series of graphs depicting the dynamic changes in HTLV-1 antibody and nucleic acid levels over time in various patient cohorts. **(A)** A HTLV-1 carrier showing persistent positive results. **(B-D)** Three patients with ATLL, each showing persistent positive antibody and nucleic acid results. **(E, F)** Two patients with ATLL who received allo-HSCT, with transient negative nucleic acid results post-transplant but persistent positive antibody results. Reference value: positive judgment criteria described by HLTV-1 test kit; optimal value: positive judgment criteria adjusted with ROC curve.

hematology department, which may not reflect the broader patient population across various medical settings. Secondly, the living areas of the patients and their corresponding positive rates of HLTV-1 testing can indicate the epidemic areas of HLTV-1 infection, but it cannot represent the infection rate in these specific regions. Thirdly, our study was limited by the availability of testing reagents, which necessitated the use of only one of the currently prevalent antibody detection methods. Moreover, the sample size used to refine the

positive criteria for antibody testing was relatively small, highlighting the need for additional research to determine the most appropriate threshold for a positive antibody test result.

In conclusion, our study emphasizes that the use of the Wantai test kit for HTLV-1 antibody screening in hospitals situated within HTLV-1 endemic areas exhibits a high degree of specificity. However, it is noted that this kit's sensitivity is insufficient when evaluated against the current standards for the interpretation of positive results. Revising the positive cutoff threshold for HTLV-1 antibody testing to 0.335 S/CO could improve the sensitivity of the assay. In clinical settings where HTLV-1 infection-associated diseases are strongly suspected, it is imperative to concurrently assess for both HTLV-1 antibodies and nucleic acids.

Data availability statement

The original contributions presented in the study are included in the article/Supplementary Material. Further inquiries can be directed to the corresponding authors.

Ethics statement

The studies involving humans were approved by Institutional Reviewer Board of the Fujian Medical University Union Hospital (Ethical Approval Number: 2024KY128). The studies were conducted in accordance with the local legislation and institutional requirements. Written informed consent for participation was not required from the participants or the participants' legal guardians/next of kin because This is a retrospective study, so the written informed consent was not required.

Author contributions

YC: Writing – original draft, Writing – review & editing, Conceptualization, Data curation, Formal Analysis, Funding acquisition, Validation. JZ: Writing – original draft, Writing – review & editing, Data curation, Investigation, Project administration, Software. YXC: Writing – original draft, Writing – review & editing, Data curation, Methodology, Software, Validation. YW: Writing – original draft, Writing – review & editing, Data curation, Methodology, Resources, Validation. JH: Writing – original draft, Writing – review & editing, Conceptualization, Funding acquisition, Methodology, Project administration. ZW: Writing – original draft, Writing – review & editing, Conceptualization, Data curation, Formal Analysis, Funding acquisition, Investigation, Methodology, Project administration, Software, Visualization. JY: Writing – original draft, Writing – review & editing, Methodology, Formal analysis, Software.

Funding

The author(s) declare that financial support was received for the research and/or publication of this article. This work was supported by National Natural Science Foundation of China (82000142), Joint Funds for the innovation of Science and Technology, Fujian province (2023Y9128), Natural Science Foundation of Fujian Province (2022J01264), Natural Science Foundation of Fujian Province (2024J01587), and Scientific Research Foundation of Xiang An Biomedicine Laboratory (2023XAKJ0102057).

Acknowledgments

We greatly appreciate all patients who supported this study.

Conflict of interest

The authors declare that the research was conducted in the absence of any commercial or financial relationships that could be construed as a potential conflict of interest.

Publisher's note

Supplementary material

The Supplementary Material for this article can be found online at: https://www.frontiersin.org/articles/10.3389/fcimb.2025.1474526/full#supplementary-material

References

Canavaggio, M., Leckie, G., Allain, J. P., Steaffens, J. W., Laurian, Y., Brettler, D., et al. (1990). The prevalence of antibody to HTLV-I/II in United States plasma donors and in United States and French hemophiliacs. *Transfusion.* 30, 780–782. doi: 10.1046/j.1537-2995.1990.30991048781.x

Chan, C. P., Kok, K. H., and Jin, D. Y. (2017). Human T-cell leukemia virus type 1 infection and adult T-cell leukemia. *Adv. Exp. Med. Biol.* 1018, 147–166. doi: 10.1007/978-981-10-5765-6_9

Chang, L, Ou, S., Shan, Z., Zhu, F., Ji, H., Rong, X., et al. (2021). Seroprevalence of human T-lymphotropic virus infection among blood donors in China: a first nationwide survey. *Retrovirology.* 18, 2. doi: 10.1186/s12977-020-00546-w

Chen, X., Liu, F., Fu, X., Feng, Y., Zhang, D., Liu, H., et al. (2019). Prevalence of human T-cell lymphotropic virus type-1 infection among blood donors in mainland China: a systematic review and meta-analysis of the last 20 years. *Expert Rev. Hematol.* 12, 579–587. doi: 10.1080/17474086.2019.1632703

Chen, Y., Lv, L., Ye, Y., Li, J., Huang, M., Hu, J., et al. (1992). Research on the morphology, immunology, cytogenetics, and clinical aspects of adult T-cell leukemia. *Chin. J. Hematology.* 08, 110.

Du, J., Chen, C., Gao, J., Xie, J., Rong, X., Xu, X., et al. (2014). History and update of HTLV infection in China. *Virus Res.* 191, 134–137. doi: 10.1016/j.virusres.2014.07.036

Fujino, R., Kawato, K., Ikeda, M., Miyakoshi, H., Mizukoshi, M., and Imai, J. (1991). Improvement of gelatin particle agglutination test for detection of anti-HTLV-I antibody. *Jpn J. Cancer Res.* 82, 367–370. doi: 10.1111/j.1349-7006.1991.tb01856.x

Gessain, A., and Cassar, O. (2012). Epidemiological aspects and world distribution of HTLV-1 infection. *Front. Microbiol.* 3, 388. doi: 10.3389/fmicb.2012.00388

Gessain, A., Ramassamy, J. L., Afonso, P. V., and Cassar, O. (2023). Geographic distribution, clinical epidemiology and genetic diversity of the human oncogenic retrovirus HTLV-1 in Africa, the world's largest endemic area. *Front. Immunol.* 14, 1043600. doi: 10.3389/fimmu.2023.1043600

Hindawi, S., Badawi, M., Fouda, F., Mallah, B., Mallah, B., Rajab, H., et al. (2018). Testing for HTLV 1 and HTLV 2 among blood donors in Western Saudi Arabia: prevalence and cost considerations. *Transfus Med.* 28, 60–64. doi: 10.1111/tme.12440

Hu, J., Lv, L., Zhang, P., Peng, Y., and Chen, Y. (1996). Gene diagnosis of adult T-cell leukemia/lymphoma. *Chin. J. Internal Med.* 9, 48–49.

Itabashi, K., Miyazawa, T., Sekizawa, A., Tokita, A., Saito, S., Moriuchi, H., et al. (2020). A nationwide antenatal human T-cell leukemia virus type-1 antibody screening in Japan. *Front. Microbiol.* 11, 595. doi: 10.3389/fmicb.2020.00595

Iwanaga, M. (2020). Epidemiology of HTLV-1 infection and ATL in Japan: an update. *Front. Microbiol.* 11, 1124. doi: 10.3389/fmicb.2020.01124

Ji, H., Chang, L., Yan, Y., and Wang, L. (2023). Development and validation of a duplex real-time PCR for the rapid detection and quantitation of HTLV-1. *Virol. J.* 20, 9. doi: 10.1186/s12985-023-01970-y

Laperche, S., Sauleda, S., Piron, M., Mühlbacher, A., Schennach, H., Schottstedt, , et al. (2017). Evaluation of sensitivity and specificity performance of elecsys HTLV-I/II assay in a multicenter study in europe and Japan. *J. Clin. Microbiol.* 55, 2180–2187. doi: 10.1128/JCM.00169-17

Luo, L., Chen, Y., Wu, Z., Huang, Y., Lu, L., Li, J., et al. (2024). Clinical characteristics, genetic alterations, and prognosis of adult T-cell leukemia/lymphoma: an 11-year multicenter retrospective study in China. *Am. J. Cancer Res.* 14, 1649–1661. doi: 10.62347/RARP1733

Nozuma, S., and Jacobson, S. (2019). Neuroimmunology of human T-lymphotropic virus type 1-associated myelopathy/tropical spastic paraparesis. *Front. Microbiol.* 10, 885. doi: 10.3389/fmicb.2019.00885

Okamura, J., Uike, N., Utsunomiya, A., and Tanosaki, R. (2007). Allogeneic stem cell transplantation for adult T-cell leukemia/lymphoma. *Int. J. Hematol.* 86, 118–125. doi: 10.1532/IJH97.07070

Proietti, F. A., Carneiro-Proietti, A. B., Catalan-Soares, B. C., and Murphy, E. L. (2005). Global epidemiology of HTLV-I infection and associated diseases. *Oncogene.* 24, 6058–6068. doi: 10.1038/sj.onc.1208968

San Martín, H., Balanda, M., Vergara, N., Valenzuela, M. A., Cartier, L., Ayala, S., et al. (2016). Human T-Lymphotropic Virus Type 1 and 2 Seroprevalence among first-time blood donors in Chile, 2011-2013. *J. Med. Virol.* 88, 1067–1075. doi: 10.1002/jmv.24428

Valcarcel, B., Enriquez-Vera, D., De-la-Cruz-Ku, G., Chambergo-Michilot, D., Calderón-Huaycochea, H., Malpica, L, et al. (2023). Epidemiological features and outcomes of HTLV-1 carriers diagnosed with cancer: A retrospective cohort study in an endemic country. *JCO Glob Oncol.* 9, e2200369. doi: 10.1200/GO.22.00369

Vallinoto, A. C. R., Cayres-Vallinoto, I., Freitas Queiroz, M. A., Ishak, M. O.G., and Ishak, R. (2019). Influence of immunogenetic biomarkers in the clinical outcome of HTLV-1 infected persons. *Viruses* 11, 974. doi: 10.3390/v11110974

Wolf, S., Vercruyssen, M., and Cook, L. (2022). HTLV-1-related adult T-cell leukemia/lymphoma: insights in early detection and management. *Curr. Opin. Oncol.* 34, 446–453. doi: 10.1097/CCO.0000000000000883

Wu, Z. J., Zheng, X. Y., Yang, X. Z., Liu, T. B., Yang, T., Zheng, Z. H., et al. (2016). Clinical characteristics and prognosis in 12 patients with adult T cell leukemia/lymphoma confirmed by HTLV-1 provirus gene detection. *Zhonghua Xue Ye Xue Za Zhi* 37, 1027–1032. doi: 10.3760/cma.j.issn.0253-2727.2016.12.003

Zhao, J., Zhao, F., and Han, W. (2020). HTLV screening of blood donors using chemiluminescence immunoassay in three major provincial blood centers of China. *BMC Infect. Dis.* 20, 581. doi: 10.1186/s12879-020-05282-2

Zuo, X., Zhou, R., Yang, S., and Ma, G. (2023). HTLV-1 persistent infection and ATLL oncogenesis. *J. Med. Virol.* 95, e28424. doi: 10.1002/jmv.28424

frontiers | Frontiers in Cellular and Infection Microbiology

TYPE Original Research
PUBLISHED 22 April 2025
DOI 10.3389/fcimb.2025.1522217

OPEN ACCESS

EDITED BY
Ariadna Petronela Fildan,
Ovidius University, Romania

REVIEWED BY
Sreya Ghosh,
Boston Children's Hospital and Harvard Medical School, United States
George Dimopoulos,
National and Kapodistrian University of Athens, Greece

*CORRESPONDENCE
Weifeng Zhao
zhaoweifeng@suda.edu.cn

RECEIVED 04 November 2024
ACCEPTED 25 March 2025
PUBLISHED 22 April 2025

CITATION
Xiao S, Xu J, Xiao H, Li Y, Chen X, Chen L and Zhao W (2025) Clinical characteristics and prognosis of COVID-19- associated invasive pulmonary aspergillosis in critically patients: a single-center study. *Front. Cell. Infect. Microbiol.* 15:1522217. doi: 10.3389/fcimb.2025.1522217

Clinical characteristics and prognosis of COVID-19-associated invasive pulmonary aspergillosis in critically patients: a single-center study

Shuang Xiao[1], Jie Xu[2], Han Xiao[3], Yonggang Li[4], Xu Chen[2], Li Chen[1] and Weifeng Zhao[1*]

[1]Department of Infectious Diseases, The First Affiliated Hospital of Soochow University, Suzhou, China, [2]Center of Clinical Laboratory, The First Affiliated Hospital of Soochow University, Suzhou, China, [3]Department of Infectious Disease, Qingdao Municipal Hospital, Qingdao, China, [4]Department of Radiology, The First Affiliated Hospital of Soochow University, Suzhou, China

Objective: A single-center retrospective study was conducted according to the latest diagnostic criteria of the European Consortium for Mycology in Medicine/International Society for Human and Animal Mycoses (ECMM/ISHAM) Consensus, which describes the clinical characteristics, factors influencing and prognosis of a group of patients with COVID-19 (Omicron variant) combined with invasive pulmonary mycoses with onset of disease at the end of 2022.

Methods: This study retrospectively analyzed data related to 58 hospitalized patients with severe pneumonia due to COVID-19 infection admitted to the ICU of critical care medicine, respiratory ICU, and ICU of the Department of Infections at the First Affiliated Hospital of Soochow University from December 1, 2022, to January 31, 2023. CAPA was defined according to the ECMM/ISHAM consensus criteria. Our study compared the clinical and microbiological characteristics and associated risk factors of fungal infections and pulmonary fungal infections and performed univariate and multivariate analyses of factors associated with mortality in patients with COVID-19-Associated Pulmonary Aspergillosis (CAPA).

Results: 17 (29.3%) of the 58 critically ill patients were diagnosed with CAPA, of which 10 (58.82%) patients were Probable CAPA and 7 (41.18%) patients were Possible CAPA. Among this *Aspergillus* strains, *Aspergillus fumigatus* strains were found in 13 cases (76.47%) and *Aspergillus niger* strains in 4 cases (23.53%). 7 (41.18%) patients had concomitant bacterial fungal infections with a mortality rate of 57.14% (4/7), of which *Acinetobacter baumannii* was the most common pathogen. Among the patients with CAPA, galactomannan assay of bronchoalveolar lavage fluid (BALF) was performed in 5 patients with a 100% (5/5) positivity rate, and two or more serum galactomannan (GM) assays were performed in 17 patients, with a probability of favorable results in both cases of 41.2% (7/17). The 60-day mortality rate in patients with CAPA was 52.9% (9/17), whereas the non-CAPA patients had a 60-day mortality rate of 24.4% (10/41), which was statistically different (P = 0.035). Diabetes mellitus (P = 0.018, OR: 5.040 (95% CI: 1.314-19.337)), renal insufficiency (P=0.002, OR: 11.259 (95% CI:

2.480-51.111)), chronic obstructive pulmonary disease (COPD) (P = 0.003, OR: 6.939 (95% CI: 1.963-24.531)), elevated interleukin-6 (IL-6) (P = 0.022, OR: 4.160 (95% CI: 1.226~14.113)), mechanical ventilation (P = 0.002, OR: 8.100 (95%CI: 2.132~30.777)), increased duration of steroids use (P = 0.022, OR: 1.071 (95%CI: 1.010~1.135)), increased cumulative dose of steroids use ((P < 0.001, OR: 1.012 (95%CI: 1.009~1.015)), use of tocilizumab (P = 0.020, OR: 11.480 (95%CI: 2.480~51.111)), and increased length of hospitalization in ICU (P = 0.021, OR: 1.038 (95% CI: 1.006 to 1.071)), and increase in the type of antibiotics used (P = 0.002, OR: 1.603 (95% CI: 1.181 to 2.176)) were the risk factors for the occurrence of fungal infections, whereas the use of steroids or not, the use of baricitinib or not, and hypertension did not have a significant effect on the occurrence of fungal infections (P > 0.05). Patients with CAPA had a higher mortality rate, and their hospitalization was prolonged compared to non-CAPA patients. The all-cause mortality rate for patients with CAPA was 52.9%. We also performed univariate and multivariate analyses of potential factors associated with mortality, including the use of mechanical ventilation (P = 0.040 OR: 10.500, (95% CI: 1.115 to 98.914)), advanced age (P = 0.043 OR: 1.212, (95% CI: 1.006 to 1.460)), and a significantly higher CRP level (P = 0.042 OR: 1.043, (95% CI: 1.002~1.078)) had a worse prognosis. Steroids use, gender, and diabetes mellitus were not associated with patient death (P > 0.05).

KEYWORDS

COVID-19, invasive pulmonary aspergillosis, mortality, influencing factors, clinical characteristics, microbiological characteristics

1 Introduction

At the end of 2022, the global COVID-19 outbreak resumed, with the Omicron variant becoming dominant. This variant has numerous mutations that boost its ability to evade humoral immunity and increase transmissibility (Rana et al., 2022). Although Omicron infections are generally less severe, the extreme transmissibility led to a surge in cases and an increase in critically ill patients (Brüssow, 2022; Wu Y. et al., 2022). COVID-19 patients in intensive care units (ICUs) face higher risks of co-infections and mortality (Binkhamis et al., 2023). Pulmonary aspergillosis, an opportunistic infection linked to mechanical ventilation, predominantly affects ICU patients with chemotherapy, transplants, or immunosuppression (Thompson et al., 2020). During COVID-19 epidemics, the virus was found to damage alveolar epithelial and tissue endothelial cells, disrupting lung barriers (Short et al., 2016). Combined with prolonged hospital stays, steroid and immunomodulator use, and the need for invasive mechanical ventilation in most patients with acute respiratory distress syndrome, this makes critically ill COVID-19 patients more prone to bacterial and opportunistic fungal lung infections (*Aspergillus*, *Candida*, *Cryptococcus*, and *Trichinella*), with *Aspergillus* being the most common (Chiurlo et al., 2021). Some studies have reported that the prevalence of CAPA in patients with severe COVID-19 ranges from 2.4% to 34.3% (Kariyawasam et al., 2022). The prognosis for severe CAPA is relatively poor, characterized by high morbidity and mortality rates that range from 22.2% to 71.4% (Kariyawasam et al., 2022; Lamoth et al., 2021; Pasquier et al., 2021). This situation poses a significant threat to public health. Since the beginning of the COVID-19 pandemic, many studies on CAPA have been reported, and the prevalence of CAPA in COVID-19 ICU patients reported in different studies varies widely, which may be related to inconsistent surveillance methods and diagnostic criteria (Chong et al., 2022). In 2020, the European Confederation of Medical Mycology/International Society for Human and Animal Mycoses consensus developed relevant diagnostic criteria and disposition consensus for CAPA. The diagnosis of *Aspergillosis* was categorized as Proven CAPA (histopathological confirmation or *Aspergillus* positive in sterile samples), Probable CAPA (host factors + clinical deterioration + mycological evidence e.g., BALF GM ≥1.0), and Possible CAPA (clinical suspicion with insufficient mycological evidence/non-specific findings), and the relevant host factors that predispose to aspergillosis were defined (Asperges et al., 2024). While this consensus aids in diagnosing and treating CAPA, it remains a clinical challenge (Skóra et al., 2023).

There are few studies on the incidence, prognosis, and associated risk factors of CAPA in the Omicron variant. This retrospective study analyzed CAPA incidence in the Omicron variant, identified risk factors, and assessed their relationship with

patient prognosis. The findings may guide future viral pneumonia treatment, reduce secondary pulmonary mycoses, and improve severe COVID-19 pneumonia survival rates.

2 Materials and methods

2.1 Study population and inclusion-exclusion criteria

We conducted a single-center retrospective observational cohort study of patients admitted to three ICUs (Intensive Care Medicine ICU, Respiratory ICU, and Infectious Disease ICU) of the First Affiliated Hospital of Soochow University between December 1, 2022 and January 31, 2023. No personally identifiable information about participants was accessed during data collection. Inclusion criteria were 1. age ≥18 years; 2. positive SARS-CoV-2 polymerase chain reaction (PCR) test on nasopharyngeal swabs or respiratory samples; and 3. patients diagnosed with COVID-19 severe pneumonia. Exclusion criteria were: 1. patients who died or were automatically discharged within 48 hours of admission; 2. patients who lacked sufficient clinical data; and 3. patients who contracted COVID-19 pneumonia during hospitalization (Table 1).

2.2 Data collection

CAPA in this study was defined according to the consensus criteria for research and clinical guidance published by ECMM/ISHAM 2020. These criteria defined CAPA cases as Proven CAPA, Probable CAPA, and Possible CAPA. This paper collects Probable CAPA and Possible CAPA.

Clinical data, as well as pathogenetic data, were collected from COVID-19 patients, including demographic characteristics, length of hospitalization, inflammatory biomarkers, fungal isolates, infectious agents (*Klebsiella pneumoniae*, *Pseudomonas aeruginosa*, *Escherichia coli*, *Enterobacter cloacae*), underlying diseases [Diabetes mellitus, Hypertension, Hepatic disease, Cardiovascular disease, Chronic kidney disease (CKD), Chronic obstructive pulmonary diseases (COPD), personal history of malignancy, whether mechanically ventilated or not, duration of mechanical ventilation]. The primary outcome indicator was to assess the incidence of proposed or Possible CAPA. Secondary outcome indicators identified CAPA risk factors and assessed the association between relevant risk factors and 60-day mortality. Detailed information on the above can be found in Table 2.

TABLE 1 Criteria for inclusion and exclusion.

Category	Criteria
Inclusion	1. Adults ≥18 years
	2. Confirmed SARS-CoV-2 infection (PCR-positive respiratory sample)
	3. Diagnosis of severe COVID-19 pneumonia
Exclusion	1. Death or self-discharge within 48 hours of admission
	2. Insufficient clinical documentation
	3. Hospital-acquired COVID-19 pneumonia

2.3 Statistical methods

Descriptive statistics were used to assess the baseline characteristics of the entire cohort; the variables involved in this study showed a skewed distribution, and the information of the skewed distribution was expressed as median (M) and interquartile ranges (IQR). Quantitative variables were compared using Student's t-test or Mann-Whitney U-test; we used the Pearson chi-square test or Fisher exact test for qualitative variables. Variables considered clinically relevant and statistically significant in the univariate analysis were included in the multivariate logistic regression analysis. All statistical analyses were performed using IBM SPSS version 22.0 software (IBM et al., USA), and a P value of < 0.05 was considered statistically significant.

3 Results

3.1 Diagnosis of CAPA and its clinical characteristics

From December 1, 2022, to January 31, 2023, a total of 67 patients were diagnosed with severe COVID-19 pneumonia and admitted to the three ICUs of our hospital (Critical Care Medicine ICU, Respiratory ICU, and Infectious Disease ICU), of which 58 patients were enrolled in this study. Among the enrolled critically ill patients with COVID-19, the incidence of CAPA was 29.3% (17/58), 10 (58.82%) patients were diagnosed with Probable CAPA, and 7 (41.18%) patients were diagnosed with Possible CAPA (Figure 1).

We performed univariate and multifactorial analyses of risk factors that may influence the occurrence of CAPA. We found that elderly male patients accounted for most CAPA and non-CAPA patients. Regarding the patients' underlying diseases, we found that the combination of diabetes (P=0.018, OR: 5.040 (95% CI: 1.314~19.337)), renal insufficiency (P=0.002, OR: 11.259 (95% CI: 2.480~51.111)), COPD (P = 0.003, OR: 6.939 (95% CI: 1.963~24.531)) was more likely to develop CAPA (Figure 2), while comorbidities such as hypertension, cerebral infarction, hematencephalon, hepatic disease, and cancer did not show statistically significant differences in whether CAPA occurred (Table 2). Among some inflammatory indicators, elevated IL-6 increased the incidence of CAPA in COVID-19 critically ill patients (P = 0.022, OR: 4.160 (95% CI: 1.226-14.113)) (Figure 2). In addition, mechanical ventilation (P = 0.002, OR: 8.100 (95% CI:

10.3389/fcimb.2025.1522217

TABLE 2 Univariate analysis of risk factors for the occurrence of CAPA.

Characteristics	CAPA (n=17)	NO CAPA (n=41)	Total (n=58)	*P* value
Demographics				
Male [Cases (%)]	12 (70.59)	32 (78.05)	44(75.86)	0.071
Age, median (IQRs)	76.0 (63.0,84.0)	78.0 (71.0,84.0)		0.991
Underlying diseases				
Diabetes [Cases (%)]	7 (41.18)	5 (12.29)	12 (20.69)	**0.034**
Hypertension [Cases (%)]	9 (52.94)	18 (43.90)	27 (46.55)	0.530
Cerebral infarction [Cases (%)]	3 (17.65)	5 (12.29)	8 (13.79)	0.681
Hematencephalon [Cases (%)]	1 (5.88)	2 (4.88)	3 (51.72)	1.000
Cardiovascular disease [Cases (%)]	2 (11.76)	6 (14.63)	8 (13.79)	1.000
Hepatic disease [Cases (%)]	2 (11.76)	5 (12.19)	7 (12.07)	1.000
Renal insufficiency [Cases (%)]	8 (47.06)	3 (7.32)	11 (18.97)	**0.001**
COPD [Cases (%)]	10 (58.82)	7 (17.07)	17 (29.31)	**0.003**
Cancer [Cases (%)]	8 (47.06)	10 (24.39)	18 (31.03)	0.089
Laboratory indicators				
High CRP (IQRs)	135.24 (88.34,219.55)	32 (45.1)		0.274
Elevated IL-6 [Cases (%)]	12 (70.59)	15 (36.59)	27(46.55)	**0.020**
Leucocyte (IQRs)	8.03 (3.76-11.26)	6.5 5(4.47-9.34)	6.68 (3.91-10.39)	0.447
Methods of treatment				
Invasive mechanical ventilation [Cases (%)]	9 (52.94)	5 (12.20)	14 (24.14)	**0.001**
Eat autonomously [Cases (%)]	12 (70.59)	26 (63.41)	38 (65.52)	0.743
Steroids [Cases (%)]	15 (88.24)	32 (78.05)	47 (81.03)	0.789
Steroids Use time, median (IQRs)	15 (10,27)	10 (6.25,16.75)		**0.026**
Cumulative steroid [mg]	89.00(75.00,101.75)	54.00 (37.50,89.00)		**<0.001**
Tolizumab [Cases (%)]	8 (47.06)	3 (7.32)	11 (18.97)	**0.001**
Baricitinib [Cases (%)]	9 (52.94)	13 (31.71)	22 (37.93)	0.153
Length of ICU stay, median (IQRs)	45(31,62)	30 (20,41)		**0.049**
Types of antibiotics (IQRs)	5(3.5-6.0)	2 (1.0-4.0)	3 (2.0-5.0)	**<0.001**
In-hospital mortality [Cases (%)]	9(52.94)	10 (24.39)	19 (32.76)	**0.035**

Statistically significant intergroup differences ($P<0.05$) are highlighted in boldface type.

2.132~30.777)), the use of tolizumab (P = 0.020, OR: 11.480 (95% CI: 2.480~51.111)), and an increase in length of hospitalization (P = 0.021, OR: 1.038 (95% CI: 1.006~ 1.071)) could all increase the risk of infection in CAPA (Figure 3). This study also found that the majority of patients with both CAPA and non-CAPA patients used steroids therapy, with 15 (88.2%) patients with CAPA using steroids within three days of admission and 32 (78.0%) patients with non-CAPA using steroids within three days of admission, and that there was no statistically significant difference between steroids use and non-use of steroids for the occurrence of CAPA, and that As the duration of

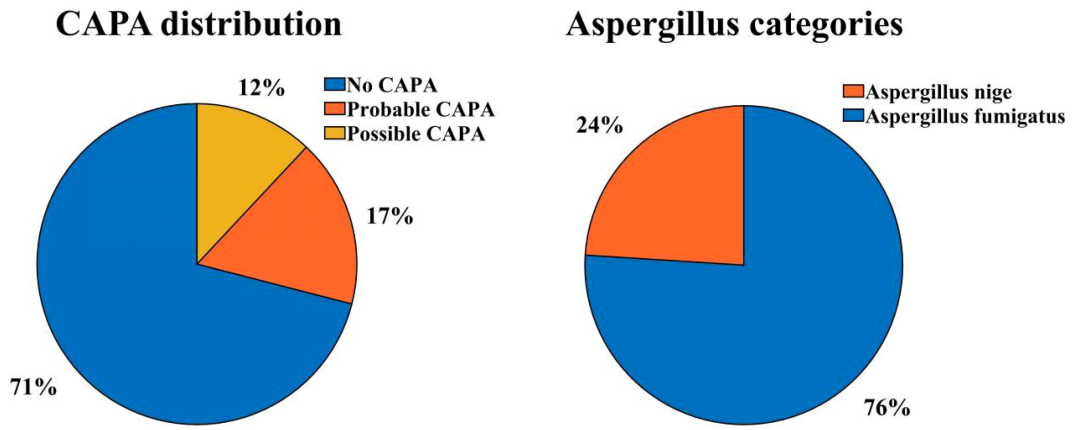

FIGURE 1
CAPA distribution and aspergillus categories.

steroids use increased, the odds of CAPA increased (P < 0.001, OR: 0.043 (95% CI: 0.008~0.221), and the cumulative amount of steroids use increased, the odds of CAPA also increased (P < 0.001, OR: 1.012 (95% CI: 1.009~1.015). At the same time, we also found that the type of antibiotics used before the occurrence of CAPA was higher in CAPA patients than in non-CAPA patients (5 (3.5-6.0) vs. 2 (1.0-4.0)) and that the occurrence of CAPA was also associated with an increase in the type of antibiotics used (P = 0.002, OR: 1.603 (95% CI: 1.181~2.176)) (Figure 2).

3.2 Pathogenetic and imaging characteristics

In this study, all patients underwent more than two sputum cultures, positive for *Aspergillus*. 5 patients underwent bronchoscopic examination, and the Bronchoalveolar Lavage Fluid (BALF) was retained and cultured to reveal *Aspergillus*. Positive strains included the *Aspergillus fumigatus* strain in 13 cases (76.47%) and the *Aspergillus niger* strain in 4 cases (23.53%). 7 (41.18%) patients had co-infections of bacterial and fungal infections, predominantly gram-negative bacteria, most frequently *Acinetobacter baumannii*, and most bacteria were multiresistant. All patients with CAPA underwent more than two serum Galactomannan (GM) tests, and the probability rate of serum mean GM index > 0.5 was 41.2% (7/17). Considering that the COVID-19 virus can be transmitted by aerosol, to safeguard the safety of medical personnel, only five patients in this study underwent BALF GM test, and the GM index were all ≥ 1.0. All CAPA patients were initiated with antifungal drugs at the time of sputum culture or BALF suggestive of *Aspergillus* positivity, and the most commonly used antifungal drug was voriconazole (9/17, 52.94%), followed by esaconazole (5/17, 29.41%) and amphotericin B (3/17, 17.65%) was also used in some patients. All patients were on broad-spectrum antibiotics prior to the onset of CAPA.

In addition, all patients underwent chest CT, and only 2 patients were seen to have vacuolar infiltrate formation in the lungs (Figure 3), while the other portion presented with a diffuse infiltrative presentation of the lungs.

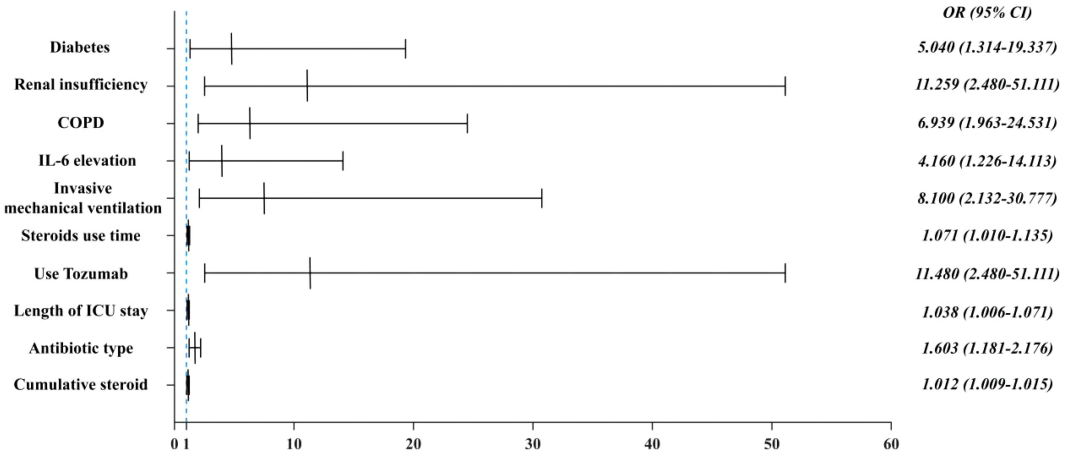

FIGURE 2
Multifactorial analysis of risk factors for the occurrence of CAPA.

10.3389/fcimb.2025.1522217

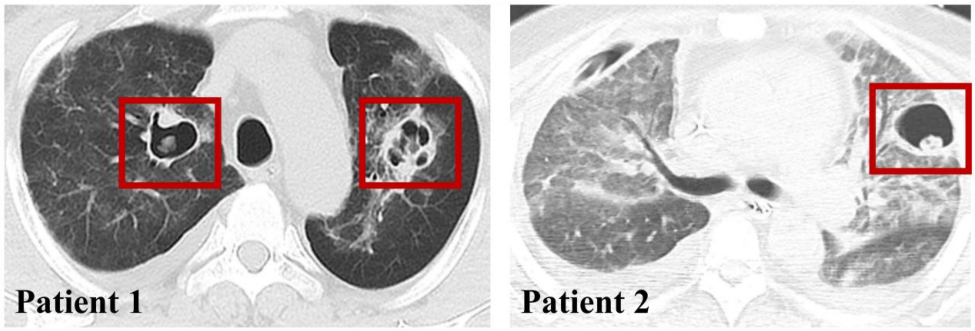

FIGURE 3
CAPA imaging presentation.

3.3 Mortality

As presented in Table 3, the 60-day mortality rate was 52.9% (9/17) in CAPA patients and 24.4% (10/41) in non-CAPA patients, with a statistically significant difference in the 60-day mortality rate between the two (P=0.004, OR: 0.287 (95% CI: 0.087-0.942)). We performed a univariate analysis of the 60-day morbidity and mortality rates by various clinical characteristics affecting patients

TABLE 3 Univariate analysis of risk factors affecting the prognosis of CAPA patients.

	Dead (n=9)	Alive (n=8)	Total (n=17)	*P* value
Male [Cases (%)]	9 (100.00)	3 (37.50)	12 (70.59)	0.090
Age, median (IQRs)	76.00 (65.00,85.00)	68.50 (50.25,84.00)	76.0 (63.0,84.0)	**<0.001**
Invasive mechanical ventilation [Cases (%)]	7 (77.78)	2 (25.00)	10 (58.82)	**0.015**
Hypertension [Cases (%)]	5(55.56)	4 (50.00)	9 (52.94)	1.000
Diabetes[Cases (%)]	5 (55.56)	2 (25.00)	7 (41.18)	0.335
Hematencephalon[Cases (%)]	1 (11.11)	0 (0.00)	2 (25.00)	1.000
COPD [Cases (%)]	7 (77.78)	3 (37.50)	10 (58.82)	0.153
Renal insufficiency [Cases (%)]	3 (33.33)	1 (12.50)	4 (23.53)	0.576
Steroids [Cases (%)]	9 (100.00)	6 (75.00)	15 (88.24)	0.206
Steroids Use time, median (IQRs)	19.00 (12.00,31.00)	12.50 (7.50, 22.75)	15 (10,27)	**<0.001**
Cumulative steroid [mg]	75.00 (74.07,118.13)	95.44 (75.19,122.25)		0.862
Tozumab [Cases (%)]	5 (55.56)	3 (37.50)	8 (47.06)	0.637
CRP, median (IQRs)	192.00 (119.54,219.55)	88.34 (36.33,134.00)	135.24 (88.34,219.55)	**<0.001**
Elevated IL-6 [Cases (%)]	7 (77.78)	5 (62.50)	12 (70.59)	0.620
Elevated PCT [Cases (%)]	9 (100.00)	6 (75.00)	15 (88.24)	0.206
Leucocytemedian (IQRs)	12.52 (8.03,11.69)	10.38 (4.84,14.32)	8.03 (3.76-11.26)	0.972
Positive GM tests [Cases (%)]	4 (44.44)	3 (37.50)	7 (41.18)	1.000
Types of antibiotics median (IQRs)	5.00 (4.00,8.00)	5.00 (4.00,7.00)	5 (3.5-6.0)	0.894
Combined bacterial infections [Cases (%)]	7 (77.78)	5 (62.50)	12 (70.59)	0.620

Statistically significant intergroup differences (P<0.05) are highlighted in boldface type.

with CAPA. The results indicated that age (P < 0.001), mechanical ventilation (P = 0.015), duration of steroids administration (P < 0.001), and elevated C-reactive protein(CRP) (P < 0.001) had statistically significant differences in whether a patient died or not. However, when these risk factors were included in a multifactorial Logistic regression analysis, the results showed that the use of mechanical ventilation (P = 0.040 OR: 10.500, (95% CI: 1.115-98.914)) (Figure 4), advanced age (P = 0.043 OR: 1.212, (95% CI: 1.006-1.460)) and CRP levels were significantly higher (P = 0.042 OR: 1.043, (95% CI: 1.002~1.078)) (Figure 4), while gender and duration of steroids use had no significant effect on prognosis (P > 0.05) (Table 3).

4 Discussion

With the global spread of COVID-19, there are more and more reports about patients with combined bacterial and fungal infections, among which fungal infections, especially *Aspergillus* infections, whose higher infection rate and mortality pose a severe threat to the life and health of patients, so it is essential to diagnose the co-infections at an early stage and to make the correct clinical interventions [14]. In our study, the incidence of COVID-19 co-infection with pulmonary mycosis was 29.3%, with a mortality rate of 52.9% (9/17) (Table 2). The mortality rate of COVID-19 patients with co-infections with bacterial fungi was as high as 57.14% (4/7). In comparison, the 90-day mortality rate of non-CAPA patients was significantly lower 24.4% (10/41) than that of patients with co-infections with fungal infections (P = 0.035) (Table 2). Graciela et al. described the clinical, microbiological, and radiological characteristics of 86 patients diagnosed with probable CAPA in a Mexican hospital. They described the mortality rate, which was as high as 60% in their CAPA patients (Hernández-Silva et al., 2024). In a meta-analysis, the incidence and mortality of CAPA in patients admitted to the ICU were estimated to be 10.2% and 54.9% (Mitaka et al., 2021), and their mortality rate remained high. A meta-analysis by Woon et al. included a total of 729 patients with COVID-19, of whom 14.9% (109/729) were diagnosed with CAPA, with a prevalence ranging from 3.3 to 34.4% between 3.3 and 34.4%, with an all-cause hospitalization mortality rate of 42.6% (OR 3.39; 95% CI,1.97-5.86; P < 0.001) (Chong et al., 2022). It is evident that despite the overall better prognosis of mildly ill patients with Omicron infections, there is a high incidence of CAPA in critically ill patients and an extremely high mortality rate in patients with CAPA.

In treating COVID-19 pneumonia, glucocorticoids, and immunosuppressants have been used as standard therapeutic tools, which play an essential role in controlling the inflammatory response and reducing the mortality of the patients. However, when steroids and immunosuppressants are applied, the risk of CAPA in patients increases. In our study, whether steroids therapy was used or not had no effect on whether CAPA occurred; however, with the prolongation of steroids use (P = 0.002, OR: 1.603 (95% CI: 1.181~2.176)) and the increase in cumulative dose of steroids use ((P < 0.001, OR: 1.012 (95% CI: 1.009~1.015) (Figure 2). The incidence of CAPA increased. Hashim et al. concluded in a meta-analysis of 21 studies and 5174 patients that the risk of CAPA was associated with the use of high-dose glucocorticoids and not significantly correlated with low-dose steroids and that patients with COVID-19 were at risk of CAPA even without steroids therapy (Hashim et al., 2023). Gregoire et al. studied 141 patients with CAPA in a single-center retrospective observational study analyzing the incidence and risk factors for COVID-19-associated pulmonary aspergillosis in an intensive care unit. In univariate analyses, patients using steroids had a higher probability of developing CAPA. However, multivariate analyses did not observe an association between steroids and CAPA development (Gregoire et al., 2021). Currently, there are conflicting results in different studies about whether steroids are a risk factor for the development of CAPA, probably because steroids were heavily used as an effective treatment during the COVID-19 period. The baseline conditions of the patients, as well as the dosage of steroids used

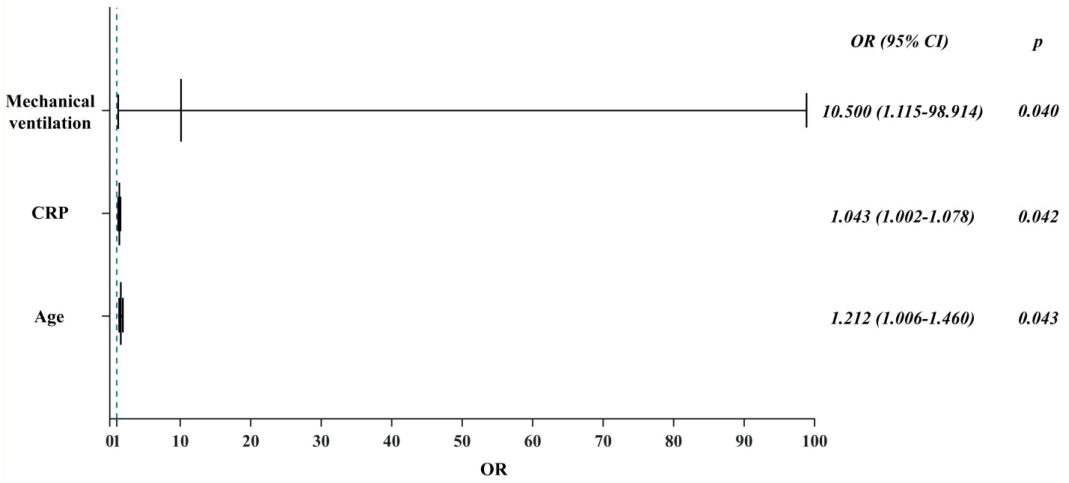

FIGURE 4
Multifactorial analysis of factors influencing the prognosis of CAPA patients.

and the duration of their use, varied in each study center, resulting in conflicting results.

In the present study, we found that the incidence of CAPA increased only when glucocorticoids were used for an extended period. This may be because the steroids were used for a shorter period and did not have a significant immunomodulatory effect on the patients. In our univariate and multivariate analyses of risk factors for CAPA mortality, we found that neither the use of steroids nor the duration of steroids use significantly affected CAPA mortality (Table 3). Tolizumab and baricitinib were also commonly used as immunomodulators during the COVID-19 pneumonia epidemic. Several previous studies have identified the use of tocilizumab as a risk factor for CAPA (Cadena et al., 2021; Prattes et al., 2022), and our study found that the use of tocilizumab (P = 0.020) increased the incidence of CAPA. In contrast, the use of baricitinib did not affect the presence of CAPA; in a retrospective study conducted at the National Institute of Respiratory Research (INER) in Mexico City, the incidence of CAPA at its center was only 4.13%. One factor contributing to its low prevalence was the rare use of immunomodulators such as tocilizumab at this center (Hernández-Silva et al., 2024). A meta-analysis showed that the combination of baricitinib with dexamethasone and anti-il-6 inhibitors significantly reduced 28-day mortality (Selvaraj et al., 2022); Albuquerque et al. found that the efficacy of baricitinib was not inferior to that of tocilizumab, and that baricitinib had a shorter half-life compared to tocilizumab, and the shorter half-life of baricitinib compared with tocilizumab was beneficial in reducing the risk of secondary infections (Albuquerque et al., 2023), and the present study found that the use of baricitinib did not increase the prevalence of CAPA as tocilizumab did, and the role that glucocorticosteroids and various types of immunosuppressants and immunomodulators have played in the treatment of COVID-19 pneumonia is well documented, and previous studies have confirmed that glucocorticosteroids may increase the prevalence of COVID-19 pneumonia and that glucocorticosteroids may reduce the risk of secondary infections. Previous studies have also confirmed that glucocorticoids can reduce the mortality rate of COVID-19 ventilated patients (Recovery: Randomised Evaluation of Covid-19 Therapy, 2020), but the side effects should be considered comprehensively, and steroids and immunomodulators can be used in the right amount and at the right time. In addition, we found that patients with diabetes mellitus (P = 0.018), renal insufficiency (P = 0.002), and COPD (P = 0.003) were more prone to CAPA. In the follow-up treatment and monitoring of clinical indicators of patients with COVID-19, we observed an increase in interleukin-6 (P = 0.022), mechanical ventilation (P = 0.002), and an increase in the hospitalization duration (P = 0.021), and increased type of antibiotic use (P = 0.002) were risk factors for the development of CAPA (Table 2).

Currently, the incidence of bacterial co-infections in patients with COVID-19 is low, but in the intensive care unit, the incidence of co-infections with bacterial infections and the mortality rate is high due to the prolonged stay in the ICU, the need for prolonged mechanical ventilation, and the high incidence of pulmonary infections in the critically ill patients (Wu H. Y. et al., 2022), and the current reports on both bacterial and fungal co-infections in COVID-19 are extremely rare, and inherently there is no accurate incidence and prognosis of the In our study, we found that the probability of COVID-19 co-infection with both fungal and bacterial infections was about 41.18%, and the mortality rate was as high as 57.14%, and the most common bacterial strain was *Acinetobacter baumannii*, and some previous studies have found that most of the co-infections with bacterial infections of COVID-19 in the ICU were gram-negative (*Pseudomonas aeruginosa*, *Enterobacteriaceae*, and *Klebsiella pneumoniae*) (Bardi et al., 2021; Naseef et al., 2022). Our findings showed that the primary co-infected strain was *Acinetobacter baumannii*. In a retrospective study by Yang et al., a total of 20 critically ill patients with COVID-19, all of whom were admitted to the ICU, were enrolled. The reasons for this may lie in the different ICU environments in different study centers, the use of antibiotics, and the small number of cases preventing a uniform conclusion. All patients with CAPA had large numbers of *Aspergillus* found on more than two sputum cultures or BALF cultures. All patients underwent a serum GM test, which had a positive rate of 41.2% (7/17), and five patients with CAPA underwent an BALF GM test, which was positive in all cases. A previous report found the sensitivity of alveolar lavage fluid GM to be 66.7% in CAPA cases, but only 21.4% were positive for serum GM (Armstrong-James et al., 2020). We can see that BALF is vital in diagnosing CAPA. However, fiberoptic bronchoscopy is rare in many healthcare institutions because the COVID-19 virus can be transmitted by aerosol. CAPA patients with negative serum GM tests are present; some CAPA patients may be underdiagnosed. Therefore, the diagnosis of CAPA should not be limited to serum GM but should be based on sputum culture, CT manifestations, clinical symptoms, and host factors of ECMM/ISHAM.

In this study, the mortality rate of CAPA patients was 57.14% (4/7), which was much higher than the 90-day mortality rate of 24.4% (10/41) in non-CAPA patients (P = 0.004, OR: 0.28, (95% CI: 0.087~0.942)) (Table 2), and among CAPA patients, the use of mechanical ventilation (P = 0.040 OR: 10.500, (95% CI: 1.115~98.914)), advanced age (P = 0.043 OR: 1.212, (95% CI: 1.006~1.460)) and significantly elevated CRP levels (P = 0.042 OR: 1.043, (95% CI: 1.002~1.078)) had a poor prognosis (Figure 3), and all CAPA patients were treated with antifungal therapy when they were found to be *Aspergillus*, and of the 17 patients with CAPA, nine patients were treated with voriconazole, five patients were treated with esaconazole, and three patients were treated with antifungal therapy with amphotericin B. However, we found that timely antifungal therapy did not significantly improve the patient's prognosis, which may be related to the patient's severe condition and prolonged disease duration. For the targets of the drugs as antifungal mainly include: 1. Clinical resolution: ≥72-hour fever remission + respiratory symptom improvement (SOFA score decrease ≥2 points); 2. Microbiological clearance: Negative fungal culture/PCR from respiratory samples on sequential testing; 3. Radiographic stabilization: ≥50% reduction in pulmonary infiltrates on CT within 14 days; 4. Inflammatory normalization: CRP <20 mg/L + IL-6 <40 pg/mL sustained for

5 days (Verweij et al., 2021). The CAPAs mainly occurred in the ICUs. In patients with prolonged disease duration and poor prognosis, their COVID-19 disease duration mainly determines their mortality rate. Antifungal therapy did not improve the prognosis of either proven CAPA, probable CAPA, or possible CAPA (Russo et al., 2024; van Grootveld et al., 2023). Therefore, preventing CAPA is essential in managing critically ill patients with COVID-19.

Our study still needs some improvement. Firstly, this study is a single-center study with a small sample size, so some of the conclusions may differ from those of other centers due to the different diagnostic methods and treatments in each treatment center. Secondly, this study needs more drug resistance monitoring of *Aspergillus* and has limited reference value for using antibiotics to treat COVID-19 combined *Aspergillus* strains. Furthermore, because all patients were COVID-19 critically ill, we excluded patients who died or were automatically discharged within 48 hours of admission. However, these patients may have had a longer course of the disease and fungal infection before admission, so our study found the CAPA incidence and mortality rates. However, they were already at a high level and may be biased compared to the facts. Finally, because critically ill COVID-19 patients are too sick to be diagnosed by histology or direct microscopy, this study was limited to patients with proposed CAPA and suspected CAPA and lacked studies of patients with confirmed CAPA.

5 Conclusions

In conclusion, we found a high prevalence of CAPA (29.3%) in cases of severe COVID-19 pneumonia and a mortality rate of 52.9% in patients with CAPA. Risk factors associated with the development of CAPA include underlying diseases such as diabetes, IL-6 elevation, renal insufficiency, and chronic obstructive pulmonary disease, as well as mechanical ventilation, tocilizumab use, and prolonged hospitalization. Previous studies on the use of glucocorticoids have been controversial, with some suggesting that the use of glucocorticoids increases the incidence of CAPA and may worsen the prognosis. In contrast, others have found that using glucocorticoids does not make a significant difference in the occurrence of CAPA and leads to a favorable prognosis. However, our study found that short-term use of glucocorticosteroids in appropriate doses did not increase the incidence of CAPA and helped to improve the prognosis of patients; when glucocorticosteroids were used for a prolonged period, they led to an increase in the incidence of CAPA. Of note, mortality is significantly higher in patients with CAPA compared with non-CAPA patients, and mechanical ventilation, advanced age, and elevated C-reactive protein levels are considered poor prognostic indicators in patients with CAPA. Prevention of CAPA through careful monitoring of high-risk patients, rational use of glucocorticoids and immunomodulators, and effective infection control measures remains a top priority in managing severe COVID-19 cases.

However, we must also note the limitations of our study, including the single-centre design, small sample size, and exclusion of specific patient groups that could have biased our findings. In order to validate our findings and gain further insight into the epidemiology, risk factors, and CAPA management strategies of critically ill COVID-19 patients, future multicenter collaborative studies with larger sample sizes are warranted.

Data availability statement

The original contributions presented in the study are included in the article/supplementary material. Further inquiries can be directed to the corresponding author.

Author contributions

SX: Conceptualization, Data curation, Formal Analysis, Investigation, Methodology, Project administration, Software, Supervision, Validation, Visualization, Writing – original draft, Writing – review & editing. JX: Data curation, Methodology, Resources, Supervision, Validation, Writing – review & editing. HX: Investigation, Methodology, Software, Validation, Writing – review & editing. YL: Resources, Software, Validation, Writing – review & editing. XC: Software, Validation, Visualization, Writing – review & editing. LC: Supervision, Validation, Writing – review & editing. WZ: Conceptualization, Data curation, Funding acquisition, Methodology, Resources, Supervision, Validation, Writing – review & editing.

Funding

The author(s) declare that financial support was received for the research and/or publication of this article. This study was supported by the Beijing Huidao Technology Project Grant (H220799).

Acknowledgments

Thanks for the clinical data provided by the First Affiliated Hospital of Soochow University.

Conflict of interest

The authors declare that the research was conducted in the absence of any commercial or financial relationships that could be construed as a potential conflict of interest.

Generative AI statement

The author(s) declare that no Generative AI was used in the creation of this manuscript.

Publisher's note

References

Albuquerque, A. M., Eckert, I., Tramujas, L., Butler-Laporte, G., McDonald, E. G., Brophy, J. M., et al. (2023). Effect of tocilizumab, sarilumab, and baricitinib on mortality among patients hospitalized for COVID-19 treated with corticosteroids: a systematic review and meta-analysis. *Clin. Microbiol. Infect.* 29, 13–21. doi: 10.1016/j.cmi.2022.07.008

Armstrong-James, D., Youngs, J., Bicanic, T., Abdolrasouli, A., Denning, D. W., Johnson, E., et al. (2020). Confronting and mitigating the risk of COVID-19 associated pulmonary aspergillosis. *Eur. Respir. J.* 56, 2002554. doi: 10.1183/13993003.02554-2020

Asperges, E., Pesare, R., Bassoli, C., Calia, M., Lerta, S., Citiolo, F., et al. (2024). The prognostic role of diagnostic criteria for COVID-19-associated pulmonary aspergillosis: A cross-sectional retrospective study. *Antibiotics.* 13, 150. doi: 10.3390/antibiotics13020150

Bardi, T., Pintado, V., Gomez-Rojo, M., Escudero-Sanchez, R., Azzam Lopez, A., Diez-Remesal, Y., et al. (2021). Nosocomial infections associated to COVID-19 in the intensive care unit: clinical characteristics and outcome. *Eur. J. Clin. Microbiol. Infect. Dis.* 40, 495–502. doi: 10.1007/s10096-020-04142-w

Binkhamis, K., Alhaider, A. S., Sayed, A. K., and Almufleh, Y. K. (2023). Prevalence of secondary infections and association with mortality rates of hospitalized COVID-19 patients. *Ann. Saudi. Med.* 43, 243–253. doi: 10.5144/0256-4947.2023.243

Brüssow, H. (2022). COVID-19: Omicron - the latest, the least virulent, but probably not the last variant of concern of SARS-CoV-2. *Microb. Biotechnol.* 15, 1927–1939. doi: 10.1111/1751-7915.14064

Cadena, J., Thompson, G. R., and Patterson, T. F. (2021). Aspergillosis: epidemiology, diagnosis, and treatment. *Infect. Dis. Clin. North. Am.* 35, 415–434. doi: 10.1016/j.idc.2021.03.008

Chiurlo, M., Mastrangelo, A., Ripa, M., and Scarpellini, P. (2021). Invasive fungal infections in patients with COVID-19: A review onpatho-genesis, epidemiology, clinical features, treatment, and outcomes. *New. Microbiol.* 44 (2), 71–83.

Chong, W. H., Saha, B. K., and Neu, K. P. (2022). Comparing the clinical characteristics and out-comes of COVID-19-associate pulmonary aspergillosis (CAPA): a systematic review and meta-analysis. *Infection.* 50, 43–56. doi: 10.1007/s15010-021-01701-x

Gregoire, E., Pirotte, B. F., Moerman, F., Altdorfer, A., Gaspard, L., Firre, E., et al. (2021). Incidence and risk factors of COVID-19-associated pulmonary aspergillosis in intensive care unit-A monocentric retrospective observational study. *Pathogens.* 10, 1370. doi: 10.3390/pathogens10111370

Hashim, Z., Nath, A., Khan, A., Gupta, M., Kumar, A., Chatterjee, R., et al. (2023). Effect of glucocorticoids on the development of COVID-19-associated pulmonary aspergillosis: A meta-analysis of 21 studies and 5174 patients. *Mycoses.* 66, 941–952. doi: 10.1111/myc.13637

Hernández-Silva, G., Corzo-León, D. E., Becerril-Vargas, E., Peralta-Prado, A. B., Odalis, R. G., Morales-Villarreal, F., et al. (2024). Clinical characteristics, bacterial coinfections and outcomes in COVID-19-associated pulmonary aspergillosis in a third-level Mexican hospital during the COVID-19 pre-vaccination era. *Mycoses.* 67, e13693. doi: 10.1111/myc.13693

Kariyawasam, R. M., Dingle, T. C., Kula, B. E., Vandermeer, B., Sligl, W. I., and Schwartz, I. S. (2022). Defining COVID-19-associated pulmonary aspergillosis: systematic review and meta-analysis. *Clin. Microbiol. Infect.* 28, 920–927. doi: 10.1016/j.cmi.2022.01.027

Lamoth, F., Lewis, R. E., Walsh, T. J., and Kontoyiannis, D. P. (2021). Navigating the uncertainties of COVID-19-associated aspergillosis: A comparison with influenza-associated aspergillosis. *J. Infect. Dis.* 224, 1631–1640. doi: 10.1093/infdis/jiab163

Mitaka, H., Kuno, T., Takagi, H., and Patrawalla, P. (2021). Incidence and mortality of COVID-19-associated pulmonary aspergillosis: A systematic review and meta-analysis. *Mycoses.* 64, 993–1001. doi: 10.1111/myc.13292

Naseef, H. A., Mohammad, U., Al-Shami, N., Sahoury, Y., Abukhalil, A. D., Dreidi, M., et al. (2022). Bacterial and fungal co-infections among ICU COVID-19 hospitalized patients in a Palestinian hospital: a retrospective cross-sectional study. *F1000Res.* 11, 30. doi: 10.12688/f1000research.74566.2

Pasquier, G., Bounhiol, A., Robert, G. F., Zahar, J. R., Gangneux, J. P., Novara, A., et al. (2021). A review of significance of Aspergillus detection in airways of ICU COVID-19 patients. *Mycoses.* 64, 980–988. doi: 10.1111/myc.13341

Prattes, J., Wauters, J., Giacobbe, D. R., Salmanton-García, J., Maertens, J., Bourgeois, M., et al. (2022). Risk factors and outcome of pulmonary aspergillosis in critically ill coronavirus disease 2019 patients-a multinational observational study by the European Confederation of Medical Mycology. *Clin. Microbiol. Infect.* 28, 580–587. doi: 10.1016/j.cmi.2021.08.014

Rana, R., Kant, R., Huirem, R. S., Bohra, D., and Ganguly, N. K. (2022). Omicron variant: Current insights and future directions. *Microbiol. Res.* 265, 127204. doi: 10.1016/j.micres.2022.127204

Recovery: Randomised Evaluation of Covid-19 Therapy (2020). *Low-cost dexamethasone reduces death by up to one third in hospitalised patients with severe respiratory complications of COVID-19*. Available online at: www.recoverytrial.net/files/recovery_dexamethasone_statement_160620_final.pdf (Accessed 17 June 2020).

Russo, A., Serraino, R., Serapide, F., Bruni, A., Garofalo, E., Longhin, F., et al. (2024). COVID-19-associated pulmonary aspergillosis in intensive care unit: A real-life experience. *Heliyon.* 10, e24298. doi: 10.1016/j.heliyon.2024.e24298

Selvaraj, V., Finn, A., Lal, A., Khan, M. S., Dapaah-Afriyie, K., and Carino, G. P. (2022). Baricitinib in hospitalised patients with COVID-19: A meta-analysis of randomised controlled trials. *EClinicalMedicine.* 49, 101489. doi: 10.1016/j.eclinm.2022.101489

Short, K. R., Kasper, J., van der Aa, S., Andeweg, A. C., Zaaraoui-Boutahar, F., Goeijenbier, M., et al. (2016). Influenza virus damages the alveolar barrier by disrupting epithelial cell tight junctions. *Eur. Respir. J.* 47, 954–966. doi: 10.1183/13993003.01282-2015

Skóra, M., Gajda, M., Namysł, M., Wordliczek, J., Zorska, J., Piekiełko, P., et al. (2023). COVID-19-associated pulmonary aspergillosis in intensive care unit patients from Poland. *J. Fungi.* 9, 666. doi: 10.3390/jof9060666

Thompson Iii, G. R., Cornely, O. A., Pappas, P. G., Patterson, T. F., Hoenigl, M., Jenks, J., et al. (2020). Invasive *aspergillosis* as an under-recognized superinfection in COVID-19. Open. *Forum. Infect. Dis.* 7, ofaa242. doi: 10.1093/ofid/ofaa242

van Grootveld, R., van der Beek, M. T., Janssen, N. A. F., Ergün, M., van Dijk, K., Bethlehem, C., et al. (2023). Incidence, risk factors and pre-emptive screening for COVID-19 associated pulmonary aspergillosis in an era of immunomodulant therapy. *J. Crit. Care* 76, 154272. doi: 10.1016/j.jcrc.2023.154272

Verweij, P. E., Brüggemann, R. J. M., Azoulay, E., Bassetti, M., Blot, S., Buil, J. B., et al. (2021). Taskforce report on the diagnosis and clinical management of COVID-19 associated pulmonary aspergillosis. *Intensive Care Med.* 47, 819–834. doi: 10.1007/s00134-021-06449-4

Wu, H. Y., Chang, P. H., Chen, K., Lin, I. F., Hsih, W. H., Tsai, W. L., et al. (2022). Coronavirus disease 2019 (COVID-19) associated bacterial coinfection: Incidence, diagnosis and treatment. *J. Microbiol. Immunol. Infect.* 55, 985–992. doi: 10.1016/j.jmii.2022.09.006

Wu, Y., Long, Y., Wang, F., Liu, W., and Wang, Y. (2022). Emergence of SARS-CoV-2 Omicron variant and strategies for tackling the infection. *Immun. Inflamm. Dis.* 10, e733. doi: 10.1002/iid3.733

frontiers | Frontiers in Cellular and Infection Microbiology

TYPE Original Research
PUBLISHED 02 May 2025
DOI 10.3389/fcimb.2025.1435970

OPEN ACCESS

EDITED BY
Diana Manolescu,
Victor Babes University of Medicine and Pharmacy, Romania

REVIEWED BY
Marie Louise Guadalupe Attwood,
North Bristol NHS Trust, United Kingdom
Emil Robert Stoicescu,
Victor Babes University of Medicine and Pharmacy, Romania

*CORRESPONDENCE
Yi Jin
hnjinyimd@163.com

RECEIVED 21 May 2024
ACCEPTED 19 March 2025
PUBLISHED 02 May 2025

CITATION
Huang J, Chen P, Zhang Z, Cheng C, Peng P, Li Y, Meng D, Liu T and Jin Y (2025) Synovial fluid fibrin degradation product can be used as a new auxiliary marker for periprosthetic joint infection diagnosis. *Front. Cell. Infect. Microbiol.* 15:1435970. doi: 10.3389/fcimb.2025.1435970

Synovial fluid fibrin degradation product can be used as a new auxiliary marker for periprosthetic joint infection diagnosis

Jincheng Huang[1], Peng Chen[2], Zhaodong Zhang[3], Cheng Cheng[1], Puji Peng[1], Yunfei Li[1], Dongfang Meng[4], Tao Liu[1] and Yi Jin[1]*

[1]Department of Orthopaedics, Henan Provincial People's Hospital, Henan University People's Hospital, Zhengzhou University People's Hospital, Zhengzhou, Henan, China, [2]Department of Orthopaedics, Second Affiliated Hospital of Luohe Medical College, Luohe, Henan, China, [3]Department of Orthopaedics, Huaihe Hospital of Henan University, Kaifeng, Henan, China, [4]Department of Traditional Chinese Orthopedics, First Affiliated Hospital of Henan University of Traditional Chinese Medicine, Zhengzhou, Henan, China

Background: While the value of blood coagulation markers, such as D-Dimer, Fibrinogen, platelet count/mean platelet volume ratio (PC/MPV), and Fibrin Degradation Product (FDP), in the diagnosis of periprosthetic joint infection (PJI) has been explored in recent years, the significance of synovial fluid coagulation markers in PJI diagnosis remains unclear. Therefore, this study aims to investigate the potential value of synovial fluid D-Dimer (sD-Dimer) and synovial fluid FDP (sFDP) in the diagnosis of PJI.

Materials and methods: In a prospective study, the levels of serum C-reactive Protein (CRP), Erythrocyte Sedimentation Rate (ESR), sD-Dimer, and sFDP were measured and compared in 56 patients with PJI (Group A) and 40 patients with aseptic loosening (Group B) who presented at our department from March 1st, 2020, to December 31st, 2023. The diagnostic efficacy of these markers in PJI diagnosis was assessed using the area under the curve (AUC) of the receiver operating characteristic (ROC) curve.

Results: The levels of CRP, ESR, sD-Dimer, and sFDP in Group A were significantly higher than the levels in Group B. The AUC values, optimal threshold values, sensitivity, and specificity for CRP, ESR, sD-Dimer, and sFDP in PJI diagnosis were as follows: CRP [0.920 (95% confidence interval (CI), 0.846–0.965), >6.77, 76.69%, 95.00%], ESR [0.905 (95% CI, 0.828–0.955), >41, 73.21%, 92.50%], sD-Dimer [0.788 (95% CI, 0.692–0.864), >738.65, 66.07%, 80.00%], and sFDP [0.869 (95% CI, 0.785–0.929), >1558.35, 91.07%, 70.00%]. Furthermore, sFDP demonstrated similar performance in PJI diagnosis to CRP

and ESR, while sD-Dimer exhibited inferior performance in PJI diagnosis compared to CRP and ESR.

Conclusions: sFDP shows promise as a valuable new adjunctive diagnostic marker for PJI. Further investigations with larger sample sizes are warranted.

KEYWORDS

prosthetic joint infection, synovial fluid, CRP, ESR, D-dimer, fibrin degradation product, diagnosis

Introduction

Despite the publication of guidelines by the 2010 American Academy of Orthopedic Surgeons (Della Valle et al., 2011), 2013 Musculoskeletal Infection Society (MSIS) (Parvizi and Gehrke, 2014), 2018 International Consensus Meeting (ICM) (Parvizi et al., 2018), 2014 European Bone and Joint Infection Society (EBJIS) (Tande and Patel, 2014), and 2021 EBJIS criteria (McNally et al., 2021) for PJI diagnosis, the timely and accurate diagnosis of periprosthetic joint infection (PJI) remains challenging.

Synovial fluid, also referred to as joint fluid, is situated within the articular joint cavity. It undergoes significant alterations during joint pathology and is considered a crucial component of the diagnostic algorithm for confirming or excluding PJI (Vale et al., 2023). Traditionally, the analysis of synovial fluid has primarily focused on parameters such as synovial leukocyte count, synovial polymorphonuclear percentage (sPMN%), and bacterial culture (Squire et al., 2011). However, the optimal thresholds and diagnostic value of synovial leukocyte count and sPMN% in PJI diagnosis remain subjects of debate (Yi et al., 2015; Pagliaccetti et al., 2021; Abdelaziz et al., 2022). Furthermore, synovial culture has demonstrated only moderate accuracy, with the confirmation or exclusion of PJI often requiring several days of culture (Carli et al., 2019). Consequently, the evaluation of numerous novel synovial markers, including calprotectin (Peng et al., 2022), interleukin-6 (Mihalic et al., 2020), S100 calcium-binding protein A8 (S100A8), S100 calcium-binding protein A9 (S100A9) (Xu et al., 2023), lactate glucose ratio (Berthoud et al., 2020), D-lactate (Karbysheva et al., 2020), and α-Defensin (Zeng et al., 2021) for diagnosing PJI has been undertaken. While some of these emerging synovial markers show promising performance in PJI diagnosis, their widespread adoption in routine clinical practice is hindered by the requirement for specialized antibodies and equipment. Therefore, it is imperative to identify convenient and efficient synovial markers for the diagnosis of PJI.

Although coagulation markers have traditionally been utilized for detecting venous thromboembolism, recent studies have indicated that elevated blood coagulation markers, such as D-Dimer (Shahi et al., 2017; Huang et al., 2019), Fibrinogen (Huang et al., 2021), platelet count/mean platelet volume ratio (PC/MPV) (Paziuk et al., 2020; Sahin et al., 2021) and Fibrin Degradation Product (FDP) (Fujimoto et al., 2018; Xu et al., 2019) may serve as indicators of PJI. Furthermore, research has shown that sFDP and sD-Dimer are markedly expressed in the synovium during inflammatory conditions like rheumatoid arthritis (Anil et al., 2022), and the expression of sD-Dimer is notably elevated in foals with septic joints compared to those without infection (Ewald, 1989). Nevertheless, the applicability of sFDP and sD-Dimer in the diagnosis of PJI remains uncertain.

As C-reactive protein (CRP) and erythrocyte sedimentation rate (ESR) are widely recommended as PJI diagnostic markers in various guidelines (Della Valle et al., 2011; Parvizi and Gehrke, 2014; Tande and Patel, 2014; Parvizi et al., 2018; McNally et al., 2021), the objective of this investigation is to assess the diagnostic utility of sD-Dimer and sFDP in the context of PJI compared with CRP and ESR. Our hypothesis posits that: (i) levels of sD-Dimer and sFDP in PJI patients will exhibit elevation compared to individuals with aseptic loosening; (ii) sD-Dimer and sFDP will demonstrate comparable diagnostic efficacy in PJI detection when compared with CRP and ESR.

Materials and methods

This study was conducted in strict adherence to the ethical guidelines outlined in the Declaration of Helsinki (Ethical Principles for Medical Research Involving Human Subjects) and received approval from the Ethics Board of Henan Provincial People's Hospital (Approval No. 202080). Prior to participation, informed consent was obtained from all participants or their legally

Abbreviations: CRP, C-reactive Protein (CRP); ESR, Erythrocyte Sedimentation Rate; sD-Dimer, synovial fluid D-Dimer; sFDP, synovial fluid Fibrin Degradation Product; AUC, Area under the curve; ROC, Receiver operating characteristics; IQR, Interquartile range; PJI, Periprosthetic joint infection; PMN, Polymorph neutrophiles; THA, Total hip arthroplasty; TJA, Total joint arthroplasty; TKA, Total knee arthroplasty; ICM, International consensus meeting; MSIS, Musculoskeletal infection society.

authorized representatives, ensuring the protection of their rights and welfare throughout the research process.

Inclusion criteria

The inclusion criteria for this study encompassed patients who presented with either chronic PJI or aseptic loosening and subsequently underwent relevant treatments, including conservative management, debridement, antibiotics, and implant retention (DAIR) surgery, prosthesis removal with antibiotic bone cement spacer implantation surgery, or revision arthroplasty at our institution between March 1, 2020, and December 31, 2023.

Exclusion criteria

The exclusion criteria for this study comprised patients who met any of the following conditions: 1) a history of anticoagulant therapy within the preceding 2 weeks; 2) recent joint dislocation or trauma occurring within the past 2 weeks; 3) presence of systemic inflammatory conditions, such as rheumatoid arthritis, systemic lupus erythematosus (SLE), psoriasis, polymyalgia rheumatica, or inflammatory bowel disease (IBD); 4) history of hypercoagulable disorders; 5) synovial fluid samples contaminated with blood; 6) initial synovial sample concentrations of sD-Dimer and sFDP falling below the lower limits of detection of the analytical instrument; 7) post-dilution of synovial samples (10-fold, 20-fold, 40-fold and 80-fold dilution were achieved by mixing the sample with respective volume of saline solution.) resulting in sD-Dimer and sFDP concentrations surpassing the upper limits of detection of the instrument; and 8) presence of tumors.

Study Population

A total of 120 patients were recruited for this study between March 1, 2020, and December 31, 2023, at our department. Among them, 16 cases were excluded due to recent anticoagulant therapy within 2 weeks, 2 cases were excluded for recent joint dislocation or trauma within the same timeframe, 3 cases were excluded for undetectable levels of (sD-Dimer or sFDP, 2 cases were excluded for systemic inflammatory conditions, and 1 case was excluded for undergoing primary joint arthroplasty for bone tumor disease. Ultimately, a cohort of 96 patients met the study's inclusion and exclusion criteria, as illustrated in Figure 1.

Definition of PJI and aseptic loosening

PJI was defined using the MSIS criteria (Della Valle et al., 2011). Aseptic loosening was defined using the criteria in our previous published paper (Ewald, 1989; Anil et al., 2022).

Measuring methods

Preoperative levels of serum CRP and ESR were assessed prior to surgery. Synovial fluid samples were obtained either before or during the surgical procedure. Following collection, the synovial fluid samples were placed in tubes containing 3.8% sodium citrate solution (at a ratio of 1:9 citrate to synovial fluid). Within the initial 2 hours post-collection, the samples underwent centrifugation at 1000× g for 10 minutes, after which the supernatants were carefully pipetted and stored at -80°C for subsequent analyses. The concentrations of sD-Dimer and sFDP were determined using an automated

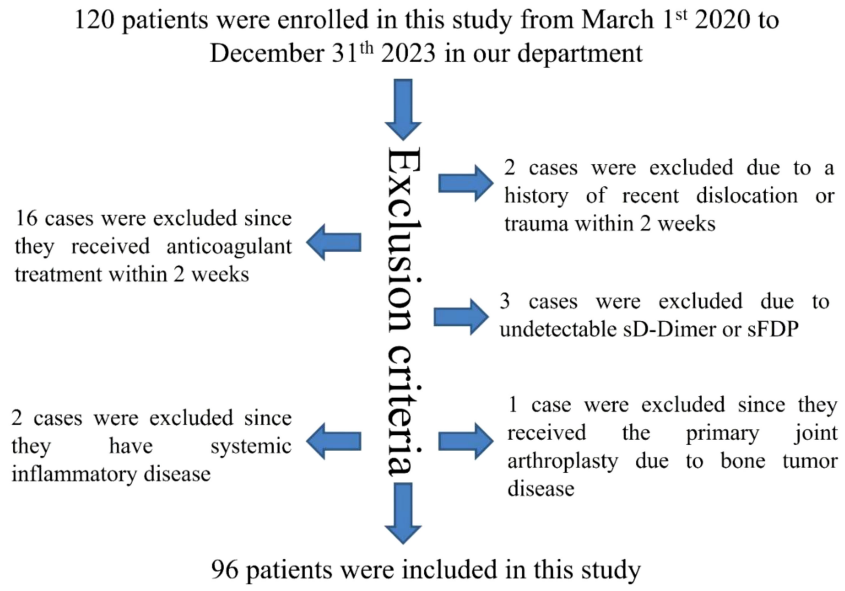

FIGURE 1
Flow diagram of included patient.

coagulation analyzer (Sysmex Europe, CS-5100) with commercially available reagents and controls as per the manufacturer's instructions. In cases where the concentrations of sD-Dimer or sFDP in the original synovial sample exceeded the upper limits of the analyzer's detection range, 10-fold, 20-fold, 40-fold and 80-fold dilution were achieved by mixing the sample with respective volume of saline solution. The reported results were adjusted by the corresponding dilution factor.

Statistical analysis

The normality of quantitative data was initially assessed using the Kolmogorov-Smirnov test. Data conforming to a normal distribution were presented as mean ± standard deviation, and between-group comparisons of quantitative data were conducted using the Independent-sample t test. Non-normally distributed data were expressed as Median (Interquartile Range), and non-parametric methods were employed for between-group quantitative comparisons. Categorical data were compared using the Chi-square test ($\chi 2$). All statistical analyses were performed using IBM SPSS Statistics (version 19, IBM SPSS Software).

The diagnostic performance of CRP, ESR, sD-Dimer, and sFDP in PJI diagnosis was evaluated through receiver operating characteristic (ROC) analyses using MedCalc 19.0.4 (MedCalc Software, Ostend, Belgium). Sensitivity, specificity, and the area under the ROC curve (AUC) were key parameters assessed. DeLong's test (DeLong et al., 1988) was utilized to compare the AUC values between CRP and ESR, CRP and sD-Dimer, CRP and sFDP, ESR and sD-Dimer, as well as ESR and sFDP. A significance level of $p < 0.05$ was considered indicative of a statistically significant difference.

Results

General information of participants

Patients were stratified into two groups: group A (comprising 56 patients with periprosthetic joint infection) and group B (comprising 40 patients with aseptic loosening). Detailed patient demographics are summarized in Table 1, showing no significant differences in baseline characteristics between the two groups.

Comparison of PJI diagnostic value of CRP, ESR, sD-Dimer and s-FDP

The levels of CRP, ESR, sD-Dimer, and sFDP in group A were significantly higher than the levels observed in Group B (Table 2). The receiver operating characteristic (ROC) curve analysis (Table 3) revealed that AUC of both sFDP and sD-Dimer were lower than CRP and ESR in PJI diagnosis. In order to know whether there was significant difference when compared the AUC among sFDP, sD-Dimer, CRP and ESR in PJI diagnosis, DeLong's test (DeLong et al., 1988) was performed and DeLong's test indicated that sFDP demonstrated comparable diagnostic performance in PJI diagnosis to CRP and ESR. However, sD-Dimer exhibited inferior diagnostic performance in PJI diagnosis compared to CRP and ESR (Table 4; Figure 2).

TABLE 1 Comparison of the general data between patients from the two different groups.

Characteristics	Group A (n=56)	Group B (n=40)	P-value
Age (years) *	66.11 ± 8.96	65.00 ± 10.22	0.575
Gender†			0.859
Male (n, %)	22 (37.29)	15 (37.50)	
Female (n, %)	34 (60.71)	25 (62.50)	
Joint†			0.187
Knee (n, %)	38 (67.86)	32 (80.00)	
Hip (n, %)	18 (32.14)	8 (20.00)	

*The values are given as the mean and standard deviation; †The values are given in terms of number of cases and percentages. P < 0.05 was considered statistically significant.

Discussion

The precise diagnosis of PJI in patients lacking typical symptoms, such as sinus tract formation, redness, swelling, fever, or persistent pain, remains a significant challenge for orthopedic surgeons. The search for reliable biomarkers for PJI diagnosis continues to be a focus of research. To our knowledge, this study represents the first investigation into the diagnostic value of sD-Dimer and sFDP in PJI diagnosis. Our findings demonstrate that sFDP performs comparably to CRP and ESR in the diagnosis of PJI. With a calculated optimal threshold value of >1558.35, sFDP exhibits a sensitivity of 91.07% and a specificity of 70.00% in PJI diagnosis. Given the rapid analysis, ease of identification, and cost-effectiveness of FDP detection, our results introduce a novel adjunct marker for PJI diagnosis.

Numerous studies have explored various biomarkers and diagnostic tools for PJI, with a particular focus on synovial fluid markers due to their proximity to the site of infection. For instance, synovial calprotectin has shown high sensitivity and specificity in

TABLE 2 Comparison of CRP, ESR, sD-Dimer, sFDP between patients from the two different groups.

Characteristics	Group A	Group B	P-value
CRP (mg/L)	Median: 35.18 (IQR: 40.37)	Median: 2.26 (IQR: 1.73)	<0.001*
ESR (mm/h)	Median: 66.55 (IQR: 54.00)	18.13 (IQR: 19.50)	<0.001*
sD-Dimer (ug/L)	Median: 1044.93 (IQR: 841.35)	454.88 (IQR: 585.99)	<0.001*
sFDP (ug/L)	Median: 3621.68 (IQR: 2138.19)	1281.04 (IQR: 1776.26)	<0.001*

*The values are given by non-parametric analysis. P < 0.05 was considered statistically significant.

TABLE 3 Diagnostic performance of CRP, ESR, sD-Dimer, sFDP in PJI diagnosis.

	AUC	95% Confidence Interval	Youden index J	Optimal threshold value	Sensitivity (%)	Specificity (%)	P value
CRP	0.920	0.846–0.965	0.7179	>6.77	76.69	95.00	<0.0001
ESR	0.905	0.828–0.955	0.6571	>41	73.21	92.50	<0.0001
sD-Dimer	0.788	0.692–0.864	0.4607	>738.65	66.07	80.00	<0.0001
sFDP	0.869	0.785–0.929	0.6107	>1558.35	91.07	70.00	<0.0001

PJI diagnosis, with some studies reporting sensitivity and specificity values of up to 95% and 97%, respectively (Zhang et al., 2020; Peng et al., 2022; Warren et al., 2022). Karbysheva et al. demonstrated that synovial fluid D-Lactate had a sensitivity of 94.3% and specificity of 78.4% in PJI diagnosis when using Musculoskeletal Infection Society criteria (Karbysheva et al., 2020). Theil et al. showed that synovial fluid pH had a strong correlation with synovial leukocyte count and can potentially serve as a diagnostic marker for chronic PJI (Theil et al., 2022). Chen et al. found that synovial fluid leukocyte esterase can used as a rapid PJI diagnostic tool, with a pooled sensitivity of 87% and specificity of 96% (Chen et al., 2019). Although these studies suggested that synovial fluid biomarkers hold promise as new diagnostic indicators for PJI, most of these published synovial fluid biomarkers often require specialized antibodies and equipment for detection, limiting their widespread adoption in routine clinical practice. Different from most of these published synovial fluid biomarkers, FDP detection is already routinely performed in clinical settings, making sFDP a more accessible and practical option for PJI diagnosis.

It is important to note that while sFDP shows promise as a valuable new adjunctive diagnostic marker for PJI, its relatively modest specificity suggests that it should be used in combination with other biomarkers. The integration of multiple parameters for PJI diagnosis has been explored in other studies, with some reporting improved diagnostic accuracy when combining different biomarkers. Lee et al. found that combining synovial fluid calprotectin with CRP and IL-6 significantly improved PJI diagnostic performance (Lee et al., 2017). Diniz et al. found that combined synovial fluid alpha-2-microglobulin and synovial fluid CRP demonstrated improved PJI diagnostic accuracy (Diniz et al., 2023). Yu et al. found that combined platelet-to-albumin ratio with CRP and ESR had a high PJI diagnostic accuracy, with sensitivity and specificity values of 93.8% and 92.5%, respectively (Yu et al., 2025). All these findings highlighted the potential of combining multiple biomarkers to improve diagnostic accuracy. Therefore, further investigations are needed to explore the synergistic use of sFDP with other established biomarkers.

However, it is imperative to interpret the findings of this study within the context of several limitations. Firstly, our study included a modest cohort of 96 patients, underscoring the need for larger, higher-quality studies to comprehensively assess the diagnostic value of sD-Dimer and sFDP in PJI diagnosis. Secondly, we did not compare the AUC values of sD-Dimer and sFDP with synovial fluid leukocyte count and sPMN% in PJI diagnosis. Consequently, we are unable to definitively ascertain whether the diagnostic performance of sD-Dimer and sFDP in PJI diagnosis surpasses that of synovial fluid leukocyte count and sPMN%. Thirdly, our exclusion criteria encompassed patients with systemic inflammatory diseases, a history of anticoagulant therapy, or recent dislocations or trauma within a two-week period, constituting approximately 20% of patients in our department. This exclusion criterion may somewhat constrain the generalizability of our conclusions in the clinical evaluation of PJI. Fourthly, due to the viscosity of synovial fluid and the relatively elevated concentrations of sD-Dimer and sFDP in PJI patients, there were instances where we had to dilute the synovial fluid with an appropriate volume of saline solution to enhance detection success rates. However, this dilution process may introduce a degree of error in

TABLE 4 Pairwise comparison of ROC curves among CRP, ESR, sD-Dimer, sFDP in PJI diagnosis.

	ESR	sD-Dimer	sFDP
CRP	Z=0.575 P=0. 5651	Z= 2.775 P= 0.0055	Z= 1.152 P= 0.2494
ESR	–	Z= 2.387 P= 0.0170	Z= 0.822 P= 0.4109
sD-Dimer	–	–	Z= 3.297 P=0.0010

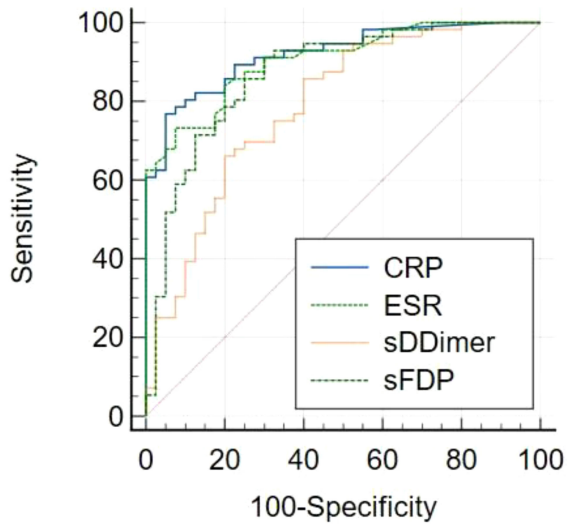

FIGURE 2
Receiver operating characteristic (ROC) curves of CRP, ESR, sD-Dimer, sFDP in PJI diagnosis.

concentration detection. Lastly, since this study primarily focuses on preoperative diagnosis, it did not aim to establish a specific minimum follow-up period. Consequently, it is plausible that some patients who were not operated on in our hospital during the study period may have been diagnosed with PJI at a later stage.

Conclusion

In conclusion, sFDP emerges as a promising adjunctive parameter for PJI diagnosis. Nonetheless, given its relatively modest specificity, the integration of sFDP with other biomarkers is recommended. The synergistic utilization of multiple parameters warrants exploration in more extensive clinical trials and holds potential utility, especially in cases where diagnoses remain inconclusive. Nevertheless, further comprehensive studies are imperative to validate and refine this combined diagnostic approach.

Future directions

The findings in this study should be interpreted with caution due to the study's limitations. Further comprehensive research is essential to confirm these results and refine the diagnostic approach for PJI using synovial fluid markers. The integration of multiple biomarkers, along with larger and more diverse patient populations, will be crucial in enhancing the reliability and clinical applicability of these diagnostic tools.

Data availability statement

The raw data supporting the conclusions of this article will be made available by the authors, without undue reservation.

Ethics statement

The studies involving humans were approved by Ethics Board of Henan Provincial People's Hospital. The studies were conducted in accordance with the local legislation and institutional requirements. The participants provided their written informed consent to participate in this study. Written informed consent was obtained from the individual(s) for the publication of any potentially identifiable images or data included in this article.

Author contributions

JH: Funding acquisition, Writing – original draft. PC: Data curation, Software, Writing – review & editing. ZZ: Methodology, Software, Writing – review & editing. CC: Methodology, Writing – original draft. PP: Formal Analysis, Writing – original draft. YL: Project administration, Writing – original draft. DM: Data curation, Supervision, Validation, Writing – review & editing. TL: Methodology, Supervision, Conceptualization, Writing – review & editing. YJ: Funding acquisition, Writing – review & editing.

Funding

The author(s) declare that financial support was received for the research and/or publication of this article. The Project Sponsored by the Advanced Scientific Research Foundation for the Returned Overseas Chinese Scholars in Henan Province (2024HNSLXRY08); Henan Provincial and Ministry Co-construction Project (SBGJ202102031); National Natural Science Foundation of China (82002840); Key Scientific and Technological Projects in Henan Province (LHGJ20240046); Overseas Training Program for Medical Science and Technology Talents in Henan Province (H20240055).

Conflict of interest

The authors declare that the research was conducted in the absence of any commercial or financial relationships that could be construed as a potential conflict of interest.

Publisher's note

References

Abdelaziz, H., Aljawabra, A., Rossmann, M., Tien, C. S., Citak, M., Klatte, T. O., et al. (2022). What is the impact of automated synovial cell counting on different aseptic causes and periprosthetic conditions associated with revision THA? *Clin. Orthop Relat. Res.* 480, 905–914. doi: 10.1097/CORR.0000000000002063

Anil, U., Singh, V., and Schwarzkopf, R. (2022). Diagnosis and detection of subtle aseptic loosening in total hip arthroplasty. *J. Arthroplasty* 37, 1494–1500. doi: 10.1016/j.arth.2022.02.060

Berthoud, O., Coiffier, G., Albert, J. D., Gougeon-Jolivet, A., Goussault, C., Bendavid, C., et al. (2020). Performance of a new rapid diagnostic test the lactate/glucose ratio of synovial fluid for the diagnosis of septic arthritis. *Joint Bone Spine* 87, 343–350. doi: 10.1016/j.jbspin.2020.03.009

Carli, A. V., Abdelbary, H., Ahmadzai, N., Cheng, W., Shea, B., Hutton, B., et al. (2019). et al: diagnostic accuracy of serum, synovial, and tissue testing for chronic periprosthetic joint infection after hip and knee replacements: A systematic review. *J. Bone Joint Surg. Am.* 101, 635–649. doi: 10.2106/JBJS.18.00632

Chen, Y., Kang, X., Tao, J., Zhang, Y., Ying, C., and Lin, W. (2019). Reliability of synovial fluid alpha-defensin and leukocyte esterase in diagnosing periprosthetic joint

infection (PJI): a systematic review and meta-analysis. *J. Orthop Surg. Res.* 14, 453. doi: 10.1186/s13018-019-1395-3

Della Valle, C., Parvizi, J., Bauer, T. W., DiCesare, P. E., Evans, R. P., Segreti, J., et al. (2011). American Academy of Orthopaedic Surgeons clinical practice guideline on: the diagnosis of periprosthetic joint infections of the hip and knee. *J. Bone Joint Surg. Am.* 93, 1355–1357. doi: 10.2106/JBJS.9314ebo

Diniz, S. E., Ribau, A., Vinha, A., Oliveira, J. C., Abreu, M. A., and Sousa, R. (2023). Simple and inexpensive synovial fluid biomarkers for the diagnosis of prosthetic joint infection according to the new EBJIS definition. *J. Bone Jt Infect.* 8, 109–118. doi: 10.5194/jbji-8-109-2023

Ewald, F. C. (1989). The Knee Society total knee arthroplasty roentgenographic evaluation and scoring system. *Clin. Orthop Relat. Res.* 248, 9–12. doi: 10.1097/00003086-198911000-00003

Fujimoto, T., Kaneko, T., Sunakawa, T., Ikegami, H., and Musha, Y. (2018). Elevation of fibrin degradation product (FDP) values prevents the negative conversion of serum CRP values after total knee arthroplasty. *J. Orthop* 15, 940–944. doi: 10.1016/j.jor.2018.08.005

Huang, J. C., Chen, X., Qiang, S., Zheng, W. D., Zheng, J., and Jin, Y. (2021). Exciting performance of plasma fibrinogen in periprosthetic joint infection diagnosis. *Orthop Surg.* 13, 812–816. doi: 10.1111/os.12964

Huang, J., Zhang, Y., Wang, Z., Dong, Y., Zhao, Y., Zheng, J., et al. (2019). The serum level of D-Dimer is not suitable for distinguishing between prosthetic joint infection and aseptic loosening. *J. Orthop Surg. Res.* 14, 407. doi: 10.1186/s13018-019-1461-x

Karbysheva, S., Yermak, K., Grigoricheva, L., Renz, N., Perka, C., and Trampuz, A. (2020). Synovial fluid d-lactate-A novel pathogen-specific biomarker for the diagnosis of periprosthetic joint infection. *J. Arthroplasty* 35, 2223–2229 e2222. doi: 10.1016/j.arth.2020.03.016

Lee, Y. S., Koo, K. H., Kim, H. J., Tian, S., Kim, T. Y., Maltenfort, M. G., et al. (2017). Synovial fluid biomarkers for the diagnosis of periprosthetic joint infection: A systematic review and meta-analysis. *J. Bone Joint Surg. Am.* 99, 2077–2084. doi: 10.2106/JBJS.17.00123

McNally, M., Sousa, R., Wouthuyzen-Bakker, M., Chen, A. F., Soriano, A., Vogely, H. C., et al. (2021). The EBJIS definition of periprosthetic joint infection. *Bone Joint J.* 103-B, 18–25. doi: 10.1302/0301-620X.103B1.BJJ-2020-1381.R1

Mihalic, R., Zdovc, J., Brumat, P., and Trebse, R. (2020). Synovial fluid interleukin-6 is not superior to cell count and differential in the detection of periprosthetic joint infection. *Bone Jt Open* 1, 737–742. doi: 10.1302/2633-1462.112.BJO-2020-0166.R1

Pagliaccetti, J., Pannu, T. S., Villa, J. M., Piuzzi, N. S., and Higuera, C. A. (2021). Variability and interpretation of synovial cell count and differential: A perspective in hip and knee arthroplasty. *Orthopedics* 44, e320–e325. doi: 10.3928/01477447-20210508-01

Parvizi, J., and Gehrke, T. (2014). International Consensus Group on Periprosthetic Joint I: Definition of periprosthetic joint infection. *J. Arthroplasty* 29, 1331. doi: 10.1016/j.arth.2014.03.009

Parvizi, J., Tan, T. L., Goswami, K., Higuera, C., Della Valle, C., Chen, A. F., et al. (2018). The 2018 definition of periprosthetic hip and knee infection: an evidence-based and validated criteria. *J. Arthroplasty* 33, 1309–1314 e1302. doi: 10.1016/j.arth.2018.02.078

Paziuk, T., Rondon, A. J., Goswami, K., Tan, T. L., and Parvizi, J. (2020). A novel adjunct indicator of periprosthetic joint infection: platelet count and mean platelet volume. *J. Arthroplasty* 35, 836–839. doi: 10.1016/j.arth.2019.10.012

Peng, X., Zhang, H., Xin, P., Bai, G., Ge, Y., Cai, M., et al. (2022). Synovial calprotectin for the diagnosis of periprosthetic joint infection: a diagnostic meta-analysis. *J. Orthop Surg. Res.* 17, 2. doi: 10.1186/s13018-021-02746-2

Sahin, E., Karaismailoglu, B., Ozsahin, M. K., Guven, M. F., and Kaynak, G. (2021). Low value of platelet count to mean platelet volume ratio to diagnose chronic PJI: A case control study. *Orthop Traumatol Surg. Res.* 107, 102899. doi: 10.1016/j.otsr.2021.102899

Shahi, A., Kheir, M. M., Tarabichi, M., Hosseinzadeh, H. R. S., Tan, T. L., and Parvizi, J. (2017). Serum D-dimer test is promising for the diagnosis of periprosthetic joint infection and timing of reimplantation. *J. Bone Joint Surg. Am.* 99, 1419–1427. doi: 10.2106/JBJS.16.01395

Squire, M. W., Della Valle, C. J., and Parvizi, J. (2011). Preoperative diagnosis of periprosthetic joint infection: role of aspiration. *AJR Am. J. Roentgenol* 196, 875–879. doi: 10.2214/AJR.10.5160

Tande, A. J., and Patel, R. (2014). Prosthetic joint infection. *Clin. Microbiol. Rev.* 27, 302–345. doi: 10.1128/CMR.00111-13

Theil, C., Ackmann, T., Gosheger, G., Puetzler, J., Moellenbeck, B., Schwarze, J., et al. (2022). Synovial fluid pH is as specific as synovial leukocyte count but less sensitive for the diagnosis of chronic prosthetic joint infection. *J. Orthop Traumatol* 23, 52. doi: 10.1186/s10195-022-00672-5

Vale, J. S., Castelo, F. S., Barros, B. S., Ribau, A. C., Carvalho, A. D., and Sousa, R. J. G. (2023). Synovial fluid biomarkers for the diagnosis of periprosthetic joint infection-A systematic review and meta-analysis of their diagnostic accuracy according to different definitions. *J. Arthroplasty* 38, 2731–2738 e2733. doi: 10.1016/j.arth.2023.06.017

Warren, J. A., Klika, A. K., Bowers, K., Colon-Franco, J., Piuzzi, N. S., and Higuera, C. A. (2022). Calprotectin lateral flow test: consistent across criteria for ruling out periprosthetic joint infection. *J. Arthroplasty* 37, 1153–1158. doi: 10.1016/j.arth.2022.01.082

Xu, Y., Ma, X., Guo, H., Tang, H., Liu, J., Wang, C., et al. (2023). Diagnostic value of synovial fluid biomarkers for periprosthetic joint infection: A prospective, double-blind trial. *Med. Sci. Monit* 29, e940842.

Xu, H., Xie, J., Huang, Q., Lei, Y., Zhang, S., and Pei, F. (2019). Plasma fibrin degradation product and D-dimer are of limited value for diagnosing periprosthetic joint infection. *J. Arthroplasty* 34, 2454–2460. doi: 10.1016/j.arth.2019.05.009

Yi, P. H., Cross, M. B., Moric, M., Levine, B. R., Sporer, S. M., Paprosky, W. G., et al. (2015). Do serologic and synovial tests help diagnose infection in revision hip arthroplasty with metal-on-metal bearings or corrosion? *Clin. Orthop Relat. Res.* 473, 498–505.

Yu, Y., Wen, Y., Xia, J., Dong, G., and Niu, Y. (2025). Blood cell ratio combinations for diagnosing periprosthetic joint infections: A preliminary study. *Infect. Drug Resist.* 18, 635–645. doi: 10.2147/IDR.S489201

Zeng, Y. Q., Deng, S., Zhu, X. Y., Sun, X. B., Feng, W. J., Zeng, J. C., et al. (2021). Diagnostic accuracy of the synovial fluid alpha-defensin lateral flow test in periprosthetic joint infection: A meta-analysis. *Orthop Surg.* 13, 708–718. doi: 10.1111/os.12966

Zhang, Z., Cai, Y., Bai, G., Zhang, C., Li, W., Yang, B., et al. (2020). The value of calprotectin in synovial fluid for the diagnosis of chronic prosthetic joint infection. *Bone Joint Res.* 9, 450–457. doi: 10.1302/2046-3758.98.BJR-2019-0329.R2

frontiers | Frontiers in Cellular and Infection Microbiology

TYPE Original Research
PUBLISHED 14 May 2025
DOI 10.3389/fcimb.2025.1578549

OPEN ACCESS

EDITED BY
Diana Manolescu,
Victor Babes University of Medicine and Pharmacy, Romania

REVIEWED BY
Young-Chul Lee,
Gachon University, Republic of Korea
Sheng Ding,
Chengdu University, China
Jose Luis Malaga Granda,
Universidad Catolica de Santa Maria, Peru
Islam Seder,
Technical University of Denmark, Denmark
Arianna Ceruti,
Leipzig University, Germany

*CORRESPONDENCE
Manoj K. Pastey
manoj.pastey@oregonstate.edu

RECEIVED 17 February 2025
ACCEPTED 23 April 2025
PUBLISHED 14 May 2025

CITATION
Prescott MA, Koesdjojo MT, Mandrell DT and Pastey MK (2025) Development of a rapid point-of-care dengue virus type 2 infection diagnostic assay using recombinase polymerase amplification and lateral flow device.
Front. Cell. Infect. Microbiol. 15:1578549.
doi: 10.3389/fcimb.2025.1578549

Development of a rapid point-of-care dengue virus type 2 infection diagnostic assay using recombinase polymerase amplification and lateral flow device

Meagan A. Prescott[1,2], Myra T. Koesdjojo[3], David T. Mandrell[3] and Manoj K. Pastey[1*]

[1]Department of Biomedical Sciences, College of Veterinary Medicine, Oregon State University, Corvallis, OR, United States, [2]Department of Microbiology, College of Science, Oregon State University, Corvallis, OR, United States, [3]Custom Integration Services, KTM Research LLC, Hubbard, OR, United States

Introduction: Dengue virus (DENV) is the most rapidly spreading arbovirus globally, with over half of the world's population at risk of infection. Early and rapid detection is crucial to ensure timely patient care, reduce healthcare burden, and prevent severe disease progression. However, conventional nucleic acid amplification techniques are often unsuitable for low-resource settings due to their equipment and procedural demands.

Methods: We evaluated a real-time reverse transcription recombinase polymerase amplification (RT-RPA) assay for the sensitive and specific detection of DENV serotype 2 (DENV2). The assay was tested using both Twista fluorometer and lateral flow detection (LFD) formats. Analytical sensitivity was determined by probit regression, while specificity was assessed against unrelated viruses and other flaviviruses. Clinical validation was performed using serum, cell culture, and FTA® card samples. Assay robustness was evaluated under varying temperatures and after freeze-thaw cycles.

Results: The RT-RPA assay reliably amplified DENV2 at concentrations as low as 50 copies per reaction, with LOD_{95} estimated at 38.48 copies (Twista) and 50.37 copies (LFD). No cross-reactivity was observed with respiratory syncytial virus, influenza, rabbit herpes virus, West Nile virus, or other DENV serotypes (DENV1, DENV3, DENV4). The assay successfully detected multiple DENV2 strains and maintained performance across 33°C–40°C and after repeated freeze-thaw cycles. RNA extracted from FTA® cards was successfully amplified. Clinical validation confirmed accurate detection in serum and cell culture samples, while DENV3-positive blood samples tested negative, reinforcing specificity.

Discussion: The RT-RPA/LFD assay offers a rapid, sensitive, and specific tool for DENV2 detection, compatible with low-resource and field-based settings. Its simplicity, robustness, and portability make it a promising approach for point-of-care diagnostics and outbreak surveillance in endemic regions.

KEYWORDS

dengue virus, real-time reverse transcription recombinase polymerase amplification, lateral flow detection (LFD), low-resource settings, point-of-care diagnostics

1 Introduction

Dengue virus (DENV) is a significant and widely distributed member of the *Flaviviridae* family. The World Health Organization (WHO) classifies dengue as a global pandemic threat and the most critical mosquito-borne viral disease worldwide (WHO, 2012). Dengue is endemic in over 100 countries across tropical and subtropical regions, with sporadic outbreaks occurring in additional locations worldwide (WHO, 2012). Since early 2023, ongoing transmission combined with an unexpected surge in dengue cases has resulted in a historic high of over 6.5 million cases and more than 7,300 dengue-related deaths (WHO, 2025). Annually, an estimated 100 to 390 million new infections occur, and alarmingly, the incidence of dengue has increased 30-fold over the last five decades (Malavige et al., 2023; Bhatt et al., 2013; WHO, 2012). Dengue outbreaks impose a substantial burden on healthcare systems and economies while contributing to morbidity and mortality. Additionally, disease underreporting and misclassification remain prevalent challenges (Malavige et al., 2023; Bhatt et al., 2013; Shepard et al., 2013; Edillo et al., 2015; Gulland, 2013; Salmon-Mulanovich et al., 2015; Shepard et al., 2014; Undurraga et al., 2015; Wichmann et al., 2011; Beatty et al., 2011). Managing dengue infections is increasingly complex, as symptoms often resemble those of other endemic diseases (Potts and Rothman, 2008). Consequently, rapid and sensitive diagnostic tests that can be administered early in disease progression are crucial for effective case management.

Dengue infection manifests along a spectrum from asymptomatic cases to severe disease. While most infections present as mild dengue fever, some progress to severe dengue hemorrhagic fever or dengue shock syndrome (Whitehorn and Simmons, 2011). The virus consists of four serotypes (DENV1-4); primary infection with one serotype confers lifelong immunity to that serotype but increases the risk of severe disease upon secondary infection with a different serotype due to antibody-dependent enhancement. Additionally, the sequence of serotype infections influences disease severity (Guzman et al., 2013; Fried et al., 2010; Endy et al., 2004; Ananta Preecha et al., 2005; de Araújo et al., 2009; Gibbons et al., 2007; Halstead, 2006; Sangkawibha et al., 1984; Thomas et al., 2008; Vaughn et al., 2000; Trivedi and Chakravarty, 2022).

Accurate and efficient DENV diagnosis is essential for surveillance, early detection, case confirmation, and differentiation from other diseases (WHO, 2009). Various diagnostic methods are available depending on the stage of infection. During the early phase (4–5 days post-infection), direct virus detection is possible, whereas serological methods are required later when the virus is no longer detectable. In general, high-confidence tests tend to be complex and time-consuming, limiting their widespread use, while rapid serological tests (based on antibody detection) often lack sensitivity or are unsuitable for early diagnosis (WHO, 2009).

Viral isolation, the gold standard for DENV detection, is impractical in clinical settings due to its time-intensive nature (Yamada et al., 2002; Medina et al., 2012). Serology-based assays, including IgM/IgG enzyme-linked immunosorbent assays (ELISA) and nonstructural protein 1 (NS1) antigen detection, are widely used due to their speed, but they exhibit reduced sensitivity and specificity (Hunsperger et al., 2014; Peeling et al., 2010; Hunsperger et al., 2009; Fernández and Vázquez, 1990; Moi et al., 2013; Paranavitane et al., 2014; Blacksell et al., 2012; Felix et al., 2012; Saito et al., 2015). Nucleic acid-based methods enable direct viral detection within a short timeframe. Real-time reverse transcription PCR (RT-PCR) has been employed for many years (Lanciotti et al., 1992; Johnson et al., 2005; Najioullah et al., 2014; Santiago et al., 2013; Zhao et al., 2024), but its complexity and resource requirements make it unsuitable for point-of-care testing. Recently, isothermal amplification techniques, such as nucleic acid sequence-based amplification (NASBA) (Wu et al., 2001) and reverse transcription loop-mediated isothermal amplification (RT-LAMP) (Sahni et al., 2013; Teoh et al., 2015), have been explored as alternatives that retain sensitivity while improving accessibility.

Recombinase polymerase amplification (RPA) is a promising isothermal amplification technique that offers advantages over traditional PCR and other isothermal methods. RPA is an extremely rapid (≤20 minutes) DNA amplification method that relies on three key enzymes: recombinases, which facilitate primer-target binding; single-stranded binding proteins (SSB), which stabilize the displaced DNA strands; and a strand-displacing polymerase, which enables DNA synthesis (Piepenburg et al., 2006). When coupled with reverse transcriptase (RT), RPA allows for RNA-to-cDNA conversion and subsequent amplification in a

single-tube reaction (Bonnet et al., 2022). Detection of amplification products can be achieved via real-time fluorescence or lateral flow devices (LFD) (Boehringer and O'Farrell, 2021; Kakkar et al., 2024). In real-time RT-RPA, a fluorescent exo-probe is included in the reaction mix, whereas LFD-based detection utilizes 5'-modified primers and a colorimetric signal upon application to the LFD. This combination enables rapid, sensitive, and equipment-free detection of specific viral targets, making it particularly well-suited for low-resource settings, outbreak response, and decentralized testing. In resource-limited regions where laboratory infrastructure is minimal, this dual-format strategy provides both flexibility and accessibility, allowing critical diagnostic testing to be brought closer to the point of care.

RT-RPA combined with LFD has been successfully used for rapid detection of various viruses, including SARS-CoV-2, influenza, and hepatitis B (Zhao et al., 2024). While pan-DENV assays exist, few target specific serotypes like DENV2, which is often linked to severe dengue in regions such as India and the Americas. Serotype-specific detection offers greater clinical and epidemiological value. To address this gap, we developed a sensitive, field-deployable RT-RPA/LFD assay for DENV2, aiming to improve rapid diagnosis and support dengue control efforts.

2 Materials and methods

2.1 Virus and RNA

DENV2 laboratory strains were grown in Vero cells, harvested, and stored at -80°C. The typical dengue virus titer from Vero cells were 10_7 PFU/mL. The laboratory strains of DENV2 used in this study were NGC, S221, and TH-36. RNA collected from these laboratory strains was extracted for RT-RPA using the NucleoSpin RNA isolation kit (Macherey-Nagel, Düren, Germany). Extractions were performed following the supplied protocols and guidelines. RNA was aliquoted into single-use tubes and stored at -80°C. Samples were processed in a Biosafety Level 2 (BSL-2) facility, ensuring safe handling of DENV2 and preventing exposure to infectious agents.

2.2 Assay design overview

2.2.1 Primers and probe design

Primers compatible with the RPA reaction were designed to specifically amplify DENV2 (Table 1; Figure 1). The primer set was designed to amplify a 316 bp segment of the DENV2 viral genome corresponding to a portion of the structural membrane (M) protein (Figure 1). The M protein gene of DENV-2 is relatively conserved among DENV-2 isolates and serves as a good target for RPA due to its moderate length and role in viral assembly. A multiple sequence alignment of DENV-2 strains was performed to confirm minimal variation in the primer and probe binding sites.

In addition, *in silico* analyses (e.g., BLAST alignment) and experimental cross-reactivity testing were conducted using unrelated viral templates, including respiratory syncytial virus, influenza (PR/8/34), and rabbit herpes virus, as well as several related flavivirus members such as West Nile virus and RNA from the other DENV serotypes.

Real-time RT-RPA generated a clear fluorescence signal using standard primers and a FAM-labeled exo probe (Figure 2A). Signal generation occurred upon probe hybridization and cleavage by Exonuclease III at the tetrahydrofuran (THF) site, separating the fluorophore from the quencher. This enabled specific and real-time detection of DENV2 amplification.

2.2.2 Real-time reverse transcription recombinase polymerase amplification

DENV2 genome amplification was performed using the TwistAmp exo RT kit (TwistDx, Ltd., Cambridge, United Kingdom) (Twist, 2018). Depending on the detection format, appropriate primers were used (Table 1; Figure 1). The kit contained a lyophilized pellet with reaction enzymes, including the RT enzyme necessary for generating complementary DNA (cDNA) from an RNA template, premeasured and distributed by the manufacturer.

The reaction pellet was dissolved following the manufacturer's instructions using a mix of rehydration buffer, diluted template, appropriate primer/probe sets, and water to a final volume of 47.5 µl. Magnesium acetate (280 nM) was used to initiate the RPA

TABLE 1 RPA and LFD primers and probe used for the rapid detection of DENV2.

Name	Sequence 5'-3'	GenBank Accession
Real-time		
DENV2_3F	ACCTTGGTGAATTGTGTGAAGACACAATCACG	PP269861.1
DENV2_1R	CCTATGGTGTATGCCAGGATTGCTGCCATTATGGT	PP269937.1
DENV2_Probe	ATGGGACTGGAGACACGAACTGAAACA[**dT(FAM)**]**G**[**THF**] A[**dT(BHQ-1**)]GTCATCAGAAGGGG	PP269903.1
LFD		
DENV2_3F_LFD	**FAM**-ACCTTGGTGAATTGTGTGAAGACACAATCACG	PP269861.1
DENV2_1R_LFD	**Biotin**-CCTATGGTGTATGCCAGGATTGCTGCCATTA TGGT	PP269937.1

Bold text within the sequence denotes modifications made to the oligonucleotides. dT(FAM): thymidine nucleotide bearing fluorescein, THF: tetrahydrofuran spacer replacing G nucleotide, and dT(BHQ-1): thymidine nucleotide bearing the black hole quencher 1.

10.3389/fcimb.2025.1578549

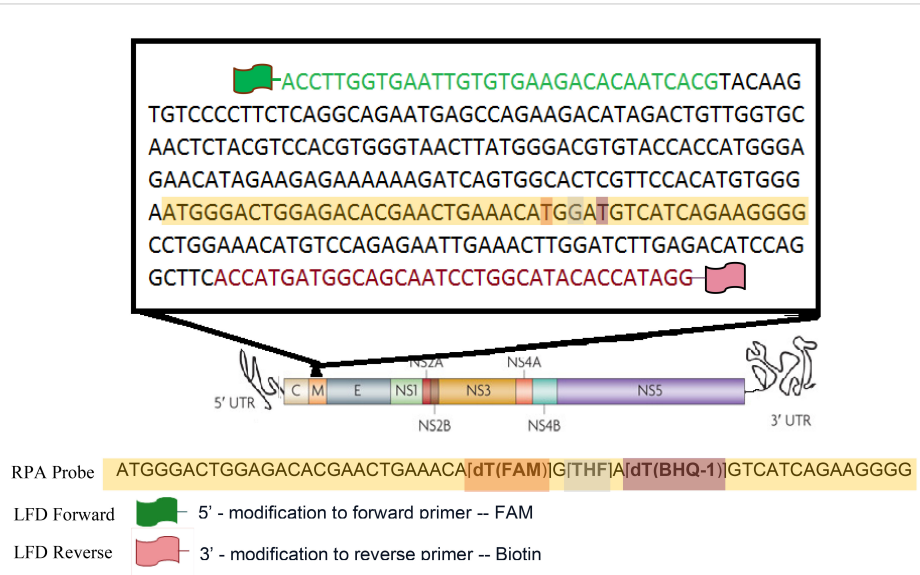

FIGURE 1
Schematic diagram of M gene showing RPA and LFD primers and probe used.

reaction, bringing the final reaction volume to 50 µl. The mixture contained 0.5 µM forward and reverse primers and 0.2 µM probe. A non-template control (water with no DNA) and a positive control using NGC DENV2 were included in each run.

2.2.3 Limit of detection

Accurate assessment of nucleic acid copy number is critical for determining the analytical sensitivity of molecular assays, such as RT-RPA. It allows for precise quantification of the target RNA or DNA, enabling the evaluation of detection limits (e.g., LoD95) and ensuring reproducibility across experiments. For assessing genome copy numbers, a ten-fold serial dilution series of DENV2 (NGC strain) RNA was prepared. Starting from a stock solution of known concentration, dilutions were made in nuclease-free water (or an appropriate buffer) to generate final concentrations of 100, 90, 80, 70, 60, 50, 40, 30, 20, and 10 copies per reaction. Each dilution was aliquoted and tested in 20 replicate reactions to determine the detection rate at each concentration (Table 2; Figure 3).

Additionally, serial dilutions of positive control plasmids, pTM-M (containing the M gene), were included. A 316 bp fragment (nt. 524–840; GenBank accession no. PP269861.1) of the membrane glycoprotein region was cloned into the pTM vector. The recombinant plasmids used as standard nucleic acids were quantified using a NanoDrop ND-1000 spectrophotometer, and the DNA copy number was calculated using the following formula:

$$DNAcopynumber(copies/\mu L)\frac{6.022x10^{23}xplasmidconcentration(ng/\mu L)}{plasmidmolecularweight(g/mol)x10^{9}}$$

The recombinant plasmid was serially diluted from 10^{1}°C to 10 copies/µL and stored at −20°C until use. The reaction was conducted at 40 °C for 20 minutes, and amplification products were visualized using either LFD or real-time fluorescence detection (data not shown).

2.2.4 Confirmation of RT-RPA amplified DENV2 DNA product

To confirm the correct DNA product was amplified, Sanger sequencing was performed at the Center for Genome Research and Biocomputing at Oregon State University. Following amplification, products were purified using a GeneJET DNA purification kit (Thermo Scientific, Waltham, MA, USA) and observed via gel electrophoresis on a 1.5% agarose gel stained with SYBR Safe (Life Technologies, Carlsbad, CA, USA) (Figure 2B). DNA band was visualized under an LED blue light transilluminator, and the 316 bp product (Figure 2B) was excised and purified using the GeneJet kit. Sequencing results were aligned to the predicted DENV2 sequence using the EMBOSS Water pairwise alignment tool.

2.2.5 Detection of amplified product

2.2.5.1 Fluorescence detection of real time RT-RPA

Real-time RT-RPA was achieved using the TwistAmp exo RT kit (TwistDx) (Twist, 2018). Reactions containing the basic RPA primers with the DENV2-specific exo-probe allowed real-time visualization of amplification products via fluorescence signal monitoring. Amplification was monitored using the portable Twista real-time fluorometer (TwistDx) (Figure 2A). For experiments involving temperature gradients, the Bio-Rad CFX96 Touch™ Real-Time PCR Detection System (Bio-Rad Laboratories, Hercules, CA, USA) was used (Figure 4). The one-step RT-RPA reaction is completed within 20 minutes.

2.2.5.2 Lateral flow device detection of RT-RPA products

Rapid detection of the DENV2 genome was also achieved by LFD. DENV2 genome amplification was conducted using the TwistAmp exo kit (TwistDx) (Twist, 2018), with the 5' modified primers replacing standard primers in the reaction mix. The

10.3389/fcimb.2025.1578549

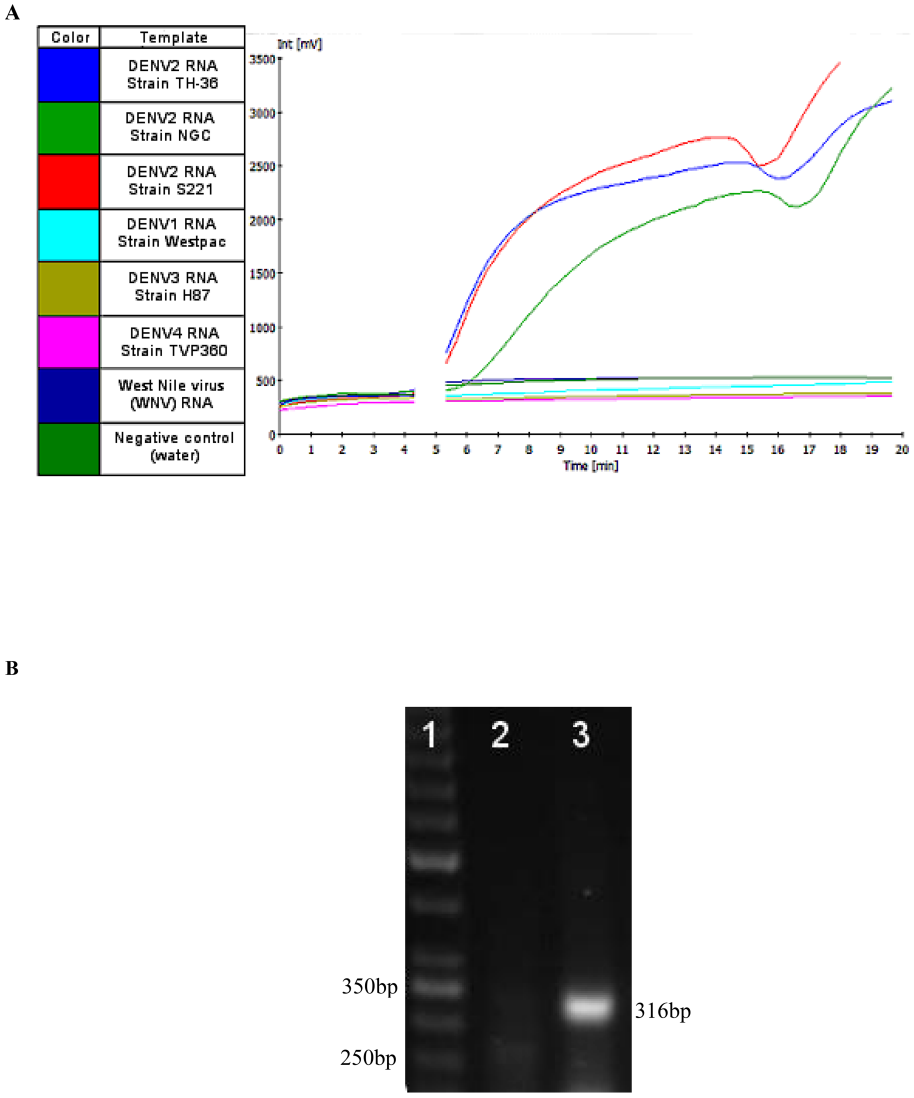

FIGURE 2
(A) A representative image of real-time RT-RPA amplification products using the Twista fluorometer. The graph depicts the fluorescent signal for each template used in the RT-RPA reactions and the key to the left indicates the template each color represents. At approximately five minutes into run time a required Magnesium acetate (280 nM) adding step, to initiate the RPA reaction, was performed resulting in signal not being generated for the duration of that step (gap in the graph). **(B)** RPA amplification of Dengue 2 M gene. The numbers in the left margin indicate selected bands of the DNA marker, and the estimated amplified product size is indicated at 316 bp in the right margin. Lane 1 is a 50bp DNA ladder (Thermo Scientific™), lane 2 is the no-template control (water as template). Lanes 3 represent RPA amplification product from 10 copies of DENV-2 genome per reaction at 37°C.

optimal concentration of labeled primers was determined to be 1.25 µM. The end products, labeled with biotin and FAM, were diluted in buffer and applied to a PCRD-2 LFD (Forsite Diagnostics, UK) (Figures 5, 6B). In brief, 5 µL of RPA products were added into 100 µL of sample buffer and mixed thoroughly. Then, 60 µL of the mixed solution was dispensed onto the lateral-flow dipsticks and results were recorded until the positive control line was visualized. A colorimetric signal indicated the presence of doubly labeled DNA at the test line (T-line) via immobilized anti-FAM and anti-biotin antibodies, with a control line (C-line) ensuring proper flow. Positive results were indicated by two lines (C-line and T-line), while negative results showed only the C-line. Tests without visible lines were considered faulty and unusable. The LFD detection format added no more than 10 minutes to the reaction time and enabled product visualization without the need for costly exo-probes or real-time detection equipment.

The lateral flow device used in this study was optimized to ensure absolute accuracy by eliminating the possibility of false positives and false negatives. The following measures were implemented: a. Every test result was verified using quantitative PCR (qPCR); b. Each sample was tested in at least three independent replicates to confirm consistency; c. The LFD assay included built-in internal controls to ensure proper test functionality; d. Key reaction parameters such as incubation time, reaction temperature, and primer concentration were systematically optimized; e. A stringent threshold for positive detection was

TABLE 2 Detection of DENV2 RNA by RT-RPA across different copy numbers.

Copies of DENV2 per reaction	Positive amplification (Twista fluorometer)	Positive amplification (LFD)
100	20/20	20/20
90	20/20	20/20
80	20/20	20/20
70	20/20	20/20
60	20/20	20/20
50	20/20	20/20
40	19/20	16/20
30	17/20	13/20
20	14/20	10/20
10	13/20	8/20

Table shows the number of positive results out of 20 replicates for each input concentration using both the Twista fluorometer and LFD.

established based on calibration with standard reference materials, ensuring that only true positives were reported, f. To assess potential cross-reactivity, the LFD assay was tested against respiratory syncytial virus (RSV), influenza (PR/8/34), and rabbit herpes virus, as well as several related flavivirus members; West Nile virus (WNV) and RNA from the other DENV serotypes (Table 3).

2.3 Clinical sample collection and ethics compliance

2.3.1 Ethics statement

Serum samples for clinical performance studies were obtained through the Dengue Surveillance System sample collection under guidelines approved by the Medical Faculty University Padjajaran (Bandung, Indonesia), M.S. Ramaiah Medical College Hospital (Bangalore, India) and Oregon State University (OSU) institutional review boards (IRB Approval #8053 on May 09, 2021). Patients did not provide verbal or written consent for this study. Samples were de-linked from patient identifiers according to IRB protocols.

A total of five acute serum samples from clinically suspected DENV-infected patients (average age: 20.3 years) were collected between 2022–2023 at Hospital Dokter Hasan Sadikin (Bandung, Indonesia) (Table 3). The RT-RPA assay was performed on a subset of these clinical samples at the Medical Faculty University Padjajaran (Bandung, Indonesia). Two samples (DENV_4, DENV_5) represent RNA extracted from cultured DENV2-positive patients confirmed by Lanciotti (RT-PCR) (Lanciotti et al., 1992). In addition, RNA from three patient serum samples (HTV093, HTV277, and HTV201) suspected to be DENV positive but previously unconfirmed were extracted using a Qiagen RNA extraction kit and tested using the DENV2-specific RT-RPA real-time assay (Table 3).

2.3.2 Patient sample collection on Watman FTA® cards

The purpose of using Flinders Technology Associates (FTA) cards for sample collection is two-fold. First, people in developing countries who live in remote villages may not be able to travel to city hospitals and the FTA card may benefit them if they are willing to send a finger pin-prick blood sample on FTA card for diagnosis. Secondly, surveillance of mosquitoes for dengue from different locations can be accomplished as the FTA card preserves RNA samples for a considerable time until processing.

Sample collection using Whatman FTA® technology (GE Healthcare Bio- Sciences Corp., USA) was also tested with both real-time and LFD (Figures 6A, B). Initial screens were prepared using spiked samples that contained 100 µl of DENV2 (NGC) virus from cell culture and applied to Indicating FTA® Micro Cards.

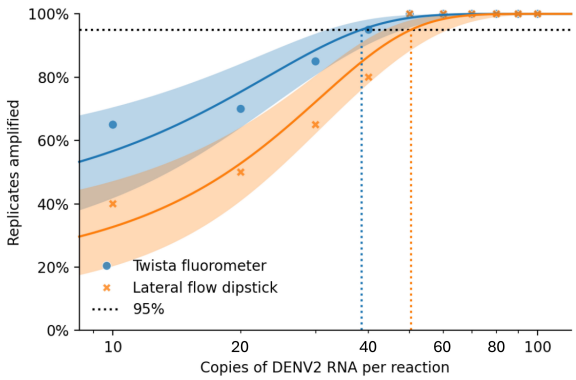

FIGURE 3
Combined Probit regression plot comparing Twista (fluorescence detection) and LFD (lateral flow): • Solid blue curve: Twista with 95% CI • Solid Orange curve: LFD with 95% CI • Blue circles: Observed Twista results • Orange cross: Observed LFD results • Dashed vertical lines show the estimated LoD at 95% detection for each method: o Twista ≈ 38.48 copies/reaction o LFD ≈ 50.37 copies/reaction.

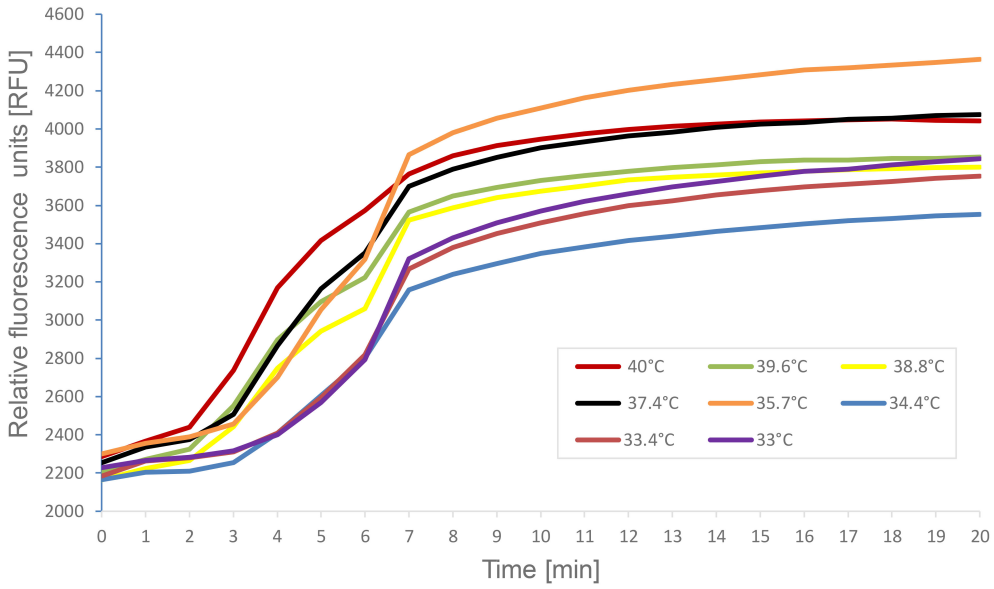

FIGURE 4
A representative image of the reaction temperature range for DENV2 specific real-time RT-RPA amplification products. Fluorescence measurements were made using the CFX96 Touch™ Real-Time PCR Detection System. The graph depicts the fluorescent signal for each of RT- RPA reactions which varied only in the temperature conditions. The key indicates the color on the graph that represents the temperature each RT- RPA reaction was run under.

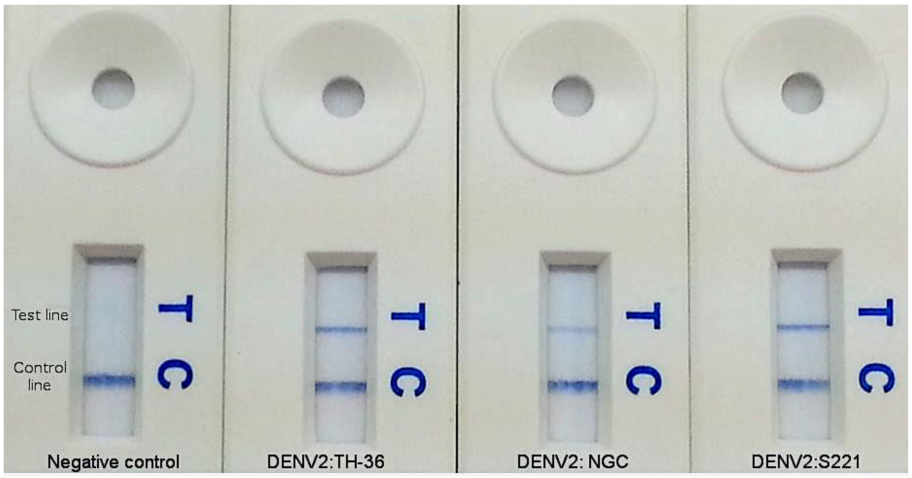

FIGURE 5
Amplification products for DENV2 RT-RPA assay visualized by LFD. Colorimetric signal at the test line (T) indicates positive amplification. Signal at control line (C) indicates a valid test.

After drying for at least 2 hours, RNA was extracted. At M.S. Ramaiah Medical College Hospital, India, a total of nine acute serum samples were collected from febrile patients during 2022–2023, suspected of having dengue 0–5 days after onset of symptoms and whose average age was 18.5 years (Figure 6C). For each of the nine patients sampled, both whole blood and serum samples were collected and applied to FTA® cards. These samples were confirmed by hospital personnel to have DENV infection by the NS1 based ELISA method (Dengue NS1 Ag Microlisa Kit, J.Mitra and Co Pvt. Ltd, India) but no information on serotype was available. Cards were stored for several months at room temperature followedby RNA extraction from the FTA® cards by the Molecular Diagnostics Laboratory at Oregon State University. Sample preparation was accomplished using the Ambion RNA Rapid Extraction solution (Life Technologies) followed by isolation using the Ambion MagMAX 96 viral RNA isolation kit (Life Technologies). The undiluted RNA was used as template in the RT-RPA assay and reactions were run in duplicate.

10.3389/fcimb.2025.1578549

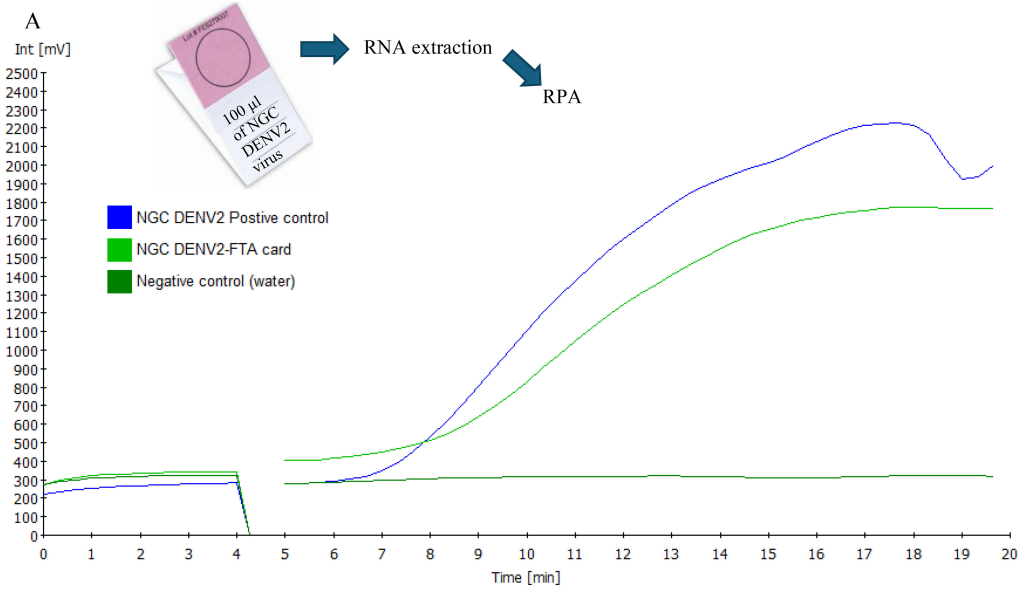

C

Summary of RPA amplification using real-time detection on the Twista fluorometer for clinical samples on FTA cards

Clinical sample	RT-RPA amplification (whole blood)	RT-RPA amplification (serum)
R335442	Negative	Negative
M519936	Negative	Negative
AK520639	Negative	Negative
V494207	Negative	Negative
PK520812	Negative	Positive
M521383	Negative	Negative
L521617	Negative	Negative
M522432	Negative	Negative
L519824	Negative	Negative

FIGURE 6
Amplification of samples from FTA cards. RNA collected from FTA® cards spiked with NGC DENV2 was amplified by our RT-RPA assay and visualized using both real-time **(A)** and LFD formats **(B)**. Following this spiked trial, the clinical samples obtained from patients in India were tested **(C)**. RNA from both whole blood and serum FTA® card samples were analyzed by RT-RPA specific to DENV2. For each of the replicates tested, one of the patient serum samples (PK520812s) was amplified by RT-RPA measured by both the real time and LFD formats **(C)**.

2.4 Assessment of DENV2 specific RT-RPA assay reaction conditions and robustness

2.4.1 Temperature tolerance

Reaction conditions were also examined for the RT-RPA assay. Using the real-time format, identical RT-RPA reactions were run under several different temperature conditions (Figure 4). The Twista reader is capable of holding the reactions at only a single temperature, therefore, the CFX thermocycler was used as a fluorometer so, samples could be subjected to a gradient ofconstant temperatures. Reactions contained 10^{-2} dilution of DENV2 (NGC) and the temperatures tested ranged from the manufacture's recommended 40°C down to 33°C. As seen in Figure 4, each temperature tested resulted in amplification products, highlighting the adaptable nature of RPA amplification in regard to temperature.

2.4.2 Carry-over and cross-contamination

To ensure the accuracy and reliability of the detection process, rigorous contamination control measures were implemented. Prior to opening the sample cap, the exterior surface was disinfected with 70% ethanol to eliminate potential contaminants. All handling and processing were conducted within a laminar flow hood to prevent environmental contamination. To evaluate possible cross-contamination of samples while performing the assay, a panel of DENV-1–4 was used at high positive (10^7 Genome Copy Equivalent (GCE/mL) and below limit of detection (LOD)(10^1 GCE/mL) concentrations, respectively. Samples below LOD are composed of normal human serum spiked with DENV to a concentration just below the LOD. Five replicates of the high positive and below LOD DENV concentrations were extracted using the Ambion MagMAX 96 viral RNA isolation kit (Life Technologies) and tested in alternating series. All negative samples tested negative (5/5) and

10.3389/fcimb.2025.1578549

TABLE 3 Summary of DENV2 RPA amplification using real-time detection on the Twista fluorometer and LFD.

Template	RT-RPA amplification	LFD detection
Laboratory samples		
DENV2: strain NGC	Positive	Positive
DENV2: strain TH-36	Positive	Positive
DENV2: strain S221	Positive	Positive
DENV1: strain Westpac	Negative	Negative
DENV1: strain TH-SMAN	Negative	Negative
DENV3: Strain H87	Negative	Negative
DENV4: Strain H241	Negative	Negative
DENV4: Strain TVP 360	Negative	Negative
WNV	Negative	Negative
RSV	Negative	Negative
Influenza	Negative	Negative
Herpes virus	Negative	Negative
Tissue culture negative	Negative	Negative
negative control (water)	Negative	Negative
Clinical samples		
DENV_4	Positive	Positive
DENV_5	Positive	Positive
HTV 201	Negative	Negative
HTV 277	Negative	Negative
HTV 337	Negative	Negative

The source of the template used in the RT-RPA reaction is indicated in the template column and the RT-RPA amplification column indicates whether amplification was observed. For LFD, positive results were indicated by two lines (C-line and T-line), while negative results showed only the C-line.

all DENV positive samples tested positive for DENV (5/5). Several below LOD samples produced CT values >39 that may correspond to detection of DENV RNA; however, these results are not 100% reproducible (data not shown).

2.4.3 Performance in fresh vs. frozen specimens

To assess the impact of temperature fluctuations on assay performance, DENV2-spiked human serum samples were tested following multiple freeze–thaw cycles. Moderate and low positive dilutions were prepared in triplicate, frozen at −80°C for 24 hours, and subjected to five consecutive freeze/thaw cycles. Once thawed, every sample was processed according to the assay protocol. Data showed a 100% qualitative agreement between the initial and post freeze/thaw cycle (1, 2, 3, 4, and 5) detection results (data not shown).

2.5 Statistical analysis

All experimental data were analyzed using appropriate statistical methods to assess the sensitivity, specificity, and reproducibility of the RT-RPA assay. The limit of detection (LOD95) was determined using probit regression analysis to estimate the viral copy number at which 95% of reactions yielded positive results (Figure 3). Specificity was evaluated by testing the assay against non-target viruses, and results were analyzed for cross-reactivity. Reproducibility was assessed by performing triplicate experiments across independent runs and calculating mean cycle threshold (Ct) values, standard deviations, and coefficients of variation. Clinical validation results were analyzed using positive percent agreement (PPA), negative percent agreement (NPA), and overall accuracy in comparison to reference methods. Data analysis was conducted using GraphPad Prism and R statistical software, with significance levels set at $p< 0.05$ where applicable.

3 Results

3.1 Sensitivity of DENV2 detection by real-time RT-RPA and LFD

3.1.1 Analytical sensitivity

The sensitivity of the RT-RPA assay was evaluated using both real-time fluorescence (Twista fluorometer) and lateral flow device (LFD) formats. Although amplification was observed at input levels as low as 10–25 copies per reaction, only the 50-copy dilution consistently yielded positive results in 100% of replicates within the 20-minute reaction window. Similarly, the LFD format detected 50 copies per reaction across all replicates, though its sensitivity declined more rapidly at lower input concentrations compared to real-time detection (Table 2).

3.1.2 Limit of detection by probit analysis

Probit regression analysis was performed to determine the 95% limit of detection (LoD_{95}) for each detection method (Figure 3). The estimated LoD_{95} was approximately 38.48 copies/reaction for the Twista fluorometer and 50.37 copies/reaction for LFD. These findings demonstrate that real-time RT-RPA offers greater sensitivity, capable of detecting lower quantities of DENV2 RNA with high confidence.

3.1.3 Strain coverage

The assay's ability to detect multiple DENV2 strains was also assessed. RNA from each strain was diluted to 10^2 copies/reaction in nuclease-free water and tested in at least three replicates. All tested DENV2 strains were successfully amplified by the RT-RPA assay and detected by both the Twista fluorometer and LFD formats (Figure 2A; Figure 5; Table 3). Representative amplification results are shown in Figures 2A and 5, confirming the assay's broad detection capability across DENV2 variants.

3.2 Specificity of DENV2 detection by real-time RT-RPA and LFD

3.2.1 Non-target testing

The specificity of the DENV2 RT-RPA assay was evaluated using both real-time fluorescence detection (Twista fluorometer) and LFD formats. A panel of non-target templates was tested in at least three replicates each to assess cross-reactivity. These included two negative controls—nuclease-free water and a tissue culture negative control—as well as a range of unrelated viral RNA templates: respiratory syncytial virus (RSV), influenza A virus (PR/8/34), and rabbit herpesvirus. In addition, several closely related flaviviruses were included: West Nile virus (WNV) and RNA from DENV serotypes 1, 3, and 4 (Table 3).

All non-target templates tested negative by both detection methods, indicating high specificity of the RT-RPA assay for DENV2.

3.2.2 Product confirmation

Amplification reactions were performed using 0.05 µL of viral cDNA in a 50-µL reaction volume. Results of the specificity evaluation are summarized in Table 1 and confirm that the selected primers are highly specific to the DENV2 genome. Amplicons from NGC samples were further analyzed by agarose gel electrophoresis (Figure 2B) and confirmed by sequencing. Sequencing results verified that the amplified products matched the expected DENV2 target region.

3.3 Detection methods of RT-RPA products

Amplification products were detected using two formats: real-time fluorescence via the Twista fluorometer and colorimetric visualization via a lateral flow device (LFD). Both detection methods yielded concordant results, with the Twista fluorometer and LFD producing identical outcomes across all tested samples. The LFD successfully generated visible positive signals for all DENV2 strains and negative results for non-DENV2 viral templates, including other flaviviruses and unrelated respiratory viruses (Figure 2A; Figure 5; Table 3). These results confirm the high specificity of the assay and its versatility across detection platforms.

LFD band intensity was observed to vary depending on reaction time, sample concentration, flow rate, and reagent interactions. Therefore, reaction conditions were standardized prior to sample testing to ensure consistency and reproducibility.

3.4 Assessment of DENV2-specific RT-RPA assay in clinical samples

3.4.1 Detection in cell culture-derived samples

The RT-RPA assay was first evaluated using RNA from cell culture-derived samples. Two samples (DENV_4 and DENV_5), obtained from patients previously confirmed to be infected with DENV2, produced clear and consistent amplification using both real-time fluorescence (Twista fluorometer) and LFD formats (Table 3). These results confirmed the assay's effectiveness in detecting DENV2 RNA under controlled sample conditions.

3.4.2 Specificity evaluation in suspected clinical samples

Three suspected dengue-positive blood samples (HTV093, HTV277, and HTV201) failed to generate amplification with the DENV2-specific RT-RPA assay in either detection format (Table 3). Subsequent RT-PCR serotyping identified all three samples as DENV3, further validating the specificity of the RT-RPA assay for the DENV2 serotype and ruling out cross-reactivity with other dengue serotypes.

3.4.3 Detection from FTA® card samples

DENV2 RNA preserved on FTA® cards was reliably detected using both Twista and LFD formats (Figures 6A, B). Clinical testing of FTA® card samples from patients in India showed that one serum sample (PK520812s) yielded a positive amplification signal across all replicates with both detection methods (Figure 6C). In contrast, the matching whole blood sample from the same patient, as well as all other clinical samples collected on FTA® cards, did not produce detectable signals.

3.5 Assessment of DENV2-specific RT-RPA assay reaction conditions and robustness

3.5.1 Temperature tolerance

The RT-RPA assay demonstrated robust performance across a range of constant temperatures (33°C to 40°C) using a 10^{-2} dilution of DENV2 RNA. Amplification was successful at all tested temperatures (Figure 4), confirming the assay's adaptability to variable field or laboratory conditions.

3.5.2 Carry-over and cross-contamination

To assess cross-contamination risk, DENV1–4 samples were tested in alternating high-positive (10^7 GCE/mL) and below-LoD (10^1 GCE/mL) concentrations. All high-positive samples tested positive, and all low-level samples tested negative (5/5), confirming the effectiveness of contamination control measures. Sporadic late signals (Ct >39) in below-LoD samples were not reproducible.

3.5.3 Freeze–thaw stability

DENV2-spiked serum samples subjected to five freeze–thaw cycles showed 100% agreement in detection across all replicates compared to fresh controls. This indicates the assay is resilient to temperature stress and suitable for use with stored or transported clinical specimens.

4 Discussion

Rapid and sensitive detection of DENV is critical to the disease management of a virus with such a prominent burden to human health (Kabir et al., 2021). The findings of this study highlight the potential of the real-time RT-RPA assay as a valuable tool for the rapid detection of DENV2. One of the primary strengths of the assay is its high sensitivity. The assay reliably amplified DENV2 at concentrations as low as 50 copies per reaction as detected by both Twista fluorometer and LFD, with probit regression estimating an LOD95 of approximately 38.48 copies per reaction for Twista fluorometer and 50.37 copies per reaction for LFD. This low detection limit is particularly promising for early diagnosis when viral loads might be low, thus facilitating prompt patient management and outbreak control. Equally important is the assay's specificity. By rigorously testing against a range of non-DENV2 viral templates—including other flaviviruses and unrelated respiratory pathogens—the study confirmed that the selected primers exclusively target DENV2 RNA. This high specificity minimizes the risk of false positives, which is critical in areas where multiple flaviviruses co-circulate.

The dual-mode detection capability—real-time fluorescence and lateral flow device (LFD) readout—greatly enhances the assay's versatility. The real-time format allows for quantitative assessments in a controlled laboratory environment, while the LFD format provides a rapid, equipment-free method suitable for point-of-care testing. This versatility is especially beneficial in resource-limited settings or during outbreak scenarios where rapid, on-site diagnostics can significantly impact public health responses.

Moreover, the assay demonstrated robust performance across a range of temperatures, from 33°C to 40°C, and after multiple freeze/thaw cycles, suggesting that it can accommodate variations in both environmental conditions and sample handling. This resilience is vital for field applications, where laboratory-grade environmental control may not be available. The ability to work effectively with samples stored on FTA® cards further supports the potential for using this assay in remote or resource-constrained regions, facilitating safe sample collection and transport.

Validation of clinical samples demonstrated that the newly developed RT-RPA/LFD assay exhibits diagnostic performance comparable to that of the gold standard real-time RT-PCR assay for routine DENV detection (Wang and Gubler, 2018), but this method simplifies the instrumentation requirements and reduces the cost. Although methods like RT-RPA (Teoh et al., 2015) and LAMP (Dauner et al., 2015; Lopez-Jimena et al., 2018) enable rapid dengue diagnosis, the novel RT-RPA/LFD assay offers notable advantages. Its lateral-flow dipstick design allows results to be read by the naked eye in 10 mins, eliminating the need for specialized equipment and trained personnel. Additionally, operating at 37°C—using body heat for amplification—it is well-suited for field use and low-resource settings, unlike other methods that require precise temperature control and power-dependent instrumentation.

The combination of RT-RPA and LFD has been successfully applied for the rapid detection of SARS-CoV-2, influenza A and B, Coxsackievirus A6, and hepatitis B virus (Liu et al., 2021; Sun et al., 2019; Xie et al., 2021; Zhang et al., 2021; Zhao et al., 2024). Additionally, RT-RPA combined with LFD and CRISPR/Cas12a has been used to detect pan-DENV serotypes (Bhardwaj et al., 2025; Xi et al., 2019; Xiong et al., 2020). However, few studies have focused specifically on serotype-specific detection of DENV2 using this format. While pan-DENV detection confirms the presence of the virus, serotype-specific detection provides critical, actionable insights that improve patient management, inform public health interventions, support vaccine development, and enhance our understanding of dengue epidemiology.

Although all four dengue serotypes circulate globally, DENV2 is often considered the most prevalent serotype, particularly in regions such as India and the Americas, where it is associated with a higher proportion of severe dengue cases (Sirisena et al., 2021). Our work addresses this gap by developing a sensitive, field-deployable RT-RPA/LFD assay specifically targeting the DENV2 serotype. The implementation of this assay may facilitate rapid serotype-specific diagnosis and contribute to improved dengue control efforts in the current global health landscape.

While initial clinical evaluations, including tests on cell culture samples and FTA® card-collected specimens, provided encouraging results, some limitations remain. For instance, the assay failed to amplify RNA from certain blood samples that were later identified as DENV3 infections, underscoring the assay's high specificity for DENV2 but also pointing to the need for multiplexing capabilities if detection of all dengue serotypes is desired in a clinical diagnostic tool. Additionally, the relatively small dataset used for probit regression to estimate the LOD95 calls for future work involving larger numbers of clinical samples to refine the detection limits and ensure reproducibility across diverse conditions.

Future research should focus on developing a multiplex RT-RPA assay that can simultaneously detect multiple dengue serotypes or other co-circulating arboviruses, such as Zika and chikungunya. Larger-scale studies across diverse geographic regions and patient populations will be essential to validate the assay's diagnostic performance and establish standardized protocols. An evaluation of the cost-effectiveness and scalability of the RT-RPA assay, compared to traditional RT-PCR methods, could facilitate its adoption in public health programs, and integrating data connectivity with the LFD format might streamline surveillance efforts and enhance data collection during outbreak monitoring.

In summary, the real-time RT-RPA assay for DENV2 exhibits considerable promise due to its high sensitivity, specificity, and operational versatility. Its adaptability to different detection formats and robustness under variable conditions position it as an attractive option for both laboratory and field-based diagnostics. With further validation, optimization, and expansion into multiplex formats, this assay could become a key tool in the early diagnosis and management of dengue outbreaks, ultimately contributing to improved patient care and more effective public health responses.

Data availability statement

The original contributions presented in the study are included in the article/supplementary material. Further inquiries can be directed to the corresponding author.

Ethics statement

The studies involving humans were approved by IRB# 8053; Human Research Protection Program and Institutional Review Board, Oregon State University. Approval letter has been uploaded under supplemental files section. Note: This approval includes the clinical samples obtained from The Medical Faculty University Padjajaran, Bandung, Indonesia, and M.S. Ramaiah Medical College, Bangalore, India. The studies were conducted in accordance with the local legislation and institutional requirements. The human samples used in this study were acquired from a by-product of routine care or industry. Written informed consent for participation was not required from the participants or the participants' legal guardians/next of kin in accordance with the national legislation and institutional requirements.

Author contributions

MAP: Conceptualization, Data curation, Formal analysis, Investigation, Methodology, Validation, Visualization, Writing – original draft, Writing – review & editing. MK: Formal analysis, Methodology, Resources, Validation, Writing – review & editing. DM: Methodology, Validation, Visualization, Writing – review & editing. MKP: Conceptualization, Data curation, Formal analysis, Funding acquisition, Investigation, Project administration, Resources, Supervision, Visualization, Writing – original draft, Writing – review & editing.

Funding

The author(s) declare that financial support was received for the research and/or publication of this article. Funding for this work was provided by KMT Research LLC, and Oregon State University College of Veterinary Medicine.

Acknowledgments

We would like to thank both Dr. Alec Hirsch and Dr. William Messer from Oregon Health and Science University (OHSU) for providing DENV2 laboratory strains used in this study. We would like to thank Dr. Dave Stein from OHSU for facilitating the transfer of virus strains and for providing technical support. We would also like to thank Dr. Indumathi, M.S. Ramaiah Medical College, Bangalore, India, for providing clinical samples on FTA cards, and Oregon State University Veterinary Diagnostic Laboratory for processing the FTA cards. We would like to thank Dr. Bachti Alisjahbana and Lidya Chaidir Medical Faculty University Padjajaran, Bandung, Indonesia, for providing and executing RPA assay experiments for Indonesian clinical samples. We would like to thank Dr. Jan Medlock for Statistical analysis.

Conflict of interest

Authors MK and DM were employed by the company KTM Research LLC.

The remaining authors declare that the research was conducted in the absence of any commercial or financial relationships that could be construed as a potential conflict of interest.

Generative AI statement

The author(s) declare that no Generative AI was used in the creation of this manuscript.

Publisher's note

References

Ananta Preecha, S., Chanama, S., A-nuegoonpipat, A., Naemkhunthot, S., Sa-Ngasang, A., Sawanpanyalert, P., et al. (2005). Serological and virological features of dengue fever and dengue haemorrhagic fever in Thailand from 1999 to 2002. *Epidemiol. Infect.* 133, 503–507. doi: 10.1017/S0950268804003541

Beatty, M. E., Beutels, P., Meltzer, M. I., Shepard, D. S., Hombach, J., Hutubessy, R., et al. (2011). Health economics of dengue: a systematic literature review and expertpanel's assessment. *Am. J. Trop. Med. Hyg* 84, 473–488. doi: 10.4269/ajtmh.2011.10-0521

Bhardwaj, P., Dhangur, P., Kalichamy, A., and Singh, R. (2025). RT-RPA assisted CRISPR/cas12a based one-pot rapid and visual detection of the pan-dengue virus. *J. Med. Virol.* 97, e70219. doi: 10.1002/jmv.70219

Bhatt, S., Gething, P. W., Brady, O. J., Messina, J. P., Farlow, A. W., Moyes, C. L., et al. (2013). The global distribution and burden of dengue. *Nature* 496, 504–507. doi: 10.1038/nature12060

Blacksell, S. D., Jarman, R. G., Gibbons, R. V., Tanganuchitcharnchai, A., Mammen, M. P., Nisalak, A., et al. (2012). Comparison of seven commercial antigen and antibody enzyme-linked immunosorbent assays for detection of acute dengue infection. *Clin. Vaccine Immunol.* 19, 804–810. doi: 10.1128/CVI.05717-11

Boehringer, H. R., and O'Farrell, B. J. (2021). Lateral flow assays in infectious disease diagnosis. *Clin. Chem.* 68, 52–58. doi: 10.1093/clinchem/hvab194

Bonnet, E., Jaarsveldt, D. V., and Burt, F. J. (2022). Rapid reverse transcriptase recombinase polymerase amplification assay for flaviviruses using non-infectious *in*

vitro transcribed RNA as positive controls. *J. Virological Methods* 299, 114351. doi: 10.1016/j.jviromet.2021.114351

Dauner, A. L., Mitra, I., Gilliland, T. Jr., Seales, S., Pal, S., Yang, S. C., et al. (2015). Development of a pan-serotype reverse transcription loop-mediated isothermal amplification assay for the detection of dengue virus. *Diagn. Microbiol. Infect. Dis.* 83, 30–36. doi: 10.1016/j.diagmicrobio.2015.05.004

de Araújo, J. M., Schatzmayr, H. G., de Filippis, A. M., Dos Santos, F. B., Cardoso, M. A., Britto, C., et al. (2009). A retrospective survey of dengue virus infection in fatal cases from an epidemic in Brazil. *J. Virol Methods* 155 1), 34–38. doi: 10.1016/j.jviromet.2008.09.023

Edillo, F. E., Halasa, Y. A., Largo, F. M., Erasmo, J. N., Amoin, N. B., Alera, M. T., et al. (2015). Economic cost and burden of dengue in the Philippines. *Am. J. Trop. Med. Hyg* 92, 360–366. doi: 10.4269/ajtmh.14-0139

Endy, T. P., Nisalak, A., Chunsuttitwat, S., Vaughn, D. W., Green, S., Ennis, F. A., et al. (2004). Relationship of preexisting dengue virus (DV) neutralizing antibody levels to viremia and severity of disease in a prospective cohort study of DV infection in Thailand. *J. Infect. Dis.* 189, 990–1000. doi: 10.1086/382280

Felix, A. C., Romano, C. M., Centrone, C., Rodrigues, C. L., Villas-Boas, L., Araújo, E. S., et al. (2012). Low sensitivity of NS1 protein tests evidenced during a dengue type 2 virus outbreak in Santos, Brazil. *Clin. Vaccine Immunol.* 19, 1972–1976. doi: 10.1128/CVI.00535-12

Fernández, R. J., and Vázquez, S. (1990). Serological diagnosis of dengue by an ELISA inhibition method (EIM). *Mem Inst Oswaldo Cruz* 85, 347–351. doi: 10.1590/S0074-02761990000300012

Fried, J. R., Gibbons, R. V., Kalayanarooj, S., Thomas, S. J., Srikiatkhachorn, A., Yoon, I. K., et al. (2010). Serotype-specific differences in the risk of dengue hemorrhagic fever: an analysis of data collected in Bangkok, Thailand from 1994 to 2006. *PloS Negl. Trop. Dis.* 4, e617. doi: 10.1371/journal.pntd.0000617

Gibbons, R. V., Kalanarooj, S., Jarman, R. G., Nisalak, A., Vaughn, D. W., Endy, T. P., et al. (2007). Analysis of repeat hospital admissions for dengue to estimate the frequency of third or fourth dengue infections resulting in admissions and dengue hemorrhagic fever, and serotype sequences. *Am. J. Trop. Med. Hyg* 77, 910–913. doi: 10.4269/ajtmh.2007.77.910

Gulland, A. (2013). Burden of dengue fever is higher than previously thought. *BMJ* 347, f6280. doi: 10.1136/bmj.f6280

Guzman, M. G., Alvarez, M., and Halstead, S. B. (2013). Secondary infection as a risk factor for dengue hemorrhagic fever/dengue shock syndrome: an historical perspective and role of antibody-dependent enhancement of infection. *Arch. Virol* 158, 1445–1459. doi: 10.1007/s00705-013-1645-3

Halstead, S. B. (2006). Dengue in the Americas and Southeast Asia: do they differ? *Rev. Panam Salud Publica* 20, 407–415. doi: 10.1590/S1020-49892006001100007

Hunsperger, E. A., Yoksan, S., Buchy, P., Nguyen, V. C., Sekaran, S. D., Enria, D. A., et al. (2009). Evaluation of commercially available anti-dengue virus immunoglobulin M tests. *Emerg Infect. Dis.* 15, 436–440. doi: 10.3201/eid1503.080923

Hunsperger, E. A., Yoksan, S., Buchy, P., Nguyen, V. C., Sekaran, S. D., Enria, D. A., et al. (2014). Evaluation of commercially available diagnostic tests for the detection of dengue virus NS1 antigen and anti-dengue virus IgM antibody. *PloS Negl. Trop. Dis.* 8, e3171. doi: 10.1371/journal.pntd.0003171

Johnson, B. W., Russell, B. J., and Lanciotti, R. S. (2005). Serotype-specific detection of dengue viruses in a fourplex real-time reverse transcriptase PCR assay. *J. Clin. Microbiol* 43, 4977–4983. doi: 10.1128/JCM.43.10.4977-4983.2005

Kabir, M. A., Zilouchian, H., Younas, M. A., and Asghar, W. (2021). Dengue detection: advances in diagnostic tools from conventional technology to point of care. *Biosensors* 11, 206. doi: 10.3390/bios11070206

Kakkar, S., Gupta, P., Singh Yadav, S. P., Raj, D., Singh, G., Chauhan, S., et al. (2024). Lateral flow assays: Progress and evolution of recent trends in point-of-care applications. *Mater Today Bio* 28, 101188. doi: 10.1016/j.mtbio.2024.101188

Lanciotti, R. S., Calisher, C. H., Gubler, D. J., Chang, G. J., and Vorndam, A. V. (1992). Rapid detection and typing of dengue viruses from clinical samples by using reverse transcriptase-polymerase chain reaction. *J. Clin. Microbiol* 30, 545–551. doi: 10.1128/jcm.30.3.545-551.1992

Liu, D., Shen, H., Zhang, Y., Shen, D., Zhu, M., Song, Y., et al. (2021). A microfluidic-integrated lateral flow recombinase polymerase amplification (MI-IF-RPA) assay for rapid COVID-19 detection. *Lab. Chip* 21, 2019–2026. doi: 10.1039/D0LC01222J

Lopez-Jimena, B., Bekaert, M., Bakheit, M., Frischmann, S., Patel, P., Simon-Loriere, E., et al. (2018). Development and validation of four one-step real-time RT-LAMP assays for specific detection of each dengue virus serotype. *PloS Negl. Trop. Dis.* 12, e0006381. doi: 10.1371/journal.pntd.0006381

Malavige, G. N., Sjö, P., Singh, K., Piedagnel, J. M., Mowbray, C., Estani, S., et al. (2023). Facing the escalating burden of dengue: Challenges and perspectives. *PloS Glob Public Health* 3, e0002598. doi: 10.1371/journal.pgph.0002598

Medina, F., Medina, J. F., Colón, C., Vergne, E., Santiago, G. A., and Muñoz-Jordán, J. L. (2012). Dengue virus: isolation, propagation, quantification, and storage. *Curr. Protoc. Microbiol* 15, 15D.2. doi: 10.1002/9780471729259.mc15d02s27

Moi, M. L., Omatsu, T., Tajima, S., Lim, C. K., Kotaki, A., Ikeda, M., et al. (2013). Detection of dengue virus nonstructural protein 1 (NS1) by using ELISA as a useful laboratorydiagnostic method for dengue virus infection of international travelers. *J. Travel Med.* 20, 185–193. doi: 10.1111/jtm.12018

Najioullah, F., Viron, F., and Césaire, R. (2014). Evaluation of four commercial real-time RT-PCR kits for the detection of dengue viruses in clinical samples. *Virol J.* 11, 164. doi: 10.1186/1743-422X-11-164

Paranavitane, S. A., Gomes, L., Kamaladasa, A., Adikari, T. N., Wickramasinghe, N., Jeewandara, C., et al. (2014). Dengue NS1 antigen as a marker of severe clinical disease. *BMC Infect. Dis.* 14, 570. doi: 10.1186/s12879-014-0570-8

Peeling, R. W., Artsob, H., Pelegrino, J. L., Buchy, P., Cardosa, M. J., Devi, S., et al. (2010). Evaluation of diagnostic tests: dengue. *Nat. Rev. Microbiol* 8, S30–S38. doi: 10.1038/nrmicro2459

Piepenburg, O., Williams, C. H., Stemple, D. L., and Armes, N. A. (2006). DNA detection using recombination proteins. *PloS Biol.* 4, e204. doi: 10.1371/journal.pbio.0040204

Potts, J. A., and Rothman, A. L. (2008). Clinical and laboratory features that distinguish dengue from other febrile illnesses in endemic populations. *Trop. Med. Int. Health* 13, 1328–1340. doi: 10.1111/j.1365-3156.2008.02151.x

Sahni, A. K., Grover, N., Sharma, A., Khan, I. D., and Kishore, J. (2013). Reverse transcription loop-mediated isothermal amplification (RT-LAMP) for diagnosis of dengue. *Med. J. Armed Forces India* 69, 246–253. doi: 10.1016/j.mjafi.2012.07.017

Saito, Y., Moi, M. L., Kotaki, A., Ikeda, M., Tajima, S., Shiba, H., et al. (2015). Detection of dengue virus nonstructural protein 1 (NS1) in urine samples using ELISA as a laboratory diagnostic method for dengue virus infection. *Jpn J. Infect. Dis.* 68 (6), 455-460. doi: 10.7883/yoken.JJID.2014.441

Salmon-Mulanovich, G., Blazes, D. L., Lescano, A. G., Bausch, D. G., Montgomery, J. M., and Pan, W. (2015). Economic burden of dengue virus infection at the household level among residents of puerto maldonado, Peru. *Am. J. Trop. Med. Hyg.* 93 (4), 684-690. doi: 10.4269/ajtmh.14-0755

Sangkawibha, N., Rojanasuphot, S., Ahandrik, S., Viriyapongse, S., Jatanasen, S., Salitul, V., et al. (1984). Risk factors in dengue shock syndrome: a prospective epidemiologic study in Rayong, Thailand. I. The 1980 outbreak. *Am. J. Epidemiol.* 120, 653–669. doi: 10.1093/oxfordjournals.aje.a113932

Santiago, G. A., Vergne, E., Quiles, Y., Cosme, J., Vazquez, J., Medina, J. F., et al. (2013). Analytical and clinical performance of the CDC real time RT-PCR assay for detection and typing of dengue virus. *PloS Negl. Trop. Dis.* 7, e2311. doi: 10.1371/journal.pntd.0002311

Shepard, D. S., Halasa, Y. A., Tyagi, B. K., Adhish, S. V., Nandan, D., Karthiga, K. S., et al. (2014). Economic and disease burden of dengue illness in India. *Am. J. Trop. Med. Hyg* 91, 1235–1242. doi: 10.4269/ajtmh.14-0002

Shepard, D. S., Undurraga, E. A., and Halasa, Y. A. (2013). Economic and disease burden of dengue in Southeast Asia. *PloS Negl. Trop. Dis.* 7, e2055. doi: 10.1371/journal.pntd.0002055

Sirisena, P. D. N., Mahilkar, S., Sharma, C., Jain, J., and Sunil, S. (2021). Concurrent dengue infections: Epidemiology & clinical implications. *Indian J. Med. Res.* 154, 669–679. doi: 10.4103/ijmr.IJMR_1219_18

Sun, N., Wang, Y., Yao, X., Chen, F., Gao, D., Wang, W., et al. (2019). Visual signal generation for the detection of influenza viruses by duplex recombinase polymerase amplification with lateral flow dipsticks. *Anal. Bioanal Chem.* 411, 3591–3602. doi: 10.1007/s00216-019-01840-zTeoh

Teoh, B., Sam, S., Tan, K., Danlami, M. B., Shu, M., Johari, J., et al. (2015). Early detection of dengue virus by use of reverse transcription-recombinase polymerase amplification. *J. Clin. Microbiol.* 53, 830-837. doi: 10.1128/jcm.02648-14

Thomas, L., Verlaeten, O., Cabié, A., Kaidomar, S., Moravie, V., Martial, J., et al. (2008). Influence of the dengue serotype, previous dengue infection, and plasma viral load on clinical presentation and outcome during a dengue-2 and dengue-4 co-epidemic. *Am. J. Trop. Med. Hyg* 78, 990–998. doi: 10.4269/ajtmh.2008.78.990

Trivedi, S., and Chakravarty, A. (2022). Neurological complications of dengue fever. *Curr. Neurol. Neurosci. Rep.* 22, 515–529. doi: 10.1007/s11910-022-01213-7

Twist, DX. (2018). *Appendix to the TwistAmpTM reaction kit manuals* (Cambridge, UK: twistdx.co.UK).

Undurraga, E. A., Betancourt-Cravioto, M., Ramos-Castañeda, J., Martínez-Vega, R., Méndez-Galván, J., Gubler, D. J., et al. (2015). Economic and disease burden of dengue in Mexico. *PloS Negl. Trop. Dis.* 9, e0003547. doi: 10.1371/journal.pntd.0003547

Vaughn, D. W., Green, S., Kalayanarooj, S., Innis, B. L., Nimmannitya, S., Suntayakorn, S., et al. (2000). Dengue viremia titer, antibody response pattern, and virus serotype correlate with disease severity. *J. Infect. Dis.* 181, 2–9. doi: 10.1086/315215

Wang, W., and Gubler, D. J. (2018). Potential point-of-Care testing for dengue virus in the field. *J. Clin. Microbiol* 56. doi: 10.1128/jcm.00203-18.https://doi.org/10.1128/jcm.00203-18

Whitehorn, J., and Simmons, C. P. (2011). The pathogenesis of dengue. *Vaccine* 29, 7221–7228. doi: 10.1016/j.vaccine.2011.07.022

WHO (2012). *Global strategy for dengue prevention and control. edited by WHO* (Geneva: WHO).

WHO (2025). Available online at: https://www.who.int/news-room/fact-sheets/detail/dengue-and-severe-dengue (Accessed February 5, 2025).

WHO and Special Programme for Research and Training in Tropical Diseases (2009). *Dengue: guidelines for diagnosis, treatment, prevention and control. edited by WHO* (Geneva: WHO).

Wichmann, O., Yoon, I. K., Vong, S., Limkittikul, K., Gibbons, R. V., Mammen, M. P., et al. (2011). Dengue in Thailand and Cambodia: an assessment of the degree of underrecognized disease burden based on reported cases. *PloS Negl. Trop. Dis.* 5, e996. doi: 10.1371/journal.pntd.0000996

Wu, S. J., Lee, E. M., Putvatana, R., Shurtliff, R. N., Porter, K. R., Suharyono, W., et al. (2001). Detection of dengue viral RNA using a nucleic acid sequence-based amplification assay. *J. Clin. Microbiol* 39, 2794–2798. doi: 10.1128/JCM.39.8.2794-2798.2001

Xi, Y., Xu, C. Z., Xie, Z. Z., Zhu, D. L., and Dong, J. M. (2019). Rapid and visual detection of dengue virus using recombinase polymerase amplification method combined with lateral flow dipstick. *Mol. Cell. Probes* 46, 101413. doi: 10.1016/j.mcp.2019.06.003

Xie, J., Yang, X., Duan, L., Chen, K., Liu, P., Zhan, W., et al. (2021). One-step reverse-transcription recombinase polymerase amplification using lateral flow strips for the detection of coxsackievirus A6. *Front. Microbiol.* 12. doi: 10.3389/fmicb.2021.629533

Xiong, Y., Luo, Y., Li, H., Wu, W., Ruan, X., and Mu, X. (2020). Rapid visual detection of dengue virus by combining reverse transcription recombinase-aided amplification with lateral-flow dipstick assay. *Int. J. Infect. diseases: IJID: Off. Publ. Int. Soc. Infect. Dis.* 95, 406–412. doi: 10.1016/j.ijid.2020.03.075

Yamada, K., Takasaki, T., Nawa, M., and Kurane, I. (2002). Virus isolation as one of the diagnostic methods for dengue virus infection. *J. Clin. Virol* 24, 203–209. doi: 10.1016/S1386-6532(01)00250-5

Zhang, B., Zhu, Z., Li, F., Xie, X., and Ding, A. (2021). Rapid and sensitive detection of hepatitis B virus by lateral flow recombinase polymerase amplification assay. *J. Virological Methods* 291, 114094. doi: 10.1016/j.jviromet.2021.114094

Zhao, Y., Wei, Y., Ye, C., Cao, J., Zhou, X., Xie, M., et al. (2024). Application of recombinase polymerase amplification with lateral flow assay to pathogen point-of-care diagnosis. *Front. Cell Infect. Microbiol* 14. doi: 10.3389/fcimb.2024.1475922

frontiers | Frontiers in Cellular and Infection Microbiology

TYPE Original Research
PUBLISHED 26 May 2025
DOI 10.3389/fcimb.2025.1534519

OPEN ACCESS

EDITED BY
Ariadna Petronela Fildan,
Ovidius University, Romania

REVIEWED BY
Nan Zheng,
Nanjing University, China
Gaurav Sutrave,
The University of Sydney, Australia

*CORRESPONDENCE
Ziyang Li
zylicsu@csu.edu.cn
Min Hu
huminjyk@csu.edu.cn

RECEIVED 26 November 2024
ACCEPTED 23 April 2025
PUBLISHED 26 May 2025

CITATION
Chen Z, Liu X, Tan L, Lyu X, Long Q, Wu W, Guo Z, Liu Z, Li Z and Hu M (2025) Comparative of metagenomic and targeted next-generation sequencing in lower respiratory tract fungal infections. *Front. Cell. Infect. Microbiol.* 15:1534519. doi: 10.3389/fcimb.2025.1534519

Comparative of metagenomic and targeted next-generation sequencing in lower respiratory tract fungal infections

Zhiyang Chen[1,2,3], Xin Liu[1,2,3], Li Tan[1,2,3], Xing Lyu[1,2,3], Qichen Long[1,2,3], Weimin Wu[1,2,3], Zhe Guo[1,2,3], Zhenni Liu[1,2,3], Ziyang Li[1,2,3]* and Min Hu[1,2,3]*

[1]Department of Clinical Laboratory, The Second Xiangya Hospital of Central South University, Changsha, China, [2]Molecular Diagnostic Technology Hunan Engineering Research Center, Changsha, China, [3]Clinical Medical Research Center for Molecular Diagnosis of Infectious Diseases in Hunan Province, Changsha, China

Objectives: This study aims to compare the diagnostic efficiency and consistency of metagenomic next-generation sequencing (mNGS) and targeted next-generation sequencing (tNGS) in patients with lower respiratory tract fungal infections.

Methods: A total of 115 patients with probable pulmonary infection between September 2022 and April 2023 were enrolled at the Second Xiangya Hospital, Changsha, China, of which 61 were clinically diagnosed with invasive pulmonary fungal infection (IPFI) and 54 were non-IPFI cases. All patients received bronchoalveolar lavage, with mNGS, tNGS, and cultures being conducted paralleled. Diagnostic effectiveness and consistency in detecting microorganisms were compared.

Results: Both mNGS and tNGS showed high sensitivity rates of 95.08% each, with specificity of 90.74% and 85.19%, respectively. They also demonstrated positive predictive values (PPVs) of 92.1% and 87.9% and negative predictive values (NPVs) of 94.2% and 93.9%, respectively, in diagnosing IPFI. The sensitivity and NPV of mNGS and tNGS were superior to that of any individual or combined conventional microbiological tests (CMTs) ($P < 0.05$). The consistency of culture with mNGS and tNGS was 48.70% and 50.43%, respectively. For fungal detection, *Pneumocystis jirovecii* (26/61, 42.6%; and 28/61, 45.9%), *Candida albicans* (19/61, 31.1%; and 21/61, 34.4%), and *Aspergillus fumigatus* (16/61, 26.2%; and 15/61, 24.6%) are most prevalent for mNGS and tNGS in enrolled cases, and the detection rate was greatly higher than that of culture. Furthermore, mNGS and tNGS were capable of diagnosing mixed infections in 65 and 55 out of the 115 cases, whereas only nine cases of bacterial-fungal infection were detected by culture.

Conclusion: The diagnostic efficacy of mNGS and tNGS was comparable to that of identified IPFI. NGS-based methodologies present a promising tool for detecting IPFI, which can be a good supplement to CMT.

KEYWORDS

mNGS, tNGS, diagnosis, invasive pulmonary fungal infection, fungal

1 Background

Despite the utilization of existing antifungal drugs, invasive fungal diseases (IFDs) are estimated to result in approximately 6.5 million incidence and 3.8 million deaths worldwide annually (Denning, 2024). Among the IFDs, invasive pulmonary fungal infections (IPFIs) are frequently observed in clinical settings, notably among individuals suffering from lung cancer, diabetes, tuberculosis, compromised immune systems, and those on prolonged antibacterial medication. In recent years, the prevalence and mortality of IPFI are generally increasing (Parums, 2022). Hence, rapid identification of pathogens is of great importance for IPFI.

At present, the conventional techniques for diagnosing IPFI encompass smears, cultures, antigen-antibody assays, and molecular biology tests. However, these existing methods are challenging to meet clinical needs due to low positivity rates and because they are time-consuming and need prior assumptions. Patients who test negative by conventional methods are treated with empirical antibiotics, which may lead to potential reinfection and adverse reactions (Huang et al., 2020). In order to meet the current need for prompt identification of pathogens and initiate timely and appropriate treatment, next-generation sequencing (NGS) has seen significant advancements this year, which becomes a front-line diagnostic in identifying rare pathogens and in the assessment of patients who may be suffering from severe infections (Wilson et al., 2014; Miller et al., 2019; Zhu et al., 2020; Zheng et al., 2021).

The common applications of NGS in diagnostic laboratories include metagenomic NGS (mNGS) and targeted NGS (tNGS). mNGS allows for the comprehensive detection of a wide range of pathogens, including viruses, bacteria, fungi, and parasites. However, the simultaneous detection of both DNA and RNA processes is economically challenging (Li et al., 2022). tNGS based on multiplex PCR amplification or probe capture enriches nucleic acid of known pathogen (Zhao et al., 2021; Singh, 2022). As a more cost-effective and high sensitivity assay, tNGS is gaining attention in clinical infectious management (Chen et al., 2024). To date, there has been a lack of comparative analysis between mNGS and tNGS in IPFI. Therefore, we conducted this retrospective study among patients with IPFI to evaluate the diagnostic efficacy of mNGS, tNGS, and conventional microbiological tests (CMTs) to assess the practical application of mNGS and tNGS in the clinical management for managing invasive IPFIs.

2 Methods

2.1 Participants and study design

This retrospective case series involved a total of 115 patients with probable pulmonary infection between September 2022 and April 2023 in the Second Xiangya Hospital, Central South University, China. All patients received bronchoalveolar lavage, with mNGS, tNGS, and cultures being conducted paralleled.

The inclusion criteria for this study were as follows: (i) patients with clinical manifestations of pulmonary infections; (ii) underwent bronchoalveolar lavage; (iii) implementation of mNGS, tNGS, and CMTs; and (iv) availability of complete clinical data. The exclusion criteria included the following: (i) individuals lacking concurrent culture, mNGS, and tNGS tests; and (ii) cases with incomplete clinical medical records.

The diagnosis of IPFI or non-IPFI was based on a composite clinical judgement by a clinician team that consists of at least two senior clinicians/professors, including clinical symptoms (fever, respiratory symptoms, fungal-related radiological changes, etc.), microbiological evidence (G test, GM test, fungal staining, molecular methods, etc.), and host factors (the presence of immunosuppression). This study was approved by the Ethics Committee of the Second Xiangya Hospital, Central South University (LYF2022229). The study was considered exempt from informed consent as it was a retrospective observational cohort study.

2.2 Data collection

Demographic and clinical data were extracted from electronic medical records, including age; gender; underlying diseases; pulmonary imaging and laboratory findings (including Erythrocyte Sedimentation Rate (ESR), C-reactive Protein (CRP), Procalcitonin (PCT), and blood routine); results of CMTs, mNGS, and tNGS; and outcome.

2.3 mNGS sequencing and analysis

The methods of mNGS were the same as that described in our previously published article (Li et al., 2024). DNA was extracted from samples using the QIAamp® UCP Pathogen DNA Kit, in which

human DNA was removed. RNA extraction was performed using the QIAamp UCP pathogen mini kit, followed by Turbo DNase treatment to deplete the host DNA background. The RNA was then reverse-transcribed and amplified using the Ovation RNA-Seq system. After fragmentation, the library was constructed using the Ovation Ultralow System V2. Sequencing was carried out on the Illumina NextSeq 550 with single-end 75-bp reads. During data analysis, low-quality reads were removed using fastp. Human sequences were identified and excluded by aligning to the hg38 genome using the Burrows-Wheeler Aligner software. The remaining microbial reads were aligned to the database using Short Nucleotide Alignment Program (SNAP) to identify pathogens. Regarding the cutoff values, for pathogens with background reads in the negative control, a given species or genus was reported as a positive detection if the reads-per-million (RPM) ratio was ≥10. The RPM ratio was calculated as the RPM of the sample divided by the RPM of the no-template control (RPMsample/RPMNTC). For pathogens without background reads in the negative control, the RPM thresholds for positive detection were set as follows: for bacteria, mycoplasma, chlamydia, DNA viruses, and fungi, ≥3 reads; for the *Mycobacterium tuberculosis* complex, ≥1 read. Finally, clinical symptoms, laboratory findings, and the immune status of patients will be taken into account to comprehensively assess whether the detected microorganisms are potential pathogens.

2.4 tNGS sequencing and analysis

2.4.1 Sample preparation

A volume of 650 µL of the sample was liquefied by combining it with an equal volume of dithiothreitol (80 mmol/L) in a 1.5-mL centrifuge tube. The sample used was from the same tube of bronchoalveolar lavage fluid (BALF) collected from the patient, and all samples were stored at −20°C and processed within 24 h after collection. The mixture was homogenized for 15 s using a vortex mixer. Meanwhile, a positive control and a negative control from the Respiratory Pathogen Detection Kit (KS608-100HXD96, KingCreate, Guangzhou, China) were set up to monitor the whole experiment process of tNGS.

2.4.2 Nucleic acid extraction

Five hundred microliters of the homogenate was utilized for total nucleic acid extraction and purification via the MagPure Pathogen DNA/RNA Kit, following the manufacturer's protocol.

2.4.3 Library construction and sequencing

We used the Respiratory Pathogen Detection Kit to construct the library. Two rounds of PCR amplification were performed with 198 pathogen-specific primers for ultra-multiplex PCR to enrich target sequences of bacteria, viruses, fungi, mycoplasma, and chlamydia (Supplementary Table 1). After amplification, PCR products were bead-purified and then amplified with primers having sequencing adapters and unique barcodes. The Qsep100 Bio-Fragment Analyzer (Bioptic, Taiwan, China) and Qubit 4.0 fluorometer (Thermo Scientific, Massachusetts, USA) were used to evaluate library quality and quantity, respectively. Library fragments were about 250–350 bp in size, and the library concentration was at least 0.5 ng/µL. The mixed library's concentration was reevaluated and diluted to 1 nmol/L. Specifically, we use the following conversion formula: $\text{nmol/L} = \frac{\text{ng/µL}\times 10^6}{\text{L}\times 660\text{g/mol}}$ (660 g/mol, which represents the average molecular weight of double-stranded DNA; L denotes the fragment length, and, for this purpose, we consider 300 bp). We dilute the final library to 1 nmol/L with nuclease-free water. Then, 5 µL of the library is mixed with 5 µL of fresh 0.1 mol/L NaOH, vortexed, centrifuged, and incubated at room temperature for 5 min. The diluted and denatured library is sequenced on an Illumina MiniSeq using a KingCreate (Guangzhou, China) universal sequencing kit (KS107-CXR). Each library generates about 0.1 million single-end 100-bp reads on average.

2.4.4 Bioinformatics analysis

Sequencing data were analyzed using the data management and analysis system (v3.7.2, KingCreate). The raw data underwent initial identification via the adapter. Reads with single-end lengths exceeding 50 bp were retained, followed by low-quality filtering to retain reads with Q30 > 75%, ensuring high-quality data. The single-ended aligned reads were then compared using the Self-Building clinical pathogen database to determine the read count of specific amplification targets in each sample. The reference sequences used for read mapping were database-curated from different sources, including GenBank database, RefSeq database, and Nucleotide database from National Center for Biotechnology Information.

2.4.5 Report results' output

According to the principle of targeted amplification of microbial sequences using specific primers, the amplicon coverage and normalized read count of detected pathogens were served as the primary result interpretation indicator. The following criteria were established to classify a microorganism as a potential pathogen: (i) bacteria (excluding *Mycobacterium tuberculosis* complex), fungi, and atypical pathogen: amplicon coverage ≥50% and normalized read count ≥50; (ii) viruses: amplicon coverage ≥50% and normalized read count ≥30; and (iii) *Mycobacterium tuberculosis* complex: normalized read count ≥10. Then, the patient's medical history, symptoms, the immune status, and other laboratory results were assessed to conduct a comprehensive assessment by two experienced clinicians or clinical microbiologist independently. Conflicting interpretations were consulted with a senior physician to achieve a consensus.

2.5 Statistical analyses

Quantitative variables were represented as medians with accompanying ranges, and categorical variables were presented as counts with percentages. Wilson's method was used to calculate 95% confidence intervals (CIs) for these proportions. The 2 × 2

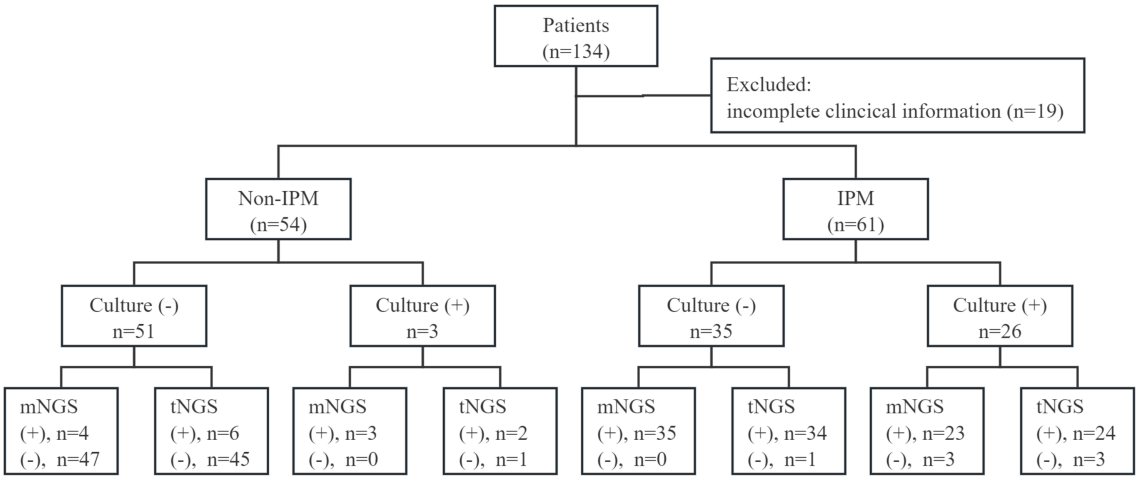

FIGURE 1
Overview of the research scheme and results of culture, mNGS, and tNGS. (+), positive; (–), negative.

contingency tables were established to determine sensitivity, specificity, positive predictive value (PPV), and negative predictive value (NPV). The McNemar's test was used for comparisons of the diagnostic performance of CMTs, mNGS, and tNGS. The SPSS 27.0.1 software was used for data analysis, and $P < 0.05$ was considered statistically significant.

3 Results

3.1 Clinical characteristics

As shown in Figure 1, a total of 134 patients with suspected lower respiratory tract infections, who underwent both BALF mNGS and tNGS, were enrolled. Of these, 19 patients had incomplete clinical information, and 115 patients were subjected to final analysis. Based on clinical diagnosis, patients were divided into non-IPFI (n = 54) and IPFI group (n = 61).

The clinical features of these two groups were analyzed and summarized in Table 1. The distribution of genders was comparable between the groups, yet the median age of the IPFI group was significantly higher than that of the non-IPFI group ($P = 0.027$). For laboratory findings, levels of C-reactive protein ($P = 0.027$), white blood cell count ($P = 0.043$), neutrophil percentage ($P = 0.001$), and the neutrophil-to-lymphocyte ratio ($P = 0.001$) were all markedly elevated in the IPFI group compared to those in the non-IPFI group. The most prevalent underlying conditions were malignancy in the non-IPFI group (35.2%) and hypertension in the IPFI group (37.7%). Regarding the typical radiological features on chest CT images, exudation was the most frequent feature in patients from both groups ($P = 0.35$). Nodules ($P < 0.01$), lymphadenopathy ($P < 0.01$), and masses ($P < 0.01$) were significantly more frequent in the non-IPFI group. In addition, ground-glass opacity was more prevalent in the IPFI group ($P = 0.025$).

3.2 Diagnostic efficacy of mNGS, tNGS, and CMT methods

As shown in Table 2, on the basis of clinical comprehensive diagnosis, mNGS identified IPFI in 58 out of the 61 patients in the IPFI group and 5 out of 54 in the non-IPFI group, showing a sensitivity of 95.08%, specificity of 90.74%, PPV of 92.1%, and NPV of 94.2%; whereas tNGS showed sensitivity of 95.08, specificity of 85.19%, PPV of 87.9%, and NPV of 93.9%. The diagnostic efficacy of mNGS and tNGS was comparable ($P > 0.05$). As for CMTs, the sensitivity of culture, G test, and immunofluorescence (IF) was 42.62%, 37.84%, and 57.14%, respectively, with the specificity of 94.44%, 80.56%, and 89.47%. The combination use of the three CMTs identified only 36 of the 61 patients with IPFI, yielding sensitivity of 59.02%, specificity of 83.33%, PPV of 80%, and NPV of 64.3%. Both mNGS and tNGS demonstrated higher sensitivity and NPV compared to either individual or combined CMTs ($P < 0.05$). Additionally, the combination of CMTs with mNGS achieved the highest sensitivity at 100%, followed by the combination of CMTs with tNGS with sensitivity of 98.36%.

3.3 Fungal detection by culture

Among the 115 enrolled cases, culture, mNGS, and tNGS observed 19, 41, and 38 potential pathogens, respectively. The overall detection distribution of pathogens is shown in Figure 2a. The sensitivity for all pathogens and fungal pathogens using culture both varied significantly from mNGS and tNGS ($P < 0.001$), with culture of 46.09% and 24.35%, mNGS of 86.96% and 54.78%, and tNGS of 85.22% and 57.39%, respectively. In addition, mNGS and tNGS were comparable ($P > 0.05$).

In 61 patients with IPFI, fungal pathogens were isolated by culture in 26 cases. *Candida albicans* (15.38%) and *Aspergillus*

TABLE 1 Demographics and clinical characteristics of the study cohort.

Characteristic	Non-IPFI group (n = 54)	IPFI group (n = 61)	*P*-value
Age, years, median (IQR)	57.22 ± 15.44	63.8 ± 15.88	0.027
Gender, male, N (%)	42 (77.8)	46 (75.4)	0.766
Laboratory findings			
ESR	56.66 ± 35.12	47.4 ± 29.65	0.174
CRP, median (IQR)	38.75 (8.79,79.80)	73.56 (20.3, 136.9)	0.027
PCT, median (IQR)	0.22 (0.07,0.84)	0.47 (0.085, 2.255)	0.123
WBC, median (IQR)	6.955 (5.805, 10.68)	9.62 (6.255, 13.61)	0.043
N%	74.667 ± 16.43	83.636 ± 13.04	0.001
L%, median (IQR)	13.70 (5.725, 24.6)	6.80 (3.25, 12.80)	0.001
NLR, median (IQR)	5.50 (2.565, 14.53)	13.13 (6.21, 28.89)	0.001
Comorbidities, N (%)			
Malignancy	19 (35.2)	14 (23.0)	0.148
Diabetes	9 (16.7)	19 (31.1)	0.071
hypertension	13 (24.1)	23 (37.7)	0.116
Chronic liver disease	9 (16.7)	11 (18.0)	0.847
Cardiovascular disease	12 (22.2)	17 (27.9)	0.486
Chronic kidney disease	10 (18.5)	20 (32.8)	0.082
Immune disease	4 (7.4)	5 (8.2)	0.875
Hemopathy	4 (7.4)	1 (1.6)	0.13
CT images, N (%)			
Exudation	33 (61.1)	32 (52.5)	0.35
Nodules	19 (35.2)	6 (9.8)	0.001
Lymphadenectasis	10 (18.5)	2 (3.3)	0.008
Mass	6 (11.1)	0 (0.0)	0.007
Cavitation	2 (3.7)	2 (3.3)	0.901
Ground-glass opacity	3 (5.6)	12 (19.7)	0.025
LOS, days, median (IQR)	17.00 (9.00, 25.25)	16.00 (10.00, 23.50)	0.638
Outcome, Death, N (%)	1 (1.9)	8 (13.1)	0.025

fumigatus (15.38%) were the most frequently detected, followed by *Aspergillus niger* (7.69%) and *Aspergillus flavus* (7.69%). Out of the 26 cases, mNGS and tNGS had a complete match in identifying pathogens in 10 cases (38.46%). Moreover, mNGS and tNGS discovered additional fungal species in comparison to culture in 13 (50.00%) cases. Specifically, mNGS additionally detected *Pneumocystis jirovecii* (eight cases), *Candida parapsilosis* (two cases), *Candida albicans* (two cases), *Aspergillus flavus* (two cases), *Candida glabrata* (one case), and *Aspergillus fumigatus* (one case). On the other hand, tNGS uniquely identified *Pneumocystis jirovecii* (six cases), *Candida parapsilosis* (three cases), *Candida albicans* (three cases), *Candida glabrata* (two cases), *Aspergillus flavus* (two cases), *Aspergillus terreus* (one case), *Aspergillus niger* (one case), and *Aspergillus fumigatus* (one case). On the contrary, three cases that identified *Candida albicans* (one case), *Aspergillus fumigatus* (one case), and *Aspergillus niger* (one case) by culture were negative via mNGS. In addition, *Candida orthopsilosis* (one case) and *Candida krusei* (one case) were identified negative via tNGS. In the non-IPFI group, three cases of *Candida* were observed by culture and were consistent with mNGS and tNGS, combined with comprehensive clinical thinking, considering colonization.

3.4 Fungal detection by mNGS

Fifty eight of the 61 patients in the IPFI group tested positive for fungal detection by mNGS (95.08%). *Pneumocystis jirovecii*

10.3389/fcimb.2025.1534519

TABLE 2 Diagnostic performance of CMTs, mNGS, and tNGS for invasive pulmonary fungal infection.

Method	Result	Non-IPFI	IPFI	Sensitivity % (95% CI)	Specificity % (95% CI)	PPV % (95% CI)	NPV % (95% CI)
Culture	POS	3	26	42.62 (30.0–55.9)[abcd]	94.44 (84.6–98.8)[cd]	89.7 (73.5–96.4)	59.3 (53.8–64.6)[abcd]
	NEG	51	35				
G test	POS	7	14	37.84 (22.5–55.2)[abcd]	80.56 (64.0–91.8)	66.7 (47.8–81.4)[ab]	55.8 (48.3–62.9)[abcd]
	NEG	29	23				
IF	POS	2	20	57.14 (39.4–73.7)[abcd]	89.47 (66.9–98.7)	90.9 (72.3–97.5)	53.1 (42.9–63.1)[abcd]
	NEG	17	15				
CMTs	POS	9	36	59.02 (45.7–71.4)[abcd]	83.33 (70.7–92.1)	80.0 (68.0–88.3)	64.3 (56.6–71.3)[abcd]
	NEG	45	25				
mNGS	POS	5	58	95.08 (86.3–99.0)	90.74 (79.7–96.9)	92.1 (83.4–96.4)	94.2 (84.4–98.0)
	NEG	49	3				
tNGS	POS	8	58	95.08 (86.3–99.0)	85.19 (72.9–93.4)	87.9 (79.2–93.2)	93.9 (83.5–97.9)
	NEG	46	3				
CMTs + mNGS	POS	12	61	100.00 (94.1–100.0)	77.78 (64.4–88.0)	83.6 (75.5–89.3)	100
	NEG	42	0				
CMTs + tNGS	POS	14	60	98.36 (91.2–100.0)	74.07 (60.3–85.0)	81.1 (73.2–87.1)	97.6 (85.1–99.6)
	NEG	40	1				

[a]The difference was significant with mNGS based on the Chi-square test ($P < 0.05$).
[b]The difference was significant with tNGS based on the Chi-square test ($P < 0.05$).
[c]The difference was significant with CMTs + mNGS based on the Chi-square test ($P < 0.05$).
[d]The difference was significant with CMTs + tNGS based on the Chi-square test ($P < 0.05$).

(42.62%) was the most frequently detected, followed by *Candida albicans* (31.15%) and *Aspergillus fumigatus* (26.23%). In all cases, the mNGS results were in complete agreement with the culture results in 56 (48.70%) cases, in partial agreement in 11 (9.57%) cases, and in complete disagreement in 48 (41.74%) cases (Figure 2b). In specific, in the IPFI group, the mNGS results were consistent with the culture results in 7 (12.07%) cases. In addition, the mNGS results were inconsistent with culture results in 41 (70.69%) cases (38 cases: mNGS was positive, whereas culture was negative, for fungal detection; and 3 cases: mNGS was negative, whereas culture was positive, for fungal detection). Among the 38 cases, mNGS detected fungal including *Pneumocystis jirovecii* (18 cases), *Candida albicans* (10 cases), *Aspergillus fumigatus* (seven cases), *Aspergillus flavus* (four cases), *Aspergillus niger* (two cases), *Cryptococcus neoformans* (one case), *Candida metapsilosis* (one case), and *Candida parapsilosis* (one cases). Five cases were identified fungal positive in the non-IPFI group, including a patient with lung cancer with *Pneumocystis jirovecii* (one case) and four cases of *Candida*.

3.5 Fungal detection by tNGS

Fifty eight of the 61 patients in the IPFI group tested positive for fungal detection by tNGS (95.08%). The top three detected pathogens of tNGS were consistent with those of mNGS; these are *Pneumocystis jirovecii* (45.90%), *Candida albicans* (34.43%), and *Aspergillus fumigatus* (24.59%). Compared with culture, in overall cases, the tNGS results were with a full consistency with the culture results in 58 (50.43%) cases, with partial consistency in 16 (13.91%) cases, and with complete inconsistency in 41 (35.65%) cases (Figure 2c). In the IPFI group, the tNGS results were in complete agreement with the culture results in 11 (18.03%) cases. Moreover, the tNGS results were in complete disagreement with culture in 35 (57.38%) cases (33 cases: tNGS was positive for fungal while culture was negative; and 2 cases: tNGS was negative, whereas culture was positive, for fungal detection). Among the 33 cases, tNGS detected fungal including *Pneumocystis jirovecii* (19 cases), *Candida albicans* (10 cases), *Aspergillus fumigatus* (four cases), *Aspergillus niger* (two cases), *Cryptococcus neoformans* (one case), *Aspergillus flavus* (one case), *Aspergillus terreus* (one case), and *Candida parapsilosis* (one case). Eight cases were identified fungal positive in the non-IPFI group, including a respiratory failure patient with one case of *Pneumocystis jirovecii* and seven cases of *Candida*.

For the comparison of mNGS and tNGS, the results in all cases were completely matched in 85 (73.91%) cases, partly matched in 15 (13.04%) cases, and mismatched in 15 (13.04%) cases (Figure 2d). Specifically, in mismatched cases, mNGS missed *Candida albicans* (two cases), *Aspergillus fumigatus* (one case), and *Pneumocystis jiroveciiwas* (one case) in four cases. Because low sequencing reads of colonized

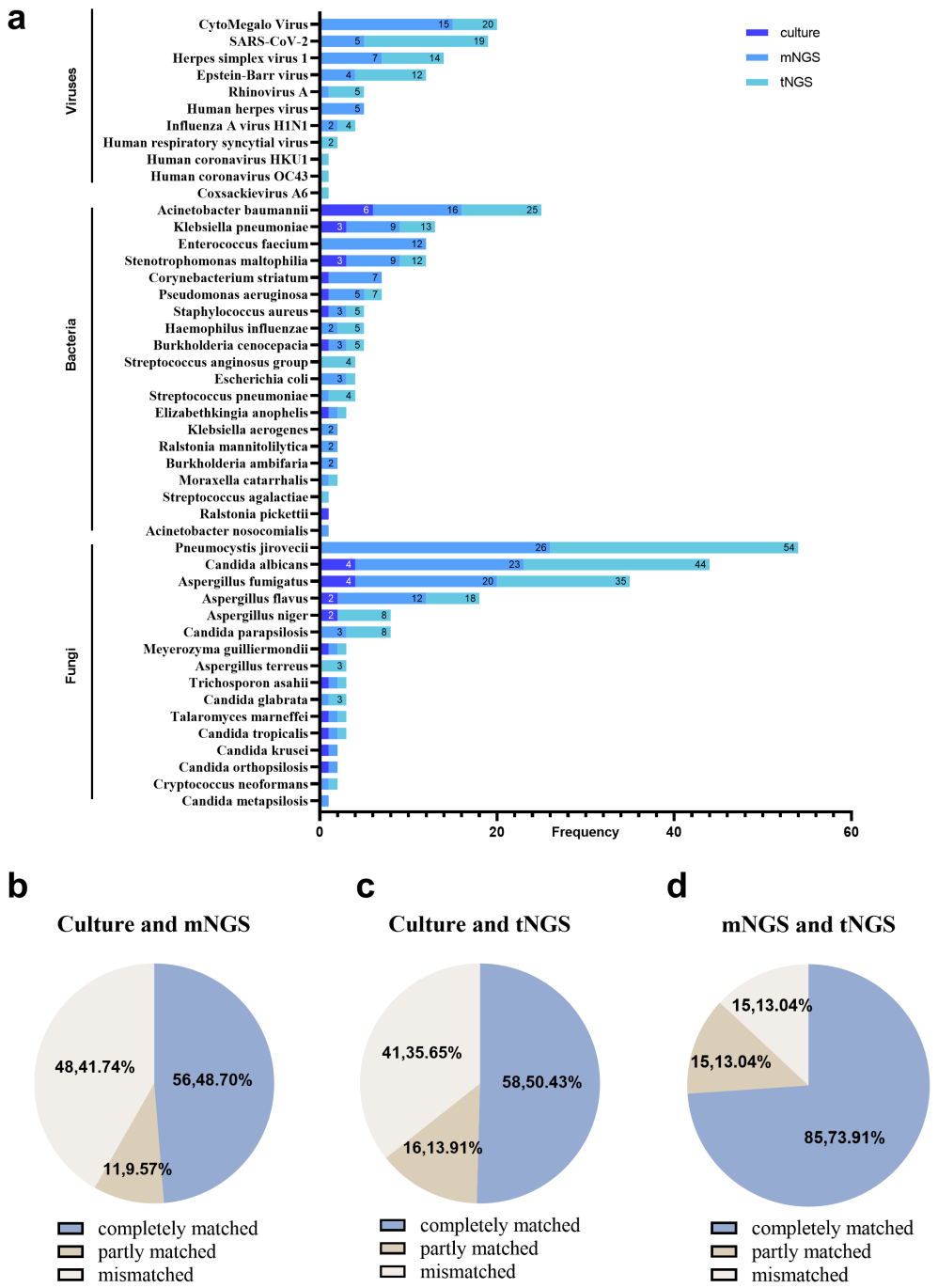

FIGURE 2
The pathogens distribution and the comparison of culture, mNGS, and tNGS in all cases. **(a)** Distribution of pathogens detected by culture, mNGS, and tNGS. **(b)** Culture and mNGS consistency. **(c)** Culture and tNGS results' consistency. **(d)** mNGS and tNGS results' consistency.

Candida was observed by mNGS, compared with the different reported rules between tNGS and mNGS, *Candida* was not reported by mNGS but tNGS in three cases. Compared with mNGS, tNGS missed *Aspergillus fumigatus* (two cases), *Pneumocystis jirovecii* (one case), and *Candida krusei* (one case). In addition, in other five cases, fungus was filtered because the detected sequence number was lower than the reported limit [*Pneumocystis jirovecii* (one case), *Aspergillus fumigatus* (one case), *Candida parapsilosis* (two cases), and *Aspergillus flavus* (one case)].

3.6 Detection of coinfections by culture, mNGS, and tNGS

In a total of 55 of the 115 patients (47.83%), coinfection was found using tNGS, increasing the detection rate of coinfection compared to that of culture (7.83%) ($P < 0.001$). It is worth noting that 10.43%, 13.04%, 11.30%, and 13.04% of patients were diagnosed as bacterial-fungal, bacterial-virus, fungal-virus, and bacterial-fungal-virus coinfections, respectively.

Sixty five out of the 115 patients (56.5%) were found coinfection using mNGS, which has no significant difference compared with tNGS. The detection rate of bacterial-fungal, bacterial-virus, fungal-virus, and bacterial-fungal-virus coinfections were 10.43%, 13.04%, 11.30%, and 13.04%, respectively (Figure 3).

4 Discussion

Patients presenting with IPFI often exhibit a range of underlying health conditions, posing a challenge in clinical management. The options for anti-fungal medications are limited, typically being both expensive and require prolonged treatment duration. Additionally, anti-fungal drugs often present significant adverse reactions and may be poorly tolerated by patients. Therefore, achieving an accurate diagnosis of IPFI is critically important.

The emergence of NGS has brought great progress to the diagnosis of infectious diseases. In recent years, mNGS has been widely accepted and used in clinical practice for early treatment or differential diagnosis of critically ill patients (Chiu and Miller, 2019; Greninger and Naccache, 2019; Chen et al., 2020). Our previous study showed that mNGS possesses greater sensitivity and a higher rate of clinical acceptance compared to culture when used as a reference for clinical diagnosis (Li et al., 2024), which was widely reported and supported by several studies. However, mNGS still has some limitations: easily influenced by human genes, expensive, and lack of standardization in experimental procedures and sequencing report interpretation. In contrast, tNGS involves the use of a panel of specific sequences from pre-selected pathogens, which offers higher specificity and cost-effectiveness and can eliminate the interference of human-derived genes (Wylie et al., 2015).

Upon reviewing relevant literature, it is found that there were few published studies compared the performance of tNGS and mNGS in lower respiratory tract infections (Huang et al., 2024; Sun L. et al., 2024; Wei et al., 2024). However, assessments of the clinical diagnostic value of tNGS in IPFI are limited. In the present study, two promising NGS-based detection methods, mNGS and tNGS, were compared in fungal diagnosis effectiveness in BALF. The tNGS panel used in this study was a primer or probe specifically constructed for 198 pathogens.

In our study, according to composite clinical judgement, 61 patients with IPFI and 54 non-IPFI cases were identified. We then compared the diagnostic efficiency and consistency between traditional culture method, mNGS, and tNGS, to assess the clinical validity of NGS in detecting fungi. In general, the diagnostic efficacy of mNGS and tNGS was comparable in identified IPFI without statistically different ($P > 0.05$), which aligns with the findings from previous studies (Li et al., 2022; Huang et al., 2024). Meanwhile, mNGS and tNGS, with their unbiased detection advantages, can identify pathogens that are difficult to detect by traditional culture methods, such as *Pneumocystis jirovecii*, *Cryptococcus neoformans*, viruses, and non-tuberculous mycobacteria. Our findings indicated that mNGS had equivalent sensitivity to tNGS, but with slightly higher specificity, PPV, and NPV compared to those of tNGS. However, tNGS identified more *A. terreus* complex, *A. niger* complex, and *C. parapsilosis* than mNGS. Moreover, in our study, the sensitivity and NPV of mNGS and tNGS were markedly higher than those of the combined CMTs, which include culture, G test, and IF, as well as traditional pathogen detection methods alone ($P < 0.05$). The combination of CMTs with mNGS identified all patients with IPFI with a NPV of 100%, whereas the combination of CMTs with tNGS missed one patient with IPFI (case 31). *A. fumigatus* was detected by mNGS (number of sequences: 6) in the 31st patient with IPFI with GM test being positive and with culture being negative. Interestingly, *P. jirovecii*, an opportunistic fungus often seen in immunocompromised patients with mixed infections, was the most

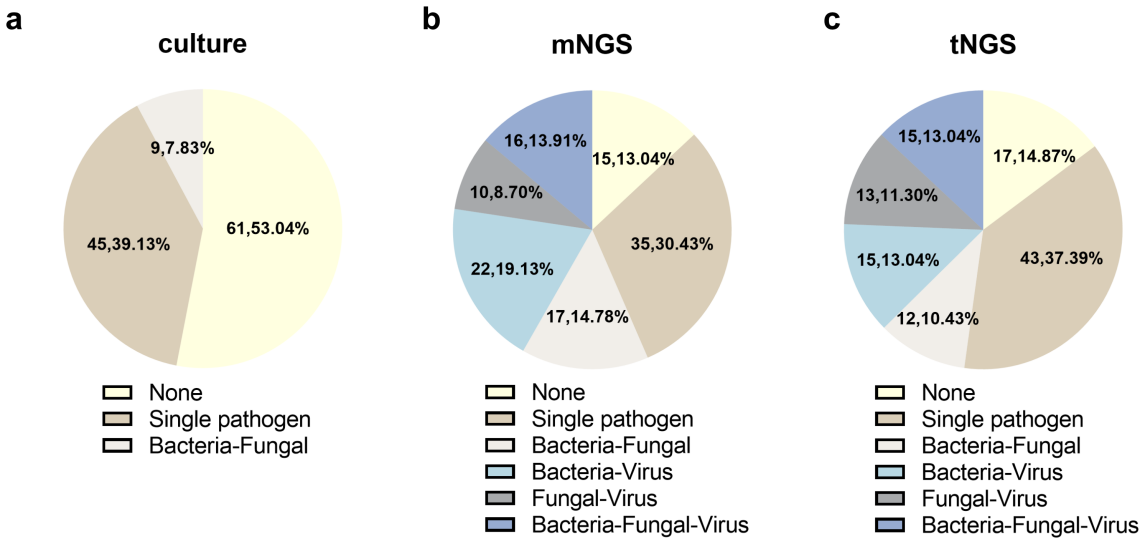

FIGURE 3
Coinfection detection of **(a)** culture, **(b)** mNGS, and **(c)** tNGS.

frequently detected in both NGS-based assays in our study. This prevalence may be associated with the older age of the patients and the presence of underlying diseases. Coinfections with *P. jirovecii*, cytomegalovirus (CMV), and Herpesviruses such as Epstein-Barr virus (EBV) have been widely reported, and our findings are in line with previous studies (Rucar et al., 2024).

The detection efficiency of two-NGS based assays is excellent; however, there are also cases that are not consistent with the positive culture results. mNGS failed to detect fungi in three patients (cases 18, 28, and 37) of *C. albicans*, *A. fumigatus*, and *A. niger* complex, respectively, whereas culture and tNGS were positive. The three cases were confirmed as true positives by traditional culture and tNGS. However, the low sequence counts detected by tNGS, which barely met the reporting threshold, suggested low pathogen loads. Therefore, we suppose the false negative values of mNGS were likely due to these low pathogen loads. In addition, tNGS missed *C. orthopsilosis* and *P. kudriavzevii*, whereas culture and mNGS were positive in case 48 and case 59, respectively. These two cases were confirmed true positive as well. Since the differences have no pattern and are not caused by the differences in the detection ranges of mNGS and tNGS, these differences may be related to reasons such as degradation of samples due to storage or wet experimental performance.

Except for fungi, the detection performance of the two NGS-based assays for bacteria and virus was similar as well, which is comparable to that in the previous studies (Li et al., 2022; Sun W. et al., 2024). As the development of tNGS products was targeting specific infectious pathogens, our BALF tNGS panel mainly focuses on lower respiratory tract infection pathogens. For bacteria, due to the broader coverage of mNGS, the detection rate of mNGS is higher than that of tNGS in our study. mNGS detected a higher number of *E. faecium*, *C. striatum*, *R. mannitolilytica*, and *B. ambifaria* compared to tNGS, whereas tNGS identified more *S. anginosus* group. *E. faecium* and *C. striatum* are the components of the normal flora of skin and mucous membranes and are often regarded as opportunistic pathogens, particularly in individuals with compromised immune function. In such cases, they may lead to severe infections, thereby possessing significant clinical implications. Although the significance of *R. mannitolilytica* and *B. ambifaria* in lower respiratory tract infections is limited, a rare case of spheroid pneumonia caused by *R. mannitolilytica* was diagnosed through mNGS as reported (Ma et al., 2023). For viruses, tNGS has a greater advantage than mNGS in the detection of RNA viruses, such as SARS-CoV-2, Rhinovirus A, human respiratory syncytial virus, human coronavirus HKU1, and OC43, which could not be detected by the mNGS DNA process. However, the detection rate of several DNA virus such as CMV was also slightly lower than that of mNGS in our study (mNGS, n = 15; and tNGS, n = 5). The missed detection of CMV by tNGS was mainly due to the filtering of the sequence number that did not meet the reporting standard.

In addition, the ability of tNGS and mNGS to simultaneously identify bacteria, fungi, and viruses was also illustrated in our study. By comparing the results of culture and these two NGS-based technologies, the coinfection rate increased from 7.83% to 47.83% and 56.5% with significant difference for tNGS and mNGS, respectively. However, there was no significant difference observed between mNGS and tNGS, suggesting that the detection capabilities of both methods in cases of mixed infection are largely comparable as well.

As advanced diagnostic tools, mNGS and tNGS often elicit high expectations in clinical practice. However, there are several issues that need attention in the result interpretation. mNGS and tNGS have differences in the presentation of the final sequence number. Since tNGS was based on ultra-multiplex PCR, which specifically increases the number and proportion of nucleic acid sequences of the target pathogen, therefore, the sequence number of tNGS in the final report tends to be higher than that of mNGS. Therefore, the results reporting rules of each pathogen of these two methods need to be combined with clinical practice to avoid false negatives or false positives that may occur in bioinformatics analysis. Accordingly, it is essential to engage in comprehensive communication with clinicians regarding the fact that the sequence counts obtained from tNGS and mNGS should not be directly compared horizontally. Moreover, because NGS-based technologies could not differentiate between colonizing and pathogenic pathogens, it is essential to consider the pathogenic significance when detecting colonizing bacteria with low sequence, such as *Candida albicans*, in BALF.

Our study had several limitations. First, it was a single-center retrospective study, which may limit the generalizability of the results and introduce potential biases related to the specific patient population. Second, the sample size was relatively small, and several cases lacked paired traditional results including G test and IF, owing to the restriction of enrolled cases.

Collectively, in our cohort of 115 patients, tNGS showed comparable diagnostic value to mNGS and was significantly superior to CMT. By focusing on specific pathogen-related gene regions, tNGS not only reduces the volume of sequencing data but also lowers costs and enhances cost-effectiveness for detecting common pathogens. In our lab, tNGS completes the process from sample processing to sequencing in just 15–16 h, compared to mNGS of 20–24 h, facilitating rapid clinical diagnosis. Additionally, for non-critical patients, targeted detection by tNGS can resolve most issues and shows higher sensitivity in detecting low-abundance pathogens, making it highly applicable in clinical settings. Given these practical advantages of tNGS in clinical microbiology, patients with lower respiratory tract infections can be referred for tNGS alongside traditional pathogen detection methods to identify common pathogens. Conversely, mNGS is more appropriate for critical illnesses, particularly in cases of unexplained infections. However, due to the variations in wet and dry experimental procedures across different laboratories, both NGS-based methods currently lack widely accepted standards and quantitative thresholds; therefore, NGS is not intended to supplant traditional diagnostic methods. Instead, NGS-based methodologies should be integrated flexibly with conventional techniques to enhance clinical diagnostic accuracy and inform treatment strategies effectively.

Data availability statement

The datasets presented in this study can be found in online repositories. The names of the repository/repositories and accession number(s) can be found below: https://ngdc.cncb.ac.cn/?lang=zh, PRJCA032778.

Ethics statement

The studies involving humans were approved by The Ethics Committee of the Second Xiangya Hospital, Central South University (LYF2022229). The studies were conducted in accordance with the local legislation and institutional requirements. The study was considered exempt from informed consent as it was a retrospective observational cohort study.

Author contributions

ZC: Funding acquisition, Writing – original draft, Writing – review & editing, Conceptualization, Data curation. XLi: Data curation, Formal Analysis, Writing – review & editing, Software. LT: Data curation, Formal Analysis, Writing – review & editing. XLy: Writing – review & editing, Methodology. QL: Writing – review & editing, Investigation. WW: Writing – review & editing, Visualization. ZG: Writing – review & editing, Software, Visualization. ZNL: Writing – review & editing, Validation. ZYL: Conceptualization, Supervision, Validation, Writing – review & editing, Visualization. MH: Conceptualization, Resources, Supervision, Validation, Writing – review & editing.

Funding

The author(s) declare that financial support was received for the research and/or publication of this article. This study was supported by Hunan Natural Science Foundation (No. 2023JJ40812; ZC), National Natural Science Foundation of China (No. 82102499; ZL), Key Research and Development Program of Hunan Province (2022SK2020; MH), Scientific Research Project for Hunan Health Commission (No. 202211003513; ZL), and the Scientific Research Launch Project for new employees of the Second Xiangya Hospital of Central South University.

Conflict of interest

The authors declare that the research was conducted in the absence of any commercial or financial relationships that could be construed as a potential conflict of interest.

Generative AI statement

The author(s) declare that no Generative AI was used in the creation of this manuscript.

Publisher's note

All claims expressed in this article are solely those of the authors and do not necessarily represent those of their affiliated organizations, or those of the publisher, the editors and the reviewers. Any product that may be evaluated in this article, or claim that may be made by its manufacturer, is not guaranteed or endorsed by the publisher.

Supplementary material

The Supplementary Material for this article can be found online at: https://www.frontiersin.org/articles/10.3389/fcimb.2025.1534519/full#supplementary-material.

References

Chen, Q., Yi, J., Liu, Y., Yang, C., Sun, Y., Du, J., et al. (2024). Clinical diagnostic value of targeted next–generation sequencing for infectious diseases (Review). *Mol. Med. Rep.* 30, 153. doi: 10.3892/mmr.2024.13277

Chen, H., Yin, Y., Gao, H., Guo, Y., Dong, Z., Wang, X., et al. (2020). Clinical utility of in-house metagenomic next-generation sequencing for the diagnosis of lower respiratory tract infections and analysis of the host immune response. *Clin. Infect. Dis.* 71, S416–S426. doi: 10.1093/cid/ciaa1516

Chiu, C. Y., and Miller, S. A. (2019). Clinical metagenomics. *Nat. Rev. Genet.* 20, 341–355. doi: 10.1038/s41576-019-0113-7

Denning, D. W. (2024). Global incidence and mortality of severe fungal disease. *Lancet Infect. Dis.* 24, e428–e438. doi: 10.1016/S1473-3099(23)00692-8

Greninger, A. L., and Naccache, S. N. (2019). Metagenomics to assist in the diagnosis of bloodstream infection. *J. Appl. Lab. Med.* 3, 643–653. doi: 10.1373/jalm.2018.026120

Huang, Z., Hu, B., Li, J., Feng, M., Wang, Z., Huang, F., et al. (2024). Metagenomic versus Targeted Next-Generation Sequencing for Detection of Microorganisms in Bronchoalveolar Lavage Fluid among Renal Transplantation Recipients. *Front. Immunol.* 15. doi: 10.3389/fimmu.2024.1443057

Huang, J., Jiang, E., Yang, D., Wei, J., Zhao, M., Feng, J., et al. (2020). Metagenomic next-generation sequencing versus traditional pathogen detection in the diagnosis of peripheral pulmonary infectious lesions. *IDR* 13, 567–576. doi: 10.2147/IDR.S235182

Li, Z., Tan, L., Zhang, J., Long, Q., Chen, Z., Xiang, Z., et al. (2024). Diagnostic performance of metagenomic sequencing in patients with suspected infection: A large-scale retrospective study. *Front. Cell Infect. Microbiol* 14. doi: 10.3389/fcimb.2024.1463081

Li, S., Tong, J., Liu, Y., Shen, W., and Hu, P. (2022). Targeted next Generation Sequencing Is Comparable with Metagenomic next Generation Sequencing in Adults with Pneumonia for Pathogenic Microorganism Detection. *J. Infect.* 85, e127–e129. doi: 10.1016/j.jinf.2022.08.022

Ma, J., Zhang, C., Dang, K., Liao, Y., Feng, X., and Zhou, P. (2023). Spherical pneumonia caused by ralstonia mannitolilytica: A case report and literature review. *BMC Pulm Med.* 23, 20. doi: 10.1186/s12890-023-02316-8

Miller, S., Naccache, S. N., Samayoa, E., Messacar, K., Arevalo, S., Federman, S., et al. (2019). Laboratory validation of a clinical metagenomic sequencing assay for pathogen detection in cerebrospinal fluid. *Genome Res.* 29, 831–842. doi: 10.1101/gr.238170.118

Parums, D. V. (2022). Editorial: the world health organization (WHO) fungal priority pathogens list in response to emerging fungal pathogens during the COVID-19 pandemic. *Med. Sci. Monit* 28. doi: 10.12659/MSM.939088

Rucar, A., Totet, A., Le Govic, Y., Demey, B., and Damiani, C. (2024). Pulmonary co-infections by pneumocystis jirovecii and herpesviridae: A seven-year retrospective study. *Ann. Clin. Microbiol Antimicrob* 23, 8. doi: 10.1186/s12941-023-00663-2

Singh, R. R. (2022). Target enrichment approaches for next-generation sequencing applications in oncology. *Diagnostics* 12, 1539. doi: 10.3390/diagnostics12071539

Sun, L., Zhang, K., Liu, Y., Che, L., Zhang, P., Wang, B., et al. (2024). Metagenomic next-generation sequencing targeted and metagenomic next-generation sequencing for pulmonary infection in HIV-infected and non-HIV-infected individuals. *Front. Cell Infect. Microbiol* 14. doi: 10.3389/fcimb.2024.1438982

Sun, W., Zheng, L., Kang, L., Chen, C., Wang, L., Lu, L., et al. (2024). Comparative analysis of metagenomic and targeted next-generation sequencing for pathogens diagnosis in bronchoalveolar lavage fluid specimens. *Front. Cell Infect. Microbiol* 14. doi: 10.3389/fcimb.2024.1451440

Wei, M., Mao, S., Li, S., Gu, K., Gu, D., Bai, S., et al. (2024). Comparing the diagnostic value of targeted with metagenomic next-generation sequencing in immunocompromised patients with lower respiratory tract infection. *Ann. Clin. Microbiol Antimicrob* 23, 88. doi: 10.1186/s12941-024-00749-5

Wilson, M. R., Naccache, S. N., Samayoa, E., Biagtan, M., Bashir, H., Yu, G., et al. (2014). Actionable diagnosis of neuroleptospirosis by next-generation sequencing. *N Engl. J. Med.* 370, 2408–2417. doi: 10.1056/NEJMoa1401268

Wylie, T. N., Wylie, K. M., Herter, B. N., and Storch, G. A. (2015). Enhanced virome sequencing using targeted sequence capture. *Genome Res.* 25, 1910–1920. doi: 10.1101/gr.191049.115

Zhao, N., Cao, J., Xu, J., Liu, B., Liu, B., Chen, D., et al. (2021). Targeting RNA with next- and third-generation sequencing improves pathogen identification in clinical samples. *Advanced Sci.* 8, 2102593. doi: 10.1002/advs.202102593

Zheng, Y., Qiu, X., Wang, T., and Zhang, J. (2021). The diagnostic value of metagenomic next-generation sequencing in lower respiratory tract infection. *Front. Cell Infect. Microbiol* 11. doi: 10.3389/fcimb.2021.694756

Zhu, N., Zhang, D., Wang, W., Li, X., Yang, B., Song, J., et al. (2020). A Novel coronavirus from patients with pneumonia in China, 2019. *N Engl. J. Med.* 382, 727–733. doi: 10.1056/NEJMoa2001017

frontiers | Frontiers in Cellular and Infection Microbiology

TYPE Original Research
PUBLISHED 16 June 2025
DOI 10.3389/fcimb.2025.1566603

OPEN ACCESS

EDITED BY
Diana Manolescu,
Victor Babes University of Medicine and Pharmacy, Romania

REVIEWED BY
Siyuan Hao,
University of Texas Southwestern Medical Center, United States
Kankan Yang,
Shenzhen Bay Laboratory, China

*CORRESPONDENCE
Shilong Chen
csl6116@163.com

RECEIVED 25 January 2025
ACCEPTED 31 May 2025
PUBLISHED 16 June 2025

CITATION
Chen X, Zhang S, Lin S, Wang S, Huang M, Chen S and Chen S (2025) A combination of recombinase polymerase amplification with CRISPR technology rapidly detects goose parvovirus with high accuracy and sensitivity. *Front. Cell. Infect. Microbiol.* 15:1566603. doi: 10.3389/fcimb.2025.1566603

A combination of recombinase polymerase amplification with CRISPR technology rapidly detects goose parvovirus with high accuracy and sensitivity

Xiuqin Chen, Shizhong Zhang, Su Lin, Shao Wang, Meiqing Huang, Shaoying Chen and Shilong Chen*

Institute of Animal Husbandry and Veterinary Medicine, Fujian Academy of Agricultural Science, Fuzhou, Fujian, China

Background: Goose parvovirus (GPV) poses a significant threat to the waterfowl industry, necessitating reliable detection methods. However, conventional techniques are often time-consuming, equipment-dependent, or lack sufficient sensitivity for detecting early-stage infection. In contrast, emerging CRISPR/Cas12a-based systems offer a promising alternative for rapid, sensitive, and on-site diagnostics.

Methods: We developed and optimized a recombinase polymerase amplification (RPA)-CRISPR/Cas12a assay targeting the conserved *VP3* gene of GPV. The analytical and diagnostic performance of this assay was rigorously validated using plasmid standards and clinical specimens from both experimentally infected and field-collected ducklings.

Results: Our developed assay combines RPA with CRISPR/Cas12a technology for rapid GPV nucleic acids detection. This method achieves a detection limit of 10 copies/μL of the *VP3* gene within one hour, demonstrating high sensitivity and rapid turnaround. The assay exhibited exceptional specificity, with no cross-reactivity against other waterfowl viruses, and showed robust reproducibility, with intra- and inter-assay coefficients of variation consistently below 5.0%. Clinical validation using 42 field samples confirmed a diagnostic sensitivity of 100% and 95.5% specificity, showing superior performance to real-time quantitative PCR (qPCR) in both metrics. Furthermore, the assay supports flexible visual readouts using portable blue light transilluminators, facilitating on-site interpretation.

Conclusions: This study established a highly field-deployable RPA-CRISPR/Cas12a assay for rapid, visual detection of GPV with outstanding sensitivity and specificity. Its capability for instrument-free on-site diagnosis via blue light transillumination makes this approach particularly promising for resource-limited settings.

KEYWORDS

goose parvovirus, CRISPR/Cas12a, recombinase polymerase amplification, nucleic acid, portable

Introduction

Waterfowl parvoviruses belong to the genus *Dependovirus* within the family Parvoviridae. They are categorized into two primary groups based on host susceptibility and complete genomic characteristics (Zádori et al., 1995). These groups comprise Muscovy duck parvovirus (MDPV) and goose parvovirus (GPV). MDPV specifically affects Muscovy ducklings (Cheng et al., 1993), while GPV is responsible for Derzy's disease in both goslings (Derzsy, 1967) and Muscovy ducklings (Cheng et al., 2008; Wang et al., 2015, 2013), as well as short beak and dwarfism syndrome (SBDS) in mule ducks and Cherry Valley ducks (Chen et al., 2016; Xiao et al., 2017). Muscovy duck-origin GPV (MDGPV) arises from natural recombination between MDPV and GPV (Liu et al., 2024; Wang et al., 2015), showing a diagnostic feature of intestinal embolism similar to that observed in Derzy's disease (Wang et al., 2020, 2019). MDPV, classical and recombinant GPV infections, can cause high morbidity and mortality in domestic waterfowl (Cheng et al., 1993; Glavits et al., 2005). Additionally, the short beak and dwarfism syndrome virus (SBDSV), a distinct GPV originating from ducks (Chen et al., 2016; Wang et al., 2016), presents a lower morbidity rate (2% to 10%) (Chen et al., 2015), yet infected ducks exhibit an average weight reduction of approximately 1 kg at slaughter compared to healthy counterparts (Chen et al., 2015). These infections have posed significant economic challenges in domestic waterfowl production across Asia, Europe, and North America (Chen et al., 2016; Cheng et al., 2008; Gough et al., 2005; Jansson et al., 2007; Poonia et al., 2006; Woolcock et al., 2000).

Traditional detection methods for GPV include virus isolation (Chen et al., 2016), serological assays such as ELISA, latex agglutination, and indirect immunofluorescence assays (IFA) (Chen et al., 2016; Takehara et al., 1999; Zhang et al., 2020), and nucleic acid-based amplification techniques (Lin et al., 2019; Luo et al., 2018). While virus isolation remains the gold standard for diagnosing GPV infection. Nevertheless, given their labor-intensive and time-consuming nature, as well as the need for highly skilled personnel, these techniques fall short in meeting the urgent demand for rapid field diagnostics. Serological tests, though rapid and user-friendly, are limited by their inability to detect the virus in early infection stages and exhibit low sensitivity (Luo et al., 2018). Molecular advancements have introduced conventional PCR and real-time quantitative PCR (qPCR), offering high sensitivity and specificity (Lin et al., 2019; Luo et al., 2018; Wozniakowski et al., 2010). However, these methods are hampered by long turnaround times and the necessity for sophisticated equipment, which restricts their applicability in resource-limited settings. Isothermal amplification techniques, such as recombinase polymerase isothermal amplification (RPA), have emerged as promising alternatives by overcoming some of these limitations (Daher et al., 2016). Nonetheless, the application of RPA in on-site detection has been impeded by the risk of false-positive results due to aerosol contamination (Hu et al., 2022).

The recent advent of the CRISPR/Cas system, particularly the trans-cleavage activity mechanism, has revolutionized nucleic acid detection (Chen et al., 2018; Gootenberg et al., 2017; Li et al., 2018). Cas12a (Cpf1), for instance, can specifically recognize and bind to target double-stranded DNA (dsDNA) or single-stranded DNA (ssDNA) with a protospacer adjacent motif (PAM) sequence, facilitated by guide RNAs (gRNAs) (Chen et al., 2018). This binding leads to the cleavage of surrounding ssDNA, resulting in the release of fluorophores and quenching groups, thereby transforming target sequence information into a detectable fluorescent signal. The integration of RPA pre-amplification with this system has led to the development of the first CRISPR-Dx platform, DETECTR, which achieves attomolar sensitivity for DNA detection (Chen et al., 2018). Unlike PCR, which requires precise thermal cycling, CRISPR-based detection operates effectively at physiological or room temperatures, making it highly adaptable for on-site use (Gootenberg et al., 2017; Hu et al., 2023; Wei et al., 2022; Wu et al., 2022). However, the application of the CRISPR/Cas12a system combined with RPA for GPV detection remains unexplored.

This study introduces a novel CRISPR/Cas12a-based assay targeting the *VP3* gene of GPV. The assay delivers rapid and accurate results within a 1-hour turnaround time, significantly expediting the diagnostic process. Moreover, the use of a portable blue light transilluminator enables visual detection without the need for sophisticated equipment, rendering the assay particularly advantageous for resource-limited settings (Figure 1). By providing a reliable and user-friendly diagnostic tool, this study paves the way for efficient surveillance and control of GPV in domestic waterfowl populations.

Materials and methods

Reagents

NEBuffer 2.1, NEBuffer 3.1, CutSmart buffer, and EnGen Lba Cas12a protein were obtained from New England Biolabs (Beijing, China). 10 × Cas12a reaction buffer was purchased from Guangzhou Magigen Biotechnology Co., Ltd. (Guangzhou, China). The nucleic acid rapid lysis solution was purchased from Shanghai Kanglang Biotechnology Co., Ltd. (Shanghai, China). The TwistAmp® Basic kit was purchased from TwistDx Ltd. (Cambridge, UK). PerfectStart® Green qPCR SuperMix and *EasyPure*® Viral DNA/RNA Kit were acquired from TransGen Biotechnology Co., Ltd. (Beijing, China).

Animals and viruses

A total of thirty-six 23-day-old healthy Muscovy ducklings were examined for waterfowl parvovirus antibodies using the previously described latex agglutination inhibition assay (LAI) (Chen et al., 2016).

The viruses used in this study include the following: SBDSV, MDGPV, classical GPV (cGPV), MDPV, Muscovy duck reovirus (MDRV), novel duck reovirus (NDRV), duck plague virus (DPV) and duck adenovirus B2 (DAdV B2). They were identified and preserved at the Institute of Animal Husbandry and Veterinary Medicine, Fujian Academy of Agricultural Sciences.

Design of RPA primers and CRISPR RNA

The complete genome nucleotide sequences of GPV were retrieved from the National Center for Biotechnology Information (NCBI)

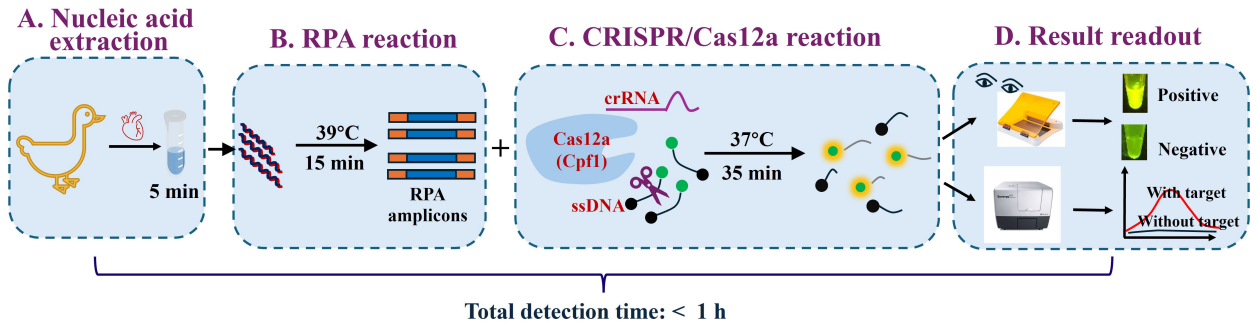

FIGURE 1
Schematic of the RPA-CRISPR/Cas12a assay for GPV detection. The workflow comprises four main steps: **(A)** Cardiac tissue is lysed in nucleic acid lysis buffer for 5 min. **(B)** The resultant lysate is directly subjected to recombinase polymerase amplification (RPA) at 39°C for 15 min to amplify the target sequence. **(C)** The CRISPR RNA (crRNA)-guided Cas12a ribonucleoprotein (RNP) specifically binds to the double-stranded DNA (dsDNA) amplicons. Formation of the RNP/dsDNA complex activates the trans-cleavage activity of Cas12a, which subsequently cleaves single-stranded DNA (ssDNA) reporter molecules, producing a fluorescent signal. **(D)** Fluorescence readouts can be visualized by the naked eye under blue light (470 nm excitation) using a portable blue light transilluminator or quantified using a multimode microplate reader.

database (http://www.ncbi.nlm.nih.gov/). The identification of conserved regions was carried out through multiple sequence alignments using the MegAlign module in the DNASTAR software (Version 7.1). This analytical approach conclusively identified the *VP3* gene as the most conserved genomic region of GPV, a finding fully consistent with prior reports (Ma et al., 2022; Dong et al., 2019; Yang et al., 2017). Three primer sets targeting the *VP3* gene were generated using Primer Premier version 5.0. software (PREMIER Biosoft, CA, USA) in accordance with the TwistAmp assay design manual, and both hairpin and cross dimer were assessed. The CRISPR RNA (crRNA) was designed to target the *VP3* gene of GPV employing the online tool Benchling (https://www.benchling.com/crispr/). NCBI-BLAST was used to conduct the specificity analysis of RPA primers. The sequence conservative analysis of crRNAs was performed using the ClustalW program (https://www.genome.jp/tools-bin/clustalw). The oligonucleotides utilized in this research were synthesized by Sangon Biotech (Shanghai, China). Detailed information regarding the designed primers and crRNA are shown in Table 1.

Establishment of RPA assay

RPA was performed following the manufacturer's protocol for pre-amplifying DNA sequences. Briefly, a 50 μL RPA mixture was prepared, consisting of 29.5 μL of rehydration buffer, 480 nM of each primer, 1 μL of target template, and 12.2 μL of sterile nuclease-free water, along with 2.5 μL of 280 nM magnesium acetate. A negative control was included by replacing the DNA template with sterile nuclease-free water. The RPA was conducted at 39°C in a water bath for 15 min, and subsequently incubated at 95°C for 5 min. Purification of the RPA products was carried out using a Universal DNA Purification Kit (TianGen, Beijing, China). Evaluation of the reaction products was conducted through gel

TABLE 1 Sequences of oligonucleotides utilized in this study.

Name	Sequence (5'to 3')	Product length	Ref.
RPA-F1	CAAGATCTTCAATGTTCAAGTCAAGGAAGTC	259 bp	This study
RPA-R1	CAATGACCGTAGCGCATTCTACTGCTTAGAG		
RPA-F2	CAAGGAAGTCACAACGCAGGATCAGACAAAG	200 bp	
RPA-R2	TACTGCACAATGCACACCAACCAGAATGGAG		
RPA-F3	CATTGCAAACAATCTCACCTCAACAATCCAAG	119 bp	
RPA-R3	GACCATGCCGCCGTTCCCGTCGGATGTCTATG		
qPCR-F	GAGGTAGACAGCAACAGAAA	343 bp	Lin et al., 2019
qPCR-R	GCTCGTCCGTGACCATA		
crRNA*	UAAUUUCUACUAAGUGUAGAUCGGAUGAUGAGCACCAACUC		This study
FQ reporter	FAM-TTATT-BHQ		This study

*The spacer sequences of the crRNA, which are responsible for recognizing and binding to the target, are marked with an underline.

electrophoresis. Primer pairs exhibiting superior performance were selected through gel electrophoresis screening.

CRISPR/Cas12a-mediaed nucleic acid detection and visualization

The LbaCas12a reaction was conducted in a total volume of 30 μL. Firstly, 100 nM Cas12a was pre-incubated with 200 nM crRNA in 10 × Magigen reaction buffer at 37°C for 5 min to form the ribonucleoprotein (RNP) complex. Subsequently, 200 nM ssDNA reporter and 1 μL of RPA amplicons were added to the RNP complex, then the solution was immediately transferred to a 384-well black polystyrene microplate (Costar). Real-time fluorescence analysis was carried out at 37°C using the multimode microplate reader Bio Tek Synergy H1, with fluorescence measurements recorded every 1 min for 30 min. The excitation and emission wavelengths were set at 485 and 525 nm, respectively. To obtain the visual detection results of the samples, the tubes were placed on a portable blue-light instrument (TianGen, Beijing, China). The visual detection results were photographed using a smartphone in a dark environment.

Evaluation of the limit of detection and specificity of the RPA-CRISPR/Cas12a assay

To assess the LOD of the RPA-CRISPR/Cas12a assay, 1 μL of 10-fold serially diluted plasmid DNA ranging from 10^0 to 10^3 copies/μL was used as templates for the RPA reaction. Subsequently, 1 μL of the positive RPA amplicons were used to trigger the CRISPR/Cas12a cleavage system. Each reaction was conducted in triplicate, with the negative RPA amplicons serving as the negative control. In terms of specificity evaluation, the DNA of five waterfowl-origin viruses, including MDPV, MDRV, NDRV, DPV, and DAdV B2, were tested.

Real-time qPCR assay

The qPCR assay (Lin et al., 2019) for GPV detection was performed following the instructions of the Roche LightCycler® 96 instrument (Roche Diagnostics, Germany). Briefly, the qPCR reaction mixtures consisted of 10 μL of PerfectStart® Green qPCR SuperMix, 0.5 μL of each forward and reverse primer (10 μM), 1 μL of DNA template, and 8 µL of nuclease-free water to a final volume of 20 μL. The qPCR amplification conditions were as follows: pre-denaturation at 95°C for 5 min, followed by 40 cycles of denaturation at 95°C for 15 s, annealing at 60°C for 10 s, and extension at 72°C for 15 s. Samples with a cycle threshold (Ct) value < 30 and a melting temperature (Tm) of 86.15 ± 0.26°C, exhibiting a distinct single peak, were considered positive for GPV.

Repeatability and reproducibility analysis of RPA-CRISPR/Cas12a assay

Three different concentrations of standard plasmid (10^6–10^4 copies/μL) were tested for the intrabatch and interbatch assays. For repeatability (intra-assay) analysis, three different concentrations of standard plasmid were tested in three independent runs. Reproducibility (inter-assay) was determined in three independent runs conducted by different individuals on different days, with results analyzed using the coefficient of variation (CV).

Validation of the RPA-CRISPR/Cas12a assay using mock/actual samples

All experimental procedures were reviewed and approved by the Institute of Animal Husbandry and Veterinary Medicine, Fujian Academy of Agricultural Science Animal Care and Use Committee (license number: MYLLSC2024-007).

To assess the practical application value of the RPA-CRISPR/Cas12a assay, thirty-six 23-d-old Muscovy ducklings were randomly allocated into two groups, each consisting of 18 ducklings. Ducklings in Group 1 received an intramuscular injection in the leg with 0.5 ml of MDGPV strain JS, a 5th-passage allantoic fluid virus with a titer of $2^{10.0}$ LA, serving as the positive control. Conversely, ducklings in Group 2 were administered 0.5 ml of sterile phosphate-buffered saline (PBS) as a mock control. All Muscovy ducklings were housed in isolators, and their clinical signs were meticulously monitored daily for a total of 14 days. Following the challenge, serum, oropharyngeal swabs, cloacal swabs, and tissue samples from the heart, lung, spleen, liver, kidney, and pancreas samples were collected from the mock-injected ducklings at 2, 5, 10, and 14 days post infection (dpi). Additionally, 42 field-isolated samples were collected from ducklings suspected of GPV infection in Tutian or Zhangzhou, Fujian Province. Nucleic acids were extracted from heart tissue samples using a rapid lysis solution, with 1 µL of the extracted nucleic acids serving as the template for both the RPA-CRISPR/Cas12a method and the qPCR assay. The results obtained were confirmed using an IFA, as previously described (Chen et al., 2016).

Statistical analysis

The statistical analysis was performed using GraphPad Prism 8.0 (GraphPad, USA). The unpaired Student's t-test was used to analyze differences between two groups. **** represents $P < 0.0001$, ** represents $P < 0.01$, and ns represents $P > 0.05$. The data were presented as mean ± SD, derived from three independent experiments. LOD, specificity, positive predictive value (PPV), and negative predictive value (NPV) were calculated using established statistical formulas. Exact 95% confidence intervals

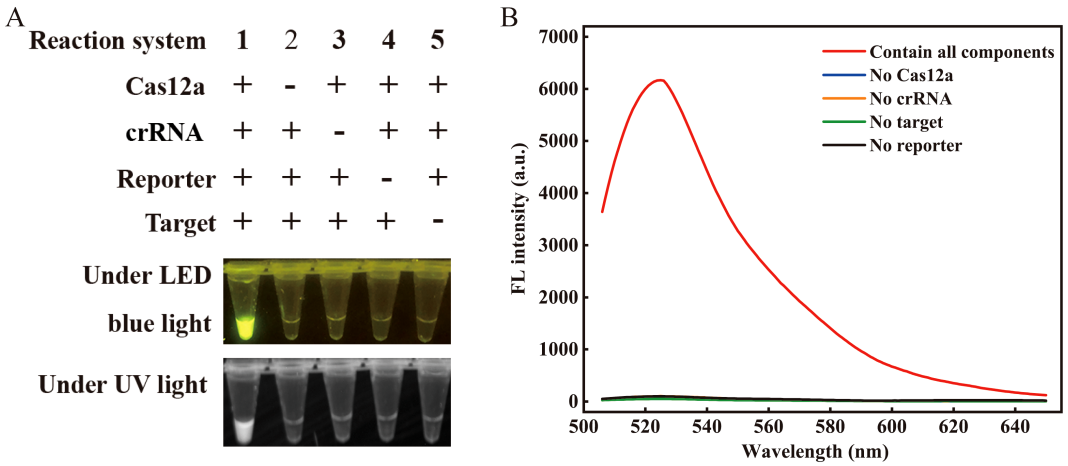

FIGURE 2
Feasibility validation of the RPA-CRISPR/Cas12a assay. **(A)** Validation of the Cas12a cleavage activity under blue light (470 nm) and UV light. The "+" refers to the presence of a reaction ingredient, while "-" represents their absence. **(B)** Spectrogram fluorescence of the RPA-CRISPR/Cas12a assay. Apart from the red curve, all other curves depict reactions where a particular single component was excluded while retaining all other components and enzymes (λex 485 nm, λem 525 nm). Target denotes the target nucleic acid sequence. The concentrations of Cas12a, crRNA, and ssDNA reporter were 100 nM, 200 nM, and 200 nM, respectively.

(CI) for these performance metrics were determined using the Clopper-Pearson method, which employs binomial probability calculations to ensure conservative interval estimates.

Results

Verification of the RPA-CRISPR/Cas12a assay for GPV detection

To examine the feasibility of the proposed assay, we prepared five reaction systems (reactions #1–5; Figure 2). A plasmid containing a 259 bp fragment of the *VP3* gene was served as the target. After a 20-minute incubation at 37°C, only reaction #1, comprising all components, showed a strong fluorescence signal when illuminated with LED blue or UV light. Conversely, the absence of certain components resulted in no detectable fluorescence signals (Figure 2A). The feasibility of the visual readout was further confirmed by measuring the fluorescent intensity (Figure 2B). These results demonstrated the feasibility of using the RPA-CRISPR/Cas12a assay for detecting GPV.

Screening of the optimal RPA primer pairs

Three pairs of RPA primers were designed to target the *VP3* gene of GPV. The optimal RPA primers were validated through agarose gel electrophoresis. As depicted in Supplementary Figure S1, the 259 bp RPA product corresponding to the first pair of primers had the brightest and clearest band, with no nonspecific bands present. Consequently, the first pair of primers was selected for further experimentation. Moreover, the Sanger sequencing result further demonstrated the efficacy of the RPA primers (Supplementary Figure S2).

Evaluation of the optimized conditions

Several parameters were optimized to enhance the analytical performance, including the concentration of Cas12a, crRNA, ssDNA reporter, and buffers. The concentration of Cas12a was found to have a significant impact on the *trans*-cleavage efficiency of the CRISPR/Cas12a. Therefore, various concentrations of Cas12a enzyme were first optimized. As shown in Figure 3A, the fluorescence intensity was highest at 200 nM Cas12a. However, the signal-to-background ratio (S/B) was lower than that at 150 nM. Therefore, the optimal concentration of Cas12a was 150 nM. Furthermore, the concentration of crRNA plays a pivotal role in determining the optimal signal readout. Therefore, the concentration of crRNA was also optimized. The optimal concentration, which yielded the highest S/B ratio, was 200 nM (Figure 3B). For the ssDNA reporter, 300 nM was the optimal concentration as it provided the highest S/B ratio despite an increase in fluorescence intensity with higher concentrations (Figure 3C). Additionally, the chemical environment of the Cas12a may impact its *trans*-cleavage efficiency. Therefore, we selected four commercial reaction buffers to investigate. We found that the Magigen buffer gave the highest S/B ratio (Figure 3D), therefore it was chosen for subsequent analyses.

LOD and specificity of the RPA-CRISPR/Cas12a assay

To assess the LOD of the Cas12a-mediated cleavage assay, 10-fold serial dilutions of the standard plasmid pMD-19T-*VP3* ranging from 10^0 to 10^3 copies/μL were used as the template. As shown in Figure 4A, the assay successfully detected plasmids containing as low as 10 copies/μL of the *VP3* gene.

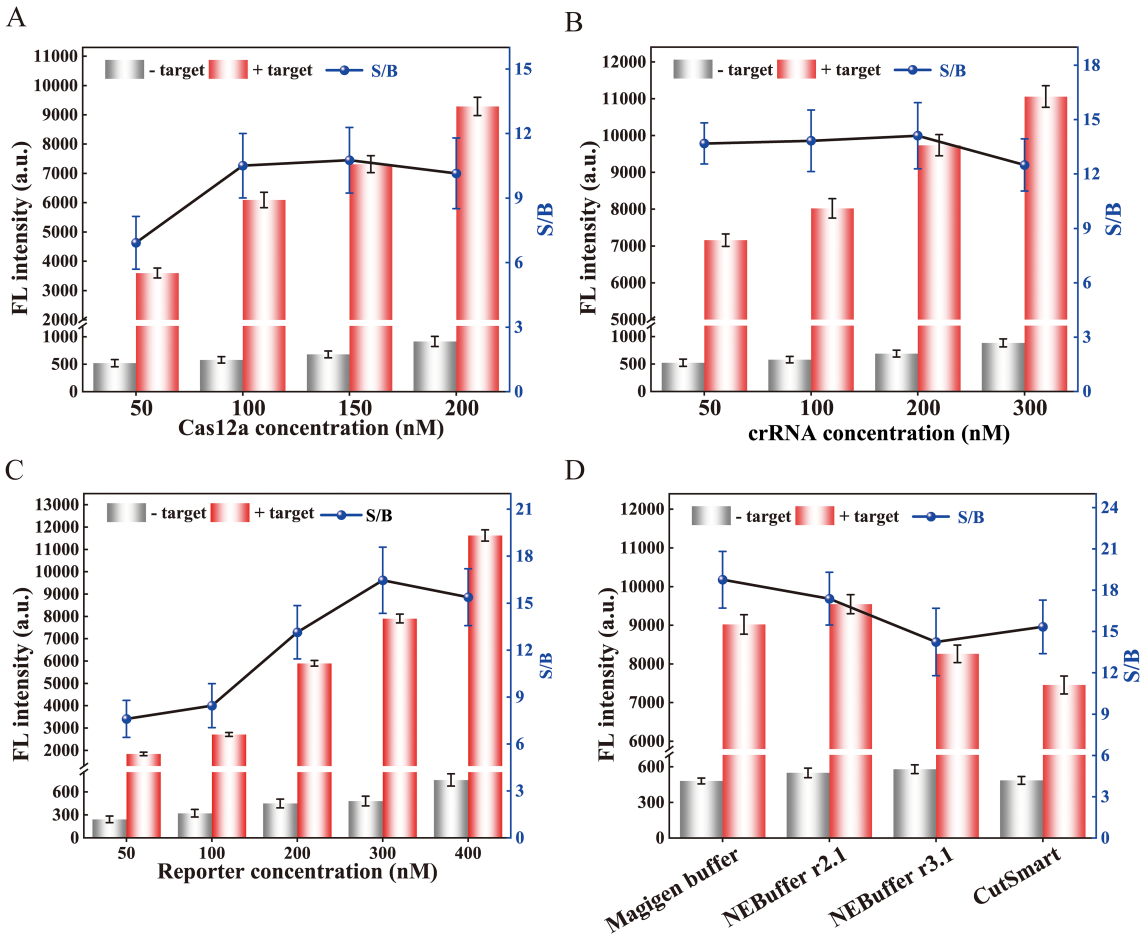

FIGURE 3
Optimization of reaction conditions for the RPA-CRISPR/Cas12a assay. Optimization of **(A)** Cas12a concentration, **(B)** crRNA concentration, and **(C)** reporter concentration. **(D)** Effect of different buffers on *trans*-cleavage efficiency of CRISPR/Cas12a. The signal-to-background ratio was determined based on the ratio of positive to negative fluorescence intensity. The fluorescence intensity at 30 min of the reaction was displayed. Error bars represent the mean of three replicates ± standard deviation (SD).

The specificity of the assay was evaluated using viruses that commonly infect ducks, including MDPV, MDRV, NDRV, DPV, and DAdV B2. As illustrated in Figure 4B, the fluorescence intensity of cGPV, MDGPV, and SBDSV were significantly higher than those of the other duck viruses, confirming that the assay had high specificity without cross reactions with non-GPV targets.

Analytical the repeatability and reproducibility of the RPA-CRISPR/Cas12a assay

To further validate the performance of the established assay, we conducted experiments to assess its repeatability and reproducibility. CVs were calculated for three different concentrations of standard plasmid in both intra-batch and inter-batch analyses. The results indicated that the constructed assay possesses excellent reproducibility and repeatability in detecting GPV, with an intra-assay CV for fluorescence intensity ranging from 1.54% to 2.46%, and an inter-assay CV ranging from 2.41% to 3.18% (Table 2).

Application of the assay on clinical samples

First, we applied the proposed strategy on multiple mock samples to evaluate its practical applicability. As shown in Table 3, the RPA-CRISPR/Cas12a assay successfully detected GPV-DNA in all tissue, blood, oropharyngeal swabs, and cloacal swabs samples at both 2 and 5 dpi. Furthermore, this assay maintained its sensitivity, detecting GPV-DNA in blood and cloacal swab samples even at 10 dpi. However, at 15 dpi, GPV-DNA was undetectable in any of the mock samples. In contrast, as shown in Table 4, the qPCR assay was only capable of detecting GPV-DNA in blood samples at 2 dpi. These results demonstrate that the RPA-CRISPR/Cas12a assay exhibits superior sensitivity than the qPCR assay for detecting GPV-DNA in clinical samples.

We further applied this strategy using 42 field-isolated duckling samples exhibiting clinical symptoms such as poor feathering (Supplementary Figure S3A) and intestinal embolism (Supplementary Figure S3B). Initial screening via IFA classified 20 samples as positive and 22 as negative (Supplementary Figure S4). Subsequent diagnostic evaluation using both the RPA-CRISPR/Cas12a and qPCR assays revealed superior performance of the CRISPR-based method. The

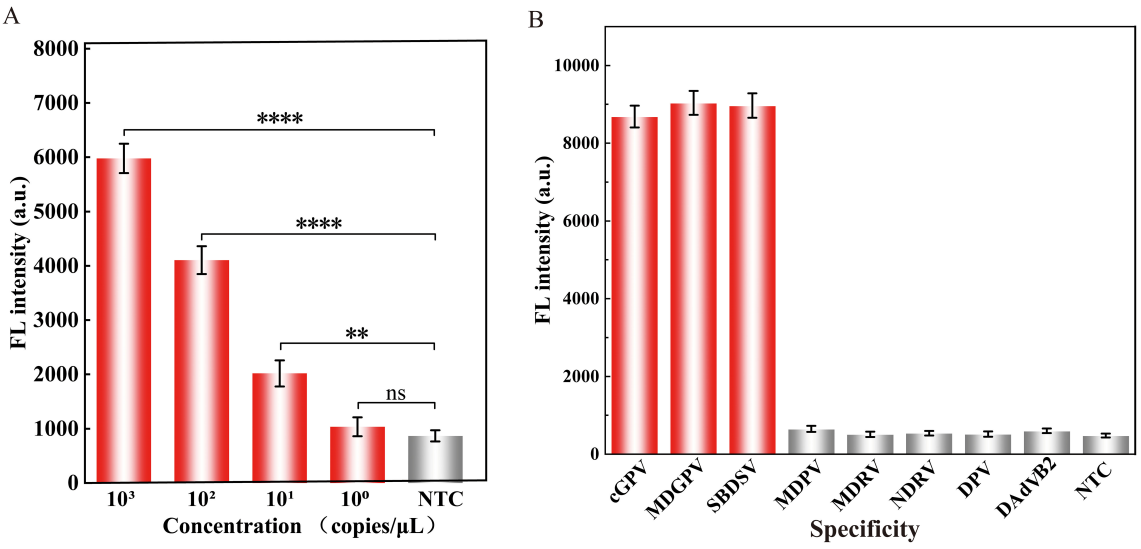

FIGURE 4
Properties evaluation of the RPA-CRISPR/Cas12a assay for detecting GPV. The **(A)** sensitivity and **(B)** specificity analysis of the proposed assay. Equal concentrations of the nucleic acids of the virus were used in all analyses. The fluorescence intensity at 30 min of the reaction was displayed. Error bars represent the mean of three replicates ± standard deviation (SD). NTC implies the absence of template control. **** represents $P < 0.0001$, ** represents $P < 0.01$, and ns represents $P > 0.05$.

RPA-CRISPR/Cas12a assay exhibited superior performance, achieving a diagnostic sensitivity of 100% (95% CI: 83.2%–100%) and 95.5% specificity (95% CI: 77.2%–99.9%), with a PPV of 95.2% (95% CI: 76.4%–99.9%) and a NPV of 100% (95% CI: 84.6%–100%) (Figure 5A). In contrast, qPCR showed reduced accuracy with a diagnostic sensitivity of 90% (95% CI: 68.4%–98.8%) and 90.9% specificity (95% CI: 73.5%–98.8%), as detailed in the comparative analysis (Figure 5B).

To develop an affordable on-site testing platform, we utilized a portable blue light transilluminator for rapid visual readouts. As depicted in Figure 5C, positive samples exhibited strong bright green fluorescence under the transilluminator, whereas negative samples showed negligible background fluorescence. This fluorescence-based interpretation exhibited complete concordance with the RPA-CRISPR/Cas12a assay results, validating the transilluminator's applicability for on-site diagnostics in resource-limited settings.

Discussion

Infectious diseases among waterfowl have surged in recent years, with significant economic implications. GPV, in particular, has been endemic in various global regions, causing notable economic losses (Chen et al., 2016). Consequently, the development of rapid and accurate diagnostic tools for GPV surveillance is of paramount importance. PCR-based methods are commonly utilized for GPV detection due to their high specificity and sensitivity. Nonetheless, these techniques are constrained to laboratory environments due to their reliance on sophisticated equipment and specialized personnel.

In this study, a visualization method combining RPA with CRISPR/Cas 12a system for rapid, simple, and highly sensitive detection of GPV was developed. The assay provides flexible detection platforms, allowing results analysis through either a real-time fluorescent PCR instrument or a multimode microplate reader. For field applications, a portable blue light transilluminator enables visual inspection, significantly enhancing on-site testing feasibility. Compared to qPCR, the RPA-CRISPR/Cas12a assay demonstrated superior diagnostic accuracy, achieving 100% sensitivity (20/20 true positives) and 95.5% specificity (21/22 true negatives) (Figure 5A). In contrast, qPCR assay showed lower sensitivity (90%, with 2/20 false negatives) and specificity (90%, with 2/22 false positives) (Figure 5B). This performance advantage was further evident in mock infection

TABLE 2 Results of repeatability and reproducibility analysis of the RPA-CRISPR/Cas12a assay.

Concentration of standard plasmid (copies/μL)	Repeatability (intra-bath assay)		Reproducibility (inter-bath assay)	
	mean ± SD	CV (%)	mean ± SD	CV (%)
10^6	9588.33 ± 147.79	1.54	9798.67 ± 210.09	2.14
10^5	8620.00 ± 165.31	1.92	8683.33 ± 252.94	2.91
10^4	7426.00 ± 182.95	2.46	7600.00 ± 242.03	3.18

Mean, the average of fluorescence intensity of three independent RPA-CRISPR/Cas12a runs.
SD, standard deviation; CV, coefficient of variation.

TABLE 3 Detection of GPV-DNA in mock samples using the RPA-CRISPR/Cas12a assay.

Days post infection	Blood	Heart	Liver	Spleen	Lung	Kidney	Pancreas	Oropharynx	Cloacal
2	+	+	+	+	+	+	+	+	+
5	+	+	+	+	+	+	+	+	+
10	+	–	–	–	–	–	–	–	+
15	–	–	–	–	–	–	–	–	–

+, positive; –, negative.

TABLE 4 Detection of GPV-DNA in mock samples using the qPCR assay.

Days post infection	Blood	Heart	Liver	Spleen	Lung	Kidney	Pancreas	Oropharynx	Cloacal
2	+	–	–	–	–	–	–	–	–
5	–	–	–	–	–	–	–	–	–
10	–	–	–	–	–	–	–	–	–
15	–	–	–	–	–	–	–	–	–

+, positive; –, negative.

experiments, where GPV-DNA was reliably detected at both high (2 dpi) and low (10 dpi) concentrations, while qPCR assay only detected GPV-DNA in blood samples at 2 dpi (Table 4). The enhanced sensitivity originates from CRISPR/Cas12a system's dual-function mechanism: crRNA-guided single-base discrimination ensures precise target recognition, whereas Cas12a's collateral ssDNase activity enables exponential signal amplification, effectively minimizing nonspecific interference common in primer-dependent methods (Chen et al., 2018).

The assay exhibited exceptional specificity with no cross-reactivity against non-GPV targets (Figure 4B), consistent with Cas12a's sequence-specific recognition. Notably, it achieved a detection limit of 10 copies/μL of for GPV plasmids DNA, outperforming existing nucleic acid amplification methods (Supplementary Table S1). For instance, Liu et al. (2019) reported an RPA-vertical flow (VF) assay for GPV detection with a LOD of 2×10^2 copies/μL, which is 20-fold lower than our method. Similarly, Yang et al. (2017) employed LAMP with Eva Green dye to reduce non-specific amplification but achieved only a LOD of 10^2 copies/μL, requiring higher amplification temperatures (65°C). Through optimized coordination between RPA primers and crRNA, we eliminated aerosol contamination risks associated with RPA-LF assays (Hu F, et al., 2022) and reduced the

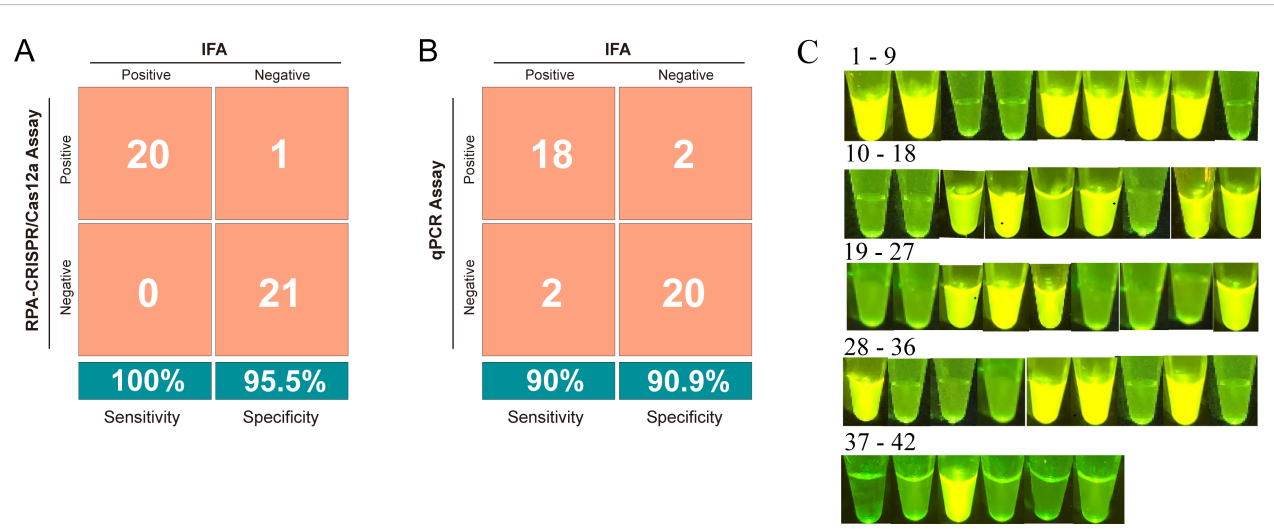

FIGURE 5
Evaluation of the RPA-CRISPR/Cas12a assay for detecting GPV in clinical samples. **(A)** Confusion matrix illustrating the comparison of results between the RPA-CRISPR/Cas12a assay and indirect immunofluorescence assay (IFA). **(B)** Confusion matrix illustrating the comparison of results between the qPCR assay and IFA. **(C)** Visual appearance of results for 42 clinical samples. The pictures were captured under blue light (470 nm) by a smartphone camera. Bright green fluorescence was observed in positive samples, whereas dim green fluorescence was detected in negative samples.

total detection time to 55 minutes, overcoming the prolonged workflows of qPCR and semi-nested PCR (Supplementary Table S1).

Buffer components play a significant role in the spontaneous formation of essential higher-level protein structures (Habimana et al., 2023). Therefore, they may influence the *trans*-cleavage efficiency of Cas12a. While previous studies generally used NEBuffer r2.1 for CRISPR/Cas reactions (Wu et al., 2022; Yang et al., 2022), our findings indicated that the Cas12a protein achieved optimal trans-cleavage efficiency in the Magigen buffer, which contains dithiothreitol (DTT) (see Supplementary Table S2) (Chen et al., 2023; Deng et al., 2022; Ding et al., 2018). DTT is crucial for stabilizing enzymes and protecting sulfhydryl groups, thereby enhancing the accuracy of CRISPR nucleic acid detection systems.

To streamline the detection process, employed a rapid nucleic acid lysis strategy, reducing the total assay time to 55 minutes (comprising 5 minutes for nucleic acid release, 15 minutes for RPA, and 35 minutes for CRISPR/Cas12a detection; see Figure 1). The use of a portable blue light transilluminator for visual observation underscores the assay's suitability for on-site GPV detection. Despite the assay's rapid detection and high specificity, several challenges persist. Primarily, the separation of nucleic acid amplification and CRISPR/Cas12a *trans*-cleavage into two distinct steps introduces complexities. While this two-step approach prevents the loss of the RPA nucleic acid template due to *cis* cleavage by CRISPR/Cas12a and avoids RPA primer degradation from CRISPR/Cas12a trans-cleavage activation (Hu F et al., 2022), it complicates manual handling and increases the risk of cross-contamination during amplicon transfer. To mitigate these risks, several strategies have been proposed, such as separating the isothermal amplification system from the Cas12/crRNA complex (Pang et al., 2020; Wang et al., 2021), utilizing photocleavable linkers (Hu M et al., 2022), or developing a PAM-free one-step assay (Yang et al., 2024). Additionally, quantifying high target concentrations using CRISPR/Cas-based assays remains challenging due to the system's high sensitivity and limited availability of reporter molecules, which can lead to an early signal plateau (Li et al., 2019). Furthermore, although our assay requires only a portable instrument, there is still a need to develop assays based on lateral flow immunoassays to fulfill the demand for even more rapid diagnostics. Nevertheless, these constraints are anticipated to be addressed in future research endeavors.

Conclusion

In summary, a novel method integrating RPA with the CRISPR/Cas12a system was successfully established for rapid, visual, and field-deployable detection of GPV. The assay demonstrates outstanding sensitivity and specificity, achieving a rapid turnaround time of only 55 min from samples collection to result generation. Notably, the system eliminates complex instrumentation requirements by incorporating a blue light transilluminator for instant visual interpretation, addressing a critical bottleneck in point-of-care testing. Collectively, this study presents an innovative, on-site approach for GPV detection, holding substantial promise for implementation in resource-limited settings where traditional laboratory infrastructure is lacking.

Data availability statement

The datasets presented in this study can be found in online repositories. The names of the repository/repositories and accession number(s) can be found in the article/Supplementary Material.

Ethics statement

The animal study was approved by Institute of Animal Husbandry and Veterinary Medicine, Fujian Academy of Agricultural Science Animal Care and Use Committee. The study was conducted in accordance with the local legislation and institutional requirements.

Author contributions

XC: Conceptualization, Data curation, Formal analysis, Funding acquisition, Methodology, Writing – original draft, Writing – review & editing. SZ: Investigation, Methodology, Writing – review & editing. SL: Funding acquisition, Writing – review & editing. SW: Funding acquisition, Methodology, Writing – review & editing. MH: Investigation, Resources, Writing – review & editing. SYC: Resources, Supervision, Writing – review & editing. SLC: Funding acquisition, Project administration, Supervision, Validation, Writing – review & editing.

Funding

The author(s) declare that financial support was received for the research and/or publication of this article. This research was funded by grants sponsored by the Scientific Research Project of Fujian Academy of Agricultural Sciences (Grant No. ZYTS2023017), the Fujian Public Welfare Project (Grant No. 2023R1024002, 2023R1024003, 2022R1026004), the "5511" Collaborative Innovation Project of Fujian Academy of Agricultural Sciences, China (XTCXGC2021018 and XTCXGC2021012) and the Central Government Guides Local Scientific and Technological Development Project (Grant No. 2022L3019).

Conflict of interest

The authors declare that the research was conducted in the absence of any commercial or financial relationships that could be construed as a potential conflict of interest.

Generative AI statement

The author(s) declare that no Generative AI was used in the creation of this manuscript.

Publisher's note

All claims expressed in this article are solely those of the authors and do not necessarily represent those of their affiliated organizations, or those of the publisher, the editors and the reviewers. Any product that may be evaluated in this article, or claim that may be made by its manufacturer, is not guaranteed or endorsed by the publisher.

Supplementary material

The Supplementary Material for this article can be found online at: https://www.frontiersin.org/articles/10.3389/fcimb.2025.1566603/full#supplementary-material

References

Chen, S., Cheng, X., Chen, S., Wang, S., Lin, F., Wu, N., et al. (2015). Short report: A new emerging disease in mule ducks caused by a novel goose parvovirus. *Fujian Agri Sci. Tech.* 7, 23–25. doi: 10.13651/j.cnki.fjnykj.2015.07.007

Chen, X., Liu, X., Yu, Y., Wang, H., Li, C., Vallée, I., et al. (2023). FRET with MoS2 nanosheets integrated CRISPR/Cas12a sensors for robust and visual food-borne parasites detection. *Sensor Actuat B-Chem.* 395, 134493. doi: 10.1016/j.snb.2023.134493

Chen, J. S., Ma, E., Harrington, L. B., Da Costa, M., Tian, X., Palefsky, J. M., et al. (2018). CRISPR-Cas12a target binding unleashes indiscriminate single-stranded DNase activity. *Science.* 360, 436. doi: 10.1126/science.aar6245

Chen, S., Wang, S., Cheng, X., Xiao, S., Zhu, X., Lin, F., et al. (2016). Isolation and characterization of a distinct duck-origin goose parvovirus causing an outbreak of duckling short beak and dwarfism syndrome in China. *Arch. Virol.* 161, 2407–2416. doi: 10.1007/s00705-016-2926-4

Cheng, X., Chen, S., Zhu, X., Chen, S., Lin, F., Wang, S., et al. (2008). Isolation and identification of goose parvovirus from Muscovy ducklings. *Fujian J. Agri Sc.i* 23, 355–358. doi: 10.19303/j.issn.1008-0384.2008.04.005

Cheng, Y., Lin, T., Hu, Q., Li, Y., Zhou, W., and Wu, Z. (1993). Isolation and identification of a Muscovy duckling parvovirus. *Chin. J. Virol.* 9, 228–235. doi: 10.13242/j.cnki.bingduxuebao.000055

Daher, R. K., Stewart, G., Boissinot, M., and Bergeron, M. G. (2016). Recombinase polymerase amplification for diagnostic applications. *Clin. Chem.* 62, 947–958. doi: 10.1373/clinchem.2015.245829

Deng, F., Li, Y., Li, B., and Goldys, E. M. (2022). Increasing trans-cleavage catalytic efficiency of Cas12a and Cas13a with chemical enhancers: application to amplified nucleic acid detection. *Sensor Actuat B-Chem.* 373, 132767. doi: 10.1016/j.snb.2022.132767

Derzsy, D. (1967). A viral disease of goslings. I. Epidemiological, clinical, pathological and aetiological studies. *Acta Vet. Acad. Sci. Hung.* 17, 443–448.

Ding, X., Kong, X., Chen, Y., Zhang, C., Hua, Y., and Li, X. (2018). Selective extraction and antioxidant properties of thiol-containing peptides in soy glycinine hydrolysates. *Molecules.* 23, 1909. doi: 10.3390/molecules23081909

Dong, J., Bingga, G., Sun, M., Li, L., Liu, Z., Zhang, C., et al. (2019). Application of high-resolution melting curve analysis for identification of Muscovy duck parvovirus and goose parvovirus. *J. Virol. Methods* 266, 121–125. doi: 10.1016/j.jviromet.2018.12.018

Glavits, R., Zolnai, A., Szabo, E., Ivanics, E., Zarka, P., Mato, T., et al. (2005). Comparative pathological studies on domestic geese (Anser domestica) and Muscovy ducks (Cairina moschata) experimentally infected with parvovirus strains of goose and Muscovy duck origin. *Acta Veterinaria Hungarica (Budapest. 1983).* 53, 73–89. doi: 10.1556/AVet.53.2005.1.8

Gootenberg, J. S., Abudayyeh, O. O., Lee, J. W., Essletzbichler, P., Dy, A. J., Joung, J., et al. (2017). Nucleic acid detection with CRISPR-Cas13a/c2c2. *Science.* 356, 438. doi: 10.1126/science.aam9321

Gough, D., Ceeraz, V., Cox, B., Palya, V., and Mato, T. (2005). Isolation and identification of goose parvovirus in the UK. *Vet. Rec.* 156, 424. doi: 10.1136/vr.156.13.424

Habimana, J. D. D., Mukama, O., Chen, G., Chen, M., Amissah, O. B., Wang, L., et al. (2023). Harnessing enhanced CRISPR/Cas12a trans-cleavage activity with extended reporters and reductants for early diagnosis of Helicobacter pylori, the causative agent of peptic ulcers and stomach cancer. *Biosens Bioelectron.* 222, 114939. doi: 10.1016/j.bios.2022.114939

Hu, T., Ke, X., Li, W., Lin, Y., Liang, A., Ou, Y., et al. (2023). CRISPR/Cas12a-enabled multiplex biosensing strategy via an affordable and visual nylon membrane readout. *Adv. Sci.* 10, 2204689. doi: 10.1002/advs.202204689

Hu, F., Liu, Y., Zhao, S., Zhang, Z., Li, X., Peng, N., et al. (2022). A one-pot CRISPR/Cas13a-based contamination-free biosensor for low-cost and rapid nucleic acid diagnostics. *Biosens Bioelectron.* 202, 113994. doi: 10.1016/j.bios.2022.113994

Hu, M., Qiu, Z., Bi, Z., Tian, T., Jiang, Y., and Zhou, X. (2022). Photocontrolled crRNA activation enables robust CRISPR-Cas12a diagnostics. *PNAS.* 119, e2092933177. doi: 10.1073/pnas.2202034119

Jansson, D. S., Feinstein, R., Kardi, V., Mato, T., and Palya, V. (2007). Epidemiologic investigation of an outbreak of goose parvovirus infection in Sweden. *Avian Dis.* 51, 609–613. doi: 10.1637/0005-2086(2007)51[609:EIOAOO]2.0.CO;2

Li, S., Cheng, Q., Liu, J., Nie, X., Zhao, G., and Wang, J. (2018). CRISPR-Cas12a has both cis- and trans-cleavage activities on single-stranded DNA. *Cell Res.* 28, 491–493. doi: 10.1038/s41422-018-0022-x

Li, L., Li, S., Wu, N., Wu, J., Wang, G., Zhao, G., et al. (2019). HOLMESv2: a CRISPR-Cas12b-assisted platform for nucleic acid detection and DNA methylation quantitation. *ACS Synth. Biol.* 8, 2228–2237. doi: 10.1021/acssynbio.9b00209

Lin, S., Wang, S., Cheng, X., Xiao, S., Chen, X., Chen, S., et al. (2019). Development of a duplex SYBR green I-based quantitative real-time PCR assay for the rapid differentiation of goose and Muscovy duck parvoviruses. *Virol. J.* 16, 6. doi: 10.1186/s12985-018-1111-7

Liu, H. W., Xu, Z. R., Wang, S., Cheng, X. X., Xiao, S. F., Zhu, X. L., et al. (2024). Identification and genome characterization of a novel Muscovy duck-origin goose parvovirus with three recombinant regions between Muscovy duck parvovirus and goose parvovirus. *Transbound Emerg. Dis.* 2024, 1018317. doi: 10.1155/2024/1018317

Liu, W., Yang, Y., Du, S., Yi, H., Xu, D., Cao, N., et al. (2019). Rapid and sensitive detection of goose parvovirus and duck-origin novel goose parvovirus by recombinase polymerase amplification combined with a vertical flow visualization strip. *J. Virol. Methods* 266, 34–40. doi: 10.1016/j.jviromet.2019.01.010

Luo, Q., Chen, B., Xu, J., Ma, W., Lao, C., Li, Y., et al. (2018). Development of a SYBR green II real-time polymerase chain reaction for the clinical detection of the duck-origin goose parvovirus in China. *Intervirology.* 61, 230–236. doi: 10.1159/000495181

Ma, H., Gao, X., Fu, J., Xue, H., Song, Y., and Zhu, K. (2022). Development and evaluation of NanoPCR for the detection of goose parvovirus. *Vet. Sci.* 9, 460. doi: 10.3390/vetsci9090460

Pang, B., Xu, J., Liu, Y., Peng, H., Feng, W., Cao, Y., et al. (2020). Isothermal amplification and ambient visualization in a single tube for the detection of SARS-CoV-2 using loop-mediated amplification and CRISPR technology. *Anal. Chem.* 92, 16204–16212. doi: 10.1021/acs.analchem.0c04047

Poonia, B., Dunn, P. A., Lu, H., Jarosinski, K. W., and Schat, K. A. (2006). Isolation and molecular characterization of a new Muscovy duck parvovirus from Muscovy ducks in the USA. *Avian Pathol.* 35, 434–435. doi: 10.1080/03079450601009563

Takehara, K., Nakata, T., Takizawa, K., Limn, C. K., Mutoh, K., and Nakamura, M. (1999). Expression of goose parvovirus VP1 capsid protein by a baculovirus expression system and establishment of fluorescent antibody test to diagnose goose parvovirus infection. *Arch. Virol.* 144, 1639–1645. doi: 10.1007/s007050050617

Wang, S., Cheng, X. X., Chen, S. Y., Lin, F. Q., Chen, S. L., Zhu, X. L., et al. (2015). Evidence for natural recombination in the capsid gene VP2 of Taiwanese goose parvovirus. *Arch. Virol.* 160, 2111–2115. doi: 10.1007/s00705-015-2491-2

Wang, S., Cheng, X., Chen, S., Xiao, S., Chen, S., Lin, F., et al. (2016). Identification of a novel goose parvovirus (GPV) recombinant associated with short beak and dwarfism syndrome in mainland Chin. *Infect. Genet. Evol.* 41, 289–291. doi: 10.1016/j.meegid.2016.04.013

Wang, S., Cheng, X., Chen, S., Zhu, X., Chen, S., Lin, F., et al. (2013). Genetic characterization of a potentially novel goose parvovirus circulating in Muscovy duck flocks in Fujian province, China. *J. Vet. Med. Sci.* 75, 1127–1130. doi: 10.1292/jvms.12-0527

Wang, J., Mi, Q., Wang, Z., Jia, J., Li, Y., and Zhu, G. (2020). Sole recombinant Muscovy duck parvovirus infection in Muscovy ducklings can form characteristic intestinal embolism. *Vet. Microbiol.* 242, 108590. doi: 10.1016/j.vetmic.2020.108590

Wang, R., Qian, C., Pang, Y., Li, M., Yang, Y., Ma, H., et al. (2021). OpvCRISPR: one-pot visual RT-LAMP-CRISPR platform for SARS-cov-2 detection. *Biosens Bioelectron.* 172, 112766. doi: 10.1016/j.bios.2020.112766

Wang, J., Wang, Z., Jia, J., Ling, J., Mi, Q., and Zhu, G. (2019). Retrospective investigation and molecular characteristics of the recombinant Muscovy duck parvovirus circulating in Muscovy duck flocks in China. *Avian Pathol.* 48, 343–351. doi: 10.1080/03079457.2019.1605145

Wei, J., Li, Y., Cao, Y., Liu, Q., Yang, K., Song, X., et al. (2022). Rapid and visual detection of porcine parvovirus using an ERA-CRISPR/Cas12a system combined with lateral flow dipstick assay. *Front. Cell. Infect. Microbiol.* 12. doi: 10.3389/fcimb.2022.879887

Woolcock, P. R., Jestin, V., Shivaprasad, H. L., Zwingelstein, F., Arnauld, C., McFarland, M. D., et al. (2000). Evidence of Muscovy duck parvovirus in Muscovy ducklings in California. *Vet. Rec.* 146, 68–72. doi: 10.1136/vr.146.3.68

Wozniakowski, G., Kozdrun, W., and Samorek-Salamonowicz, E. (2010). Detection and differentiation of waterfowl parvoviruses by PCR. *Bull. Veterinary Institute Pulawy.* 54, 283–288.

Wu, C., Chen, Z., Li, C., Hao, Y., Tang, Y., Yuan, Y., et al. (2022). CRISPR-Cas12a-empowered electrochemical biosensor for rapid and ultrasensitive detection of SARS-CoV-2 delta variant. *Nano-Micro Lett.* 14, 159. doi: 10.1007/s40820-022-00888-4

Xiao, S., Chen, S., Cheng, X., Lin, F., Wang, S., Zhu, X., et al. (2017). The newly emerging duck-origin goose parvovirus in China exhibits a wide range of pathogenicity to main domesticated waterfowl. *Vet. Microbiol.* 203, 252–256. doi: 10.1016/j.vetmic.2017.03.012

Yang, J., Chen, H., Wang, Z., Yu, X., Niu, X., Tang, Y., et al. (2017). Development of a quantitative loop-mediated isothermal amplification assay for the rapid detection of novel goose parvovirus. *Front. Microbiol.* 8. doi: 10.3389/fmicb.2017.02472

Yang, L., Chen, G., Wu, J., Wei, W., Peng, C., Ding, L., et al. (2024). A PAM-free one-step asymmetric RPA and CRISPR/Cas12b combined assay (OAR-CRISPR) for rapid and ultrasensitive DNA detection. *Anal. Chem.* 96, 5471–5477. doi: 10.1021/acs.analchem.3c05545

Yang, B., Shi, Z., Ma, Y., Wang, L., Cao, L., Luo, J., et al. (2022). LAMP assay coupled with CRISPR/Cas12a system for portable detection of African swine fever virus. *Transbound Emerg. Dis.* 69, E216–E223. doi: 10.1111/tbed.14285

Zádori, Z., Stefancsik, R., Rauch, T., and Kisary, J. (1995). Analysis of the complete nucleotide sequences of goose and Muscovy duck pervoviruses indicates common ancestral origin with adeno-associated virus 2. *Virology.* 212, 562–573. doi: 10.1006/viro.1995.1514

Zhang, S., Yang, J., Wang, Z., Chen, L., Diao, Y., and Tang, Y. (2020). Research note: development of an ELISA to distinguish between goose parvovirus infection and vaccine immunization antibodies. *Poult Sci.* 99, 1332–1340. doi: 10.1016/j.psj.2019.12.012

frontiers | Frontiers in Cellular and Infection Microbiology

TYPE Original Research
PUBLISHED 23 June 2025
DOI 10.3389/fcimb.2025.1521641

OPEN ACCESS

EDITED BY
Diana Manolescu,
Victor Babes University of Medicine and Pharmacy, Romania

REVIEWED BY
Hongsheng Wang,
Chinese Academy of Medical Sciences and Peking Union Medical College, China
Brahmchetna Bedi,
Emory University, United States

*CORRESPONDENCE
Xianzhi Xiong
xxz0508@hust.edu.cn
Jianchu Zhang
zsn0928@163.com

†These authors have contributed equally to this work and share first authorship

‡These authors have contributed equally to this work and share last authorship

RECEIVED 02 November 2024
ACCEPTED 02 June 2025
PUBLISHED 23 June 2025

CITATION
Zhou M, Sun S, Chen L, Xu H, Liu L, Lv J, Zhang J and Xiong X (2025) The impact of bronchoalveolar lavage fluid metagenomics next-generation sequencing on the diagnosis and management of patients with suspected pulmonary infection.
Front. Cell. Infect. Microbiol. 15:1521641.
doi: 10.3389/fcimb.2025.1521641

The impact of bronchoalveolar lavage fluid metagenomics next-generation sequencing on the diagnosis and management of patients with suspected pulmonary infection

Mei Zhou[1†], Shengwen Sun[2†], Long Chen[1], Huan Xu[3], Lanlan Liu[1], Jiaxi Lv[1], Jianchu Zhang[1*‡] and Xianzhi Xiong[1*‡]

[1]Department of Respiratory and Critical Care Medicine, NHC Key Laboratory of Pulmonary Diseases, Union Hospital, Tongji Medical College, Huazhong University of Science and Technology, Wuhan, Hubei, China, [2]Department of Critical Care Medicine, Union Hospital, Tongji Medical College, Huazhong University of Science and Technology, Wuhan, Hubei, China, [3]Department of Scientific Affairs, Vision Medicals for Infectious Diseases, Guangzhou, Guangdong, China

Objectives: This study aimed to enhance the comprehension of the practical utility of bronchoalveolar lavage fluid (BALF) metagenomic next-generation sequencing (mNGS) in the clinical management of patients with suspected pneumonia.

Methods: We retrospectively analyzed 296 individuals who underwent BALF mNGS and conventional microbial tests (CMTs) for suspected pneumonia. We compared the clinical characteristics between patients with pulmonary infection (PI) and those without pulmonary infection (NPI). The detection rate of mNGS and CMTs in different groups of patients were compared. The Sankey diagram was used to present the results of the influence of mNGS on diagnosis and treatment.

Results: Comparison between PI and NPI showed that individuals with fever, concurrent malignant tumors, consolidation or ground-glass opacity on chest CT(Computed tomography) images, and elevated inflammatory markers on blood tests were more likely to develop lung infections. Analysis of the rate of positive detection between CMTs and mNGS in various subgroups revealed that mNGS had a significantly higher positive detection rate in patients with pulmonary infections (87.95% vs. 71.06%, $p<0.001$), in immunocompetent patients (86.91% vs. 68.08%, $p<0.001$), and in patients with malignant tumors (92.31% vs. 69.23%, $p=0.035$). Furthermore, mNGS helped initiate appropriate antibiotic treatment and confirmed the effectiveness of empirical treatment. Compared to immunocompetent patients, BALF mNGS in immunocompromised individuals with suspected lung infections yielded higher rates of accurate diagnosis (62.86% vs. 42.79%, $p = 0.027$) and more effective treatment (71.43% vs. 58.56%, $p = 0.148$).

Conclusions: BALF mNGS identified a greater variety of pathogens than CMTs. Immunocompromised patients with suspected pneumonia may benefit more from BALF mNGS.

KEYWORDS

BALF, mNGS, pulmonary infection, diagnosis, management

Introduction

Infectious disease remains to be a global health concern. Despite significant improvements in microbiological testing techniques and medical treatment, the mortality rate remains high (Bloom and Cadarette, 2019). Rapid and accurate etiological diagnosis of pulmonary infection is the fundamental way to control infection, reduce mortality, and prevent the development of drug-resistant bacteria. At present, the primary approach for identifying the etiological pathogens of pulmonary infectious disease is microbial culture. Although it is effective in addressing certain clinical issues, conventional microbiological tests still suffer from some limitations, such as low positive rate, insufficient reliability, and long turnaround time (Li et al., 2019; Sin et al., 2014). In recent years, several rapid diagnostic techniques for identifying the causes of infectious diseases have been applied in healthcare settings. These approaches include antigen/antibody assays and polymerase chain reaction-based nucleic acid detection of specific pathogens (Subramony et al., 2016). However, these tests are typically restricted to healthcare professionals who anticipate potential disease-causing agents, and their outcomes are frequently influenced by thresholds (Dimech, 2021).

Metagenomic next-generation sequencing (mNGS) based on high-throughput sequencing technology has emerged as a solution. Initially, because of its high price and complex operating procedures, mNGS was only used in some scientific research fields (Chiu, 2013; Lloyd-Price et al., 2016). With the display of its superior performance and the reduction of detection cost (van Nimwegen et al., 2016), next-generation sequencing has quickly entered clinical practice, and its application in tumor diagnosis and individualized therapy (Coombs et al., 2018; Tsoulos et al., 2017) and prenatal diagnosis (Xu and Shi, 2014) have been reported. The first application of mNGS in the diagnosis of infectious diseases was reported in the New England Journal in 2014, in which mNGS was used to diagnose an infectious 14-year-old patient with severe combined immunodeficiency syndrome (Wilson et al., 2014). Since then, an increasing number of case reports and clinical studies have pointed out the value of mNGS in the diagnosis of infectious diseases, and research is no longer limited to central nervous system infections (Guan et al., 2016; Yao et al., 2016). Studies on the osteoarticular system (Ruppe et al., 2017), the respiratory system (Leo et al., 2017; Ruppe et al., 2016), and other systems have also been reported.

As a new detection method, mNGS has obvious advantages compared with traditional pathogenic detection methods: (1) It can detect all pathogenic microorganisms simultaneously and quickly; (2) It can quickly detect pathogens that are time-consuming or difficult in traditional pathogenic culture, such as Mycobacterium tuberculosis; (3) Diagnosis of rare and emerging pathogens. At present, there are several challenges in the clinical application of mNGS for diagnosing infectious diseases, such as the absence of standardized protocols, the complexity of interpreting test results, and relatively high expenses (Han et al., 2019). Moreover, it should be noted that the respiratory system is not a sterile environment, which adds complexity to the interpretation of the data. Numerous clinical studies have been published on the utility of mNGS in diagnosing pulmonary infections. However, most of these studies had small sample sizes and were limited to specific populations or pathogens (Lin et al., 2023; Shen et al., 2023; Sun et al., 2022; Wang et al., 2023). BALF mNGS has been used in our department for many years to assist in the diagnosis of pathogens of pulmonary infection. In actual clinical work, we have observed that BALF mNGS has indeed provided great help for the diagnosis and treatment of most patients, but we are not clear about which patients are more suitable for this examination or benefit more. There is a scarcity of studies on the direct impact of BALF mNGS on the diagnosis and treatment of patients with suspected pulmonary infections, including both mild and severe cases. This study was conducted to gain a deeper understanding of the practical application of mNGS in clinical practice.

Methods

Study design and patient population

This retrospective study recruited 317 patients from the Department of Respiratory and Critical Care Medicine, between May 2020 and August 2021. This study was conducted in accordance with the principles of the Declaration of Helsinki and approved by the Ethics Committee of Tongji Medical College of Huazhong University of Science and Technology (Grant No. IORG0003571). Given the retrospective nature of the study and the use of anonymized data, the need for written informed consent was waived by the Ethics Committee. All patient information was de-identified prior to analysis to protect patient confidentiality. The

inclusion criteria were (1) age≥14 years, (2) suspected pneumonia, and (3) mNGS results. The exclusion criteria were as follows: (1) sample failure to pass the quality control of mNGS, or (2) incomplete clinical data. Based on our inclusion and exclusion criteria, 296 participants were included in the study, while 21 were excluded due to incomplete clinical data caused by random errors in retrieving hospitalization information, such as untraceable or incorrect hospitalization numbers in mNGS reports. No systematic bias related to clinical characteristics (e.g., disease severity or follow-up status) was identified in these exclusions.

In this study, suspected cases of pneumonia met both criteria: (1) new-onset symptoms, such as fever, cough, expectoration, or dyspnea, and (2) new-onset abnormal chest imagine features (Lin et al., 2022). Pulmonary infection was diagnosed using a comprehensive reference standard that included all microbiological tests and clinical adjudication. The reference was based on the diagnostic criteria for community-acquired pneumonia (CAP) (Metlay et al., 2019) and hospital-acquired pneumonia (HAP) (Kalil et al., 2016).

We retrospectively analyzed 296 individuals who underwent BALF mNGS and conventional microbial tests (CMTs) for suspected pneumonia. We compared the clinical characteristics between patients with pulmonary infection (PI) and those without pulmonary infection (NPI). Then the detection rate of mNGS and CMTs in different groups of patients were compared (Figure 1). In this part, patients were considered immunocompromised if they met any of the following criteria (Ramirez et al., 2020): (1) primary immune deficiency diseases; (2) active malignancy or malignancy within 1 year of CAP, excluding localized skin cancers or early-stage cancers; (3) receiving cancer chemotherapy; (4) HIV infection with a CD4 T-lymphocyte count < 200 cells/μL or a percentage < 14%; (5) solid organ transplantation; (6) hematopoietic stem cell transplantation; (7) receiving corticosteroid therapy with a dose ≥20 mg prednisone or equivalent daily for ≥14 days, or a cumulative dose >600 mg of prednisone; (8) receiving biological immune modulators; (9) receiving disease-modifying antirheumatic drugs or other immunosuppressive drugs. The clinical impact of mNGS was assessed according to the Supplementary Table 1 and Supplementary Table 2 (Xu C. et al., 2023).

Taking clinical composite diagnosis as the reference standard, we use manual case-by-case analysis to analyze the influence of mNGS on diagnosis and treatment. The Sankey diagram was used to present the results of data classification and statistics.

Conventional microbiological tests

In this study, clinicians make preliminary judgments and make necessary CMTs according to the condition and clinical manifestations. Clinical specimens, such as sputum, BALF, blood, pleural effusion, tissue, and bone marrow, were collected. The sputum, BALF, and blood can be used for smear examinations, such as acid-fasting staining (*Mycobacterium. Spp*). An indirect fluorescence immunoassay was used to detect five pathogenic IgM antibodies in the blood, including adenovirus (ADV), Respiratory Syncytial Virus (RSV), *Chlamydia pneumonia* (CP), *Mycoplasma pneumonia* (MP), and Coxsackievirus B5. The blood T-SPOT test, BLAF X-pert test, and acid-fasting staining were performed to detect *Mycobacterium tuberculosis* (MTB). Blood 1, 3-β-D glucan assay (BGD) was performed to detect fungal infection, and blood and BALF galactomannan were used to detect *Aspergillus.* spp infection.

mNGS of BALF

Specimens such as bronchoalveolar lavage fluid (BALF) must first undergo wall breaking. One gram of glass beads (a diameter of 0.5 mm was added to the wall-breaking tube, followed by 0.6 ml specimen, which was oscillated at a high speed of 2800–3200 rpm for 30 min. and then 300μl was taken for nucleic acid extraction according to the instructions of the Tiangen trace sample genome extraction kit (DP316). 500ng of extracted DNA was taken, and procedures such as interruption, terminal repair, joint addition, amplification, database construction, and sequencing were performed according to standard procedures and sequenced on an Illumina NextSeq 550 sequencer using a 75-cycle single-end sequencing strategy (Huang et al., 2024). The sequence number of the respiratory tract specimens must be greater than 5M. At the same time, internal reference, negative and positive controls were set. The resulting data were stripped of sequences of low quality and too short in length (less than 35bp) to obtain high-quality sequences, which were then compared with the human reference genome (H19) using Burrows-Wheeler Alignment software. After removing human sequences, the sequences were compared with four databases of bacteria, fungi, viruses, and parasites respectively to obtain a sequence number that could match a certain pathogen. Possible pathogens were determined according to the sequence number and other clinical tests.

Interpretation of mNGS results

Given the lack of a standard method for interpreting mNGS results and the variety of reporting parameters among different sequencing platforms, we used the following criteria, which were derived and revised from prior literature on mNGS, to define clinically significant microbes (CSMs) (Miao et al., 2018; Xu et al., 2023). The threshold of sequenced reads in mNGS data analysis distinguishes true pathogens from background noise by enhancing specificity, reducing false positives caused by contamination or low-abundance commensals (Jia et al., 2021; Carbo et al., 2022; Du et al., 2022). Clinically, it ensures reliable pathogen identification, guiding targeted therapy while minimizing overdiagnosis.

1. Parasites: the reads number was ≥100 because of their large molecular weight and many broken fragments (Qin et al., 2021).

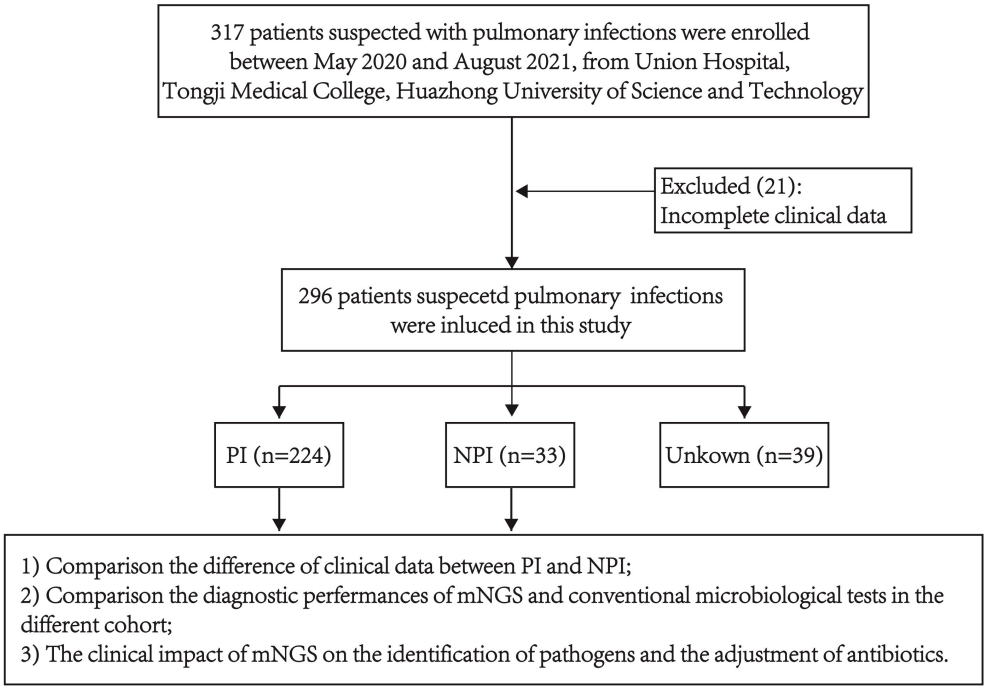

FIGURE 1
The flowchart of the patients.

2. Other pathogens: the reads number was ≥3 (Miao et al., 2018; Xu et al., 2023).
3. For strictly pathogenic microorganisms such as *Mycobacterium tuberculosis* (MTB), Nocardia, Mycoplasma, and Aspergillus, the read number was ≥1 (Xu et al., 2023).
4. Intracellular bacteria such as *M. tuberculosis*, Legionella, and brucellosis: the read number was ≥1 because of their relatively low release into body fluids, leading to low detection sensitivity (Xu et al., 2023).
5. Some pathogenic microorganisms with thicker cell walls, such as fungi, the read number was ≥1 because nucleic acid extraction efficiency is low, resulting in a low clinical detection rate and sensitivity (Qin et al., 2021).

Clinical composite diagnosis as the reference standard

The clinical composite diagnosis was determined by integrating clinical manifestations, laboratory tests, chest radiology, microbiological results (CMTs and mNGS), and treatment response, guided by the diagnostic criteria of CAP (Metlay et al., 2019) and HAP (Kalil et al., 2016). Two pulmonary infection specialists independently reviewed records of 296 patients (after excluding 21 with incomplete data from 317 enrolled). Etiology and pathogens were assessed, with disagreements resolved through discussion or consultation with a senior infectious disease expert. This yielded 224 pulmonary infections, 33 non-pulmonary infections, and 39 unexplained cases (Figure 1). Discordant mNGS and CMT results were reviewed by the expert panel to ensure clinical relevance, forming the reference standard for comparing pathogen detection rates.

Statistical analysis

SPSS (version 26.0) was used to analyze the data. Continuous variables following a normal distribution were described as mean ± standard deviation, and the dependent t-test was used to compare between the groups. Continuous variables that did not follow a normal distribution were described as median (Q1, Q3), and the Wilcoxon rank test was used to compare between the groups. Categorical variables are described as n (%), and the chi-square test or Fisher's exact test was used for categorical variables, as appropriate. Statistical significance was set at 5% ($p < 0.05$). GraphPad Prism (version 9.3) and Origin (version 9.9) were used to generate the graphs.

Results

Clinical characteristics

We compared and analyzed the sex, age, length of hospitalization, clinical manifestations, immune status, and comorbidities of the patients in the pulmonary infection group (PI) and the non-pulmonary infection group (NPI); the proportion of patients with fever (32.1% vs. 3%, p=0.001) was significantly

TABLE 1 Clinical characteristics of the patients.

Clinical characteristics	Total (257)	PI(224)	NPI(33)	P value
Sex(male)	**167 (65%)**	150 (67%)	17 (51.5%)	0.082
Age	55.49 ± 13.88	55.25 ± 14.26	57.15 ± 10.97	0.463
LOH(days)	12.72 ± 6.96	12.95 ± 7.2	11.18 ± 4.78	0.173
Clinical manifestation				
Fever	73 (28.4%)	72 (32.1%)	1 (3%)	**0.001**
Cough	178 (69.3%)	154 (68.8%)	24 (72.7%)	0.644
Expectoration	134 (52.1%)	116 (51.8%)	18 (54.4%)	0.767
Dyspnea	96 (37.4%)	80 (35.7%)	16 (48.5%)	0.157
Chest pain	53 (20.6%)	49 (21.9%)	4 (12.1%)	0.196
Chest distress	61 (23.7%)	53 (23.7%)	8 (24.2%)	0.942
Hemoptysis	37 (14%)	33 (14.7%)	3 (9.1%)	0.59
Immune deficiency	**35 (13.6%)**	33 (14.7%)	2 (6.1%)	0.275
Complication				
Hypertension	50 (19.5%)	43 (19.2%)	7(21.2%)	0.814
Cardiovascular disease	23 (8.9%)	20(8.9%)	3(9.1%)	1
Diabetes	36 (14%)	31(13.8%)	5(15.2%)	0.839
Malignant tumor	26 (10.1%)	26(11.6%)	0	**0.032**
Chronic pulmonary disease	69 (26.8%)	64 (28.4%)	5(15.2%)	0.104
Chronic renal disease	8 (3.1%)	8(3.6%)	0	0.601
Cerebrovascular disease	30 (11.7%)	27 (12.1%)	3 (9.1%)	0.777
Digestive diseases	8 (3.1%)	6 (2.7%)	2 (6.1%)	0.274

LOH, length of hospitalization.
The bold values indicate that the P-value is less than 0.05.

higher in the PI group, and the proportion of patients with tumors (11.6% vs. 0, p=0.032) was significantly higher in the PI group (Table 1).

We also compared and analyzed the characteristics of pulmonary CT images and bronchoscopy and found that the proportional of bilateral lesions (63.4% vs. 81.8%, p=0.037), ground-glass opacity (21% vs. 45.5%, p=0.002), and interstitial lesions (17% VS 60.6%, p<0.001) was higher in the NPI group, whereas consolidation (29% vs. 9.1%, p=0.15) was higher in the PI group (Table 2). The bronchoscopy characteristics included normal, mucosal hyperemia, purulent and serous secretions, bronchial stenosis, and neoplasm, with no statistical difference between the two groups.

In the blood routine, compared to the NPI group, the PI group exhibited significantly lower levels of hemoglobin (Hb, 118.85 g/L vs. 129.64 g/L, p=0.006), red blood cell (RBC, 4.01 10^12/L vs 4.35 10^12/L, p=0.005), and hematocrit (Hct, 35.66 vs. 29.19, p=0.002); and higher levels of inflammatory markers, including C-reactive protein (CRP, 19.35 mg/L vs. 3.13 mg/L, p<0.001), erythrocyte sedimentation rate (ESR, 33 mm/60 min vs. 9.5 mm/60 min, p=0.004), ferritin (239.2 ng/mL vs. 134.5 ng/mL, p=0.009), and serum amyloid A (SAA, 31.9 mg/L vs. 4.1 mg/L, p=0.003). In the biochemical test, the PI group showed a significant increase in γ-glutamyl transpeptidase (γGT, 28 U/L vs. 21 U/L, p=0.013) and a decrease in serum albumin (ALB, 36.6 g/L vs. 39.5 g/L, p=0.01). Regarding coagulation function, the PI had significantly elevated fibrinogen levels (FIB, 4.76 g/L vs. 3.6 g/L, p<0.001) (Table 3).

Pathogen profiles

Using the final clinical diagnosis as the reference standard, mNGS achieved a sensitivity of 87.95% (95% CI: 86.83%–94.46%) and a specificity of 39.39% (95% CI: 22.91%–57.86%), while CMT demonstrated a sensitivity of 69.64% (95% CI: 63.17%–75.59%) and a specificity of 63.64% (95% CI: 45.12%–79.60%) (Table 4). Concordance analysis of CMT and mNGS results showed that 148 patients (57.59%) were double-positive, 20 (7.78%) were double-negative, 69 (26.85%) were positive for mNGS but negative for CMT, and 20 (7.78%) were positive for CMT but negative for mNGS (Figure 2A). Among 148 double-positive patients, 23 (15.54%) were completely matched between mNGS and CMT, 57 (38.51%) were partially matched, and 68 (45.94%) were mismatched.

10.3389/fcimb.2025.1521641

TABLE 2 Radiographic findings of the patients.

Radiographic finding and bronchoscopy	Total (257)	PI (224)	NPI (33)	P value
Radiographic finding				
Bilateral lesions	169 (65.8%)	142 (63.4%)	27 (81.8%)	**0.037**
Consolidation	68 (26.5%)	65 (29%)	3 (9.1%)	**0.015**
GGO	62 (24.1%)	47 (21%)	15 (45.5%)	**0.002**
Pleural effusion	50 (19.5%)	45 (20.1%)	5 (15.2%)	0.504
Patchy shadow	78 (30.4%)	69 (30.8%)	9 (27.3%)	0.68
Nodule	129 (50.2%)	114 (50.9%)	15 (45.5%)	0.56
Emptiness	28 (10.9%)	26 (11.6%)	2 (6.1%)	0.549
Interstitial lesion	58 (22.6%)	38 (17%)	20 (60.6%)	**0**
Bronchiectasis	49 (19.1%)	45 (20.1%)	4 (12.1%)	0.277
Mass shadow	35 (13.6%)	33 (14.7%)	2 (6.1%)	0.275
Bronchoscopy				
Normal	33 (12.8%)	30 (13.4%)	3(9.1%)	0.78
Mucosal hyperemia	132 (51.4%)	112 (50%)	20 (60.6%)	0.255
Secretion				0.076
Purulent secretion	40 (15.6%)	39 (17.4%)	1 (3%)	
Serous secretion	31 (12.1%)	27 (12.1%)	4 (12.1%)	
Bronchial stenosis	22 (8.6%)	21 (9.4%)	1 (3%)	0.224
Neoplasm	4 (1.6%)	3(1.3%)	1 (3%)	0.425

GGO, ground glass nodules.
The bold values indicate that the P-value is less than 0.05.

As shown in Figures 2C~E, we counted the number of pathogens detected by CMT and mNGS and showed the number of detected fungi, bacteria, viruses, and atypical pathogens in the form of bar charts, respectively. The most frequently identified pathogens were *Mycobacterium tuberculosis*, *Aspergillus* spp., *Pneumocystis jiroveci*, *Candida albicans*, *Pseudomonas aeruginosa*, *Klebsiella pneumonia*, and *Acinetobacter baumannii*. Multiple species, including *Nocardia* spp., *Streptococcus constellatus*, *Enterococcus faecalis*, *Streptococcus pneumoniae*, *Haemophilus influenzae*, non-tuberculous Mycobacterium tuberculosis, *Chlamydia psittaci*, *Legionella pneumophila*, were detected solely by mNGS.

Comparison of positive rates among different groups

We categorized patients with pulmonary infection (PI groups) (Figure 3A) into various subgroups based on their immune status and comorbidities. The subgroups included immunocompromised patients (Figure 3B), immunocompetent patients (Figure 3C), patients with hypertension (Figure 3D), patients with diabetes (Figure 3E), patients with malignant tumors (Figure 3F), patients diagnosed with pulmonary tuberculosis (Figure 3G), and patients diagnosed with pulmonary aspergillosis (Figure 3H). We also compared the detection positive rates between CMT and mNGS in various subgroups, which showed that the overall positive rate of mNGS was significantly higher in patients with pulmonary infections (87.95% vs. 71.06%, $p<0.001$). The positive rate of mNGS was significantly higher in immunocompetent patients (86.91% vs. 68.08%, $p<0.001$) and malignant tumors (92.31% vs. 69.23%, $p=0.035$). The detection rate was not significantly different between CMT and mNGS in immunocompromised patients (93.94% vs. 78.79%, $p=0.066$), in patients with hypertension (90.70% vs. 76.74%, $p=0.08$), in patients with diabetes (83.87% vs. 77.42%, $p=0.52$), pulmonary tuberculosis (93.24% vs. 89.19%, $p=0.384$), or pulmonary aspergillosis (92.31% vs. 82.05%, $p=0.176$).

The impact of mNGS on the diagnosis and treatment

The pathogens reported by the mNGS results may not always be the causative agents. Therefore, the positive rate of mNGS cannot be used as an objective measure to assess its impact on the diagnosis and treatment of patients with suspected lung infections. To further explore the impact of mNGS results on diagnosis and treatment in actual clinical practice, we carefully categorized the various possible impacts; the detailed classifications are listed in Supplementary Table 1 and Supplementary Table 2. For pathogen diagnosis, mNGS has three clinical impacts: positive impact, non-impact, and negative impact. The positive impact can be categorized into three categories: D1, mNGS result was quicker than CMT; D2, co-infection was diagnosed based on mNGS; and D3, mNGS result contributed to pathogen identification. The non-impact also had three categories: D4, mNGS results were negative; D5, mNGS detected the same pathogens as CMT and did not detect them earlier than CMT; and D6, the microbes detected by mNGS were assessed as unlikely pathogens. The negative impact had only one category: D7, Lung infection pathogens were undetected by mNGS and without suspected pathogen detection. Regarding pathogen treatment, mNGS had only two clinical impacts: positive impact and non-impact. The positive impact was divided into four categories: T1, initiation of appropriate antibiotic treatment; T2, guidance of antimicrobial escalation; T3, guidance of antimicrobial de-escalation; and T4, confirmation of empiric treatment. The non-impact had two categories: T5, mNGS results were positive but treatment was not adjusted; T6, mNGS results was negative but treatment was not adjusted.

10.3389/fcimb.2025.1521641

TABLE 3 Laboratory findings of the patients.

Laboratory findings	Total (257)	PI(224)	NPI(33)	P value
WBC(G/L)	6.37 (4.97, 8.49)	6.5 (5.02, 8.69)	6.04 (4.85, 7.17)	0.105
RBC(T/L)	4.05 ± 0.69	4.01 ± 0.69	4.35 ± 0.55	**0.006**
Hb(g/L)	120.25 ± 20.5	118.85 ± 20.42	129.64 ± 18.8	**0.005**
Hct(%)	36.12 ± 6.12	35.66 ± 6.18	39.19 ± 4.67	**0.002**
PLT(G/L)	254.22 ± 102.21	257.75 ± 103.99	230.45 ± 87.07	0.153
Neutrophils(%)	67.92 ± 12.97	68.48 ± 13.16	64.16 ± 10.99	0.074
Lymphocyte(%)	21.38 ± 10.97	20.89 ± 11.06	24.63 ± 9.85	0.067
CRP(mg/L)	14.5 (3.14, 52.18)	19.35 (3.64, 59.8)	3.13 (3.11, 5.11)	**0**
PCT(ng/ml)	0.13 (0.13, 0.15)	0.13 (0.13, 0.15)	0.13 (0.13, 0.13)	0.36
ESR(mm/h)	27 (8, 63.5)	33 (10, 66)	9.5 (5.75, 31.75)	**0.004**
Fer(ug/L)	218.5 (93.4, 428.2)	239.2 (98.25, 442.4)	134.5 (54.7, 175.4)	**0.009**
SAA(mg/L)	16.35 (4.4, 194.15)	31.9 (4.9, 278.7)	4.1 (2.1, 17)	**0.003**
TB(umol/L)	10.96 ± 5.3	10.95 ± 5.49	11.04 ± 3.9	0.929
DB(umol/L)	3.81 ± 2.26	3.86 ± 2.35	3.46 ± 1.42	0.342
ALT(U/L)	26.72 ± 25.9	27.46 ± 27.1	21.82 ± 15.25	0.244
AST(U/L)	21 (17, 28)	21 (17, 28)	22 (17, 27.5)	0.944
ALP(U/L)	75 (63, 95.75)	75 (61, 98)	74 (68, 87.5)	0.849
γGT(U/L)	26 (15, 45)	28 (15, 49)	21 (14, 27)	**0.013**
TP(g/L)	63.52 ± 7.45	63.38 ± 7.64	64.41 ± 6.05	0.461
ALB(g/L)	37.2 (32.4, 40.78)	36.6 (31.8, 40.5)	39.5 (37.2, 41.8)	**0.01**
Cr(umol/L)	76.04 ± 83.42	77.22 ± 88.92	68.25 ± 25.53	0.566
BUN(mmol/L)	5.52 ± 3.9	5.58 ± 4.11	5.14 ± 1.94	0.543
UA(umol/L)	290.71 ± 101.55	287.37 ± 98.41	312.87 ± 119.75	0.179
Cystatin C(mg/L)	1.06 ± 1.03	1.09 ± 1.1	0.92 ± 0.24	0.488
BG(mmol/L)	5.41 ± 1.6	5.4 ± 1.52	5.46 ± 2.02	0.865
CK(U/L)	69.87 ± 78.17	67.46 ± 81.33	86.43 ± 49.62	0.278
LDH(U/L)	250.28 ± 129.86	250.46 ± 134.48	249 ± 92.55	0.96
D-dimer(mg/L)	0.68 (0.32, 1.86)	0.72 (0.32, 1.96)	0.42 (0.29, 0.92)	0.054
FIB(g/L)	4.51 (3.37, 6.09)	4.76 (3.48, 6.18)	3.6 (2.99, 4.23)	**0**
PT(s)	13.49 ± 1.05	13.54 ± 1.07	13.19 ± 0.77	0.09
APTT(s)	39.16 ± 5.04	39.37 ± 5.15	37.61 ± 3.85	0.072

WBC, white blood cell count; RBC, red blood cell count; Hb, hemoglobin; Hct, hematocrit; PLT, platelet count; CRP, C-reactive protein; PCT, procalcitonin; ESR, erythrocyte sedimentation rate; Fer, ferritin; SAA, serum amyloid A; TB, total bilirubin; DB, direct bilirubin; ALT, alanine aminotransferase; AST, aspartate aminotransferase; ALP, alkaline phosphatase; γGT, γ -glutamyl transpeptidase; TP, total protein; ALB, albumin; Cr, creatinine; BUN, blood urea nitrogen; UA, uric acid;BG, blood glucose; CK, creatine kinase; LDH, lactate dehydrogenase; FIB, fibrinogen; PT, prothrombin time; APTT, activated partial thromboplastin time.
The bold values indicate that the P-value is less than 0.05.

A total of 222 immunocompetent patients were suspected to have a pulmonary infection. The mNGS assay had a positive impact on the final diagnosis of the causative agent in 95 patients, representing 42.79% of immunocompetent patients. Among these patients, D1, D2, and D3 accounted for 4.5%, 13.06%, and 25.23%, respectively. The mNGS assay did not have an impact on the diagnosis in 115 patients, in which D4, D5, and D6 had proportions of 17.12%, 16.67%, and 18.02%, respectively. It had a negative impact on the diagnosis in 12 patients (D7, 5.41%) (Figure 4A). The mNGS assay had a positive impact on pathogen treatment in 130 (58.56%) immunocompetent patients but had no impact in 92 (41.44%) patients. Among patients with a positive impact, T1 accounted for the largest proportion (37.84%), whereas T5 had the highest proportion of patients with no impact (24.32%) (Figure 4C). In our

study, there were 35 immunocompromised patients, in which the mNGS assay had a positive impact, non-impact, and negative impact on the final diagnosis in 22 patients (62.86%), 9 patients (25.71%), and 4 patients (11.43%), respectively. The positive impact was mainly categorized as D2 (45.71%) and the non-impact as D6 (11.43%) (Figure 4B). The positive impact and non-impact of the mNGS assay on the treatment of immunocompromised patients were observed in 25 and 10 patients, respectively (Figure 4D).

To thoroughly compare the impact of mNGS results on diagnosis and treatment outcomes between immunocompromised and immunocompetent patients, we combined the categories of negative impact and non-impact to serve as the control group for positive impact. Chi-square tests were performed to evaluate differences. Compared to immunocompetent patients, mNGS in immunocompromised individuals with suspected lung infections demonstrated significantly higher rates of accurate diagnosis (62.86% vs. 42.79%, p = 0.027) and a trend toward more effective treatment outcomes (71.43% vs. 58.56%, p = 0.148), though the latter did not reach statistical significance.

Discussion

Our study revealed a significantly higher prevalence of fever (32.1% vs. 3%, p=0.001) among patients diagnosed with pulmonary infections than among those without pulmonary infections. Patients with malignant tumors (11.6% vs. 0, p=0.032) were more prone to developing pulmonary infections than those with hypertension, cardiovascular disease, and diabetes. However, in this study, the number of patients with pulmonary infections complicated by malignant tumors is relatively small (n=26). Therefore, this finding is considered as exploratory, and further validation with larger clinical samples is needed to confirm the correlation between pulmonary infections and tumors. The likelihood of infection is significantly elevated in the presence of fever and abnormal lung infiltration. A comparative analysis of pulmonary CT images between the PI and NPI groups showed that consolidation (29% vs. 9.1%, p=0.15) was more prevalent in patients with lung infections. In contrast, bilateral involvement (63.4% VS 81.8%, p<0.001), ground-glass opacity (21% vs. 45.5%, p=0.002), and interstitial lesions (17% VS 60.6%, p<0.001) were more common in non-pulmonary infections. The comparative analysis of blood routine, biochemical and other blood test results indicated that patients in the lung infection group exhibited lower levels of Hb (118.85 g/L vs. 129.64 g/L, p=0.006) and serum albumin (36.6 g/L vs. 39.5 g/L, p=0.01), as well as higher levels of inflammatory markers, including CRP (19.35 mg/L vs. 3.13 mg/L, p<0.001), ESR (33 mm/60 min vs. 9.5 mm/60 min, p=0.004), ferritin (239.2 ng/mL vs. 134.5 ng/mL, p=0.009), SAA (31.9 mg/L vs. 4.1 mg/L, p=0.003), and FIB (4.76 g/L vs. 3.6 g/L, p<0.001). These findings demonstrate that, in our clinical practice, patients who exhibited fever, had malignant tumors and abnormalities such as consolidation on CT images, and showed elevated inflammatory markers on blood tests were more likely to have lung infections. These findings are consistent with observations in clinical practice and have been documented in published studies (Akinosoglou et al., 2013; Aliberti et al., 2021; Musher and Thorner, 2014; Valvani et al., 2019). It may also have a certain guiding significance for selecting appropriate patients with suspected pulmonary infections to perform BALF mNGS in the future.

Several published studies have shown that the positive rate and sensitivity of mNGS are superior to those of CMT, especially in the diagnosis of mixed infections, critically ill patients, and immunocompromised individuals (Deng et al., 2022; Parize et al., 2017; Zhong et al., 2023). A prospective multicenter study demonstrated that untargeted next-generation sequencing detected significantly more clinically relevant viruses and bacteria than conventional methods (36% vs 11%, p<0.001) in immunocompromised adults, with high negative predictive value (64/65, 95% CI 0.95-1), highlighting its diagnostic potential (Parize et al., 2017). Deng et al. (2022) compared the diagnostic performance of bronchoalveolar lavage fluid (BALF) mNGS versus CMT in pediatric pneumonia. Their results showed that mNGS had significantly higher overall pathogen detection rates (91.3% vs. 59.2%, p<0.001), with superior sensitivity for bacterial and viral infections. However, mNGS exhibited lower sensitivity for *Mycoplasma pneumoniae* (42.1% vs. 100%) compared to CMT. Additionally, mNGS identified virus-bacteria co-infections as the most prevalent polymicrobial pattern. Zhong et al. (2023) found that mNGS showed significantly higher detection rates than conventional culture (93.3% vs. 29.3%, p<0.0001) in AIDS patients with pulmonary infections. mNGS also identified polymicrobial infections in 60% of these patients, further emphasizing its superior diagnostic value. Nevertheless, Peng et al. (2021) retrospectively analyzed 60 critically ill immunocompromised patients with suspected pneumonia and compared the diagnostic performance of BALF mNGS and CMTs. Their study found that the overall diagnostic accuracy was similar between mNGS and CMTs. While mNGS was better at identifying viral pneumonia, it was less accurate for fungal infections. The authors suggested that combining mNGS and CMTs may be the optimal diagnostic strategy.

TABLE 4 Comparison of diagnostic performance between mNGS and CMTs in patients with suspected pneumonia.

Methods	Results	Clinical diagnosis positive	Clinical diagnosis negative	Accuracy	Sensitivity	Specificity
mNGS	Positive	197	20	81.71% (76.43%–86.24%)	87.95% (86.83%–94.46%)	39.39% (22.91%–57.86%)
	Negative	27	13			
CMT	Positive	156	12	68.87% (62.82%–74.48%)	69.64% (63.17%–75.59%)	63.64% (45.12%–79.60%)
	Negative	68	21			

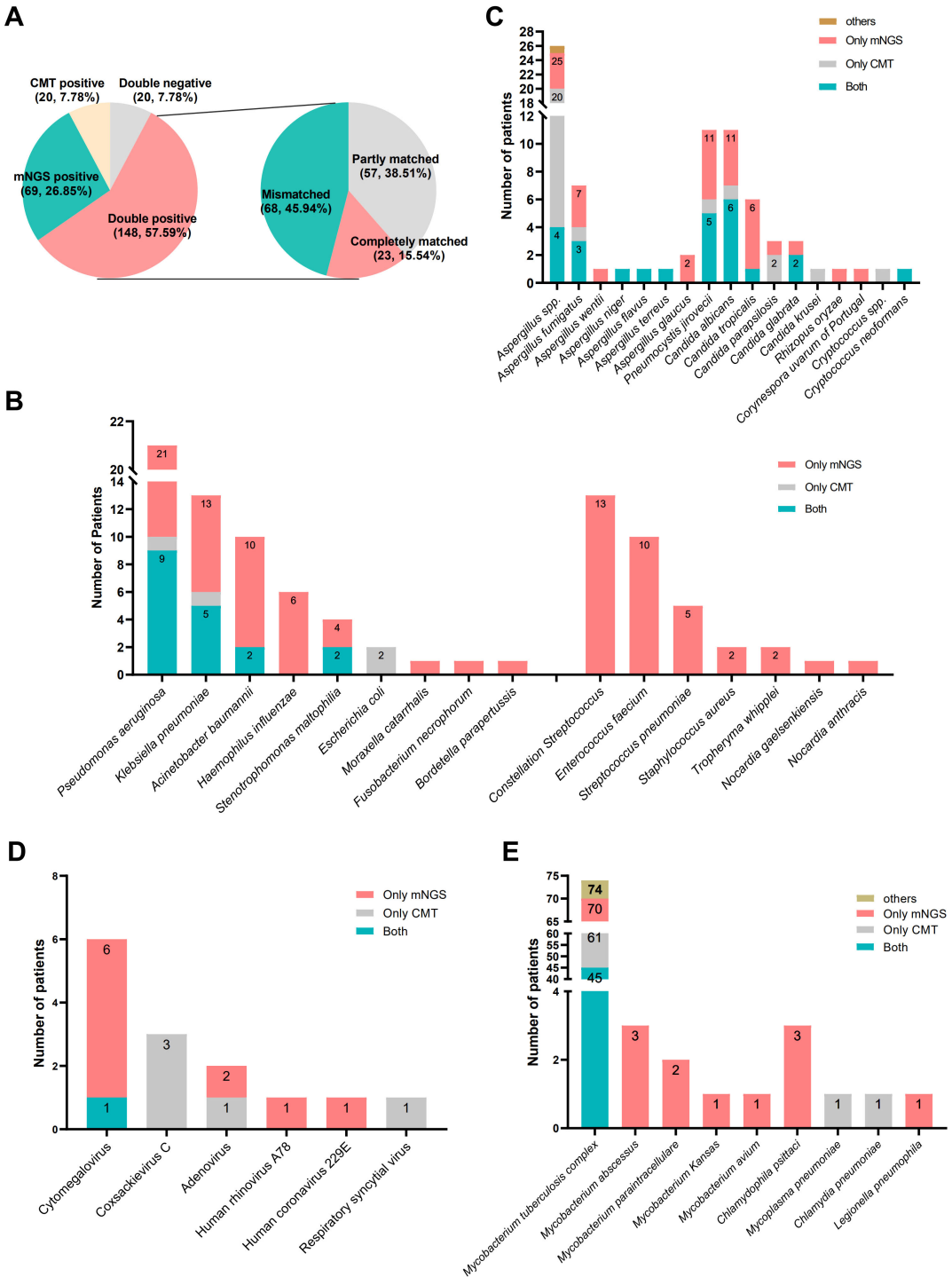

FIGURE 2
Pathogen profiles. **(A)** The concordance analysis of CMT and mNGS; **(B)** types and number of fungi detected by CMT and mNGS; **(C)** types and number of bacteria detected by CMT and mNGS; **(D)** types and number of virus detected by CMT and mNGS; **(E)** types and number of atypical pathogens detected by CMT and mNGS.

Collectively, the diagnostic effectiveness of mNGS varies depending on the specific types of pathogens, types of specimens being tested, and patient characteristics. Regardless of cost, the combination of mNGS and CMT remains the most effective diagnostic method (Qu et al., 2022).

For certain pathogens that lack rapid and effective diagnostic methods in some medical institutions, such as *C. psittaci*, *P. jirovecii*, NTM, *L. pneumophila*, mNGS detection methods also have unique benefits (Chen et al., 2023; Du et al., 2023; Huang et al., 2023; Tang et al., 2023), which is consistent with our findings

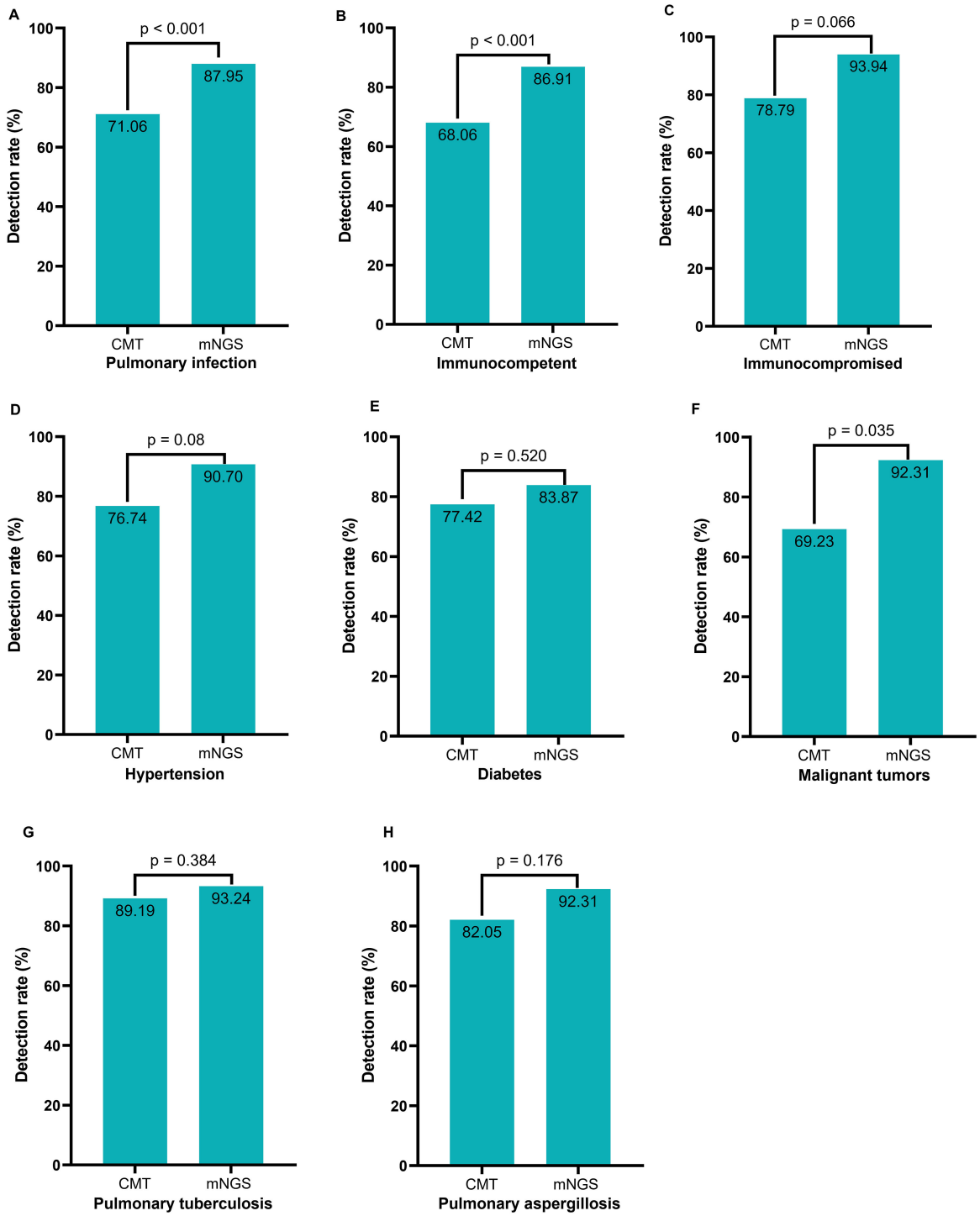

FIGURE 3
Comparison of positive rates among various subgroups between CMT and mNGS. **(A)** All pulmonary infection patients; **(B)** Pulmonary infection patients with normal immune function; **(C)** Pulmonary infection patients with compromised immune function; **(D)** Pulmonary infection patients with hypertension; **(E)** Pulmonary infection patients with diabetes; **(F)** Pulmonary infection patients with tumor; **(G)** Pulmonary tuberculosis patients; **(H)** Pulmonary aspergillosis patients.

(Figure 2). This study showed that mNGS can detect a wider range of pathogens compared to CMT. It was able to identify pathogens that typically require advanced culture conditions, such as *S. pneumoniae*, *H. influenzae*, *S. constellatus*, *Nocardia* spp.

Although both mNGS and CMT showed a high positive rate in patients with suspected lung infections, mNGS showed a significantly higher rate (Figure 3A). There was also a relatively high level of disagreement between the two methods (Figure 2A),

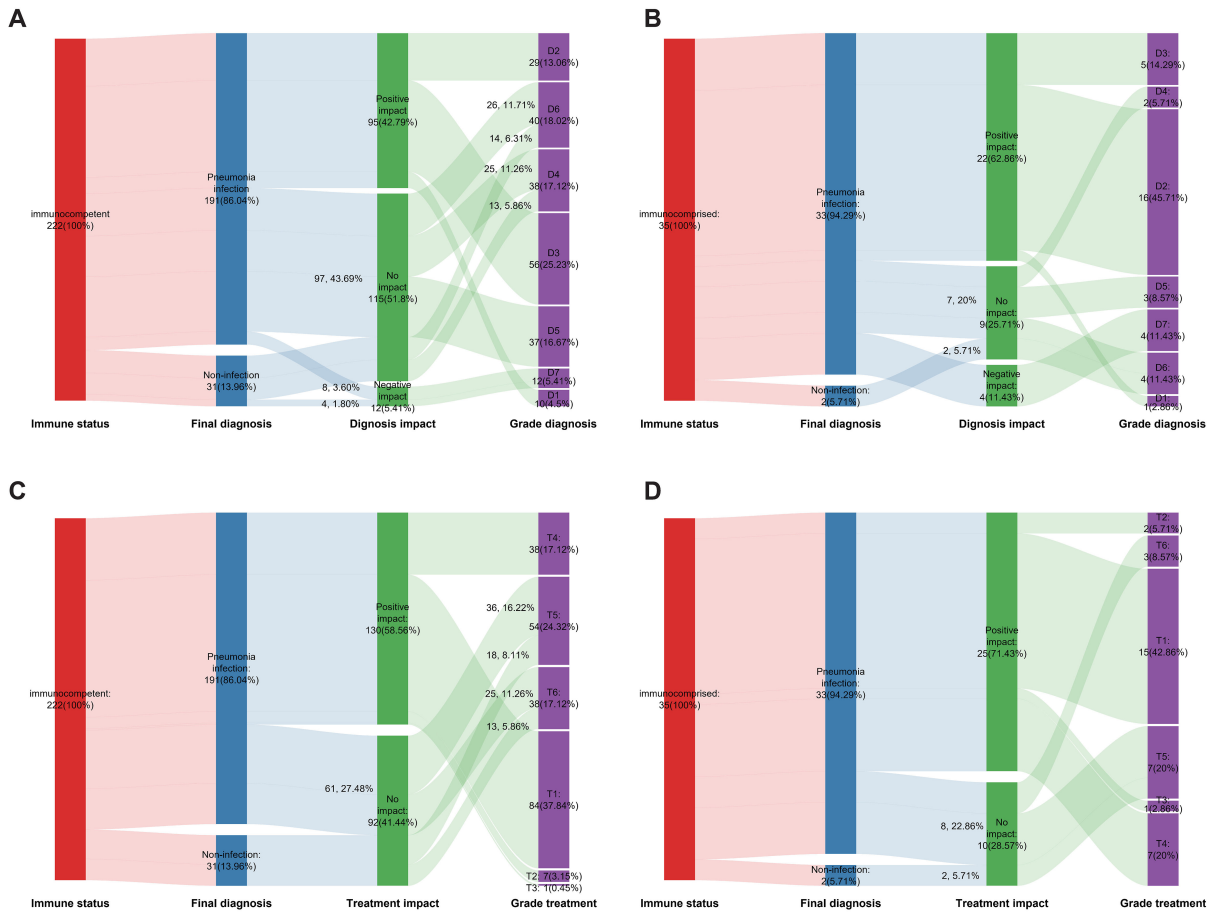

FIGURE 4
The impact of mNGS on the diagnosis and treatment. **(A)** The effect of mNGS on pathogen diagnosis among immunocompetent patients; **(B)** The effect of mNGS on pathogen diagnosis among immunocompromised patients; **(C)** The effect of mNGS on treatment among immunocompetent patients; **(D)** The effect of mNGS on treatment among immunocompromised patients.

which could be due to the broad range of tests included in the CMT, such as the T-SPOT, sputum culture, BALF GM test, and blood G test. CMT positivity cannot completely confirm the corresponding pathogen infection but will be included in the positive statistical results.

This study found comparable detection rates for *M. tuberculosis* and Aspergillus between mNGS and CMT (Figures 3G, H). CMT, including sputum smear, BALF X-pert, T-SPOT, and galactomannan tests, is cost-effective for routine cases. But mNGS excels in complex scenarios, detecting *M. tuberculosis* in atypical or CMT-negative cases and identifying Aspergillus species for targeted therapy. mNGS also detects co-infections, enhancing diagnostic scope. While CMT is preferred for routine tuberculosis screening, mNGS may be more economical when invasive procedures are needed. mNGS is not recommended for routine use but adds value in challenging cases. However, subgroup analyses are often underpowered (Supplementary Table 3), with most sample sizes below those required for 80% power, except for immunocompetent and pulmonary infection subgroups. Thus, subgroup findings are exploratory, requiring larger studies for validation. Unlike previous studies, we conducted an analysis to assess the impact of the mNGS test on the final diagnosis and adjustment of the treatment regimen for each patient to gain a deeper understanding of its impact on actual clinical diagnosis and therapy. The mNGS diagnosis impact (D1–D7) and treatment impact (T1–T6) classifications were enhanced by evaluating inter-rater reliability, yielding Cohen's kappa values of 0.866 (95% CI: 0.796–0.937) for diagnosis (Supplementary Table 4) and 0.868 (95% CI: 0.783–0.953) for treatment (Supplementary Table 5), indicating strong agreement. Our results show that BALF mNGS has several beneficial effects on diagnosis and treatment. Specifically, mNGS assists in the diagnosis of mixed infections and identification of infectious pathogens. Moreover, it aided in initiating appropriate antibiotic treatment and confirmed the effectiveness of empirical treatment. Further subgroup analysis showed that BALF mNGS in immunocompromised patients suspected of having pulmonary infection could have more positive effects on diagnosis (42.79% vs. 62.86%, p= 0.0267) and treatment (58.56% vs. 71.43%, p= 0.148).

Liang and colleagues (Liang et al., 2022) conducted a study to analyze the effect of BALF mNGS on the treatment of patients with suspected lower respiratory tract infections. The results showed that 3.6% of patients were degraded by antibiotics (reducing the antibacterial spectrum or reducing the types of antibiotics), 23.6%

were upgraded (increasing the types of antibiotics or changing to broad-spectrum antibiotics), 60.7% remained unchanged, and 12.1% were transferred to a lung hospital. Studies have shown that the majority of patients do not adjust their treatment plan following mNGS testing; however, the mNGS results verify the accuracy of empirical treatment, which is consistent with our research results (Figure 4). We are confident that the results of mNGS will have a positive impact on this particular group of patients. Xiao and colleagues (Jin et al., 2022) also found that the ultimate diagnosis and treatment adjustment of cases primarily relied on the combined findings of mNGS, CT, other tests, and clinical features. Modifications and adjustments were made solely based on the results of mNGS in 32 (32/246, 13.01%) and 23 (23/246, 9.35%) cases, respectively. These modifications have beneficial effects on the disease progression and prognosis of these patients. Most of these patients were infected with *M. tuberculosis*, NTM, or atypical pathogens.

Han and his colleagues (Han et al., 2023) discovered that the results of plasma mNGS had a positive effect on 83 patients (57.1%). This was achieved by accurately diagnosing or excluding infections and initiating targeted therapies. However, only 32.4% (11/34) of the negative mNGS tests showed a positive impact, suggesting that plasma mNGS testing alone may not be a powerful tool for ruling out infections in clinical settings.

Although the tested samples and classification criteria for the impact on diagnosis and treatment may vary, our study classified a negative result from the NGS test as having no effect on the clinical diagnosis. However, our results showed that for suspected pneumonia patients with normal immunity, approximately half of the mNGS results had a positive impact on the diagnosis and treatment. More clinical trials and studies are required to gain a deeper understanding of the appropriate individuals to test, the optimal timing for testing, and how to optimize the diagnostic efficiency and socioeconomic benefits of mNGS for pulmonary infectious diseases. Furthermore, this manual classification system prioritizes diagnostic context over automated interpretation. Retrospective design allows granular analysis but limits real-time clinical generalizability. Current framework requires specialized expertise, making it less suitable for emergency settings where rapid decision-making predominates.

In clinical practice, we frequently encounter patients presenting with either radiological pulmonary abnormalities and/or respiratory symptoms, which necessitates comprehensive clinical evaluation to differentiate true pulmonary infections from other pathologies and decide on antimicrobial therapy initiation. Our study specifically addressed this diagnostic challenge through rigorous case selection criteria (detailed in "Study design and patient population"), where the cohort potentially included non-infectious pulmonary conditions such as interstitial lung disease, pulmonary edema, and neoplastic lesions. Critical analysis revealed that patients demonstrating specific clinical features (e.g., febrile presentation), comorbid conditions (particularly malignancies), characteristic CT findings (consolidation or ground-glass opacities), and laboratory abnormalities (elevated inflammatory markers) showed significantly higher probabilities of confirmed pulmonary infections. These findings systematically validate our clinical experience through three key dimensions: 1. Diagnostic Triangulation: Integration of microbiological, radiological, and laboratory evidence. 2. Risk Stratification: Identification of high-yield clinical predictors for infection likelihood. 3. Diagnostic Stewardship: Guidance for judicious antimicrobial use in ambiguous cases. This evidence-based alignment between empirical clinical judgment and systematic research outcomes reinforces the necessity of multidimensional assessment in pulmonary infection diagnosis. The concordance observed provides scientific validation for current diagnostic protocols.

Compared to CMTs, mNGS has a higher initial cost. This is due to the expensive sequencer, sophisticated reagents, and significant computational resources required for data analysis. As a result, the cost of a single mNGS test is often several times higher than that of traditional methods. However, mNGS provides a comprehensive view of the microbial community in a sample within a relatively short time, typically within 24–48 hours. This rapid turnaround time can potentially reduce the overall cost of care by enabling more targeted and timely treatment, thereby avoiding prolonged and inappropriate empirical therapy (Miller and Chiu, 2021). In contrast, CMTs have limitations in detecting fastidious or unculturable pathogens. For example, many viruses and some intracellular bacteria are difficult to identify using conventional culture methods, which can lead to misdiagnosis or delayed diagnosis. This, in turn, affects the effectiveness of treatment and patient outcomes. In contrast, mNGS can detect a wide range of pathogens, including novel and emerging ones, without prior knowledge of the causative agent. This enhanced diagnostic capability can lead to more effective treatment strategies and improved patient prognosis. In summary, while the initial costs of implementing NGS technologies in infectious disease diagnostics are high, the potential for improved diagnostic accuracy, reduced hospital stays, and more effective patient management can justify these expenses. The continued development and refinement of NGS technologies, alongside advances in bioinformatics and data analysis, are expected to further enhance their cost-effectiveness and clinical utility in the future (Liu and Ma, 2024; Haslam, 2021).

This study has several limitations. First, most patients underwent only mNGS DNA testing, potentially missing RNA viruses. Second, as a single-center study with few immunocompromised patients, generalizability is limited. Third, the retrospective design introduced selection bias, as mNGS was often used for complex cases or patients with better socioeconomic status, restricting applicability to broader populations. Fourth, missing data in routine tests or CMTs, particularly in milder cases, may have affected precision. A complete case analysis (Supplementary Table 6), including only patients with complete data, confirmed robust results. Fifth, the lack of standardized mNGS interpretation criteria and unblinded diagnostic adjudication may have introduced bias, though mitigated by expert consensus and predefined thresholds. Finally, cost-effectiveness was not evaluated. Future prospective, multicenter

studies with larger cohorts, standardized criteria, blinded adjudication, and cost analyses are needed to validate our findings.

Data availability statement

The raw sequence data reported in this paper have been deposited in the Genome Sequence Archive (Genomics, Proteomics & Bioinformatics 2021) in National Genomics Data Center (Nucleic Acids Res 2022), China National Center for Bioinformation / Beijing Institute of Genomics, Chinese Academy of Sciences (GSA: CRA026168) that are publicly accessible at https://ngdc.cncb.ac.cn/gsa.

Ethics statement

The studies involving humans were approved by The Ethics Committee of Tongji Medical College, Huazhong University of Science and Technology (IORG No: IORG0003571). The studies were conducted in accordance with the local legislation and institutional requirements. The human samples used in this study were acquired from Test results in normal clinical diagnosis and treatment. Written informed consent for participation was not required from the participants or the participants' legal guardians/next of kin in accordance with the national legislation and institutional requirements.

Author contributions

MZ: Writing – original draft, Writing – review & editing. SS: Data curation, Methodology, Writing – original draft. LC: Data curation, Formal Analysis, Investigation, Writing – original draft. HX: Data curation, Formal Analysis, Writing – original draft. LL: Project administration, Resources, Writing – original draft. JL: Methodology, Resources, Writing – original draft. JZ: Conceptualization, Supervision, Writing – review & editing. XX: Conceptualization, Funding acquisition, Supervision, Writing – review & editing.

Funding

The author(s) declare that financial support was received for the research and/or publication of this article. This article was funded by Jointown Caritas Fund of Hubei Red Cross Foundation and the Free Innovation Pre-Research Fund of Union Hospital (No.2020xhyn029).

Conflict of interest

The authors declare that the research was conducted in the absence of any commercial or financial relationships that could be construed as a potential conflict of interest.

Generative AI statement

The author(s) declare that no Generative AI was used in the creation of this manuscript.

Publisher's note

All claims expressed in this article are solely those of the authors and do not necessarily represent those of their affiliated organizations, or those of the publisher, the editors and the reviewers. Any product that may be evaluated in this article, or claim that may be made by its manufacturer, is not guaranteed or endorsed by the publisher.

Supplementary material

The Supplementary Material for this article can be found online at: https://www.frontiersin.org/articles/10.3389/fcimb.2025.1521641/full#supplementary-material

References

Akinosoglou, K. S., Karkoulias, K., and Marangos, M. (2013). Infectious complications in patients with lung cancer. *Eur. Rev. Med. Pharmacol. Sci.* 17, 8–18.

Aliberti, S., Dela, C. C., Amati, F., Sotgiu, G., and Restrepo, M. I. (2021). Community-acquired pneumonia. *Lancet* 398, 906–919. doi: 10.1016/S0140-6736(21)00630-9

Bloom, D. E., and Cadarette, D. (2019). Infectious disease threats in the twenty-first century: strengthening the global response. *Front. Immunol.* 10. doi: 10.3389/fimmu.2019.00549

Carbo, E. C., Sidorov, I. A., van Rijn-Klink, A. L., Pappas, N., van Boheemen, S., Mei, H., et al. (2022). Performance of five metagenomic classifiers for virus pathogen detection using respiratory samples from a clinical cohort. *Pathogens* 11. doi: 10.3390/pathogens11030340

Chen, H., Liang, Y., Wang, R., Wu, Y., Zhang, X., Huang, H., et al. (2023). Metagenomic next-generation sequencing for the diagnosis of pneumocystis jirovecii pneumonia in critically pediatric patients. *Ann. Clin. Microbiol. Antimicrob.* 22. doi: 10.1186/s12941-023-00555-5

Chiu, C. Y. (2013). Viral pathogen discovery. *Curr. Opin. Microbiol.* 16, 468–478. doi: 10.1016/j.mib.2013.05.001

Coombs, C. C., Gillis, N. K., Tan, X., Berg, J. S., Ball, M., Balasis, M. E., et al. (2018). Identification of clonal hematopoiesis mutations in solid tumor patients undergoing unpaired next-generation sequencing assays. *Clin. Cancer Res.* 24, 5918–5924. doi: 10.1158/1078-0432.CCR-18-1201

Deng, W., Xu, H., Wu, Y., and Li, J. (2022). Diagnostic value of bronchoalveolar lavage fluid metagenomic next-generation sequencing in pediatric pneumonia. *Front. Cell Infect. Microbiol.* 12. doi: 10.3389/fcimb.2022.950531

Dimech, W. (2021). The standardization and control of serology and nucleic acid testing for infectious diseases. *Clin. Microbiol. Rev.* 34, e3521. doi: 10.1128/CMR.00035-21

Du, J., Zhang, J., Zhang, D., Zhou, Y., Wu, P., Ding, W., et al. (2022). Background filtering of clinical metagenomic sequencing with a library concentration-normalized model. *Microbiol. Spectr.* 10, e0177922. doi: 10.1128/spectrum.01779-22

Du, R., Feng, Y., Wang, Y., Huang, J., Tao, Y., and Mao, H. (2023). Metagenomic next-generation sequencing confirms the diagnosis of legionella pneumonia with rhabdomyolysis and acute kidney injury in a limited resource area: a case report and review. *Front. Public Health* 11. doi: 10.3389/fpubh.2023.1145733

Guan, H., Shen, A., Lv, X., Yang, X., Ren, H., Zhao, Y., et al. (2016). Detection of virus in csf from the cases with meningoencephalitis by next-generation sequencing. *J. Neurovirol* 22, 240–245. doi: 10.1007/s13365-015-0390-7

Han, D., Li, Z., Li, R., Tan, P., Zhang, R., and Li, J. (2019). Mngs in clinical microbiology laboratories: on the road to maturity. *Crit. Rev. Microbiol.* 45, 668–685. doi: 10.1080/1040841X.2019.1681933

Han, D., Yu, F., Zhang, D., Yang, Q., Xie, M., Yuan, L., et al. (2023). The real-world clinical impact of plasma mngs testing: an observational study. *Microbiol. Spectr.* 11. doi: 10.1128/spectrum.03983-22

Haslam, D. B. (2021). Future applications of metagenomic next-generation sequencing for infectious diseases diagnostics. *J. Pediatr. Infect. Dis. Soc.* 10, S112–S117. doi: 10.1093/jpids/piab107

Huang, Z., Hu, B., Li, J., Feng, M., Wang, Z., Huang, F., et al. (2024). Metagenomic versus targeted next-generation sequencing for detection of microorganisms in bronchoalveolar lavage fluid among renal transplantation recipients. *Front. Immunol.* 15. doi: 10.3389/fimmu.2024.1443057

Huang, W., Wang, F., Cai, Q., Xu, H., Hong, D., Wu, H., et al. (2023). Epidemiological and clinical characteristics of psittacosis among cases with complicated or atypical pulmonary infection using metagenomic next-generation sequencing: a multi-center observational study in China. *Ann. Clin. Microbiol. Antimicrob.* 22. doi: 10.1186/s12941-023-00631-w

Jia, X., Hu, L., Wu, M., Ling, Y., Wang, W., Lu, H., et al. (2021). A streamlined clinical metagenomic sequencing protocol for rapid pathogen identification. *Sci. Rep.* 11, 4405. doi: 10.1038/s41598-021-83812-x

Jin, X., Li, J., Shao, M., Lv, X., Ji, N., Zhu, Y., et al. (2022). Improving suspected pulmonary infection diagnosis by bronchoalveolar lavage fluid metagenomic next-generation sequencing: a multicenter retrospective study. *Microbiol. Spectr.* 10. doi: 10.1128/spectrum.02473-21

Kalil, A. C., Metersky, M. L., Klompas, M., Muscedere, J., Sweeney, D. A., Palmer, L. B., et al. (2016). Management of adults with hospital-acquired and ventilator-associated pneumonia: 2016 clinical practice guidelines by the infectious diseases society of America and the American thoracic society. *Clin. Infect. Dis.* 63, e61–e111. doi: 10.1093/cid/ciw353

Leo, S., Gaia, N., Ruppe, E., Emonet, S., Girard, M., Lazarevic, V., et al. (2017). Detection of bacterial pathogens from broncho-alveolar lavage by next-generation sequencing. *Int. J. Mol. Sci.* 18. doi: 10.3390/ijms18092011

Li, G., Sun, J., Pan, S., Li, W., Zhang, S., Wang, Y., et al. (2019). Comparison of the performance of three blood culture systems in a chinese tertiary-care hospital. *Front. Cell Infect. Microbiol.* 9. doi: 10.3389/fcimb.2019.00285

Lin, P., Chen, Y., Su, S., Nan, W., Zhou, L., Zhou, Y., et al. (2022). Diagnostic value of metagenomic next-generation sequencing of bronchoalveolar lavage fluid for the diagnosis of suspected pneumonia in immunocompromised patients. *BMC Infect. Dis.* 22. doi: 10.1186/s12879-022-07381-8

Lin, T., Tu, X., Zhao, J., Huang, L., Dai, X., Chen, X., et al. (2023). Microbiological diagnostic performance of metagenomic next-generation sequencing compared with conventional culture for patients with community-acquired pneumonia. *Front. Cell Infect. Microbiol.* 13. doi: 10.3389/fcimb.2023.1136588

Liang, M., Fan, Y., Zhang, D., Yang, L., Wang, X., Wang, S., et al. (2022). Metagenomic next-generation sequencing for accurate diagnosis and management of lower respiratory tract infections. *Int. J. Infect. Dis.* 122, 921–929. doi: 10.1016/j.ijid.2022.07.060

Liu, Y., and Ma, Y. (2024). Clinical applications of metagenomics next-generation sequencing in infectious diseases. *J. Zhejiang Univ Sci. B* 25, 471–484. doi: 10.1631/jzus.B2300029

Lloyd-Price, J., Abu-Ali, G., and Huttenhower, C. (2016). The healthy human microbiome. *Genome Med.* 8, 51. doi: 10.1186/s13073-016-0307-y

Metlay, J. P., Waterer, G. W., Long, A. C., Anzueto, A., Brozek, J., Crothers, K., et al. (2019). Diagnosis and treatment of adults with community-acquired pneumonia. An official clinical practice guideline of the American thoracic society and infectious diseases society of america. *Am. J. Respir. Crit. Care Med.* 200, e45–e67. doi: 10.1164/rccm.201908-1581ST

Miao, Q., Ma, Y., Wang, Q., Pan, J., Zhang, Y., Jin, W., et al. (2018). Microbiological diagnostic performance of metagenomic next-generation sequencing when applied to clinical practice. *Clin. Infect. Dis.* 67, S231–S240. doi: 10.1093/cid/ciy693

Miller, S., and Chiu, C. (2021). The role of metagenomics and next-generation sequencing in infectious disease diagnosis. *Clin. Chem.* 68, 115–124. doi: 10.1093/clinchem/hvab173

Musher, D. M., and Thorner, A. R. (2014). Community-acquired pneumonia. *N Engl. J. Med.* 371, 1619–1628. doi: 10.1056/NEJMra1312885

Parize, P., Muth, E., Richaud, C., Gratigny, M., Pilmis, B., Lamamy, A., et al. (2017). Untargeted next-generation sequencing-based first-line diagnosis of infection in immunocompromised adults: a multicenter, blinded, prospective study. *Clin. Microbiol. Infect.* 23, 571–574. doi: 10.1016/j.cmi.2017.02.006

Peng, J. M., Du, B., Qin, H. Y., Wang, Q., and Shi, Y. (2021). Metagenomic next-generation sequencing for the diagnosis of suspected pneumonia in immunocompromised patients. *J. Infect.* 82, 22–27. doi: 10.1016/j.jinf.2021.01.029

Qin, H., Peng, J., Liu, L., Wu, J., Pan, L., Huang, X., et al. (2021). A retrospective paired comparison between untargeted next generation sequencing and conventional microbiology tests with wisely chosen metagenomic sequencing positive criteria. *Front. Med. (Lausanne)* 8, 686247. doi: 10.1080/22221751.2022.2035194

Qu, J., Zhang, J., Chen, Y., Huang, Y., Xie, Y., Zhou, M., et al. (2022). Aetiology of severe community acquired pneumonia in adults identified by combined detection methods: a multi-centre prospective study in china. *Emerg. Microbes Infect.*. 11, 556–566. doi: 10.1080/22221751.2022.2035194

Ramirez, J. A., Musher, D. M., Evans, S. E., Dela Cruz, C., Crothers, K. A., Hage, C. A., et al. (2020). Treatment of community-acquired pneumonia in immunocompromised adults. *Chest.* 158, 1896–1911. doi: 10.1016/j.chest.2020.05.598

Ruppe, E., Baud, D., Schicklin, S., Guigon, G., and Schrenzel, J. (2016). Clinical metagenomics for the management of hospital- and healthcare-acquired pneumonia. *Future Microbiol.* 11, 427–439. doi: 10.2217/fmb.15.144

Ruppe, E., Lazarevic, V., Girard, M., Mouton, W., Ferry, T., Laurent, F., et al. (2017). Clinical metagenomics of bone and joint infections: a proof of concept study. *Sci. Rep.* 7, 7718. doi: 10.1038/s41598-017-07546-5

Shen, Z., Wang, Y., Bao, A., Yang, J., Sun, X., Cai, Y., et al. (2023). Metagenomic next-generation sequencing for pathogens in bronchoalveolar lavage fluid improves the survival of patients with pulmonary complications after allogeneic hematopoietic stem cell transplantation. *Infect. Dis. Ther.* 12, 2103–2115. doi: 10.1007/s40121-023-00850-w

Sin, M. L., Mach, K. E., Wong, P. K., and Liao, J. C. (2014). Advances and challenges in biosensor-based diagnosis of infectious diseases. *Expert Rev. Mol. Diagn.* 14, 225–244. doi: 10.1586/14737159.2014.888313

Subramony, A., Zachariah, P., Krones, A., Whittier, S., and Saiman, L. (2016). Impact of multiplex polymerase chain reaction testing for respiratory pathogens on healthcare resource utilization for pediatric inpatients. *J. Pediatr.* 173, 196–201. doi: 10.1016/j.jpeds.2016.02.050

Sun, H., Wang, F., Zhang, M., Xu, X., Li, M., Gao, W., et al. (2022). Diagnostic value of bronchoalveolar lavage fluid metagenomic next-generation sequencing in pneumocystis jirovecii pneumonia in non-hiv immunosuppressed patients. *Front. Cell Infect. Microbiol.* 12. doi: 10.3389/fcimb.2022.872813

Tang, M., Zeng, W., Qiu, Y., Fang, G., Pan, M., Li, W., et al. (2023). Clinical features of rare disseminated mycobacterium colombiense infection in nine patients who are hiv-negative in guangxi, China. *Int. J. Infect. Dis.* 128, 321–324. doi: 10.1016/j.ijid.2023.01.002

Tsoulos, N., Papadopoulou, E., Metaxa-Mariatou, V., Tsaousis, G., Efstathiadou, C., Tounta, G., et al. (2017). Tumor molecular profiling of nsclc patients using next generation sequencing. *Oncol. Rep.* 38, 3419–3429. doi: 10.3892/or.2017.6051

Valvani, A., Martin, A., Devarajan, A., and Chandy, D. (2019). Postobstructive pneumonia in lung cancer. *Ann. Transl. Med.* 7, 357. doi: 10.21037/atm.2019.05.26

van Nimwegen, K. J., van Soest, R. A., Veltman, J. A., Nelen, M. R., van der Wilt, G. J., Vissers, L. E., et al. (2016). Is the $1000 genome as near as we think? A cost analysis of next-generation sequencing. *Clin. Chem.* 62, 1458–1464. doi: 10.1373/clinchem.2016.258632

Wang, J., Xu, H., Wang, X., and Lan, J. (2023). Rapid diagnosis of non-tuberculous mycobacterial pulmonary diseases by metagenomic next-generation sequencing in non-referral hospitals. *Front. Cell Infect. Microbiol.* 12. doi: 10.3389/fcimb.2022.1083497

Wilson, M. R., Naccache, S. N., Samayoa, E., Biagtan, M., Bashir, H., Yu, G., et al. (2014). Actionable diagnosis of neuroleptospirosis by next-generation sequencing. *N Engl. J. Med.* 370, 2408–2417. doi: 10.1056/NEJMoa1401268

Xu, C., Chen, X., Zhu, G., Yi, H., Chen, S., Yu, Y., et al. (2023). Utility of plasma cell-free DNA next-generation sequencing for diagnosis of infectious diseases in patients with hematological disorders. *J. Infect.* 86, 14–23. doi: 10.1016/j.jinf.2022.11.020

Xu, L., and Shi, R. (2014). Noninvasive prenatal diagnosis using next-generation sequencing. *Gynecol Obstet Invest.* 77, 73–77. doi: 10.1159/000355693

Yao, M., Zhou, J., Zhu, Y., Zhang, Y., Lv, X., Sun, R., et al. (2016). Detection of listeria monocytogenes in csf from three patients with meningoencephalitis by next-generation sequencing. *J. Clin. Neurol.* 12, 446–451. doi: 10.3988/jcn.2016.12.4.446

Zhong, J., Liu, Y., Luo, N., Wei, Q., Su, Q., Zou, J., et al. (2023). Metagenomic next-generation sequencing for rapid detection of pulmonary infection in patients with acquired immunodeficiency syndrome. *Ann. Clin. Microbiol. Antimicrob.* 22. doi: 10.1186/s12941-023-00608-9

frontiers | Frontiers in Cellular and Infection Microbiology

TYPE Original Research
PUBLISHED 13 August 2025
DOI 10.3389/fcimb.2025.1560870

OPEN ACCESS

EDITED BY
John S. Spencer,
Colorado State University, United States

REVIEWED BY
Kai Ling Chin,
Universiti Malaysia Sabah, Malaysia
Hua Chen,
Guangzhou Chest Hospital, China

*CORRESPONDENCE
Ying-Chun Xu
xycpumch@139.com
Qi-Wen Yang
yangqiwen81@vip.163.com

†These authors have contributed equally to this work

RECEIVED 15 January 2025
ACCEPTED 22 July 2025
PUBLISHED 13 August 2025

CITATION
Yi Q-L, Wu Y, He S, Feng M-L, Liu X-Y, Zhou X-Z, Gao H-T, Zhang Y-F, Yang Q-W and Xu Y-C (2025) Development and evaluation of a multiplex molecular point-of-care assay for direct identification of *Mycobacterium tuberculosis* and prioritized non-tuberculous mycobacteria. *Front. Cell. Infect. Microbiol.* 15:1560870. doi: 10.3389/fcimb.2025.1560870

Development and evaluation of a multiplex molecular point-of-care assay for direct identification of *Mycobacterium tuberculosis* and prioritized non-tuberculous mycobacteria

Qiao-Lian Yi[1†], Yun Wu[1,2†], Shuang He[3], Meng-Li Feng[3], Xiao-Yu Liu[1], Xin-Zhu Zhou[1,2], Hao-Tian Gao[1], Yu-Fan Zhang[3], Qi-Wen Yang[1,4*] and Ying-Chun Xu[1,4*]

[1]Department of Laboratory Medicine, Peking Union Medical College Hospital, Chinese Academy of Medical Sciences and Peking Union Medical College, Beijing, China, [2]Graduate School, Chinese Academy of Medical Sciences and Peking Union Medical College, Beijing, China, [3]R&D Department Genewise Bio Co., Ltd, Beijing, China, [4]State Key Laboratory of Complex, Severe, and Rare Diseases, Chinese Academy of Medical Sciences and Peking Union Medical College, Beijing, China

Objective: This study aimed to establish a multiplex molecular point-of-care assay called *fastNTM* incorporating an ultra-fast sample pre-treatment for direct identification of *Mycobacterium tuberculosis* complex (MTBC) and 8 non-tuberculous Mycobacteria (NTM) commonly prioritized in clinical settings, and to evaluate its performance in 149 clinical confirmed mycobacterial-positive samples.

Methods: The study was divided into two stages: a pilot study to establish the methodology and a clinical validation study to evaluate its performance. In the pilot study, we established the *fastNTM* and analyzed its performance regarding limits of detection, reproducibility, specificity and efficiency. The clinical validation study was performed using 149 clinical confirmed mycobacterial-positive samples, with 16S rRNA identification as the reference standard. The complete process, from patient to result, was accomplished within 90 minutes.

Results: Of the 149 positive clinical mycobacterial cultures analyzed, 136 were within the designed targets. Among these 136 cultures, 133 samples were correctly identified by *fastNTM*, achieving an accuracy rate of 97.79%.

Conclusions: This study demonstrates that *fastNTM* with its high accuracy rate are capable to rapidly and effectively differentiate between MTBC and the major NTM species.

KEYWORDS

non-tuberculous mycobacteria, *Mycobacterium tuberculosis*, pathogen identification, point-of-care testing, molecular diagnosis

Introduction

Non-tuberculous mycobacteria (NTM) represent a diverse group of near 200 species, distinct from the *Mycobacterium tuberculosis* complex (MTBC) and *Mycobacterium leprae* (LPSN, 2025). Recognized as opportunistic pathogens, NTM are more likely to colonize the respiratory tracts of hosts. The global significance of NTM diseases has been escalating due to a rising trend in their occurrence (Kumar and Loebinger, 2022; Cristancho-Rojas et al., 2024). Pulmonary infections caused by NTM present symptoms similar to those of tuberculosis (TB), including persistent cough, weight loss, and fatigue (Dahl et al., 2022). Misdiagnosing NTM infections as recurrent TB or drug-resistant TB often leads to inappropriate empiric treatment, potentially contributing to the development of TB drug resistance (Gopalaswamy et al., 2020). Therefore, rapidly distinguishing between MTBC and NTM, and identifying the specific NTM species, is crucial for the implementation of TB control strategies and patient clinical outcomes.

The diversity of NTM isolated from pulmonary samples varies widely by geographical region. Globally, about one-half of NTM species isolated from human specimens belongs to the M. avium complex (MAC) (Hoefsloot et al., 2013). However, in China, *M. abscessus* and the *M. avium* complex account for up to 52.6% and 23.2% of all NTM-caused infections, respectively (Tan et al., 2021). Despite these regional differences, *M. avium*, *M. abscessus*, *M. fortuitum* and *M. kansasii* remain the most relevant species for NTM pulmonary disease (Kim et al., 2019; Ratnatunga et al., 2020; Dahl et al., 2022; Nguyen et al., 2024). *M. avium* and *M. intracellulare* have higher infection rates among non-AIDS patients (Pasipanodya et al., 2017). Other species, such as *M. scrofulaceum*, *M. gordonae*, *M. marinum* and *M. ulcerans*, although relatively rare in pulmonary infections, have shown a relatively high isolation rate in clinical settings. These species can cause infections not only in the immunocompromised hosts, but also in otherwise healthy individuals (Van der Werf et al., 1999; Chang et al., 2021; Canetti et al., 2022). Pulmonary *M. scrofulaceum* disease has mainly occurred in patients with chronic pulmonary diseases (Suzuki et al., 2016; Wilson et al., 2019).

The conventional methods for identifying NTM in clinical settings, which rely on smear microscopy and culture. Sputum culture, while sensitive and considered the gold standard, is laborious and time-consuming, with a requirement of 10–42 days for results (Forbes et al., 2018). Clinical practices for rapid identification, such as Gene Xpert, are primarily focus on detecting MTBC with limited capacity to identify NTM (Opota et al., 2016). Other reported available assays for the direct identification of NTM in clinical specimens, including the LightCycler Mycobacterium Detection Kit (Omar et al., 2011), Genoscholar™ NTM+MDRTB II (Mitarai et al., 2012), and the GenoType Mycobacteria Direct test (Franco-Álvarez De Luna et al., 2006), still necessitate additional manual operations, sample processing and nucleic acid extraction. Advanced methods such as targeted next-generation sequencing (tNGS) and metagenomic next-generation sequencing (mNGS) can detect a broader range of strains and minimize the risk of missed detections (Schwab et al., 2024). However, limitations of these sequencing-based detection methods are obvious, including the need for costly sequencing instruments, and skilled personnel for high-quality nucleic acid extraction. Otherwise, Mass spectrometry relies on databases for identification. Current databases may not have comprehensive entries for all mycobacterial species, leading to potential misidentification, especially for rare or closely related species (Alcaide et al., 2018). Rapid testing options, while offering faster results, are often limited in the breadth of detectable species or involve complex operational steps.

For species identification, the intergenic transcribed spacer (ITS) region, located between the 16S rRNA and 23S rRNA genes, is a highly conserved yet variable genetic region that has emerged as a crucial target for the detection and identification of genotypically similar bacteria such as non-tuberculous mycobacteria (NTM). The presence of unique sequences within the ITS region allows for the design of highly specific primers and probes, reducing the likelihood of cross-reactivity with other bacterial species (Ngan et al., 2011). To address these challenges, we developed a multiplex PCR-based point-of-care assay called *fastNTM* for MTBC and NTM discrimination along with an ultrafast sample pretreatment method. Given the diverse range of NTM species and their various distribution, eight prevalent NTM species were selected, including *M. avium*, *M. abscessus*, *M. fortuitum*, *M. kansasii*, *M. intracellulare*, *M. scrofulaceum*, *M. gordonae*, and *M. marinum/ulcerans*.

The objective of this study was to evaluate the clinical performance of this panel in differentiating MTBC and key NTM based on multiplex molecular POCT and ultrafast sample pretreatment. By offering a "sample-in, result-out" solution, *fastNTM* represents a significant advancement in the rapid and accurate diagnosis of TB and NTM infections, potentially reducing the time to treatment and enhancing patient outcomes.

Materials and methods

Primer and probe design

The assay enables the simultaneous detection of 9 targets in a single reaction, allowing for the concurrent identification of the *M. tuberculosis* complex and 8 NTM. It was achieved by multiplex quantitative PCR platform combined with asymmetric PCR and multicolor melting curve analysis (MMCA) (Elenitoba-Johnson et al., 2001). It targets the intergenic transcribed space (ITS) region between the 16S rRNA and 23S rRNA genes of mycobacteria, using a pan-mycobacterial primer set: By downloading over 20 sequences for each species from the NCBI database, conserved regions were identified through sequence alignment, while overlapping regions with other species were excluded. Specific primers for each species were designed to target theses specific regions using Oligo7 and NCBI BLAST. The NCBI Primer-BLAST was used to verify optimized oligonucleotide sequences for specificity. The species-specific primers exhibited varying melting temperatures and the sequences of the primers-probe pairs are presented in Supporting Information Table S1 (Supplementary Material).

Establishment of *fastNTM*

The PCR amplification system is carefully calibrated with primer concentrations of 0.6 μM for the *M. tuberculosis* complex and 0.2 μM for restrictive NTM primers, along with 4 μM for non-restrictive primers, ensuring specific detection. The probe concentration is set at 0.1 μM to facilitate the identification of amplified products through fluorescence during the reaction. The multiplex molecular identification is performed in a cartridge. The cartridge comes preloaded with magnetic beads, lysis solution, wash solution, elution buffer, and freeze-dried detection reagents, integrating nucleic acid extraction, RT-PCR amplification, and target detection (Figure 1).

Operation procedure of multiplex molecular point-of-care panel

The overall operation procedure of *fastNTM* is illustrated in Figure 1. Initially, 0.5 mL of the original clinical specimen, such as sputum, is transferred to the pretreatment cartridge, mixed with an equal volume of pretreatment solution. The ultrasound-assisted disruption is then activated for 1 minute to homogenize the sample. Following this, 0.5 mL of the liquefied sample is aspirated into the detection cartridge. The analysis is subsequently performed automatically by the NAT - 3000 Pro system (Genewise Bio Co., Ltd, Beijing, China), which completes the process within 85–90 minutes. MTBC determination is characterized by cycle threshold (Ct) value and that of NTM is melting temperature (Tm). The total turnaround time from sample to result is within 90 minutes.

Sample preparation

Low, medium, and high concentration tests. Inactivated *M. tuberculosis* was added to mycobacterial-negative sputum samples at low (40 CFU/mL), medium (1000 CFU/mL), and high concentrations (1,000,000 CFU/mL). For each concentration, 20 replicate tests were conducted for both the pretreated and untreated samples to compare the results.

Limit of detection (LOD) tests. The LoD was determined using serial dilutions of MTBC and NTM species. For each of the eight NTM species, concentrations of 100, 300, 500, 750 and 1000 CFU/mL were prepared. While for MTBC, concentrations of 10, 30, 50, 75, and 100 CFU/mL inactivated *M. tuberculosis* were prepared. Those bacterial suspensions were added to mycobacterial-negative sputum samples. Ten replicates were prepared for each species. Mycobacterial-negative sputum samples without additional mycobacterial templates served as negative controls. In each experimental group, both Ct and Tm values included internal controls (IC).

Comparison with Xpert MTB/RIF Ultra assay. TB-suspected sputum samples were collected from clinical settings, and different levels of MTB are confirmed by Xpert MTB/RIF Ultra Assay, including 15 MTB not detected, 1 MTB detected very low, 6 MTB detected low, and 8 MTB detected medium. Each sputum sample was divided into two aliquots: one was processed according to the manufacturer's instructions for the Xpert MTB/RIF Ultra Assay and tested using the GeneXpert® System, while the other was processed according to the *fastNTM* operation procedure as shown in Figure 1.

Clinical mycobacterial cultures preparation

A total of 149 clinical mycobacterial cultures in mycobacteria growth indicator tube (MGIT) originally cultured from 142 respiratory (sputum, tracheobronchial aspirate, bronchoalveolar lavage fluid, endotracheal aspirate) and 7 non-respiratory routine samples (tissue, lymphaden, body fluid) were randomly collected in the Clinical Microbiology Laboratory, Peking Union Medical College Hospital in Beijing, China, between 2021 and 2023. The clinical information of original specimens was shown in Table 1. All cultures were frozen samples accumulated over the years, and positive for MGIT system (BD BACTEC MGIT960 system, Becton Dickinson, Franklin Lakes, NJ, USA). Clinical workflow of positive mycobacterial cultures confirmation was presented in Supporting Information Figure S1 (Supplementary Material).

Each clinical mycobacterial MGIT-positive culture was divided into two portions for further analysis. One portion was directly tested with the multiplex molecular POCT panel, while the other underwent nucleic acid extraction and then being sent for 16S rRNA sequencing to obtain species-level identification. Results of 16S rRNA identification were regarded as the reference standard. For strains that cannot be identified by 16S rRNA, further identification is performed using the *hsp*65 gene.

Statistical analyses

We compared the rates of positive results of both *fastNTM* and reference methods using Cohen's Kappa Statistic. The 95% confidence intervals (95% CI) were calculated using the Wilson score method. Cohen's Kappa values for quantify agreement were calculated using GraphPad QuickCalcs (https://www.graphpad.com/quickcalcs/kappa1/) with 95% CIs.

Results

Performance of ultrafast pretreatment procedure

An ultrafast sample pretreatment procedure utilizing ultrasound-assisted enzymatic homogenization was implemented in the *fastNTM* assay. To evaluate the impact of this pretreatment

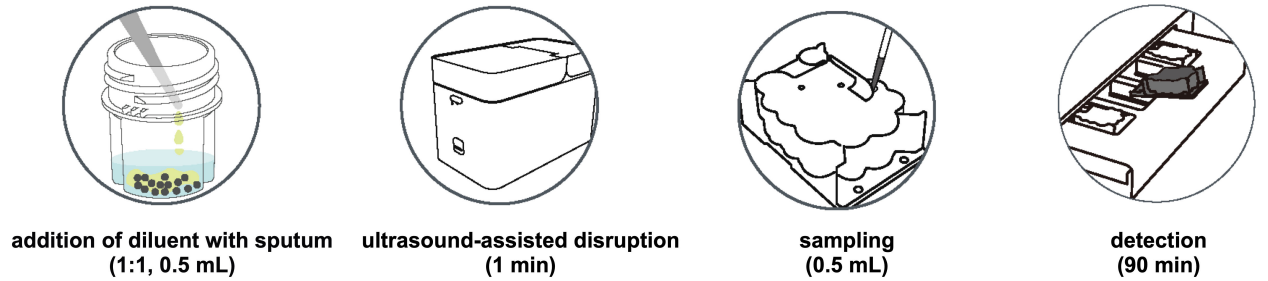

FIGURE 1
The overall operation procedure of *fastNTM*: Step1. Transfer 0.5 mL of specimen to the pretreatment cartridge with the equal volume of pretreatment solution. 2. Turn on the ultrasound-assisted disruption for 1 minute. 3. Aspirate 0.5 mL of the liquefied sample to the panel. 4. Multiplex PCR will be performed within 85–90 minutes.

method on detection outcomes, a controlled experiment was conducted using simulated samples with low, medium, and high concentrations of inactivated *M. tuberculosis*. The findings are presented in Figure 2a. The treated samples displayed cycle threshold (Ct) values of (21.561 ± 0.386, 31.687 ± 0.684, 34.892 ± 0.592) for the high, medium, and low concentration groups, respectively. Conversely, the untreated samples exhibited Ct values of 26.464 ± 0.562, 35.288 ± 0.653, and 38.122 ± 0.652 for the corresponding concentration groups. Within each group, a significant reduction in Ct values was observed, with the low concentration group showing that four samples did not yield detectable nucleic acid levels without treatment. This pretreatment process enhanced the efficiency of nucleic acid release.

Limit of detection for *fastNTM*

The lowest concentration level that achieved a 100% positive detection rate was determined as the LOD, and this was verified. The final LOD for the *fastNTM* was determined to be 500 copies/mL for *M. tuberculosis* and 500 copies/mL for each NTM species. The coefficients of variation (CV) for the Ct values of *M. tuberculosis* and the Tm values of the eight NTM species were calculated, as well as the IC. The percentage of positive assays for the MTB and 8 NTM in the LoD groups was 100%. The CV for the Tm values of the eight NTM species was less than 1%, the CV for the Ct values of M. tuberculosis was 1.14%, the CV for the IC Ct values was less than 1.8%, and the CV for the IC Tm values was less than 1% (Supplementary Material, Supporting Information Table S2). The negative samples showed no amplification.

Comparison of *fastNTM* to GeneXpert

To demonstrate that a 1-minute pretreatment process can achieve the same detection efficiency as a conventional 20-minute procedure, we conducted a comparative analysis using sputum specimens tested with the GeneXpert system. As there are currently no similar products available for *fastNTM*, we have relied solely on the detection results for *M. tuberculosis* as a reference. The comparative results between the *fastNTM* assay and the Xpert MTB/RIF Ultra Assay are presented in Figure 2b. It showed a high level of concordance in terms of both negative and positive results. Additionally, the Ct value distribution for *M.*

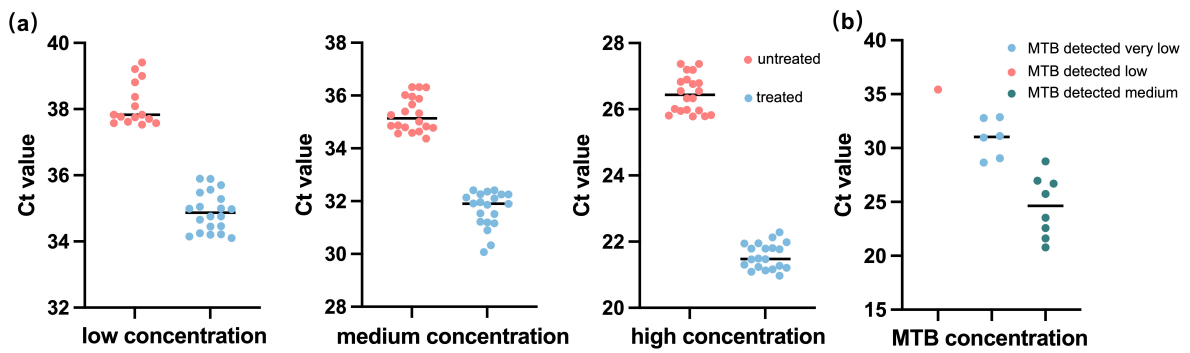

FIGURE 2
Performance of the ultrafast sample pretreatment procedure in sample detection. **(a)** Comparison results between *fastNTM* with and without the ultrafast sample pretreatment procedure among low (40 CFU/mL), medium (1000 CFU/mL), and high concentrations (1,000,000 CFU/mL). **(b)** Detection results of *fastNTM* using the ultrafast sample pretreatment procedure with the Xpert MTB/RIF Ultra Assay TB-confirmed sputum sample.

TABLE 1 Clinical information of 149 mycobacterial cultures.

Issues	Number (*n*)	Percentage(%)
Gender, female	99	66.44%
Age distribution		
0-20	4	2.68%
21-40	24	16.11%
41-60	54	36.24%
61-80	56	37.58%
≥81	11	7.38%
Sample type		
Sputum	109	73.15%
Tracheobronchial aspirates	22	14.77%
Bronchoalveolar lavage fluid	9	6.04%
Skin and tissue	3	2.01%
Tracheal intubation aspirates	2	1.34%
Vertebral puncture tissue	1	0.67%
Node biopsy	1	0.67%
Other respiratory specimens	1	0.67%
Other body fluids	1	0.67%
Department Distribution		
Department of Infection	72	48.32%
Respiratory Medicine Clinic	47	31.54%
Respiratory medical wards	20	13.42%
Department of cardiology	10	6.71%

tuberculosis detected by the *fastNTM* assay is consistent with the concentration trends obtained by the Xpert MTB/RIF Ultra Assay, suggesting a strong correlation between the two methods, indicating that the 1-minute pretreatment process can achieve the same detection efficiency as a conventional 20-minute procedure.

Multiplex molecular POCT analysis of clinical mycobacterial cultures

Of the 149 clinical mycobacterial cultures analyzed in the study, 15 mycobacterial species were identified by 16S rRNA sequencing. The results of *fastNTM* evaluation are presented in Tables 2, 3. A total of 145 cultures were positive detected by *fastNTM*, and 16 cultures showed discrepancies with the established identification results. Among these, cultures of *M. lentiflavum* and *M. shinjukuense* were not detected by *fastNTM*. Cultures of *M. malmoense* and *M. paragordonae* were mis-identified as *M. fortuitum* and *M. gordonae*, respectively. Cultures of *M. colombiense* and *M. marseillense* were identified as *M. intracellulare*. Additionally, one culture of *M. kansasii* were not detected by *fastNTM*, and 2 *M. intracellulare* were identified as *M. avium* (Table 2).

Among the 149 cultures, 2 were identified for multiple mycobacterial species by *fastNTM*. Thus, subcultures were performed to obtain single colony. A follow-up 16S rRNA sequencing were identified individually for those single species. The identification results for these sub-cultures showed consistent with *fastNTM*.

Results of 136 cultures confirmed by 16S rRNA identification were within the detection range of this panel, account for 91.28%. Among these 136 cultures, *fastNTM* results of 133 cultures showed concordant identification with the sequencing data, achieving an overall accuracy rate of 97.79%. The sensitivity and specificity of *fastNTM* for each targeted species were showed in Table 3. The specificities of all 9 targets were above 95%. Except for *M. kansasii*, the remaining 8 targets showed sensitivities above 96%.

Discussion

Here we introduced a multiplex molecular point-of-care panel that utilizes one minute of sample processing to simultaneously detect the presence of eight clinically dominant NTM species and MTBC was developed. This method allows for the amplification of multiple targets in a single reaction by using differentially labeled probes for each target. Asymmetric PCR ensures that one strand of the target DNA is preferentially amplified, which enhances the efficiency of probe hybridization. The MMCA then allows for the differentiation of these targets based on their unique melting temperatures. The assay employs an ultrafast sample pretreatment method, reducing the conventional 20-minute process, and achieves automated PCR detection and result analysis within 90 minutes from patient to result. This streamlined protocol achieved an overall accuracy rate of 97.79%.

In this study, the selection of eight prevalent NTM species was primarily based on strain isolation rates (Huang et al., 2020) and epidemiological investigations. Our selection took into account both isolation frequency and clinical pathogenicity. However, this approach may have led to the omission of some clinically significant but less prevalent NTM species, or the inclusion of those with high isolation rates but lower clinical relevance. Our goal is to quickly provide the most probable TB/NTM results to clinicians. This aids in rapid screening and diagnosis, particularly for slowly growing NTM. Among these, *M. marinum* and *M. ulcerans* with high phylogenetic relatedness (i.e., >99.8% 16S rRNA sequence similarity) (Röltgen et al., 2012) were not differentiated in this study. While infections due to *M. marinum* can usually be treated with antimycobacterial drugs, very few cases of *M. ulcerans* infection respond favorably to antimicrobial therapy (Franco-Paredes et al., 2018). One of limitations of this study is that, differentiation of these two species needs further test such as whole-genome method.

In this study we utilized ITS as the target for MTBC and NTM detection. However, when it comes to species-level identification of more NTMs, the ITS region does have certain limitations. For instance, five samples initially identified as *M. fortuitum* by *fastNTM* were later confirmed to be *M. mageritense* through

TABLE 2 Identification of clinical mycobacterial cultures.

16S rRNA-identified Results	Number of cultures	Number of *fastNTM*-matched cultures	Description of mismatches
M. intracellulare	61	59	2 identified as *M. avium* by *fastNTM*
M. abscessus	34	34	
M. avium	12	12	
M. fortuitum	11	11	
M. gordonae	7	7	
M. kansasii	6	5	1 undetected by *fastNTM*
M. mageritense	6	0	identified as *M. fortuitum*, not the target of *fastNTM*
M. paragordonae	2	0	identified as *M. gordonae*, not the target of *fastNTM*
M. lentiflavum	2	0	negative result, not the target of *fastNTM*
M. intracellulare & *M. gordonae*	1	1	
M. intracellulare & *M. abscessus*	1	1	
M. marinum/ulcerans	1	1	
M. tuberculosis	1	1	
M. scrofulaceum	1	1	
M. colombiense	1	0	identified as *M. intracellulare*, not the target of *fastNTM*
M. marseillense	1	0	identified as *M. intracellulare*, not the target of *fastNTM*
M. shinjukuense	1	0	negative result, not the target of *fastNTM*

hsp65 gene sequencing. To achieve more precise differentiation, additional genes such as *hsp65*, *sodA*, *recA*, and *rpoB* are recommended for NTM identification (Adékambi and Drancourt, 2004). Moving forward, if our research involves the identification of a broader range of NTM species, we will incorporate more genes into our primer design to enhance the accuracy and specificity of our detection method.

All nine detection targets in our study demonstrated specificities above 95%, indicating a high level of accuracy in identifying the targeted mycobacterial species. Except for *M. kansasii*, the remaining eight targets showed sensitivities above 96%, which is a significant benchmark for effective diagnostic testing. However, it is important to note that the sample sizes for *M. kansasii*, *M. marinum*/*ulcerans* and *M. scrofulaceum* were less than ten, which could potentially impact the statistical confidence of the sensitivity analysis for these specific targets. This consideration is crucial as smaller sample sizes can lead to less precise estimates of sensitivity and specificity, and may not fully capture the performance characteristics of the detection targets. Therefore, while the high specificity and sensitivity rates are promising, further testing with larger sample sizes for these four targets is necessary to confirm the observed performance metrics.

Besides, among all misidentifications observed in the study, several non-targeted mycobacterial species were incorrectly identified. Specifically, six strains of *M. mageritense*, not within the target range of our assay, were incorrectly identified as *M. fortuitum*. *M. mageritense* was first discovered in 1997 and further study showed its phenotypic and clinical similarity to isolates of the *M. fortuitum* third biovariant complex (sorbitol positive) (Wallace et al., 2002). Without specific method, isolates of *M. mageritense* are likely to go undetected. Two strains of *M. paragordonae* were identified as *M. gordonae*. *M. paragordonae* is an emerging pathogen in human pulmonary disease, first discovered in 2014 (Li et al., 2022). The phylogenetic tree of the 16S rRNA gene sequences showed that the *M. paragordonae* isolates were most closely related to the *M. gordonae* ATCC 14470 T strain, with up to a 99.0% gene match; however, the DNA–DNA affinity comparison between those two isolates was only 46.52%. One strain each of *M. marseillense* and *M. colombiense* were identified as *M. avium*. Both species belong to the *M. avium* complex (MAC). *M. marseillense* was firstly described as a new species within the MAC in 2009 (Salah et al., 2009). One strain of *M. shinjukuense* and two strains of *M. lentiflavum*, which do not belong to MAC, were identified as negative. These misidentifications underscore the complexities in differentiating between closely related mycobacterial species and the necessity for continuous refinement of diagnostic assays to enhance specificity and inclusivity.

To date, in our country, there are three certified commercially available kits for NTM species identification, including the CapitalBio Mycobacterium identification array assay (CapitalBio Corp., Beijing), PCR-REBA Myco-ID assay (Yaneng BioSciences,

TABLE 3 Statistical results of *fastNTM* compared with reference results.

Species	True positive	False positive	False negative	True negative	Kappa	SE of kappa	95% CI	sensitivity	specificity
M. intracellulare	61	2	2	84	0.945	0.027	0.892-0.998	0.9683	0.9767
M. abscessus	35	0	0	114	1	0	1.0-1.0	1	1
M. avium	12	2	0	135	0.916	0.059	0.8-1.0	1	0.9854
M. fortuitum	11	6	0	132	0.765	0.091	0.585-0.944	1	0.9565
M. gordonae	8	2	0	139	0.882	0.082	0.72-1.0	1	0.9858
M. kansasii	5	0	1	143	0.906	0.904	0.722-1.0	0.8333	1
M. marinum/ ulcerans	1	0	0	148	1	0	1.0-1.0	1	1
M. tuberculosis	1	0	0	148	1	0	1.0-1.0	1	1
M. scrofulaceum	1	0	0	148	1	0	1.0-1.0	1	1

*SE: standard error.

Shenzhen), and the MeltPro Myco assay (Zeesan Biotech, Xiamen). While these kits offer advantages in terms of the number of species they can identify, they are limited by complex manual operations and varying clinical relevance. CapitalBio Mycobacterium identification array assay uses DNA microarray technology to identify 17 species of mycobacteria. However, it requires samples to be cultured and confirmed as mycobacterial positives before further species identification (Liu et al., 2012). PCR-REBA Myco-ID assay, based on 16S rRNA sequencing and nucleic acid probes with reverse blot hybridization, can identify 22 species of mycobacteria (Zhang et al., 2021). The entire detection process requires a total of 6 hours. Those two kits are more laborious compared to PCR-based methods due to the complex manual operations involved in DNA hybridization.

MeltPro Myco Assay uses multicolor melting curve analysis to identify 19 clinically relevant mycobacterial species. While it offers a higher number of identifiable species (19 vs. 9) and a lower limit of detection (300 CFU/mL vs. 500 CFU/mL), it still requires extensive sample preparation. The patient's sputum must undergo decontamination, neutralization, centrifugation, resuspension, and DNA extraction before the final DNA detection. The turnaround time for this qPCR-based method is within 3 hours, compared to our 90-minute process (Xu et al., 2019). Besides, the qPCR instrument requires the capability to perform PCR-high resolution melting (PCR - HRM) analysis. Our fastNTM assay addresses these limitations by offering a streamlined, rapid, and clinically relevant detection method. It enables direct detection of TB and NTM from raw patient samples within 90 minutes, significantly improving the speed and reliability of mycobacterial identification in clinical settings.

In this study, among the 149 mycobacterial-positive cultures, 43 (28.86%; 43/149) showed negative smear results despite being positive in the MGIT system. According to our hospital's protocol, further sub-culture on Löwenstein-Jensen medium was performed for these MGIT960-positive cultures. This means that for these 43 samples, there are an average delay of 15.59 ± 10.38 days in confirming NTM positivity for these samples, with a median delay of 12.5 days and the longest extension reaching 41 days after MGIT960 positive-alert. Notably, all 43 of these cultures were detected by *fastNTM*, without the need for further cultivation. Excluding four samples that were outside the target range, f*astNTM* achieved a 100% accuracy rate in detecting these cultures (Supplementary Material, Information of NTM.xlsx). This highlights the superior sensitivity and efficiency of f*astNTM* in identifying NTM-positive samples compared to traditional smear methods.

Additionally, the ultrafast sample pretreatment procedure introduced here that requires only one minute, significantly enhancing overall detection efficacy. For instance, in our tests, the LoD for MTBC is 50 copies. However, in pure bacterial suspensions without a negative sputum matrix, a concentration of 40 copies can achieve 100% detection after undergoing the sample pretreatment. In contrast, untreated suspensions resulted in four instances of no detection. Experimental results compared with GeneXpert confirm that the detection efficiency achieved with this one-minute preprocessing is comparable to that of conventional 20-minute process. This advancement not only streamlines the diagnostic workflow but also improves the speed and reliability of NTM identification in clinical settings. Our approach offers a significant advancement in the field by enabling direct detection of TB and NTM from raw patient samples within 90 minutes. This represents a major improvement over traditional culture methods, which typically require at least ten days or more. The *fastNTM* technology not only accelerates the diagnostic process but also enhances sensitivity and specificity, as demonstrated.

In conclusion, the multiplex detection capability of *fastNTM* enables the simultaneous identification of multiple targets in a single reaction. This feature is especially advantageous in clinical settings, where rapid and accurate diagnosis is essential for effective patient management. The ability to quickly detect MTB and NTM

empowers physicians to make critical decisions regarding patient care and therapy during a single medical encounter, thereby enhancing the efficiency and efficacy of treatment.

Data availability statement

Data available on request due to ethical restrictions.

Ethics statement

The study was conducted in accordance with the Declaration of Helsinki, and granted a waiver of informed consent. Only de-identified clinically obtained bacterial isolates were used in this study. No human subjects participated in this study. The patient's clinical information didn't include identifiable information such as the patient's name, ID card, and so on. It was approved by the Research Ethics Committee of Peking Union Medical College Hospital, Chinese Academy of Medical Sciences (reference number HS-3136, September 2021).

Author contributions

QY: Conceptualization, Data curation, Formal Analysis, Investigation, Methodology, Validation, Visualization, Writing – original draft, Writing – review & editing. YW: Data curation, Formal Analysis, Investigation, Methodology, Validation, Visualization, Writing – original draft, Writing – review & editing. SH: Writing – original draft, Writing – review & editing. MF: Writing – original draft, Writing – review & editing. XL: Writing – original draft, Writing – review & editing. XZ: Writing – original draft, Writing – review & editing. HG: Writing – original draft, Writing – review & editing. YZ: Writing – original draft, Writing – review & editing. QY: Writing – original draft, Writing – review & editing. YX: Writing – original draft, Writing – review & editing.

Funding

The author(s) declare financial support was received for the research and/or publication of this article. The work was supported by grants from National High Level Hospital Clinical Research Funding (2022-PUMCH-B-074) and Peking Union Medical College Hospital Talent Cultivation Program - Category D (No.UHB12289).

Acknowledgments

All authors made substantial contributions to conception and design, acquisition of data, or analysis and interpretation of data and took part in drafting the article or revising it critically for important intellectual content. And all authors have read and agreed to the published version of the manuscript.

Conflict of interest

Q-LY, Y-CX, and M-LF are coinventors of the rapid sample pretreatment process employing ultrasound-assisted enzymatic homogenization, for which a patent has been filed by China National Intellectual Property Administration 202310961352.2. Q-LY, YW, Y-CX, Q-WY, X-YL, SH, M-LF, and Y-FZ are coinventors of the invention relates to primer probe combination, kit, identification method and application of mycobacterium species identification, for which a patent has been filed by China National Intellectual Property Administration 2025100224462. SH, M-LF, and Y-FZ are employees of Genewise Bio Co., Ltd, a company that commercializes the technology and intellectual property described herein.

The remaining author declares that the research was conducted in the absence of any commercial or financial relationships that could be construed as a potential conflict of interest.

Generative AI statement

The author(s) declare that no Generative AI was used in the creation of this manuscript.

Publisher's note

All claims expressed in this article are solely those of the authors and do not necessarily represent those of their affiliated organizations, or those of the publisher, the editors and the reviewers. Any product that may be evaluated in this article, or claim that may be made by its manufacturer, is not guaranteed or endorsed by the publisher.

Supplementary material

The Supplementary Material for this article can be found online at: https://www.frontiersin.org/articles/10.3389/fcimb.2025.1560870/full#supplementary-material

References

Adékambi, T., and Drancourt, M. (2004). Dissection of phylogenetic relationships among 19 rapidly growing Mycobacterium species by 16S rRNA, hsp65, sodA, recA and rpoB gene sequencing. *Int. J. Syst. Evol. Microbiol.* 54, 2095–2105. doi: 10.1099/ijs.0.63094-0

Alcaide, F., Amlerová, J., Bou, G., Ceyssens, P. J., Coll, P., Corcoran, D., et al. (2018). How to: identify non-tuberculous Mycobacterium species using MALDI-TOF mass spectrometry. *Clin. Microbiol. Infection* 24, 599–603. doi: 10.1016/j.cmi.2017.11.012

Canetti, D., Riccardi, N., Antonello, R. M., Nozza, S., and Sotgiu, G. (2022). Mycobacterium marinum: A brief update for clinical purposes. *Eur. J. Intern. Med.* 105, 15–19. doi: 10.1016/j.ejim.2022.07.013

Chang, H.-Y., Tsai, W.-C., Lee, T.-F., and Sheng, W.-H. (2021). Mycobacterium gordonae infection in immunocompromised and immunocompetent hosts: A series of seven cases and literature review. *J. Formosan Med. Assoc.* 120, 524–532. doi: 10.1016/j.jfma.2020.06.029

Cristancho-Rojas, C., Varley, C. D., Lara, S. C., Kherabi, Y., Henkle, E., and Winthrop, K. L. (2024). Epidemiology of mycobacterium abscessus. *Clin. Microbiol. Infection* 30, 712–717. doi: 10.1016/J.CMI.2023.08.035

Dahl, V. N., Mølhave, M., Fløe, A., van Ingen, J., Schön, T., Lillebaek, T., et al. (2022). Global trends of pulmonary infections with nontuberculous mycobacteria: a systematic review. *Int. J. Infect. Dis.* 125, 120–131. doi: 10.1016/j.ijid.2022.10.013

Elenitoba-Johnson, K. S. J., Bohling, S. D., Wittwer, C. T., and King, T. C. (2001). Multiplex PCR by multicolor fluorimetry and fluorescence melting curve analysis. *Nat. Med.* 7, 249–253. doi: 10.1038/84708

Forbes, B. A., Hall, G. S., Miller, M. B., Novak, S. M., Rowlinson, M.-C., Salfinger, M., et al. (2018). Practical guidance for clinical microbiology laboratories: mycobacteria. *Clin. Microbiol. Rev.* 31, 1–66. doi: 10.1128/CMR.00038-17

Franco-Álvarez De Luna, F., Ruiz, P., Gutiérrez, J., and Casal, M. (2006). Evaluation of the GenoType mycobacteria direct assay for detection of Mycobacterium tuberculosis complex and four atypical mycobacterial species in clinical samples. *J. Clin. Microbiol.* 44, 3025–3027. doi: 10.1128/JCM.00068-06

Franco-Paredes, C., Marcos, L. A., Henao-Martínez, A. F., Rodríguez-Morales, A. J., Villamil-Gómez, W. E., Gotuzzo, E., et al. (2018). Cutaneous mycobacterial infections. *Clin. Microbiol. Rev.* 32(1), e00069-18. doi: 10.1128/CMR.00069-18

Gopalaswamy, R., Shanmugam, S., Mondal, R., and Subbian, S. (2020). Of tuberculosis and non-tuberculous mycobacterial infections - A comparative analysis of epidemiology, diagnosis and treatment. *J. BioMed. Sci.* 27, 1–17. doi: 10.1186/s12929-020-00667-6

Hoefsloot, W., van Ingen, J., Andrejak, C., Ängeby, K., Bauriaud, R., Bemer, P., et al. (2013). The geographic diversity of nontuberculous mycobacteria isolated from pulmonary samples: an NTM-NET collaborative study. *Eur. Respir. J.* 42, 1604–1613. doi: 10.1183/09031936.00149212

Huang, J., Li, Y., Zhao, Y., Yang, W., Xiao, M., Kudinha, T., et al. (2020). Prevalence of nontuberculous mycobacteria in a tertiary hospital in Beijing, China, January 2013 to December 2018. *BMC Microbiol.* 20, 158. doi: 10.1186/s12866-020-01840-5

Kim, S.-Y., Mi Moon, S., Woo Jhun, B., Jung Kwon, O., Jae Huh, H., Yong Lee, N., et al. (2019).Species Distribution and Macrolide Susceptibility of Mycobacterium fortuitum Complex Clinical Isolates. *Antimicrob Agents Chemother*. 63, 10.1128/aac.02331-18. doi: 10.1128/aac.02331-18

Kumar, K., and Loebinger, M. R. (2022). Nontuberculous mycobacterial pulmonary disease: clinical epidemiologic features, risk factors, and diagnosis: the nontuberculous mycobacterial series. *Chest* 161, 637–646. doi: 10.1016/j.chest.2021.10.003

Li, Y., Zhang, W., Zhao, J., Lai, W., Zhao, Y., Li, Y., et al. (2022). Mycobacterium paragordonae is an emerging pathogen in human pulmonary disease: clinical features, antimicrobial susceptibility testing and outcomes. *Emerg. Microbes Infect.* 11, 1973–1981. doi: 10.1080/22221751.2022.2103453

Liu, J., Yue, J., Yan, Z., Han, M., Han, Z., Jin, L., et al. (2012). Performance assessment of the CapitalBio Mycobacterium identification array system for identification of mycobacteria. *J. Clin. Microbiol.* 50, 76–80. doi: 10.1128/JCM.00320-11

LPSN (2025). Available online at: https://www.bacterio.net/genus/mycobacterium (Accessed March 19, 2025).

Mitarai, S., Kato, S., Ogata, H., Aono, A., Chikamatsu, K., Mizuno, K., et al. (2012). Comprehensive multicenter evaluation of a new line probe assay kit for identification of Mycobacterium species and detection of drug-resistant Mycobacterium tuberculosis. *J. Clin. Microbiol.* 50, 884–890. doi: 10.1128/JCM.05638-11

Ngan, G. J. Y., Ng, L. M., Jureen, R., Lin, R. T. P., and Teo, J. W. P. (2011). Development of multiplex PCR assays based on the 16S-23S rRNA internal transcribed spacer for the detection of clinically relevant nontuberculous mycobacteria. *Lett. Appl. Microbiol.* 52, 546–554. doi: 10.1111/j.1472-765X.2011.03045.x

Nguyen, M.-V. H., Haas, M. K., Kasperbauer, S. H., Calado Nogueira de Moura, V., Eddy, J. J., Mitchell, J. D., et al. (2024). Nontuberculous mycobacterial pulmonary disease: patients, principles, and prospects. *Clin. Infect. Dis.* 79, e27–e47. doi: 10.1093/cid/ciae421

Omar, S. V., Roth, A., Ismail, N. A., Erasmus, L., Ehlers, M., Kock, M., et al. (2011). Analytical performance of the roche Lightcycler® Mycobacterium detection kit for the diagnosis of clinically important mycobacterial species. *PloS One* 6(9), e24789. doi: 10.1371/journal.pone.0024789

Opota, O., Senn, L., Prod'hom, G., Mazza-Stalder, J., Tissot, F., Greub, G., et al. (2016). Added value of molecular assay Xpert MTB/RIF compared to sputum smear microscopy to assess the risk of tuberculosis transmission in a low-prevalence country. *Clin. Microbiol. Infection* 22, 613–619. doi: 10.1016/j.cmi.2016.04.010

Pasipanodya, J. G., Ogbonna, D., Deshpande, D., Srivastava, S., and Gumbo, T. (2017). Meta-analyses and the evidence base for microbial outcomes in the treatment of pulmonary Mycobacterium avium-intracellulare complex disease. *J. Antimicrobial Chemotherapy* 72, ii3–ii19. doi: 10.1093/jac/dkx311

Ratnatunga, C. N., Lutzky, V. P., Kupz, A., Doolan, D. L., Reid, D. W., Field, M., et al. (2020). The rise of non-tuberculosis mycobacterial lung disease. *Front. Immunol.* 11. doi: 10.3389/fimmu.2020.00303

Röltgen, K., Stinear, T. P., and Pluschke, G. (2012). The genome, evolution and diversity of Mycobacterium ulcerans. *Infection Genet. Evol.* 12, 522–529. doi: 10.1016/j.meegid.2012.01.018

Salah, I.B., Cayrou, C., Raoult, D., and Drancourt, M. (2009). Mycobacterium marseillense sp. nov., Mycobacterium timonense sp. nov. and Mycobacterium bouchedurhonense sp. nov.,members of the Mycobacterium avium complex. *Int. J. Syst. Evol. Microbiol.* 59, 2803–2808. doi: 10.1099/ijs.0.010637-0

Schwab, T. C., Perrig, L., Göller, P. C., Guebely de la Hoz, F. F., Lahousse, A. P., Minder, B., et al. (2024). Targeted next-generation sequencing to diagnose drug-resistant tuberculosis: a systematic review and meta-analysis. *Lancet Infect. Dis.* 24, 1162–1176. doi: 10.1016/S1473-3099(24)00263-9

Suzuki, S., Morino, E., Ishii, M., Namkoong, H., Yagi, K., Asakura, T., et al. (2016). Clinical characteristics of pulmonary Mycobacterium scrofulaceum disease in 2001–2011: A case series and literature review. *J. Infection Chemotherapy* 22, 611–616. doi: 10.1016/j.jiac.2016.06.006

Tan, Y., Deng, Y., Yan, X., Liu, F., Tan, Y., Wang, Q., et al. (2021). Nontuberculous mycobacterial pulmonary disease and associated risk factors in China: A prospective surveillance study. *J. Infection* 83, 46–53. doi: 10.1016/j.jinf.2021.05.019

Van der Werf, T. S., van der Graaf, W. T., Tappero, J. W., and Asiedu, K. (1999). Mycobacterium ulcerans infection. *Lancet* 354, 1013–1018. doi: 10.1016/S0140-6736(99)01156-3

Wallace, R. J., Brown-Elliott, B. A., Hall, L., Roberts, G., Wilson, R. W., Mann, L. B., et al. (2002). Clinical and laboratory features of mycobacterium mageritense. *J. Clin. Microbiol.* 40, 2930–2935. doi: 10.1128/JCM.40.8.2930-2935.2002

Wilson, J. W., Jagtiani, A. C., and Wengenack, N. L. (2019). Mycobacterium scrofulaceum disease: experience from a tertiary medical centre and review of the literature. *Infect. Dis.* 51, 602–609. doi: 10.1080/23744235.2019.1634281

Xu, Y., Liang, B., Du, C., Tian, X., Cai, X., Hou, Y., et al. (2019). Rapid identification of clinically relevant mycobacterium species by multicolor melting curve analysis. *J. Clin. Microbiol.* 57, 1–12. doi: 10.1128/JCM.01096-18

Zhang, Q., Xiao, H., and Yan, L. (2021). PCR-reverse blot hybridization assay in respiratory specimens for rapid detection and differentiation of mycobacteria in HIV-negative population. *BMC Infect. Dis.* 21 (1), 264. doi: 10.1186/s12879-021-05934-x

frontiers | Frontiers in Cellular and Infection Microbiology

TYPE Original Research
PUBLISHED 10 October 2025
DOI 10.3389/fcimb.2025.1572936

OPEN ACCESS

EDITED BY
Diana Manolescu,
Victor Babes University of Medicine and Pharmacy, Romania

REVIEWED BY
Jia-Yuh Chen,
Chung Shan Medical University, Taiwan
Jill Roberts,
University of South Florida, United States

*CORRESPONDENCE
Dhammika H. Navarathna
dhammika.navarathna@va.gov

RECEIVED 07 February 2025
ACCEPTED 19 September 2025
PUBLISHED 10 October 2025

CITATION
Berger B, Lukey J, Jinadatha C and Navarathna DH (2025) Impact of discontinuing automatic reflex urine culture after urinalysis: a diagnostic and antibiotic stewardship initiative. *Front. Cell. Infect. Microbiol.* 15:1572936. doi: 10.3389/fcimb.2025.1572936

Impact of discontinuing automatic reflex urine culture after urinalysis: a diagnostic and antibiotic stewardship initiative

Blaine Berger[1,2], Janell Lukey[1], Chetan Jinadatha[3,4] and Dhammika H. Navarathna[1*]

[1]Department of Pathology and Laboratory Medicine Services, Central Texas Veterans Health Care System, Temple, TX, United States, [2]Department of Pathology and Laboratory Medicine, Baylor Scott & White Medical Center, Temple, TX, United States, [3]Department of Medicine, Central Texas Veterans Health Care System, Temple, TX, United States, [4]Department of Medical Education, School of Medicine, Texas A&M University, Bryan, TX, United States

Introduction: This study aims to assess the impact of discontinuing reflex urine cultures based on urinalysis results (positive for nitrates and/or leukocyte esterase) on diagnostics,antibiotic usage, and laboratory efficiency at the Central Texas Veterans' HealthCare System (CTVHCS). It seeks to evaluate whether stopping reflex testing reducesunnecessary antibiotic use, enhances antibiotic stewardship, and improves theprocessing of clinically relevant specimens.

Methods: A 6-year retrospective analysis was conducted, comparing data from 3 years before and 3 years after the 2018 policy change, which discontinued reflex urine culture unless specifically requested by healthcare providers suspecting urinary tract infection (UTI) symptoms. The study analyzed the number of processed urine cultures, positivity for uropathogens, and antibiotic usage trends before and after the policy change.

Results: The policy change resulted in a significant reduction in processed urine cultures. There was also a notable decrease in ciprofloxacin usage and an increase in the use of nitrofurantoin,indicating a shift towards narrower-spectrum antibiotics.

Discussion: Stopping reflex testing reduced the lab burden by focusing on clinically relevant cases of UTIs and supported improved antibiotic stewardship. This enabled healthcare providers toselectively order culture and sensitivity, targeting true UTIs.

KEYWORDS

asymptomatic bacteriuria, urinalysis reflex, UTI, uropathogen, urine culture

1 Introduction

Urinary tract infections (UTIs) due to bacterial pathogens are a very common global issue that draws more than 10 million physicians' visits and approximately 2 million emergency department visits annually (Schappert and Rechtsteiner, 2011). The most common organisms causing UTIs are *Escherichia coli*, *Enterococcus*, *Klebsiella*, *Enterobacter*, and *Proteus* spp., along with *Staphylococcus saprophyticus* and *Streptococcus agalactiae* (GBS) (Yarbrough; Flores-Mireles et al., 2015).

Early detection of UTI and its etiology along with antibiotic susceptibility helps providers with better patient management. The appropriate method to diagnose UTI is by performing laboratory culture and sensitivity testing of urine samples submitted from patients exhibiting UTI symptoms such as dysuria, urgency, and frequency, which may be associated with systemic symptoms such as fever and chills (Hooton and Stamm, 1997). Laboratory practices and algorithms largely vary across the country. In most hospitals in the USA, after a provider orders a urinalysis (UA) for non-UTI-related conditions, the urine is often automatically reflexed for culture and sensitivity based on hospital-specific criteria (Advani et al., 2019). This usually occurs when abnormalities are detected in leukocyte esterase, nitrite, or white blood cell (WBC) count, to rule out a UTI. There are no prescribed standard/s for urine reflex testing, and each individual healthcare facility makes their own policy for what is the best practice for their patient population and their available laboratory resources. Sometimes, the local laboratory practices conflict with diagnostic and antibiotic stewardship practices at the facility and successful diagnostic stewardship interventions are based on local patient populations and individual patient-based interventions (Advani and Vaughn, 2021).

The Veterans Affairs (VA) healthcare systems including our institution, similar to many other institutions, historically adopted UA with reflex to culture as a strategy to improve the diagnosis of UTIs. This approach was reported to be useful in emergency departments (EDs), where rapid decision-making is critical, making early urine sample collection and processing advantageous (Chironda et al., 2014). Additionally, in adult intensive care units (ICUs), reflex urine culturing has been associated with a reduction in the number of urine cultures ordered, although its impact in other clinical areas remains uncertain (Sarg et al., 2016). Despite limited setting-specific data and variable patient populations, many healthcare systems continue to rely on the UA reflex to culture method as a standard diagnostic protocol (Advani and Vaughn, 2021). Our institution undertook a process improvement policy change at reducing inappropriate treatment of asymptomatic bacteriuria focusing on optimizing urine test utilization. Our hospital has a strong antibiotic stewardship working group composed of infectious disease (ID) physicians, clinical pharmacists, an infection preventionist, and a microbiologist. ID specialists raised the issue of indiscriminate antibiotics used for asymptomatic bacteriuria and suggested the possibility of UA reflex hard stop. As our pregnant patient population is very low, the lab agreed to pursue this. Our microbiology lab classifications and workup of potential uropathogens in nonsterile urines are based on the Clinical Microbiology Procedures Handbook. Gram-negative Bacilli, *Staphylococcus aureus*, *Enterococcus* spp., beta-hemolytic *Streptococcus, Neisseria gonorrhoeae*, and yeasts are considered uropathogens (Yarbrough).

Here, we describe the effect of policy change to discontinue reflex urine testing from all positive UA samples in our facility. Five years post policy change, we examined our retrospective data to understand the impact of our process improvement measures on both diagnostic and antibiotic stewardship fronts.

2 Material and methods

2.1 Facility

The Central Texas Veterans' Health Care System (CTVHCS) provides healthcare services at 11 locations serving central Texas. Our hospitals are the Olin E. Teague Veterans Medical Center in Temple and the Doris Miller VA Medical Center in Waco. We also operate a stand-alone multispecialty clinic in Austin, and nine community-based outpatient clinics in various small cities in central Texas locality. We serve approximately 250,000 patients in 39 counties in central Texas.

2.2 Study material and samples

2.2.1 Sample collection and processing

Midstream, clean-catch urine specimens were collected in sterile, wide-mouthed, leak-proof containers according to standard microbiological procedures. Samples were transported to the laboratory within 2 h of collection, or stored at 4 °C and processed within 24 h when immediate inoculation was not feasible.

2.2.2 Primary culture

Each urine specimen was mixed thoroughly, and 1 µL of uncentrifuged urine was inoculated onto UriSelect™ chromogenic agar (Bio-Rad, France) using a calibrated loop. Plates were incubated aerobically at 35 ± 2 °C for 18–24 h. Colony counts were recorded as colony-forming units per milliliter (CFU/mL) and interpreted according to established diagnostic thresholds.

2.2.3 Colony morphology and preliminary identification

Chromogenic reactions on UriSelect agar were observed for preliminary differentiation of bacterial species based on colony color and morphology (e.g., *Escherichia coli*—pink to burgundy colonies; *Enterococcus* spp.—turquoise colonies; *Klebsiella*, *Enterobacter*, and *Citrobacter*—blue colonies; *Proteus* spp.—brown colonies). Mixed cultures were noted and isolated further as required.

2.2.4 Definitive identification by MALDI-TOF MS

Representative colonies were subjected to species-level identification using MALDI-TOF mass spectrometry (MS Prime system) (bioMérieux, France).

2.2.5 Antimicrobial susceptibility testing

Isolates were subjected to antimicrobial susceptibility testing (AST) using the Vitek 2 system (bioMérieux, France). A 0.5 McFarland standard suspension was prepared in sterile saline and inoculated into appropriate Vitek 2 AST cards (e.g., GN or GP panels depending on organism type).

All urine culture testing is done at the central microbiology laboratory located at our main campus in Temple, TX. Specimen requirement by the lab is clean-catch or catheterized urine samples to be transported to the laboratory as soon as possible. If a delay in transport is expected, the specimen may be transferred to a preservative tube that may be held at room temperature or refrigerated for up to 48 h. Urine specimens are held refrigerated for 2 days after setting up for culture and susceptibility testing. A urine culture is considered positive if it grows up to two organisms >10 colonies in our lab using 1 µL of inoculating loop (1×10^4/mL). For freshly voided urine, a culture of ≥100 CFU (1×10^5/mL) from a single organism type is considered the cutoff. If the CFU range is between 10 and 100, evaluation will be based on the specimen type and clinical status. Samples will not be worked up for less than 10 CFUs except for cystoscopic or kidney/suprapubic aspirates. As part of continuous process improvement, in August 2014, we switched to nonselective chromogenic culture medium from a conventional culture method to process urine samples. This was considered more time-saving with reliable detection, easy enumeration, presumptive identification, and easy recognition of mixed cultures (Hengstler et al., 1997).

CTVHCS uses the Sysmex UN-series, an automated UA system for screening and initial clinical workup of a variety of renal and lower urinary tract disorders. From late 2013 to mid-August 2018, our central lab located at the Olin E. Teague Veterans Medical Center in Temple, TX received urine specimens showing positive UA results for nitrates, and/or leukocyte esterase, which were subsequently subjected to reflex culture and sensitivity. Negative reflex cultures would be reported with "no significant bacterial growth" while positive cultures would be reported with ID and sensitivity with a comment entered as "CLO" (culture indicated by UA, laboratory ordered) on the laboratory order. In 2018, reflex testing was abandoned in favor of provider-requested urine culture. Since 6 August 2018, the hospital's microbiology lab has ceased performing reflex urine cultures. According to the guidelines of the United States Preventive Services Task Force, screening for asymptomatic bacteriuria is only recommended for pregnant women (Henderson and Bean, 2019). This recommendation is mirrored by the latest IDSA Clinical Practice Guideline for the Management of Asymptomatic Bacteriuria except in older persons residing in long-term care facilities (Nicolle et al., 2019). All our pregnant women and veterans in long-term care are examined by the women's clinic or their providers who directly ordered urine culture and sensitivity testing. Consequently, leukocyte esterase- and nitrite-positive UA results were no longer reflexively sent for culture and sensitivity testing, and the "CLO" comment was not included in patient charts. A laboratory memo was distributed to all providers to notify them of the changes made, informing them not to assume that UA will automatically reflex for future cultures and emphasizing the requirement to place a separate culture order for suspected UTIs.

2.3 Data collection

Using the patient electronic medical record system and TheraDoc (Premier, Inc., Charlotte, NC), an electronic clinical surveillance system, positive urine culture results were collected. We examined retrospective urine culture results for the 3 years before and 3 years after July 2018, which marks an inflection point where UA reflex to culture ceased. To analyze the impact on antibiotic utilization, we collected data on patients diagnosed as having UTI and treated with antibiotics (dose per patient) 3 years before and 3 years after July 2018. The hospital antibiotic usage percentages for UTI therapy before and after the policy decision are depicted in Figure 1.

2.4 Statistics analysis

Analysis of contingency tables with major uropathogens (Table 1) was performed by using the chi-square test and antibiotic usage trend using Fisher's exact test in GraphPad Prism version 10.1.2 for Windows (GraphPad Software, San Diego, CA; www.graphpad.com).

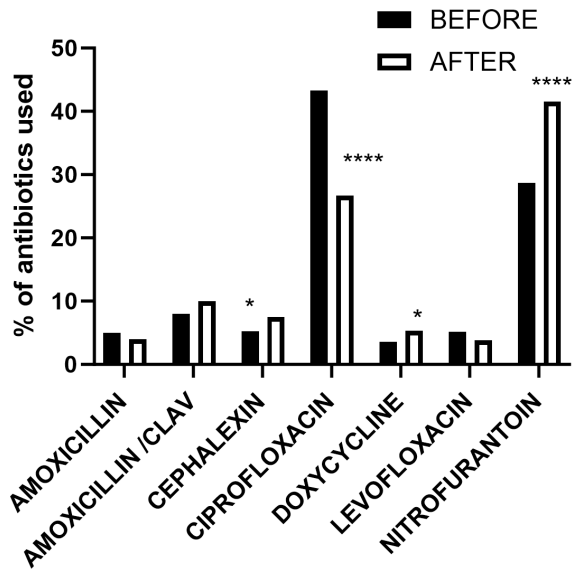

FIGURE 1
Patient's records of administered or prescribed antibiotics dose regimen per patient in the 3 years preceding and following the implementation of hard stop urine reflex policy. *$p < 0.05$; ****$p < 0.0001$.

10.3389/fcimb.2025.1572936

TABLE 1 Total number of real uropathogens reported from the urine culture and sensitivity (C&S) workup in 3 years before and 3 years after the hard stop on urinalysis reflex to culture and percent reduction.

Uropathogen	# Pre-decision urine C&S	# Post-decision urine C&S	% Reduction
S.agalactia	768	187	76
S.aureus	309	92	70
E faecalis	1840	742	60
E coli	4794	2310	52
K. pneumoniae	968	666	31
P mirabilis	564	300	47

is shorten abbreviation for number.

3 Results

3.1 Comparison of all urine cultures ordered pre and post 3 years from stop reflex decision

We examined the total number of urine culture orders received at the microbiology lab for culture and sensitivity for 3 years before and 3 years after July 2018. Three years before the policy change, our microbiology lab processed 47,288 total urine samples. In the subsequent 3 years following the intervention, the number of samples processed dramatically reduced to 27,366 urine samples, which is a 42% decline.

3.2 Comparison of all positive urine cultures reported pre and post 3 months from stop reflex decision

First, we examined all reported positive urine cultures 3 months pre and post decision date, spanning a total of 6 months (Table 2). We noticed a huge reduction in the number of urine cultures processed in our laboratory. Our lab reported 1,511 positive urine cultures during the 3 months immediately before the policy was changed to stop reflex-based UA reports. Three months after implementing the new policy, the lab only reported 409 positive urine cultures. Reports of positive cultures from normal flora in the urine show that the *Lactobacillus* and *Streptococcus* viridans group had a dramatic reduction from 47 and 41 to 9 and 4, respectively (Table 2). In addition, there were 16 candida and non-candida yeast reported in the 3 months pre-decision period, while only 2 were reported after the policy was changed. We also noticed a significant reduction in the major uropathogens ($p < 0.05$) in terms of *E. coli*, *K. pneumoniae*, *Proteus* spp., *Enterococcus* spp., coagulase-positive *Staphylococcus*, and group B streptococcus (Table 2).

3.3 Comparison of major uropathogens reported pre and post 3 years from stop reflex decision

After our initial pan comparison of all UTI reports for the 6-month time frame, we examined the trends of major pathogens of concern (Flores-Mireles et al., 2015) by extending the 3 years pre and 3 years post decision to stop reflexing (Table 1) from the total cultures processed and mentioned in section 3.1. As expected, we found a significant reduction of all listed pathogens ($p < 0.0001$). *S. agalactiae* (GBS) was the least reported, with a reduction of 76% of cases from pre to post intervention. *K. pneumoniae*, being a real uropathogen, had a 31% reduction in reported culture positivity.

3.3.1 Antibiotic utilization trend before and after policy implementation

We identified 1,249 patient records (dose regimen/patient used for UTI only) with administered or prescribed antibiotics in the 3 years preceding policy implementation and 1,633 patient records post-implementation as shown in Table 3. Analyzing the data (Figure 1) using Fisher's exact test, we observed a significant reduction in ciprofloxacin usage ($p < 0.0001$) post-implementation, while nitrofurantoin usage increased significantly ($p < 0.0001$). Additionally, cephalexin and doxycycline usage showed significant increases ($p < 0.05$) after policy implementation.

4 Discussion

UA is often considered an unreliable tool for diagnosing UTIs because of its low positive predictive value (PPV) when compared to urine culture. For instance, the PPV of pyuria in identifying culture-positive infections has been reported to be as low as 4% and up to 32% in various studies (Humphries and Dien Bard, 2016). The absence of standardized criteria for reflexive urine culture testing has recently become a subject of investigation. UA is one of the oldest diagnostic tests in medicine, and today, many laboratories utilize UA as a preliminary screening method to decide whether further bacterial culture is necessary. While reflex urine culture is now a common practice, there is a lack of evidence-based guidelines to define optimal criteria and workflows for these procedures (Chambliss and Van, 2022). Prior research has highlighted similar challenges, noting that inappropriate treatment of asymptomatic bacteriuria is often linked to the overuse of UA reflex to urine cultures. The findings revealed that halting reflex urine culture practices significantly reduced the number of cultures performed and showed a tendency toward lower antibiotic usage (Dietz et al., 2016). The purpose of this study was to evaluate the effects of

10.3389/fcimb.2025.1572936

TABLE 2 Total number of each organism reported from the culture and sensitivity (C&S) workup in 3 months before and after the hard stop on urinalysis reflex.

UTI organism	# Reported pre decision on C&S	# Reported post decision on C&S
E. coli *	597	152
E. faecalis *	185	56
K. pneumoniae *	152	46
S. agalactiae *	92	21
S. epidermidis **	88	18
P. mirabilis *	59	26
Lactobacillus **	47	9
S. viridans **	41	4
S. anginosus **	32	16
E. cloacae *	25	13
S. aureus *	23	11
C. koseri *	22	4
K. oxytoca *	21	5
P. aeruginosa *	13	8
S. marcescens *	12	2
S. haemolyticus **	12	2
K. aerogenes *	8	3
C. braakii **	7	0
P. stuartii **	7	2
M. morganii *	6	5
S. saprophyticus **	5	0
S. alactolytus **	4	0
S. mutans ***	4	0
S. simulans ***	4	0
E. gallinarum ***	4	0
Corynebacterium **	4	0
P. rettgeri **	4	1
R. planticola *	4	0
S. gallolyticus **	4	1
S. warneri ***	3	0
A. baumannii *	3	0
E. faecium *	3	2
C. glabrata *	8	1
C. albicans *	8	0
C. tropicalis *	0	1

Uropathogen* Opportunistic** Non-pathogen***.

TABLE 3 Total antibiotics classes (dose regimen/patient) prescribed 3 years before and 3 years after discontinuing reflex testing (dose regimen/patient).

Antibiotic name	# Used for UTI before* decision	# Used for UTI after* decision
AMOXICILLIN	65	69
AMOXICILLIN/CLAV	104	171
CEPHALEXIN	66	123
CIPROFLOXACIN	541	435
DOXYCYCLINE	45	87
LEVOFLOXACIN	65	62
NITROFURANTOIN	358	679
FOSFOMYCIN	1	3
CEFTRIAXONE	4	4
Total # of Antibiotics used for	1249	1633

is shorten abbreviation for number. * is for discontinuing reflex testing.

discontinuing reflex urine cultures, and these results align with previous studies on the subject (Dietz et al., 2016; Chambliss and Van, 2022).

Uropathogens in urine culture may not be an indication of UTI in many cases. In ICU trauma patients, Stovall et al. found that a negative UA rules out a catheter-associated UTI in virtually all cases due to its high negative predictive value and sensitivity of 100% (Stovall et al., 2013). A positive UA was defined as positive leukocyte esterase, positive nitrite, WBC > 10/high-power field, or the presence of bacteria. A positive urine culture was defined as growth of ≥10 (5) CFU of an organism irrespective of the UA result or ≥10 (3) CFU in the setting of a positive UA. A UTI was defined as positive urine culture without an alternative cause for the fever (Stovall et al., 2013). Cultures performed without additional diagnostics tests that aid in the correct clinical interpretation of urine cultures is a common practice. A study of isolated urine cultures in 2009–2013 found that 20.2% of urine cultures were performed without a UA or urine microscopy (Carlson et al., 2017). This number may vary from institution to institution based on protocols, but this can add up to a large volume of urine cultures, especially at larger hospitals and healthcare systems. According to Stovall et al (Stovall et al., 2013), many of these urine cultures could be prevented by implementing a policy of not performing urine cultures on a patient with a negative UA because even in cases of positive urine cultures, a negative UA ruled out catheter-associated UTI in patients with a fever. We find that this practice of discontinuing reflex of positive UA to culture may further lead to a significant reduction in urine culture volume, with the most benefit seen in larger institutions with higher volumes of patients and specimens. This decreases the burden on the lab and allows the staff to focus on processing more critical specimens instead of working up cultures that may not be clinically relevant. A positive urine culture may extend a patient's stay and cause them to receive additional treatments and is also a detriment to antibiotic stewardship efforts. In cases where these positive urine cultures likely do not represent an underlying UTI, the patient may receive unnecessary antibiotic treatment and have a prolonged ICU or hospital stay (Grein et al., 2016). This leads to increased chances of patients developing healthcare-related infections or other harm, increasing patient morbidity and mortality. Unnecessary antibiotics can promote the development of antibiotic-resistant bacteria. These antibiotic-resistant bacteria can pose significant harm to patients and become challenging to treat, increasing patient morbidity and mortality (Ventola, 2015). Although targeted antibiotics for UTIs were used more frequently than non-specific antibiotics (at the discretion of the provider, as is common practice at our institution), some providers treated UTIs without ordering a urine culture. This practice may have contributed to the increased total number of antibiotics used (shown in Table 3), which is a limitation of this study. Our electronic health record system cannot specifically isolate cases where a urine culture and sensitivity was performed for UTI diagnosis and treated accordingly. Once we stopped reflexing, we only reported antibiotic sensitivity results from the patients who had orders. In addition, the annual hospital antibiogram, which includes ESBL prevalence, provides good insight into locally resistant trends based on those results for individual physicians to make a therapeutic choice. Therefore, targeted therapy and empirical therapy were both impacted by the policy of stopping UA reflexes to culture, and we believe that the trend shift in antibiotic use occurred because of this.

In addition to the financial burden to the patient and the hospital system, another considerable factor is that the hospitals are not reimbursed for treatment of catheter-associated UTIs. Therefore, it is very important for patient safety that results are accurate and reliable in these diagnoses (Morgan et al., 2012).

Larger healthcare systems are most affected by these inefficiencies and will see the greatest benefit from policy changes to reduce unnecessary urine cultures. Urine cultures can be falsely positive due to improper collection, improper handling, improper storage conditions, and contamination. Therefore, in addition to revisiting reflex criteria, as recommended by Stovall et al (Stovall et al., 2013), UA of suspected culture-positive patients will also have an added benefit. However, the latter option comes at an additional cost. Standardizing these procedures and ensuring proper quality

control help increase efficiency and decrease false positives. The significant increase in nitrofurantoin usage post-implementation serves as a clear indication of the successful introduction of narrower-spectrum antibiotics, which aligns with the principles of antibiotic stewardship. This shift towards more targeted antibiotic therapy reflects a conscious effort to minimize the use of broad-spectrum antibiotics and mitigate the risk of antibiotic resistance. In addition to the seven common antibiotics we used for this study (Figure 1), trimethoprim/sulfamethoxazole and ceftriaxone (included in Table 3) are commonly used for simple UTI. In complicated UTI or kidney infection, fluoroquinolone is used if there are no other treatment options (Jancel and Dudas, 2002). Another limitation in our data is not including empirical use of antibiotics before the culture results were available. Another limitation was that our electronic data system could not retrieve purely culture-based antibiotics therapy data. As a result, we computed total antibiotic dose data per UTI case diagnosed through cultures and symptomatic evaluations.

Moreover, the implementation of selective reporting of antibiotic sensitivity due to formulary restriction and the latest CLSI updates may have played a role in reducing the use of targeted antibiotics such as ciprofloxacin. By providing healthcare providers with more precise information on antibiotic susceptibility, selective reporting promotes the use of antibiotics that are most effective against specific pathogens, thereby optimizing targeted antibiotic therapy and reducing unnecessary antibiotic use by skipping asymptomatic bacteriuria. We believe that our report will help other organizations to revisit their policies, in turn aiding in cost cutting, improving patient safety, and promoting antibiotic stewardship. Urinary cultures should only be performed when there is a high clinical suspicion for infection rather than a reflex testing of every abnormal UA.

Data availability statement

The original contributions presented in the study are included in the article/supplementary material. Further inquiries can be directed to the corresponding author.

Ethics statement

This is an observational process improvement study which used deidentified patient data and ethical approval is not required. However, institutional Associate Chief of Staff - Research has been notified of the pending submission and received approval. for the studies on humans because Institutional Associate Chief of Staff - Research has been notified of the pending submission and received approval. The studies were conducted in accordance with the local legislation and institutional requirements. Written informed consent for participation was not required from the participants or the participants' legal guardians/next of kin in accordance with the national legislation and institutional requirements. The human samples used in this study were acquired from a by- product of routine care or industry.

Author contributions

BB: Investigation, Methodology, Visualization, Writing – original draft, Writing – review & editing. JL: Data curation, Project administration, Resources, Writing – original draft, Writing – review & editing. CJ: Conceptualization, Resources, Visualization, Writing – original draft, Writing – review & editing. DN: Conceptualization, Data curation, Formal analysis, Funding acquisition, Investigation, Methodology, Project administration, Resources, Software, Supervision, Validation, Visualization, Writing – original draft, Writing – review & editing.

Funding

The author(s) declare financial support was received for the research and/or publication of this article. This work was supported by the Central Texas Veterans Health Care System, Temple, TX.

Acknowledgments

The authors would like to express their gratitude to CTVHCS for providing access to the necessary data and resources for this study. This material is the result of work supported with resources and the use of facilities at the Central Texas Veterans Health Care System.

Conflict of interest

The authors declare that the research was conducted in the absence of any commercial or financial relationships that could be construed as a potential conflict of interest.

Generative AI statement

The author(s) declare that no Generative AI was used in the creation of this manuscript.

Any alternative text (alt text) provided alongside figures in this article has been generated by Frontiers with the support of artificial

intelligence and reasonable efforts have been made to ensure accuracy, including review by the authors wherever possible. If you identify any issues, please contact us.

Publisher's note

All claims expressed in this article are solely those of the authors and do not necessarily represent those of their affiliated organizations, or those of the publisher, the editors and the reviewers. Any product that may be evaluated in this article, or claim that may be made by its manufacturer, is not guaranteed or endorsed by the publisher.

Author disclaimer

The opinions expressed here are those of the authors and do not represent the views of Department of Veterans Affairs or of Central Texas Veterans Health Care System, Temple, TX.

References

Advani, S. D., Gao, C. A., Datta, R., Sann, L., Smith, C., Leapman, M. S., et al. (2019). Knowledge and practices of physicians and nurses related to urine cultures in catheterized patients: an assessment of adherence to IDSA guidelines. *Open Forum Infect. Dis.* 6. doi: 10.1093/ofid/ofz305

Advani, S., and Vaughn, V. M. (2021). Quality improvement interventions and implementation strategies for urine culture stewardship in the acute care setting: advances and challenges. *Curr. Infect. Dis. Rep.* 23. doi: 10.1007/s11908-021-00760-3

Carlson, A. L., Munigala, S., Russo, A. J., McMullen, K. M., Wood, H., Jackups, R., et al. (2017). Inpatient urine cultures are frequently performed without urinalysis or microscopy: findings from a large academic medical center. *Infect. Control Hosp Epidemiol.* 38, 455–460. doi: 10.1017/ice.2016.311

Chambliss, A. B., and Van, T. T. (2022). Revisiting approaches to and considerations for urinalysis and urine culture reflexive testing. *Crit. Rev. Clin. Lab. Sci.* 59, 112–124. doi: 10.1080/10408363.2021.1988048

Chironda, B., Clancy, S., and Powis, J. E. (2014). Optimizing urine culture collection in the emergency department using frontline ownership interventions. *Clin. Infect. Dis.* 59, 1038–1039. doi: 10.1093/cid/ciu412

Dietz, J., , T., Lo, S., and Hammer, K., and Zegarra, M.. (2016). Impact of eliminating reflex urine cultures on performed urine cultures and antibiotic use. *Am. J. Infect. Control* 44, 1750–1751. doi: 10.1016/j.ajic.2016.04.232

Flores-Mireles, A. L., et al. (2015). Urinary tract infections: epidemiology, mechanisms of infection and treatment options. *Nat. Rev. Microbiol.* 13, 269–284. doi: 10.1038/nrmicro3432

Flores-Mireles, A. L., Walker, J. N., Caparon, M., and Hultgren, S. J.. (2016). Treatment for positive urine cultures in hospitalized adults: A survey of prevalence and risk factors in 3 medical centers. *Infect. Control Hosp Epidemiol.* 37, 319–326. doi: 10.1017/ice.2015.281

Henderson, J., and Bean, S. (2019). Screening for asymptomatic bacteriuria in adults: an updated systematic review for the U.S. Preventive services task force. W.E. doi: 10.1001/jama.2019.10060

Hengstler, K. A., Hammann, R., and Fahr, A. M. (1997). Evaluation of BBL CHROMagar orientation medium for detection and presumptive identification of urinary tract pathogens. *J. Clin. Microbiol.* 35, 2773–2777. doi: 10.1128/jcm.35.11.2773-2777.1997

Hooton, T. M., and Stamm, W. E. (1997). Diagnosis and treatment of uncomplicated urinary tract infection. *Infect. Dis. Clin. North Am.* 11, 551–581. doi: 10.1016/S0891-5520(05)70373-1

Humphries, R. M., and Dien Bard, J. (2016). Point-counterpoint: reflex cultures reduce laboratory workload and improve antimicrobial stewardship in patients suspected of having urinary tract infections. *J. Clin. Microbiol.* 54, 254–258. doi: 10.1128/JCM.03021-15

Jancel, T., and Dudas, V. (2002). Management of uncomplicated urinary tract infections. *West J. Med.* 176, 51–55. doi: 10.1136/ewjm.176.1.51

Morgan, D. J., Meddings, J., Saint, S., Lautenbach, E., Shardell, M., Anderson, D., et al. (2012). Does nonpayment for hospital-acquired catheter-associated urinary tract infections lead to overtesting and increased antimicrobial prescribing? *Clin. Infect. Dis.* 55, 923–929. doi: 10.1093/cid/cis556

Nicolle, L. E., Gupta, K., Bradley, S. F., Colgan, R., DeMuri, G. P., Drekonja, D., et al. (2019). Clinical practice guideline for the management of asymptomatic bacteriuria: 2019 update by the infectious diseases society of americaa. *Clin. Infect. Dis.* 68, e83–e110. doi: 10.1093/cid/ciz021

Sarg, M., , G., Waldrop, E., , M., Beier, A., , E., Heil, L., , K., Thom, A., , M., Preas, A., et al. (2016). Impact of changes in urine culture ordering practice on antimicrobial utilization in intensive care units at an academic medical center. *Infect. Control Hosp Epidemiol.* 37, 448–454. doi: 10.1017/ice.2015.334

Schappert, S. M., and Rechtsteiner, E. A. (2011). Ambulatory medical care utilization estimates for 2007. *Vital Health Stat. 13* 169, 1–38.

Stovall, R. T., Haenal, J. B., Jenkins, T. C., Jurkovich, G. J., Pieracci, F. M., Biffl, W. L., et al. (2013). A negative urinalysis rules out catheter-associated urinary tract infection in trauma patients in the intensive care unit. *J. Am. Coll. Surg.* 217, 162–166. doi: 10.1016/j.jamcollsurg.2013.02.030

Ventola, C. L. (2015). The antibiotic resistance crisis: part 1: causes and threats 40, 277–283.

Yarbrough, M. L (2023). "Urine Cultures," in *ClinMicroNow*, WILEY, Hoboken, NJ, 1–19.

Frontiers in
Cellular and Infection Microbiology

Investigates how microorganisms interact with their hosts

Explores bacteria, fungi, parasites, viruses, endosymbionts, prions and all microbial pathogens as well as the microbiota and its effect on health and disease in various hosts.

Discover the latest Research Topics

See more →

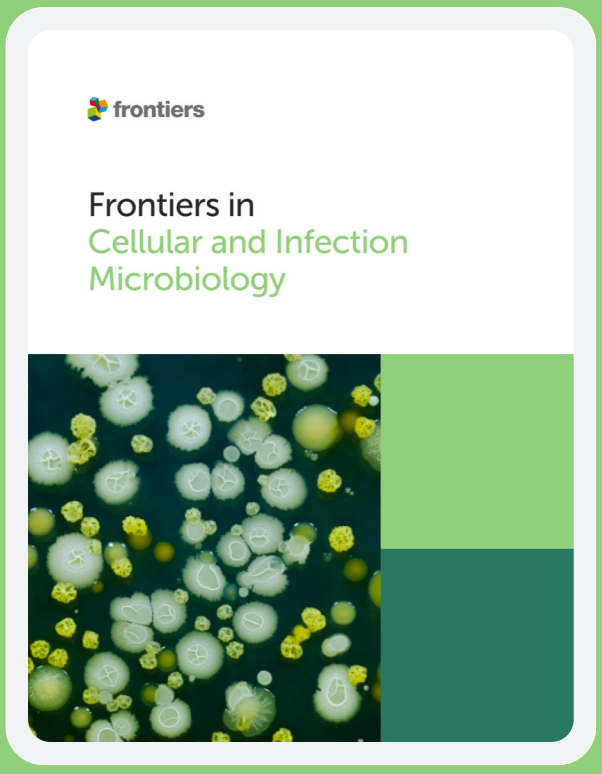

Frontiers

Avenue du Tribunal-Fédéral 34
1005 Lausanne, Switzerland
frontiersin.org

Contact us

+41 (0)21 510 17 00
frontiersin.org/about/contact